NATO Security through Science Series - C:
Environmental Security

Combined and Hybrid Adsorbents

Fundamentals and Applications

Edited by
José Miguel Loureiro
Mykola T. Kartel

Springer

NATO
OTAN

This publication is supported by:

The NATO Programme for Security through Science

Combined and Hybrid Adsorbents

NATO Security through Science Series

This Series presents the results of scientific meetings supported under the NATO Programme for Security through Science (STS).

Meetings supported by the NATO STS Programme are in security-related priority areas of Defence Against Terrorism or Countering Other Threats to Security. The types of meeting supported are generally "Advanced Study Institutes" and "Advanced Research Workshops". The NATO STS Series collects together the results of these meetings. The meetings are co-organized by scientists from NATO countries and scientists from NATO's "Partner" or "Mediterranean Dialogue" countries. The observations and recommendations made at the meetings, as well as the contents of the volumes in the Series, reflect those of participants and contributors only; they should not necessarily be regarded as reflecting NATO views or policy.

Advanced Study Institutes (ASI) are high-level tutorial courses to convey the latest developments in a subject to an advanced-level audience

Advanced Research Workshops (ARW) are expert meetings where an intense but informal exchange of views at the frontiers of a subject aims at identifying directions for future action

Following a transformation of the programme in 2004 the Series has been re-named and re-organised. Recent volumes on topics not related to security, which result from meetings supported under the programme earlier, may be found in the NATO Science Series.

The Series is published by IOS Press, Amsterdam, and Springer, Dordrecht, in conjunction with the NATO Public Diplomacy Division.

Sub-Series

A. Chemistry and Biology	Springer
B. Physics and Biophysics	Springer
C. Environmental Security	Springer
D. Information and Communication Security	IOS Press
E. Human and Societal Dynamics	IOS Press

http://www.nato.int/science
http://www.springer.com
http://www.iospress.nl

Series C: Environmental Security

Combined and Hybrid Adsorbents

Fundamentals and Applications

edited by

José Miguel Loureiro
LSRE/DEQ/FEUP, University of Porto,
Portugal

and

Mykola T. Kartel
ISPE/NASU,
Kiev, Ukraine

Published in cooperation with NATO Public Diplomacy Division

Proceedings of the NATO Advanced Research Workshop on
Combined and Hybrid Adsorbents: Fundamentals and Applications
Kiev, Ukraine
15–17 September 2005

A C.I.P. Catalogue record for this book is available from the Library of Congress.

ISBN-10 1-4020-5171-9 (PB)
ISBN-13 978-1-4020-5171-5 (PB)
ISBN-10 1-4020-5170-0 (HB)
ISBN-13 978-1-4020-5170-8 (HB)
ISBN-10 1-4020-5172-7 (e-book)
ISBN-13 978-1-4020-5172-2 (e-book)

Published by Springer,
P.O. Box 17, 3300 AA Dordrecht, The Netherlands.

www.springer.com

Printed on acid-free paper

TABLE OF CONTENTS

Preface xi

PART I – HYBRID ADSORPTIVE MATERIALS AND SPECIAL INORGANIC ADSORBENTS

Synthesis, Structure and Adsorption Properties of Functionalized Polysiloxane Materials 3
Yuriy L. Zub and Alexey A. Chuiko

Design, Synthesis and Characterization of Ordered Mesoporous Materials for Environmental Applications 23
Mietek Jaroniec

Selective Removal of Radionuclides from Nuclear Waste Effluents using Inorganic Ion Exchangers 37
Risto Koivula, Risto Harjula and Jukka Lehto

Experimental Approach to the Synthesis of Hybrid Adsorbents on the basis of Polysiloxane Xerogels Functionalized with Calix[4]arenes and their Derivatives 49
Olga V. Kuchma and Yuriy L. Zub

Hybrid Polymer-Silica Adsorbent for Chromatography 55
Olimjon N. Ruzimuradov

Design and Characterization of Novel Zeoadsorption Media derived from Surface Coating with Functional Hydrocarbons 63
Eva Chmielewská and Wlodzimierz Tylus

Regulation of Lignocellulose Materials Sorption Properties by Modification for Environmental Application 71
Galina Telysheva, Tatiana Dizhbite, Galina Lebedeva, Natalia Zaimenko and Sergey Popovs

Hydrothermostability of Mesoporous Mesophase Materials of MCM-41 and SBA-3 type 77
Mikhail E. Malyshev, Maxim S. Mel'gunov, Alexander N. Shmakov, Elena A. Mel'gunova and Vladimir B. Fenelonov

Uranium Sorption by Organozeolites and Ferromagnetic Organozeolites from Waste Water of Special Laundry 85
V.A. Nikashina, E.M. Kats, I.B. Serova and Peter A. Gembitski

Template Effect of the M^{3+}-Cations in the Course of the Synthesis of High Dispersed Titanium and Zirconium Phosphates 93
Igor Z. Zhuravlev and Vladimir V. Strelko

New Spherically Granulated Inorganic Ion Exchangers on the basis of Titanium Phosphate 99
Anna A. Zaitseva, Valentin A. Kanibolotsky, Valeriy I. Yakovlev and Vladimir V. Strelko

Iron-based Nanoadsorbents for the Removal of Metal Ions from Water 105
E.A. Deliyanni, E.N. Peleka and K.A. Matis

Preliminary Study on the Adsorption of the Cationic Dye Astrazon Red by a Portuguese Bentonite 111
Sílvia C. R. Santos, Rui A. R. Boaventura and Álvaro F. M. Oliveira

PART II – ACTIVATED CARBON, COMBINED ADSORBENTS AND OTHER ORGANIC ADSORBENTS

Morphology and Surface Chemistry of Chemically Treated Activated Carbons 119
Krisztina László

Porous Carbons in Gas Separation and Storage 133
Francisco Rodríguez-Reinoso

Carbonaceous Materials as Desulfurization Media 145
Teresa J. Bandosz

Combined Adsorption Preparations from Active Carbons, Clay Minerals and Natural Plant Products 165
Mykola T. Kartel, Volodymyr V. Strelko, Svetlana S. Stavitskaya, Valentina K. Mardanenko and Lidia A. Kupchik

Synthesis of New Low Density Carbon Materials with Molecular Sieving Properties 181
Svetlana S. Stavitskaya, Mykola T. Kartel, Valentina E. Goba, Olga N. Bakalinskaya and Ninel M. Koval

Granular Activated Carbon from Deciduous Wood Lignocellulose 187
Janis Rizhikovs, J. Zandersons, M. Puke, N. Vedernikovs, G. Dobele, A. Tardenaka and B. Spince

Synthesis of Activated Carbon from Spent Lubricating Oil and Application for Adsorption of Cadmium and Lead Ions from Aqueous Solution 195
Reyad Shawabkeh, Abdulaziz Khlaifat, Omar Khashman and Salah Tarawneh

Synthesis and Catalytic Properties of N-Containing Synthetic Carbons on a basis of Copolymer of Styrene and Divinylbenzene 201
Sergey V. Zhuravsky, Mykola T. Kartel and Olexander M. Puziy

Adsorption Properties of Modified Filtration Materials in Water Treatment 207
Yuriy I. Tarasevich, Zinaida M. Shkavro, Olena O. Shevchuk and Yuriy L. Zub

Properties of Combined Sorbent - "Zeolite in Fiber" 213
V.A. Nikashina, G.V. Myasoedova, E.V. Kulbachevskaya, E.M. Kats, V.L. Tziperman and R.K. Idiatulov

Enhancement of Adsorption Capacity by Use of Phase Change Material (PCM) as Additive in an Activated Carbon (AC) Fixed Bed Adsorber 219
W. Zimmermann and J.U. Keller

Thermochemical Activation of Lignins for Obtaining Effective Sorbents 225
Galina Dobele, Galina Telysheva and Nikolai Bogdanovich

An Opportunity for Reduction of the Influence of Diffusion Resistance when Carrying out Catalytic and Adsorption Processes by using Porous Wall Tubes made of Activated Carbon 231
Ljutzkan Ljutzkanov and Nikolai Kolev

Use of Active Carbon to Phenol Reduction from Water Solution 237
Anna Wolborska

Removal of Hydrogen Sulfide, Ammonia and Nitrite Ions from Water Solutions using Modified Active Carbons 243
T. Lupascu, Raisa Nastas, M. Ciobanu, Tatiana Arapu and V. Rusu

Adsorption of Chromium Ions from Aqueous Solution using Activated Carbo-Aluminosilicate Material 249
Reyad Awwad Shawabkeh

Modified Natural Sorbents for Binding Heavy Metal Ions 255
Alina A. Nikolaychuk, Lidia A. Kupchik and Mykola T. Kartel

Influence of Adsorption of Viruses of Plants on Electric Properties of Porous Silicon 261
Yuri A. Vashpanov and Igor P. Konup

Adsorption Study of Lead by *Ascophyllum Nodosum* using a Factorial Experimental Design 269
Olga Freitas, Rui Boaventura and Cristina Delerue-Matos

Application of Chitin Containing Sorbents for Treatment of Water Solutions 275
Tatyana Solodovnik

Biosorption Performance of a Binary Metal Mixture by Algal Biomass: Column Experiments 281
Vítor Vilar, Cidália Botelho and Rui Boaventura

Removal of Selenium and Antimony species from Aqueous Solutions by means of a Weakly Basic Ion Exchanger 287
Mercy S. Dzul Erosa and Wolfgang H. Höll

PART III – MODELING ADSORBENTS, ADSORPTION AND ADSORPTION PROCESSES

The Porous Structure of Hard and Deformed Adsorbents and Mobility of Adsorbed Molecules 295
R.Sh. Vartapetyan and E.V. Khozina

Characterization of Hard and Soft Porous Materials and Tissue Scaffolds 309
Sergey V. Mikhalovsky, Lyuba I. Mikhalovska, Stuart L. James, Paul E. Tomlins, Paul V. Grant, Pankaj Vadgama and Vlad M. Gun'ko

Modeling Gas Phase Adsorption in Industrial and Military Applications 321
Peter Lodewyckx

Focusing Materials Research through Process Modeling 337
José Miguel Loureiro, Ana Mafalda Ribeiro and Sónia Adriana Figueiredo

Some Aspects of Physical and Chemical Adsorption on Surface of Amorphous Solid 349
Tamaz A. Marsagishvili, M.N. Machavariani and S.A. Kirillov

Breakthrough Behavior of Water Vapor on Activated Carbon Filters.....357
Ana Mafalda Ribeiro and José Miguel Loureiro

List of Participants.....361

Index.....365

PREFACE

Adsorption is a separation process playing a fundamental role in several industrial areas, being used in both purification and bulk separations. The adsorbent used is the main parameter controlling the effectiveness of the process. Emerging new separations and the improvement of existing ones constitute the driving force for the development of new adsorbents with improved adsorbing properties. With this objective, recent research directions include the development of hybrid organic-inorganic and combined adsorbents.

These Combined and Hybrid Adsorbents have progressively found their place, gaining importance for adsorptive applications and, consequently, for economy. They encompass significant scientific advances, pointing to the development of some directions of modern technology in the near future. This is confirmed by the impressive growth of the number of scientific publications dedicated to the subject in the last few years.

The progresses in the development of these materials, the increased environmental and terrorism concerns, the needs for the integration between science and technology and the new analytical techniques available, enabling the complete characterization of these new materials, led us to the organization of a Research Workshop, aiming at making an up-to-date review of the latest achievements and an exchange of ideas between people working in several fields of this research area.

This volume includes the key lectures and participants' contributions delivered at the NATO-funded Advanced Research Workshop *Combined and Hybrid Adsorbents: Fundamentals and Applications*, held in Pushcha-Voditsa, Kiev, Ukraine, from the 15th to the 17th of September 2005, and attended by 49 participants from 19 countries.

The purpose of the workshop was three-fold, according to the three parts in which this book is divided. The first part includes contributions reporting the dramatic progress in the field of hybrid organic-inorganic adsorptive materials prepared by sol-gel and template methods as well as their applications; special inorganic adsorbents and their applications, including the removal of radionuclides from nuclear waste effluents, are included in this first part. The second part concerns the synthesis, properties and applications of carbon and combined adsorbents, including enterosorbents for the effective elimination of toxic metals and radionuclides from the human organism; other organic adsorbents, including chitin and algal biomass, are included in the second part. Finally, the third part is dedicated to the modeling of adsorbents, adsorption and

adsorption processes, including the simulation of carbon masks used both for civil and military protection purposes.

This book is addressed to a wide readership. Specialized workers in the field should find the updated materials on several areas of this topic very useful. University teachers could use the material in this book for introductory or graduate courses, and those who have a general interest in the subject should find the offered overviews particularly interesting. There are extensive literature references for further detailed studies.

Many people have contributed to the success of the ARW on which this volume is based. We wish to thank especially the ARW secretary, Ana Mafalda Ribeiro, for her outstanding work, availability and kindness and also Olga Bakalinskaya for her competent assistance in the organization of the meeting. We thank of course all the participants, mainly the invited key speakers, for their contributions to a stimulating intellectual dialogue atmosphere throughout the duration of the Workshop. Finally, it is a great pleasure to acknowledge the financial support provided by the NATO Public Diplomacy Division.

José Miguel Loureiro
Mykola T. Kartel

PART I

HYBRID ADSORPTIVE MATERIALS AND SPECIAL INORGANIC ADSORBENTS

SYNTHESIS, STRUCTURE AND ADSORPTION PROPERTIES OF FUNCTIONALIZED POLYSILOXANE MATERIALS

YURIY L. ZUB* AND ALEXEY A. CHUIKO
Institute of Surface Chemistry, National Academy of Sciences of Ukraine, 17 General Naumov Str., Kyiv 03164, Ukraine

Abstract. A consideration has been given to salient features of synthesis of functionalized polysiloxane xerogels using one-, two-, and three-component (in terms of alkoxysilanes) systems. Possibilities have been revealed for potentialities of physical methods for characterizing nature of functional groups, types of structural units that form these xerogels and surface layer structure. Adsorption properties of such hybrid organic-inorganic materials have been described in detail.

Keywords: sol-gel method; hybrid organic-inorganic materials; functionalized polysiloxane xerogels; synthesis; structure; sorption properties

1. Introduction

During the last few years the chemistry of organic-inorganic materials saw a rapid progress, which is due to both broad possibilities for their design and ample scope for their application in various fields.[1] Among these materials, one can distinguish several large classes, with a special interest being avoked by a class of functionalized polysiloxane materials. Many of them possess a porous structure and find much use as sorptive materials.

The synthesis of these materials is most often effected by the sol–gel method.[2] A use is usually made of its variant that is based on reaction of hydrolytic polycondensation of corresponding silicon derivatives (Schemes

* To whom correspondence should be addressed. Dr. Yu.L. Zub, Head of Hybrid Materials Laboratory, Institute of Surface Chemistry, NAS of Ukraine, 17 General Naumov Str., Kyiv 03164, Ukraine; e-mail: zub@public.icyb.kiev.ua

J.M. Loureiro and M.T. Kartel (eds.), Combined and Hybrid Adsorbents, 3–21.

1 and 2).[3–5] This reaction proceeds in the presence of water and a catalyst (e.g., OH^-, H^+, F^-). The appropriate treatment of the formed gels (their ageing, washing, drying, etc.) results in functionalized polysiloxane xerogels (FPX).

Preparation of FPX is most often effected using two-component systems (Scheme 2). This approach employs tetraalkoxysilane [usually tetraethoxysilane (TEOS), $Si(OC_2H_5)_4$] in the capacity of a structure-forming agent while the second component (trifunctional silane) is used to introduce a necessary functional (ligand) group R′.

$$Na[O(HO)_2SiCH_3] \xrightarrow[-NaCl]{+HCl} (HO)_3SiCH_3 \xrightarrow[-H_2O]{} (O_{3/2}SiCH_3)_x \quad (1)$$

$$Si(OR)_4 + (RO)_3SiR' \xrightarrow[-ROH]{+H_2O,\ catalyst} Si(OH)_4 + (HO)_3SiR' \xrightarrow[-H_2O]{}$$

$$\rightarrow (SiO_2)_x \cdot (O_{3/2}SiR')_y \quad (2)$$

Application of the sol–gel method for synthesizing functionalized polysiloxane materials offers a number of advantages over other methods. The main of these advantages consists in the possibility to use multicomponent (in terms of alkoxysilanes) systems. Of importance is the fact that it is possible to vary the nature of both structure-forming agents [$E(OR)_n$ (E = Si, Al, etc.) or $(RO)_3Si–R''–Si(OR)_3$] and trifunctional silanes $(RO)_3SiR'$. In the last case one can prepare polysiloxane xerogels whose surface layer contains simultaneously functional groups R′ differing in their nature. The possibility of making a wide choice of conditions that are acceptable for effecting the hydrolytic polycondensation reaction allows one to exert a rather strict control over properties of final products (xerogels). The above-stated relates, in the first place, to parameters of their porous structure. One of the obvious advantages of the sol–gel method resides in the the fact that it involves a one-stage process. In other words, formation of xerogel particles and their functional layer takes place at one stage of the synthesis. Besides, the sol–gel method makes it possible to prepare xerogels whose content of functional groups is close to a preassigned content. Moreover, the total content of such groups may be by an order of magnitude greater than that attained in the situation with modified silicas. Thus, application of the sol–gel method offers ample scope for creation of both the sorptive polysiloxane materials themselves and their surface.[4–8]

This paper was intended to consider the results that were achieved during the past years. These results refer, first of all, to salient features of

synthesis, structure, and adsorption properties of polysiloxane xerogels with functional groups containing N, P, O, and S.

2. Synthesis and Identification of Functionalized Polysiloxane Xerogels

2.1. SYNTHESIS WITHOUT USING A STRUCTURE-FORMING AGENT

The hydrolytic polycondensation only of carbofunctional silico-organic monomers with a composition of $X_3SiR''Y$ or $(X_3SiR'')_2Y$, where Y is a ligand group; X is Cl, OR, OCOR, or NR_2; R is CH_3 or C_2H_5; R″ is $(CH_2)_m$, etc., found wide use in works of the team headed by Voronkov which were aimed to synthesize sulfur-containing polysiloxane sorbents.[6,9] The hydrolysis of the majority of silico-organic monomers was carried out for 1–10 h in an aqueous media (pH 8–11, KOH) at the boiling temperature of the reaction mixture and was accompanied by a practically quantitative yield of the formed polymers. The precipitates obtained were dried at 100–110 °C. Sometimes the synthesis involved application of nonaqueous solvents (e.g., dioxane, alcohols), and KOH solutions were replaced by ammoniac media. The above-described procedure gave a number of polyalkylsilsesquioxanes with common formulas $[O_{3/2}Si(CH_2)_mY]_n$ (Y = SH, NHC(O,S)Me, NHC(S)NHC(O)Me, $S(CH_2)_2NH_2$, etc.; m = 2 or 3) and $[O_{3/2}Si(CH_2)_mY(CH_2)_mSiO_{3/2}]_n$ (Y = S, SCH_2S, NHC(O,S)NH, $NHC(O)C_6H_4C(O)NH$, $NHC(S)(CH_2)_2C(S)NH$, NHSSNH, $NHS(O)NH$, $NHS(O_2)NH$, etc.). In some cases (e.g., during the course of the synthesis of the polymer with a link of $O_{3/2}SiCH_2SH$) the hydrolysis of the starting alkoxysilane was effected in an acidic medium alcohol–dioxane, with the subsequent condensation being performed in an alkaline medium.[10,11] It should be noted that polycondensation of $(CH_3O)_3SiCH_2SH$ in acetone takes place with participation of mercaptomethyl groups.[11]

In order to prepare polymers containing sulfoacidic fragments it was necessary to perform a preliminary oxidation of trialkoxysilylalkanethiols by a 70% solution of hydrogen peroxide in dioxane at –5 °C (Scheme 3).[12] The same method was also applied for producing polymers with groups $–NHC(SO_2)NH–$ and $–NHC(SO_2)NHC(O)CH_3$ (in this case a 45% solution of H_2O_2 was used).[9]

$$(RO)_3Si(CH_2)_mSH + 3H_2O_2 \xrightarrow[-3ROH]{} (HO)_3Si(CH_2)_mSO_3H \xrightarrow[-1.5H_2O]{}$$

$$\rightarrow 1/n\left[O_{3/2}Si(CH_2)_mSO_3H\right]_n \qquad (m = 1-3) \qquad (3)$$

It was supposed that the final products should contain a spatially cross-linked skeleton. The supposition was corroborated by the fact that they were nonswelling and insoluble in water and organic solvents. These polymers were thermally stable at temperatures up to 200–280 °C and chemically stable in concentrated solutions of mineral acids and ammonia, which allows their use under severe conditions. Their content of functional groups can reach large values (e.g., 12.3 mmol g^{-1} in the case of $\equiv SiCH_2SH$[11]). It was shown[10] that the reductive capacity of a polymer with thiol groups depends on the size of its particles.

The approach advanced for synthesizing sorbents is rather simple. At the same time, the differences present in the structure of functional groups Y give rise to differences in rates and completeness of transitions of starting mono-mers. Therefore, in some cases the production of cross-linked polymeric products became highly hampered.[9] One of the drawbacks of the offered approach is the absence of any possibility for varying the content of functional groups in the polymers under consideration. Besides, the hydrolytic polycondensation of alkoxysilanes under such conditions gives precipitates but not gels. Hence, the set of factors that may be employed in the situation with such systems to exert an effect on properties of final products becomes substantially smaller in number.

The above-mentioned polymers include also the product of hydrolysis of ester $(C_2H_5O)_3Si(CH_2)_2P(O)(OC_2H_5)_2$ in boiling HCl. This product is a fragile substance with a composition of $[O_{3/2}Si(CH_2)_2P(O)(OH)_2]_x$ which was described as early as 1960.[13] The xerogels contained (thio)phosphoryl groups were also prepared using $(S,O)P[C_6H_4Si(OPr^i)_3]_3$.[14] In this case the catalyst was *n*-toluenesulfonic acid or HCl. In the last case the process resulted in the formation of highly porous xerogels.

Monocomponent systems were used to obtain xerogels containing cyclam.[15] It was shown that the parameters of their porous structure depend on the nature of the catalyst, the solvent, the composition of the hydrolyzing groups [$Si(OEt)_3$ or SiH_3] and the temperature of the gel treatment.

2.2. SYNTHESIS WITH PARTICIPATION OF TETRAALKOXYSILANE AS A STRUCTURE-FORMING AGENT

As early as 1966 a method was offered for producing 'aminoorganosilicagel' by hydrolysis of APTES, $(C_2H_5O)_3Si(CH_2)_3NH_2$ (or its mixtures with TEOS) in an alkaline medium.[16] Later on the xerogel obtained was the subject of inquiry in detail.[17-24] The aim of numerous works was to find methods of synthesis which could result in a sorbent with a highly extended surface and maximum content of amine groups.[18,23,24] These methods usually involved a hydrolytic polycondensation reaction of

TEOS and APTES at their molar ratio of 2:1; the alkaline medium was created after addition of water. In the case of such a system the gel was formed in several minutes. After ageing for 24 h the gel was subjected to drying (in vacuum at 100–105 °C) followed by washing with water and repeated drying. The procedure made it possible to prepare xerogels with a reproducible composition $[(SiO)_{2.6}(O_{3/2}Si(CH_2)_3NH_2)\cdot H_2O]$ and main characteristics.[24] Depending on the synthesis conditions the content of amine groups was in the interval from 2.8 to 4.2 mmol g^{-1}. From the SEM micrograph (Figure 1) it is seen that such materials consist of particles of irregular shapes. According to the TEM data[5] these xerogels have a three-dimensional skeleton formed by condensed spherical globules with a diameter of ~20 nm (Figure 1).

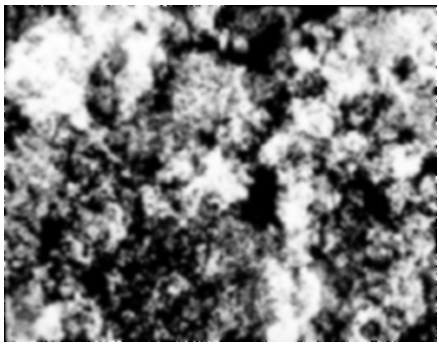

SEM: the scale bar (5 mm) is 5 μm

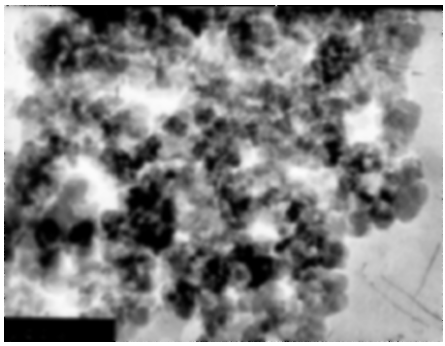

TEM: the scale bar (15 mm) is 100 nm

Figure 1. Micrographs of the sorbent with $\equiv Si(CH_2)_3NH_2$ groups.[24]

The above-considered approach involved application of ethanol (which often allowed to avoid appearance of two phases) employed for producing xerogels with such functional groups as secondary amine, ethylenediamine, imidazolyl groups, etc.[24,25] The authors described the synthesis of a xerogel sample with ethylenediamine groups.[21,26,27] It was mentioned that the synthesis did not involve any solvent. However any parameters of the porous structure of the xerogel were not presented. Zub et al.[25] showed that at a ratio of alkoxysilanes of 2(TEOS):1 such xerogel is formed practically non-porous. This agrees with the data of Silva and Airoldi.[28] Synthesis of the xerogel with an aniline group (or its derivatives) was considered (catalyst – HF, solvent – ethanol).[29-32] Obtaining low-density xerogels containing aminogroups of various nature was analyzed.[33] The authors described a synthesis of porous xerogels with a bifunctional surface layer composed of $\equiv Si(CH_2)_3NH_2/CH_3$ (or C_6H_5).[25,34] The ingredient ratio in the initial solution was 1:1:1. Earlier[35] it was shown that an introduction of

methyl groups increases mechanical strength of spheres of xerogels (0.2 – 1.5 mm) with amine groups. Obtaining monodispersed colloid particles containing aminogroups was considered.[36]

This approach was also used for synthesizing xerogels with (thio)urea groups NHC(O,S)NH (F^-/Si = 1/100).[37] At the TEOS/trifunctional silane ratio of 2:1 the xerogels formed had a monofunctional surface layer and possessed hydrophobic properties while at a ratio of 4:1 (or 8:1) they possessed hydrophilic properties. The xerogel surface acquired hydrophilic properties also in the case of introduction of additional amine groups. Synthesis of xerogels with malonamide ligands was considered.[38]

Becker and Unger[39] described the synthesis of xerogels using 1,2-epoxy-3-propoxypropyltriethoxysilane. Initially, polyethoxysiloxane was prepared from TEOS by acid hydrolysis. Homogeneity of the reaction medium in the second stage was maintained by addition of sodium or ammonium hydroxide, therefore the final product contained either 1,2-dihydroxyl-3-propoxypropyl or hydroxylamine functional groups.

Synthesis of xerogels with groups $\equiv Si(CH_2)_3SH$ is usually performed using such catalysts as $(n\text{-}Bu)_2Sn(CH_3COO)_2$[17,19] or HCl.[40,41] However, according to the NMR spectroscopy data,[19,22] the polysiloxane skeleton of these xerogels does not have any effective cross-linking. Besides, the polymeric matrix composition includes tin.[26] Moreover, these systems are noted for appearance of two phases, and the xerogel formed is practicvally non-porous.[42] These drawbacks could be avoided by using methanol as a solvent and F^- as a catalyst.[42] The xerogel obtained possessed an extended porous structure (the content of HS groups was equal to 4.5 mmol g^{-1}). The authors described also preparation of xerogels which contained a bifunctional surface layer of the SH/NH_2 type.[42] The destruction of the surface layer in such xerogels begins at a temperature above 300 °C, which seems to give evidence for appearance of a synergetic effect. Earlier synthesis of analogous xerogels was considered.[40] Obtaining xerogel with a ligand group that contained sulphide, amine and thiol centers was also considered.[43] A comparative characteristic of sorbents with SH-groups is given in Lee et al.[41] and Im et al.[44]

The xerogel with groups $\equiv Si(CH_2)_2COOH$ was synthesized by the acid hydrolysis of $(C_2H_5O)_3Si(CH_2)_3CN$ in the presence of TEOS.[45] Later on this approach was considered by the authors.[46,47] Synthesis of xerogels with ligand – EDTA analogue was described.[48]

Parish and co-workers[26] proposed several approaches to obtain xerogels containing $\equiv Si(CH_2)_{2\ or\ 3}PPh_2$ groups (catalyst - $(n\text{-}Bu)_2Sn(CH_3COO)_2$, solvent – ethanol or toluene). Later these syntheses were reproduced in methanol.[49] The xerogels containing additional groups (amine or thiol) were also described. Partial oxidation of P(III) atom was observed in all

cases.[49] Obtaining xerogels with phosphine ligands was considered in detail by Lindner.[50]

Aliev et al.[51] and Jurado-Gonzalez et al.[52] synthesized xerogels $[SiO_{n/2}(OEt)_{4-n}]_x \cdot [(EtO)_{3-n}O_{n/2}Si(CH_2)_mPO(OEt)_2]_y$ (m = 2 or 3) using HCl as a catalyst. A porous structure was characteristic of the xerogels prepared at a TEOS/trifunctional silane ratio of 10:1. When sols were allowed to stand at 60 °C for 16 days[52] or F^- was used as a catalyst,[53] the porous structure has been already formed at the ratio of 2:1 or 6:1. Boiling of the xerogel samples in HCl leads to the conversion of groups $–PO(OEt)_2$ to $–P(O)(OH)_2$ and made it possible to synthesize porous xerogels even in the case of the ratio of 2:1.[53] Preparation P=O-containing xerogels with more complicated spacers was considered.[54]

Obtaining xerogel-anion-exchanger with functional group of $\equiv Si(CH_2)_3N(CH_3)_3^+Cl^-$ composition was described by Yang et al.[19] and Yacoub-George et al.[35] (acid medium, solvent – alcohol), and one with 3-n-propyl-1-azonia-4-azabicyclo[2.2.2]octanechloride was described by Arenas et al.[55]

2.3. SYNTHESIS WITH PARTICIPATION OF BIS(TRIALKOXYSILANES) AS STRUCTURE-FORMING AGENTS

By now hybrid materials of the class of polysilsesquioxanes have been a matter of a rather careful consideration.[56,57] However, functionalized xerogels whose preparation involved application of bis(trialkoxysilanes) $(RO)_3Si–R''–Si(OR)_3$ in the capacity of structure-forming agents have been studied scantily. Thus, for example, alkoxysilane with R" = $–(CH_2)_2–$ (HCl as a catalyst) was used when synthesizing P=O-containing xerogels.[51] However, these xerogels turned to be practically non-porous, and porous samples were obtained only in the case of conversion $–P(O)(OEt)_2 \rightarrow –P(O)(OH)_2$. Jurado-Gonzalez et al.[58] showed that gelation of alkoxysilane $(EtO)_3SiCH_2CH[PO(OEt)_2]CH_2CH_2Si(OEt)_3$ in the medium of 1 M HCl/THF for 11 days led to a transparent monolithic sample whose boiling in concentrated HCl yielded a xerogel with $–P(O)(OH)_2$ groups.

These results provide evidence for the fact that the proceeding of the hydrolytic polycondensation reaction in such systems is noted for some particularities. The Shvaikovska et al.[59] studied the particularities observed in the case of the synthesis of xerogels with 3-aminopropyl groups and showed that in order to avoid nonhomogeneous gelation it was necessary to use ethanol, to effect a preliminary hydrolysis of $(C_2H_5O)_3Si(CH_2)_2Si(OC_2H_5)_3$ (with F^- as a catalyst), and to enlarge the time for gel ageing (up to 30 days). The synthesis under these conditions allowed one to produce xerogels with such functional groups as $–NH_2$,

$-NH(CH_2)_2NH_2$, $=NH$,[60,62] and $-SH$.[61,62] A use was made of bis(triethoxysilanes) with R" = $-(CH_2)_2-$ and $-C_6H_5-$. The molar ratio 'structure-forming agent/functionalizing agent' was equal to 4:1 or 2:1. The content of ligand groups ranged from 1.0 to 2.7 mmol g^{-1}. AFM micrographs of synthesized xerogels are presented in Figure 2. It is brought about by the existence of aggregates of primary particles which in terms of their shape resemble ellipsoids. Their size was 30–65 nm.

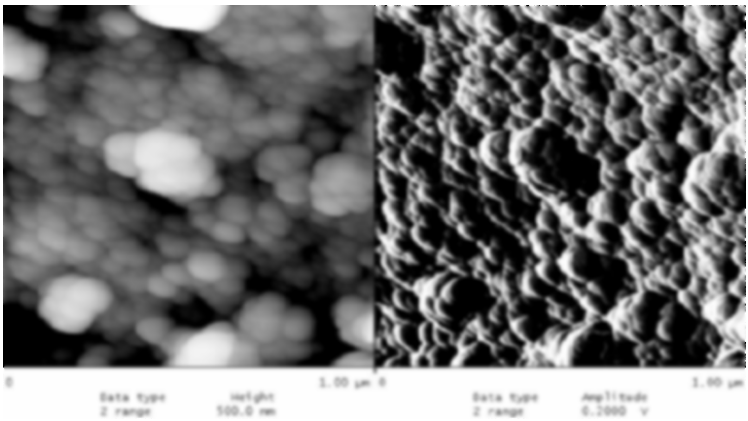

Figure 2. AFM micrograph of NH_2-containing xerogel (R″ = -$(CH_2)_2$-).[62]

3. Application of Physical Methods for Determining Composition and Structure of Functionalized Polysiloxane Xerogels

3.1. VIBRATIONAL SPECTROSCOPY

IR spectroscopy is known to be a traditional technique that makes it possible to ascertain that in the xerogels obtained there are (a) introduced functional groups (and/or products of their transformation during the course of synthesis), (b) siloxane bonds, (c) silanol groups, (d) water and/or nonaqueous solvents, (e) systems of hydrogen bonds. However, in a number of cases any characteristic bands of absorption in an IR spectrum of a xerogel could not be detected because they are already of low intensity in an IR spectrum of a starting trifunctional silane (e.g., ν(SH)). At the same time, in Raman spectra the line attributed to this vibration is much more intense. Therefore, this line is readily identified even when the ratio of groups $-(CH_2)_3SH/-(CH_2)_3NH_2$ in a xerogel sample makes up 0.36:1.[5]

Absorption bands for functional groups in IR spectra of xerogels may be masked by the presence of water in these xerogels. Thus, in IR spectra of

amine-containing xerogels in the region above 3000 cm^{-1} there is always an intense and broad band of absorption ν(OH).[24,25] In the background of this band it is possible to identify two weak absorption bands $\nu_{s,as}$(NH) at ~3300 and ~3370 cm^{-1} ascribed to amine groups participating in hydrogen bonds. This observation is corroborated by the fact that in the region 1500–1600 cm^{-1} there are two (or one) weak absorption bands related to $\delta(NH_2)$. An analogous situation is also observed for xerogels with (thio)urea groups,[37] namely the absorption band ν(OH) for water masks ν(NH) for amide fragment. However, the presence of intense characteristic bands of absorption in the region 1400–1700 cm^{-1} (one in the case of thiourea groups and two in the case of urea groups) allows one to detect easily the presence of (thio)urea fragments.

The IR spectra recorded for all the polysiloxane xerogels in the region 1000–1200 cm^{-1} contain a most intense absorption band with a shoulder on the side of more high frequencies. The appearance of this band is typical for a three-dimensional skeleton of siloxane bonds (≡Si–O–Si≡) which bears carbofunctional groups.[63] This region for xerogels with phenyl groups has two maximum of practically the same intensity, which can be employed for their identification.[24,25]

The absence of absorption bands ν(C≡N) in the region 2200–2300 cm^{-1} of the IR spectra for carboxyl-containing xerogels[5] gives evidence for the complete saponification of nitrile groups. At the same time in these spectra there appears an intense band of absorption in the region 1720–1730 cm^{-1} that is characteristic of COOH groups which are bound with OH groups by hydrogen bonds.[64] Besides, nearby this absorption band there appears a band at ~1640 cm^{-1}, which provides evidence for formation of some carboxyl groups of ester bonds. Hence, the IR spectroscopy makes it possible to identify also transformations of some functional groups.

The application of IR spectroscopy for the purpose of studying xerogels whose synthesis involved participation of bis(trialkoxysilanes)[60–62] enabled one to reveal the presence of both noncondensed silanol groups (in the spectra there is a sharp band of absorption at ~3730 cm^{-1}) and some nonhydrolyzed ≡Si–OC_2H_5 (and/or ≡Si–OCH_3) groups.

3.2. SOLID-STATE NMR SPECTROSCOPY

Solid-state NMR spectroscopy can furnish valuable additional information about structure of xerogels and their surface layers. In the first place this relates to nature of structural units (T^n and Q^m). Thus, ^{29}Si CP/MAS NMR spectra for amine-containing xerogels contain several sets of resonance signals in the spectrum interval from −110 to −50 ppm (Figure 3).[19] In the first region there are, as a rule, three signals at about −110, −100, and −90

ppm that are related to $(SiO)_4\mathbf{Si}$ (Q^4), $(SiO)_3\mathbf{Si}OH$ (Q^3) and $(SiO)_2\mathbf{Si}(OH)_2$ (Q^2), respectively.[65] The presence of the second region is characteristic of samples with phenyl groups (signal at −80.3 ppm with a shoulder at −78.0 ppm). It provides evidence for existence of such structural units as $(SiO)_3\mathbf{Si}C_6H_5$ (T^3) and $(SiO)_2\mathbf{Si}(OH)C_6H_5$ (T^2). The third region also contains one signal at −66 ppm with a shoulder at −57 ppm, which can be ascribed to the structural units of the previous type, that is to $(SiO)_3\mathbf{Si}(CH_2)_3NH_2$ (T^3) and $(SiO)_2\mathbf{Si}(OH)(CH_2)_3NH_2$ (T^2) (the samples described by Zub et al.[25] do not contain alkoxysilyl groups).

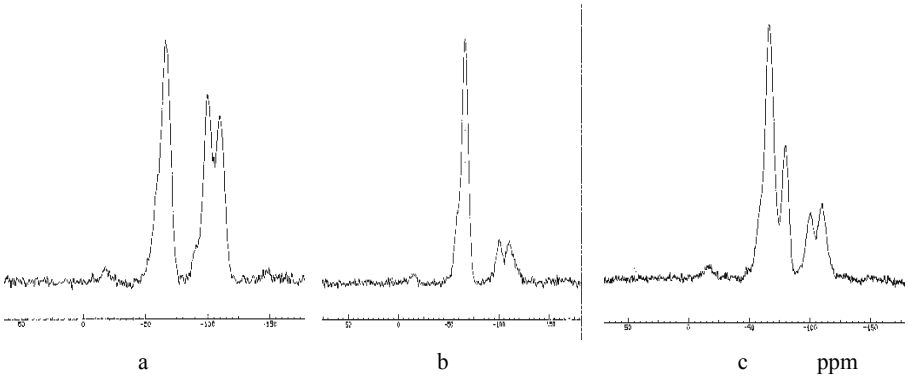

Figure 3. ^{29}Si CP/MAS NMR spectra for xerogels containing such functional groups as $\equiv Si(CH_2)_3NH_2$ (a), $\equiv Si(CH_2)_3NH_2/\equiv SiCH_3$ (b), and $\equiv Si(CH_2)_3NH_2/\equiv SiC_6H_5$ (c).[27]

Figure 4 displays the ^{13}C CP/MAS NMR spectra for the same xerogels. All of them contain signals at about 10 ppm ($Si\mathbf{C}H_2$), 22 ppm ($C\mathbf{C}H_2C$), and 43 ppm ($\mathbf{C}H_2NH_2$). The rest of the signals are attributed to phenyl groups (Figure 4c). It should be noted that in the case of xerogels containing $-CH_3$ and $-C_6H_5$ radicals the signal assigned to the central carbon atom of the propyl chain ($\equiv SiCH_2[\mathbf{C}H_2]CH_2NH_2$) has a shoulder at about 25–26 ppm. It is known that the chemical shift value for this atom points to the amine group state. In the spectrum registered for single APTES this resonance line is at 26–29 ppm while in the situation with protonation of the amine group the line is shifted towards the strong field region (21–22 ppm).[59] Thus, the amine group observed on the surface of the xerogels under consideration should have been protonated (at least partially). However, this is inconsistent with the IR spectroscopy data. Therefore, they participate in formation of hydrogen bonds with silanol groups, which is corroborated by the data presented by Maciel.[22] However, in the case of the xerogels with bifunctional surface layers some amine groups take part in formation of hydrogen bonds which, by their nature, are similar to bonds that are present in liquid APTES. These inferences will not contradict the

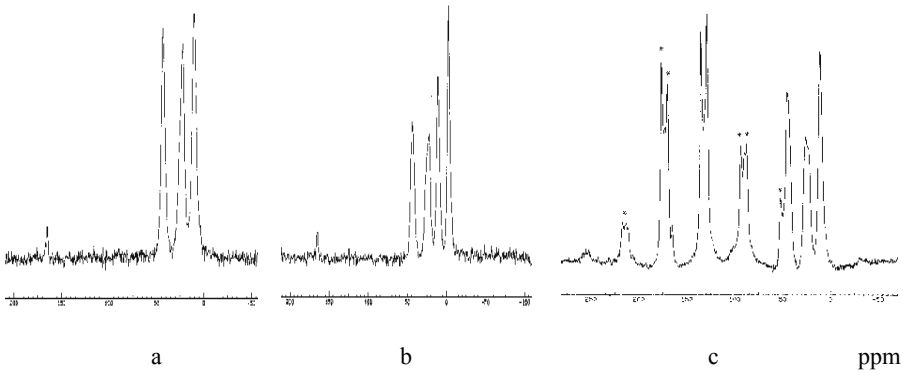

Figure 4. ^{13}C CP/MAS NMR spectra for xerogels containing such functional groups as $\equiv Si(CH_2)_3NH_2$ (a), $\equiv Si(CH_2)_3NH_2/\equiv SiCH_3$ (b), and $\equiv Si(CH_2)_3NH_2/\equiv SiC_6H_5$ (c).[19]

^{13}C CP/MAS NMR spectroscopy data on the assumption that the formation of such hydrogen bonds as $\equiv Si(CH_2)_3NH_2\cdots HOSi\equiv$ (including hydrogen bonds with water molecules) gives rise to the same shift of the signal assigned to the central carbon atom of the propyl radical towards strong fields, as it was the case for protonation of amine groups.

Our analysis of the ^{29}Si CP/MAS NMR spectra for the xerogels prepared on the basis of bis(triethoxysilanes) (Figure 5) permits us to make an inference that during the course of the hydrolytic polycondensation reaction their ≡Si–C bonds are stable because in the region of structural units Q^m (from –90 ppm to –110 ppm) there are no signals. The fact that in the spectra there is a set of intense resonance signals (in the region from –48 ppm to –66 ppm for samples with ethylene bridges and in the region from –60 ppm to –80 ppm for samples with phenylene bridges) provides evidence for existence of such structural units as T^n (n = 1–3) in these xerogels.[60–62] Therefore, the structure of these xerogels is a combination of structural units T^1, T^2, and T^3 connected by siloxane bonds.

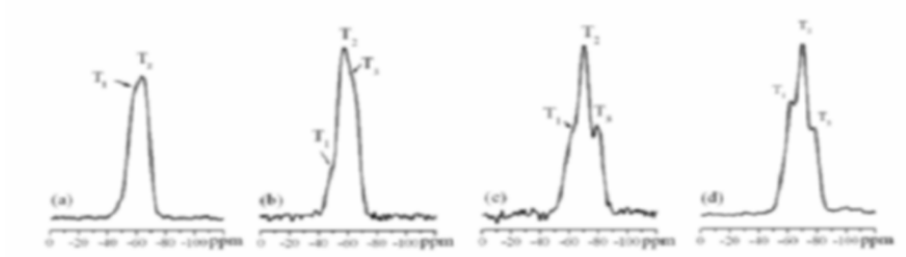

Figure 5. ^{29}Si CP/MAS NMR spectra for the xerogels synthesized using various systems: a, $-C_2H_4-/-NH_2$=2:1; b, $-C_2H_4-/-SH$=2:1; c, $-C_6H_4-/-NH_2$=2:1; d, $-C_6H_4-/-SH$=2:1.[61,62]

One of the salient features of the ^{13}C CP/MAS NMR spectra for the xerogels in question is the presence of two signals at 15–18 and 57–59 ppm.[60–62] Since all the xerogels were dried in a high vacuum, these signals give evidence for the presence of residual ethoxysilyl groups. The region where the signal assigned to the middle atom of a 3-aminopropyl link is situated (~23 ppm) and the broadening of this signal point to the participation of amine groups in nonhomogeneous hydrogen bonds.[22]

3.3. METAL MICROPROBE TECHNIQUE

For the purpose of studying surface topography of FPX, Stechenko et al.[66-68] employed the metal microprobe technique. In particular, the subject of inquiry was sorption of Cu(II) ions by amine-containing xerogels from acetonitrile solutions. It was found that irrespective of the degree of surface coverage by the metal on the surface there proceeded formation of complexes of the same composition (CuO_2N_2). The composition of these complexes was also independent of the nature of amine groupings as well as of the structure-adsorption characteristics of the sorbent. It gave grounds to infer that such polyaminosiloxane xerogels were noted for a similar structure of their surface. It also provided evidence for the fact that on their surface there could exist oligomers with the above-mentioned aminopropyl groupings that were formed during the course of the hydrolytic polycondensation reaction. In the simplest case they could be dimers with a composition of $=O_2=Si[(CH_2)_3NH_2]–O–Si(OH)[(CH_2)_3NH_2]–O–$.

4. Adsorption Properties of Functionalized Polysiloxane Xerogels

4.1. SOME FACTORS CONTRIBUTING TO STRUCTURE AND ADSORPTION PROPERTIES OF FUNCTIONALIZED POLYSILOXANE XEROGELS

In the situation when xerogels were prepared using one-component systems, the influence of conditions of synthesis on parameters of their porous structure was not considered in detail. Pozhidaev[9] indicated that the specific surface area (by *n*-hexane) of such xerogels took a value in the interval 340–540 $m^2\ g^{-1}$.

In the case when xerogels were prepared using two-component systems (with TEOS as a structure-forming agent), the subject of inquiry included such conditions of their synthesis as relative sizes of functional group R′, ratio of reacting alkoxysilanes, amount of reaction water, nature of the nonaqueous solvent, temperature of synthesis, gel ageing time, modes of washing and drying. By way of example, consider amine-containing

xerogels. It was shown[5,24] that (1) all the samples obtained are classified among mesoporous adsorbents (for the majority of them their values of S_{sp}, V_s, and d fall within the interval 92–315 $m^2\ g^{-1}$, 0.12–1.38 $cm^3\ g^{-1}$, 3.7–17.7 nm, respectively); (2) in all the cases introduction of a nonaqueous solvent brings about a decrease in S_{sp} and V_s and an increase in d; (3) with decreasing TEOS/APTES ratio the porosity of samples decreases substantially (at a ratio of 1:1 the xerogel becomes practically nonporous); (4) a similar effect is exerted by relative increase of geometric sizes of the functional group and by a decrease in the amount of water taken for the hydrolysis; (5) increase in the gel ageing time (from 1 to 7 days) makes an insignificant effect on the porous structure parameters; (6) drying of xerogels at atmospheric pressure leads to large-pored sorbents; (7) washing of xerogels with water (before repeated vacuum drying) results in fine-pored adsorbents while washing with abundant amounts of water considerably increases sizes of pores. As far as the xerogels with a bifunctional surface layer (NH_2/CH_3 or C_6H_5) are concerned, it was shown[24,25,34] that appearance of hydrophobic groups on the surface led to formation of globules of larger sizes and of loosely packed structures, which causes a substantial decrease in the specific surface area of samples. Thus, the results achieved provide evidence for the fact that by laying down conditions of synthesis it is possible to prepare xerogels with desired parameters of their porous structure.

For xerogels with thiourea groups it was found[37] that at the TEOS/trifunctional silane ratio of 2:1 there occurs formation of practically nonporous samples. When this ratio increases (e.g., from 2:1 to 8:1), S_{sp} of the xerogels obtained increases gradually and reaches ~300 $m^2\ g^{-1}$.

Functionalized polysilsesquioxane xerogels attract attention because of their high values of S_{sp}, namely from 510 to 840 $m^2\ g^{-1}$ for xerogels with ethylene bridges and from 650 to 970 $m^2\ g^{-1}$ for xerogels with phenylene bridges.[60–62] The type of isotherms of these xerogels (Figure 6) depends, in the first place, on the nature of functional groups (amine or thiol groups). In the first case the isotherms for xerogels with ethylene bridges are S-shaped and have a distinct hysteresis loop (in contrast to xerogels with phenylene bridges) while isotherms in the second case are more like Langmuir isotherms. According to the curves presented in Figure 6, PSDs are rather narrow in character.

Zub et al.[60-62] found that the parameters of the porous structure of such xerogels were substantially affected by the nature of a spacer, relative size of the functional group, ratio of reacting alkoxysilanes, and gel ageing time.

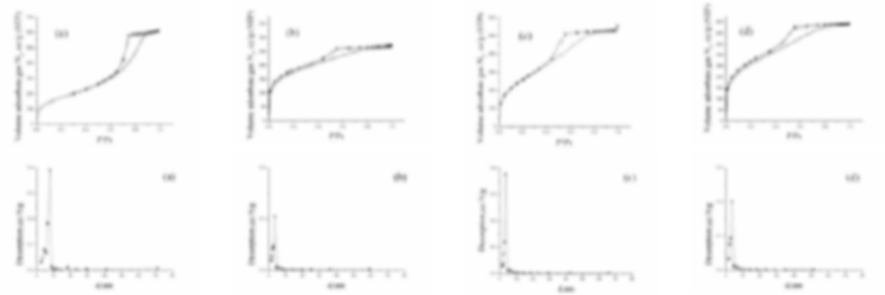

Figure 6. Isotherms of N_2 adsorption/desorption and PSDs for the xerogels synthesized using the following systems: a, -C_2H_4-/-NH_2=2:1; b, -C_2H_4-/-SH=2:1; c, -C_6H_4-/-NH_2=2:1; d, -C_6H_4-/-NH_2=2:1.[60-62]

4.2. ADSORPTION CHARACTERISTICS OF XEROGELS WITH REFERENCE TO IONS OF METALS

The adsorption properties characteristics of functionalized polysiloxane materials prepared on the basis of one-component systems with reference to a wide range of ions of metals have been a subject of comprehensive studies.[6,9] The sorptive potentialities of the xerogels prepared using two-component systems have been studied to a lesser extent. Parish[17,27] studying absorption of Ni, Co, Cu, Zn(II) by aminocontaining xerogels showed that an equilibrium in such systems is reached at least in 15 h. In acid medium these xerogels absorb Cu(II) ions best of all that is in agreement with data.[69] Xerogels with PPh_2 groups[26] absorb metal ions (Co and Ni(II)) from their ethanol solution more slowly. However a part of functional groups of xerogels does not take part in complex formation.[17,26,27,70] This agrees with data.[71] Pavan et al.[29] point at equilibrium attainment at metal ions absorption during 20-30 min. In[72] studying sorption of Au(III) microquantities by xerogels containing in surface layer thiourea groups it was shown that an increase of solution temperature (up to 50°C) decreases significantly time of an attainment of sorption equilibrium (up to 5 min) and increases degree of gold extraction. Xerogels of this group were used the most often to study sorption of 3d-metals[29,69,43]. However recently a range of investigated metals has been extended (Hg(II)[41,44,69,73]; Ca(II)[48]; Zn(II)[48]; Cd(II)[41,48]; Pb(II)[41]; Pd(II)[48]; UO_2(II)[74]; Ln(III)[75], Am(III), Pu(IV)[38,75]). It is interesting that a separation of Ni(II) and Cu(II) is possible on xerogels with bifunctional surface layer (ethylenediamine and vinyl groups)[27]. In the work of Melnyk et al.[72] a consideration has been given to sorption of microquantities of Au(III) from acidic solutions by xerogels whose surface layers contain thiourea (and amine) groups. It has been found that the

maximum degree of extraction of Au(III) is characteristic of the sorbent with a bifunctional surface layer. Besides, this xerogel has a high efficiency in sorbing mercury(II) from acidic solutions.[24]

Finally it should be noted that sol-gel method has a great potential at synthesis of sorbents "with memory" for metal ions[76] or for their analytical determination.[77]

5. Conclusions

The above-exposed approaches to the synthesis of hybrid organo-inorganic sorptive materials with regulated porosity and functionality of their surface layers offer ample scope for sorptive technology, chromatography, catalysis, organic and inorganic chemistry involving interactions of the 'guest–host' type. The possibility of using multicomponent systems during the hydrolytic polycondensation reaction is a powerful means for designing both supports themselves and their surfaces. Introduction of additional functional groups into a surface layer is a potent key to exert control over reactivity of surface in such novel materials. Therefore, there is no doubt that this line of researches in chemistry will henceforth maintain a rapid pace of its progress.

ACKNOWLEDGMENT

This research is partially sponsored by the NATO's Scientific Affairs Division in the framework of the Science for Peace Programme (Grant SfP-978006).

REFERENCES

1. *Functional Hybrid Materials*, edited by P. Gomez-Romero and C. Sanchez (Wiley-VCH, Weinheim, 2004).
2. C.J. Brinker and G.W. Scherer, *Sol-Gel Science: The Physics and Chemistry of Sol-Gel Processing* (Academic Press, San Diego, 1990).
3. I.B. Slinyakova and T.I. Denisova, *Organo-silicon Adsorbents: Production, Properties, and Application* (Naukova Dumka, Kyiv, 1988) (in Russ.).
4. Yu.L. Zub and R.V. Parish, Functionalized polysiloxane sorbents: preparation, structure, properties and use, *Stud. Surf. Sci. Catal.* 99, 285-299 (1996).
5. Yu.L. Zub and A.A. Chuiko, in: *Colloidal Silica: Fundamentals and Applications*, edited by H.E. Bergna (Marcel Dekker, Washington, DC, 2005), pp. 397-424.
6. M.G. Voronkov, N.N. Vlasova, Yu.N. Pozhidaev, Organosilicon ion-exchange and complexing adsorbents, *Appl. Organometal. Chem.* 14, 287-303 (2000).
7. D. Avnir, L.C. Klein, D. Levy, U. Schubert, and A.B. Wojcik, in: *The Chemistry of Organic Silicon Compounds*, edited by Z. Rappoport and Y. Apeloig (Wiley, Chichester, Vol. 2, 1998), pp. 2317 - 2362.
8. T.N. Yakubovich, Yu.L. Zub, A.A. Chuiko, in: *Chemistry of Silica Surface*, edited by A.A. Chuiko (Institute of Surface Chemistry, Kyiv, Vol. 1, 2001), pp. 54 – 97 (in Russ.).

9. Yu.N. Pozhidaev, Carbofunctional polyalkylsilsesquioxanes with ion-exchange and complexing properties, *Synopsis of Thesis for a Doctor's Degree* (IrIC, SB of RAN, Irkutsk, 2004) (in Russ.).
10. L.P. Finn, I.B. Slinyakova, M.G. Voronkov, N.N. Vlasova, F.P. Kletsko, A.I. Kirillov, and T.V.Shklyar, Structure and properties of polymercaptomethylsilsesquioxane xerogel, *Dokl. AN SSSR* 235(6), 1426-1429 (1977) (in Russ.).
11. L.P. Finn, I.B. Slinyakova, M.G. Voronkov, and N.N. Vlasova, Study of structure and adsorption properties of sulfur-containing polyorganosiloxane xerogels, *Adsorbtsiya i Adsorbenty* (8), 98-102 (1980) (in Russ.).
12. N.N. Vlasova, L.M. Stanevich, A.I. Kirillov, and M.G. Voronkov, Poly(ω-sulfoalkylsilsesquioxanes). Synthesis and sorption properties, *Izvestiya SO AN SSSR. Ser. Khim. Nauk* 2(1), 107-109 (1987) (in Russ.).
13. G.H. Barnes, Jr. and M.P. David, Synthesis and hydrolytic stability of some organosilicon phosphonate esters*, J. Org. Chem*. 25, 1191-1194 (1960).
14. J.-P. Bezombes, C. Chuit, R.J.P. Corriu, and C. Reye, Preparation and characterization of new organic-inorganic hybrid materials incorporating phosphorus centers, *J. Mater. Chem.* 8, 1749-1759 (1998).
15. G. Dubois, R.J.P. Corriu, C. Reye, S. Brandes, F. Denat, and R. Guilard, First organic-inorganic hybrid materials with controlled porosity incorporating cyclam units, *Chem. Commun.* 2283-2284 (1999).
16. A.A. Chuiko, G.Ye. Pavlik, G.B. Budkevich, and I.Ye. Neimark, A method of preparation of silica gels containing aminoalkyl groups, *USSR Certificate of Authorship No 182719,* 1966 (in Russ.).
17. I.S. Khatib and R.V. Parish, Insoluble ligands and their applications. I. A comparison of silica-immobilized ligands and functionalized polysiloxane, *J. Organomet. Chem.* 369, 9-16 (1989).
18. Yu.L. Zub, L.S. Kovaleva, B.V. Zhmud', S.N. Orlik, I. Uzunov, D. Simeonov, D. Klisurski, and I. Teocharov, Rhodium complexes fixed on polysiloxane and silica matrices with nitrogen-containing functional groups in a reaction of acetylene hydroformylation, *Proc. 7th Int. Symp. Heterog. Catal.* (Bourgas, Bulgaria, Vol. 1, 1991), pp. 567-571.
19. J.J. Yang, I.M. El-Nahhal, and G.E. Maciel, Synthesis and solid-state NMR structural characterization of some functionalized polysiloxanes, *J. Non-Crystal. Solids.* 204, 105-117 (1996).
20. B.V. Zhmud and J. Sonnefeld, Aminopolysiloxane gels: production and properties, *J. Non-Crystal. Solids.* 195, 16-27 (1996).
21. J.J. Yang, I.M. El-Nahhal, I-S. Chuang, and G.E. Maciel, Synthesis and solid-state NMR structural characterization of polysiloxane-immobilized amine ligands and their metal complexes, *J. Non-Crystal. Solids* 209, 19-39 (1997).
22. G.E. Maciel, in: *Solid State NMR of Polymers*, edited by I. Ando and T.Asakura (Elsevier, Amsterdam, 1998), pp. 923-984.
23. O.K. Matkovskii, G.R. Yurchenko, O.V. Stechenko, and Yu.L. Zub, Influence of solvent nature on structure-adsorption characteristics of poly(3-aminopropyl)siloxanes, *Naukovi Zapysky Ternopil's'kogo Derzhav.Pedagog. Univer., Series 'Khimiya'* (4), 40-45 (2000) (in Ukrain.).
24. Yu.L. Zub, Surface chemistry of new hybrid organic-inorganic materials, *Synopsis of Thesis for a Doctor's Degree* (ISC, NAS of Ukraine, Kyiv, 2002) (in Ukrain.).
25. Yu.L. Zub, A.A. Chuiko, and O.V. Stechenko, Synthesis, structure and structure-adsorption characteristics of some polyaminosiloxanes, *Doklady NAN Ukrainy* (4), 150-155 (2002) (in Russ.).

26. R.V. Parish, D. Habibi, and V. Mohammadi, Insoluble ligands and their applications. II. Polysiloxane-phosphine ligands, their complexes, and hydrogenation catalysts, *J. Organomet. Chem.* 369, 17-28 (1989).
27. I.M. El-Nahhal and R.V. Parish, Insoluble ligands and their applications. III. Polysiloxane diaminoethane derivatives, *J. Organometal. Chem.* 452, 19-22 (1993).
28. C.R. Silva and C. Airoldi, Acid and base catalysts in the hybrid silica sol-gel process, *J. Colloid Interf. Sci.* 195, 381-387 (1997).
29. F.A. Pavan, I.S. Lima, E.V. Benvenutti, Y. Gushikem, and C. Airoldi, Hybrid aniline/silica xerogel cation adsorption and thermodynamics of interaction, *J. Colloid Interf. Sci.* 275, 386-391 (2004).
30. F.A. Pavan, W.F. de Mahalhaes, M.A. de Luca, C.C. Moro, T.M.H. Costa, and E.V. Benvenutti, A characterization study of xerogel silicapropylaniline powders, *J. Non-Crystal. Solids* 311, 54-60 (2002).
31. F.A. Pavan, L. Franken, C.A. Moreira, T.M.H. Costa, E.V. Benvenutti, and Y. Gushikem, Synthesis of a thermal stable silica/p-anisidine sol-gel powdered material, *J.Colloid Interf. Sci.* 241, 413-416 (2001).
32. D.R. Azolin, C.C. Moro, T.M.H. Costa, and E.V. Benvenutti, Effects of organic content and H_2O/TEOS molar ratio on the porosity and pore size distribution of hybrid naphthaleneaminepropylsilica xerogel, *J. Non-Cryst. Solids* 337, 201–206 (2004).
33. C. Alie, F. Ferauche, R. Pirard, A.J. Lecloux, and J.-P. Pirard, Preparation of low-density xerogels by incorporation of additives during synthesis, *Microporous and Mesoporous Materials* 70, 57-62 (2004).
34. O.V. Stechenko, G.R. Yurchenko, O.K. Matkovskii, and Yu.L. Zub, Adsorption properties of some polyaminosiloxanes, *Naukovyi Visnyk Uzhgor. Univer., Series 'Khimiya'* (5), 107-112 (2000) (in Ukrain.).
35. E. Yacoub-George, E. Bratz, and H.Tiltscher, Preparation of functionalized polyorgano-siloxane spheres for the immobilization of catalytically active compounds, *J. Non-Cryst. Solid*s 167, 9-15 (1994).
36. V. van Blaaderen and A. Vru, Synthesis and characterization of monodisperse colloidal organo-silica shperes, *J. Colloid Interf. Sci.* 156, 1-18 (1993).
37. Yu.L. Zub, I.V. Melnyk, A.A. Chuiko, D. Cauzzi, and G. Predieri, Design of functionalized polysiloxanes: synthesis and investigation of sulfur-containing xerogels with mono- and bifunctional surface layer, *Chemistry, Physics and Technology of Surface* 7, 35-45 (2002).
38. J.-C. Broudic, O. Conocar, J.J.E. Moreau, D. Meyer, and M.W. C.Man, New hybrid silica based materials for the solid-liquid extraction of actinides*, J. Mater. Chem*. 9, 2283-2285 (1999).
39. N. Becker and K. Unger, Synthesis and properties of chemical modified dihydroxy-, hydroxyamino- and amino-functional silica packings in adsorption chromatography, *Fresenius Z. Anal. Chem.* 304, 374-381 (1980).
40. I.M. El-Nahhal, J.J. Yang, I-S. Chuang, and G.E. Maciel, Synthesis and solid-state NMR structural characterization of polysiloxane-immobilized thiol and thiol-amine ligands, *J. Non-Cryst. Solids* 208, 105-118 (1996).
41. J.S. Lee, S. Gomes-Salazar, and L.L. Tavlarides, Synthesis of thiol functionalized organo-ceramic adsorbent by sol-gel technology, *React. Funct. Polym.* 49, 159-172 (2001).
42. I.V. Melnyk (Seredyuk), Yu.L. Zub, A.A. Chuiko, and P. Van Der Voort, Novel polyorganosiloxane xerogels with a bifunctional $\equiv Si(CH_2)_3SH/\equiv Si(CH_2)_3NH_2$ surface layer, *Chemistry, Physics and Technology of Surface* 8, 125-133 (2002).

43. C. Airoldi and L.N.H. Arakaki, Immobilization of ethylenesulfide on silica surface through sol-gel process and some thermodynamic data of divalent cation interaction, *Polyhedron* 20, 929-936 (2001).
44. H.-J. Im, C. E. Barnes, S. Dai, and Z. Xue, Functionalized sol–gels for mercury(II) separation: a comparison of mesoporous materials prepared with and without surfactant templates, *Microporous and Mesoporous Materials* 70, 57-62 (2004).
45. A.A. Chuiko, G.Ye. Pavlik, and I.Ye. Neimark, Method of preparation of organosilica gel, *USSR Certificate of Authorship No 164680,* 1964.
46. N.A. Prybora, L.S. Dzyubenko, Yu.L. Zub, and M. Jaroniec, Synthesis of the polysiloxane containing butyric acid residue on its surface layer, *Khimichni Nauky. Collected Sci. Papers of Nat. Training M.P.Dragomanov's Univ.* 41-47 (1999) (in Ukrain.).
47. N.A. Prybora, Yu.L. Zub, A.A. Chuiko, and M. Jaroniec, Synthesis and properties of some polycarboxylsiloxane sorbents, *Abstr. 2nd Int. Conf. on Silica Science and Technol.* (Mulhouse, France, 2001), p. 171.
48. P. Tien and L.-K. Chau, Novel sol-gel-derived material for separation and optical sensing of metal ions: propyl-ethylenediamine triacetate functionalized silica, *Chem. Mater.* 11, 2141-2147 (1999).
49. J.J. Yang, I.M. El-Nahhal, I-S. Chuang, and G.E. Maciel, Synthesis and solid-state NMR structural characterization of polysiloxane-immobilized phosphine, phosphine-amine and phosphine-thiol ligand systems, *J. Non-Cryst. Solids* 212, 281-291 (1997).
50. Z. Lu, E. Lindner, and H.A. Mayer, Applications of sol-gel-processed interphase catalysts, *Chem. Rev*. 102, 3543-3578 (2002).
51. A. Aliev, D.L. Ou, B. Ormsby, and A.C.Sullivan, Porous silica and polysilsesquioxane linked phosphonates and phosphonic acids, *J. Mater. Chem*. 10, 2758-2764 (2000).
52. M. Jurado-Gonzalez, D. Lou, A.C. Sullivan, and J.R.H. Wilson, Synthesis, characterization and catalytic activity of porous vanadyl phosphonate-modified silicas, *J. Mater. Chem.* 12, 3605-3609 (2002).
53. O.A. Dudarko, I.V. Mel'nyk, Yu.L. Zub, A.A.Chuiko, and A. Dabrowsli, Synthesis of polysiloxane xerogels using teraethoxysilane/(diethylphosphatoethyl)triethoxysilane system, *Kolloid. Zh*. 67, 753-758 (2005) (in Russ.).
54. C. Carbonneau, R. Frantz, J.-O. Durand, M. Granier, G.F. Lanneau, and R.J.P. Corriu, Studies of the hydrolysis of ethyl and tert-butyl phosphonates covalently bonded to silica xerogels, *J. Mater. Chem.* 12, 540-545 (2002).
55. L.T. Arenas, T.A.S. Aguire, A. Langaro, Y. Gushikem, E.V. Benvenutti, and T.M.H. Costa, 3-n-propyl-1-azonia-4-azabicyclo[2.2.2]octanechloride/silica hybrid polymer. A morphologic study in relation to the organic content, *Polymer* 44, 5521-5525 (2003).
56. D.A. Loy, and K.J. Shea, Bridged polisilsesquioxanes. Highly porous hybrid organic-inorganic materials, *Chem. Rev.* 95, 1431-1442 (1995).
57. R.J.P. Corriu, The control of nanostructured solids: a challenge for molecular chemistry, *Eur. J. Inorg. Chem.* 1109-1121 (2001).
58. M. Jurado-Gonzalez, D.L. Ou, B. Ormshy, A.C. Sullivan, and J.R.H. Wilson, A new solid acid catalyst: the first phosphonate and phosphonic acid functionalised microporous polysilsesquioxanes, *Chem. Commun.* 67-68 (2001).
59. N.V. Shvaikovska, I.V. Mel'nyk, G.R. Yurchenko, O.K. Matkovski, and Yu.L. Zub, Synthesis and structure–adsorption characteristics of bridged polysilsesquioxanes with aminopropyl groups, *Chemistry, Physics, and Technology of Surface* 10, 80–84 (2004) (in Russ.).

60. Yu.L. Zub, A.A. Chuiko, N.V. Stolyarchuk, I.V. Mel'nyk, and A. Dabrowski, New amine-containing adsorbents on the basis of bridged polysilsesquioxanes, *Dopov. NAN Ukrainy*, (2), 117-122 (2005) (in Russ.).
61. Yu.L. Zub, N.V. Stolyarchuk, I.V. Melnyk, A.A. Chuiko, A. Dabrowski, and M. Barczak, New adsorbents based on bridged polysilsesquioxanes containing 3-mercaptopropyl functional groups, *Mendeleev Commun.* 15(4), 168-170 (2005).
62. A.Dabrowski, M.Barczak, N.V. Stolyarchuk (Shvaykovka), I.V.Melnyk, Yu.L.Zub, Bridged polysilsesquioxane xerogels functionalizated by amine- and thiol-groups: synthesis, structure, adsorption properties, *Adsorption* 11, 497-513 (2005).
63. L.P. Finn, and I.B. Slinyakova, Structure and thermodestruction of polyorganosiloxane xerogels were shown by IR spectroscopy, *Kolloid. Zh.* 37, 723-729 (1975) (in Russ.).
64. D. Lin-Vien, N.B. Colthup, W.G. Fateley, and J.G. Grasselly, *The Handbook of Infrared and Raman Characteristic Frequencies of Organic Molecules* (Academic Press, San Diego, CA, 1991).
65. G. Engelhardt, and D. Michel, *High-resolution Solid-state NMR of Silicates and Zeolites* (Wiley, Chichister, 1987).
66. O.V. Stechenko, T.N. Yakubovich, V.V. Teslenko, Yu.L. Zub, and A.A. Chuiko, Study of copper(II) absorption by some polyaminosiloxanes from acetonitrile solutions, *Chemistry, Physics and Technology of Surface.* 2, 62-67 (1997) (in Ukrain.).
67. Ye.V. Stechenko, T.N. Yakubovich, V.V. Teslenko, B.K. Veisov, Yu.L. Zub, and A.A. Chuiko, Copper(II) adsorption from acetonitrile solutions by nitrogencontaining polysiloxanes, *Chemistry, Physics and Technology of Surface* 3, 46-50 (1999) (in Russ.).
68. Ye.V. Stechenko, T.N. Yakubovich, V.V. Teslenko, Yu.L. Zub, and A.A. Chuiko. Copper(II) ions adsorption from acetonitrile solutions by polyaminosiloxane xerogel with bifunctional surface layer, *Ukr. Khim. Zh*. 69, 19 – 24 (2003) (in Russ.).
69. A.R. Cestari, E.F.S. Vieira, J. de A. Simoni, and C. Airoldi, Thermochemical investigation on the adsorption of some divalent cations on modified silicas obtained from sol-gel process, *Thermochimica Acta*, 348, 25-31 (2000).
70. I. Ahmed and R.V. Parish, Insoluble ligands and their applications. IV. Polysiloxane-bis(2-aminoethyl)amine ligands and some derivatives, *J. Organomet. Chem.* 452, 23-28 (1993).
71. I.M. El Nahhal, M.M. Chehimi, C. Cordier, and G. Dodin, XPS, NMR and FTIR structural characterization of polysiloxane-immobilized amine ligand system, *J. Non-Cryst. Solids* 275, 142-146 (2000).
72. I.V. Melnyk, V.Ya. Demchenko, Yu.L. Zub, and A.A. Chuiko, Sorption of auric-ions(III) using polysiloxane xerogels functionalized with thiourea groups, *Chemistry, Physics, and Technology of Surface* 9, 31-36 (2003) (in Ukrain.).
73. K.H. Nam, S. Gomez-Salazar, and L.L. Tavlarides, Mercury(II) adsorption from wastewaters using a thiol functional adsorbent, *Ind. Eng. Chem. Res.* 42, 1955-1964 (2003).
74. F. Caprasse, D. Leroy, L. Martinot, J.P. Pirard, J. Guillaume, C. Jerome, and R. Jerome, New silica based polymeric systems designed for the solid-liquid extraction of uranyl ions, *J. Mater. Chem.* 12, 137-142 (2002).
75. S. Bourg, J.-C. Broudic, O. Conocar, J.J.E. Moreau, D. Meyer, and M.W.C. Man, Tailoring of organically modified silicas for the solid-liquid extraction of actinides, *Chem. Mater.* 13, 491-499 (2001).
76. S. Dai, Hierarchically imprinted sorbents, *Chem. Eur. J.* 7, 763-768 (2001).
77. M.M. Collinson, Analytical applications of organically modified silicates, *Mikrochim. Acta* 129, 149-165 (1998).

DESIGN, SYNTHESIS AND CHARACTERIZATION OF ORDERED MESOPOROUS MATERIALS FOR ENVIRONMENTAL APPLICATIONS

MIETEK JARONIEC*
Kent State University, Kent OH 44242, USA

Abstract. Since the first report on the MCM-41 silica in 1992 several thousands of papers have been published on ordered mesoporous materials (OMMs). These novel materials, prepared either by soft- or hard-templating syntheses, become more and more important in many fields of science and technology such as adsorption, catalysis, separations, environmental processes, nanotechnology and biotechnology. The aim of this article is to provide a brief review on the OMMs design and synthesis as well as to show potential of these materials for various environmental applications such as sequestration of carbon dioxide, removal of gaseous organic and inorganic pollutants via adsorption and catalytic degradation, removal of heavy metal ions from contaminated water, and so on. The scope of environmental applications of OMMs is broad and continuously growing. The soft- and hard-templating syntheses create great opportunities for the design of OMMs such as ordered mesoporous silicas, organosilicas and carbons with desired surface and structural properties and for their use in various environmental processes.

Keywords: adsorption; carbon dioxide sequestration; heavy metal ions; ordered mesoporous silicas; ordered mesoporous carbons; mesoporous organosilicas

1. Introduction

Since the first report on the MCM-41 silica in 1992,[1,2] several thousands of papers have been published on ordered mesoporous materials (OMMs). An

* Chemistry Dept., Kent State University, Kent OH 44242, USA; e-mail: jaroniec@kent.edu

J.M. Loureiro and M.T. Kartel (eds.), Combined and Hybrid Adsorbents, 23–36.

impressive progress has been achieved in the synthesis of novel OMMs via self-assembly of various organic and inorganic species. A wide variety of ordered inorganic, organic and hybrid mesostructures with tailored pore size, morphology and surface properties have been synthesized (see reviews by Sayari and Liu,[3] Stein et al.,[4] Sayari and Hamoudi,[5] Schuth and Schmidt,[6] Soler-Illia et al.,[7] Stein,[8] and references therein). OMMs such as silicas and organosilicas with hexagonal, cubic and cage-like structures and tailored mesopore widths have been prepared by adjusting synthesis conditions and using proper templates such as surfactants,[1,2] oligomers[9] and block copolymers.[10] These organics have been used as soft templates in the self-assembly of organic and inorganic species. The removal of soft templates from those organic/inorganic mesostructured composites via extraction and/or calcination opens porosity, which can be used for adsorption and related applications. In addition, the resulting OMMs can be used as hard templates to prepare other ordered mesoporous materials such as inorganic oxides, carbons and polymeric adsorbents, the self assembly synthesis of which is difficult or sometimes impossible. Thus, the soft- and hard-templating syntheses are commonly used to prepare OMMs with desired pore size, high surface area and large adsorption capacity.

This review article is focused on the OMMs design and synthesis as well as on their environmental applications such as sequestration of carbon dioxide, removal of gaseous organic and inorganic pollutants via adsorption and catalytic degradation, removal of heavy metal ions from contaminated water, and so on. It consists of two main chapters; one of them is related to ordered mesoporous silicas and organosilicas and their environmental applications, whereas the other one is devoted to ordered mesoporous carbons.

2. Ordered Mesoporous Silicas and Organosilicas

2.1. SYNTHESIS AND BASIC CHARACTERITICS

The surface and structural properties of OMMs, especially silicas can be easily tailored to achieve the high adsorption affinity, desired pore size and pore volume. As it was mentioned in introduction the morphology, porous structure, pore size and pore volume of OMMs, especially ordered mesoporous silicas (OMSs), can be easily tailored by adjusting synthesis conditions and using proper templates. While the aforementioned properties are important in some environmental applications, the major advantage of these materials is the easiness of tailoring their surface properties. This feature makes OMSs very attractive materials for various environmental applications.

The desired surface functionality of OMSs can be achieved by using one of the following approaches: (i) post-synthesis modification of the template-free OMSs by using different organosilanes with or without subsequent attachment of additional organic functionalities (see articles by Jaroniec et al.,[11] Antochshuk et al.,[12] Stein et al.,[4] Sayari and Hamoudi,[5] and references therein), (ii) direct reaction of the silica-template mesostructures with organosilanes, which utilizes a unique interfacial reactivity of the self-assembled mesostructures towards organosilanes,[13,14] and (iii) one-pot synthesis involving co-condensation of tetraethyl orthosilicate (TEOS) and organotriethoxysilanes in the presence of surfactant and/or polymeric templates (see articles by Stein et al.,[4] Sayari and Hamoudi,[5] Kruk et al.,[15] and references therein). The first procedure usually employs calcined samples and does not affect significantly their mesopore structure. However, this procedure has some disadvantages such as relatively low ligand coverage in the resulting materials, which is associated with relatively high amount of residual silanols. Also, calcination process can lead to the structure deterioration. The second procedure does not require the template removal via calcination, which makes it attractive from the viewpoint of green chemistry. This procedure utilizes the silica reactivity towards organosilanes, which leads to the displacement of surfactant or polymeric template from the self-assembled silica-template mesostructure and to the formation of covalent bonding with the silica surface (see Figure 1). This displacement process preserves the mesostructural ordering, avoids the structure shrinkage and simultaneously allows achieving high coverage of bonded ligands and desired surface functionality.[13,14]

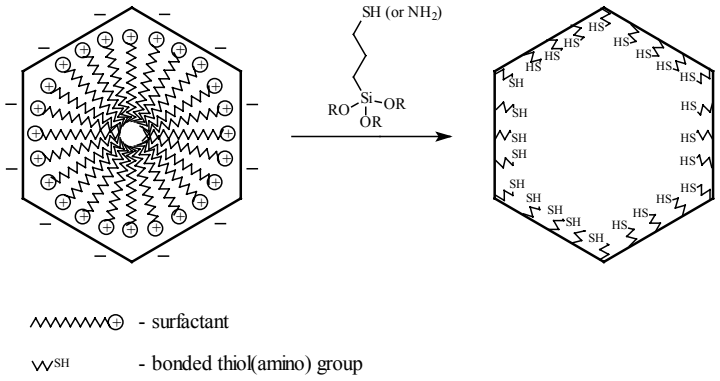

Figure 1. Schematic illustration of the reaction of as-synthesized surfactant-templated OMS with organosilane containing SH or NH_2 groups.[12]

The one-pot synthesis seems to be an attractive way to functionalize mesoporous silicas because it does not require their prior calcination, but its

shortcomings lie often in providing materials of broad pore size distributions and lower structural ordering. Although these shortcomings can be reduced or even eliminated by proper selection of organosilanes and adjustment of the synthesis conditions, the one-pot synthesis remains to be less flexible to introduce a complex surface functionality in comparison to the post-synthesis functionalization. However, there is no doubt that the one-pot synthesis is extremely promising for preparation of novel organic-inorganic hybrid materials of uniformly distributed organic segments in the entire inorganic framework.[16-23] The development of these hybrid materials is regarded as a major achievement in the OMM synthesis. For the first time, there is an opportunity to custom-tailor framework properties, surface properties and pore structures of organic-inorganic composites. The pore structure and pore size can be tailored via proper selection of supramolecular templates and/or synthesis conditions.

The control of framework properties can be achieved by judicious selection of suitable organosilanes and/or their mixing with appropriate amount of tetraethyl orthosilicate (TEOS) (see Table 1). Surface properties can be tailored by using the aforementioned methods, but also there is a vast opportunity for chemical modification of periodic mesoporous organosilicas via reaction with organosilanes. In addition, as shown in the last row of Table 1 organosilanes with bridged and terminal organic groups can undergo co-condensation giving materials with both framework and pendent organic groups.[19]

TABLE 1. Formation of different OMSs by co-condensation of organosilanes in the presence of surfactant and polymeric templates

Type of OMS formed	Organosilanes used in self-assembly process
Silica framework	$Si(-OC_2H_5)_4$
Surface-modified silica	$Si(-OC_2H_5)_4$ + $R\text{-}Si(-OC_2H_5)_3$
Framework-modified silica	$(H_5C_2O\text{-})_3Si\text{-}R'\text{-}Si(-OC_2H_5)_3$
Surface and framework modified silica	$(H_5C_2O\text{-})_3Si\text{-}R'\text{-}Si(-OC_2H_5)_3$ + $R\text{-}Si(-OC_2H_5)_3$

R and R' denote organic groups in organosilanes.

2.2. ENVIRONMENTAL APPLICATIONS OF OMS

There are three main types of environmental applications of ordered mesoporous silicas and organosilicas: (i) sequestration of carbon dioxide, (ii) removal of other gaseous organic and inorganic pollutants via adsorption and/or catalytic degradation, and (iii) removal of heavy metal ions, toxic organics and other pollutants from contaminated water. In addition, specially designed OMSs can be used for the development of sensors to detect organic and inorganic pollutants in air and water. This

section is focused on the application of functionalized OMSs for sequestration of carbon dioxide and removal of heavy metal ions from aqueous solutions.

2.2.1. *OMS adsorbents for carbon dioxide sequestration*

Various OMSs with modified surface properties were tested as adsorbents for sequestration of carbon dioxide. Xu et al.[24,25] used polyethylenimine-modified MCM-41materials for CO_2 adsorption and achieved adsorption capacity about 250 mg of this adsorbate per gram of the adsorbent. La_2O_3-modified MCM-41 materials were tested for CO_2 adsorption by Shen et al.[26] Also, CO_2 adsorption was studied on Al, Fe, Cu and Zn-containing MCM-41 materials by Macario et al.[27] as well as on the pore-expanded MCM-41 by Franchi et al.[28] While MCM-41 exhibits two-dimensional (2D) arrangement of hexagonally ordered mesopores (*P6mm* symmetry group), MCM-48 is a 3D cubic structure of *Ia3d* symmetry.[2] MCM-48 samples modified with metal species were tested as CO_2 adsorbents by Macario et al.;[27] however, adsorption of CO_2 on amine-modified MCM-48 samples was studied by Huang et al.[29] and Kim et al.[30]

There are several reports on the use of polymer-templated materials such as amine-modified SBA-15 for sequestration of carbon dioxide.[31-34] SBA-15 is a large pore OMS with 2D hexagonal arrangement of cylindrical channels, which in contrast to MCM-41 contain complementary irregular micropores in the walls of ordered mesopores.[35] Due to the presence of interconnecting micropores SBA-15 can be considered as 3D microporous and mesoporous network. The aforementioned studies showed that amine-functionalized SBA-15 materials are promising adsorbents for carbon dioxide. The reported adsorption capacities were analogous to those achieved for MCM-41-type materials.

2.2.2. *OMS adsorbents for volatile organic compounds and other gaseous pollutants*

OMSs are promising adsorbents for removal of volatile organic compounds (VOCs).[36-41] Zhao et al.[36] showed that some typical VOCs such as benzene, carbon tetrachloride, and *n*-hexane were captured by the MCM-41 type materials and showed better performance in comparison to some microporous adsorbents such as zeolites and activated carbons. A comparative study of isopentane and toluene adsorption on surfactant-templated and polymer-templated OMSs such as MCM-41 and SBA-15 was reported by Serrano et al.[40] Ueno et al.[38,39] studied adsorption of benzene, toluene and xylene on SBA-15 and SBA-16; the latter is a cage-like OMS with *Im3m* symmetry. They found that the OMSs studied showed higher selectivity towards benzene than toluene and xylene. In addition,

they were able to tune benzene selectivity by proper thermal treatment of these OMSs. In 2002 Ueno et al.[37] reported a microfluidic device containing OMS powder for detection of benzene, toluene and *o*-xylene mixture. By introducing to this device SBA-16 powder it was possible to achieve benzene detection limit of about 100 ppb.[38]

A unique 3D mesoporous-microporous structure of SBA-15 and related polymer-templated OMSs make those materials attractive adsorbents for various hydrocarbons. Van Bavel et al.[41] investigated plugged SBA-15 materials for adsorption of hexane, heptane and methylpentane because these materials are more stable than the conventional micellar templated structures known so far and possess a tunable amount of open and plugged pores as well as exhibit high microporosity. Newalkar et al.[42,43] examined SBA-15 as potential adsorbent for light hydrocarbons such as methane, ethane, ethylene, acetylene, propane, and propylene. They found that adsorption capacities for ethylene and propylene are higher than those for the corresponding alkanes. Their study suggested a higher affinity of SBA-15 framework for alkenes over corresponding alkanes due to the presence of complementary micropores in the SBA-15 mesostructure. It was shown that the SBA-15 sample with higher microporosity displayed strong affinity for ethylene, which was comparable with that reported for π-complexation-based adsorbents. Thus, these studies indicate that adsorption of various hydrocarbons on polymer-templated OMSs such as SBA-15 as well as separation of alkane/alkene and aromatic/aliphatic mixtures can be controlled by tuning microporosity in these materials.

Also, the OMS-type materials were used for adsorption of other gaseous pollutants. For instance, amine-modified MCM-48 and polyethylenimine-modified MCM-41 were used to adsorb H_2S.[29,44] Bhargava and Akolekar[45] studied Al-containing MCM-41 materials as potential adsorbents for NO and CO; however, Al-containing SBA-15 was examined as adsorbent for various carcinogenic nitrosamines.[46]

2.2.3. *Decomposition of gaseous pollutants on OMS materials*

Although adsorption is commonly used to remove various toxic compounds and pollutants, this approach has several disadvantages. First of all, adsorbents loaded with toxic compounds are hazardous materials, which need to be properly stored, disposed or regenerated after reaching adsorption capacity. One of the best alternatives to the removal of toxic compounds via adsorption is combination of this process with catalytic or photocatalytic transformation (degradation/decomposition) of these pollutants into less hazardous species or environmentally friendly chemicals. This rapidly growing research area is primarily focused on the design of catalytic activity of materials, while the development of their

porosity is a secondary issue. An integrative approach that addresses both issues seems to be promising as evidenced by some recent studies. For instance, Hudson et al.[47-49] used OMSs such as MCM-48 and SBA-15 for incorporation of catalytic species and employed the resulting nanostructured composites for trapping (adsorption) and decomposition of toxic gases. OMSs modified with sodium persulfate and 2,6-bis(benzoxazolyl) pyridine were used for decomposition of hydrogen cyanide and cyanogens.[48,49]

The use of nanostructures for trapping and catalytic degradation of toxic compounds is expected to grow rapidly. There is a growing interest in the development of smart nanomaterials that can simultaneously sense and destroy harmful chemical contaminants.[50] The review article by Kamat and Meisel[50] highlights some recent advances of nanoscience in the area of environmental remediation. In particular, nanostructured composites are promising materials for photocatalytic degradation of various air pollutants. Also, there is a tremendous interest in photocatalytic degradation of toxic compounds in water (e.g., see review article by Bhatkhande[51] and references therein).

2.2.4. *OMS adsorbents for removal of heavy metal ions*

There are numerous reports on the design and synthesis of OMSs with attached organic groups of high affinity towards heavy metal ions, especially for mercury ions. These materials were shown to be effective adsorbents for heavy metal ions from aqueous solutions because they have high surface area, large pore volume, tailorable pore size and good pore connectivity. Moreover, there are indications that the well-defined porous structure may contribute to the high loading capacities and remarkable selectivity of OMS-based adsorbents.[52,53]

Silicas with hexagonally ordered mesopores such as MCM-41 were initially decorated with mercaptopropyl groups and used for adsorption of mercury ions from water.[52,53] Later other OMSs such as MCM-48 and SBA-15 as well as more complex ligands such as 1-allyl-3-propylthiourea and benzoylthiourea were bonded to the pore walls to improve adsorption capacity and affinity towards mercury ions.[54-56] It was shown that incorporation of 1-benzoyl-3-propylthiourea ligand into mesopores of MCM-41 and MCM-48 afforded materials with high ligand concentration (~ 1.5 mmol/g), high surface area and pore width of ~3.0 nm. The maximum loading of mercury ions from aqueous solutions on these materials was between 5.0-7.0 mmol Hg^{2+}/g and exceeded significantly the capacity of the previously known samples. A further improvement in the development of these materials can be achieved by incorporation of

multifunctional bridging groups into the OMS framework[57,58] or by designing mesostructures with both surface and bridging groups.[23]

There is also a great interest in the development of OMS-based adsorbents for other heavy metal ions. Mesoporous silicas with amine functionality were used to study adsorption of cadmium (II) ions.[59] Also, a cage-like OMS, FDU-1, was employed to incorporate humic acid and tested for removal of cadmium (II) ions from water.[60] SBA-15 materials with thiol and imidazole ligands were investigated as adsorbents for Pd^{2+} and Pt^{2+} ions.[61,62] Adsorption of chromium (III) ions was studied on OMSs with phosphonic functionality.[63] The aforementioned adsorbents have been prepared by post-synthesis modification of OMSs or direct incorporation of desired ligands via co-condensation of proper organosilanes. Recently, Sayari et al.[64] proposed to obtain novel adsorbents for removal of Co^{2+} Cu^{2+} and Ni^{2+} ions from aqueous solutions by post-synthesis expansion of mesoporous structure of as-synthesized MCM-41 using *N*,*N* dimethyldecylamine. This process affords materials with open pore structure and readily accessible amine groups able to attract several metal ions.

3. Ordered Mesoporous Carbons

An important achievement in the area of OMMs was the use of ordered mesoporous silicas and colloidal crystals as templates to create new periodic mesoporous and macroporous materials, including carbons,[65-68] polymers,[69] metals[70] and inorganic oxides.[71,72] Although there are numerous works in this area, only a few references are provided to illustrate the hard templating method for synthesis of various ordered nanoporous materials. This method has been used with a great success to develop ordered mesoporous carbons.[66,72,73] In this case, the templating process involves the formation of hard templates such as ordered mesoporous silicas or colloidal crystals (step a in Figure 2), infiltration of the porous template with a fluid-type carbon precursor (step b in Figure 2) and its carbonization followed by removal of the template (step c in Figure 2). The resulting ordered carbon is an inverse replica of the template used.

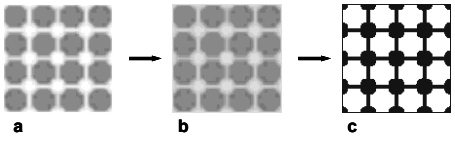

Figure 2. Schematic illustration of the templating synthesis of ordered mesoporous carbons; a - ordered siliceous template, b - template filled with carbon precursor, and c - ordered mesoporous carbon being inverse replica of the template used.[74]

An attractive alternative to the synthesis of novel carbons by templating process is imprinting of silica colloids or silica particles with either ordered or disordered porosity in large pitch particles.[75-77] This method involves imprinting of colloids or particles in pitch particles, eventual stabilization of pitch particles followed by carbonization and dissolution of silica particles (see Figure 3). It was shown by Li and Jaroniec[75,76] that the colloidal imprinting is very promising for the synthesis of mesoporous carbons with uniform spherical pores and tailored surface area and pore volume. This process can be also used to disperse catalytic particles in the carbon by using them together with silica colloids.[75]

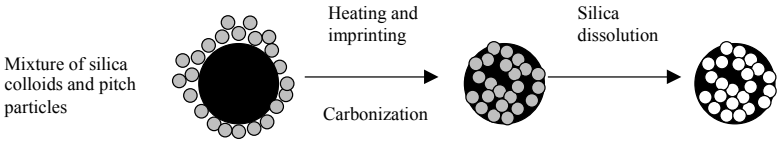

Figure 3. Schematic illustration of the imprinting process, which involves silica colloids and pitch particles.[78]

Since ordered mesoporous carbons (OMCs) were reported by Ryoo et al.[65] at the end of 1999, the research in this area has been concentrated on the synthesis of novel carbon structures. The current efforts on applications of OMCs are focused mainly on the double layer capacitors,[73,79] fuel cells[80,81] and hydrogen storage.[82,83] It is expected that environmental applications of OMCs in adsorption and catalysis related processes will grow too.

4. Conclusions

This short review illustrates that ordered mesoporous materials exhibit a remarkable propensity to be tailored in desired forms, including thin films, fibers, monoliths, spheres, and nanoparticles. There are available methods for the synthesis of OMMs with tailored surface and structural properties allowing design of materials for specific applications including traditional areas such as adsorption, catalysis and environmental cleanup as well as nanotechnology and biotechnology. It is shown that recent achievements in the synthesis of novel OMSs and especially in their functionalization have a pronounced impact on the advancement of environmental remediation processes.

ACKNOWLEDGMENT

The author acknowledges support by NSF Grants CTS-0086512 and CHE-0093707.

REFERENCES

1. C.T. Kresge, M.E. Leonowicz, W.J. Roth, J.C. Vartuli, and J.S. Beck, Ordered mesoporous molecular-sieves synthesized by a liquid-crystal template mechanism, *Nature* 359, 710-712 (1992).
2. J.S. Beck, J.C. Vartuli, W.J. Roth, M.E. Leonowicz, C.T. Kresge, K.D. Schmitt, C.T.-W. Chu, D.H. Olson, E.W. Sheppard, S.B. McCullen, J.B. Higgins, and J.L. Schlenker, A new family of mesoporous molecular sieves prepared with liquid crystal templates, *J. Am. Chem. Soc.* 114, 10834-10843 (1992).
3. A. Sayari, and P. Liu, Non-silica periodic mesostructured materials: recent progress, *Microporous Mater.* 12, 149-177 (1997).
4. A. Stein, B.J. Melde, and R.C. Schroden, Hybrid inorganic-organic mesoporous silicates – nanoscopic reactors coming of age, *Adv. Mater.* 12, 1403-1419 (2000).
5. A. Sayari, and S. Hamoudi, Periodic mesoporous silica-based organic-inorganic nanocomposite materials, *Chem. Mater.* 13, 3151-3168 (2001).
6. F. Schuth, and W. Schmidt, Microporous and mesoporous materials, *Adv. Mater.* 14, 629-638 (2002).
7. G.J.A.A. Soler-Illia, C. Sanchez, B. Lebeau, and J. Patarin, Chemical strategies to design textured materials: from microporous and mesoporous oxides to nanonetworks and hierarchical structures, *Chem. Rev.* 102, 4093-4138 (2002).
8. A. Stein, A. Advances in microporous and mesoporous solids, *Adv. Mater.* 15, 763-775 (2003).
9. C.J. Brinker, Y. Lu, A. Sellinger, and H. Fan, Evaporation-induced self-assembly: nanostructures made easy, *Adv. Mater.* 11, 579-585 (1999).
10. D. Zhao, J. Feng, Q. Huo, N. Melosh, G.H. Fredrickson, B.F. Chmelka, and G.D. Stucky, Triblock copolymer syntheses of mesoporous silica with periodic 50 to 300 angstrom pores, *Science* 279, 548-552 (1998).
11. C.P. Jaroniec, M. Kruk, M. Jaroniec, and A. Sayari., Tailoring surface and structural properties of MCM-41 silicas by bonding organosilanes, *J. Phys. Chem. B* 102, 5503-5510 (1998).
12. V. Antochshuk, and M. Jaroniec., Adsorption, thermogravimetric and NMR studies of FSM-16 materials functionalized with alkylmonochlorosilanes, *J. Phys. Chem. B* 103, 6252-6261 (1999).
13. V. Antochshuk, and M. Jaroniec., Functionalized mesoporous materials obtained via interfacial reactions in self-assembled silica-surfactant systems, *Chem. Mater.* 12, 2496-2501 (2000).
14. V. Antochshuk, A.S. Araujo, and M. Jaroniec, Functionalized MCM-41 and CeMCM-41 materials synthesized via interfacial reactions, *J. Phys. Chem. B* 104, 9713-9719 (2000).
15. M. Kruk, T. Asefa, M. Jaroniec, and G.A. Ozin, Metamorphosis of ordered mesopores to micropores: periodic silica with unprecedented loading of pendant reactive organic groups transforms to periodic microporous silica with tailorable pore size, *J. Am. Chem. Soc.* 124(22), 6383-6392 (2002).
16. S. Inagaki, S. Guan, Y. Fukushima, T. Ohsuna, and O. Terasaki, Novel mesoporous materials with a uniform distribution of organic groups and inorganic oxide in their framework, *J. Am. Chem. Soc.* 121, 9611-9614 (1999).

17. B.J. Melde, B.T. Holland, C.F. Blanford, and A.A. Stein, Mesoporous sieves with unified hybrid inorganic/organic frameworks, *Chem. Mater.* 11, 3302-3308 (1999).
18. T. Asefa, M.J. MacLachlan, N. Coombs, G.A. and Ozin, Periodic mesoporous organosilicas with organic groups inside the channel walls, *Nature* 402, 867-871 (2000).
19. T. Asefa, M. Kruk, M.J. MacLachlan, N. Coombs, H. Grondey, M. Jaroniec, and G.A. Ozin, Novel bifunctional periodic mesoporous organosilicas, BPMOs: synthesis, characterization, properties and in-situ selective hydroboration – alcoholysis reactions of functional groups, *J. Am. Chem. Soc.* 123, 8520-8530 (2001).
20. S. Inagaki, S. Guan, T. Ohsuna, and O. Terasaki, An ordered mesoporous organosilica hybrid material with a crystal-like wall structure, *Nature* 416, 304-307 (2002).
21. M. Kuroki, T. Asefa, W. Whitnal, M. Kruk, C. Yoshina-Ishii, M. Jaroniec, and G.A. Ozin, Synthesis and properties of 1,3,5-benzene periodic mesoporous organosilica (PMO): Novel aromatic PMO with three point attachments and unique thermal transformations, *J. Am. Chem. Soc.* 124, 13886-13895 (2002).
22. J.R. Matos, M. Kruk, L.P. Mercuri, M. Jaroniec, T. Asefa, N. Coombs, G.A. Ozin, T. Kamiyama, and O. Terasaki, Periodic mesoporous organosilica with large cagelike pores, *Chem. Mater.* 14, 1903-1905 (2002).
23. O. Olkhovyk, S. Pikus, and M. Jaroniec, Bifunctional periodic mesoporous organosilica with large heterocyclic bridging groups and mercaptopropyl ligands, *J. Mater. Chem.* 15, 517-1519 (2005).
24. X. Xu, C. Song, J.M. Andresen, B.G. Miller, and A.W. Scaroni, Novel polyethylenimine-modified mesoporous molecular sieve of MCM-41 type as high-capacity adsorbent for CO_2 capture, *Energy & Fuels* 16, 1463-1469 (2002).
25. X. Xu, C. Song, J.M. Andresen, B.G. Miller, and A.W. Scaroni, Preparation and characterization of novel CO_2 ‘‘molecular basket’’ adsorbents based on polymer-modified mesoporous molecular sieve MCM-41, *Microporous Mesoporous Mater.* 62, 29-45 (2003).
26. S.C. Shen, X. Chen, and S. Kawi, CO_2 Adsorption over Si-MCM-41 materials having basic sites created by postmodification with La_2O_3, *Langmuir* 20, 9130-9137 (2004).
27. A. Macario, A. Katovic, G. Giordano, F. Iucolano, D. Caputo, Synthesis of mesoporous materials for carbon dioxide sequestration, *Microporous Mesoporous Mater.* 81, 139-147 (2005).
28. R. Franchi, P.J.E. Harlick, and A. Sayari, A high capacity, water tolerant adsorbent for CO_2: diethanolamine supported on pore-expanded MCM-41, *Stud. Surf. Sci. Catal.* 156, 879-886 (2005).
29. H.Y. Huang, R.T. Yang, D. Chinn, and C.L. Munson, Amine-grafted MCM-48 and silica xerogel as superior sorbents for acidic gas removal from natural gas, *Ind. Eng. Chem. Res.* 42, 2427-2433 (2003).
30. S. Kim, J. Ida, V.V. Guliants, and Y.S. Lin Jerry, Tailoring pore properties of MCM-48 silica for selective adsorption of CO_2, *J. Phys. Chem. B* 109, 6287-6293 (2005).
31. A.C.C. Chang, S.S.C. Chuang, M.M. Gray, and Y. Soong, In-situ infrared study of CO_2 adsorption on SBA-15 grafted with ç-(aminopropyl)triethoxysilane, *Energy & Fuels* 17, 468-473 (2003).
32. N. Hiyoshi, K. Yogo, and T. Yashima, Adsorption of carbon dioxide on amine modified SBA-15 in the presence of water vapor, *Chem.Lett.* 33, 510-511 (2004).
33. R.A. Khatri, S.S.C. Chuang, Y. Soong, and M.M. Gray, Carbon dioxide capture by diamine-grafted SBA-15: a combined Fourier transform infrared and mass spectrometry study, *Ind. Eng. Chem. Res.* 44, 3702-3708 (2005).

34. F. Zheng, D.N. Tran, B.J. Busche, G.E. Fryxell, R.S. Addleman, T.S. Zemanian, and C.L. Aardahl, Ethylenediamine-modified SBA-15 as regenerable CO_2 sorbent, *Ind. Eng. Chem. Res.* 44, 3099-3105 (2005).
35. M. Kruk, M. Jaroniec, C.H. Ko, and R. Ryoo, Characterization of porous structure of SBA-15, *Chem. Mater.* 12, 1961-1968 (2000).
36. X.S. Zhao, Q. Ma, and G.Q.(M.) Lu, VOC removal: comparison of MCM-41 with hydrophobic zeolites and activated carbon, *Energy & Fuels* 12, 1051-1054 (1998).
37. Y. Ueno, T. Horiuchi, M. Tomita, O. Niwa, H.-S. Zhou, T. Yamada, and I. Honma, Separate detection of BTX mixture gas by a microfluidic device using a function of nanosized pores of mesoporous silica adsorbent, *Anal. Chem.* 74, 5257-5262 (2002).
38. Y. Ueno, T. Horiuchi, A. Tate, O. Niwa, H. Zhou, T. Yamada, and I. Honma, Effect of the calcination temperature of self-ordered mesoporous silicate on its adsorption characteristics for aromatic hydrocarbons, *New J. Chem.* 29, 504-508 (2005).
39 Y. Ueno, A. Tate, O. Niwa, H.S. Zhou, T. Yamada, and I. Honma, High benzene selectivity of mesoporous silicate for BTX gas sensing microfluidic devices, *Anal. Bioanal. Chem.* 382, 804-809 (2005).
40. D.P. Serrano, G. Calleja, J.A. Botas, and F.J. Gutierrez, Adsorption and hydrophobic properties of mesostructured MCM-41 and SBA-15 materials for volatile organic compound removal, *Ind. Eng. Chem. Res.* 43, 7010-7018 (2004).
41. E. Van Bavel, V. Meynen, P. Cool, K. Lebeau, E.F. Vansant, Adsorption of hydrocarbons on mesoporous SBA-15 and PHTS materials, *Langmuir* 21, 2447-2453 (2005).
42. B.L. Newalkar, N.V. Choudary, P. Kumar, S. Komarneni, and T.S.G. Bhat, Exploring the potential of mesoporous silica, SBA-15, as an adsorbent for light hydrocarbon separation, *Chem. Mater.* 14, 304-309 (2002).
43. B.L. Newalkar, N.V. Choudary, U.T. Turaga, R.P. Vijayalakshmi, P. Kumar, S. Komarneni, and T.S.G. Bhat, Potential adsorbent for light hydrocarbon separation: Role of SBA-15 framework porosity, *Chem. Mater.* 15, 1474-1479 (2003).
44. X. Xu, I. Novochinskii, and C. Song, Low-temperature removal of H_2S by nanoporous composite of polymer-mesoporous molecular sieve MCM-41 as adsorbent for fuel cell applications, *Energy & Fuels,* ASAP article (2005).
45. S.K. Bhargava, and D.B. Akolekar, Adsorption of NO and CO over transition-metal-incorporated mesoporous catalytic materials, *J. Coll. and Inter. Sci.* 281, 171-178 (2005).
46. C.F. Zhou, Y.M. Wang, J.H. Xu, T.T. Zhuang, Y. Wang, Z.Y. Wu, and J.H. Zhu, New efficient Al-containing SBA-15 materials for removing nitrosamines in mild conditions, In: *Stud. Surf. Sci. Catal.* 156, 907-916 (2005).
47. M.J. Hudson, D.B. Jackson, J.L. Ward, and M.J. Chinn, Peroxides in ordered nanoporous silicas: clean alternatives to transition metal oxidants for the removal of toxic gases, *Chem. Commun.* 2970-2971 (2003).
48. M.J. Hudson, D.B. Jackson, J.L. Ward, M.J. Chinn, and M. Stockenhuber, Peroxydisulfate in MCM-48 silicas: powerful and clean materials for the removal of toxic gases, *J. Mater. Chem.* 14, 1180-1186 (2004).
49. M.J. Hudson, J.P. Knowles, P.J.F. Harris, D.B. Jackson, M.J. Chinn, and J.L. Ward, The trapping and decomposition of toxic gases such as hydrogen cyanide using modified mesoporous silicates*, Microporous Mesoporous Mater.* 75, 121-128 (2004).
50. P.V. Kamat, and D. Meisel, Nanoscience opportunities in environmental remediation, *Comptes Rendus Chimie* 6, 999-1007 (2003).

51. D.S. Bhatkhande, V.G. Pangarkar, and A.A.C.M. Beenackers, Photocatalytic degradation for environmental applications - a review, *J. Chem. Technol. Biotechnol.* 77, 102-116 (2002).
52. X. Feng, G.E. Fryxell, L.Q. Wang, A.Y. Kim, J. Liu, and K. Kemner, Functionalized monolayers on ordered mesoporous supports, *Science* 276, 923-930 (1997).
53. L. Mercier, and T.J. Pinnavaia, Access in mesoporous materials: Advantages of a uniform pore structure in the design of a heavy metal ion adsorbent for environmental remediation, *Adv. Mater.* 9, 500-503 (1997).
54. V. Antochshuk, and M. Jaroniec, 1-Allyl-3-propylthiourea modified mesoporous silica for mercury removal, *Chem. Commun.* 258-259 (2002).
55. V. Antochshuk, O. Olkhovyk, M. Jaroniec, I.-S. Park, and R. Ryoo, Benzoylthiourea-modified mesoporous silica for mercury(II) removal, *Langmuir* 19, 3031-3034 (2003).
56. O. Olkhovyk, V. Antochshuk, and M. Jaroniec, Benzoylthiourea-modified MCM-48 mesoporous silica for mercury(II) adsorption from aqueous solutions, *Colloids & Surfaces, A* 236, 69-72 (2004).
57. L. Zhang, W. Zhang, J. Shi, Z. Hua, Y. Li, and J. Yan, A new thioether functionalized organic-inorganic mesoporous composite as a highly selective and capacious Hg^{2+} adsorbent, *Chem. Commun.* 210-211 (2003).
58. O. Olkhovyk, and M. Jaroniec, Periodic mesoporous organosilica with large heterocyclic bridging groups, *J. Am. Chem. Soc.* 127, 60-61 (2005).
59. Y.-K. Lu, and X.-P. Yan, An imprinted organic-inorganic hybrid sorbent for selective separation of cadmium from aqueous solution, *Anal. Chem.* 76, 453-457 (2004).
60. L.C. Cides da Silva, G. Abate, N. Andrea, M.C.A. Fantini, J.C. Masini, L.P. Mercuri, O. Olkhovyk, M. Jaroniec, and J.R. Matos, Microwave synthesis of FDU-1 silica with incorporated humic acid and its application for adsorption of Cd^{2+} from aqueous solutions, In: *Stud. Surf. Sci. Catal.* 156, 941-950 (2005).
61. T. Kang, Y. Park, and J. Yi, Highly selective adsorption of Pt^{2+} and Pd^{2+} using thiol-functionalized mesoporous silica, *Ind. Eng. Chem. Res.* 43, 1478-1484 (2004).
62. T. Kang, Y. Park, K. Choi, J.S. Lee, and J. Yi, Ordered mesoporous silica (SBA-15) derivatized with imidazole-containing functionalities as a selective adsorbent of precious metal ions, *J. Mater. Chem.* 14, 1043-1049 (2004).
63. K.H. Nam, L.L. and Tavlarides, Synthesis of a high-density phosphonic acid functional mesoporous adsorbent: application to Chromium(III) removal, *Chem. Mater.* 17, 1597-1604 (2005).
64. A. Sayari, S. Hamoudi, and Y. Yang, Applications of pore-expanded mesoporous silica. 1. Removal of heavy metal cations and organic pollutants from wastewater, *Chem. Mater.* 17, 212-216 (2005).
65. R. Ryoo, S.H. Joo, and S. Jun, Synthesis of highly ordered carbon molecular sieves via template-mediated structural transformation, *J. Phys. Chem. B* 103, 7743-7746 (1999).
66. R. Ryoo, S.H. Joo, M. Kruk, and M. Jaroniec, Ordered mesoporous carbons, *Adv. Mater.* 13, 677-681 (2001).
67. S. Jun, S.H. Joo, R. Ryoo, M. Kruk, M. Jaroniec, Z. Liu, T. Ohsuna, and O. Terasaki, Synthesis of new nanoporous carbon with hexagonally ordered mesostructure, *J. Am. Chem. Soc.* 122, 10712-10713 (2000).
68. M. Kang, S.H. Yi, H.I. Lee, J.E. Yie, and J.M. Kim, Reversible replication between ordered mesoporous silica and mesoporous carbon, *Chem. Commun.* 1944-1945 (2002).
69. C. Liu, J.B. Lambert, and L. Fu, A novel family of ordered, mesoporous inorganic/organic hybrid polymers containing covalently and multiply bound microporous organic hosts, *J. Am. Chem. Soc.* 125, 6452-6461 (2003).

70. Z. Liu, Y. Sakamoto, T. Ohsuna, K. Hiraga, O. Terasaki, C.H. Ko, H.J. Shin, and R. Ryoo, TEM studies of platinum nanowires fabricated in mesoporous silica MCM-41, *Angew. Chem.* 39, 3107-3110 (2000).
71. S.C. Laha, and R. Ryoo, Synthesis of thermally stable mesoporous cerium oxide with nanocrystalline frameworks using mesoporous silica templates, *Chem. Commun*. 2138-2139 (2003).
72. H. Yang, and D. Zhao, D., Synthesis of replica mesostructures by the nanocasting strategy, *J. Mater. Chem.* 15, 1217-1231 (2005).
73. J. Lee, S. Han, and T. Hyeon, Synthesis of new nanoporous carbon materials using nanostructured silica materials as templates, *J. Mater. Chem.* 14, 478-486 (2004).
74. M. Jaroniec, Ordered Mesoporous Materials: Synthesis, Structure and Interfacial Properties, *Annals Polish Chem. Soc.* 2, 1098-1102 (2003).
75. Z. Li, and M. Jaroniec, Colloidal imprinting: a novel approach to the synthesis of mesoporous carbons, *J. Am. Chem. Soc.* 123, 9208-9209 (2001).
76. Z. Li, and M. Jaroniec, Synthesis and adsorption properties of colloid-imprinted carbons with surface and volume mesoporosity, *Chem. Mater.* 15, 1327-1333 (2003).
77. Z. Li, M. Jaroniec, Y.-J. Lee, and L.R. Radovic, High surface area graphitized carbon with uniform mesopores synthesized by a colloidal imprinting method, *Chem. Commun.* 1346-1347 (2002).
78. M. Jaroniec, and Z. Li, in: *Adsorption Science and Technology: Proceedings of the Third Pacific Basin Conference*, edited by Chang-Ha Lee (World Scientific, Singapore, 2003) pp. 136.
79. H.S. Zhou, S.M. Zhu, M. Hibino, and I. Honma, Electrochemical capacitance of self-ordered mesoporous carbon, *J. Power Sources* 122, 219-223 (2003).
80. S.H. Joo, S.J. Choi, I. Oh, J. Kwak, Z. Liu, O. Terasaki, and R. Ryoo, Ordered nanoporous arrays of carbon supporting high dispersions of platinum nanoparticles, *Nature* 412, 169-172 (2001).
81. A.B. Fuertes, and T.A. Centeno, Mesoporous carbons with graphitic structures fabricated by using porous silica materials as templates and iron-impregnated polypyrrole as precursor, *J. Mater. Chem.* 15, 1079-1083 (2005).
82. E. Terres, B. Panella, T. Hayashi, Y.A. Kim, M. Endo, J.M. Dominguez, M. Hirscher, H. Terrones, and M. Terrones, Hydrogen storage in spherical nanoporous carbons, *Chem. Phys. Lett.* 403, 363-366 (2005).
83. L.C. Chen, R.K. Singh, and P.A. Webley, Synthesis, characterization and hydrogen storage on ordered carbon adsorbents, *Stud. Surf. Sci. Catal.* 156, 603-608 (2005).

SELECTIVE REMOVAL OF RADIONUCLIDES FROM NUCLEAR WASTE EFFLUENTS USING INORGANIC ION EXCHANGERS

RISTO KOIVULA*, RISTO HARJULA AND JUKKA LEHTO
Laboratory of Radiochemistry, A.I. Virtasen aukio 1, P.O. Box 55, 00014 University of Helsinki, Finland

Abstract. The development of ion exchange processes and materials focuses on selective separation. R&D on inorganic materials for selective separation processes has been strong for several years. The superior selectivity of some inorganic ion exchangers compared to other sorption materials presently used in the separation processes has been the major initiative for continuing research. High selectivity is the key to fulfilling the strict regulations concerning waste effluents and to enhancing the energy efficiency of separation processes. Several selective inorganic ion exchange materials have been developed at the Laboratory of Radiochemistry for decontamination of low and intermediate radioactive waste solutions, and some of those materials have found industrial applications. One of them is extremely cesium selective ($k_{Cs/Na}$=1,500,000) a transition metal hexacyanoferrate (CsTreat®) which is granular and has a wide operational pH range (pH 1 to 13). These physical properties are one of the key factors for ion exchange materials in their conventional separation processes and are atypical for the most of selective inorganic materials. About 900 m^3 of high-salt (~240 g/L $NaNO_3$) evaporator concentrates have been decontaminated with only 112 liters of CsTreat® at Loviisa nuclear power plant, Finland, in ten years. For the second most important fission product, strontium, a granular sodium titanate (SrTreat®) material has been developed. It has a high selectivity ($k_{Sr/Na}$=200,000) but rather limited pH range (above 9) and it is also sensitive to calcium. Large numbers of metal oxides with various doping elements have been developed for selective separation of activated corrosion products. For radioactive cobalt and nickel

* To whom correspondence should be addressed; e-mail: risto.koivula@helsinki.fi

J.M. Loureiro and M.T. Kartel (eds.), Combined and Hybrid Adsorbents, 37–47.

very effective materials have been found: titanium oxide, (CoTreat®) and tin antimonates, respectively.

Keywords: selective; separation; ion exchange; radioactive; waste; inorganic

1. Introduction

The spectrum of radioactive wastes produced by nuclear industry is extremely diverse with respect to their radionuclide content, concentrations of interfering salts and acidity/alkalinity. High radioactive solutions can be saturated with salts and nitrates or they can be very low salt, almost pure aqueous solutions. Separation of radionuclides from solutions of low salt content can be quite straight forward by means of conventional ion exchange processes utilizing organic resins or inorganic materials of low selectivity, such as zeolites. However decontamination of solutions with large excesses of inactive salts by conventional separation methods is unfeasible. Typically radionuclides are in trace concentrations in waste solutions, much below micromoles per litre, and only in the most highly radioactive waste solutions radionuclides are in the millimolar range. However, the concentrations of inactive salts in those solutions can be as high as 7 moles per litre. Therefore, effective separation of radionuclides cannot be accomplished with ordinary organic ion exchangers from most nuclear waste solutions since the resins do not exhibit the required selectivity for any metal ions.

This paper discusses the use of selective inorganic ion exchangers in nuclear waste effluent treatment. The focus is on new, highly selective, ion exchange materials that have been developed in the Laboratory of Radiochemistry, University of Helsinki. Highly selective materials, such as transition metal hexacyanoferrate exchangers for cesium removal and a sodium titanate exchanger for strontium removal, are discussed in detail since they have found use in large scale applications. Also the latest development on selective separation of activated corrosion products, such as ^{60}Co and ^{63}Ni, is presented due to their importance on radiation dose and regulation limits on final disposal.

1.1. SELECTIVITY OF ION EXCHANGER

Broadly speaking, two main features of ion exchange material have a direct effect on the selectivity of ion exchange: affinity and accessibility.

Electrostatic attraction has a major effect on the affinity of an ion exchange material towards ions of opposite charge, and it can be manipulated in the material synthesis. In some cases also the material tendency towards a lower energy level will determine the affinity. The structure of the material usually determines whether the ion exchange sites are accessible for a certain ion or not. In three dimensional ion exchange materials steric hindrance restricts movement of ions and this can exclude certain ions from the exchange sites as in the case of zeolites (ion sieve effect). Combining and adjusting the affinity and accessibility of an ion exchange material alters its selectivity. For example, the affinity can be increased so that electrostatic attraction will break the hydration layer of metal cation, which in turn allows the metal ion to enter the inner structure of the material where the ion exchange sites are located.

1.1.1. *Ion exchange capacity and selectivity*

Ion exchange capacity and selectivity are two important properties that contribute to the efficiency of an ion exchanger. In the following, Cs/Na exchange is taken as an example to discuss the effect of these properties on the performance of an ion exchanger in radionuclide removal. Sodium is usually the most abundant cation in nuclear waste effluents and ^{137}Cs is often the radionuclide of major concern.

1.1.2. *Selectivity coefficient*

The selectivity coefficient is usually used to measure the ion exchange equilibrium. For the Cs/Na exchange the selectivity coefficient $k_{Cs/Na}$ is defined as:

$$k_{Cs/Na} = \frac{[Cs]_S [Na]_L}{[Cs]_L [Na]_S} \quad (1)$$

where subscript letters S and L refer to the equilibrium ion concentrations in the solid and in the liquid phases, respectively. The selectivity coefficient may depend on the degree of loading of Cs in the exchanger, and also changes with the ionic strength of solutions at high concentrations where the activity coefficient ratio γ_{Cs}/γ_{Na} can deviate strongly from unity.

1.1.3. *Distribution coefficient*

The efficiency of an ion exchanger is often measured, especially so in radionuclide removal, by the distribution coefficient K_d, i.e.

$$K_d = \frac{[Cs]_S}{[Cs]_L} \quad (2)$$

The distribution coefficient can be measured by a static batch or dynamic column experiment. Under the same equilibrium conditions these two measurements are equivalent, so K_d measured under batch conditions can be used to estimate column performance. When the cesium concentration in the exchanger is expressed in mol/kg and in solution in mol/L, the distribution coefficient thus gives the maximum theoretical processing capacity of the ion exchanger, i.e. the maximum volume of water that can be purified per mass of exchanger. This maximum capacity is reached when the column is completely exhausted, in other words when the breakthrough of cesium from the column is 100%.

By combining Eqs. 1 and 2, and inserting $[Na]_S = Q - [Cs]_S$ Eq. 3 is obtained after some manipulation for K_d (and theoretical processing capacity).

$$K_d = \frac{Q}{\frac{[Na]_L}{k_{Cs/Na}} + [Cs]_L} \quad (3)$$

In low-activity waste streams the activity concentration of ^{137}Cs is typically in the range of 3.7–370 kBq/l. This corresponds to a chemical cesium concentration of about 10^{-11} – 10^{-9} mol/L. The concentration of sodium is almost always very much higher than that of cesium (> 10^{-3} mol/L) so that $[Na]_L/k_{Cs/Na} >> [Cs]_L$ in Eq. 3. Under these circumstances the concentration of cesium does not have effect on the value of K_d, and Eq. 3 can be presented in the familiar logarithmic form:

$$\log K_d = \log(k_{Cs/Na}\, Q) - \log[Na]_L \quad (4)$$

In this case (uni-univalent exchange, cesium present as a trace) K_d and theoretical processing capacity are inversely proportional to the concentration of sodium in the solution. Selectivity ($k_{Cs/Na}$) is the key factor in determining the maximum processing capacity. The ion exchange capacity Q is typically in the range of 1–5 meq/g of dry exchanger (Na-form) for commercial materials and the upper limit of this range is close to the 'theoretical' maximum. Selectivity, on the other hand, has no theoretical maximum. This means that in making efficient exchangers for radionuclide removal, one should aim to produce materials with high selectivity – trying to maximize ion exchange capacity is less important.

2. Results and Discussions

A number of selective inorganic ion exchange materials have been developed and reported in the literature. Although laboratory tests of these materials have been promising only a few materials have shown good results in large scale installations. In the following sections only materials developed in the Laboratory of Radiochemistry, Helsinki, are discussed.

2.1. SELECTIVE REMOVAL OF CESIUM

One extremely selective material group for cesium uptake is hexacyanoferrates (HCF). Insoluble transition metal hexacyanoferrates have been known for decades, used as precipitants at large scales already in the 1940s, and as effective agents for the removal of radioactive cesium.[1] However, their use in columns has been prohibited due to lack of granular form of the material.

The first industrial scale process utilizing hexacyanoferrates in packed bed columns was at the Loviisa Nuclear Power Plant, Finland, where a hexacyanoferrate product developed at the Laboratory of Radiochemistry was taken into use in 1991.[2,3] During the following ten years a total of 900 m^3 of alkaline (pH 11.5), high-salt (240 g/L $NaNO_3$) evaporator concentrate has been purified with average decontamination factor of about 2000, using only fourteen 8-liter hexacyanoferrate columns. This level of decontamination of cesium from solutions of large excess of competing, inactive ions is only possible with a highly selective ion exchange material. In the case of transition metal hexacyanoferrates the selectivity is proposed to originate from the size of tunnels in the material structure where the ion exchange sites are located. The diameter of these tunnels corresponds closely to the diameter of cesium ions.[4] Ions larger than cesium cannot enter the tunnel structure and so are excluded from the ion exchange sites while smaller ions create strain to the structure when exchanged. The performance of CsTreat® is not affected by the presence of common alkali and alkaline earth metal in the water. Only high concentrations of potassium and ammonium ions are known to interfere markedly with cesium removal, but only at concentration levels which are atypical for waste solutions.

CsTreat® removes cesium effectively not only from concentrated waste effluents but also from dilute solutions. It has been used at Callaway NPP, USA, and Olkiluoto NPP, Finland, in the purification of dilute waste solutions.[6] In a laboratory scale column test with a Callaway waste simulant (pH 6, 320 mg/L Na and 17 mg/L Ca) 300,000 bed volumes were purified without any breakthrough. This means that the annual amount of

the hexacyanoferrate needed to purify all the dilute waste effluents from an NPP is very small, being only some tens of liters.

TABLE 1. Selectivity coefficients for Cs/Na exchange in commercial ion exchange materials[5]

Ion Exchange Material	Concentration of Na (mol/L)	Selectivity coefficient $k_{Cs/Na}$
Sulphonic acid resin	not known	< 10
Resorcinol-formaldehyde resin	6.0	11,400*
Zeolite (mordenite)	0.1	450
Silicotitanate (CST)	5.7	18,000
CsTreat®	5.0	1,500,000

* selectivity coefficient calculated from measured distribution coefficient of 5450 ml/g.

We have also studied crystalline silicotitanate (CST) that has high selectivity for cesium but is also fairly selective for strontium. The framework of CST is formed of four corner-sharing TiO_6 octahedra bridged by SiO_4 tetrahedra in the a- and b-axes resulting in a tetragonal unit cell (a = b = 7.8 Å, c ≅ 12 Å) and tunneled structure. The tunnel size is suitable for cesium ions and CST has been considered as one of the most promising materials for cesium separation.[7,8] At high alkalinities the interference of sodium on cesium uptake is significant, but selectivity for cesium can be enhanced by substitution of Nb^{5+} ions for Ti^{4+}. This, in turn, will reduce the ion exchange capacity of the material.

2.2. SELECTIVE REMOVAL OF STRONTIUM

Sodium titanate based SrTreat has proved to be highly effective in the removal of radioactive strontium from alkaline nuclear waste solutions. This exchanger is especially suited for the decontamination of alkaline concentrated sodium nitrate solutions that are characteristic of neutralized stored wastes from some nuclear fuel reprocessing plants. SrTreat removes strontium very efficiently also from both concentrated and dilute solutions. The optimum pH range of this material is 10 and above, and it is efficient even in the highest pH values found in waste solutions. High potassium, lithium, magnesium and ammonium concentrations do not interfere with the strontium uptake, whereas calcium ions have a strong or even limiting effect on it[9] (Figure 1). However, the interference by calcium is not regarded as a major problem because the optimal pH range of SrTreat is so high. At high pH values virtually all of the calcium is precipitated as calcium carbonate if the solution has been in contact with the atmosphere.

2.3. SELECTIVE REMOVAL OF ACTIVATED CORROSION PRODUCTS

Our recent focus has been on the selective removal of activated corrosion products, primarily cobalt and nickel. Cobalt has been of the most concern and thus the most studied activated corrosion product due to its big contribution to dose at NPPs. Recently nickel too has drawn a lot of attention because of its long half life with respect to low and intermediate level waste disposal after decommissioning NPPs, and because it has been very difficult to selectively remove from these wastes. Metal oxides have demonstrated good selectivity for transition metals and a large number of different oxides have been tested in our laboratory. Tin antimonates have shown good nickel and cobalt uptake properties and their selectivity is based on material structure.

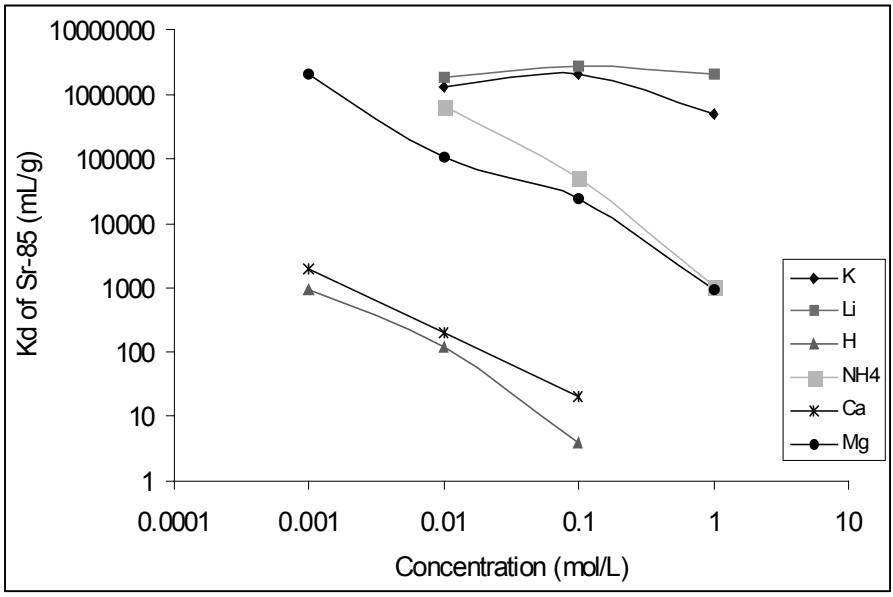

Figure 1. Distribution coefficient of ^{85}Sr for SrTreat in different salt solutions as a function of solution concentration. SrTreat was in the same ionic form as the solution cation.[9]

A good example of the relation of material structure to selectivity is the difference between the selectivity of cobalt and nickel from 0.1 M HNO_3 solution on pyrochlore structured tin antimonates (solid solutions that retain a pyrochlore structure of Sb_2O_5 with up to 35% Sn for Sb substitution). The differences in selectivity are most probably the result of different physical properties of the exchanging ions and steric hindrance of the exchangers. The hydrated ionic radii of cobalt and nickel are 2.95 and 3.02 Å, respectively.[10] The tunnel size of pyrochlore antimony pentoxide is 6 Å,

which generates an ion sieve effect which can be observed as a difference in metal uptake levels between the otherwise very similar metals. Progressive Sn for Sb substitution results in an increase in the lattice parameter (a) that increases the K_d values of cubic, pyrochlore-structured materials (Figure 2). Higher K_d values are associated with easier access of exchanging ions to the inner ion exchange sites (inside tunnels and cavities) of the materials. The K_d values rise sharply with the increase in lattice parameter from 10.34 Å to 10.39 Å.[11]

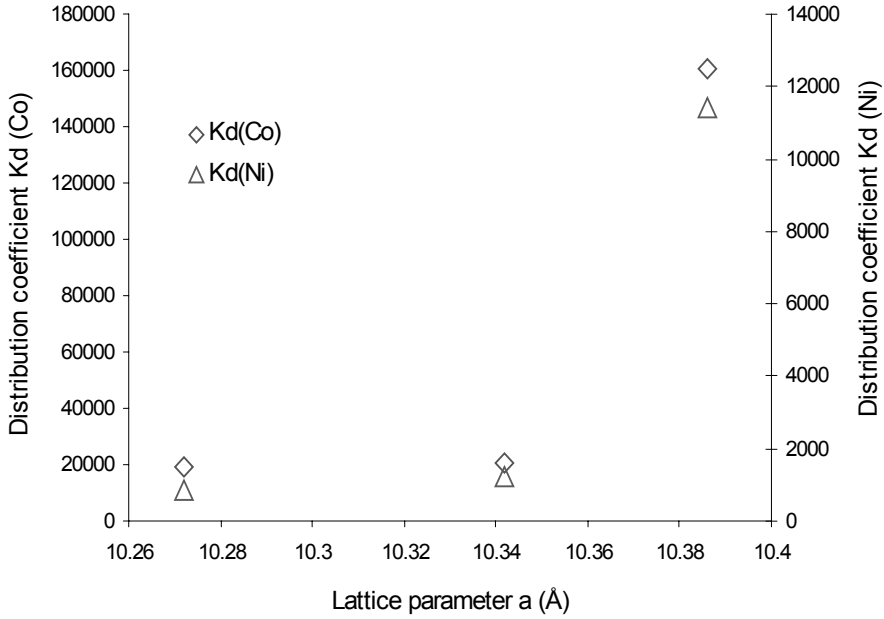

Figure 2. Distribution coefficients (mL/g) of ^{57}Co and ^{63}Ni in 0.1 M HNO_3 solution as a function of the lattice parameter of tin antimonates with pyrochlore structure.[11]

The combination of different types of ion exchange sites in one material can also have strong influence on selectivity due to kinetic reasons, particularly in dynamic column experiments. The presented K_d-values of tin antimonates (Figure 2) indicate substantially higher cobalt uptake than nickel uptake. In the column experiments, however, uptake of the two metals on tin antimonate is surprisingly similar. There are two types of ion exchange sites in pyrochlore materials: on the surface of the material and in tunnels and cavities inside the material. The latter are responsible for most of the ion exchange capacity of the materials.[12,13] The high uptake of cobalt in batch experiments may be associated with ion exchange inside the material, whereas the uptake of nickel takes place on outer surfaces of the material. The kinetic constraints of dynamic column experiments will favor

metal uptake on the surfaces rather than inside the tunnels of the material, the surfaces being more favorable for nickel uptake than cobalt uptake. This preference is evident in the column experiment done with the tin antimonate exchanger where the two metals were in the same solution (0.01 M $Ca(NO_3)_2$, used to simulate neutral bond water) and the pH of the eluent was changed (Figure 3). This experiment also demonstrated the change in the selectivity sequence with pH. In addition, the marked differences in the BT-levels of the metals suggest that nickel and cobalt might themselves be separated through variation in acid concentration of the eluent. This finding agrees with the reported enthalpies of the ion exchange reaction on crystalline antimony pentoxide ($\Delta H°$ of $M^{2+} \rightarrow H^+$ is 9.0, 79.5 and 159.1 kJ eq^{-1} for Ca, Ni and Co, respectively).[14]

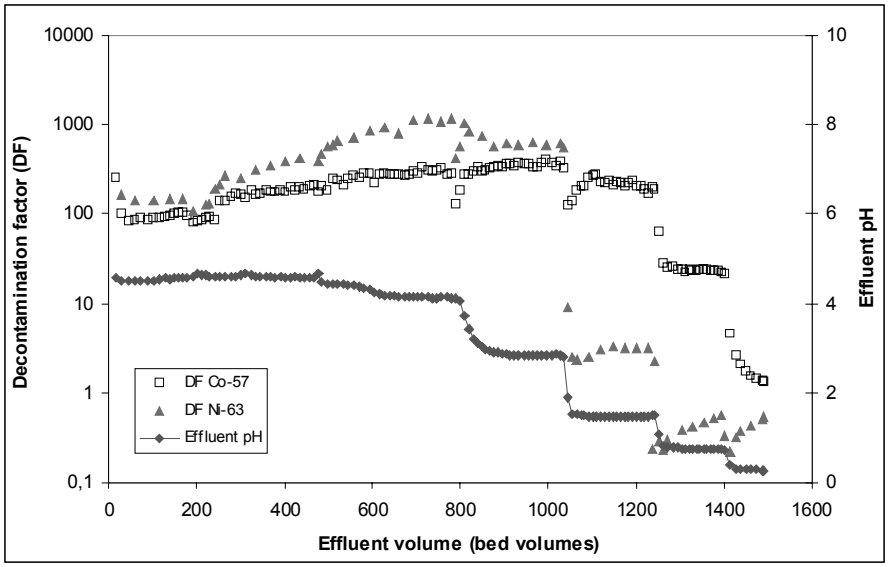

Figure 3. Decontamination curves of ^{57}Co (□) and ^{63}Ni (▲) for tin antimonate in 0.01 M $Ca(NO_3)_2$ solution.[11]

The third ion exchange material in the Treat-family is Co-Treat®. This titanium oxide based material was originally developed for removal of ionic cobalt but it was noticed that several other corrosion products could be removed at the same time. Test results indicate that decontamination factors from 10 to 1000 can be achieved with CoTreat® for different activated corrosion products. Also combining different Treat-materials results in excellent decontamination (Figure 4).

3. Conclusions

Selective inorganic ion exchange materials perform optimally in separation of radioactive nuclides from waste solutions. They are not only superior in selectivity but their physical characters, such as resistance to ionizing radiation and thermal stability is well suited for radioactive waste management and for waste minimization in particular.

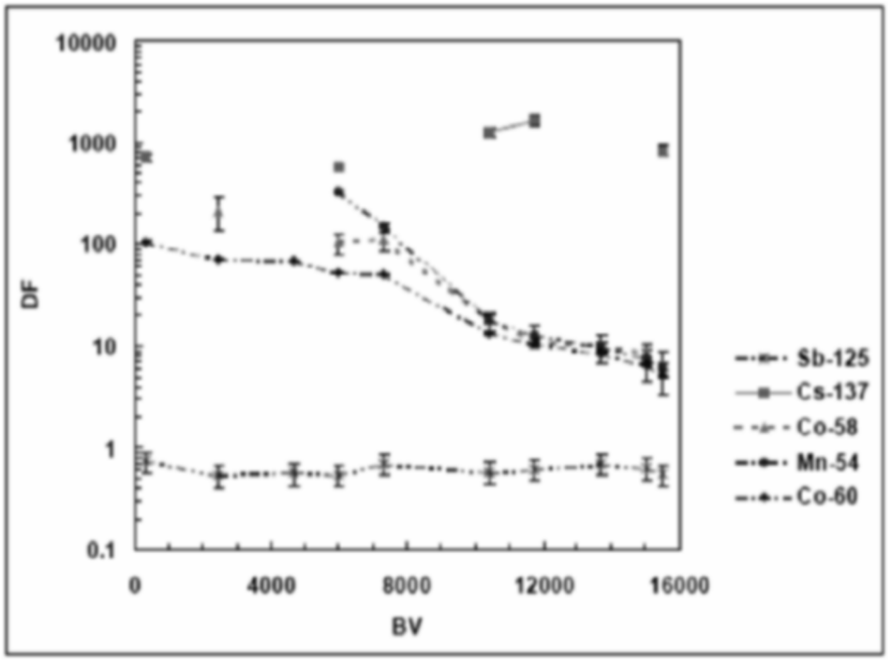

Figure 4. Column DF for different radionuclides as a function of bed volumes processed (BV) for Harris NPP Floor Drain Water. Water was prefiltered (0.45 μm) before column run. One CoTreat column and one CsTreat column in series (each BV = 0.5 ml). Flow rate 12-13 mL/h (24-26 BV/h).[15]

There are two main advantages which can be attained by using highly selective ion exchangers. First, environmental releases can be reduced considerably since the exchanger is able to remove radionuclides from effluents that contain excesses of common alkali and alkaline earth metal ions, which do not practically interfere with the ion exchange. The second advantage of the high selectivity, gained through high processing capacities, is the reduction of final waste volumes. This will result in large reductions in waste disposal costs and usually also in the over all waste treatment costs.

Future developments in selective inorganic ion exchangers will extend to selective anion exchange. Early results on selective separation of

radioactive $^{124,125}Sb$ and ^{99}Tc have been most encouraging.[16] These radionuclides are usually present in solutions as oxy-anions, such as TcO_4^-, and the strategy in their selective separation has been the reduction in oxidation state of the metal resulting in cationic or neutral species which are fixed on the solid material by adsorption or cation exchange.

REFERENCES

1. M. Streat, and D.L. Jacobi, in: *Ion Exchange Technology*, edited by A.K. Sengupta (Technomic Publishing Co, Lancaster, 1995) pp. 193-224.
2. E. Tusa, A. Paavola, R. Harjula, and J. Lehto, *Nuclear Technology* 107, 279-284 (1994).
3. R. Harjula, J. Lehto, E. Tusa, and A. Paavola, *Nuclear Technology* 107, 272-278 (1994).
4. L.H. Baestlé, D. Van Deyck, and D. Huys, *J. Inorg. Nucl. Chem*. 27, 683-695 (1965).
5. E. Tusa, A. Paavola, R. Harjula, and J. Lehto, in: *Proceedings of the 8th International Conference on Waste Management and Environmental Remediation*, Bruges, Belgium, Sept. 30 – Oct. 4, 2001.
6. R. Harjula, J. Lehto, L. Saarinen, A. Paajanen, and E. Tusa, in: *Proceedings of the Waste Management '96 Symposium,* Tucson, Arizona, USA, February 25-29, 1996.
7. D.M. Poojary, R.A. Cahill, and A. Clearfield, *Chem. Mater*. 6, 2364-2368 (1994).
8. J.F. Walker Jr., P.A. Taylor, and D.D. Lee, *Sep. Sci. Technol*. 34 (6&7), 1167-1181 (1999).
9. J. Lehto, L. Brodkin, and R. Harjula, *Nuclear Technology* 127, 81-87 (1999).
10. Y.J. Marcus, *Chem. Soc., Faraday Trans*. 83, 2985-2992 (1987).
11. R. Koivula, R. Harjula, and J. Lehto, *Sep. Sci. Technol.* 38(15), 3795-3808 (2003).
12. V. Veselý, and V. Pekárek, *Talanta* 19, 219-262 (1972).
13. A. Clearfield, *Solv. Extr. Ion Exch*. 18(4), 655-678 (2000).
14. M. Abe, in: *Inorganic Ion Exchange Materials*, edited by A. Clearfield (CRC Press, Boca Raton, FL, 1982) pp. 197-242.
15. R. Harjula, J. Lehto, A. Paajanen, L. Brodkin, and E. Tusa, in: *Proceedings of the Waste Management '99 Symposium*, Tucson, Arizona, USA, February 28 - March 4, 1999.
16. R. Harjula, H. Myllymaa, and R. Koivula, in: *Proceedings of the Waste Management '05 Symposium*, Tucson, Arizona, USA, February 27 - March 3, 2005.

EXPERIMENTAL APPROACH TO THE SYNTHESIS OF HYBRID ADSORBENTS ON THE BASIS OF POLYSILOXANE XEROGELS FUNCTIONALIZED WITH CALIX[4]ARENES AND THEIR DERIVATIVES

OLGA V. KUCHMA AND YURIY L. ZUB*
Institute of Surface Chemistry, National Academy of Sciences of Ukraine, 17 General Naumov Str., Kyiv 03164 Ukraine

Abstract. Polysiloxane xerogels with immobilized calix[4]arenes and covalently bonded calix[4]arene-crown-6 were obtained by sol-gel method. The presence of functional groups introduced in the structure of xerogels was confirmed by FTIR spectroscopy. The synthesized materials are characterized by the developed specific surface area (120-643 m^2/g) and are able to extract cesium ions in acid medium. It was determined that the quantity of functional groups that take part in this process is 40% maximum.

Keywords: Calixarenes; Calixcrowns; Immobilization; Sol-gel method; Solid-phase extraction; Cesium

1. Introduction

The wide application of chemical technologies that use various radioactive elements leads to an accumulation of solid and liquid radioactive wastes representing a serious danger for the environment.[1,2] The solid-phase extraction of radioactive isotopes with the following regeneration of the sorbent is one of the approaches to decrease the liquid radioactive waste quantity.[3,4] From this viewpoint a creation of sorbents based on silicon

* To whom correspondence should be addressed. Dr. Yu.L.Zub, Head of Hybrid Materials Laboratory, Institute of Surface Chemistry, NAS of Ukraine, 17 General Naumov Str., Kyiv 03164 Ukraine; e-mail: zub@public.icyb.kiev.ua

J.M. Loureiro and M.T. Kartel (eds.), Combined and Hybrid Adsorbents, 49–54.

dioxide functionalized with macrocyclic compounds of calixarene type and their crown-ether derivatives (calixcrowns) is very promising. The advantages of such systems are the presence of a pre-given cation-binding capability of the anchored ligands causing high selectivity, a reduction to minimum of their loss during extraction, and radiation stability.[5,6] In the present study it is considered the use of one-step sol-gel method for immobilization of 25,26,27,28-tetrahydroxycalix[4]arene (THC) in the polysiloxane matrix and, for comparison, the same method for covalently functionalization of xerogels with 26,28-dipropoxy-5,17-bis[3-(triethoxysilyl)propyl]-calix[4]arene-crown-6 (DBCC) being derivative of THC. Moreover, structure-adsorption characteristics of the obtained xerogels and their sorption properties toward cesium cations are investigated.

2. Experimental

The content of functional groups was set by the concentration of macrocycles in the initial solution. Xerogels with content of THC functional groups about 0.1 (sample **I**), 0.5 (sample **II**) and 1.0 mmol/g (sample **III**) were obtained. In case of xerogels functionalized with DBCC samples with concentrations of calixcrowns around 0.1 (sample **IV**) and 0.5 (**V**) mmol/g were synthesized. It should be noted that in all cases such strong nucleophile as fluoride-ion (F/Si =1/100 (mol.)) which is easily washed out from xerogels was used as a catalyst.

*Typical method of synthesis (sample **I**).* To a solution of 0.042 g (0.1 mmol) THC in DMF/THF (21:7 cm^3) at stirring a solution of NH_4F (0.0063 g in 1.22 cm^3 H_2O) was added. After stirring for 5 min, 3.7 cm^3 (0.017 mol) TEOS was dropped to the mixture. Gelation time was 25 min. After 6 days the gel was powdered and dried in vacuum at 20 ºC during 1 hour, at 100 ºC for 2 hours and at 120 ºC during 4 hours. Then the xerogel was washed out with 0.5 L of water and dried in vacuum again: 1 hour at 20 ºC and 5 hours at 100 ºC. The yield of a light yellow powder was 1.066 g.

The sorption ability of the synthesized samples toward cesium cations in 1M HNO_3 in the static conditions and at room temperature was investigated. The volume of initial solution was 15 cm^3. The mass of sorbent was 0.1 g, time of sorption process was 1 hour and 24 hours. The molar ratio of functional groups:cesium ion was 1:2. After attaining sorption equilibrium the solid phase was separated by filtration and washed out with water. The residual quantity of cesium in the filtrate was determined by atomic adsorption spectrophotometry.

3. Results and Discussions

The reaction of hydrolytic polycondensation of tetraalkoxysilanes in the presence of organic compounds allows their easy incorporation into the polysiloxane matrixes.[7] One of the restrictions of this approach is the solubility degree of the organic compound in solvents promoting the above mentioned reaction. It is clear that it is practically impossible to reach a wide range of organic components content in polysiloxane matrixes for components of low solubility. Moreover an addition of tetraalkoxysilanes and an appearance in reacting mixture of the products of their hydrolysis and polycondensation (alcohols and water) may decrease the solubility of the organic component. However the solubility of THC in the mixture of such non-aqueous solvents as THF and DMFA was sufficient for obtaining polysiloxane xerogels with THC content in the range of 0.1 – 1.0 mmol/g (samples **I** – **III**). DBCC is characterized by higher solubility owing to the presence of organic radicals in the low and upper positions of the THC framework. Therefore only DMF (samples **IV** and **V**) was used as solvent. However in this case it was impossible to obtain a sample with content of DBCC > 0.5 mmol/g. Comparing the gelation and ageing time with the concentration of calixarenes in the initial solution denotes increasing this time with increasing concentration of macrocycles. Thus, in case of sample **III** the ageing time was 50 days, while for sample **I** this time was only 6 days. Probably, an increase of geometrical sizes of immobilized molecules with simultaneous increasing of its concentration in initial solution made impossible to obtain samples with content of DBCC > 0.5 mmol/g. Elemental analysis shows that the content of THC and DBCC functional groups in synthesized materials are higher than estimated by their concentration in the initial solutions. For example the content of functional groups in sample **V** is 1.5 mmol/g. It should be noted that this sample has about three DMF molecules on a single functional group.

Synthesized xerogels were identified by IR spectroscopy (data not shown). The most intensive absorption band with the shoulder in high-frequency is identified in the region 1086-1073 cm^{-1} in IR spectra of all samples. Its appearance associates with the presence of the three-dimensional frame of ≡Si-O-Si≡ bonds in the xerogels.[8] The three low-intensity absorption bands in the region of 2880-2977 cm^{-1} indicate the presence of calixarenes functional groups. These bands are typical for stretching vibrations $\nu_{s,as}$(CH) of CH_2-groups that bonding aromatic rings. Thus intensity of these bands is increased with the increase of relative quantity of the incorporated macrocyclic molecules. In the region of 1660-1665 cm^{-1} in the spectra of samples **I-III** the medium intensive absorption band is observed that is typical for vibrations ν(C=O) of DMF that was

used as a solvent in the synthesis. In the IR spectra of the xerogels **IV** and **V**, unlike the spectra of the samples **I-III**, the intensive absorption bands in the region of 808 and 460 cm^{-1} that are typical for stretching vibrations ν_s(COC) and deformation δ(COC) vibrations of crown-6-ether moiety of DBCC are observed. All obtained xerogels include water. The wide intensive absorption band characteristic for ν(OH) vibrations of water molecules that take part in hydrogen bond is determined higher 3000 cm^{-1}.

Figure 1 shows nitrogen adsorption-desorption isotherms of all synthesized xerogels. The isotherms of the samples **I** and **III** belong to the Langmuir type (type I according to IUPAC[9]). The isotherm of xerogel **II** belongs to the Langmuir type also, though it has the legibly defined hysteresis loop in the P/P_0 0.4-0.8. The isotherm of sample **IV** belongs to type II, while the isotherm of **V** has S-like character and belongs to type IV. Well-defined hysteresis loop has rather step-like character in case of sample **V** and can testify not only about the presence of mesopores in this sample, but also about its biporosity.

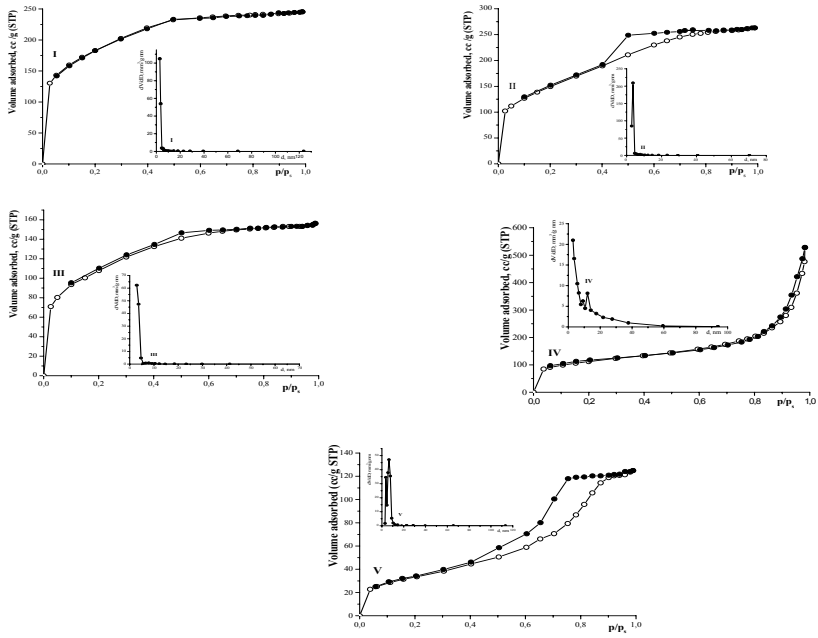

Figure 1. Nitrogen adsorption-desorption isotherms of **I-V** and their PSD.

These conclusions agree with structure-adsorption characteristics of the obtained xerogels (Table 1). The analysis of data presented in Table 1 shows that an increase of content of immobilized macrocycles in the xerogels determines gradual decrease of the value of specific surface area. It may be explained by increasing primary particles sizes of the xerogels. Also a decrease of the sorption volume of pores is observed. It is possible to

assume that it is caused by increasing the functional groups quantity in the surface layer. However, the average pore size increases. Thus, the pore sizes of samples **I** and **IV** are typical of materials at the limit between micro- and mesoporosity, and samples **II** and **V** are typical mesoporous xerogels.

The pore size distribtion curves (Figure 1) specify the existence of biporous structure in case of the samples **IV** and **V**. In conclusion, comparing structural-adsorption characteristics of the samples **I** and **IV, II** and **V** (Table 1), it is possible to conclude that at the same content of macrocycles in the polysiloxane matrix the size of functional groups essentially influences on the structure of the xerogels.

Sorption of Cs^+ from 1M HNO_3 was investigated for all xerogels. The results of sorption investigations are listed in Table 1. From data of this table it is obvious that sorption equilibrium was attained after 1 hour.

TABLE 1. Structure-adsorption characteristics and sorption data of cesium ions from 1M HNO_3 of the synthesized xerogels

Sample	S_{sp}, m^2/g	V_s, cm^3/g	d, nm	Maximum quantity of groups taking part in sorption, %		Degree of Cs^+ sorption, Q, %
				1 hour	24 hours	
I	643	0.39	3.0	11	10	5
II	531	0.41	3.7	18	20	9
III	381	0.24	3.7	41	40	21
IV	383	0.80	(2.9) 12.0	9	10	7
V	120	0.20	3.6; 6.5	33	33	18

With increasing the incorporated molecules the quantity of fixed cesium (Q, %) grows (the idle experiment shows that the xerogel without immobilized macrocycles does not extract cesium cations at similar conditions). However no more than 40% of functional groups take part in the cesium sorption process. Thus an appreciable part of the incorporated macrocycles is inaccessible to cesium cations. The fact that xerogels with covalently bound macrocycles extract cesium ions better than the xerogels with immobilized macroligands deserves attention (Table 1).

4. Conclusions

Using the reaction of hydrolytic polycondensation of TEOS in the presence of THC and DBCC it is possible to obtain porous polysiloxane xerogels with immobilized or covalently bound macrocycles. It was determined that

with increasing concentration of the macrocyclic ligands in initial solution and increasing their geometric sizes the gelation and ageing time increases significantly. Consequently, the attempt to achieve considerable concentrations of the incorporated DBCC (>1 mmol/g) obtaining gel in such systems is problematic. The synthesized xerogels are characterized by a developed porous surface (120-643 m^2/g). It was shown that the increasing content of the macrocycles in the xerogels causes considerable decreases both in the value of specific surface area and of the sorption volume of pores and also increases the pore size; in case of DBCC it causes formation of biporous structures. Sorption properties of the synthesized xerogels toward cesium cations were investigated. It was determined that the sorption equilibrium is attained after 1 hour. At the increasing content of the immobilized macrocyclic ligands in the xerogels the cesium ions sorption degree ascends. However, the quantity of functional groups that take part in this process is 40% maximum. It was determined that sorption properties of the synthesized xerogels depend on content of functional groups in the matrix; however, there is no influence of structure-adsorption characteristics of the xerogels on its sorption capability toward cesium ions.

ACKNOWLEDGEMENTS

The authors thank the NATO programme «Science for Peace» (Grant 978006) for financial support of this work.

REFERENCES

1. S.V. Nesterov, Crown ethers in radiochemistry. Achivements and prospects, *Uspekhi Khimii* 69 (9), 840-855 (2000) (in Russ.).
2. A. Casnati, S. Barboso, H. Rouquette, New Efficient Calixarene Amide Ionophores for the Selective Removal of Strontium Ion from Nuclear Waste: Synthesis, Complexation, and Extraction Properties, *J. Am. Chem. Soc.* 123, 12182-12190 (2001).
3. J. Kim, S. Kim, J. Ko, Selective transport of cesium ion in polymeric CTA membrane containing calixcrown ethers, *Talanta* 52, 1143–1148 (2000).
4. T.L. Yost, B.C. Fagan, Crown ethers-doped sol-gel materials for strontium(II) separation, *Anal. Chem.* 72, 5516-5519 (2000).
5. V.V. Makhlyarchuk, S.V. Zatonskii, Radiation chemistry of crown compounds, *Uspekhi Khimii* 61(5), 883-909 (1992) (in Russ.).
6. J.D. Lamb, M.D. Christenson, Macrocyclic ligands in separations, *J. Incl. Phenom. Mol. Rec. Chem.* 32, 107-110 (1998).
7. *Handbook of Sol-Gel Science and Technology: Processing, Characterization, and Applications*, edited by S. Sakka (Kluwer, Dordrecht, 1-3, 2005).
8. I.P. Finn, I.B. Slinyakova, Structure and thermodestruction of polyorganosiloxane xerogels according to IR spectroscopy data, *Colloid J.* 37(4), 723-729 (1975) (in Russ.).
9. K.S.W. Sing, D.H. Everett, R.A.W. Haul, J. Rouquerol, T. Siemieniewska, Reporting physisorption data for gas/solid systems with special reference to the determination of surface area and porosity, *Pure Appl. Chem.* 57, 603-619 (1985).

HYBRID POLYMER-SILICA ADSORBENT FOR CHROMATOGRAPHY

OLIMJON N. RUZIMURADOV*
Scientific-Technological Complex "Science and Progress", Tashkent State Technical University 7a, Mirza Golib str., Tashkent, 700174, Uzbekistan

Abstract. This report describes the synthesis and some properties of hybrid Poly (acrylonitrile) – silica nanocomposites having potential as chromatography sorbents. The focus is on the fact that the properties of such nanostructures can depend not only on the chemical nature of their components, but also on the synergy of these components. The sol–gel approach involved the hydrolysis and condensation of tetraethoxysilane, with smaller amounts of acrylonitrile polymerized in such a way as to generate polymer dispersed in the continuous silica phase. The resulting polymer–modified silica materials were characterized by infrared spectroscopy, scanning electron microscopy and chromatographic analysis.

Keywords: Sol–gel; acrylonitrile; tetraethoxysilane; nanohybrid material; sorbent; morphology

1. Introduction

The sol–gel process has been a remarkably successful route for incorporating ceramic–like phases into hybrid organic–inorganic nanocomposites.[1–14] One of the methods consists of incorporation of monomers at the initial stage of a sol–gel reaction and polymerizing the monomers simultaneously with the formation of silica gels (hydrolysis and condensation of a tetraalkoxysilane).[1–3] It is frequently possible to obtain multi–phase materials (polymer modified ceramics or ceramic modified

* To whom correspondence should be addressed. Olimjon N. Ruzimuradov, Scientific-Technological Complex "Science and Progress", Tashkent State Technical University 7a, Mirza Golib str., Tashkent, 700174, Uzbekistan; e-mail: Ruzimuradov@rambler.ru

J.M. Loureiro and M.T. Kartel (eds.), Combined and Hybrid Adsorbents, 55–62.

polymers) with dimensions of the phases in the nanometer range, with correspondingly novel properties.[7]

To synthesize homogeneous polymer hybrids, organic polymers with functional groups that have specific interaction with silica gel are introduced into the sol–gel reaction solution.[4–6] The example chosen here was poly(acrylonitrile) (PAN), since it contains cyano functional groups that can form hydrogen bonds with silanol groups on the ceramic phase.[15-17] Also, PAN may be modified, with 3-(trimethoxysilyl)propyl methacrylate for example, so that it can be covalently bonded to the silicate network in the resulting hybrid material.[18] These types of bonding can be important with regard to both the nature of the nanocomposite produced and its various other properties. The ultimate goal of the material being prepared here is its possible use as a novel sorbent in chromatographic separations.[10,15]

In this paper, we report the synthesis of PAN/silica hybrid composites using *in situ* radical polymerization of the acrylonitrile monomer during the simultaneous hydrolytic polycondensation of a starting material well-known in sol–gel technology, tetraethoxysilane (TEOS) [$Si(OC_2H_5)_4$]. The structure of the hybrids was determined using Fourier infrared spectroscopy (FTIR). Elemental analysis was carried out on an EDS analyzer. Morphology of the composites was studied using scanning electron microscopy (SEM). A chromatographic property of the materials was evaluated with a liquid chromographic equipment.

2. Experimental

2.1. STARTING MATERIALS

Acrylonitrile (Aldrich) was washed with 5 wt % sodium hydroxide solution to remove the inhibitor and washed with distilled water to remove the basic impurities, and then dried over calcium chloride and distilled under reduced pressure. The middle fraction of the distillate was used. TEOS (Gelest) was used without further purification. Potassium persulfate ($K_2S_2O_8$) and Sodium bisulfite ($NaHSO_4$) were obtained from Baker Chemical Co. and were recrystallized by ethanol. All other reagents were used as received.

2.2. SYNTHESIS

The silica–like network was generated from the TEOS in the presence of ethanol as a co–solvent with the water required for the sol–gel reaction. Silica gel prepared according to the method in Kabulov et al.[19] The desired polymer–silica hybrid material was prepared as follows: 11 g of TEOS and

11 g of acrylonitrile were loaded into a 250 mL three–neck flask. During mixing, 1 mL of ammonia, 6 mL of ethanol, and 150 mL of distilled water were added. The solution was then heated to 40°C, under a stream of nitrogen gas. After 10 min, a solution of 0.15 g of the free–radical generator, $K_2S_2O_8$, in 10 mL of water was gradually added from a dropping-funnel. After one minute, a solution of 0.075 g of $NaHSO_4$ in 10 mL of water was introduced. The reaction was continued for about 3 hrs, after which the resulting suspension was filtered, washed with water (in a centrifuge), and then dried under vacuum at 60 °C to constant weight.

2.3. METHODS OF CHARACTERIZATION

The Fourier transform infra red spectra of samples were recorded on Perkin Elmer IR (Spectrum One) System 2000 equipment, in the 4000–400 cm^{-1} range. Measurements were made in solid phase using KBr pellets. Elemental analysis was carried out on an Oxford EDS analyser. Morphology of the samples was studied with a scanning electron microscope SEM Hitachi S–4000 apparatus.

The samples were analyzed by HPLC on a microcolumn liquid Milikhrom 1A chromatograph (Russia) equipped with a variable-wavelength UV detector. Column was packed with a specially designed instrument for packing HPLC columns at high pressures. To feed the solvent into the column, we used a piston pump from a Varian liquid chromatograph, which provided a pressure up to 500 atm. Before column packing the sorbent was treated with ultrasound and subjected to sedimentation purification from submicron particles. Columns 60x2 mm in size were packed with Polyacrylonitrile-silica sorbent under optimal conditions (p=150 atm, V=180 mL/h, t=15-20 min).

The column selectivity α was determined from the ratio of the normalized retention times for two peaks:[16]

$$\alpha=(t_{R2}-t_{st}) / (t_{R1}- t_{st}),$$

where t_R is the retention time for the compound under study and t_{st} is the retention time of the standard compound.

The values of relative Gibbs free energy of adsorption were calculated from the expression:[17]

$$\Delta(\Delta G) = RT \ln(t_R/t_{st})$$

3. Results and Discussion

A schematic representation for preparing PAN–silica hybrid materials is summarized in Figure 1. IR spectroscopy has been one of the most utilized tools to study the structure of hybrid materials. FTIR spectra of PAN–silica composite and silica gel sample are shown in Figure 2.

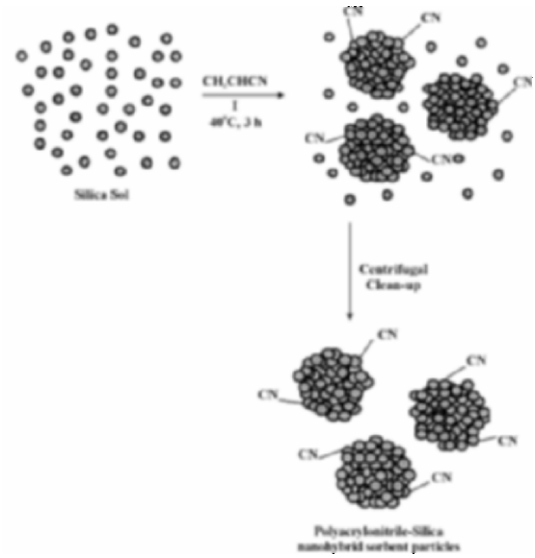

Figure 1. Preparation scheme of PAN-Silica nanohybrid sorbent.

IR spectra of silica gel show absorption bands of the stretching and bending modes of hydroxyl groups belonging to water molecules and silica gel and absorption bands belonging to hydrogen bonds between them. In the spectral range below 1200 cm^{-1}, the bands of stretching and bending vibrations of silica gel skeleton and adsorbed water molecule bending vibrations are located. The strong absorption band in the 950–1200 cm^{-1} range belongs to Si–O–Si asymmetric bond stretching vibration. The peaks at 796 and 460 cm^{-1} are related to a Si–O–Si symmetric bond stretching vibration and a Si–O–Si bending vibration, respectively. A spectral window free of the silica gel and water bands, which can be used to record the spectra of organic compounds, is located within 2000–3000 cm^{-1}.

The specific peak at 2243 cm^{-1}, falling into this window, demonstrates that the hybrid material did possess CN groups from the PAN. The formation of the silica structure in the hybrid material was confirmed by the appearance of the absorption peak at 820 cm^{-1} for Si–O–Si bonds.

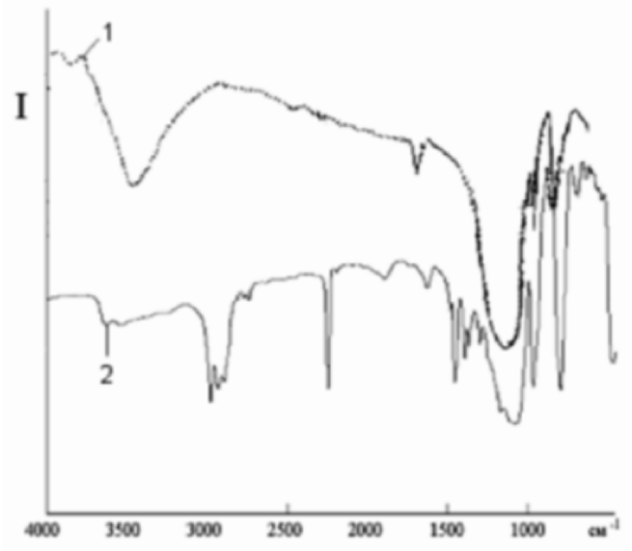

Figure 2. IR spectra of the silica gel (1) and nanohybrid PAN-Silica sorbent (2).

The presence of silanol groups on the silica networks is evidenced by the appearance of the hydroxyl peaks at 3000–3700 cm^{-1} and the Si–OH stretching peak at 950 cm^{-1}. The observation that the weak adsorption band at 3700 cm^{-1} (belonging to silanol groups free of hydrogen bonding) disappears after the process suggests that strong hydrogen bonds are formed between silica and PAN due to the orientation of the dipolar PAN units with their negative poles towards surface silanol groups:

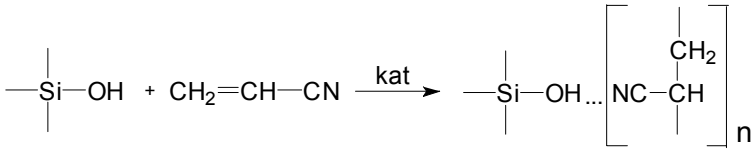

The IR data confirmed the structure of the hybrid composite resulting from the free–radical polymerization and the sol–gel reaction.

The elemental analysis results confirmed the presence of PAN within the silica network. The contents of the elements Si, C, and N were 41.98, 27.96, and 12.61 %, respectively.

The scanning electron microscopy (SEM) results used to obtain information on the morphology of the hybrid materials are shown in Figure 3. Every particle is a porous material with pore sizes up to 100 nm, consisting of spherical primary particles from 50 to 200 nm (Fig. 3b). This porosity should be very important with regard to applications such as chromatographic separations.[20]

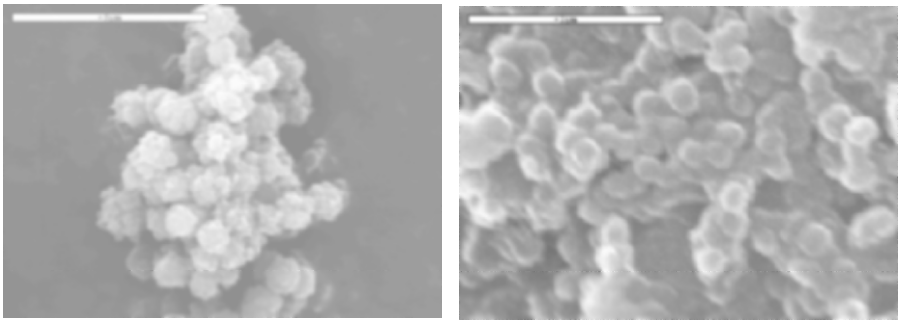

a b

Figure 3. SEM micrograph of the PAN-Silica nanohybrid sorbent with image magnification about 10000 (a) and 50000 (b).

The chromatographic properties of thin polymer layers deposited on the silica gel surface are determined by the properties of the silica gel surface and polymer macromolecules. The ability of PAN to participate in specific intermolecular interactions results from an enhanced electronic density on the nitrogen atom of the nitrile group. The synthesized sorbents were tested in HPLC separations of artificial mixtures of nitroaniline isomers. The retention time t_R, selectivity α with respect to *o* - nitroaniline, and relative Gibbs free energy $\Delta(\Delta G)$ of adsorption were determined at 290 nm from the ratio between the characteristics of the compound studied and *o* - nitroaniline under the same conditions (Table 1). The order of retention times for the isomers follows the trend: *o* - < *m* - < *p* – nitroanilines.

TABLE 1. HPLC data for the separation of nitroaniline isomers on the Poly (acrylonitrile)-silica sorbent (5-7 μm). The eluent was a 70/22/8 hexane/chloroform/isopropanol mixture eluted at a flow rate of 50 ml/min

Isomer	t_R, s	α	Δ (ΔG), J/mol
o	210	1,0	-
m	420	2,0	-1700
p	600	2,85	-2575

In this case the ortho-isomer retains weaker than other isomers because its intermolecular interaction with polar sorbent is relaxed by intramolecular interaction between substitutes disposed near in the nitroaniline molecule ($-NH_2 \ldots NO_2$). High selectivity of separation is observed for the nitroaniline isomers differing by the space constitution and the distribution of the electronic density in adsorbate molecule. The separation occurs because of differences in specific intermolecular interaction between the polar groups of sorbent. The selectivity is increased from 1.0 to 2.85. The increase of the selectivity of the sorbent leads to

weakening of adsorbate adsorption because of unspecific intermolecular interactions of adsorbate molecules and eluent with sorbent which are not very different. It is possibly determined by change of the free energy from -1700 to -2575 J/mol owing to specific intermolecular interaction of benzene ring with polar groups of the modified sorbent surface.

4. Conclusions

The results of this study demonstrate the successful synthesis of poly(acrylonitrile)–silica nanocomposites having improved thermal stability and a type of porous structure that could be extremely useful in the area of chromatographic separations. It was found that the hydrogen bonding interaction and/or physical entrapment of monomers in the silica matrix are strong enough to afford homogeneous polymer hybrid materials. Vinyl monomer is initially introduced to sol–gel reaction mixtures and then subjected to polymerization by free–radical initiators.

ACKNOWLEDGMENTS

It is a pleasure to acknowledge the financial support provided by the U. S. National Science Foundation through the COBASE Grant Program. The author is also grateful to Prof. J.E. Mark for sincerely helping and supporting the organization of my research visit to his Research Group.

REFERENCES

1. G. Philipp, and H. Schmidt, New materials for contact lenses prepared from Si- and Ti-alkoxides by the sol-gel process., *J. Non–Cryst. Solids* 63, 283- 287 (1984).
2. B.M. Novak, 'Inverse' Organic-Inorganic Composite Materials 2. Free Radical Routes into Nonshrinking Sol-Gel Composites, *Macromolecules* 24, 5481- 5483 (1991).
3. B.M. Novak, Hybrid Nanocomposite Materials-Between Inorganic Glasses and Organic Polymers, *Adv. Mater.* 5, 422-427 (1993).
4. H. Schmidt, Sol-gel derived nanoparticles as inorganic phases polymer-type matrices. *Macromol. Symp.* 159, 43-55 (2000).
5. Y. Wei, J.-M. Yeh, D. Jin, X. Jia, J. Wang, G.-W. Jang, C. Chen, and R.W. Gumbs, Composites of Electronically Conductive Polyaniline with Polyacrylate-Silica Sol-Gel Materials, *Chem. Mater.* 7, 969-974 (1995).
6. P. Judenstein, and C. Sanchez, Hybrid organic-inorganic materials: a land of multidisciplinarity. *J. Mater. Chem.* 6, 511-525 (1996).
7. J.E. Mark, Ceramic-Reinforced Polymers and Polymer-Modified Ceramics, *Polym. Eng. Sci.* 36, 2905-2916 (1996).
8. S. Yano, M. Kodomari, and T. Furukawa, Preparation and properties of Poly(vinyl acetate) /silica-gel hybrids obtained by sol-gel process, *Key Eng. Mater.* 150, 219-223(1998).
9. R. Tamaki, K. Naka, and Y. Chujo, Synthesis of poly(N,N-dimethylacrylamide)/silica gel polymer hybrid by in situ polymerization method, *Polym. J.* 30, 60- 64 (1998).

10. H. Ihara, Sh. Okazaki, K. Ohmori, Sh. Uemura, Ch. Hirayama, and Sh. Nagaoka, Polymer-silica hybrids: evaluation of grafted Poly(acrylonitrile) as organic phase for High Performance Liquid Chromatography, *Anal. Sci.* 14, 349-354 (1998).
11. Y.G. Hsu, and F.J. Lin, Organic-inorganic composite materials from acrylonitrile-butadiene-styrene copolymers and silica through an in situ sol-gel process, *J. Appl. Polym. Sci.* 75, 275-283 (2000).
12. R.M. Laine, C. Sanchez, E. Giannelis, and C.J. Brinker, Eds., *Organic/Inorganic Hybrid Materials–2000*, Vol. 628 (Materials Research Society, Warrendale, PA, 2001).
13. R.J. Hjelm, A.I. Nakatani, M. Gerspacher, and R. Krishnamoorti, Eds., *Filled and Nanocomposite Polymer Materials*, Vol. 661 (Materials Research Society, Warrendale, PA, 2001).
14. C. Sanchez, R.M. Laine, S. Yang, and C.J. Brinker, Eds., *Organic/Inorganic Hybrid Materials–2002*, Vol. 726 (Materials Research Society, Warrendale, PA, 2002).
15. B.D. Kabulov, O.N. Ruzimuradov, G. Bekmirzaeva, D.T. Satibaldieva, S.V. Zalyalieva, and S.Sh. Rashidova, Kinetic and structural features of the modification of silica sorbents for HPLC with Polyacrylonitrile, *Russ. J. Phys. Chem.* 76, 1512-1514 (2002).
16. E.L. Styskin, L.B. Itsikson, and E.V. Braude, *Practical High-Performance Liquid Chromatography* (Khimiya, Moscow, 1986).
17. A.V. Kiselev, *Mejmolekulyarnie Vzaimodeystviya v Adsorbtsii i Xromatografii* (Visshaya Shkola, Moscow, 1986), p. 284.
18. Y. Wei, D. Yang, and L. Tang, Synthesis of new Polyacrylonitrile-silica hybrid sol-gel materials and their thermal properties, *Makromol. Chem. Rapid Commun.* 14, 273-278 (1993).
19. B.D. Kabulov, T.A. Grabovskaya, and S.V. Zalyalieva, Microspherical silica for HPLC, *Russ. J. Phys. Chem.* 10, 2070-2072 (1993).
20. O.N. Ruzimuradov, B.D. Kabulov, V.Pak, S.Sh. Rashidova, and J.E. Mark, Sol-gel method for preparation of nanohybrid Polyacrylonitrile-silica sorption material, Proceedings of Intern. Conf. "*Nanochemistry: new approaches to creation of polymeric systems with specific properties*" Tashkent, 2003, 62-63.

DESIGN AND CHARACTERIZATION OF NOVEL ZEOADSORPTION MEDIA DERIVED FROM SURFACE COATING WITH FUNCTIONAL HYDROCARBONS

EVA CHMIELEWSKÁ*
Faculty of Natural Sciences, Comenius University, Mlynská dolina, 842 15 Bratislava, Slovakia

WLODZIMIERZ TYLUS
Wroclaw University of Technology, Institut of Inorganic Technology, Wyb. Wyspiańskiego 27, 50-370 Wrocław, Poland

Abstract. The paper deals with fabrication of carbonized and hydrophobized clinoptilolite-rich tuff using organic carbon rich substances, which were pyrolytic combusted and covered the external zeolite surface. Hydrophobization of the zeolite external surface was accomplished by octadecylammonium surfactant. Both surface modified clinoptilolite-rich tuffs were tested and compared to each other in regard to organic (phenol) and inorganic (chromate, arsenate) pollutants removal from aqueous solutions and so far elaborated composites with surface adsorbed pollutant species were analyzed by X-ray photoelectron spectroscopy (XPS).

Keywords: clinoptilolite-rich tuff; hydrophobization; carbonization, chromate; arsenate oxyanions and phenol adsorption; XPS

1. Introduction

Surface and interface structure incl. composition are the primary factors controlling chemical, electronic or mechanical properties of materials in

* To whom correspondence should be addressed. Eva Chmielewska, Faculty of Natural Sciences, Comenius University, Mlynská dolina, 842 15 Bratislava, Slovakia; e-mail: chmielewska@fns.uniba.sk

J.M. Loureiro and M.T. Kartel (eds.), Combined and Hybrid Adsorbents, 63–70.

many technologically important applications. Potential applications of such a fabricated material with specific surface deposition in nanoelectronics and nanoinformatics for ultrahigh density of magnetic recording or in biological sensor production are another important field of interest.[1,2,3]

The objective of our study was to characterize the interfacial phenomena and the surface architecture of novel organic - inorganic clinoptilolite-rich tuff based adsorption materials prepared by means of hydrophobization and carbonization of the external zeolitic surface using the XPS spectral analytical techniques. Above surface modified polyoxide based organoinorganic adsorbents have been used for removal of chromate and arsenate from aqueous model solutions.

Hydrophobization of the clinoptilolite external surface was done with primary octadecylamine. Carbonization was accomplished with the waste vegetable substratum inside a high temperature pyrolytic combustion chamber installed at the laboratory.[4,5]

The adsorption isotherms of the systems chromate, arsenate, phenol vs. hydrophobized and carbonized zeolites are drawn to confirm and quantify the adsorption functionalities of the examined zeolite samples.

2. Experimental

2.1. MATERIALS

The natural clinoptilolite dominated zeolite crushed and grinded into the fraction of 0.4 - 1 mm (35-16 mesh) has been supplied for lab-experiments by ZEOCEM, Share Holding Company, mining at the East-Slovakian repository Nižný Hrabovec. The mineralogical and chemical compositions of the raw zeolite is published elsewhere.[5]

2.2. METHODS

The specific C-rich waste substratum carbonization inside a high temperature pilot combustion chamber installed at the laboratory used direct heating by exhaust gas flow in an oxygen free atmosphere. The process had a lot of similarities with biomass pyrolysis. During carbonization inside an oven at lower temperatures (~350 °C) the main process was cracking producing liquid hydrocarbons and tars, then at about 650 °C hydrogen was formed, while finally at about 700 °C carbon char was produced instead of ash. The heat from the process was recuperated.[4]

Hydrophobization of clinoptilolite with ODA-surfactant to enable chromate and arsenate removal was thoroughly described in a previous work.[3]

Equilibrium adsorption and isotherm measurements at the laboratory were done with aqueous model solutions of phenol, arsenate or chromate salts incl. surface modified (hydrophobized, carbonized) *vs.* natural clinoptilolite with the solid-to-liquid ratio 1g/100 ml, at T = 23 ± 0.1 °C. All experiments were run in triplicate, keeping the suspensions equilibrated up to 7 hrs.

2.3. ANALYTICAL PROCEDURE

Aqueous phenolic solutions were analyzed by means of Diode Array Spectrophotometer Hewlett Packard 8452A (USA) in UV spectral band at 286 nm against the calibration curve, measured in analogous conditions by distilled water pH-value.

Chromate and arsenate concentrations in aqueous solutions were analyzed by atomic absorption spectrometry (AAS) with flame atomization on a Perkin-Elmer apparatus, model 1100 (USA).

X-ray photoelectron spectral (XPS) measurements were carried out on the Specs Phoibos-100 hemispherical analyzer operating at constant analyzer energy mode. The measurements were performed at room temperature using 100 W (wide scans) and 250 W (narrow scans) of X-ray Mg anode. The base pressure in UHV chamber was below 2 x 10^{-10} mbar. The spectrometer energy scale was calibrated using Au $4f_{7/2}$ and Cu $2p_{3/2}$. Sample charging was compensated by an electron flood at 0.5 mA current and 0.1±0.01 eV energy. The detection angle was normal to the surface. The samples as a powder in the as received state were pressed into a molybdenum sample holder. The C1s peak of the contamination carbon, at 284.6 eV was taken as reference in calculating BEs and accounting effects. The spectra were collected and processed by SpecsLab software. Experimental peaks were decomposed into components (75% Gaussian, 25% Lorenzian) using a non linear, least squares fitting algorithm and a Shirley baseline.

3. Results and Discussion

The simplified principles of both anionic and non ionic species bounds onto surface of hydrophobized or carbonized clinoptilolite dominated zeolite were thoroughly discussed in previous works.[3,4]

Several laboratory bench-scale trials designed for adsorption-desorption characterization testified a higher efficiency of inorganic oxyanions

removal from aqueous solutions by ODA hydrophobized zeolite, where the anionic species remained irreversibly adsorbed, than by the carbonized zeolite (Figure 1).

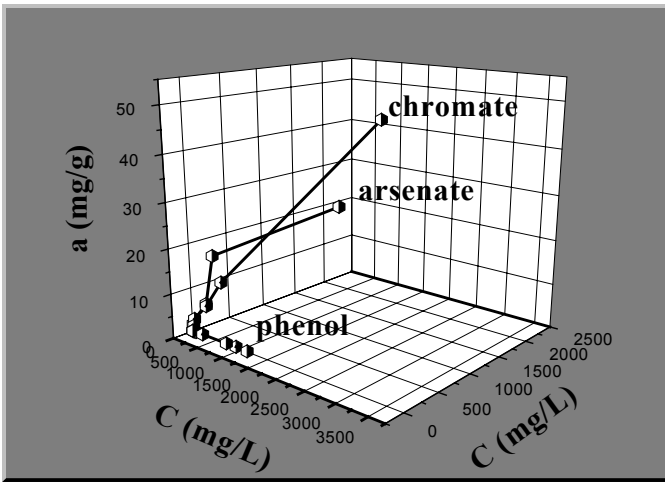

Figure 1. Phenol adsorption on carbonized and chromate, arsenate adsorption on ODA-hydrophobized clinoptilolite-rich tuff.

Nevertheless, a satisfying abatement of phenol concentration by means of the carbonized clinoptilolite-rich tuff in respect to the active charcoal (Slovak industrial product trademark HYS-N) has been achieved at laboratory scale, testing numerous aqueous model solutions in static and dynamic arrangements. Obviously, no adsorption of phenol was observed by means of an untreated clinoptilolite dominated zeolite.

Currently, surface composition and sorption complexes of above mentioned samples were studied on a very powerful XPS (alternatively ESCA - electron spectrometry for chemical analysis) technique. This surface analytical and thin film technique enables to investigate not only quantitative elemental composition of solids surfaces incl. surface Si/Al and bulk Si/Al ratios important in zeolite chemistry, but also various diffusion, oxidation and other processes and reactions on zeolite composites, concentration and distribution profiles of host species, microstructural irregularities, surface interfaces and bounding energies. Studies on zeolite surface phenomena and their surface microtopography by means of this ultra high vacuum technique became well established in the recent years.[6,7]

Binding energies (BEs) represented in Figures 2, 3 and 4, are element specific, containing chemical information as well, due to the dependence of the core electrons energy levels on the element's chemical state. Usually,

the BE increases with the increasing oxidation state or with the elevated electronegativity of the ligands.

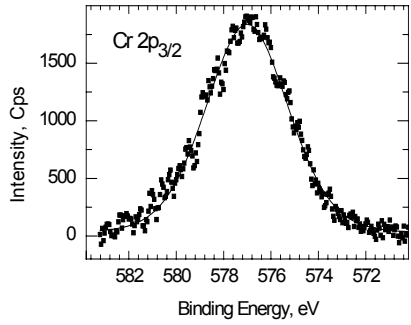

Figure 2. XPS Cr $2p_{3/2}$ spectra of ODA-clinoptilolite adsorbed with chromate.

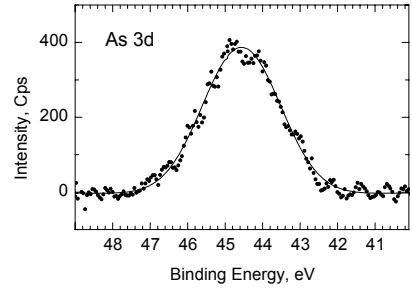

Figure 3. XPS As 2p spectra of ODA-clinoptilolite adsorbed with arsenate.

In coincidence with this rule, the highest BEs were observed for chromium and oxygen elements. Among the studied metals, a higher binding energy component was assigned to tetrahedrally coordinated Cr(VI) than to the similarly coordinated As(V) on the ODA-clinoptilolite.

Some traces of arsenic in the oxidation state As(III) and some of Cr(III) were detected too, consequently to the vacuum reduction process, affection by surrounded CO or X-ray irradiation in the XPS system as well.

Due to the recorded XPS N1s spectra deconvoluted by all samples regularly in about 2:3 concentration ratios of the ODA-nitrogen bounds, this analysis enabled to identify two forms of bounds, i.e. probably the lower energy interacted octadecylammonium *vs.* alumosilicate skeleton on the one side and on the another the higher energy interacted octadecylammonium *vs.* metal oxyanions, attached on the outer layer (Figure 4). According to this figure XPS N1s (a) spectrum for the pure ODA chemical demonstrates very clearly this deconvolution into C-N and N-H bounds only.

As Table 1 indicates, the surface Si/Al ratios of both AODAC and CHODAC samples are determined to be 3.5, which only slightly corresponds with the bulk stoichiometric ratios published for clinoptilolites (2.7 - 5.6 Slovakian mainly 4.8 - 5.2).[5]

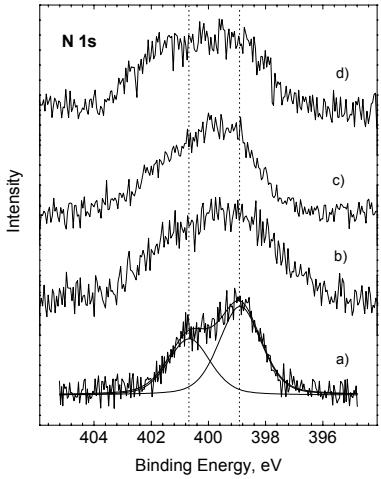

Figure 4. The XPS N 1s core level of ODA (a), ODA-clinoptilolite (b), ODA-clinoptilolite adsorbed with chromate (c), ODA-clinoptilolite adsorbed with arsenate (d).

Furthermore, XPS method confirmed that the whole surface of ODA-modified zeolite composites was covered with carbon, without differentiation whether surface or bulk carbon is present. There were no or only traces of C-O or C=O bounds.

TABLE 1. Surface composition of elements in the studied samples determined by XPS and calculated values of compounds according to the theoretical formulas in %

Element/Sample	C	N	O	Al	Si	Cr	As
Arsenate on ODA-clinoptilolite (AODAC)	51.2	1.5	29.9	3.7	13.2	-	0.4
Chromate on ODA-clinoptilolite (CHODAC)	48.5	1.5	31.6	4.0	14.1	0.2	-
$(ODA)_2CrO_4$	65.7	4.3	9.7	-	-	7.9	-
$(ODA)_3AsO_4$	68.1	4.4	6.7	-	-	-	7.9
Carbonized clinoptilolite (CACL)	71.4	5.8	20.8	-	2	-	-

Regarding C-element contents of XPS studied zeolite samples *vs.* theoretically calculated C-contents of $(ODA)_2CrO_4$ and $(ODA)_3AsO_4$ complexes, both values are more or less comparable (Table 1).

On the other hand, chromium and arsenic elements on the ODA-modified zeolites differ from the theoretically predicted values considerably. On the base of predominantly mesoporous nature of Slovakian clinoptilolite structure the oppositively charged ammonium group of ODA chains may insert and shift the electrostatically attached arsenate or chromate in the mesoporous structure of clinoptilolite much deeper than allows the XPS surface analysis. The lowering of the above metal concentrations in regard to the theoretically predicted values may be caused also by some clustered sorption pattern, i.e. by the agglomerations of the surfactant molecules with the adsorbed chromate or arsenate anions, confirmed by SEM, TEM and UV-VIS analyses so far.[3]

Consequently to that, the XPS measurements testified a massiver agglomeration of chromium and arsenic complexes on the zeolite surface than the values 10-20 nm of the layer thickness and thus the range of XPS detection represents.

A higher concentration of oxygen on the zeolite composite up to 3.5 times relatively to its content in above oxyanions complexes was found, probably due to oxygen presence in the composite matrix, i.e. in AlO_4^{5-} and SiO_4^{4-} structural skeleton.

Recorded XPS spectra indicated mostly C-element occurrence (71.4%) beside which oxygen by 20.8%, nitrogen by 5.8% and silicon by 2% appear on the carbonized zeolite surface (Table 1).

The carbonized surface of zeolite (carbon char) had the character of active charcoal. In the case of each combusted material (currently combusted waste starch and vegetable residues), the char remained its texture from original material.

According to the XPS C1s core levels of ODA- and carbonized clinoptilolite-rich tuffs, a broader spectrum and thus more variously C-bounds are present in the carbonized surface than in the ODA-hydrophobized. Especially, alcoholic, aldehydic and ketonic oxygen contributed probably to about 20% content in the XPS scanned carbonized clinoptilolite sample.

ACKNOWLEDGEMENTS

The authors acknowledge partial support of the research by the National Science Council GAV under contract Nos.: 1/1373/04 and 1/1385/04. Also bilateral Slovak-Italian project under the No. 09105 was devoted to the discussed research.

REFERENCES

1. K.G. Varshney, *Solid State Phenomena* (445), 90 - 91 (2003).
2. S.E. Manahan, *Environmental Chem*., 6th Ed. (Lewis Publishers Boca Raton 1994).

3. E. Chmielewská, K. Jesenák, and K. Gáplovská, Arsenate and chromate removal on cationic surfactant-loaded and cation-exchanged clinoptilolite rich tuff vs. montmorillonite, *Collection of Czechoslovak Chemical Communications* 68 (4), 823-836 (2003).
4. E. Chmielewská, and M. Morvová, Advanced nanosized composite based on the zeolitic tectosilicate carbonisation as alternative for phenol recovery, *Proceedings of the 9th Int. Environmental Protection Conf.*, Ostrava - Poruba, 319-322 (2005).
5. K. Pilchowski, and E. Chmielewská, Adsorptive Separation of 1,2-Dichloroethane from Model Waste Water on Natural Clinoptilolite, *Acta hydrochimica et hydrobiologica* 31 (3), 249-252 (2003).
6. M. Stöcker, X-Ray photoelectron spectroscopy on zeolites and related materials, *Microporous Materials* (6), 235-246 (1996).
7. S.L. Peterson, Pacific Northwest Lab., US Depart. Of Energy, Innov. Concepts Program 195240, Albuquerque, NM 1994.

REGULATION OF LIGNOCELLULOSE MATERIALS SORPTION PROPERTIES BY MODIFICATION FOR ENVIRONMENTAL APPLICATION

GALINA TELYSHEVA*, TATIANA DIZHBITE, GALINA LEBEDEVA, NATALIA ZAIMENKO AND SERGEY POPOVS
Latvian State Institute of Wood Chemistry, Dzerbenes str., 27, Riga, LV-1006, Latvia

Abstract. The changes in sorption properties of products obtained by modification of water insoluble lignins, wood chemical processing wastes, with silicon containing oligomers and bactericide cations: quaternary ammonium and Cu^{2+}, were characterized by nitrogen adsorption/desorption, hydrophilic-oleophilic properties, model tests towards different organic contaminants, incl. microorganisms. Goal oriented modification of lignin with Si- and N- containing compounds providing appearance in its structure of novel functional groups, reaction sites and variation in matrix rigity allowed to regulate products porous structure and in prospective to obtain efficient sorbents for terrestrial and water ecosystems able to sequestrate and inhibit action of hazardous contaminants and promote biodegradation. Combination of Si-modified lignin, used as a matrix, with inorganic cation Cu^{2+} (a guest phase) results in obtaining of organic-inorganic (OI) hybrid material with an additional dimension to their properties: improved sorption capability towards organic contaminants and high antipathogenic activity. The latter was exemplified by model tests with *E.Coli* and *B.Subtilis*: the vital activity of all bacteria sorbed was suppressed.

Keywords: Lignin; sorption properties; modification; environment decontamination

* To whom correspondence should be addressed. Galina Telysheva, Latvian State Institute of Wood Chemistry, Dzerbenes str. 27, Riga, LV-1006, Latvia; e-mail: ligno@edi.lv

J.M. Loureiro and M.T. Kartel (eds.), Combined and Hybrid Adsorbents, 71–76.

1. Introduction

The key role in stability of terrestrial and water ecosystems, sequestration and inhibition of hazardous substances and promotion of their biodegradation belongs to humic substances. The use of plant biomass originated materials for decontamination of environmental objects is extensively studied.[1,2] The similarity of hypothetic structures of lignin (one of the main components of plant tissue in nature, and phytomass chemical processing waste in industry) and humic substances was the motivation for the development of lignin-based sorption active products for ecosystem remediation. Lignin, which is considered as non specific soil organic matter, could potentially fulfill all functions of humic substances: accumulative, transport, regulative, protective and physiological.[3] Using different modes of modification it is possible to develop lignin properties responsible for the definite type of activity.

With the aim to confirm high potential of the water-insoluble commercial lignins as raw materials for design of sorbents intended for decontamination of soil and water from various pollutants and hazardous microorganisms, a set of products on the basis of commercial kraft and hydrolysis lignins as a matrix was obtained by non-covalent interactions with silicon-containing oligomers and bactericide ions: quaternary ammonium (hexadecyl-trimethyl ammonium) and Cu^{2+} cations.

2. Experimental

In the present work commercially available hydrolysis lignin residue (HL) and kraft lignin (Curan) were used as raw material for modifications.

Porous structure of lignin samples was characterized by nitrogen gas sorption-desorption (Sorptometer KELVIN 1042). The surface fractal dimensionality, d_{fs}, calculated in accordance with the Neimark' approach,[4] was applied for quantitative characterization of microsurface structural transformation caused by lignin modification.

Using vacuum-static method, the isotherms of adsorption-desorption of water and normal hydrocarbons vapors were obtained to assess hydrophilic-oleophilic properties of lignin products surface.

ESR spectra of lignin products were recorded at room temperature on a RE-1306 X-band spectrometer at 9.5 GHz with following operating conditions: 100 kHz field modulation, 4.01 G modulation amplitude and 10 ms time constant.

The sorption capacity of starting and modified lignin matrices towards 2,4-D was studied by sorption isotherms method using the batch equilibrium procedure. Soil incubation experiments on degradation of

^{14}C-ring-labeled 2,4-D in the presence of lignin-based products were performed using the peat soil in glass vials submitted with hermetically closed caps. Aliquots of the NaOH trapping solution were analyzed for $^{14}CO_2$ using Beta Multicounter System RISO GM-25-6 (Denmark).

2-days cell cultures of bacteria were used to assess the sorption properties of lignin-based products towards bacteria.

3. Results and Discussion

The results obtained have shown that both the modifications with Si-oligomers and quaternary ammonium cation increase hydrophobic properties of lignin matrices, however the porous structure of products obtained (Si-lignin and HDTMA-lignin), characterized by nitrogen adsorption, is changed in different manner depending on the modifier applied (Table 1).

TABLE 1. Characterization of porous structure of lignin products in terms of low temperature nitrogen gas adsorption

Sample	Volume of pores, mm^3/g			BET specific surface, m^2/g
	Total	Mesopores	Macropores	
Curan	15.8	11.7	4.1	3.6
HDTMA-Curan	9.4	2.8	6.5	2.1
Si-Curan	27.0	24.2	2.7	12.6

Modification with HDTMA cation results in the decrease of specific surface of lignin matrix owing to mesopores reduction. Macropores share increases and formation of a mobile phase of hydrocarbon chains is observed, which can serve as a two-dimensional solvent for organic molecules. The incorporation of siloxane bridges into lignin matrix, decreasing its rigidity, results in the development of new pore systems with uniform pore size distribution (mesopores with size of 4-5 nm) and more than threefold increase in specific surface (Figure 1).

The further improvement of Si-lignin sorption properties was achieved by introduction of Cu^{2+} cations. Thus for Si-HL the twofold increase in surface area and pore volume, accompanied with micropores formation was observed. Consideration of the surface fractal dimensionality values (Table 2) showed the slight increasing complexity of lignin matrix microsurface as the result of modification with Si-oligomers: d_{fs} changes from 2.46 (the value typical for isolated lignins) to 2.57. The following treatment of Si-lignin with Cu^{2+} lead to a further significant increase in this microsurface parameter (up to 2.79), that reveals increasing complexity of hybrid material surface and its inclining to three-dimensional surface.

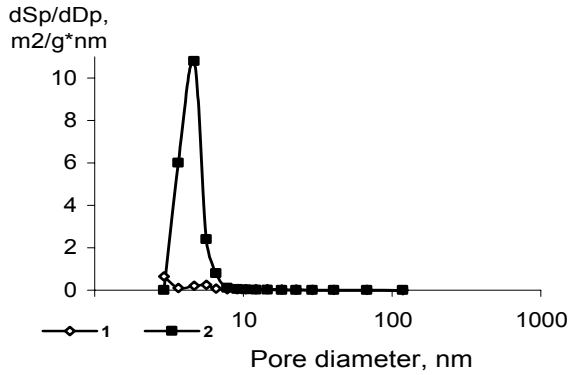

Figure 1. Effect of modification with Si-oligomers on pore area distribution in lignin matrix. 1 – non-modified Curan; 2 – Si-Curan.

TABLE 2. Surface fractal dimensionality of lignin products

Sample	Surface fractal dimensionality, d_{fs}
HL	2.46
Cu-HL	2.35
Si-HL	2.57
Cu-Si-HL	2.79

The ESR spectroscopy data (Table 3) have shown the presence of Cu^{2+} in Si-lignin matrix mostly in the form of associates of Cu^{2+} complexes, whereas in the case of Cu-HL products, the mononuclear complexes of hydrated Cu^{2+} ions[5] are detected.

TABLE 3. Parameters of ESR spectra of Cu^{2+} in lignin products

Sample	$g_{\perp}$	$g_{//}$	"G"
Cu-HL	2.07	2.36	5.1
Cu-Si-HL	2.08	2.28	3.5

$g_{\perp}$ and $g_{//}$ - diagonal components of Cu^{2+} g-tensor: $g_{\perp}$ - perpendicular to magnetic field B vector, $g_{//}$ - parallel to B, "G" = $(2-g_{//})/(2-g_{\perp})$ – a parameter, which characterizes exchange interaction between metal ions: if $G > 4$ the exchange interaction is low, if $G < 4$ considerable exchange interaction exists in the solid complexes.

Lignin products obtained by interaction with both quaternary ammonium and Cu^{2+} cations revealed the high sorption capacity (more than 80%) towards gramnegative and grampositive pathogenic bacteria (*E. coli and B. subtilus*). Non-modified lignins are capable to sorb 45 – 60 % of these bacteria and do not decrease vitality of sorbed microorganisms. HDTMA, well-known antimicrobial agent, after inclusion into lignin matrix was able only to limit the vital activity of sorbed microorganisms. At the same time, Cu-containing Si-modified lignins are characterized with the

highest sorption activity towards both bacteria and totally suppressed the vital activity of bacteria sorbed.

Lignin products, owing to their microstructure and diversity of sorption centers, can realize simultaneous sorption of organic pollutant molecules and microorganisms-degraders and thus activate the process of pollutant biodegradation on interfaces. The most effective sorption in the model experiment was demonstrated by Si- and HDTMA-modified lignin (Table 4).

TABLE 4. Sorption of 2,4-D and its bacterium degrader (*Burholderia cepacia* LMMK 626) by lignin products

Sorbent	Pre-sorbed 2,4-D, mg/g	Bacteria sorbed on the samples containing 2,4-D, cells 10^6/g
HL	2.8	7.0
HDTMA-HL	2.9	20.2
Si-HL	2.9	14.0

Testing of effects of lignin-based products on mineralization of ^{14}C-ring-labeled 2,4-D incubated in unplanted soil shows that Si-lignin provides rapid complete mineralization (Figure 2).

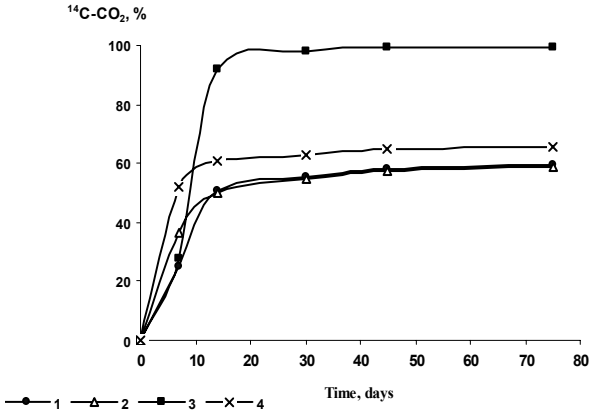

Figure 2. The effect of lignin products on mineralization of ^{14}C-ring-labeled 2,4-D in unplanted peat soil (pH 4.5). 1 – soil without additives, 2 – with HL addition, 3 – with Si-HL addition, 4- with HDTMA-HL addition.

The maximally rapid 2,4-D biodegradation during the first ten days of incubation was observed when the HDTMA-HL, which is characterized with the quantitative irreversible sorption of the pesticide, was added to the soil. Obviously, the decreased rigidity of the matrix after the modification, which resulted in more sorption capacity towards bacteria–degraders of 2,4-D, provides more benevolence conditions for microorganisms interaction on the interfaces with sorbed pesticide molecules. Despite the accelerating effect on the 2,4-D mineralization, the total amount of 2,4-D mineralized in

the presence of HDTMA-HL is lower than that of Si-HL (Figure 2). The practically exhaustive level of 2,4-D biodegradation achieved in two weeks in the presence of the Si-modified product, could be ascribed to the activation of soil microbiota development.[6]

4. Conclusions

Goal oriented modification of lignin with Si- and N-containing compounds allowed to regulate products porous structure and obtain efficient sorbents for terrestrial and water ecosystems able to sequestrate and inhibit action of hazardous contaminants and promote biodegradation. Interaction of modified and non-modified lignins with Cu^{2+} cations led to obtaining of hybrid materials with improved sorption ability and antipathogenic activity. When Si-modified lignin was used as a matrix for design of Cu-containing hybrid material, the vital activity of pathogenic bacteria (exemplified by *E. Coli* and *B. Subtilis*) was totally suppressed. The results obtained show that lignins, incl. rich-in-lignin plant processing waste, have a high potential for design of sorbents for ecosystem objects decontamination.

ACKNOWLEDGEMENT

The financial supports from the EU 6th Framework Programme, Contract IRRISEASOIL, and the Latvian budget, Research grant 1564, are gratefully acknowledged. The kind help by V. Nikolaeva, Assistant Professor of LU (microbiological tests), O. Lebedeva and E. Ponomarenko, Master Students of LU (mathematical calculation and chemical analysis) is highly appreciated.

REFERENCES

1. G. Telysheva, G. Lebedeva, T. Dizhbite, N Zaimenko, J. Ammosova, and U. Viesturs, The use of Si-containing products for *in-situ* soil bioremediation, in: *Remediation of Hazardous Waste Contaminated Soils* (Marcel Dekker, New York, 2000), pp. 699-727.
2. S.E. Bailey, T.J. Olin, R.M. Bricka, and D.D. Adrian, A review of potentially low-cost sorbents for heavy metals, Wat. Res. 33 (11), 2469-2479 (1999).
3. F.J. Stevenson, *Humus Chemistry* (John Wiley, New York, 1994).
4. A.V. Neimark, Determination of the surface fractal dimensionality from the results of an adsorption experiment, *Russian J. Phys. Chem.* 64 (10), 2593-2605 (1990).
5. J. Zhang, and D.P. Kamdem, EPR spectroscopic study of copper amine treated southern pine in wood preservation, *Holzforschung* 54 (4), 343-348 (2000).
6. G. Telysheva, T. Dizhbite, G. Lebedeva, G. Rossiskaya, V. Jurkjane, O. Treikale, U. Viesturs, and M. Daugavietis, Lignin-based soil amendment stimulating phytoremediation, *Acta Biotechnol.* 22 (1-2), 167-173 (2002).

HYDROTHERMOSTABILITY OF MESOPOROUS MESOPHASE MATERIALS OF MCM-41 AND SBA-3 TYPE

MIKHAIL E. MALYSHEV, MAXIM S. MEL'GUNOV, ALEXANDER N. SHMAKOV, ELENA A. MEL'GUNOVA AND VLADIMIR B. FENELONOV*
Boreskov Institute of Catalysis, 5 Acad. Lavrentiev Av., Novosibirsk 630090, Russia

Abstract. A method of silica mesoporous mesophase material (***MMM***) of SBA-3 type hydrothermostability (***HTS***) improvement by its post-synthesis hydrothermal treatment (***HTT***) in ammonia solution has been investigated. The effects of treatment duration and ammonia concentration on the structural and textural parameters of ***MMM*** have been determined. A mechanism of ***MMM*** transformation under ***HTT*** conditions is suggested.

Keywords: mesoporous mesophase material; post-synthesis hydrothermal treatment; hydrothermostability; mechanism of formation

1. Introduction

It is known that efficiency of zeolite applications as hydrocarbon transformation catalysts depends strongly of geometrical size of their channels and windows. This size does not exceed 1.3 nm for all known zeolites. This fact seems to be one of the reasons of the huge interest to new silica materials that appeared at the beginning of the 90s and show zeolite-like system of calibrated pores whithin the size range of 2-10 nm and higher.

These materials were discovered by Mobile collaborators in 1992.[1,2] These materials have *mesophase structure* with *short-range order* similar to

* To whom correspondence should be addressed. Vladimir B. Fenelonov, Boreskov Institute of Catalysis, 5 Acad. Lavrentiev Av., Novosibirsk 630090, Russia; e-mail: fenelon@catalysis.ru

J.M. Loureiro and M.T. Kartel (eds.), Combined and Hybrid Adsorbents, 77–83.

amorphous systems and *long-range order* of mesopore packing similar to usual crystals. Highly organized pore structure with long-range order can be easily observed on electron microscopy images and on X-ray diffraction patterns at small angles (with no diffraction peaks at wide angle region).

The general feature of these mesophases is that their pore size corresponds to mesopore range, so these materials are often called as *mesoporous zeolites*. The inventors called these materials as M41S family, there are a set of other names, and we call them *mesoporous mesophase materials* or shortly ***MMM*** regarding both to their size and structure.[3,4]

The simplest and most wide spread types of ***MMM*** such as MCM-41 and SBA-3 possess hexagonal (honeycomb-like) structure with amorphous walls and highly ordered arrangement of channels. These ***MMM***s differ one from another only by synthesis conditions. Their specific surface area is about 1100-1300 m^2/g (i.e. 2-3 times greater than for usual zeolites), channel size can be varied within the range 3-5 nm and wall thickness is about 1 nm.

At present, ***MMM***s are considered as prospective catalysts for organic molecules transformation or as catalyst supports, adsorbents and molecular sieves for separation or storage of biologically active substances, nanoelectronics materials, standards for measurement device calibration or size effect research in nanometer scale and so on. However, these materials appear to be thermostable in dry air with regard to calcination up to 700-800 °C but do not have sufficient hydrothermostability (***HTS***), i.e. stability with regards to calcination in water steam, and destroy under water steam treatment or boiling. Low ***HTS*** limits the area of possible applications of ***MMM***s. In this connection the problem of ***HTS*** of ***MMM***s becomes one of the most important in investigation of this new class of mesoporous materials.

The structure of mesophase consists of irregular packing of SiO_4 tetrahedra where each pair of neighboring tetrahedra is connected by a common oxygen atom at the top. These oxygen atoms form silanol Si–O–Si bonds and the structural instability is attributed to the hydrolysis of these bonds due to the interaction with water molecules. Thus, hydrolysis results in breaking of the bond between neighboring tetrahedra and increase of broken bonds number is followed by destruction of hexagonal packing order and finally by complete decomposition of mesophase.

Correspondingly, the strategy to ***HTS*** increase can be based on formation of protecting hydrophobic film on mesopore surface, increase of wall thickness, increase of SiO_2 polycondensation degree in the walls and additional post-synthesis treatment that results in removing areas with most strained Si–O–Si bonds which are likely to be hydrolyzed.

This work presents investigation of post-synthesis treatment of dried but not calcined mesophases in ammonia solution that, we believe, should prevent the formation of strained silanol bonds.

2. Experimental

The subjects of our investigation were ***Si-MMM*** with hexagonal arrangement of pores. These materials are analogous to MCM-41 and SBA-3 types with respect to their structural and textural characteristics. The initial sample ***Si-MMM*** was synthesized using $Na_2Si_2O_5$ as silica source and surfactant ***CTAB*** ($C_{16}H_{33}N(CH_3)_3Br$) as structure directing agent.[3,4]

The synthesis of ***Si-MMM*** was carried out at pH~1-5. Hydrothermal treatment (***HTT***) was done at 50 °C during 24 h. The synthesized materials were filtered, washed, dried in air at 60 °C. Further these samples were treated in autoclave by NH_3 solution for different times (1-10 days) at 120 °C (***NH_3-HTT***). NH_3 concentration was varied within the range 0-2 M in amount of 50 cm^3 of solution to 1 g of air-dried sample. The treated samples were filtered, dried, calcined in air at 300 °C for 3 h and then at 600 °C for another 3 h for complete thermooxidizing removal of surfactant.

To control ***HTS*** a fraction of each calcined sample was boiled in water for 1 h and other fraction was additionally calcined at 900 °C for 3 h. All samples were investigated by X-ray diffraction (XRD) and nitrogen adsorption at 77 K.

Electron microscopy (TEM) measurements were done on transmission electron microscope JEM 2010 (resolution 0.14 nm, accelerating voltage 200 kV). The images obtained were typical of MCM-41 and SBA-3 systems with highly ordered mesopore arrays and one example is shown in Figure 1.

XRD patterns were obtained at Siberian Synchrotron Radiation Center on high resolution powder diffractometer using wavelength of radiation of 0.154 nm within angular range 0.5-8.0 degrees. The N_2 adsorption isotherms were measured using ASAP 2400 Micromeritics. Textural parameters were calculated including specific surface area A_{me}, volume V_{me}, diameter d_{me}, of mesopores and mean wall thickness h_{me} between the mesoporoes.[3,4] Additionally the pore size distribution (***PSD***) was calculated by the Barret-Joiner-Halenda method.

3. Results and Discussion

The initial sample without ***NH$_3$-HTT*** has A_{me}~900 m^2/g, V_{me}~ 0.8 cm^3/g and d_{me} ~ 4 nm. There was only one reflection (100) on XRD pattern, but TEM provides evidence that it is a typical ***MMM*** with regular pore arrays.

N_2-isotherm seems to look like standard isotherm for MMM with characteristic raise corresponding to capillary condensation region (Figure. 2). ***NH$_3$-HTT*** leads to narrowing this region in all cases and consequently to narrowing of the ***PSD*** without any change of A_{me} and V_{me}.

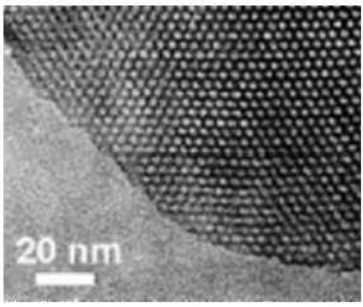

Figure 1. TEM image of ***Si-MMM*** synthesized under weak acidic conditions using ***CTAB*** surfactant.

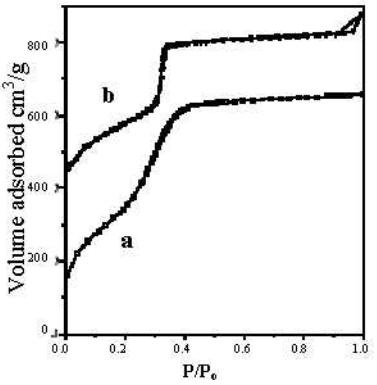

Figure 2. N_2-isotherm of ***Si-MMM*** a) before and b) after ***NH$_3$-HTT.***

One can see from Figure 3 that intensity of reflection (100) increases with increase of ***NH$_3$-HTT*** duration and NH_3 concentration. Additional reflections (110) and (200) of hexagonal arrangement of mesopore arrays appear on XRD patterns. The increase of reflection number and intensity evidences the improvement of the structure regularity of the samples after ***NH$_3$-HTT***.

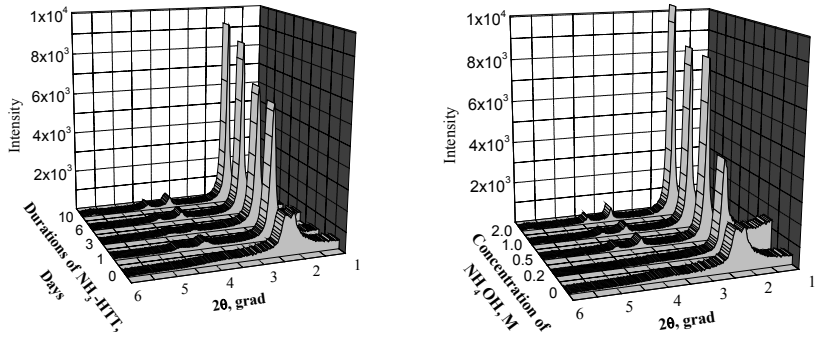

a) b)

Figure 3. XRD patterns of samples after NH_3-HTT at different a) duration τ (C_{NH3}=1.0 M) and b) concentration of NH_3 (τ = 6 days).

As it follows from XRD and adsorption data the ***NH₃-HTT*** leads to the narrowing of XRD reflection width while lattice constant a_0, mesopore diameter d_{me} and wall thickness h_w do not change. It should be noted that structure changes do not depend on ***NH₃-HTT*** duration τ for τ>1.0 day and ***NH₃*** concentration for C_{NH3}>0.2 M. This means that some kind of internal "tuning" of the structure appears in samples during ***NH₃-HTT***.

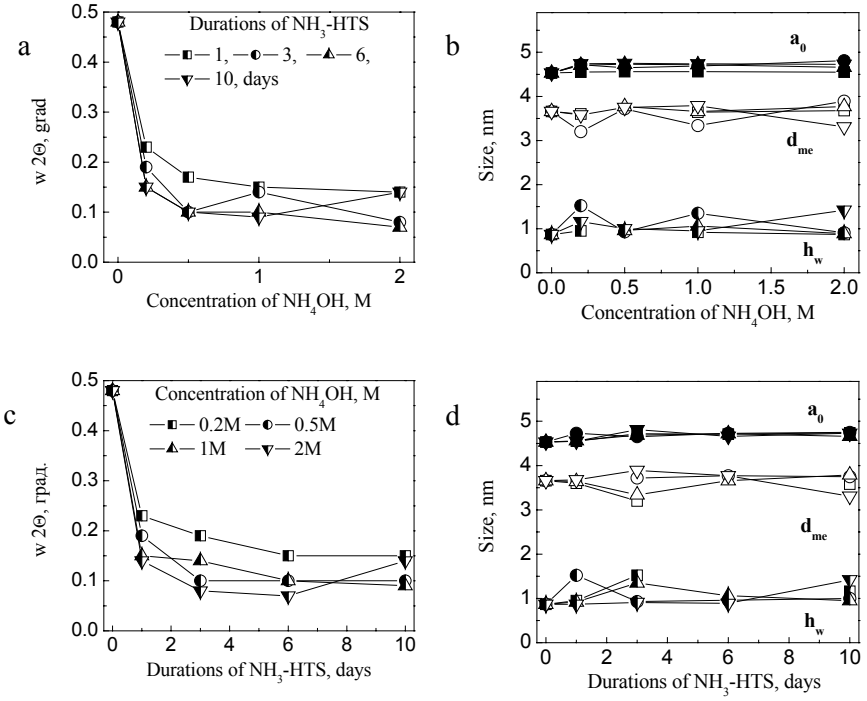

Figure 4. Effect of ***NH₃-HTT*** conditions on structural and textural parameters.

Tests on ***HTS*** by boiling in water and calcination at 900 °C showed that parameters a_0, d_{me}, h_w as well as A_{me} and V_{me} do not change essentially. Similar testing of non-treated sample showed about 30% lost of A_{me} and practically unchanged XRD pattern.

Thus ***NH₃-HTT*** increases not only the structure perfection of ***MMM*** but increases ***HTS*** of the samples as well. We explain the increase of structure perfection and ***HTS*** by the scheme that includes mechanism of ***MMM*** formation and structure re-arrangement under ***NH₃-HTT***.

It is known that self-assembling of hexagonal ***MMM*** phase in the presence of siliceous species $\mathbf{I_m}$ takes place at a surfactant concentration **S** higher than the critical concentration of micelle formation but lower than

the concentration of self-assembling to hexagonal phase. It means that self-assembling of ***MMM*** is the result of interaction of oppositely charged surfactant micelles $\mathbf{S_m^+}$ and siliceous species $\mathbf{I_m}$. According to the supramolecular chemistry law of J.-M. Lehn,[5] the interaction of oppositely charged species of **S** and **I** types supposes the selection of different variants of interaction partner with self-assembly of partners corresponding to the principle of *dual complementarity*, i.e. with extremely high correspondence of partner morphology and charge maps on their surfaces. Under equilibrium conditions uniform self-assembling can be expected according to the scheme on Figure 5 (b) with spontaneous formation of most equilibrium configuration. Under these conditions siliceous species link each other by siloxane bonds Si–O–Si with angles and interatomic distances similar to that of equilibrium ones.

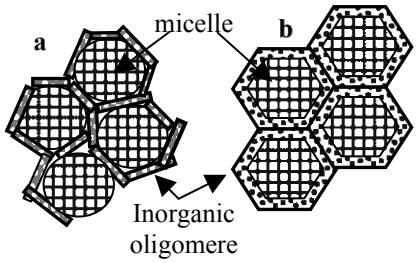

Figure 5. Scheme of irregular (**a**) and regular (**b**) arrangement of siliceous species on surfactant micelles.

Under real experimental conditions there is greater probability of formation of less regular structure built from different oligomers SiO_2 placed at random (Figure 5, a). Bonds between these oligomers can be non-equilibrium or strained due to their random orientation. Calcination of this structure fixes inorganic framework which demonstrates low HTS.

NH_3-HTT leads to hydrolysis of most strained Si–O–Si bonds, makes bonds of siliceous species and micelle weaker, providing transformation from structure **a** to structure **b** (Figure 5).

More thorough description of this transformation mechanism based on analysis of published experimental data concerning ***HTS*** increase of ***MMM***s will be presented in separate detailed report.

REFERENCES

1. C.T. Kresge, M.E. Leonowicz, W.J. Roth, J.C. Vartuli, and J.C. Beck, *Nature* 359, 710-712 (1992).
2. J.C. Beck, J.C. Vartuli, W.J. Roth, M.E. Leonowicz, C.T. Kresge, K.D. Schmitt, C.T-W. Chu, D.H. Olson, E.W. Sheppard, S.B. McCullen, J.B. Higgins, and J.L. Schlenker, *J. Amer. Chem. Soc.* 114, 10834-10843 (1992).
3. V.B. Fenelonov, V.N. Romannikov, and A.Yu. Derevyankin, *Micropor. Mesopor Mater.* 28, 57-72 (1999).

4. V.B. Fenelonov, A.Yu. Derevyankin, S.D. Kirik, L.A. Solovyov, A.N. Shmakov, J.-L. Bonardet, A. Gedeon, and V.N. Romannikov, *Micropor. Mesopor Mater.* 44-45, 33-40 (2001).
5. J-M. Lehn, *Supramolecular Chemistry, Concepts and Perspectives* (VCH, Weinheim, 1995).

URANIUM SORPTION BY ORGANOZEOLITES AND FERROMAGNETIC ORGANOZEOLITES FROM WASTE WATER OF SPECIAL LAUNDRY

V.A. NIKASHINA*, E.M. KATS, I.B. SEROVA
Vernadsky Institute of Geochemistry and Analytical Chemistry, Russian Academy of Sciences, Kosygin str. 19, Moscow 119991, Russia

PETER A. GEMBITSKI
Institute of Ecological and Technological Problems, Krivoroschskaya str. 33, Moscow 117638, Russia

Abstract. The selectivities of the new sorbents - organozeolites based on natural zeolite (sorbent 1) and magnetized natural zeolite (sorbent 2), modified by polyhexamethyleneguanidine chloride (PGMG), to carbonate complex of uranium from the CO_3^{2-}-bearing waste water of special laundry were studied. The equilibrium and kinetic characteristics of the carbonate uranium complex-ions sorption by organozeolites (sorbent 1 and 2) were determined. The high distribution coefficients for the carbonate uranium complex-ions and film-diffusion kinetic mechanism of sorption for sorbent 1 and sorbent 2 were established. The mathematical model describing this process in dynamic conditions was chosen based on obtained equilibrium and kinetic characteristics of sorbents 1 and 2. The calculation of the breakthrough times was carried out for various solution flow rates, degree of waste water decontamination, and other parameters.

Keywords: organozeolites; carbonate uranium complex; selectivity; distribution coefficient; film-diffusion kinetics; mathematical model; breakthrough times

* To whom correspondence should be addressed. V.A. Nikashina, Vernadsky Institute of Geochemistry and Analytical Chemistry, Russian Academy of Sciences, Kosygin str. 19, Moscow 119991, Russia; e-mail: nikashina@geokhi.ru

J.M. Loureiro and M.T. Kartel (eds.), Combined and Hybrid Adsorbents, 85–92.

1. Introduction

Pollution of the environment by organic contaminants, heavy metals, radionuclides including uranium and transuranium elements has created a need to develop inexpensive sorbents with a combination of various properties helping to solve these problems. We developed organozeolites based on the natural zeolites and earlier obtained ferromagnetic (preliminary magnetized) natural zeolites using polyhexamethyleneguanidine (PGMG) as modifier and epichlorohydrin (ECH) as a crosslinker.[1-3] These sorbents are characterized simultaneously by cation-exchange, anion-exchange, adsorption capacities and bactericidal activity, and also by the high selectivity to oxygen-bearing anions (CrO_4^{2-}, AsO_4^{2}, etc.),[4,5] and to the carbonate complexes of uranium such as $UO_2(CO_3)_2^{2-}$ and $UO_2(CO_3)_3^{4-}$ present in surface carbonate-containing drinking waters.[6,7] Uranium is present in CO_3-bearing solutions as strong complex-anions which contain $UO_2(CO_3)_2^{2-}$ and $UO_2(CO_3)_3^{4-}$. Therefore it was interesting to investigate U-sorption by organozeolites from CO_3-bearing solutions with a more complicated content, for example, CO_3-bearing waste water of a special laundry.

2. Materials and Methods

The investigated sorbents: sorbent 1 (or CT-PGMG) – organozeolite based on clinoptilolite-containing tuff of Tedzami deposit (Georgia), of known chemical composition, modified by a 15% solution of polyhexametyleneguanidine chloride (PGMG) according to the method previously described;[2] and sorbent 2 (or CT-FM-PGMG) – organozeolite based on the ferromagnetic clinoptilolite-containing tuff modified by PGMG according to the same method. The total cation-exchange capacity of the organozeolites was 0.9-1.1 meq/g. The total anion-exchange capacity was 0.23 meq/g (sorbent 1) and 0.20 meq/g (sorbent 2). The grain size of sorbents was 0.1–0.25 mm. The magnetic susceptibility of sorbent 2 was 8.2×10^{-3} CGSM units. The compositions of the studied solutions in mg/L were: U = 0.2-0.5, Cl = 10.0, SO_4^{2-} = 65.0, HCO_3^{2-} = 400.0**,** CO_3^{2-} = 610.0, PO_4^{3-} = 372.0, Na^+ = 500.0, NH_4^+ = 312.0, Ca^{2+} = 3.0, with pH=9.5.

The ionic strength of the solutions was regulated by addition of different quantities of NaCl. The NaCl concentration in these solutions was altered from 0.04 N to 0.26 N. The uranium sorption isotherm for organozeolite was obtained from mixtures having different ratios of solution volume to sorbent weight (V/m) at 20°C in static conditions. The appropriate distribution coefficients of carbonate uranium complex ions (CUC) were calculated from the isotherm also depending on the ionic strength of

solution ($G=A_{eq}/C_{eq}$, where G is the distribution coefficient [mL/g]; A_{eq} is the equilibrium concentration of uranium in the sorbent [mg/g]; and C_{eq} is the equilibrium concentration of uranium in the solution [mg/L]). The "the breakthrough curves" method was used to estimate the kinetic mechanism in the ion-exchange process studied.[8,9] The breakthrough curves of CUC for these solutions were obtained using 0.25 g of organozeolite at various solution flowrates. The content of uranium in solutions was determined by the photometry method with arsenaso-3[10] and by the method of standard additions.

3. Results and Discussion

3.1. THE EQUILIBRIUM CHARACTERISTICS OF CUC-IONS SORPTION ON CT-PGMG AND CT-FM-PGMG

Previously the distribution coefficients of CUC (uranium) depending on ionic strength of solution were determined in static conditions for evaluation of selectivity of organozeolites to uranium from CO_3-containing solutions. Table 1 represents the data obtained.

TABLE 1. The distribution coefficients of carbonate uranium complex–ions on organozeolite depending on the solution ionic strength

$C_{NaCL,}$ (N)	C_{eq} (mg/L)	A_{eq} (mg/g)	G (mL/g)
0.04	0.26	3.16	$1.2\ 10^4$
0.18	1.01	1.66	$1.6\ 10^3$
0.26	1.10	1.48	$1.3\ 10^3$

As Table 1 shows, a decrease in values of the distribution coefficient is observed. For example, a 6.5-fold increase in the total salt content solution decreases the value of the distribution coefficient 10 times (from $1.2x10^4$ to $1.3x10^3$ mL/g). Nevertheless the organozeolite retains a sufficiently high selectivity to CUC even in 0.26 N NaCl.

As follows from the ion-exchange theory, the quantitative description of sorption process in dynamic conditions requires the determination of the equilibrium and kinetic coefficients of the ion-exchange process studied. The equilibrium characteristics were obtained from the CUC-isotherm on the organozeolite and ferromagnetic organozeolite. Figure 1 represents the isotherms of CUC-sorption on the organozeolite (sorbent 1 - CT-PGMG) and ferromagnetic organozeolite (sorbent 2 - CT-FM-PGMG).

As shown in Figure 1, the ion-exchange isotherms of CUC (uranium) from special laundry waste water are convex and have a linear section at uranium concentration < 0.5 mg/L. The distribution coefficients of CUC-

ions in the linear section for CT-PGMG and CT-FM-PGMG are $5.7x10^4$ mL/g and $2x10^5$ mL/g respectively. The values of the uranium distribution coefficients obtained are both higher than the value obtained earlier for CT-PGMG from surface drinking waters ($G=1.1x10^4$ mL/g).[7] The equilibrium quantities of the sorbed uranium (A_{eq}) at C_{eq} = 3 mg/L was 30 mg/g on organozeolite CT-PGMG showing the high efficiency of the studied organozeolites for decontamination of special laundry waste waters from uranium.

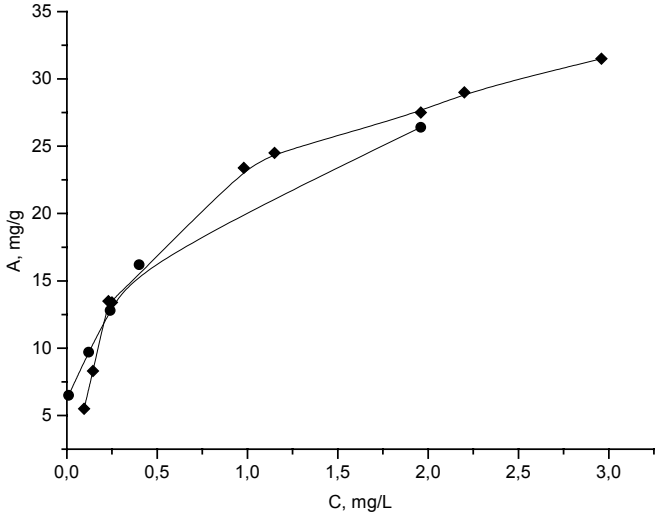

Figure 1. Uranium sorption isotherms from the special laundry waste water on CT-PGMG (♦-♦) and on CT-FM-PGMG (●-●).

3.2. KINETIC CHARACTERISTICS OF CUC-IONS SORPTION BY CT-PGMG AND CT-FM-PGMG

The kinetic characteristics of the CUC-ions sorption by CT-PGMG and CT-FM-PGMG were obtained by the method of dynamic breakthrough curves.[8,9] Figure 2 represents some of the experimental breakthrough curves of CUC-ions on CT-PGMG and CT-FM-PGMG. A comparison of the experimental breakthrough curves with a set of theoretical breakthrough curves for various models of ion-exchange dynamics (film and particle diffusion kinetics for linear isotherm, etc.) showed that they almost coincide if the model considering linear isotherm and film-diffusion kinetics is used. This means that the film-diffusion kinetics determines the rate of the ion exchange process on the studied organozeolites.

The calculation of the film-diffusion kinetic coefficients of CUC-ions, β, was carried out by comparison of the experimental breakthrough curves

obtained for the different solution flow rates, with a set of theoretical breakthrough curves for the models of ion-exchange dynamics including film diffusion kinetics and linear isotherm.[8,9] Figure 3 represents the results of calculations of film-diffusion kinetic coefficient β and its dependence on the solution flow rate.

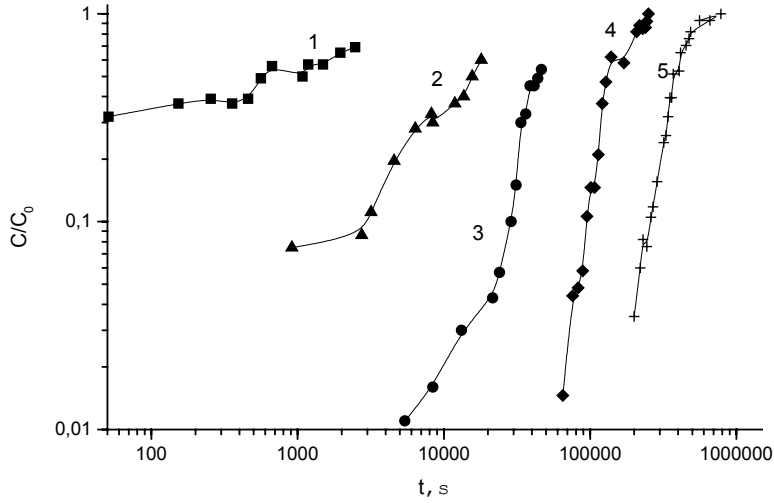

Figure 2. Breakthrough curves of CUC-ions on CT-PGMG and CT-FM-PGMG for various solution flow rates V; column cross-section = 0.78 cm^2, sorbent mass = 0.25 g; curve 1: V=0.63 cm/s, curve 2: V= 0.14 cm/s, curve 3: V= 0.05 cm/s, curve 4: V= 0.016 cm/s, curve 5: V= 0.007 cm/s (CT-FM-PGMG).

As Figure 3 shows, the experimental dependence observed on the solution flow rate V, $\beta \approx V^{0.51}$, correlates well with the theoretically predicted $\beta = V^n$ (where n=0.4-0.6). The adequacy of the model selected to real dynamic ion-exchange process was verified by comparison of the calculated and experimental curves for a solution flow rate corresponding to V=0.01 cm/s. The data obtained is presented in the Figure 4.

As Figure 4 shows, the calculated curve coincides very closely with the experimental curve. It suggests that the mathematical model selected may be used for calculation of the process investigated and allows to simulate and calculate the breakthrough curves of CUC–ions on the organozeolites studied for various operating conditions. The evaluation of the breakthrough time of the organozeolite filter depending on the solution flow rate, bed depth, different decontamination degrees in the process of the decontamination of a special laundry waste water from uranium was carried out on the basis of the selected mathematical model using obtained equilibrium and kinetic coefficients. Some of those data are listed in Table 2.

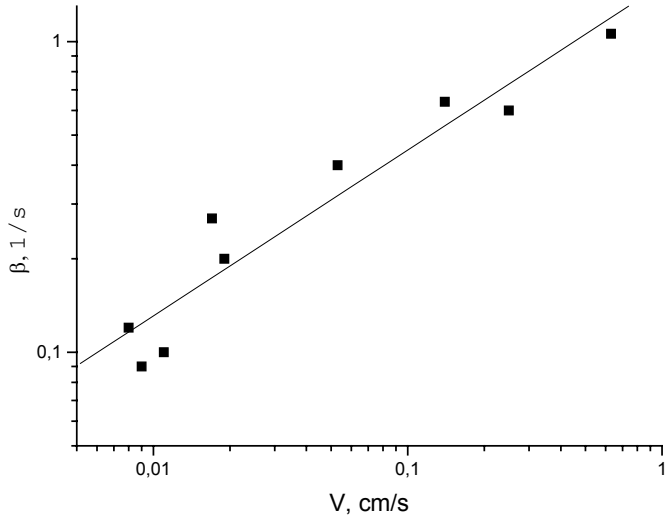

Figure 3. Film-diffusion coefficient **β** of CUC-ions *vs.* solution flow rate (V) for its sorption from the waste water of the special laundry by CT-PGMG and CT-FM-PGMG.

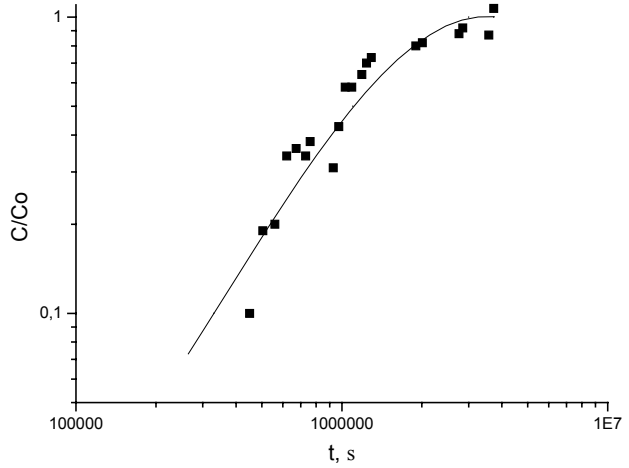

Figure 4. Experimental (square symbols) and calculated (line) breakthrough curves of carbonate complexes of uranium on organo-treated zeolitic tuff (CT-PGMG - sorbent 1) from the waste water of special laundry. The sorbent mass is 0.75 g. The feed uranium concentration is 0.23 mg/L, the solution flow rate is 0.01 cm/s.

TABLE 2. Breakthrough time (days) *vs.* column operating conditions for removal of uranium from waste water of special laundry*

C/C_o	V=6.0 m/hour	V= 1.0 m/hour	V=0,33 m/hour
0,01	254	1500	4600
0,05	259	1510	4616
0,1	261	1514	4630

* bed depth of 1 m.

As shown in Table 2, a 1 m bed depth of organozeolite provides a two orders of magnitude decontamination of the special laundry waste water from uranium during 254-4600 days (≈12.5 years) depending on the solution flow rate and the decontamination degree.

4. Conclusions

The selectivity of organozeolites studied (CT-PGMG and CT-FM-PGMG) for the carbonate uranium complex ions is preserved rather high over a fairly wide range of the solution ionic strength variations.

The equilibrium and kinetic characteristics of the dynamic process of the carbonate uranium complex ions exchange from special laundry waste waters by CT-PGMG and CT-FM-PGMG were obtained.

The obtained equilibrium (G) and kinetic (β) coefficients allow to select the mathematical model (linear isotherm and film-diffusion kinetics) describing the process in dynamic conditions.

The evaluation of the breakthrough time of the commercial organozeolite filter depending on sorbent bed depth and solution flow rates in the process of decontamination of special laundry waste waters from carbonate uranium complex ions was carried out on the basis of the selected mathematical model.

The data obtained may be useful in developing the technology of simultaneous purification of waste water both from carbonate uranium complex ions and from cationic pollutants.

REFERENCES

1. I.B. Serova, V.A. Nikashina, B.A. Rudenko, and S.S. Meshalkin, in : *Natural Zeolites-Sofia'95,* edited by G.Kirov, L.Filizova and O.Petrov (Pensoft, Sofia-Moscow, 1997), pp. 115-120.
2. V.A. Nikashina, E.M. Kats, P.A. Gembitskii, L.F. Boksha, and A.Kh. Galuzinskaya, Organomineral sorbents based on clinoptilolite-containing tuffs. 1. Preparation of organomineral anion-exchangers using polyhexamethyleneguanidine, *Russ. Chem. Bull.* 43, 1462-1465 (1994).

3. V.A. Nikashina., E.M. Kats, and P.A. Gembitskii, Organomineral sorbents based on clinoptilolite-containing tuffs. 2. Study of ion-exchange and technological properties of organomineral sorbents, *Russ. Chem. Bull.* 43, 1466-1468 (1994).
4. P. Misaelides, V.A. Nikashina , A. Godelitsas, P.A. Gembitskii, and E.M. Kats, Removal of As(V) anions from aqueous solutions using organomineral natural zeolitic materials, *J. Radioanal. Nucl. Chem.* 227, 183-186 (1998).
5. E.M. Kats, and V.A Nikashina, in: *Natural Zeolites for the Third Millennium*, edited by C.C. Colella and F.A. Mumpton (Lit. Editrice "A. De Frede", Italy, 2000), pp. 387-393.
6. V.V. Shatalov, N.P. Stupin, I.A. Busakina, and S.V. Molchanov, in: *Uranium Chemistry*, (Nauka, Moscow, 1989), p.206 (in Russian).
7. V.A. Nikashina, E.M. Kats, and I.B.Serova, in: *Zeolite' 02 Book of Abstracts*, edited by P. Misaelides, (Thessaloniki, Greece, 2002), pp. 251-252.
8. V.A. Nikashina, N.K. Galkina, and M.M. Senyavin, The calculating of the sorption of metals by ion-exchange filter, Russian Institute of Scientific and Technical Information, Moscow, Article No. 3668, 1977, 44 pp. (in Russian).
9. M.M. Senyavin, R.N. Rubinstein, E.V. Venitsianov, N.K. Galkina, I.V. Komarova, and V.A. Nikashina, *Fundametals of Calculation and Optimization of Ion-Exchange Processes* (Nauka, Moscow, 1972), 172 pp (in Russian).
10. Method of determination of U-content, GOST (State Standard) 18921-73. Drinking Water. Methods of analysis (Moscow, 1976), pp 120-125 (in Russian).

TEMPLATE EFFECT OF THE M^{3+}- CATIONS IN THE COURSE OF THE SYNTHESIS OF HIGH DISPERSED TITANIUM AND ZIRCONIUM PHOSPHATES

IGOR Z. ZHURAVLEV* AND VLADIMIR V. STRELKO
Institute for Sorption and Problems of Endoecology, NAS of Ukraine, General Naumov str., 13, Kiev, 03164, Ukraine

Abstract. An explanation of the template effect of the M^{3+}-cations in the course of the sol-gel synthesis of high dispersed titanium and zirconium phosphates is presented. Some ways to vary and to control the porous structure of such phosphates are shown and proposed.

Keywords: Sol-gel synthesis; templates; three charge cations; titanium and zirconium phosphates; ion-exchangers; porous structure; gels; amorphous materials

1. Introduction

For a long time we have been investigating the sol-gel synthesis of titanium and zirconium phosphates with the objectives of elaborating the laboratory, semi-pilot and industrial technologies for these phosphates production as spherically granulated beads with controlled beads diameter, porous structure and ion-exchange properties.[1] Unfortunately, such sol-gel synthesis has essential restrictions, the main of which is the high speed of the gel forming. Traditionally used organic inhibitors as a rule remain in the material after washing. Besides the porosity of such adsorbents is low.[2] The use of the three-charge cations for the sol-gel reaction control, for the first time suggested by us, allowed essentially increasing the porosity and improving the ion-exchange properties of the gels.[3,4]

* To whom correspondence should be addressed. Igor Z. Zhuravlev, Institute for Sorption and Problems of Endoecology, NAS of Ukraine, General Naumov str., 13, Kiev, 03164, Ukraine; e-mail: zhuravlev@ispe.kiev.ua

J.M. Loureiro and M.T. Kartel (eds.), Combined and Hybrid Adsorbents, 93–98.

2. Experimental

The investigated phosphates were prepared by mixing water solutions of the corresponding inorganic salts and acids ($TiCl_4$, $ZrOCl_2$, $Zr_2O_3Cl_2$, NaH_2PO_4, H_3PO_4, HCl, $AlCl_3$, $FeCl_3$, etc.).[3,4] Before mixing, the dissolved salts of the template three charge cations were added to one of two reaction solutions. After formation of the gels the template cations were removed by the acidic washing. Syntheses occurred in the glass vessel or in the granulate column utilizing known technology for preparation of the granulated adsorbents.[3,4]

The porous structure of the investigated phosphates was studied with the automatic Gemini-2 Micromeritics porosimeter, nitrogen adsorption. Outgas temperature was 160 ^oC. Specific surface area was measured via the thermal desorption of argon. In addition, the desiccator's method was utilized for investigation of the pore volumes by water and benzene.

3. Results and Discussion

When investigating the sol-gel process of gelation of the titanium and zirconium phosphates in the presence of such well-known inhibitors as glycerin and hydrogen peroxide, the need for the replacement of these inhibitors became obvious for us. In this connection there was the idea of using plus three charged cations such as Al^{3+}, Fe^{3+}, etc. to slow down the sol-gel reaction. As the prerequisite to this idea were the following thoughts:

1. Acidic phosphates of plus three charged cations are soluble in water and are also quite strong phosphatic complexes.[5] 2. Acidic phosphates of titanium and zirconium have low solubility in water and in mineral acids (which do not form strong complexes).[6] 3. When mixing the water solutions of phosphoric acid (phosphates of alkaline metals) and zirconium (titanium) salts the rapid sol-gel reaction occurs and formation of the corresponding phosphates takes place.[6] 4. Stability of the phosphatic complexes of zirconium and titanium is higher, than that of the M^{3+}-cations phosphates.[7]

We have supposed that if instead of phosphoric acid as an initial reagent we take the soluble phosphate of a trivalent metal, at its introduction in reaction there will be a gradual step replacement of a three-charged cation from a phosphatic complex with formation of the zirconium (titanium) phosphate instead of the first.[4] It should be accompanied by a delay of the sol-gel transition, and it is just necessary for the technology of granulation of the zirconium and titanium phosphates. At introduction of the M^{3+}-cations in the M^{4+} salt solution there is the same step replacement of the

M^{3+} from phosphate and also the sol-gel transition is accompanied by a delay. As a whole it can be presented by the Scheme 1:

$$\left.\begin{array}{l}[H_3PO_4 + MCl_3] + Zr(Ti)OCl_2 \\ H_3PO_4 + [MCl_3 + Zr(Ti)OCl_2]\end{array}\right\rangle \rightarrow Zr(Ti)\ \text{phosphate - gel} \qquad (1)$$

If we enter M^{3+}-cations into an initial solution of phosphate it is possible to neutralize completely or partially the acid anions, entered together with the M^{3+}-cations, for example:

$$FeCl_3 + 3\ NaH_2PO_4 \rightarrow Fe(H_2PO_4)_3 + 3\ NaCl \qquad (2)$$

The synthesis can also be carried out without preliminary neutralization of the initial solution [MCl_3 + H_3PO_4].

We have investigated the change of the gelation speed (visually, by the loss of the solution fluidity) as a function of the initial M^{3+}/M^{4+} ratio in a reacting mixture for the Al^{3+} and Fe^{3+}-cations. These curves are shown in the Figure 1.

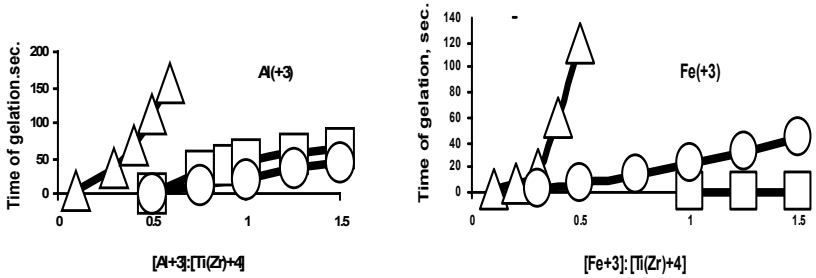

Figure 1. Time of gelation as a function of the initial M^{3+}/M^{4+} ratio. [H_3PO_4 + MCl_3] + $TiCl_4$ ($ZrOCl_2$, $Zr_2O_3Cl_2$), where M = Fe^{3+}, Al^{3+};Δ- $TiCl_4$, □- $ZrOCl_2$, ○- $Zr_2O_3Cl_2$; T = 4 °C.

Figure 1 shows that the time of the sol-gel transition varies with the change of the M^{3+}/M^{4+}ratio and that, by changing the amount of the entered M^{3+}, it is possible to control the sol-gel transition parameters. It is obvious, that the presence of M^{3+} will influence the formation of the porous structure of the gel, and that a, so-called, ionic imprinting (templating) by the M^{3+} cations-templates will take place. After formation of the gel the M^{3+} cations-templates are removed from the gel by washing with the acid. As a whole this process can be presented by the simplified Scheme 3:

$$ZrOCl_2 + AlCl_3 + H_3PO_4 \rightarrow Al - Zr - \text{phosphate} + HCl \rightarrow Zr - \text{phosphate} + AlCl_3 \qquad (3)$$

Thus in a matrix of gel the specific ion-exchange centers generated by the M^{3+}-cations remain. Thus the ultraporous structure of the gels with increased ion-exchange selectivity towards certain ions (for example to template-ions) is formed. Besides we have determined that, using the

trivalent cations-templates during the synthesis, gels with larger mesopores are formed in comparison with similar materials synthesized without M^{3+}-templates.[4]

These results are presented in comparison with known analogs in Table 1.

TABLE 1. Comparison of the porous structures of the templated with M^{3+}-cations titanium and zirconium phosphates and known analogs*

N	Ionite	V_S, cm^3/g water	V_S, cm^3/g benzene	Humidity, %	S, m^2/g (N_2)	Mean pore diam., Å
1	TiFePH	0.33	0.33	33.8	130	50÷100 (100%)
2	TiAlPH	0.35	0.33	30.3	139	50÷120 (35%) 120÷250 (60%)
3	TiPH	0.25	0.12	-	175	100 (100%)
4	ZrAlPH	0.25	0.22	35.2	305	15÷50 (90%)
5	ZrFePH	0.23	0.21	32.3	381	15÷50 (90%)
6	ZrPH	0.07	0.01	-	30	n. d.

* Abbreviations in the Table show the chemical composition of the investigated materials. TiPH and ZrPH - ionites which have not been templated with the M^{3+}-cations.[2]

The increase of the mesopores diameters of the titanium and zirconium phosphates at synthesis with the M^{3+}-templates is possible to explain as follows. As mentioned above, when forming such titanium and zirconium phosphates the stepped replacement of three charged cations from phosphatic complexes takes place. Initially these phosphates as the disconnected fragments of the structure – domains – are formed. Domains initially are presented as a colloidal solution. In the process of sol-gel reaction, domains react chemically between themselves, forming a three-dimensional network of gel. It is obvious, that the displaced three charged cations will migrate onto the surface of domains. As a result the chemical bonding of domains will occur appreciably through three charged cations. As it has already been marked, acidic M^{3+}-phosphates are considerably less stable than acidic phosphates of titanium and zirconium. Besides, after forming the gel at acidic washing the M^{3+}-phosphates are substantially dissociated, resulting in the destruction of a part of already formed bonds between domains. In result, in case of drying such synthesized phosphate hydrogel, compression of the matrix of gel appears smaller than in similar phosphates without M^{3+}. Compression of a skeleton of hydrogel in case of drying also decreases via repulsion of free acidic phosphate groups because their total quantitative increasing at acidic washing. The wet stage of such pores formation can be presented by the simplified scheme shown in Figure 2. This scheme shows the interface between two domains where the hydrated aluminum cations are situated. Before acidic washing these cations are bonded to phosphate groups. After acidic washing these cations

are removed and the resulting free acidic phosphate groups repulse each other. This is the first step of the increased mesopores formation.

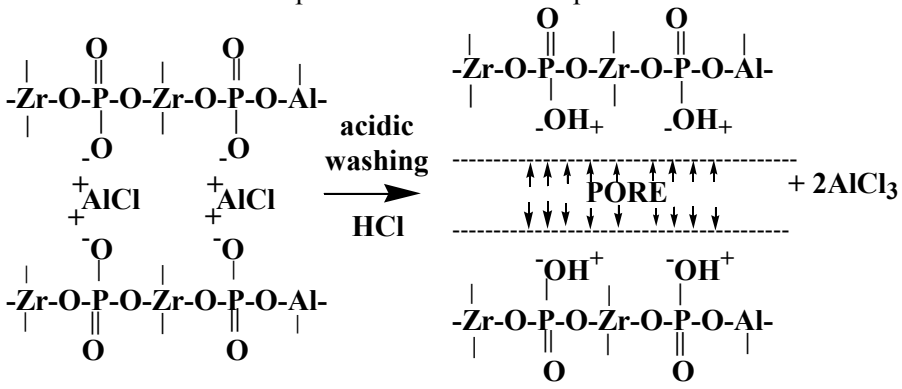

Figure 2. The first step of the mesopores formation after acidic washing in the M^{3+}-templated gel of zirconium phosphate. The second step – drying – is not presented.

Finally, after drying, the porosity of the xerogels of zirconium and titanium phosphates templated by M^{3+} -cations appears higher than in similar materials synthesized without M^{3+}-cations.

4. Conclusions

A new approach for the preparation of spherically granulated zirconium and titanium phosphates in the sol-gel technology has been proposed. Due to the utilization of three charged cations as template agents, the actual problem of the spherical beads preparation was solved via the control of the sol-gel transfer time. Using three charged cations, spherically granulated gels with larger mesopores are formed. The template M^{3+}-cations can be easily removed from adsorbents by acidic washing.

An explanation of the template effect of three charged cations on the sol-gel synthesis of high dispersed zirconium and titanium phosphates was presented. Some ways to vary and to control the porous structure of such phosphates have been shown and proposed.

REFERENCES

1. V.V. Strelko, New inorganic ion exchangers and feasibilities for their use for the treatment of industrial wastewaters, in: *Chemistry Role in the Environmental Protection* (Naukova Dumka, Kiev, 1982), pp. 179-189.
2. A.I. Bortun, and V.V. Strelko, Synthesis sorption properties and application of spherically granulated titanium and zirconium hydroxophosphates, *Proc. of the 4th Intern. Conf. on Fundamentals of Adsorption*, Kyoto, 58-65, (1992).

3. I.Z. Zhuravlev, O. Zakutevsky, T. Psareva, V. Kanibolotsky, V. Strelko, M. Taffeta, and G. Gallios, Uranium sorption on amorphous titanium and zirconium phosphates modified by Al^{3+} or Fe^{3+} ions, *J. Radioanal. Nucl. Chem.* 254, 85-89, (2002).
4. I.Z. Zhuravlev, Sol-gel synthesis and properties of ionites based on composite phosphates of polyvalent metals and silica, *Ph.D. Thesis* (Chemistry), Kiev, Ukraine, 2005.
5. D.E.C. Corbridge, *Phosphorus: an Outline of its Chemistry and Technology* (Elsevier, New York, 1980).
6. C.B. Amphlett, *Inorganic Ion Exchangers* (Elsevier, New York, 1964).
7. T. Kanazava, *Inorganic Phosphate Materials* (Elsevier, Amsterdam, 1989).

NEW SPHERICALLY GRANULATED INORGANIC ION EXCHANGERS ON THE BASIS OF TITANIUM PHOSPHATE

ANNA A. ZAITSEVA*, VALENTIN A. KANIBOLOTSKY, VALERIY I. YAKOVLEV AND VLADIMIR V. STRELKO
Institute for Sorption and Problems of Endoecology, NAS of Ukraine, General Naumov str., 13, Kiev, 03164, Ukraine

Abstract. New gel method of synthesis of spherically granulated titanium phosphate materials from technical $TiOSO_4$ solution has been developed. The influence of additional hydrothermal treatment of synthesized materials in the adsorption properties, crystal structure and chemical stability is studied.

Keywords: Titanium phosphate; hydrothermal treatment; structure characteristics

1. Introduction

Ion exchange technology is widely used for water and waste treatment, in medicine, environmental protection, etc.[1] It was found that the inorganic ion exchangers can operate in extreme conditions (high temperature or strong radiation fields, in the presence of organic solvents and oxidants and in a great excess of competitive ions), where organic resins fail to work efficiently.[1,2]

Inorganic ion exchangers on the basis of amorphous titanium phosphate due to their high sorption capacity and selectivity towards heavy metals ions are candidate materials for purification of industrial wastes and process solutions.[3,4] Producing these materials in spherically granulated form allow their use in column operation. One of the main requests for these materials is chemical (hydrolytic) stability. It is known[5,6] that properties of titanium

* To whom correspondence should be addressed. Anna A. Zaitseva, Institute for Sorption and Problems of Endoecology, NAS of Ukraine, General Naumov str., 13, Kiev, 03164, Ukraine; e-mail: zaitseva@ispe.kiev.ua

J.M. Loureiro and M.T. Kartel (eds.), Combined and Hybrid Adsorbents, 99–104.

phosphate ion exchangers depend on the way of synthesis and on the subsequent treatment.

2. Experimental

Spherically granulated titanium phosphates (TiP) were synthesized by an original gel method in the form of spherical granules.[7] A 2.5 M H_3PO_4 solution and a technical 1.5 M $TiOSO_4$ solution (industrial half-product of TiO_2 pigment production) were used as initial reagents. The reaction mixture (with molar ratio P/Ti =1.0, 1.5, 2.0) was dispersed into a vertical column filled with paraffin oil. The gelation time was from 3 to 10 s. In the column the preparation of spherical granules took place – drops of the reaction mixture transforming into spherical granules of titanium phosphate hydrogel are formed in the organic liquid. After separation from the organic liquid the granules of gel were thoroughly washed with distilled water and then dried in air.

The hydrothermal treatment of TiP samples were done in a Teflon lined autoclave in the temperature range from 130 ºC to 225 ºC during 3, 8 and 24 hours into the water. After treatment, samples were washed by distilled water at pH 3.5-4.0 and dried in the air.

The hydrolytic stability of TiP samples was studied using 0.1 N NaCl-NaOH model solutions at room temperature, in the ratio solid:liquid=1:100, duration of contact 48 h at constant shaking.

Nitrogen adsorption-desorption isotherms were collected at 77 K in a Micrometrics ASAP 2010 analyzer. Pore size distributions were calculated using the Cranston and Inkley method for cylindrical pores, the pore volumes V_s ($cm^3 \cdot g^{-1}$) were determined by exsiccater method with H_2O and C_6H_6 vapors.

X-ray diffraction spectra were recorded on a Siemens diffractometer using CuK_α radiation and germanium monochromator.

3. Results and Discussion

Amorphous titanium phosphate (TiP) samples have been obtained in the spherically granulated form by sol-gel technology as described above from $TiOSO_4$ and H_3PO_4 solutions with different initial molar ratio P/Ti=1.0 (TiP-1), 1.5 (TiP-1.5), 2.0 (TiP-2). The synthesized TiP samples were found to be mesoporous materials (V_s= 0.58-0.74 cm^3/g) with narrow pore size distribution (d_{av}= 150-180 Å) and high enough surface area (S_{spec}= 280–300 m^2/g). The influence of the hydrothermal treatment conditions in some structural characteristics is shown in Table 1. As can be seen from the

data presented (Table 1) the values of pore volume and surface area of hydrothermally treated TiP samples depend on initial composition of TiP samples, duration of process and temperature at which the treatment is conducted. It should be noted that in all cases, in the temperature range from 130 to 180 ºC, the TiP granules were not destroyed. The increase of either the duration of treatment (more than 48 h) or temperature (more than 180 ºC) leads to partial or total destruction of them. It was found that hydrothermal treatment of TiP-samples with low phosphorus contents (TiP-1) during 3-6 hours leads to increasing of mesopore volume (from 0.65 to 1.15 cm^3/g), but longer (from 6 to 24 hours) treatment results in decreasing of mesoporous volume to 0.85 cm^3/g. For samples with higher phosphorus contents (TiP-2) the dependence of mesoporous volume on the treatment duration was found to be different: the hydrothermal treatment results on constant decreasing of porous volume and in obtaining TiP samples with V_s=0.2-0.27 cm^3/g. In the whole temperature range studied we found

TABLE 1. Conditions of hydrothermal treatment and physical-chemical characteristics of obtained TiP-samples

n	Initial sample	Duration of treatment, h	T, ºC	Vs, micro, cm^3/g	Vs, meso, cm^3/g	Humidity, %	S_{spec}, m^2/g	$R_{ef}=2V_s/S$, nm
1	TiP-1	0	-	0.26	0.69	53	295	4.68
2	TiP-1.5	0	-	0.21	0.65	60	300	4.30
3	TiP-2	0	-	0.25	0.58	46	290	4.00
4	TiP-1	3	130	0.21	1.00	11	190	10.50
5	TiP-1.5	3	130	0.22	0.74	16	195	7.60
6	TiP-2	3	130	0.23	0.47	14	130	7.20
7	TiP-1	6	130	0.22	1.15	7	175	13.10
8	TiP-1.5	6	130	0.27	0.83	10	140	11.80
9	TiP-2	6	130	0.23	0.54	9	105	10.20
10	TiP-1	24	130	0.18	0.85	13	140	12.10
11	TiP-1.5	24	130	0.21	0.48	12	105	9.10
12	TiP-2	24	130	0.20	0.28	11	85	6.60
13	TiP-1	3	160	0.18	1.10	10	200	11.00
14	TiP-1.5	3	160	0.21	0.46	13	195	4.70
15	TiP-2	3	160	0.20	0.43	14	130	6.60
16	TiP-1	24	160	0.12	0.53	3	120	8.80
17	TiP-1.5	24	160	0.10	0.31	3	95	6.50
18	TiP-2	24	160	0.05	0.20	3	75	5.30
19	TiP-1	48	160	0.10	0.24	2	90	5.30
20	TiP-1.5	48	160	0.07	0.27	2	65	5.50
21	TiP-2	48	160	0.04	0.20	2	55	5.45

decreasing of surface area with increasing either duration or temperature of treatment. As shown in Table 1 (n=13-21) the influence of the treatment at a higher temperature on the physical-chemical characteristics of TiP samples is analogous to the one described earlier.

X-ray spectrum of hydrothermally treated TiP-1, TiP-1.5 and TiP-2 samples during 6 h at 130 ºC are presented in Figure 1. It should be noted that all the initial TiP samples were found to be amorphous materials. From the analysis of the data presented it can be seen that the hydrothermal treatment leads to the formation, development and increasing of the amount of crystalline phases in the structure of TiP samples. It is seen (Figure 1) that the TiP-1 (line 1) and TiP-1.5 (line 2) samples after 6 hours treatment are still amorphous materials, but for TiP-2 sample (line 3) good crystallized peaks are presented. It should be noted that calcinations of TiP samples in air leads to the formation of crystalline material at temperatures over 650 ºC. It is found that crystallization occurs easily for samples with higher phosphorus contents – after 6 hours treatment TiP-1 and TiP-1,5 samples are still amorphous (Figure 1, lines 1 and 2), but for TiP-2 (Figure 1, line 3) two crystalline phases, of titanium phosphate $(TiO)_2P_2O_7$ and titanium dioxide TiO_2 (rutile) in mass ratio 3:1 are found. In our opinion this result is connected with the different initial polymer structure of the studied materials. Composition of samples is determined by competition between the going on processes of hydrolysis of phosphate groups (that results in TiO_2 phase formation) and crystallization of polyphosphate phase. From X-ray data it was found that after 24 hours treatment all studied samples were crystalline materials with different ratio of polyphosphate $(TiO)_2P_2O_7$ and dioxide TiO_2 phases. For TiP-1 samples the ratio of $(TiO)_2P_2O_7$ to TiO_2 (rutile) was found to be 2:1, for TiP-1.5 – 3:1, and for TiP-2 – 5:1. It is seen that the amount of the phosphate containing phase is larger in the samples with higher phosphorus content in the starting material. The difference between the compositions of TiP-2 samples after 6 and 24 hours treatment is due to the formation of a product with higher quantity of $(TiO)_2P_2O_7$ phase because of the continuation of the crystallization of the amorphous part that could still be present in the sample after 6 hours treatment.

From comparison of X–ray data and adsorption measurement it can be seen that during the initial stages of hydrothermal treatment (τ=3-6 hours) – crystal nucleus formation stage – the pore structure with predominance of large size pores (r_{ef} > 10 nm) is forming. In our opinion, during this treatment stage the particles consolidation and decrease of dispersity degree can be going on, the results of which is changing of pore forms and obtaining of wide porous materials with spherical shape of pores. This

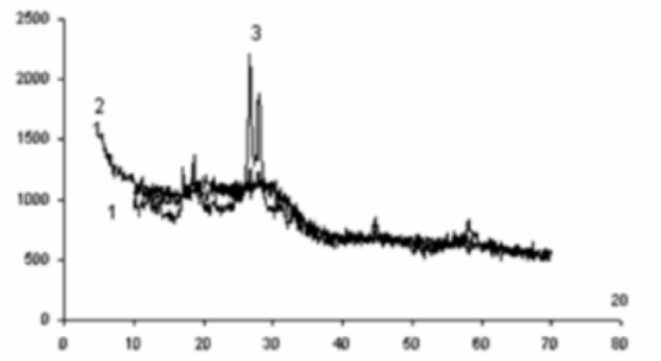

Figure 1. X-ray spectra of hydrothermally treated TiP samples: TiP-1 (line 1), TiP-1.5 (line 2), TiP-2 (line 3) during 6 h at 130 ºC.

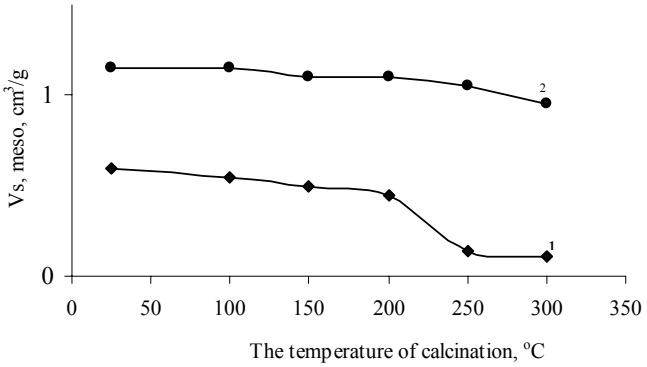

Figure 2. Dependence of mesoporous volumes on calcination temperatures of TiP samples: 1 – initial TiP sample, 2 – hydrothermally treated TiP sample (130 ºC, 24 h).

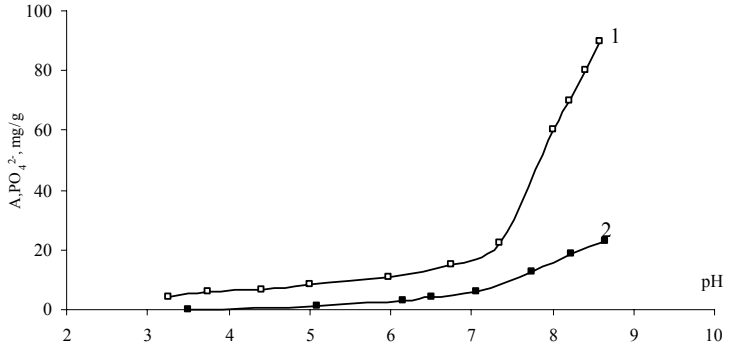

Figure 3. Dependence of hydrolytic stability of TiP samples on pH of solution: 1 – initial TiP sample, 2 – hydrothermally treated TiP sample (130 ºC, 24 h).

process causes rising of pore volume and decreasing of surface area. At longer treatment times, with increasing of crystallization processes of TiO_2 and TP phases, the pore size decreases, which results in pore volume decreasing.

It was found that hydrothermal treatment leads to increasing thermal and chemical (hydrolytic) stability of synthesized materials. For initial TiP samples it was observed that calcinations result in the decrease of mesoporous volumes (Figure 2, line 1), which was not observed for the hydrothermally treated TiP samples (Figure 2, line 2). It was found that during calcinations in the temperature range 100-300 ºC the values of mesoporous volumes of hydrothermally treated TiP samples do not change as much as for the initial TiP samples. From the data presented on the dependence degree of hydrolysis (amount of desorbed PO_4^{2-} anions) anions of TiP samples on pH (Figure 3) it is seen that the hydrolytic stability decreases with increasing of solution pH both for initial and hydrothermal treated samples (TiP-12 in Table 1). But the hydrothermally treated sample is much more chemically stable in alkali and neutral media; in our opinion this is connected with the formation of a semicrystalline or crystalline structure in the TiP samples.

4. Conclusions

The crystallization processes that occur during hydrothermal treatment of TiP samples determine the character of changing of their adsorption properties, giving the opportunity to a strong regulation of the TiP structure geometries and of increasing the thermal and chemical stability of synthesized materials.

REFERENCES

1. A. Clearfield, Role of ion exchange in solid state chemistry, *Chemical Reviews* 88, 125-158 (1988).
2. E.V. Egorov, and S.V. Makarova, *Ion exchange in radiochemistry* (Atomizdat, Moskow, 1971).
3. C.B. Amphlett, *Inorganic ion exchangers* (Elsevier, New York, 1964).
4. A. Clearfield, A.I. Bortun, V.V. Khainakov, and V.V. Strelko, Spherically granulated titanium phosphates as exchanger for toxic heavy metals, *Waste Management* 18, 203-210 (1998).
5. A. Clearfield, G.N. Nancollas, and R.H., New inorganic ion exchangers, *Ion Exchange and Solvent Extraction* 5, 1-120 (1973).
6. V. Vesely, and V. Pekarek, Synthetic inorganic ion exchangers –I. Hydrous oxides and acidic salts of multivalent metals, *Talanta* 19, 219-262 (1972).
7. V.V. Strelko, V.I. Yakovlev, V.A. Kanibolotsky, and H.O. Zaitseva, Synthesis of spherically granulated sorbent, Ukrainian Patent № 40389 A (16.07.2001).

IRON-BASED NANOADSORBENTS FOR THE REMOVAL OF METAL IONS FROM WATER

E.A. DELIYANNI, E.N. PELEKA* AND K.A. MATIS
School of Chemistry, Aristotle University of Thessaloniki, Greece

Abstract. Considering the harmful effects of heavy metals, it is necessary to remove them from liquid wastes at least to a limit accepted by regulatory agencies before their discharge to the environment – i.e. there is a need for a capable, cost-effective treatment method. The application of an innovative, simple and low cost method was tested for the preparation of nanocrystalline iron hydroxides and oxyhydroxides; different iron precursors have been earlier used and combined to different volatile precipitating agents. The examined in the present product, akaganéite [beta-FeO(OH)], had high surface area and definite pore size distribution. Main aim of this study was to evaluate the efficiency of the prepared material in the removal of heavy metal ions, like cadmium cations and arsenate oxyanions, metals that constitute priority pollutants. Batch and column experiments were conducted in current research to investigate metal ions removal.

Keywords: akaganéite; cadmium; arsenic; adsorption; wastewater

1. Introduction

The control and removal of contaminants produced by the technological activities of mankind has become an important issue due to increased significance of related pollution aspects and to water scarcity. Large quantities of process streams in chemical and metallurgical industries

* To whom correspondence should be addressed. E.N. Peleka, Laboratory of General & Inorganic Chemical Technology, Department of Chemistry, Aristotle University, GR54124, Thessaloniki, Greece; e-mail: peleka@chem.auth.gr

J.M. Loureiro and M.T. Kartel (eds.), Combined and Hybrid Adsorbents, 105–110.

contain rather moderate concentrations of toxic metal ions, which have to be removed or recovered, following severe environmental constraints. Cadmium-polluted wastewaters are generated, for instance, by a number of industries that include mainly metal-finishing, electroplating, ceramics and inorganic pigments production and acid mine drainage. Several adsorbents have been applied for the removal of cadmium, such as zeolites, bentonite, clay, dead biomass, chitosan, seaweed, different barks, modified wool, nut shell, xanthate, etc.[1] Cost is an important parameter for comparing adsorbents and iron-based materials certainly belong to the category of low-cost ones.

Arsenic is a contaminant in the groundwater of some regions. It is "famous" for its high toxicity and its ability to induce skin cancer on long-term ingestion.[2] Arsenic occurrence and mobility in natural water and its removal in water treatment have also become the focus of increasing attention.[3] The most common technique for arsenic removal is coagulation with ferric salts followed by filtration.[4]

Hydrous oxides and oxyhydroxides have been known to control trace elements removal,[5] although their use has been limited, mostly due to competition with the commercially available aluminum oxides[6] or active carbon.[7] Various methods for their artificial synthesis have been reported.[8] These materials are available only as fine powders or are generated in aqueous suspensions as a hydroxide floc or gel; in these forms they retain their desirable sorptive properties for trace elements.

The aim of the present review paper is the investigation of nanocrystalline iron oxyhydroxides and hydroxides, synthesized by a novel method; various chemical reagents were tested as feed giving different products. These materials, being well characterized, have been applied to wastewater treatment in order to remove by sorption metal ions, either cations or oxyanions. The reasons for selecting these bonding materials, like akaganéite (and goethite), are that they are cheap, easily prepared and presenting low risks for adding a further pollutant to the treated aqueous system.

2. The Adsorbent Material

The synthesis of the examined materials involves the hydrolysis of aqueous solutions of ferric salts followed by membrane purification and freeze drying of the products.[9] Three different precursors were used and combined to three different volatile precipitating agents. The obtained products were of the following types: akaganéite [β-FeO(OH)], goethite [α-FeO(OH)] and iron(III) hydroxide. Irrespective of the starting materials used, all products presented some very interesting and unique features and morphology.

Akaganéite (denoted as Ak) was prepared in the laboratory from an aqueous solution of iron(III) chloride salt and ammonium carbonate as precipitation agent. The crystal structure of the synthesized sample was examined by X-ray diffraction - see Figure 1. The material that appeared in the form of powder had BET surface area of 330 m^2/g, pore sizes in the meso- and micropore regions, and narrow pore size distribution (Figure 2). Figure 3 shows a SEM micrograph, which revealed that the material grains had all about similar morphology and an average size between 30-100 μm.[10] Its average crystallite size was 2.6 nm, estimated by TEM, as shown in Figure 4. Thus, the applied technique produced samples with a crystallite size much smaller than previously reported applications.[8] This small size resulted in a well-defined electron diffraction pattern. The aforementioned data from TEM measurements were also in accordance with the crystallite size estimated (by the Scherrer equation) of the respective XRD pattern. FTIR spectra of the material for its characterisation were taken, too. Electrokinetic measurements were also conducted, expressed traditionally as ζ–potential values. The point of zero charge of akaganéite after the sorption of cadmium cations was slightly shifted from 7.3 to 8 approximately.

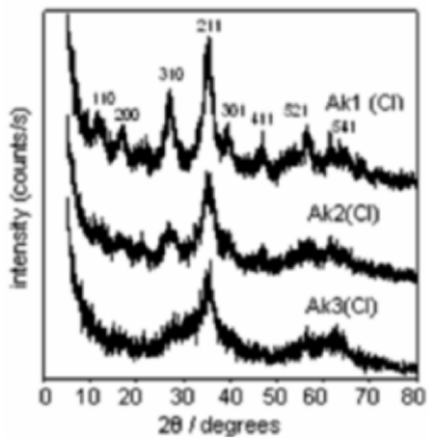

Figure 1. XRD patterns of akaganéite and other iron oxy-hydroxide samples prepared. Reprinted with permission from ref. 9; copyright Elsevier.

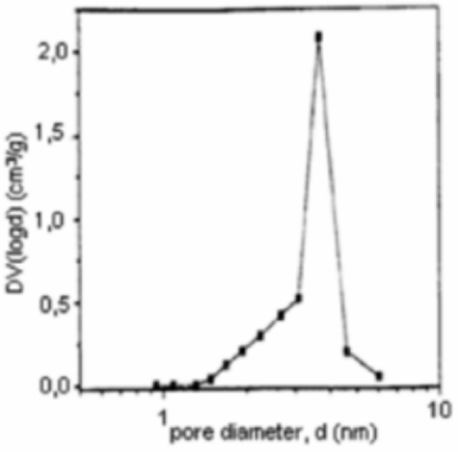

Figure 2. Desorption DV(logd) graph of akaganéite. Reprinted with permission from ref. 8; copyright Elsevier.

3. Sorption of Cadmium and Arsenic

It is known that adsorption due to electrostatic forces (physical sorption) is very fast, of the order of few seconds. The shift of the point of zero charge indicates a weak chemisorption or perhaps, a combination of physical and chemical sorption. At pH values lower than the p.z.c. the majority of the surface sites of the adsorbent material will be positively charged. The surface charge is due to the dissociation reactions of akaganéite, which has an ampholytic character.

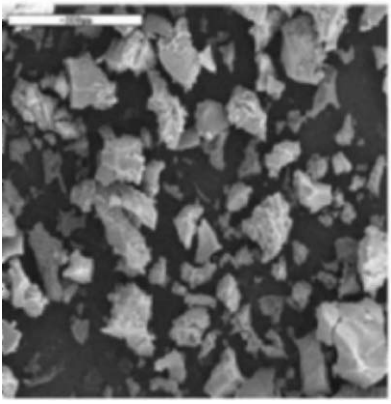

Figure 3. SEM photograph of the material (following Cd sorption). Reprinted with gratitude from ref. 10; copyright Technical Faculty Bor, Univ. Belgrade.

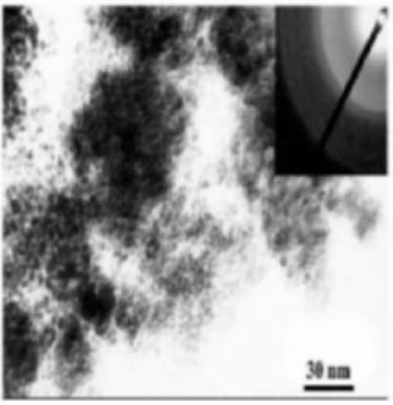

Figure 4. TEM micrograph and O-ring pattern (top right) of akaganéite as prepared. Reprinted with permission from ref. 8; copyright Elsevier.

Testing in detail the effect of sorbent amount, quantities greater than 1 g/L gave constant removals. The latter was greatly affected by solution pH (see Fig. 5). Cadmium removals were changing from almost 0 to 95% inside a pH change of 2.5 units. The known Langmuir and Freundlich models were then examined;[10] both gave quite good fitting (with correlation coefficient, R^2, respectively 0.994 and 0.997).

From the distribution of surface species of the adsorbent it can be noticed that in this pH range there is also an increase in the concentration of surface species of SOH type (neutral form); the curve of increase of SOH surface sites keeps up with that of pH change. So, the following possible reaction could be written: $SOH + Cd^{2+} \leftrightarrow SOCd^{+} + H^{+}$. In the case of a surface chemisorption going on (which was the probable mechanism), the species SO^{-} of akagenéite appear at pH greater than 8. Figure 5 presents the influence of ionic strength of solution, showing cadmium removal to be slightly decreased with increasing ionic strength. These macroscopic

observations were used to differentiate between the kinds of adsorption.[11] X-ray photoelectron spectroscopy (XPS) has been recently applied to this area, revealing also useful information on the mechanism.[12]

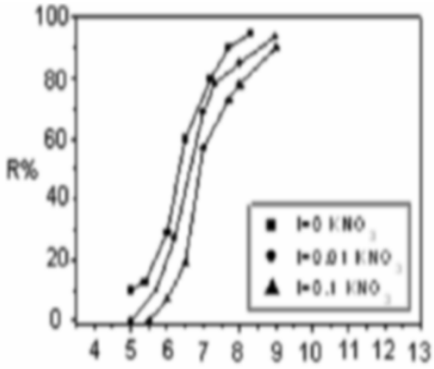

Figure 5

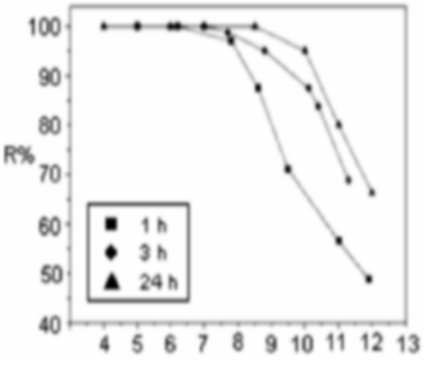

Figure 6

Figure 5. Effect of pH on the adsorption of cadmium onto akaganéite, for different values of ionic strength. Reprinted with gratitude from ref. 10; copyright Technical Faculty Bor, Univ. Belgrade.

Figure 6. Effect of pH on As(V) removal for different contact time. Reprinted with permission from ref. 13; copyright Elsevier.

This synthesized inorganic material was also effectively tested as an adsorbent of arsenates, Figure 6.[13] Adsorption isotherms were found to fit sufficiently the known Langmuir equation, with maximum sorption capacity of the order of ~120 mg/g. In general, the removal of arsenate oxyanions with the same adsorbent was significantly better than that for cadmium ion.

The amount of arsenate adsorption increased by lowering the pH of the system and by increasing the amount of the sorbent and the ionic strength of the solution. The system achieved equilibrium in the order of few hours, which possibly indicates a specific adsorption of arsenic species on akaganéite.

The possibility of using a packed-bed in column configuration of akaganéite to remove As(V) oxyanions and Cd cations from aqueous solutions was, finally, the aim of another study.[14] Synthesized akaganéite was used in two forms, i.e. in fine powder of nanocrystals and in the form of grains, as granular. The main examined parameters were the quantity of sorbent in the column and the presence (or not) of ionic strength. The Bed Depth-Service Time (BDST) equation has been applied to the sorption results in order to model the column operation.

ACKNOWLEDGEMENTS

Many thanks are due to the organisers of this meeting for their invitation and hospitality in Kiev; also, to our colleague at the Laboratory of General and Inorganic Chemical Technology, Dr. D.N. Bakoyannakis for his help.

REFERENCES

1. S.E. Bailey, T.J. Olin, R.M. Bricka, and D.D. Adrian, A review of potentially low-cost sorbents for heavy metals, *Wat. Res.* 33, 2469-2479 (1999).
2. W. Lepkowski, Graduate studies need to get back to basics*, Chem. Eng. News* 76(46), 27-29 (1998).
3. M.L. Pierce, and C.B. Moore, Adsorption of arsenite and arsenate on amorphous iron hydroxide, *Wat. Res.* 16, 1247-1253 (1982).
4. R.C. Cheng, N.C. Wang, and M.D. Beahler, Enhanced coagulation for arsenic removal, *J. AWWA* 86(9), 79-90 (1994).
5. Trace Inorganic Substances (TIS) Research Committee, A Review of Solid-Solution Interactions and Implications for the Control of Trace Inorganic Materials in Water Treatment, *J. AWWA* 80(10), 56- (1988).
6. M.A. Anderson, J.F. Ferguson, and J.J. Gavis, Arsenate adsorption on amorphous aluminum hydroxide, *J. Coll. Interface Sci.* 54, 391-398 (1976).
7. G. McKay, *Use of Adsorbents for the Removal of Pollutants from Wastewaters* (CRC Press, Boca Raton, 1995).
8. E.A. Deliyanni, D.N. Bakoyannakis, A.I. Zouboulis, K.A. Matis, and L. Nalbandian, Akaganėite-type β-FeO(OH) nanocrystals: preparation and characterization*, Microporous Mesoporous Mater.* 42, 49-57 (2001).
9. D.N. Bakoyannakis, E.A. Deliyanni, A.I. Zouboulis, K.A. Matis, L. Nalbandian, and Th. Kehagias, Akaganeite and goethite-type nanocrystals: synthesis and characterization, *Microporous Mesoporous Mater.* 59, 35-42 (2003).
10. E.A. Deliyanni, D.N. Bakoyannakis, A.I. Zouboulis, and K.A. Matis, Development and study of iron-based nanoadsorbents, in: *Proc. 36th Intl. October Conf. Mining Metal.*, Bor Serbia, 2004.
11. K.F. Hayes, Ch. Papelis, and J.O. Leckie, Modelling ionic strength effects on anion adsorption at hydrous oxide/solution interfaces, *J. Coll. Interface Sci.* 125, 717-726 (1988).
12. E.A. Deliyanni, and K.A. Matis, Sorption of Cd ions onto akaganeite-type nanocrystals*, Sep. Purif. Tech,* in press.
13. E.A. Deliyanni, D.N. Bakoyannakis, A.I. Zouboulis, and K.A. Matis, Sorption of As(V) ions by akaganeite-type nanocrystals, *Chemosphere* 50, 155-163 (2003).
14. E.A. Deliyanni, D.N. Bakoyannakis, A.I. Zouboulis, and E.N. Peleka, Removal of arsenic and cadmium by akaganéite fixed-beds*, Sep. Sci. Tech.* 38, 3967-3981 (2003).

PRELIMINARY STUDY ON THE ADSORPTION OF THE CATIONIC DYE ASTRAZON RED BY A PORTUGUESE BENTONITE

SÍLVIA C.R. SANTOS*, RUI A.R. BOAVENTURA
Laboratory of Separation and Reaction Engineering (LSRE), Dep. Eng. Química, Faculdade de Engenharia da Universidade do Porto, Rua Dr. Roberto Frias, 4200-465 Porto, Portugal.

ÁLVARO F.M. OLIVEIRA
Laboratório do Instituto Nacional de Engenharia, Tecnologia e Inovação (INETI), Rua da Amieira, 4465 S. Mamede Infesta, Portugal

Abstract. The adsorption of Astrazon Red (C.I. Basic Red 46) in aqueous solution by a bentonite clay from Benavila, Portugal, was studied. The bentonite sample was mainly composed of montmorillonite, Na-Feldspar and calcite (XRD analysis). The texture characteristics were determined by Hg and He porosimetry and the specific surface area by the methylene blue adsorption method. A kinetic experiment was carried out at 15 ºC to determine the time required to reach equilibrium. Experimental data were well described by the pseudo-second order kinetic model. Adsorption equilibrium isotherms were determined at different temperatures and the results fitted to Langmuir and Freundlich models. According to Langmuir model, the adsorption capacities were 141.0, 148.7 and 157.8 mg/g at 15, 25 and 35 ºC, respectively.

Keywords: Adsorption; Textile dyes; bentonite clay; kinetics; equilibrium

* To whom correspondence should be addressed. Sílvia Santos, Laboratory of Separation and Reaction Engineering (LSRE), Departamento de Engenharia Química, Faculdade de Engenharia da Universidade do Porto, Rua Dr. Roberto Frias, 4200-465 Porto, Portugal; e-mail: silviacs@fe.up.pt

J.M. Loureiro and M.T. Kartel (eds.), Combined and Hybrid Adsorbents, 111–116.

1. Introduction

Industrial effluents are one of the major causes of environmental pollution. Textile industries discharge a large quantity of highly colored wastewaters due to unfixed dyes on fibers.

Conventional chemical, physical and biological processes are usually ineffective for color removal. Adsorption has been shown to be a good alternative and systems using activated carbon have been successful.[1] As costs associated with replacement and regeneration of activated carbon are high, agricultural waste residues,[2] natural materials containing chitin,[3] biomaterials like algae,[4] fly ash,[5] hydroxide metal sludge,[6] sewage sludge,[7] and clays[8,9] have been investigated as potential adsorbents.

Clay materials such as bentonite, zeolite, sepiolite, dolomite and Fuller´s earth, have high specific area, high chemical and mechanical stability, high cationic exchange capacities and surface and structural properties,[8] which make them used.

Bentonite clay is mainly composed of montmorillonite, which is a 2:1 type alluminosilicate. Bentonite or montmorillonite have been used in adsorption investigations, both in natural and modified forms as homoionic bentonites (prepared by cations saturation), organophilic bentonites (with quaternarium ammonium compounds) and acid activated bentonites. The specific surface area and surface acidity of clays could be greatly increased by acid activation.[8]

In this preliminary study, natural bentonite clay was used to adsorb a cationic textile dye in aqueous solution.

2. Materials and Methods

2.1. ADSORBATE AND ADSORBENT PROPERTIES

The selected dye Astrazon Red FBL 200% 03 (C.I. Basic Red 46) was kindly offered by Dystar. It is an azoic dye and its chemical structure is presented in Figure 1. The wavelength corresponding to maximum absorbance (λ_{max}) is 525 nm.

The bentonite was collected in Benavila, Alentejo, Portugal. The clay was manually disaggregated, sieved, dried at 102 ºC and stored in a desiccator. The fraction 0.150-0.300 mm was used.

The mineralogical composition of the natural bentonite was determined by X-ray diffraction (XRD) analysis and the textural characteristics by Hg and He porosimetry (Table 1).

The specific surface area of the bentonite was estimated by the Methylene Blue adsorption method. Assuming the area covered by one methylene blue molecule as 130 $Å^2$, we obtained an adsorption capacity of 97.16 mg/g and a specific surface area of 238 m^2/g.

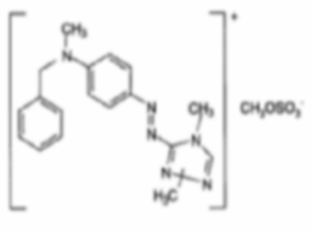

Figure 1. Chemical structure of Astrazon Red.

TABLE 1. Composition and physical texture characterization by Hg and He porosimetry of the bentonite clay

Composition		Physical characterization by porosimetry		
Minerals	% by weight		Hg	He
Montmorillonite	35	Mean pore diameter (μm)	0.218	
Na-Feldspar	21	Median pore diameter (μm)	1.49	
Calcite	18	Apparent density (g/cm^3)	2.17	
Amphibole	15	Real density (g/cm^3)		2.57
Chlorite	8	Intraparticle porosity (%)	11.4	
Quartz	3	Total porosity (%)	12.8	15.8

2.2. KINETIC EXPERIMENT

An amount of 1 g of bentonite was added to 1 L of Astrazon Red solution (110 mg/L), and stirred in a jacketed reactor at a constant temperature of 15±0.3 ºC. Samples were taken at different contact times to determine the time required to reach equilibrium. After centrifugation at 13400 rpm (Mini Spin Eppendorf centrifuge), the absorbance of the supernatant was measured at 525 nm (Helius-α UV-Vis spectrophotometer) and then converted into concentration.

2.3. EQUILIBRIUM EXPERIMENTS

Adsorption isotherms were determined at 15, 25 and 35 ºC by shaking 100 mL of Astrazon Red solutions of different concentrations with 0.100 g of bentonite in 100 mL flasks at constant temperature. The solution pH was initially adjusted to 7 with NaOH. After eight hours of contact to guarantee

that equilibrium was attained, samples were centrifuged and the dye concentration determined in the supernatant.

3. Results and Discussion

3.1. KINETIC STUDY

Pseudo-first order and pseudo-second order rate expressions are given by Eq. (1) and Eq. (2), respectively,

$$\frac{dq}{dt} = k_1 \cdot \left(q_{eq} - q\right) \tag{1}$$

$$\frac{dq}{dt} = k_2 \cdot \left(q_{eq} - q\right)^2 \tag{2}$$

where q (mg/g) is the amount of dye adsorbed at time t (min), k_1 (min^{-1}) and k_2 (g/mg/min) are the rate constants and q_{eq}(mg/g) is the amount of dye adsorbed at equilibrium. Experimental data were fitted to the integrated forms of these equations, respectively,

$$q = q_{eq} \cdot \left[1 - \exp\left(-k_1 \cdot t\right)\right] \tag{3}$$

$$q = q_{eq} \frac{q_{eq} \cdot k_2 \cdot t}{1 + q_{eq} \cdot k_2 \cdot t} \tag{4}$$

Experimental data and model curves are plotted in Figure 2.

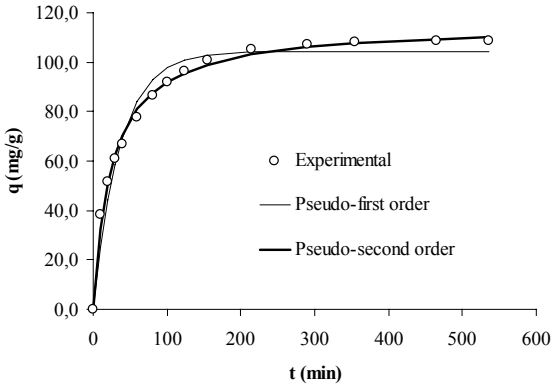

Figure 2. Effect of contact time on the adsorption of Astrazon Red by bentonite at 15ºC.

Adsorption was initially quite rapid: after 30 min contact time, more than 50% of the ultimate adsorption had occurred (Figure 2). For practical purposes equilibrium was considered to be achieved in 6 hours. Fitting data to kinetic models was performed by non-linear regression (software Fig P from Biosoft). Model parameters, k_1 and q_{eq}, obtained from pseudo-first order fit are 2.74×10^{-2} min^{-1} and 104.5 mg/g, respectively. From pseudo-second order model fit, the obtained values of k_2 and q_{eq} are 3.39×10^{-4} g/min/mg and 115.4 mg/g. The correlation coefficients (r^2) for pseudo-first and pseudo-second order fits were found to be 0.974 and 0.995, respectively.

3.2. EQUILIBRIUM STUDY

Equilibrium experimental data at 15, 25 and 35 ºC were fitted to Langmuir and Freundlich models and the respective parameters are shown in Table 2. Equilibrium isotherm at 25 ºC is presented in Figure 3.

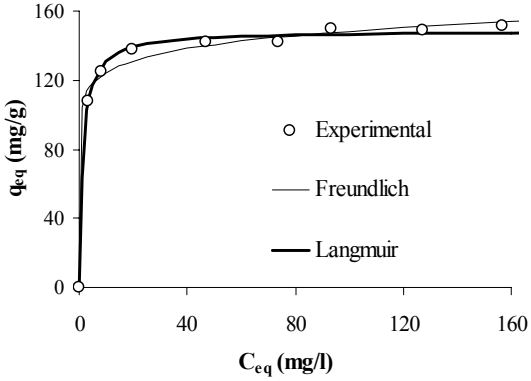

Figure 3. Equilibrium isotherm at 25 ºC.

TABLE 2. Equilibrium isotherm parameters at 15, 25 and 35 ºC

T (ºC)	Langmuir Model			Freundlich Model		
	q_{max} (mg/g)	K_L (L/mg)	r^2	K_F ($mg.g^{-1}.(mg.L^{-1})^{-1/n}$)	n	r^2
15	141.0	1.13	0.997	102.8	13.8	0.992
25	148.7	0.74	0.996	104.3	13.1	0.993
35	157.8	0.86	0.995	114.0	14.3	0.981

Langmuir model fits better the experimental data than Freundlich model. Maximum adsorption capacity (q_{max}) slightly increases with temperature. The same tendency is shown by the values of K_F. The affinity of the dye to the adsorbent decreases as temperature increases from 15 to 25 ºC and then remains practically constant. The values of n, greater than one, indicate a favorable adsorption.

4. Conclusions

The adsorption capacities obtained in the present study are greater than that found using commercial activated carbon Chemviron Carbon, UK (106 mg/g), but smaller than the value obtained with a carbon developed from sewage sludge (188 mg/g).[7]

ACKNOWLEDGMENTS

The authors wish to thank *Fundação para a Ciência e Tecnologia* (FCT) for the scholarship and financial support.

REFERENCES

1. K. Kadirvelu, C. Karthika, N. Vennilamani, and S. Pattabhi, Activated carbon from industrial solid waste as an adsorbent for the removal of Rhodamine-B from aqueous solution: Kinetic and equilibrium studies, *Chemosphere* 60, 1009-1017 (2005).
2. T. Robinson, B. Chandran, and P. Nigam, Removal of dyes from an artificial textile dye effluent by two agricultural waste residues, corncob and barley husk, *Environ. Int.* 28, 29-33 (2002).
3. S.A. Figueiredo, R.A. Boaventura, and J.M. Loureiro, Color removal with natural adsorbents: modelling, simulation and experimental, *Sep. Purif. Technol.* 20, 129-141 (2000).
4. Z. Aksu and S. Tezer, Biosorption of reactive dyes on the green alga Chlorella vulgaris, *Process Biochem.* 40, 1347-1361 (2005).
5. B. Acemioğlu, Adsorption of Congo red from aqueous solution onto calcium-rich fly ash, *J. Colloid Interface Sci*. 274, 371-379 (2004).
6. S. Netpradit, P. Thiravetyan, and S. Towprayoon, Adsorption of three azo reactive dyes by metal hydroxide sludge: effect of temperature, pH, and electrolytes, *J. Colloid Interface Sci.* 270, 255-261 (2004).
7. M. J. Martin, A. Artola, M. D. Balaguer, and M. Rigola, Activated carbons developed from surplus sewage sludge for the removal of dyes from dilute aqueous solutions, *Chem. Eng. J.* 94, 231-239 (2003).
8. A. S. Özcan, and A. Özcan, Adsorption of acid dyes from aqueous solutions onto acid-activated bentonite, *J. Colloid Interface Sci.* 276, 39-46 (2004).
9. R. Wibulswas, Bach and fixed bed sorption of methylene blue on precursor and QUACs modified montmorillonite, *Sep. Purif. Technol*. 39, 3-12 (2004).

PART II

ACTIVATED CARBON, COMBINED ADSORBENTS AND OTHER ORGANIC ADSORBENTS

MORPHOLOGY AND SURFACE CHEMISTRY OF CHEMICALLY TREATED ACTIVATED CARBONS

KRISZTINA LÁSZLÓ*
Department of Physical Chemistry, Budapest University of Technology and Economics, Budapest 1521, Hungary

Abstract. Microporous activated carbons were prepared from poly(ethyleneterephthalate). This carbon was functionalized to different degrees by cold and hot nitric acid treatment combined with subsequent heating in inert atmosphere to obtain samples with different surface chemistry. According to studies using complementary techniques (e.g., low temperature nitrogen adsorption or small angle X-ray scattering, SAXS) the greatest reduction in the surface area due to the treatment is 75 %, but the pore size distribution in the micropore range is hardly affected. The surface chemistry was characterized in nonaqueous (X-ray photoelectron spectroscopy, XPS) and aqueous medium (pH, pH_{PZC}, Boehm titration). The importance of the surface chemistry is illustrated in standard SAXS combined with contrast variation, as well as in a wide variety of adsorption processes.

Keywords: nanoporous carbon; nitrogen adsorption; X-ray photoelectron spectroscopy (XPS); small angle X-ray scattering (SAXS); functional groups; interaction; adsorption, acid/base properties, pH, phenol adsorption; DA model

1. Introduction

Activated carbons (AC), owing to their versatility, are the most frequently employed adsorbents. Their outstanding performance stems from a unique combination of geometrical and chemical properties. Recognition of the

* E-mail: klaszlo@mail.bme.hu

J.M. Loureiro and M.T. Kartel (eds.), Combined and Hybrid Adsorbents, 119–132.

role of surface area and pore hierarchy in the performance of ACs has stimulated the commercialization of carbon adsorbents with tailor-made porosity. The different size and shape of pores, as well as pits, vacancies and steps are responsible for the geometrical heterogeneities of the carbon surface. Their design at the nanoscale level, however, has revealed the importance of an additional basic parameter, namely their surface chemistry.

The adsorption properties and the catalytic activity of these systems are both influenced by heteroatoms located along the edges of the turbostratic graphene layers, or within them. The role of the different compounds of oxygen, nitrogen, sulfur, phosphorus, boron, etc., formed with the carbonaceous matrix has been thoroughly studied over the past two decades.[1-11] The band gap of the graphene sheets may be tuned by in-built heteroatoms,[3] which form stable non-stoichiometric surface compounds. The polarities of the functional groups are influenced by the proximity of neighboring chemical structures. Polarity distribution functions, rather than discrete bond polarity values, should therefore be used to characterize these systems.

Different functional groups and various surface contaminants at a surface are associated with the chemical heterogeneity of the ACs. The amount and the chemical forms of these heteroatoms depend on the origin of carbon and the history of its preparation and treatment conditions.

Chemical treatment, as well as impregnation or doping techniques, are often used to enhance the performance of porous carbons or to prevent certain potential failings of the application. Boron doping of graphites leads to a reduction of the graphitic sp^2 components and transformation into a sp^3 dominated network, thus reducing chemical erosion.[4] Substitutional boron acts both as a catalyst and as an inhibitor in carbon oxidation[5,6] by three possible mechanisms: (i) graphitization enhancement, (ii) formation of a boron oxide-oxygen diffusion barrier and site blocking film, and (iii) complex disruption of the delocalized π-electrons in the graphene layer and redistribution of the electrons.[7] In the case of phosphorus doping, the dominant oxidation inhibition mechanism suggested is active site blocking by the formation of C-P-O or C-O-P bonds at graphene edges.[7] The possibility that P becomes part of the aromatic system is, however, controversial.[9] Recently, pyrolytic carbon – silica (C – SiO_2) membranes with excellent gas separation properties were prepared from two-phase copolymers containing an aromatic imide domain and a siloxane domain.[10] Silicon doping, however, is often coupled with high temperature sintering ($T > 1400 – 1450$ °C), resulting in the formation of SiC. These materials have high strength, good oxidation and corrosion resistances, high thermal conductivity, and good thermal shock resistance.

The diversity of the O- and N-containing functional groups has been reviewed in detail.[12-14] The most frequent heteroatom in the carbon matrix is oxygen, which is generally bonded along the edges of the turbostratic graphite crystallites (Fig. 1a). Oxygen may be present in various forms, such as carboxyls, carbonyls, phenols, lactones, aldehydes, ketones, quinones, hydroquinones, anhydrides or ethereal structures.[12,18] As these groups can also interact with each other, their properties may therefore differ from those of their individual organic analogs. These groups and the delocalized electrons of the graphitic structure determine the apparent acid/base character of the AC surface.[12] Carbonyl, carboxyl, phenolic hydroxyl, lactonic and quinonoid groups are acidic, while pyrone and chromene are basic.[16-19]

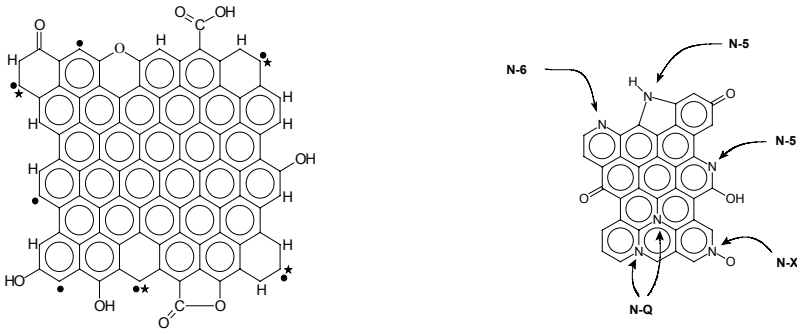

Figure 1. (a) Schematic representation of a graphene layer including the oxygen-containing functional groups at the edges. • and •* mean unpaired σ electron and in-plane σ pair (where * is a localized π electron), respectively;[13] (b) Schematic representation of N-containing functional groups on carbon surfaces N-6: pyridinic, N-5: pyrrolic/pyridone, N-Q: quaternary, N-X: N-oxide.[14]

The distribution of the surface functionalities is thus of fundamental importance in AC-based processes. However, the π electrons of the graphite planes are of great importance as well, as they act as Lewis basic sites accepting protons.[20] Although N also induces basic sites, part of the basicity of the carbon surface is nevertheless explained in terms of the π sites of the carbon basal plane. The Lewis basicity of π electrons is strongly influenced by the interaction between the aromatic system and the localizing effects of oxygen-containing groups.[13, 20]

Several methods are available for the qualitative and quantitative characterization of the chemical properties of the dry and wet carbon surfaces. No single one, however, yields a complete description of the chemistry of the surface. Owing to the complex surface chemistry of carbon, only a broad-based characterization of the surface can describe the behavior of the carbon under certain conditions, according to the

application planned.[21] Dry and/or wet techniques should be used depending on whether water may be present, as functional groups exhibit specific interactions with water even when it is present in the vapor phase.[22,23] That is, the surface of the ACs can also be modified in situ, e.g., by the pH of the aqueous medium in which the carbon is used for separation.

A series of microporous AC samples chemically modified to varying degrees of oxidation with nitric acid was prepared from a polyester precursor, in order to avoid inorganic impurities from the raw materials. The similarity of their morphology on different distance scales was proved by microscopy, gas adsorption and small angle X-ray scattering observations. The surface chemistry of the carbons described in this paper was characterized by various techniques. The goal of this presentation is to highlight the importance of the chemical properties of the carbon in physical characterization and in diverse applications.

2. Sample Preparation

Granular activated carbon (APET) was prepared from 2×3 mm poly(ethyleneterephthalate) (PET) pellets in a two-step physical activation process as described elsewhere.[24] The surface chemistry and morphology of the precursors were characterized previously.[23,25,26] The steam-activated carbon, obtained at 900 °C, was treated for 3 - 6 hours with concentrated nitric acid either at room temperature or at the boiling point of the carbon – acid suspension to achieve different degrees of surface functionalization. The acidic samples were washed with distilled water and extracted in a Soxhlet apparatus until neutral pH was attained. For some samples a second heat treatment was applied at 700 ^{o}C for 30 min in a high-purity nitrogen flow.[23]

Scanning electron microscopy (SEM), low temperature nitrogen adsorption/desorption isotherms, helium pycnometry and small angle X-Ray scattering (SAXS) were applied for morphological characterization. X-ray Photoelectron Spectroscopy (XPS) and various acid/base titration methods were used to describe the complex chemical feature of the surface.[15,27]

3. Morphological and Surface Chemical Consequences of the Surface Treatment of the Polymer Based Carbon

3.1. MORPHOLOGY

The influence of the acidic treatment on the morphology and the chemistry of the surface was systematically studied. In this chapter results will be shown on samples treated for 3 h at ambient temperature (APETA) and at

the boiling point of the nitric acid – carbon suspension (APETB) and thoroughly washed (see Experimental). Virgin APET after washing in water is used for comparison (APETW).

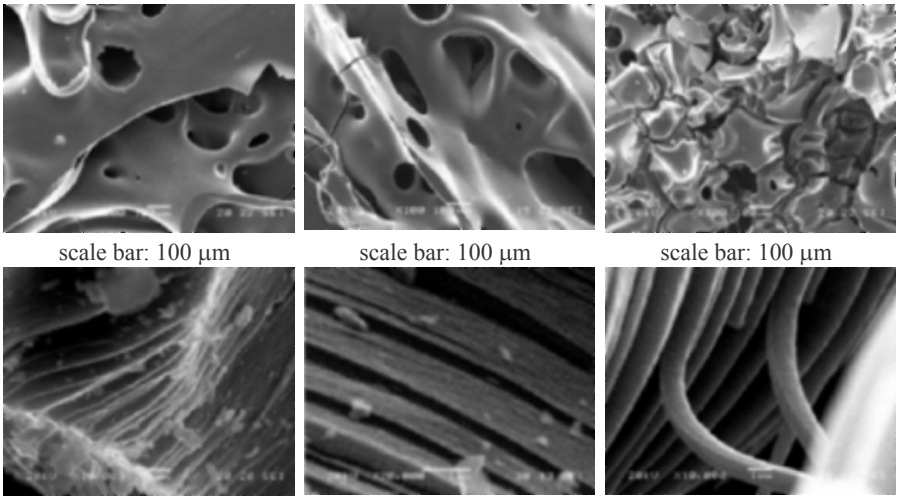

Figure 2. Low and high magnification SEM images of the water and acid treated carbon samples; (a) APETW, (b) APETA, (c) APETB.

The room temperature acid treatment, as illustrated in the SEM images (Fig. 2b, upper row), does not affect significantly the surface structure on a macroscopic scale, even with an extended treatment time.[28] Increasing the temperature of the treatment produces a much more dramatic effect than extending the duration: the carbon obtained after the boiling point treatment has a much more fractured surface (Fig. 2c, upper row).

The finer scale micrographs (Fig. 2, lower row) reveal an alternating pattern of characteristic size about 1 μm. The carbons display an apparent surface fractal dimension of $D_s = 2.4$ in the wave vector range 0.001 $Å^{-1}$ - 0.02 $Å^{-1}$ as deduced from the initial slope of the SAXS curves (Figure 3c).[25] The apparent Guinier radius R_G, mean separation L between the basic structural units (BSU) as well as the surface area S_X were deduced (Table 1).

The isotherms of the same carbons in Figure 3a reveal a typically microporous structure with a very narrow hysteresis loop. The higher density value in Table 1 means that previously closed pores also become accessible to the nitrogen. The treatment is more destructive at elevated temperature, which reduces the surface area, but the remaining structure is still strongly microporous.

The discrepancy between the adsorption and SAXS derived surface areas is generally attributed to inaccessible porosity.[22]

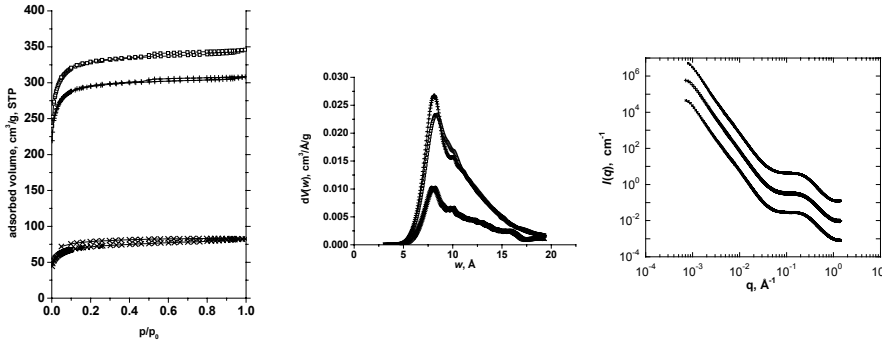

(a) (b) (c)

Figure 3. Low temperature nitrogen adsorption isotherm (a), HK micropore distribution (b) and the SAXS response (c) of the water- and acid-treated samples (□) APETW (+) APETA and (**x**) APETB. The extended power law behavior at low q, i.e., $I(q) \propto q^{-m}$, where the exponent m $(3.5 \leq m \leq 4)$ indicates scattering from surfaces.

TABLE 1. Selected data derived from the low temperature nitrogen isotherms and the SAXS response of the powdered samples*

		APETW	APETA	APETB
Nitrogen adsorption	S_{BET}, m^2/g	1156	1114	304
	V_{tot}, cm^3/g	0.50	0.48	0.14
	W_0, cm^3/g	0.48	0.46	0.12
	W_0/V_{tot}	0.96	0.96	0.86
	S_{DR}, m^2/g	1352	1293	337
	S_{BET}/S_{DR}	0.86	0.86	0.90
	w_{ads}, Å	8.6	8.6	9.2
	w_{DR}, Å	8.4	8.6	11.0
	d_{He}, g/cm3	1.74	1.82	1.50
SAXS	R_G, Å	6.1	5.8	5.8
	L, Å	19.6	19.1	18.9
	S_X, m^2/g	2000	1970	860
	$w_{min}=2V_{tot}/S_X$, Å	5.0	4.9	3.3

* S_{BET}, S_{DR} and S_X: surface area calculated from the BET, DR model and SAXS data, respectively; V_{tot}: the total pore volume from the amount of nitrogen vapor adsorbed at a relative pressure, $p/p_0 \approx 1$; $w_{ads}(=2V_{tot}/S_{BET})$; W_0: micropore volume from DR model; w_{DR}: micropore width; d_{He}: helium density.

The control sample, which was in contact with water only but not with acid, displays a micrometer scale layered structure under SEM. It is

strongly microporous: 96% of its pores contribute to the 0.48 cm^3/g micropore volume.

The polydisperse pore size distribution shows a dominant peak at 8.4 Å (Figure 3b). The average width of the slit-shaped pores derived from the Dubinin-Radushkevich (DR)-plot is 8.4 Å and the minimum slit width available for nitrogen is 5.1 Å from the X-ray and pore volume data. It is composed of randomly packed turbostratic basic structural units separated by an average distance L = 19.6 Å. The surface area derived from X-rays, S_X, measured in air is about 2000 m^2/g.

The SEM images of the APETA sample show a more pronounced step-like surface. Both the adsorption and the X-ray derived surface areas are practically unchanged. The marginally smaller micropore volume (0.46 cm^3/g) amounts to the same fraction of the total porosity. In the Horváth-Kawazoe (HK) pore size distribution, in addition to the main peak around 8 Å, a second peak appears at 10 Å, but the average and the minimum slit widths as well as the separation of the basic structural units are virtually unaffected.

The severe damage caused by the boiling acid reveals an underlying fiber-like structure in the SEM image with a typical diameter of 1 μm. A drastic loss of about 75 % in all the measured surface areas is observed. Two new peaks appearing at 15.6 Å and 18.7 Å in the semi-empirical HK pore size distribution, correspond to a doubling of some of the interlayer distances, as is also revealed by the increase in the average slit width to 11 Å. The weakening of the pore walls is sensed by the low helium density or the pronounced low pressure hysteresis.

3.2 SURFACE CHEMISTRY

The O/C ratios for the granular samples increase with increasing severity of the acid treatment (Table 2), but extended room temperature treatment does not further increase the overall surface oxygen content.[23] No significant difference was found between the distribution of the different functional groups in the granular and the powdered samples. This indicates that the chemical treatment was not confined to the outer surfaces of the granules but acted uniformly throughout the internal surfaces.

Since in aqueous media the interaction between water and carbon modifies the surface properties, the pH and the pH_{PZC} of the carbon samples were tested by standard methods.[16] The initial pH values of the carbon suspensions are summarized in Table 3. The measured pH values differ significantly from the pH of the Millipore water in which the powdered carbon samples were immersed (pH = 5.9) due to protolytic processes taking place during the immersion. The acidic treatment significantly

decreases the pH of the carbons. The low pH indicates H^+ release from the acid treated samples, which may originate from the dissociation of acidic groups formed on the carbon surface during the oxidative treatment.
Further samples will be characterized in the application section.

TABLE 2. Elemental analysis from the XPS and the resolution of the carbon signal*

	APETW	APETA	APETB
C atomic %	94	91	79
O atomic %	6	9	21
O/C %	6.4	9.9	26.6
Peak I	49.5	48.8	50.9
Peak II	26.0	26.4	23.7
Peak III	9.2	11.3	6.1
Peak IV	8.2	7.9	15.3
Peak V	7.1	5.6	4.0

Best fit of the asymmetric peak of the C1s core spectrum obtained by decomposing into five Gaussian peaks: graphitic carbon (Peak I, BE = 284.2 - 284.4 eV), carbon in phenolic, alcohol or ether groups (Peak II, BE = 284.7 - 285.2 eV), carbonyl or quinone groups (Peak III, BE = 286.1 - 286.8 eV), carboxyl or ester groups (Peak IV, BE = 288.3 – 288.7 eV), and shake-up satellite peaks due to π - π transitions in aromatic systems (Peak V, BE = 290.3 - 290.9 eV).

TABLE 3. pH and pH_{PZC} of selected PET based carbons (25 °C; sd = ± 0.1)

	pH	pH_{PZC}
APETW	6.8	9.2
APETA	4.0	4.5
APETB	3.5	2.7

From the data presented in this subchapter we conclude that surface functionalization of the PET based by exposure to nitric acid modifies the chemistry of the solid material, to a degree that depends on the severity of the treatment. At the same time, the change in the morphology is surprisingly undramatic: only hot acid treatment reduces the available surface area, but the microporus character is conserved.

4. The Role of the Surface Chemistry in the Interactions of ACs

4.1. FORMALDEHYDE REMOVAL AT RH 45%[23]

The concentration of several pollutants including aldehyde compounds in indoor air is much higher than in the atmosphere. Formaldehyde (FA), e.g., comes mainly from cigarette smoke, decoration materials, paint, synthetic fiber carpets, etc.

The kinetics of FA adsorption were studied on two PET-based AC with similar morphology but different surface oxygen content (Table 4). To mimic real conditions humid air (relative humidity, RH = 45%) was used. The adsorption of FA by both carbons was relatively fast, but the estimated surface concentration of the FA molecules is smaller than expected owing to the competition between FA and the water molecules. In the APET2 sample the conditions for water adsorption are so enhanced that even its rate of uptake was measurable, albeit an order of magnitude slower than that for FA (τ_1 in Table 5 can be attributed to FA adsorption and the slower effect (τ_2) may be due to water molecules). The fitted parameters as well as the estimated FA uptake are given in Table 5. The total coverage in both carbons is below the theoretical monolayer.

TABLE 4. Selected characteristic data of the APET based carbons used in this experiment

Sample	S_{BET} m^2/g	V_{tot} cm^3/g	Carbon[a] atomic %	Oxygen[a] atomic %	Acidic groups[b] μeq/g	Basic groups[b] μeq/g	$\frac{\text{functional group}^{c}}{100\ nm^2}$
APET1	1440	0.65	95.7	4.3	118	401	21.7
APET2	1509	0.64	90.0	10.0	380	328	28.3

[a] from XPS; [b] titrated by the Boehm method, using NaOH and HCl, respectively; [c] from the ratio of the acidic + basic functional groups to S_{BET}

TABLE 5. Kinetic parameters of FA removal. Time constants τ_i found from fit to $y = y_0 + Aexp(-x/\tau)$ (APET1) and to $y = y_0 + A_1exp(-x/\tau_1) + A_2exp(-x/\tau_2)$ (APET2)

Sample	Time constants, min	Concentration limit[a], ppm	Adsorption capacity[b], μl/g carbon	$\frac{\text{functional group}}{100\ nm^2}$ [c]
APET1	$\tau_1 = 4.43$	0.32	13.5	15.7
APET2	$\tau_1 = 2.35;\ \tau_2 = 26.4$	0.21	14.0	15.5

[a] concentration in the gas phase at equilibrium; [b] estimated from the initial (2.3 ppm) and final concentrations of FA, the adsorption volume and the mass of carbon; [c] from ratio of previous column to S_{BET}

4.2. INTERACTION IN LIQUID PHASE

4.2.1. *Non-aqueous media*

The surface area of ACs is most often deduced from adsorption measurements. This technique, however, may be perturbed by size exclusion and kinetic hindrance effects or the cross-sectional area of the

probe molecule. What is more, the evaluation of the surface area depends on the model employed for the calculations. SAXS is often employed on porous systems as an alternative to determine internal surface area. If the question of closed porosity also arises, immersing the porous material into a contrast modifying fluid provides an elegant means of investigating the structure of the carbon.[28,29] In Table 6 SAXS data calculated for three carbon samples characterized earlier show how the hydrophobic/ hydrophilic nature of the contrast variant liquid as well as the polar character of the carbon surface influence the average separation distance L of the BSUs or the internal surface area.[26]

TABLE 6. Parameters derived from SAXS measurements with different contrast variants

	APETW			APETA			APETB		
solvent	R_G Å	L Å	S_X m^2/g	R_G Å	L Å	S_X m^2/g	R_G Å	L Å	S_X m^2/g
air	6.1	20	1930	5.8	19	1810	5.7	19	920
i-octane	5.5	20	2080	5.5	19	2020	8.0	34	620
i-propanol	5.5	20	1850	5.5	20	1910	7.8	23	810

Although estimates of the surface area, S_X, are less sensitive to variations in the nature of the solvent, strong solvent-dependent effects are visible in the case of the most oxidized sample APETB. This sample, because of the weakening of the pore walls noted earlier, even displays appreciable local swelling in i-octane,[26] as can be concluded from the comparison of L values in different liquids. The fractal surface structure of the sub-grains in sample APETB (surface fractal dimension $D_S = 6\text{-}m = 2.5$ in air) is also deformed by the liquids. In the presence of non-polar solvents it becomes smoother (m = 3.5 in i-propanol and 3.75 in i-octane, respectively), thus the amphiphilic i-propanol stabilizes the rough fractal surface.

We can conclude that in contrast variation techniques the interaction between the solid (carbon) and the liquid phase may significantly affect the distribution of the pore-filling molecules within the pores. The strength of the generally non-specific interaction may (e.g., APETB) or may not (APETW, APETA) influence the surface area and/or other parameters deduced.

4.2.2. *Adsorption from dilute aqueous solutions*

As mentioned earlier, when carbon is placed in contact with aqueous solutions, the interaction with water modifies its surface properties: the functional groups act as acid/base centers.[13] Each of the functional groups can be characterized by a pK_a distribution influenced by inter- and

intralayer neighbors. Due to its acid/base feature, the performance of the same AC is sensitive to the pH of the environment.

The uptake of phenol (pK_a = 9.89, cross sectional area,[30] σ = 0.30-0.42 nm^2) was investigated on microporous carbons listed in Table 7 from aqueous solutions with different pH at room temperature.[31] The Dubinin-Astakhov (DA) adsorption-isotherm equation was used to evaluate parameters characterizing the adsorption (adsorption capacity n_m, characteristic energy of phenol adsorption E_{os}, calculated cross sectional area σ_a, surface coverage, etc.). Adsorption energy E_{12} distribution functions $F(E_{12})$ were calculated by the INTEG algorithm, based on a regularization method.[32]

TABLE 7. Selected characteristics of APET-based carbons for adsorption of phenol from aqueous media

Sample	S_{BET} m^2/g	V_{tot} cm^3/g	pH_{PZC}	Acidic groups[a] μeq/g	Basic groups[a] μeq/g	Ratio of the basic groups	$\frac{\text{functional group}}{100\ nm^2}$ [b]
APET3	1214	0.52	9.3	80	420	0.84	25
APET4	1320	0.57	4.5	640	196	0.23	38
APET5	1382	0.60	7.1	442	319	0.42	33
APET6	1488	0.64	7.1	380	328	0.46	29

[a]titrated by the Boehm method, using NaOH and HCl, respectively; [b]from the ratio of the acidic + basic functional groups to S_{BET}

APET3 was studied in four different media. Increasing the pH gradually enhances the strength of the interaction as well as the adsorption performance (Table 7, first data set).

The sequence of the energy-distribution peaks obtained by the regularization method (Figure 4), in order of increasing energy E_{12} correlates well with that of the parameter, E_{os}, of the DA equation. The strongest interactions of phenol with the surface occur for the unbuffered solution, and the weakest for the solution with pH = 3. The peaks are "lower" and "broader" for the unbuffered solution, which indicates the largest spread of interactions between the carbon surface and phenol.

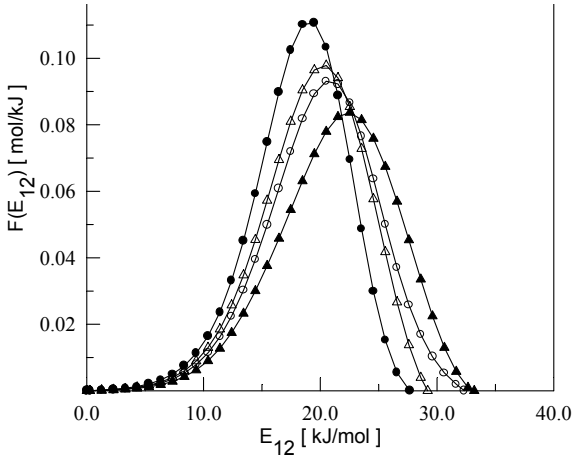

Figure 4. Adsorption energy distribution functions for phenol on APET3 from aqueous solutions of different pH. ●: pH =3, Δ: pH =4, ○: pH =5, ▲: unbuffered.

TABLE 8. Selected parameters derived from the DA isotherm

Carbon	Medium	n_m mmol/g	E_{os}	σ_a [a] nm^2	functional group / 100 nm^2	$E_{12,\,max}$ kJ/mol
APET3	pH = 3	2.83	20.16	0.712	140	19.09
	pH = 4	2.90	21.77	0.695	143	20.45
	pH = 5	2.94	22.56	0.686	145	21.06
	unbuffered	2.97	23.30	0.679	147	22.41
APET4	pH = 3	2.12	21.62	1.034	96	20.51
	unbuffered	2.29	22.06	0.957	104	20.72
APET5	pH = 3	2.72	21.39	0.844	118	20.08
	unbuffered	2.97	22.49	0.773	129	21.03
APET6	pH = 3	2.76	22.19	0.895	111	21.02
	unbuffered	3.22	22.35	0.767	130	21.45

[a] $\sigma_a = S_{BET}/(n_m N_A)$, N_A is Avogadro's number

Adsorption of phenol from aqueous media was also studied on carbons of similar morphology but different surface chemistry. As in APET3, the distribution peaks were sharper in the buffered medium. The uptake of phenol is always larger for the unbuffered solution than that for a lower pH (Table 8). The broader energy distribution suggests that phenol is adsorbed by several mechanisms in the unbuffered systems. The comparison of the reference and calculated cross-sectional area reflects strong competition between phenol species and the water molecule. The adsorption of the latter is preferred as the ratio of the basic surface groups increases.

ACKNOWLEDGEMENTS

Access to the small angle beamline BM2 at the European Synchrotron Radiation Facility is gratefully acknowledged. The author is indebted to K. Marthi for the SEM micrographs, E. Geissler for the SAXS characterization and K. Josepovits for XPS analysis and to A. Dąbrowski and P. Podkościelny for the mathematical evaluation of the phenol adsorption isotherms.

Warm thanks are extended to E. Fülöp and G. Bosznai for technical assistance. This research was supported by the Hungarian National Research Fund (OTKA, grant No. T 046532) and EU - Hungarian Government joint fund (GVOP - 3.2.2 - 2004 - 07 - 0006/3.0).

REFERENCES

1. S. Biniak, G. Szymanski, J. Siedlewski, and A. Swiatkowski, The characterization of activated carbons with oxygen and nitrogen surface groups, *Carbon* 35(12), 1799-1810 (1997).
2. Y. J. Lee, Y. Uchiyama, and L. R. Radovic, Effects of boron doping in low- and high-surface-area carbon powders, *Carbon* 42(11), 2233-2244 (2004).
3. V. V. Strelko, V. S. Kuts, and P. A. Thrower, On the mechanism of possible influence of heteroatoms of nitrogen, boron and phosphorus in a carbon matrix on the catalytic activity of carbons in electron transfer reactions, *Carbon* 38(10), 1499-1503 (2000).
4. A. Schenk, B. Winter, C. Lutterloh, J. Biener, U. A. Schubert, and J. Kueppers, The origin of reduced chemical erosion of graphite based materials induced by boron doping, *J. Nucl. Mater.* 220-222, 767-770 (1995).
5. Y. J. Lee, H. J. Joo, and L. R. Radovic, Preferential distribution and oxidation inhibiting/catalytic effects of boron in carbon fiber reinforced carbon (CFRC) composites, *Carbon* 41(13), 2591–2600 (2003).
6. L. R. Radovic, M. Karra, K. Skokova, and P. A. Thrower, The role of substitutional boron in carbon oxidation, *Carbon* 36(12), 1841–1854 (1998).
7. L. E. Jones, and P. A. Thrower, The effect of boron on carbon fiber microstructure and reactivity, *J. Chim. Phys.* 84(11-12), 1431–1438 (1987).
8. S. G. Oh, and N. M. Rodriguez, In situ electron microscopy studies of the inhibition of graphite oxidation by phosphorus, *J. Mater. Res.* 8(11), 2879–2888 (1993).
9. Y. J. Lee, and L. R. Radovic, Oxidation inhibition effects of phosphorus and boron in different carbon fabrics, *Carbon* 41(10), 1987–1997 (2003).
10. H. B. Park, and Y. M. Lee, Pyrolytic carbon–silica membrane: a promising membrane material for improved gas separation, *J. Membrane Sci.* 213(1-2), 263–272 (2003).
11. J. F. Yang, G. J. Zhang, N. Kondo, and T. Ohji, Synthesis and properties of porous Si3N4/SiC nanocomposites by carbothermal reaction between Si3N4 and carbon, *Acta Mater.* 50(19), 4831–4840 (2002).
12. C. A. Leon y Leon, and L. R. Radovic, in: *Chemistry and Physics of Carbon* Vol. 24, edited by P. A. Thrower (Marcel Dekker Press, New York, 1994), pp. 213-310.
13. L. R. Radovic, in: *Surface Chemistry of Activated Carbon Materials: State of the Art and Implications for Adsorption, Surfaces of Nanoparticles and Porous Materials*, edited by J. A. Schwarz and C. I. Contescu (Marcel Dekker, New York, 1999), pp. 529-565.

14. F. Kapteijn, J. A. Moulijn, S. Matzner, and H. P. Boehm, The development of nitrogen functionality in model chars during gasification in CO_2 and O_2, *Carbon* 37(7), 1143-1150 (1999).
15. H. P. Boehm, in: *Advances in Catalysis* Vol. 16, edited by D. D. Eley, H. Pines, and P. B. Weisz, (Academic Press, New York, 1966), pp. 179-274.
16. M. V. Lopez-Ramon, F. Stoeckli, C. Moreno-Castilla, and F. Carrasco-Marin, On the characterization of acidic and basic surface sites on carbons by various techniques, *Carbon* 37(8), 1215-1221 (1999).
17. E. Papirer, S. Li, and J. B. Donnet, Contribution to the study of basic surface groups on carbons, *Carbon* 25(2), 243-247 (1987).
18. A. Bismarck, C. Wuertz, and J. Springer, Basic surface oxides on carbon fibers, *Carbon* 37(7), 1019-1027 (1999).
19. D. Suárez, J. A. Menéndez, E. Fuente, and M. A. Montes-Morán, Contribution of pyrone-type structures to carbon basicity: an ab initio study, *Langmuir* 15(11), 3897-3904 (1999).
20. A. Contescu, M. Vass, C. Contescu, K. Putyera, and J.A. Schwarz, Acid buffering capacity of basic carbons revealed by their continuous pK distribution, *Carbon*, 36(3), 247-258 (1998).
21. T. J Bandosz, M. J Biggs, K. E. Gubbins, Y. Hattorl, T. Iiyama, K. Kaneko, J. Pikunic, and K. T. Thomson, in *Chemistry and Physics of Carbon* Vol. 28, edited by L. R. Radovic (Marcel Dekker Press, New York, 2003), pp. 41.
22. K. László, and E. Geissler, Surface chemistry and contrast-modified SAXS in polymer-based activated carbons, *Carbon*, submitted.
23. K. László, Characterization and adsorption properties of polymer based microporous carbons with different surface chemistry, *Micropor. Mesopor. Mat.* 80(1-3), 205–211 (2005).
24. K. László, A. Bóta, and L. G. Nagy, Characterization of activated carbons from waste materials by adsorption from aqueous solutions, *Carbon* 35(5), 593-598 (1997).
25. K. László, K. Marthi, C. Rochas, F. Ehrburger-Dolle, F. Livet, and E. Geissler, Morphological investigation of chemically treated PET based activated carbons, *Langmuir* 20(4), 1321-1328 (2004).
26. K. László, O. Czakkel, K. Josepovits, C. Rochas, and E. Geissler, Influence of surface chemistry on the SAXS response of polymer-based activated carbons, *Langmuir* 21(18), 8443–8451 (2005).
27. K. László, E. Tombácz, and K. Josepovits, Effect of activation on the surface chemistry of carbons from polymer precursors, *Carbon* 39(8), 1217-1228 (2001).
28. J. D. F. Ramsay, Applications of neutron scattering in investigations of adsorption processes in porous materials, *Pure & Appl. Chem.* 65(10), 2169-2174 (1993).
29. M. M. Antxustegi, P. J. Hall, and J. M. Calo, Development of porosity in Pittsburgh no. 8 coal char as investigated by contrast-matching small-angle neutron scattering and gas adsorption techniques, *Energ. Fuel.* 12(3), 542–546 (1998).
30. K. László, and A. Szűcs, Surface characterization of polyethyleneterephthalate (PET) based activated carbon and the effect of pH on its adsorption capacity from aqueous phenol and 2,3,4-trichlorophenol solutions, *Carbon* 39(13), 1945-1953 (2001).
31. K. László, Adsorption from aqueous phenol and aniline solutions on activated carbons with different surface chemistry, *Colloid. Surface. A* 265(1-3), 32-39 (2005).
32. K. László, P. Podkościelny, and A. Dąbrowski, Heterogeneity of activated carbons with different surface chemistry in adsorption of phenol from aqueous solutions, *Appl. Surf. Sci.*, in press.

POROUS CARBONS IN GAS SEPARATION AND STORAGE

FRANCISCO RODRÍGUEZ-REINOSO*
Laboratorio de Materiales Avanzados, Departamento de Química Inorgánica, Universidad de Alicante, Alicante, Spain

Abstract. The porous structure of activated carbon, the micropores of which are slit-shaped, makes this adsorbent ideal for processes such as gas separation and gas storage. In the first application, the homogeneous and uniform microporosity of carbon molecular sieves is used to separate gases with relatively similar molecular dimensions but different shape, or gases with similar molecular dimensions but different adsorption kinetics. In the second application, the slit-shaped microporosity is responsible for a larger packing density of adsorbed molecules relative to cylindrically-shaped pores of the same dimensions, thus facilitating the adsorption of high amounts of gas adsorbed per unit volume of carbon, with a high packing density of the adsorbate.

Keywords: Activated carbon; carbon molecular sieves; porosity; microporosity; adsorption; immersion calorimetry; adsorption kinetics; gas separation/gas storage

1. Introduction

Activated carbon is an excellent and versatile adsorbent[1] because of its immense capacity for adsorption from gas and liquid phases, this capacity being due to a highly developed porosity, which ranges from micropores (< 2 nm entrance dimensions) to mesopores (2-50 nm) and macropores (>50 nm). Although more than 90% of the adsorption takes place into the micropores, meso- and macropores are very important because they serve as passages to the molecules that are to be adsorbed into the micropores, thus conditioning the kinetics of the adsorption process. The adsorptive properties of activated carbon are a simultaneous function of the porosity

* To whom correspondence should be addressed. Francisco Rodríguez-Reinoso, Laboratorio de Materiales Avanzados, Departamento de Química Inorgánica, Universidad de Alicante, Apartado 99, E-03080 Alicante, Spain; e-mail: reinoso@ua.es

J.M. Loureiro and M.T. Kartel (eds.), Combined and Hybrid Adsorbents, 133–144.

and the chemical nature of the carbon surface, although there are some applications which can be more directly related to the porosity, without significant contribution from the chemical nature. This is the case for the adsorption of non polar or non polarizable molecules.

Extensive research activity has been carried out in recent years to discover activation methods needed to develop suitable pore size distributions for specific applications. This applies to the separation of gases, where the micropore dimension (width) is able to differentiate between the kinetics of adsorption of two molecules with similar dimensions, and the storage of natural gas, where a precisely defined micropore size is needed to produce a high packing density of adsorbed molecules.

This paper concentrates on the analysis of the porosity and more specifically on the microporosity of activated carbons prepared for the two specific applications mentioned above, *viz* separation and storage of gases.

2. Microporosity in Activated Carbon

The structure of microporosity in activated carbon has been the subject of many investigations and many models can be found in the literature. The model more generally accepted is based in the concept of Oberlin,[1,2] by which activated carbon resembles crumpled paper thus facilitating the interconnectivity and transport of adsorbate molecules, the thickness of the paper probably being no more than two or three carbon layers. The more-or-less slit shaped space between the graphene sheets constitutes the microporosity. The three-dimensional network of microporosity in activated carbon can also be described as a labyrinth,[1] in which a continuous connection between the lines throughout the labyrinth exists as the carbon atoms form part of a continuous graphene sheet.

The slit shape of the micropores is very important for the separation of molecules as a function of the molecular shape and dimensions. Imagine a carbon in which the separation between the graphene sheets is 0.4 nm and that the adsorption of disc-type molecules such as benzene (kinetic dimensions: 0.37 nm thickness and 0.57 nm diameter) has to compete with the adsorption of a spherical molecule with a dimension of 0.57 nm. It is obvious (Figure 1) that only the benzene molecule can be adsorbed inside the micropore because the second molecule is too large for the micropore width. Of course this situation is the opposite to that found in a 4A zeolite in which the 0.4 nm micropores are cylindrical. In this case a spherical molecule of 0.37 nm diameter will be adsorbed whereas a molecule such as benzene will not be adsorbed. In both adsorbents there is a selectivity based upon the shape and the dimensions of the molecules. In addition to this

straightforward case of gas separation by microporous carbon based on shape and dimension selectivity, there are other cases in which separation is carried out on the basis of kinetics (rates) because the adsorption uptake of the gas components is similar under equilibrium conditions.

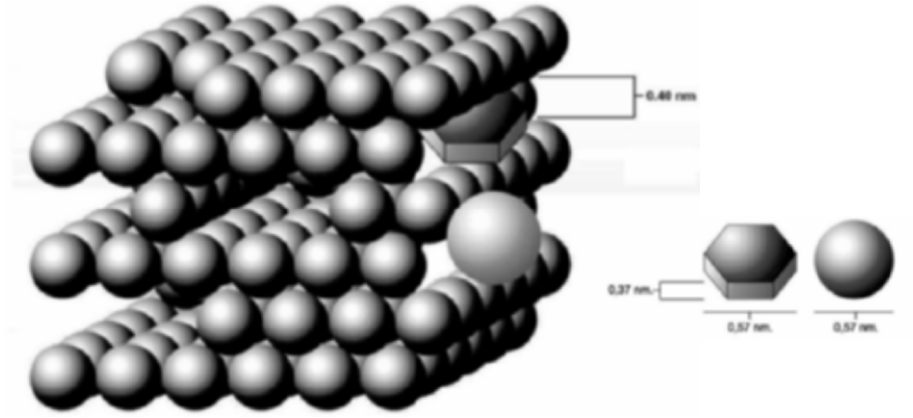

Figure 1. Model to show the selectivity for the adsorption of molecules in activated carbon.

The slit-shaped microporosity is also very important for the storage of, e.g., natural gas. In this application the main factor is the packing density of adsorbed molecules inside the microporosity, which is a function of the shape and dimensions of the micropores.[4]

Figure 2 is an indication of the effect of pore size and shape on the packing density of spherical molecules in cylinders and slits. The degree of packing is expressed as a percentage of the packing density in the corresponding closed-packed state. It is clearly indicated that the packing density of spherical molecules such as methane is much larger in slit-shaped micropores than in cylindrical pores of the same dimension. This is the reason why the adsorbent of choice for gas storage must have slit-shaped micropores.

In what follows the preparation and characterization of activated carbons for these two applications is described to show the important role of the slit-shaped microporosity in activated carbon.

3. Gas Separation

Gas separation by molecular sieves is an important industrial process, the more common sieves being zeolites and, more recently, carbon molecular

sieves (CMS). The advantages of CMS for many processes can be summarized as follows: shape selectivity for planar molecules, higher hydrophobicity, high resistance to acidic and basic media and thermal stability (of course, in the absence of oxygen). As mentioned above, there are CMS able to separate the components of a gas mixture on the basis of molecular size and shape. In other cases (e.g., separation of nitrogen from air), separation is carried out on the basis of adsorption kinetics (rates) because two gases for which the equilibrium adsorption would be very similar can be separated because one of them is able to diffuse much more rapidly through the pore entrance than the other.

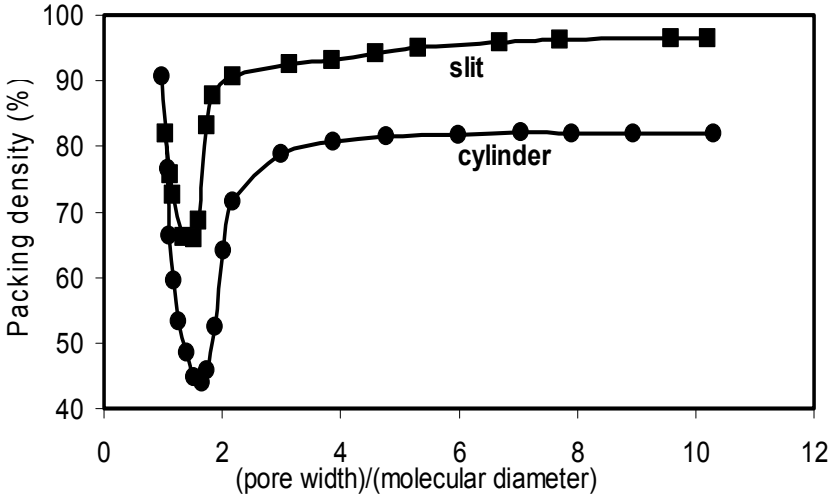

Figure 2. Packing of spherical molecules in model micropores. Adapted from reference 4, with permission from Elsevier.

Commercial CMS are manufactured by depositing amorphous carbon (by CVD from, for instance, benzene) on the entrance of the micropores until the required dimension is reached. The main problem with this procedure is the difficulty in controlling the deposition process because if it takes place additionally inside the pore it will reduce the adsorption capacity. On the other hand, the attrition of the CMS particles may partially break the deposited carbon at the entrance of the micropores, thus modifying the separation ability.

In addition to the conventional CVD process,[5] our research group has used other procedures for the preparation of CMS: i) controlled uncatalyzed gasification of chars obtained from lignocellulosic precursors; ii) mild oxidation of a char and subsequent removal of formed oxygen surface groups (as CO and CO_2 species), this widening the entrance of the micropores where the groups formed; and iii) mild oxidation of an activated carbon or a CMS of larger dimensions, followed by a mild heat treatment

under inert gas so that the remaining oxygen surface groups partially block the entrance of the micropores.

In the first of these procedures, the lignocellulosic precursor (coconut shells or peach stones) is washed with a diluted solution of sulphuric acid to remove mineral matter of the precursor and is then carbonized in a controlled manner to get the highest possible yield. The char is then slowly gasified with a flow of carbon dioxide in the 750-800ºC range (this is possible because the gasification will not be catalyzed by the mineral matter that was removed by washing) to controlled burn-offs.[6] Many different CMS, covering a wide range of micropore dimensions, from about 0.3 to 0.7 nm, could be prepared by this procedure. It has to be mentioned that if the precursor were washed with distilled water, the gasification rate was much higher and the microporosity of the resultant carbons was also wider.

The oxidation of a char (for instance by nitric acid) followed by removal of part of the oxygen surface groups formed upon oxidation is a controlled way to open the microporosity. The removal is carried out by heat treatment under an inert gas, the higher the temperature used the more oxygen surface groups removed and the larger is the widening of the pore entrance. Oxidation can also be carried out by treating the char with oxygen at around 250 ºC so that it is chemisorbed at active sites located at the entrances of the pores and then removed (as CO and CO_2), thus widening the microporosity; this process can be repeated until the required micropore size is reached.[6] Oxidation followed by heat treatment to remove the less stable and more acidic oxygen surface groups can also locate part of the remaining surface groups at the entrance of micropores, thus partially blocking them.[6]

The porosity of the prepared CMSs was analyzed by adsorption of N_2 (77 K) and CO_2 (273 K) and by immersion calorimetry of the CMS into liquids of different molecular dimensions (dichloromethane 0.33 nm; benzene 0.37 nm; cyclohexane 0.48 nm; 2,2-dimethylbutane 0.56 nm and α-pinene 0.7 nm). Adsorption kinetics were studied for individual gases (nitrogen, oxygen, methane, carbon dioxide) by introducing 0.1 MPa of the gas into the adsorption cell and following the evolution of adsorption as a function of time. Selectivity for the two couples of gases (nitrogen-oxygen and methane-carbon dioxide) was determined by calculating the ratio of amount adsorbed for each gas after 120 seconds of adsorption. A typical plot for adsorption kinetics is given in Figure 3 for a CMS prepared by the first procedure, activation of the acid-washed char with carbon dioxide.[7]

Separation of the above two mixtures was found to be optimum for a series of CMSs prepared using the three methods described above. Selectivity values for the nitrogen-oxygen mixture in the range 11-14 were obtained with the preparation methods used, although higher selectivities

were found for the methane-carbon dioxide mixture. Many CMSs with selectivity above 100 could be prepared. Since one could perhaps question the stability of CMS prepared by any of the oxidation procedures, cycles of adsorption-desorption for methane and carbon dioxide were carried out in some of the CMSs. The results were satisfactory because the uptake was kept constant after several cycles.[6]

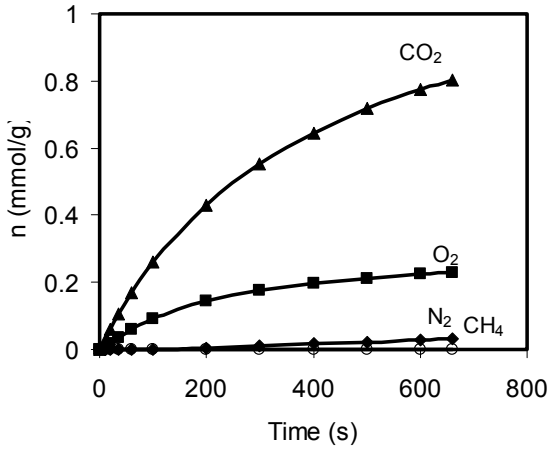

Figure 3. Typical adsorption kinetics for a CMS prepared by direct activation of an acid-washed coconut shell char. Adapted from reference 7, with permission from Elsevier.

As mentioned above, CMSs were also prepared using viscous rayon cloth or felt as precursor. In this case a controlled carbonization under nitrogen to increase the yield as much as possible, followed by a controlled gasification under carbon dioxide at slow reaction rate yield CMS with excellent selectivity for the methane-carbon dioxide separation. The additional advantage of using CMS in the form of cloth or felt is that the constituent carbon fibres have their microporosity open to the surface, this meaning a faster adsorption kinetics in respect to conventional granular CMS, for which the molecules to be adsorbed have to enter the granule through the macro- and mesopores. At the same time the use of cloth or felt ensures a much lower pressure drop produced by the circulation of the gases to be separated.

4. Gas Storage

In the case of carbons for gas storage (methane in this particular instance) one needs a very high adsorption capacity coupled with a high bulk density because the important parameter is the adsorption capacity expressed per unit volume. From the point of view of gas storage the porous carbon bed

can be divided into three well-defined volumes: i) carbon skeleton; ii) volume of meso- and macropores plus the interparticle space or voids; and iii) volume of micropores. Since the optimum packing of methane molecules in narrow micropores has been calculated by molecular simulation to be for pores in which two layers of molecules could be adsorbed (see Figure 2), it is clear that the volume of interest for storage is the microporosity of around 0.8 nm width. Consequently, an optimum adsorbent should exhibit a high volume of micropores and a low volume for the rest of spaces, thus facilitating a high volume of gas adsorbed per unit of volume of the carbon.

Of the different methods that can be used in the preparation of activated carbon, chemical activation would be the one to be preferred when a high yield is needed, as in this application. The three chemical agents more commonly used for chemical activation, zinc chloride, phosphoric acid and potassium hydroxide, have been used to prepare activated carbons for methane storage. The two former follow somewhat similar mechanisms, a typical example of the evolution of yield and porosity being plotted in Figure 4[8] for phosphoric acid activation as a function of the amount of phosphorous used in the impregnations solution, X_P. There is a fast development of microporosity as from low concentrations, this being the predominant porosity up to $X_P = 0.3$. For higher concentrations the development of microporosity is negligible, the main development corresponding to mesoporosity, which reaches values higher than the micropore volume. This chemical exhibits a concentration range in which the development of microporosity is coupled with a high yield, the latter decreasing when mesoporosity is being developed.

Impregnation with phosphoric acid and zinc chloride produces reactions leading to the fragmentation of cellulose and other components of the botanic precursor as hemicellulose and lignin. Although the two chemicals produce a relatively similar pattern along impregnation, the lower acidity of zinc chloride and the absence of phosphates differentiate both processes. However, there is a moment in which the impregnated particles become elastic and suffer some swelling; at the same time the conversion to carbon starts, as detected by the presence of tar at the surface of the particles. In both cases the reaction of the chemical with the precursor takes place at temperatures up to 450-500 ºC.

There are no visual changes observed during impregnation with KOH, with no formation of tar, because the reaction starts above 700 ºC, after the pyrolysis of the precursor. This is the main difference with the other two chemicals mentioned above.

According to the changes produced into the precursor upon impregnation, the impregnated material can be conformed under pressure to

produce solid monoliths without the need of a binder. The only point is to carry out the conforming at a temperature at which enough amount of tars is produced around the particles.

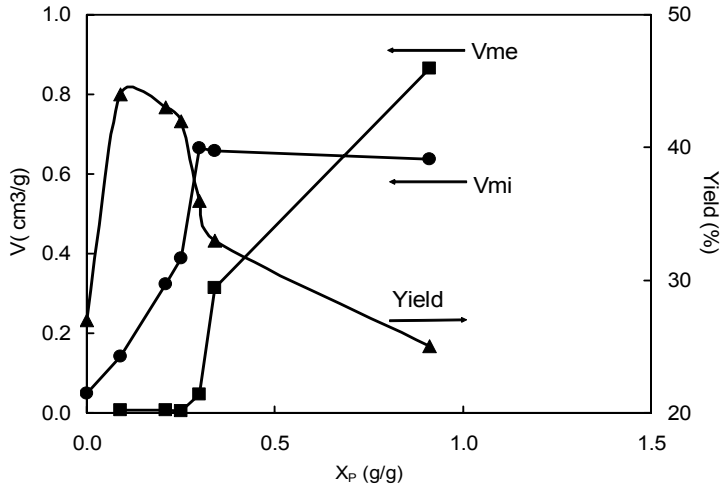

Figure 4. Evolution of microporosity, mesoporosity and yield for the activation with phosphoric acid of peach stones. Adapted from reference 8, with permission from Elsevier.

By using monoliths prepared by conforming the impregnated precursor at 100-200 ºC one can drastically reduce the fraction of the volume corresponding to interparticle space and voids. If the density of the monolith is adequate it is possible to reach high values of methane stored at the standard pressure of 3.4 MPa by unit of volume of monolith. In this case the monoliths were shaped as discs of around 2 cm diameter and 1 cm height. In order to have a better description of the discs, the different types of volume described above are calculated and plotted as a function of the concentration used for the impregnation of the lignocellulosic precursor. Such a plot (in the form of a histogram) can be found in Figure 5 for the case of phosphoric acid activation and in Figure 6 for activation with zinc chloride. Although the general behavior is relatively similar for the two chemicals there are clear differences between the volumes of the discs.

Increasing degree of activation with phosphoric acid (Figure 5) produces a slight decrease in the volume occupied by the carbon skeleton and a simultaneous increase in porosity, at first micropores and then meso- and larger pores. It is important to note that the volume of meso- and macropores decreases with increasing impregnation ratio, this reflecting the change in elasticity of the impregnated precursor.[9] Only at higher values of X_P there is an important volume of large pores, caused by the extensive attack by the acid. For the disc prepared by activation with $X_P = 0.35$, the

volume of micropores is near 90% of the total porosity and more than 50% of the total volume occupied by the carbon disc.

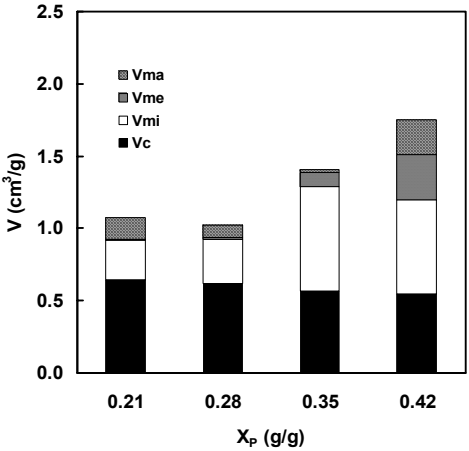

Figure 5. Distribution for volumes in discs prepared by phosphoric acid activation (V_C carbon skeleton; V_{mi} volume of micropores; V_{me} volume of mesopores; V_{ma} volume of macropores, including voids). Adapted from reference 8, with permission from Elsevier.

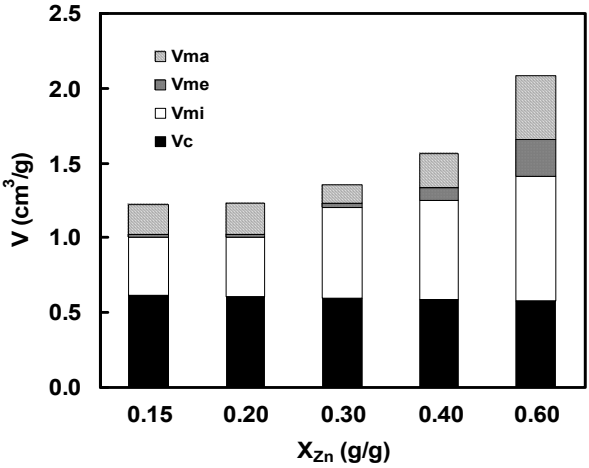

Figure 6. Distribution for volumes in discs prepared by zinc chloride activation (V_C carbon skeleton; V_{mi} volume of micropores; V_{me} volume of mesopores; V_{ma} volume of macropores, including voids). Adapted from reference 8, with permission from Elsevier.

The evolution is similar for discs prepared by zinc chloride activation[10] (Figure 6). The volume of micropores continuously increases with X_{Zn}, as it does the volume of mesopores, which is small. The volume of large pores initially decreases due to the elasticity of the impregnated precursor and increases at larger values of $X_{Zn,}$ where the attack of the chemical is more

intensive. The volume of micropores for the disc prepared at $X_{Zn} = 0.30$ is 80% of the total porosity and 50% of the volume occupied by the disc.

The comparison of Figures 5 and 6 indicates that both activating chemicals lead to discs with similar volume of carbon skeleton and a large volume of micropores in respect to other volumes of pores. It is important to note that the bulk density of the discs prepared at $X_P = 0.35$ and $X_{Zn} = 0{,}30$ are 0.71 and 0.74 g/cm^3, respectively, rather high values.

Adsorption of methane at 25 ºC on the discs was carried out up to a pressure of 3.4 MPa in a volumetric adsorption equipment (from VTI).The volume corresponding to the microporosity and the amount of methane adsorbed are related but the correlation among data is not total. The largest uptakes were 185 and 150 cm^3/g for $X_P = 0.35$ and $X_{Zn} = 0.40$, whereas the largest volume of micropores corresponds to the disc prepared at $X_{Zn} = 0.60$. Since it is more important to know the volume of methane adsorbed in a given volume of adsorbent, the bulk density of the discs has to be used. In this case the maximum methane uptakes at 3.4 MPa measured for the discs correspond to the values of 131 cm^3/cm^3 for $X_P = 0.35$ and 96 cm^3/cm^3 for $X_{Zn} = 0.40$, respectively.

In an attempt to increase the amount of methane adsorbed by the discs, they were further carbonized under a flow of nitrogen up to 800 ºC before being subjected to activation under a flow of carbon dioxide at 725 ºC. Carbonization at 800 ºC produces a weight loss in the discs (they were heat treated originally at 450 ºC for discs impregnated with phosphoric acid and 500 ºC for discs impregnated with zinc chloride) of around 10 wt%. This weight loss is accompanied by a contraction of the discs, this resulting in an increase in bulk density and a loss of microporosity. When the discs are activated under carbon dioxide there is an increase in the amount of methane adsorbed.

Figure 7 includes the plots of methane adsorbed at 3.4 MPa as a function of burn-off reached during activation for the case of phosphoric acid activation.[9] The increase in micropore volume upon activation corresponds with the increase in the amount of methane adsorbed, both coupled with a decrease in bulk density, as expected. Values for the discs prepared by only impregnation (0 wt% burn-off) are included in Figure 7 for the sake of comparison. There is a good relationship between the tendencies for the evolution of bulk density and methane uptake at 3.4 MPa.

By combination of the methane adsorption and the bulk density of the discs it is possible to obtain the plots of Figure 8 for the adsorption capacity expressed per unit volume.

The values (V/V) for the initial discs are plotted at 0 wt% burn-off. Activation under carbon dioxide produces an increase in the adsorption of

methane, large for the lower impregnation ratios used. Thus for $X_P = 0.21$ the highest methane uptake corresponds to 150 cm^3/cm^3, above the maximum value (131 cm^3/cm^3) obtained by direct chemical activation at $X_P = 0.35$. The increase in adsorption capacity is smaller when the discs prepared using higher concentrations of phosphoric acid are further activated under carbon dioxide.

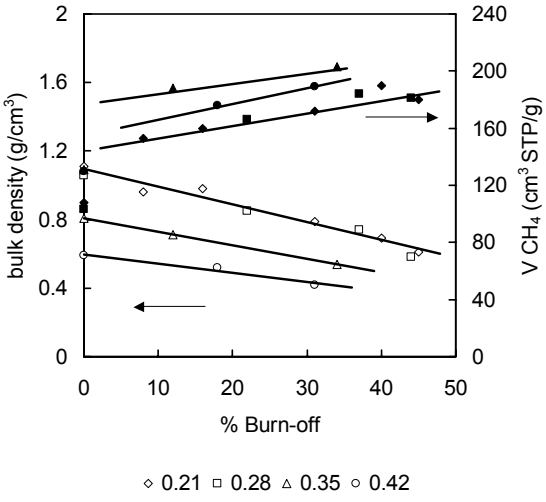

Figure 7. Evolution of bulk density and volume of methane adsorbed as a function of carbon dioxide activation (burn-off). Adapted from reference 9, with permission from Elsevier.

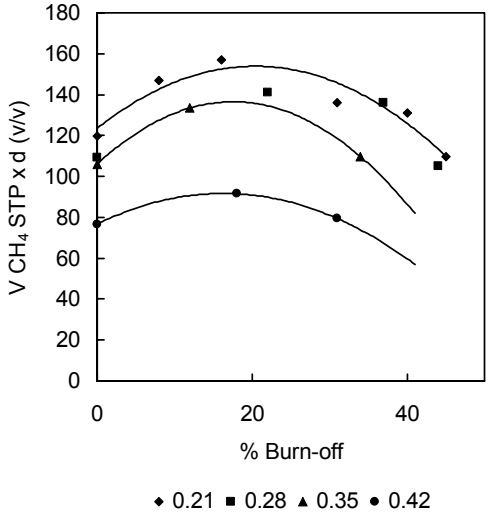

Figure 8. Evolution of methane capacity as a function of activation burn-off under carbon dioxide. Adapted from reference 9, with permission from Elsevier.

5. Conclusions

As shown above, the slit-shaped microporosity in activated carbon can be used favorably in two relatively new applications, gas separation and storage. The main problem in these two cases is the manufacture of the specific microporosity needed, but this can be overcome by using the right precursor and the appropriate activation mode. The CMS presented here have been prepared from very common lignocellulosic precursors and by using rather simple activation methods, thus reducing the final cost of the adsorbent. In the case of carbons for gas storage, the use of chemical activation permits a good control of the development of microporosity and also allows for the preparation of binder less monoliths, the only solution to reach high capacity values for natural gas (methane) storage.

REFERENCES

1. H. Marsh, and F. Rodríguez-Reinoso, *Activated Carbon* (Elsevier, in press).
2. A. Oberlin, TEM studies of carbonization and graphitization, in*: Chemistry and Physics of Carbon*, edited by P.A. Thrower (Marcel Dekker, New York, 1989), pp. 1-143.
3. F. Rodríguez-Reinoso, The role of carbon materials in heterogeneous catalysis, *Carbon* 36, 159-175 (1998).
4. F. Rouquerol, J. Rouquerol, and K. Sing, *Adsorption by Powders and Porous Solids* (Academic Press, London, 1999).
5. C. Gómez de Salazar, A. Sepúlveda-Escribano, and F. Rodríguez-Reinoso, Preparation of carbon molecular sieves by pyrolytic carbon deposition, *Adsorption* 11, 663-667 (2005).
6. C. Gómez de Salazar, A. Sepúlveda-Escribano, and F. Rodríguez-Reinoso, Preparation of carbon molecular sieves by controlled oxidation treatments, *Carbon* 38, 1889-1892 (2000).
7. C. Gómez de Salazar, A. Sepúlveda-Escribano, and F. Rodríguez-Reinoso, Use of immersion calorimetry to evaluate the separation ability of carbon molecular sieves, in: *Studies in Surface Science and Catalysis*, vol. 128, edited by K.K. Unger et al. (Elsevier, Amsterdam, 2000), pp. 303-312.
8. M. Molina-Sabio, and F. Rodríguez-Reinoso, Role of chemical activation in the development of carbon porosity, *Colloids & Surfaces A: Physicochem, Eng. Aspects* 241, 15-25 (2004).
9. M. Molina-Sabio, C. Almansa, and F. Rodríguez-Reinoso, Phosphoric acid activated carbon discs for methane adsorption, *Carbon* 41, 2113-2119 (2003).
10. C. Almansa, M. Molina-Sabio, and F. Rodríguez-Reinoso, Adsorption of methane into $ZnCl_2$-activated carbon derived discs, *Microp. Mesop. Mater.* 76, 185-191 (2004).

CARBONACEOUS MATERIALS AS DESULFURIZATION MEDIA

TERESA J. BANDOSZ*
Department of Chemistry, The City College of CUNY, 138th Street and Convent Ave, New York, NY 10031, USA

Abstract. Activated carbon-based materials have proven to work efficiently as adsorbents of sulfur containing species such as hydrogen sulfide, sulfur dioxide, methyl mercaptans from gas phase. This is owing to their surface feature such as functional groups, ash constituents, and high volume of small pores. In the pore system, sulfur containing species are oxidized to either elemental sulfur, sulfur dioxide or dimethyldisulfide depending on the chemistry of the species to be removed. Oxygen and nitrogen containing functional groups and catalytic metals such as iron or calcium are involved in this process. Presence of water film ensures sufficient conditions for dissociation providing that the local pH of the surface is greater than pK_a of the adsorbate. In this brief review the emphasis is placed on the role of activated carbons surfaces, either unmodified or modified in the processes of adsorption and catalytic oxidation of sulfur containing pollutants.

Keywords: activated carbon; adsorption; catalytic oxidation; desulfurization; hydrogen sulfide; sulfur dioxide; methyl mercaptan; DBT; surface chemistry; porosity

1. Introduction

Removal of sulfur compounds is usually addressed as desulfurization. To remove these species one has to either physically separate them, impose chemical reaction to improve separation or decompose them before separation. For separation physical adsorption, reactive adsorption on various sorbents (from the gas or liquid phase), extraction and precipitation are generally used. Imposing chemical reaction/decomposition includes

* E-mail: tbandosz@ccny.cuny.edu

J.M. Loureiro and M.T. Kartel (eds.), Combined and Hybrid Adsorbents, 145–164.

selective oxidation/catalytic oxidation on the surface of adsorbents, conventional hydrodesulfurization (HDS) on $CoMo/Al_2O_3$ catalysts, or catalytic distillation. Here only examples of the process are listed and the readers are referred to excellent reviews on desulfurization of fuels by Babich and Moulijn[1], Song[2], and the book by Stirling.[3]

To be in agreement with environmental law and to remove small, but sometimes persistent, concentrations of pollutants, activated carbons seem to be the media of choice. They are relatively inexpensive, easy to obtain, and owing to their enormously high surface area and pore volume,[4] they are able to remove and retain even traces of air and water pollutants. Activated carbons, due to their unique tailorable surface chemistry act not only as adsorbents but also as catalysts for oxidation of inorganic and organic species.[5]

This paper provides a brief summary of surface science involved in the application of activated carbon for removal of sulfur containing species. The emphasis is placed on the role of activated carbon surfaces, either unmodified or modified in the processes of adsorption and catalytic oxidation of these pollutants.

2. Removal of Hydrogen Sulfide

One of the leading malodorants arising from sewage treatment facilities and geothermal vents is hydrogen sulfide.[6] Traditionally, activated carbons used for removal of high concentrations of H_2S in sewage treatment plants are those impregnated with caustic materials such as NaOH or KOH.[6-9] The residual H_2S quickly reacts with the strong base and is immobilized. The presence of humidity facilitates the reaction.[10-13] The removal capacity of such carbon estimated using accelerated ASTM D6646-01 test[14] exceeds 0.140 g/cm^3 of the carbon bed.

The shortcoming in the applications of caustic impregnated carbon is the fact that impregnation decreases the ignition temperature of the carbon and poses a hazard of self-ignition.[8,9] Moreover, the activity of caustic carbons toward H_2S oxidation is exhausted when the caustic is consumed and the carbon pores are blocked by sulfur and sodium or potassium salts.[12]

The catalytic action of NaOH impregnated carbon can be summarized by the following reactions:[12]

$$NaOH + H_2S \rightarrow NaHS + H_2O \quad (1)$$

$$2NaOH + H_2S \rightarrow Na_2S + H_2O \quad (2)$$

$$NaHS + 0.5O_2 \rightarrow S + NaOH \quad (3)$$

$$Na_2S + 0.5O_2 + H_2O \rightarrow S + 2\ NaOH \quad (4)$$

$$HS^- + H_2O \rightarrow H_2S + OH^- \quad (5)$$

$$S^{2-} + H_2O \rightarrow HS^- + OH^- \quad (6)$$

$$2\ NaOH + H_2SO_4 \rightarrow Na_2SO_4 + 2H_2O \quad (7)$$

Both, advantages and disadvantages of caustic impregnated carbons directed the attention of researchers toward other impregnants, which can sustain basic properties with less exothermic reaction in the system. An example is potassium carbonate.[15,16] It was proposed that hydrogen sulfide dissolves more favorably in aqueous solution of K_2CO_3 than in water. H_2S, owing to its small size, is able to access the small micropores as KHS, which instantly decomposes to H_2S. That H_2S located in small pores reacts with oxygen forming elemental sulfur.

This risk of self-ignition of the carbon bed along with hazardous conditions of working with high pH carbons caused that virgin (unimpregnated) activated carbons[18-48] or carbon with specific surface modifications, such as nitrogen-enriched,[49-56] were investigated as H_2S removal media. Although extensive studies on such carbon were performed their industrial application is not yet common. This may be related to a relatively low capacity of virgin carbon compared to caustic impregnated one. Moreover, the mechanism on unimpregnated carbons seems to be more complex and very detailed features of carbon surfaces play a role in adsorption and catalytic oxidation.

A simple mechanism of adsorption/oxidation of hydrogen sulfide was first proposed by Hedden and co-workers.[30] According to them, dissociation of hydrogen sulfide occurs in the film of adsorbed water at the virgin carbon surface and then hydrogen sulfide ions, HS^-, are oxidized by oxygen radicals to elemental sulfur. Since then many studies have been done to account for such factors as a role of water,[25,31,33,35,36,39,47,48] role of oxygen,[17-26] autocatalysis by sulfur,[26,27] influence of pore sizes,[18,28,32,34,33,37] role of carbon surface chemistry,[40-43] the effects of ash,[48,57-60] and last but not least, speciation of surface oxidation products.[40-45]

As mentioned above, the film of water is necessary for dissociation of hydrogen sulfide, if pH of the surface allows it, and thus for its oxidation. It is well known that hydrophobic nature[61] of the activated carbon surface is the result of a high degree of aromatization and the presence of graphene-like sheets. Adsorption of water can be enhanced when functional groups containing oxygen or nitrogen exist at the edges of graphene-like sheets.[62,63] It was reported that on some carbons the prehumidification could improve the capacity as much as 80 times.[48] On the other hand, the amount of water adsorbed on the surface should not be too large and the affinity for water adsorption should not be greater than 5%[40,48] to reach the maximum capacity. It is likely that, when the carbon surface becomes too hydrophilic,

the small pores are filled by condensed water and the direct contact of HS^- with carbon surface in the smallest pores is limited. Another factor that plays a role is the degree of carbon oxidation.[40-43,62,63] When more oxygen groups are present, the surface becomes more acidic suppressing dissociation of hydrogen sulfide.

A role of oxygen in the kinetics of the H_2S adsorption/oxidation was studied by Tollefson and co-workers,[17-26] Steijn and co-workers[28] and Meeyoo and co-workers[25]. In general, the experiments were performed with low concentrations of H_2S (<3 %) in wide temperature (398 K-473 K) and pressure ranges (230-3200 kPa). The results showed that optimum temperature for high H_2S conversion and low SO_2 production is 448 K with O/H_2S ratio 10.05 times the stoichiometric ratio.[22] The rate-limiting step for catalytic oxidation reactions was defined as either adsorption of oxygen or hydrogen sulfide from the bulk phase on the activated carbon surface. Physical nature of adsorption was confirmed by Bandosz and co-workers when adsorption on H_2S was studied at elevated temperature (< 400 K) in the absence of air or water.[46] At those conditions, the heat of H_2S adsorption (between 40 and 50 kJ/mol) depends only on the pore sizes. This was an indirect proof that oxygen chemisorbed on the surface or present as functional groups is not active enough to oxidize hydrogen sulfide.[46] On the other hand, Mikhalovsky and Zaitsev[38] found using XPS that surface oxygen-containing functional groups contribute significantly to the formation of SO_2 in H_2S oxidation.

An interesting effect of autocatalysis by deposited sulfur was described by Steijns and co-workers.[26,27] They found that deposition of sulfur at the beginning of the removal process increases the catalytic activity of the carbon. Elemental sulfur was proposed to be rather in the form of radical chains than S_8 rings and the catalytic activity per square meter of total surface area was found to be approximately proportional to the amount of adsorbed sulfur.[27]

In all studies of hydrogen sulfide adsorption the presence of micropores is indicated as an important factor. Although the opinions about the first location of adsorbed sulfur vary,[17,18] the filling of micropores by elemental sulfur or sulfides seems to be the limiting factor of activated carbon capacity.[40,44,45,47] Steijn and Mars found that the strong sulfur adsorption is in carbons having pores between 0.5-1 nm.[18] Moreover, when sulfur is adsorbed in such small pores the presence of large polymers is unlikely, and isolated adsorbed sulfur radicals are further oxidized to SO_2 and then SO_3. On such carbons, sulfuric acid is the important product of surface reaction.[40] It was also found that when the H_2S capacity of carbons is normalized to their pore volume, the comparable capacities are obtained[40,47] (Figure 1).

A role of surface chemistry was for long time ignored in the study of hydrogen sulfide adsorption/oxidation. However, Kaliva and Smith[36] indicated that water likely forms complexes with oxygen thus taking part in the surface reaction, the effect of carbon surface chemistry, besides the influence of ash, was not discussed in details. It is well known that the degree of acid dissociation depends on the pH of the system, and dissociation is feasible when pH is greater than pK_a of an acid under study. Since hydrogen sulfide is a weak acid, analysis of the performance of carbons showed the dependence of the capacity on the acidity of carbon.[37,40,47] Moreover, threshold values were found on the dependence of the parameters describing the acidity of carbons and the normalized (for pore volumes) H_2S breakthrough capacities[47] (Figure 1). The threshold value derived from the analysis of the data was found to be around 4.5.[40] The justification for this threshold in surface pH is based on the steps of hydrogen sulfide adsorption/oxidation on unmodified carbons.[40,48] They are as follows: (1) H_2S adsorption on the carbon surface, (2) its dissolution in a water film, (3) dissociation of H_2S in an adsorbed state in the water film, (4) and surface reaction with adsorbed oxygen.

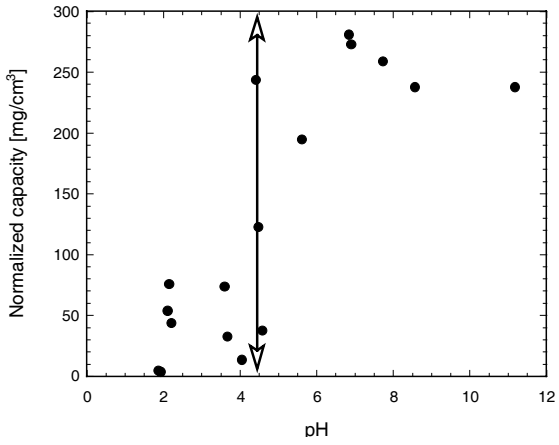

Figure 1. Normalized H_2S breakthrough capacity versus pH of carbon surface[14]. Reprinted with permission from T.J. Bandosz, *J. Colloid Interface Sci.,* 246, 1 (2002).

The effect of ash can be considered as an extension of the effect of surface chemistry. It was found that presence of iron oxides or metals ions from group 6-8 has an effect on hydrogen sulfide adsorption.[18,48,57,59] These metals affect not only the amount adsorbed but also the extent of oxidation. According to Steijn and Mars,[18] iron oxide promotes formation of SO_2 when removal process occurs at elevated temperatures. That effect was also noticed for removal of hydrogen sulfide on carbons at ambient conditions.[31,48] The study of hydrogen sulfide removal on coal fly ash

showed the noticeable adsorption/oxidation on mullite, hematite and magnetite, all containing iron oxides.[57,58] This effect was also clearly seen when carbonaceous materials derived from sewage sludge were tested as hydrogen sulfide adsorbents.[64] On them, an exceptionally high adsorption capacity, higher than that on coconut shell-based carbon was found. That superior performance was attributed to the catalytic reactions on ash, in particular on iron, copper and zinc oxides. On the other hand the catalytic effect of calcium and magnesium oxides dispersed within the carbon matrix was found to be in their basicity and insolubility in water.[60] Hydrogen sulfide dissociates on these oxide active centers where it is oxidized to elemental sulfur. The close proximity of a carbon phase enables sulfur migration to the pore system and thus regeneration of the active centers. On such materials (Midas®) capacity as high as 60% was reported.[60]

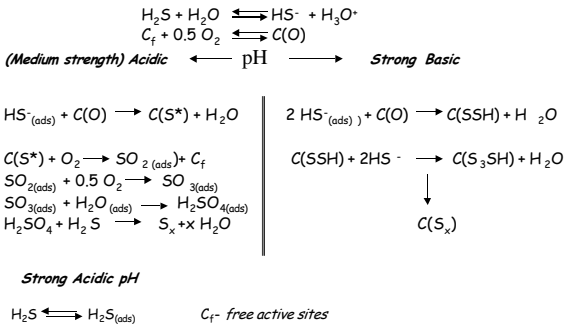

Figure 2. Proposed pathways of H_2S oxidation on unmodified activated carbons[14]. Reprinted with permission from T.J. Bandosz, J. Colloid Interface Sci., 246, 1 (2002).

Analysis of the above factors helped to formulate to the pH dependent mechanism of hydrogen sulfide adsorption on activated carbons[40,47] (Figure 2). When the environment is moderately basic an increase in the concentration of HS^- occurs. When the pH is distinctively acidic, the concentration of hydrogen sulfide ions is very low. In such situation hydrogen sulfide ions - when adsorbed in small pores - are oxidized and converted to highly dispersed sulfur. These separated sulfur "islands" are susceptible to further oxidation to SO_2 and SO_3. When the pH is less acidic (more basic) the concentration of HS^- is much higher, which forces the created sulfur atoms to be close to each other, capable of forming polysulfides.[27] Then their polymerization to stable chain or cyclic sulfur molecules such as S_8 occurs. The best conditions leading to oxidation of hydrogen sulfide to S^{4+} or S^{6+} exist when the concentration of HS^- is just right (not too high, not too low) to be oxidized to highly dispersed sulfur. On the other hand, when the content of H_2SO_4 rises in the course of the

experiment, it suppresses the dissociation of hydrogen sulfide and inhibits the adsorption process.

The described above mechanism is also true for adsorption of hydrogen sulfide on nitrogen containing carbons.[49-56] Such materials were introduced by Calgon Carbon in their proprietary process of Centaur® preparation.[52] Thermal treatment with nitrogen compounds results in the presence of quaternary and pyridine-like nitrogen in the small pores.[56] Basicity of such species, in the presence of moisture, enhances hydrogen sulfide dissociation, adsorption, oxidation, formation of radicals and then their oxidation to sulfuric acid. However, the total capacity of Centaur® is not exceptionally high (0.060 g/cm^3),[56] its surface conversion of H_2S to H_2SO_4 is almost complete. This makes regeneration of spent materials using simple water washing feasible.[49,50] Although oxidation to sulfuric acid makes Centaur® a superior product, high costs and risks related to the removal of concentrated acid from the surface limits its industrial applications in favor of caustic impregnated or virgin activated carbons.[9]

3. Removal of Sulfur Dioxide

An increase in the acidity of natural waters, fast rate of abrasion of buildings and monuments and associated with this health problems caused that desulfurization of fossil fuels along with removal of SO_2 from stock gases became strategic tasks. Efficient media for removal of sulfur dioxide are activated carbons[31,65-81] and activated carbon fibers[69,75,79]. Numerous studies indicate good efficiency of SO_2 removal on these materials either at low[69,71,73,74] or high temperatures.[67,68,77,78] Process of SO_2 adsorption has been studied extensively and, as in the case of H_2S, such parameters as porosity,[65-74,79,83] surface chemistry,[65,68,70,72,74,75,77,89] and constituents of ash[88-90] were taken into consideration. The products of surface reactions were analyzed from the point of view of removal efficiency and the feasibility of regeneration.[71,80] Since usually the process is carried out in the presence of moisture and oxygen, it is generally accepted that sulfur dioxide is oxidized to sulfuric acid as a final product of the reaction. That acid is strongly retained in the pore system of activated carbons.[73] Adsorption/oxidation of SO_2 in oxygen atmosphere and in the presence of water occurs as follows:

$$SO_{2\,gas} \rightarrow SO_{2\,ads} \tag{8}$$

$$O_{2\,gas} \rightarrow 2\,O_{ads} \tag{9}$$

$$SO_{2\,ads} + O_{ads} \rightarrow SO_{3\,ads} \tag{10}$$

$$H_2O_{gas} \rightarrow H_2O_{ads} \tag{11}$$

$$SO_{3\,ads} + H_2O_{ads} \rightarrow H_2SO_{4\,ads}, \quad (12)$$

where indices "gas" and "ads" refer to the presence of reactants in the gas phase and the adsorbed state, respectively. It was also found that three forms of adsorbed sulfur oxides (weakly adsorbed SO_2, physically adsorbed SO_3 - after oxidation of SO_2 -, and strongly adsorbed H_2SO_4[71-75]) could be present in such a situation.

In the case of adsorption of sulfur dioxide it was demonstrated that oxidation to sulfur trioxide occurs mainly in the 0.7 nm pores.[73] With an increase in the size of pores less SO_2 is converted which results in smaller uptake of sulfur dioxide. No correlation was found between the amount of SO_2 adsorbed in the presence of oxygen and the volume of micropores.

A significant effect of very small micropores on SO_2 adsorption was also noticed by Bandosz and co-workers[82] (Figure 3). The evidence on adsorption of sulfur dioxide in micropores in the absence of oxygen was found by Molina-Sabio and co-workers.[74] While calculating the micropore volumes of various carbons using CO_2, N_2, and SO_2, a relatively good agreement in the values was obtained. A small discrepancy found in the case of SO_2 was explained by its polarity. Similar effect on micropore filling mechanism was also noticed by Wang and Kaneko.[83]

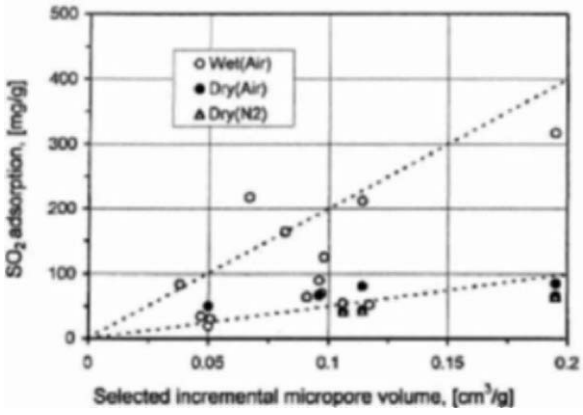

Figure 3. Dependence of SO_2 adsorption capacity on the pore volume between 0.679 nm and 0.858 nm (calculated from DFT). Reprinted with permission from Ref. 82. Copyright (2002) American Chemical Society.

Although effects of porosity are crucial for physical adsorption, when weak adsorption forces exist, the importance of the catalytic effects of surface chemistry increases. In the case of acidic gases such as SO_2, the positive effect on adsorption should be observed when the basicity of surface increases. It was found that heat treatment of activated carbons or activated carbon fibers at temperatures about 1300 K results in an increase in the amount of sulfur dioxide adsorbed.[65-71] Such treatment, besides

removal of oxygen containing acidic groups, should increase carbon basicity.[5] When basic groups containing oxygen are present on the carbon surface the adsorption of SO_2 is significantly enhanced[70,72] and these groups (pyronic and pyronic-like type) are responsible for strong physical adsorption of sulfur dioxide.

The strong adsorption of sulfur dioxide is enhanced by the presence of oxygen.[65,78,70,72,75] These oxygen-containing sites are proposed to act as catalytic centers for oxidation of SO_2 to SO_3.[76] According to Davini oxygen present in the system plays an important role in the variations of SO_2 adsorbed.[68,70] The negative role of oxygen in the amount of SO_2 adsorbed is linked to its ability to react with a carbonaceous matrix, formation of surface groups, which decrease the surface area of adsorbent. On the other hand, Daley and co-workers found that when dry SO_2 was adsorbed, the presence of oxygen containing functional groups significantly enhanced the performance at temperature smaller than 348 K.[75] That enhancement was explained by surface reactions of quinines with SO_2 and water forming diol and sulfuric acid. The effect of surface chemistry on SO_2 oxidation was also discussed in detail by Raymundo-Pinero and co-workers.[73] They confirmed that removal of oxygen from the surface forms new high-energy adsorption/oxidation centers.

An increase in the uptake of SO_2 upon oxidation of carbon was found by Lisovskii and co-workers.[71] They proposed that surface acidic groups are the catalysts for SO_2 oxidation. Moreover, the presence of strong basic functionality was suggested as not beneficial for the process of sulfur dioxide removal due to an increase in the retention of sulfuric acid.[71]

Basic nitrogen species present on the surface of activated carbons or carbon fibers, were found to enhance the sulfur dioxide uptake. PAN based activated carbon fibers are examples of good adsorbents for SO_2 removal.[79,84] Although role of nitrogen present in the carbon matrix was not emphasized by Lee and co-workers in their studies of SO_2 adsorption on PAN based activated carbon fibers,[85] Kawabuchi and co-workers noticed a significant increase in the sorption capacity when activated carbon fibers were modified with pyridine and basic nitrogen functionalities were introduced to the surface.[84] Pyridine provided basic functionality, which increased catalytic removal of SO_x. The effect is even more pronounced when those groups are present in small pores.[73,82] The only negative part related to the application of these materials is strong adsorption of sulfuric acid leading to the difficulty in adsorbent regeneration, which was mentioned earlier by Lisovskii and co-workers.[71]

As in the case of hydrogen sulfide, the presence of ash and its composition should have an effect on the amount of SO_2 retained on the surface.[86] The enhancement in the oxidation of SO_2 due to the presence of

active inorganic matter was also found by Bandosz and co-workers on carbonaceous adsorbents derived from sewage sludge.[87] In those materials, a high content of CaO was identified as a favorable factor. The effect of calcium was also studied when fly ash mixtures with calcium hydroxide were tested as SO_2 adsorbents.[88] It was found that $Ca(OH)_2$ enhances the dispersion of calcium reagent and thus improves the efficiency of the adsorbent.

4. Removal of Methyl Mercaptan

Although mercaptans present in air or gaseous fuel can cause similar environmental and catalyst poisoning effects as hydrogen sulfide, their adsorption on activated carbons has been addressed less frequently in the scientific literature.[31,53,89-96]

The main difference between hydrogen sulfide and methyl mercaptan (MM) is the presence of hydrocarbon moiety in the case of the latter compound. It causes that MM molecule is much stronger adsorbed by physical forces on the surface of activated carbons than hydrogen sulfide. The likely surface oxidation product is dimethyldisulfide (DMDS) not elemental sulfur or sulfur dioxide.

An extensive study of the effects of the carbon surface features on adsorption-oxidation of methyl mercaptan at ambient temperature was performed by Bandosz and co-workers.[92-96] To evaluate the effects of porosity, surface area and surface chemistry, activated carbons with a broad range of pore sizes were chosen (from very microporous to mesoporous) and with various surface chemical heterogeneity (oxygen or nitrogen containing surface groups, ash constituents).

Analysis of the surface oxidation products using either TA or GC/MS indicated that the predominant product of surface oxidation is dimethyldisulfide, however traces of methyl methane thiosulfonate ($C_2H_6O_2S_2$) were detected.[94] It can be the product of the reaction of DMDS with oxygen:

$$C_2H_6S_2 + 2\ O^* \rightarrow C_2H_6O_2S_2 \qquad (13)$$

or the disproportionation of sulfonic acid:

$$3CH_3SO_2H \rightarrow C_2H_6O_2S_2 + CH_3SO_3H + H_2O \qquad (14)$$

Support for the presence of these oxidation products was only less than 3 pH units decrease in the pH, which excluded the formation of sulfonic acid.[93] The overall effect of oxidation on the capacity was mixed and it was believed that the observed changes were the results of the combined influence of the surface chemistry and porosity. More acidic was the

surface, less strong was the sorption of MM, which was reflected in the amount of desorbed MM by air purging after the adsorption process.

New light on the importance of the specific surface features on the feasibility of removal of methyl mercaptan on activated carbon was thrown after study of nitrogen-enriched carbons as MM removal media.[95,97] The capacity on carbons modified with urea was much higher than that on the as received adsorbents and even ten times enhancement can be obtained using this route of surface modification. The enhanced performance is attributed to the effect of basic nitrogen incorporated within the carbon matrix. The results indicated the maximum in the capacity at C/N content about 0.02. It confirms the results obtained by Strelko and coworkers[98] who found using the quantum chemical calculation of model nitrogen-containing carbon clusters that at an atomic concentration of quaternary nitrogen within the carbon matrix between 2 and 3 % the minimum of the band gap occurs. The lowest width of the band gap indicates the highest catalytic activity in electron transfer reactions.

The importance of basicity was also demonstrated when the density of basic groups on the surface determined using Boehm titration method was linked to the MM removal capacity. The majority of carbons used for that research followed the linear trend. The discrepancy in some case was caused by the differences in the content of catalytically active phase, iron oxide, which will be addressed later in this section.

On the basis of the systematic study[92-95] and the ability of CH_3SH to dissociate, the following scheme of CH_3SH adsorption/oxidation on the nitrogen containing carbons was proposed: 1) methyl mercaptan is first adsorbed from the gas phase on the carbon surface, where due to the presence of water film, it is dissolved and, depending on the pH, it can dissociate with the formation of thiolate ions and protons; 2) since the positively charged quaternary nitrogen enhances the ion exchange properties of activated carbons, thiolate ions are adsorbed in the vicinity of the nitrogen center; 3) then nitrogen accept an electron from sulfur and transfer it to the oxygen adsorbed on the surface; 4) as a result, thiolate radicals and superoxide ions O_2^- can be formed with the latter triggering the formation of hydroxyl radicals; 5) the final step of the oxidation process is formation of DMDS and water. The reaction proceeds until all the pores with positively charged nitrogen centers, and other active centers of the carbon surface are filled with the reaction products, and then only physical adsorption of MM takes place. It occurs mainly in pores smaller than 5 nm which are active in the adsorption of water at the ambient conditions (80 % humidity).[62,63,99]

A dual role of water in the process of methyl mercaptan adsorption on activated carbons was suggested.[94] DMDS, which is the main product of

surface reactions, has to compete with water for adsorption sites. However, the competition exists, DMDS is always a "winner" owing to its strong adsorption on carbons. On the other hand, the formation of significant amount of DMDS would not be possible without the presence of water in the system. Water facilitates dissociation of methyl mercaptan leading to its oxidation by oxygen, mainly from air.

Analyzing the effect of surface chemistry one should not forget about the effects of porosity. In fact the pores are significant assets of activated carbons used in environmental applications. As mentioned above, pores smaller than 5 nm should be especially active in the adsorption process due to the possibility to accommodate water together with MM molecules and thus due to formation of microreactors for DMDS synthesis. The dependence of the amount of DMDS formed on the carbon on their volume of pores less than 5 nm is plotted in Figure 4. A good linear agreement with slope equal to 1.02 was found for samples for which the saturation conditions were reached.

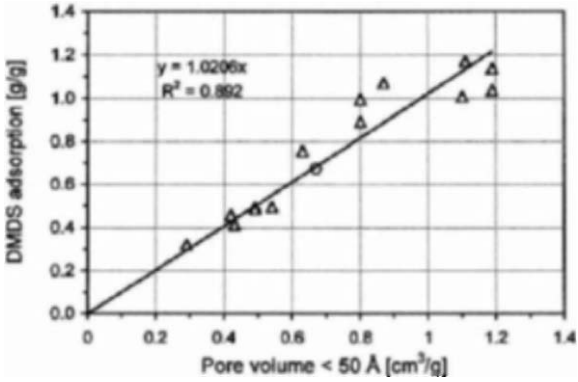

Figure 4. Dependence of the amount of DMDS adsorbed at saturation conditions on the volume of pores smaller than 5 nm. Reprinted with permission from Ref. 94. Copyright (2002) American Chemical Society.

Besides porosity, surface chemistry of the carbonaceous matrix, inorganic matter in activated carbon and its chemical specification have shown to be important for the process of MM adsorption/oxidation.[96] While potassium, which is the natural component of coconut shell-based carbon enhances capacity by shifting the dissociation of MM to the right, iron plays a role for catalytic oxidation via redox reactions. It is almost always present in an inorganic matter of carbons from such natural sources as coal, wood, or peat and its effect on MM adsorption /oxidation can be summarized in the following sequence of reactions (in the presence of moisture and oxygen).[96]

$$CH_3SH \rightarrow CH_3S^- + H^+ \quad (15)$$

$$Fe^{3+} + CH_3S^- \rightarrow Fe^{2+} + CH_3S^{\cdot} \quad (16)$$

$$2CH_3S^{\cdot} \rightarrow CH_3SSCH_3 \quad (17)$$

$$Fe^{2+} + O_2 + H^+ \rightarrow Fe^{3+} + HO_2^{\cdot} \quad (18)$$

$$CH_3S^- + HO_2^{\cdot} \rightarrow CH_3S^{\cdot} + HO_2^- \quad (19)$$

$$HO_2^- + H^+ \rightarrow H_2O_2 \quad (20)$$

$$2CH_3SH + H_2O_2 \rightarrow 2\ CH_3S^{\cdot} + 2\ H_2O \quad (21)$$

The effect of inorganic matter for adsorption of MM was also pointed out when removal of MM was investigated on coal and wood fly ash. The adsorbents chosen contained about 8 and 18 % of carbon, respectively with high pH over 12 and around 1 % of iron. With very low surface area (40 m^2 g^{-1} or less) the adsorbents were able to oxidize MM to DMDS without significant catalytic decay.[58]

All the results described above led to the conclusion about the importance of surface chemistry for adsorption/oxidation of methyl mercaptan. To explain apparent dependence of the capacity on the surface pH, two different mechanisms of adsorption/oxidation process were taken into consideration. In both cases it was supposed that adsorbed MM reacts with oxygen and then it is stored in the pore system in the form of DMDS.[94,95] Taking into account the chemical nature of MM, the removal mechanism should be different at dry conditions ("dry" mechanism) and wet conditions. At the latter, adsorption may occur either, on the dry carbon surface or on the water clusters ("island" mechanism).

In the "dry" mechanism it is assumed that MM and oxygen are adsorbed from a gas phase on the dry carbon surface, where reaction takes place. Water and DMDS are the reaction products. The latter species is adsorbed on the carbon surface while the former one is desorbed.

The "island" mechanism assumes that adsorption takes place in wet conditions and H_2O adsorbed on the carbon surface, is able to create water clusters or small water islands, where MM and oxygen first are dissolved in molecular form and later, depending on the pH, MM can dissociate to thiolate ion. Oxidation occurs due to the surface reaction between adsorbed thiolate ions and dissociatively adsorbed oxygen in water "islands" and/or between adsorbed MM and oxygen on a dry part of the carbon surface. The product of reaction, DMDS, is adsorbed in a molecular form on the carbon surface.

Taking into account the equilibrium constants of the all processes mentioned in two mechanisms, the simplified expression suggests that for

all carbons with the average surface pH greater than 7.5 concentration of CH_3S^- in the adsorbed state is equal to CH_3SH in a gas phase (100% dissociation + adsorption), which is required for effective CH_3SH removal.[95] It is about 2.7 pH units less than for simple dissociation in water. These results support the significance of the activated carbon surface and its effect on physicochemical processes taking place in the pore system.

Since basicity is an important factor for efficient removal of MM on activated carbons, the performance of materials can be also enhanced by impregnation of a virgin carbon surface with basic compounds.[6,90,91] As impregnants, NaOH, Na_2CO_3, KOH, and K_2CO_3 are usually used. In spite of blocking some pore volume, they are able to enhance the capacity of carbons for MM removal by a factor of two.[90]

Besides basic compounds, an improved capacity for MM removal can be also obtained by surface impregnation with compounds, which are able to promote redox surface reaction. It was found that the modification of the activated carbon surface with Fe_2O_3, KI and KIO_3 (all about 4 wt%) increased the capacity of activated carbon by a factor 3–5.[91, 96]

The oxidation mechanism of methanethiol on activated carbon fibers (ACF) in the presence of H_2S and iron catalyst was proposed by Katoh and coworkers.[31] According to them the process is initiated by $O_2^- \bullet$, which, through chain reactions with an iron catalyst involved, forms $\bullet OH$ radicals. Those radicals not only extract hydrogen from polysufide, form chain sulfur radicals, which accelerate the H_2S oxidation but also oxidize DMDS formed by partial oxidation. As a product, methane sulfonic acid is expected. This mechanism is true only for the complex system with a mixed supply of the sulfur containing gases.

5. Conclusions

Numerous published results indicate that complex processes take place on the surface of carbonaceous materials leading to adsorption of sulfur containing compounds, their oxidation and deposition of oxidation products in the pore system. For all of these, it is the surface features of activated carbon that govern the desulfurization processes. In the majority of cases it is impossible to separate the role of porosity, pore sizes and pore volume from the role of surface chemistry. Since their coexistence is a must, the way in which they affect the feasibility of desulfurization is a synergy, which opens the way for the application of carbonaceous materials in environmental remediation.

REFERENCES

1. I.V. Babich, and J.A. Moulijn, Science and technology of novel processes for deep desulfurization oil refinery streams: a review, *Fuel* 82, 607-631(2003).
2. Ch. Song, An overview of new approaches to deep defulfurization for ultra-clean gasoline, diesel fuel and jet fuel, *Catalysis Today* 86, 211-263 (2003).
3. D. Stirling, *The Sulfur Problem: Cleaning up Industrial Feedstocks* (RCS, Cambridge, 2000).
4. R.C. Bansal, J.B. Donnet, and F. Stoeckli, *Active Carbon* (Marcel Dekker, New York, 1988).
5. C.A. Leon y Leon, and L.R. Radovic, in: *Chemistry and Physics of Carbon*; Vol. 24, edited by P.A. Thrower (M. Dekker, New York, 1992), pp. 213-310.
6. A.Turk, S. Sakalis, J. Lessuck, H., Karamitsos, and O. Rago, Ammonia injection enhances capacity of activated carbon for hydrogen sulfide and methyl mercaptan, *Environ. Sci. Technol.* 33, 1242-1245 (1989).
7. A. Turk, K. Mahmood, and J. Mozaffari, Activated carbon for air purification in New York City's sewage treatment plants, *Wat.Sci. Tech*. 27, 121-126 (1993).
8. A. Turk, T. J. Bandosz, in: *Odours in Wastewater Treatment: Measurement, Modeling and Control*, edited by R.M. Stuetz and F-B. Frechen, (IWA, London, 2000), pp. 354-364.
9. T.J. Bandosz, A. Bagreev, F. Adib, and A.Turk, Unmodified versus caustics-impregnated carbons for control of hydrogen sulfide emissions from sewage treatment plants, *Environ. Sci. Technol*. 34, 1069-1074 (2000).
10. R. Yan, D.T. Liang, L. Tsen, and J.H. Tay, Kinetics and mechanisms of H_2S adsorption by alkaline activated carbon, *Environ. Sci. Technol* 36**,** 4460-4466 (2002).
11. H-L. Chiang, J-H. Tsai, C-L. Tsai, and Y-C. Hsu, Adsorption characteristics of alkaline activated carbon exemplified by water vapor, H_2S and CH_3SH gas, *Sep. Sci. Technol*. 35**,** 903-918 (2000).
12. A. Bagreev, and T. J. Bandosz, A role of sodium hydroxide in the process of hydrogen sulfide adsorption/oxidation on caustic-impregnated activated carbons, *Ind. Eng. Chem. Res*. 41, 672-679 (2002).
13. ASTM Standards, Vol. 15.01, *Refractories; Carbon and Graphite Products; Activated Carbon; Advanced Ceramics*, ASTM D6646-01, 1998.
14. T.J. Bandosz, On the adsorption/oxidation of hydrogen sulfide on activated carbons, *J. Colloid Interface Sci.* 246 , 1-20 (2002).
15. J. Przepiorski, and A. Oya, K_2CO_3-loaded deodorizing activated carbon fibre against H_2S gas: factors influencing the deodorizing efficiency and the regeneration method, *J. Mat. Sci. Lett.* 17, 679-682 (1998).
16. J. Przepiorski, S. Yoshida, and A. Oya, Structure of K_2CO_3-loaded activated carbon fiber and its deodorization ability against H_2S gas, *Carbon* 37, 1881-1890 (1999).
17. I. Coskun, and E. L. Tollefson, Oxidation of low concentrations of hydrogen sulfide over activated carbons, *Can. J. Chem. Eng.* 58, 72-76 (1986).
18. M. Steijns, and P. Mars, Catalytic oxidation of hydrogen sulfide. Influence of pore structure and chemical composition of various porous substances, *Ind. Eng. Chem. Prod. Res. Dev.* 16, 35-41 (1977).
19. T.K. Ghosh, and E.L. Tollefson, A continous process for recovery of sulfur from natural gas containing low concentrations of hydrogen sulfide, *Can. J. Chem. Eng.* 64, 960-968 (1986).

20. T.K. Ghosh, and E.L. Tollefson, Kinetics and reaction mechanism of hydrogen sulfide oxidation over activated carbon in the temperature range of 125-200 ^{o}C, *Can. J. Chem. Eng.* 64, 969-976 (1986).
21. A.K. Dalai, M. Majumadar, A. Chowdhury, and E.L. Tollefson, The effects of pressure and temperature on the catalytic oxidation of hydrogen sulfide in natural gas and regeneration of the catalysts to recover the sulfur produced, *Can. J. Chem. Eng.* 71, 75-82 (1993).
22. A. Yang, E.L Tollefson, and A.K. Dalai, Oxidation of low concentrations of hydrogen sulphide: process optimization and kinetics studies, *Can. J. Chem. Eng.* 76**,** 76-86 (1998).
23. A.K. Dalai, and E.L. Tollefson, Kinetics and reaction mechanism of catalytic oxidation of low concentrations of hydrogen sulfide in natural gas over activated carbon, *Can. J. Chem. Eng.* 64, 902-914 (1986).
24. A.K. Dalai, A. Majumdar, and E.L. Tollefson, Low temperature catalytic oxidation of hydrogen sulfide in sour produced wastewater using activated carbon catalysts, *Environ. Sci. Technol*. 33, 2241-2246 (1999).
25. V. Meeyoo, D.L. Trimm, and N.W. Cant, Adsorption-reaction processes for the removal of hydrogen sulphide from gas streams, *J. Chem. Tech. Biotechnol*. 68, 411-416 (1997).
26. M. Steijns, F. Derks, A. Verloop, and P. Mars, The mechanism of the catalytic oxidation of hydrogen sulfide. II Kinetics and mechanism of hydrogen sulfide oxidation catalyzed by sulfur, *J. Catal.* 42**,** 87-95 (1976).
27. M. Steijns, P. Koopman, B. Nieuwenhuijse, and P. Mars, The mechanism of the catalytic oxidation of hydrogen sulfide. III. An electron spin resonance study of the sulfur catalyzed oxidation of hydrogen sulfide, *J. Catalysis* 42, 96-106 (1976).
28. M. Steijns, and P. Mars, The role of sulfur trapped in micropores in the catalytic partial oxidation of hydrogen sulfide with oxygen, *J. Catalysis* 35**,** 11-17 (1974).
29. J. Klein, and K-D. Henning, Catalytic oxidation of hydrogen sulphide on activated carbons, *Fuel* 63, 1064-1067 (1984).
30. K. Hedden, L. Humber, and B.R. Rao, Adsorptive reinigung von schwefel was ser stoffhaltigen abgasen, VDI-Bericht Nr. 253 S. 37/42, VDI-Verlag, 1976.
31. H. Katoh, I. Kuniyoshi, M. Hirai, and M. Shoda, Studies of the oxidation mechanism of sulphur-containing gases on wet activated carbon fibre, *Appl. Catal. B: Environmental* 6, 255-262 (1995).
32. S. Tanada, T. Kita, K. Boki, and Y. Kozaki, Preparation of narrow pores carbon suitable for hydrogen sulfide adsorption, *J. Environ. Sci. Health* A20, 87-96 (1985).
33. J. Choi, M. Hirai, and M Shoda, Catalytic oxidation of hydrogen sulphide by air over an activated carbon fibre, *App. Catal. A*, 79, 241-248 (1991)
34. R. Sreeramamurthy, and P.G. Menon, Oxidation of H_2S on active carbon catalysts, *J. Catalysis* 37, 287-296 (1975).
35. A. Primavera, A. Trovarelli, P. Andreussi, and G. Dolcetti, The effect of water in the low-temperature catalytic oxidation of hydrogen sulfide to sulfur over activated carbon, *Appl. Catal. A: Gen*. 173, 185-192 (1998).
36. A.N. Kaliva, and J. W. Smith, Oxidation of low concentrations of hydrogen sulfide by air on a fixed activated carbon bed, *Can. J. Chem. Eng.* 61, 208-212 (1983).
37. L.M. Le Lauch, A. Subrenat, and P. Le Cloirec, Hydrogen sulfide adsorption and oxidation onto activated carbon cloth: applications to odorous gaseous emission treatments, *Langmuir* 19**,** 10869-10877 (2003).
38. S.V. Mikhalovsky, and Yu.P. Zaitsev, Catalytic properties of activated carbons I. Gas-Phase oxidation of hydrogen sulphide, *Carbon* 35, 1367-1374 (1997).

39. T.J. Bandosz, Effect of pore structure and surface chemistry of virgin activated carbon on removal of hydrogen sulfide, *Carbon* 37, 483-491 (1999).
40. F. Adib, A. Bagreev, and T. J. Bandosz, Analysis of the relationship between H_2S removal capacity and surface properties of unmodified activated carbons, *Environ. Sci. Technol.* 34, 686-692 (2000)
41. F. Adib, A. Bagreev, and T.J. Bandosz, Effect of surface characteristics of wood based activated carbons on removal of hydrogen sulfide, *J. Coll. Interface Sci*. 214, 407-415 (1999).
42. F. Adib, A. Bagreev, and T.J. Bandosz, Effect of pH and surface chemistry on the mechanism of H_2S removal by activated carbons*, J. Coll. Interface Sci.* 216, 360-369 (1999).
43. F. Adib, A. Bagreev, and T.J. Bandosz, On the possibility of regeneration of unimpregnated activated carbons used as hydrogen sulfide adsorbents, *Ind. Eng. Chem. Res*. 39, 2439-2446 (2000).
44. A. Bagreev, H. Rahman, and T.J. Bandosz, Wood-based activated carbons as adsorbents of hydrogen sulfide: a study of adsorption and water regeneration process, *Ind. Eng. Chem. Res*. 39, 3849-3855 (2000).
45. A. Bagreev, H. Rahman, and T.J. Bandosz, Study of H_2S adsorption and water regeneration of coconut-based activated carbon, *Environ. Sci. Technol*. 34, 4587-4592 (2000).
46. A. Bagreev, F. Adib and T.J. Bandosz, Initial heats of H_2S adsorption on activated carbons: effect of surface features, *J. Coll. Interface Sci*. 219, 327-332 (1999).
47. A. Bagreev, F. Adib, and T.J. Bandosz, pH of the activated carbon surface as an indication for its suitability for removal of hydrogen sulfide from wet air streams, *Carbon* 39, 1987-1905 (2001).
48. A. Bagreev., and T.J. Bandosz, H_2S adsorption/oxidation on unmodified activated carbons: importance of prehumidification, *Carbon* 39, 2303-2311 (2001).
49. R.A. Hayden, Process for making catalytic carbon, *U.S. Patent 5,444,031*, (1995).
50. A. Bagreev, J.A. Menendez, I. Dukhno, Y. Tarasenko, and T.J. Bandosz, Bituminous coal-based activated carbons modified with nitrogen as adsorbents of hydrogen sulfide, *Carbon* 42, 469-476 (2004).
51. R.A. Hayden, Process for regenerating nitrogen-treated carbonaceous chars used for hydrogen sulfide removal, *International patent WO 95/26230* (1995).
52. T.M. Matviya, and R. A. Hayden, Catalytic carbon, *U.S. Patent 5,356,849* (1994).
53. A. Turk, E. Sakalis, O. Rago, and H. Karamitsos, Activated carbon systems for removal of light gases, *Annals New York. Academy of Sciences* 661, 221-228 (1992).
54. J.P. Boudou, M. Chehimi, E. Broniek, T. Siemieniewska, and J. Bimer, Adsorption of H_2S or SO_2 on an activated carbon cloth modified by ammonia treatment, *Carbon* 41, 1999-2007 (2003).
55. Q.H. Yang, J.T. Zheng, Y. Li, M.Z. Wang, and B.J. Zhang, Adsorption and conversion of hydrogen sulfide over PAN-based ACF, *Carbon* 37, 2078-2080 (1999).
56. F. Adib, A. Bagreev, and T.J. Bandosz, Adsorption/oxidation of hydrogen sulfide on nitrogen modified activated carbons, *Langmuir* 16, 1980-1986 (2000).
57. J.R. Kastner, K.C. Das, and N.D. Melear, Catalytic oxidation of gaseous reduced sulfur compounds using coal fly ash, *J. Haz. Mat.* B95, 81-90 (2002).
58. J.R. Kastner, K.C. Das, Q. Buquoi, and N.D. Melear, Low temperature catalytic oxidation of hydrogen sulfide and methanethiol using wood and coal fly ash, *Environ. Sci. Technol*. 37, 2568-2574 (2003).

59. M.P. Cal, B.W. Strickler, and A.A. Lizzio, High temperature hydrogen sulfide adsorption on activated carbon. I. Effect of gas composition and metal addition, *Carbon* 38, 1757-1765 (2000).
60. A. Bagreev, and T.J. Bandosz, On the mechanism of hydrogen sulfide adsorption/oxidation on catalytic carbons, *Ind. Eng. Chem. Res.* 44, 530-538 (2005).
61 R.C. Bansal, J.B. Donnet, and F. Stoeckli. *Active Carbon*. (Marcel Dekker, New York, 1988).
62. I.I. Salame, and T.J. Bandosz, Study of water adsorption on activated carbons with different degrees of surface oxidation, *J. Coll. Interface Sci*. 210, 367-374 (1999).
63. I.I. Salame, and T.J. Bandosz, Revisiting the effect of surface chemistry on adsorption of water on activated carbons, *J. Phys. Chem*. 103, 3877-3884 (1999).
64. A. Bagreev, S. Bashkova, D.C. Locke, and T.J. Bandosz, Sewage sludge derived materials as efficient adsorbents for removal of hydrogen sulfide, *Environ. Sci. Technol*. 35, 1537-1543 (2001).
65. J. Rodriguez-Mirasol, T. Cordero, and J.J. Rodriguez, Effect of oxygen on the adsorption of SO_2 on activated carbon, Abstract of 23rd Biennial Conference on Carbon, 18-23 July 1997, College Park, PA, p. 376.
66. C. Moreno-Castilla, F. Carrasco-Marin, E. Utrera-Hidalgo, and J. Rivera-Utrilla, Activated carbons as adsorbents of sulfur dioxide in flowing air. Effect of their pore texture and surface basicity, *Langmuir 9*, 1378-1383 (1993).
67. A. Lisovskii, G.E. Shter, R. Semiat, and C Aharoni, Adsorption of sulfur dioxide by active carbon treated by nitric acid: II Effect of preheating on the adsorption properties, *Carbon* 35**,** 1645-1648 (1997).
68. P. Davini, SO_2 adsorption by activated carbons with various burnoffs obtained from bituminous coal, *Carbon* 39**,** 1387-1393 (2001).
69. L. Mochida, S. Miyamoto, K. Kuroda, S.I. Kawano, S. Yatsunami, Y. Korai, A. Yatsutake, and M. Yashikawa, Adsorption and adsorbed species of SO_2 during its oxidative removal over pitch-based activated carbon fibers, *Energy Fuels* 13**,** 369-373 (1999).
70. P. Davini, Adsorption and desorption of SO_2 on active carbon: the effect of surface basic groups, *Carbon* 28, 565-571 (1990).
71. A. Lisovskii, R. Semiat, and C. Aharoni, Adsorption of sulfur dioxide by active carbon treated by nitric acid: I Effect of the treatment on adsorption of SO_2 and Extractability of the acid formed, *Carbon* 35, 1639-1643 (1997).
72. C.A. Anurov, Physicochemical aspects of the adsorption of sulfur dioxide by carbon adsorbents *(Uspekhi Khimii) Russian Chemical Reviews* 65, 663-676 (1996).
73. E. Raymundo-Piñero, D. Cazola-Amorós, C. Salinas-Martinez de Lecea, and A. Linares-Solano, Factors controlling the SO_2 removal by porous carbons: relevance of the SO_2 oxidation steep, *Carbon* 38, 335-344. (2000).
74. M. Molina-Sabio, M.A. Muñecas, F. Rodriguez-Reinoso, and B. McEnaney, Adsorption of CO_2 and SO_2 on activated carbons with a wide range of micropore size distribution, *Carbon 33*, 1777-1782 (1995).
75. M.A. Daley, C.I. Mangun, J.A. DeBarr, S. Riha, A.A. Lizzio, G.L. Donnals, and J. Economy, Adsorption of SO_2 onto oxidized and heat-treated activated carbon fibers (ACFS) *Carbon* 35**,** 411-417 (1997).
76. A.A. Lizzio, and J.A. DeBarr, Mechanism of SO_2 removal by carbon, *Energy Fuels* 11, 284-291 (1997).
77. B. Rubio, and M.T. Izquierdo, Influence of low-rank coal char properties on their SO_2 removal capcity from flue gases: I non-activated chars. *Carbon* 35, 100-1011 (1997).

78. B. Rubio, M.T. Izquierdo, and A.M. Mastral, Influence of low-rank coal char properties on their SO_2 removal capacity from flue gases. 2. Activated chars, *Carbon* 36, 263-268 (1998).
79. I. Mochida, Y. Korai, M. Shirahama, S. Kawano, T. Hada, Y. Seo, M. Yoshikawa, and A. Yasutake, Removal of SO_x and NO_x over activated carbon fibers, *Carbon 38*, 227-239 (2000).
80. P. Davini, and G. Stoppato, SO_2 adsorption on active carbons: the effect of certain metal compounds, Abstract of 23rd Biennial Conference on Carbon, 18-23 July 1997, College Park, PA, p. 316.
81. M.C. Roman, T. Takarada, Y. Suzuki, and A. Linares, SO_2 interaction with a Ca-exchanged-coal, Abstract of 23rd Biennial Conference on Carbon, 18-23 July 1997, College Park, PA, p. 324.
82. A. Bagreev, S. Bashkova, and T.J. Bandosz, Adsorption of SO_2 on activated carbons: the effect of nitrogen functionality and pore sizes, *Langmuir* 18, 1257-1264 (2002).
83. Z-M. Wang, and K. Kaneko, Effect of pore width on micropore filling mechanism of $S0_2$ in carbon micropores, *J. Phys. Chem. B* 102, 2863-2868 (1998).
84. Y. Kawabuchi, S. Sotowa, K. Kuroda, S. Kawano, D. Whitehurst, and I. Mochida, Preparation of active carbon fiber with basic properties, Abstracts, Int. Conf. on Carbon, Carbon'96, Newcastle, UK, 1996, p.431.
85. J.K. Lee, H.J. Shim, J.C. Lim, G.J. Choi, Y.D. Kim, B. Minand, and D. Park. Influence of tension during oxidative stabilization on SO_2 adsorption characteristics of polyacrylonitrile (PAN) based activated carbon fibers, *Carbon* 35, 837-843 (1997).
86. G.Q. Lu, and D.D. Do, Retention of sulfur dioxide as sulfuric acid by activated coal reject char, *Sep. Technol.* 3, 106-110. (1993).
87. S. Bashkova, A. Bagreev, D.C. Locke, and T.J. Bandosz, Adsorption of SO_2 on sewage sludge-derived materials, *Environ. Sci. Technol*. 35, 3263-3269 (2001).
88. C-S. Ho, and S-M. Shih, $Ca(OH)_2$/fly ash sorbents for SO_2 removal, *Ind. Eng. Chem. Res*. 31**,** 1130-1135 (1992).
89. A.K. Dalai, E.L. Tollefson, A. Yang, and E. Sasaoka, Oxidation of methyl mercaptan over an activated carbon in a fixed-bed reactor, *Ind. Eng. Chem. Res.* 36, 4726-4733 (1997).
90. H-L. Chiang, J-H. Tsai, C-L. Tsai, and Y-C. Hsu, Adsorption characteristics of alkaline activated carbon exemplified by water vapor, H_2S and CH_3SH gas, *Sep. Sci. Technol.* 35, 903-918 (2000).
91. C.S. Shin, K.H. Kim, S.H. Yu, and S.K. Ryu, Adsorption of methyl mercaptan and hydrogen sulfide on the impregnated activated carbon fiber and activated carbon, presented at Fundamentals of Adsorption 7, Nagasaki, Japan, May 20-25, 2001.
92. S. Bashkova, A. Bagreev, and T.J. Bandosz, Adsorption of methyl mercaptan on activated carbons, *Environ. Sci. Technol.* 36, 2777-2782 (2002).
93. S. Bashkova, A. Bagreev, and T.J. Bandosz, Effects of surface characteristics on adsorption of methyl mercaptan on activated carbons, *Ind. Eng. Chem. Res.* 41, 4346-4352 (2002).
94. A. Bagreev, S. Bashkova, and T.J. Bandosz, Dual role of water in the process of methyl mercaptan adsorption on activated carbons, *Langmuir* 18, 8553-8559 (2002).
95. S. Bashkova, A. Bagreev, and T.J. Bandosz, Adsorption/oxidation of CH_3SH on activated carbon containing nitrogen, *Langmuir* 19, 6115-6121 (2003).
96. S. Bashkova, A. Bagreev, and T.J. Bandosz, Catalytic properties of activated carbon surface in the process of adsorption/oxidation of methyl mercaptan, *Catalysis Today* 99, 323- 328 (2005).

97. A. Bagreev, J.A. Menendez, I. Dukhno, Y. Tarasenko, and T.J. Bandosz, Adsorption of methyl mercaptan on nitrogen modified bituminous coal-based activated carbon, *Carbon* 43, 195-213 (2005).
98. V.V. Strelko, V.S. Kuts, and P.A. Thrower, On the mechanism of possible influence of heteroatoms of nitrogen, boron and phosphorus in a carbon matrix on the catalytic activity of electrons in electron transfer reactions, *Carbon* 38, 1499-1503 (2000).
99. C.L. McCallum, T.J. Bandosz, S.C. McGrother, E.A. Muller, and K.E. Gubbins, A molecular model for adsorption of water on activated carbon: comparison of simulation and experiment, *Langmuir* 15, 533-544 (1999).

COMBINED ADSORPTION PREPARATIONS FROM ACTIVE CARBONS, CLAY MINERALS AND NATURAL PLANT PRODUCTS

MYKOLA T. KARTEL*, VOLODYMYR V. STRELKO, SVETLANA S. STAVITSKAYA, VALENTINA K. MARDANENKO AND LIDIA A. KUPCHIK
Institute for Sorption and Problems of Endoecology, NASU, General Naumov str., 13, Kiev, 03164, Ukraine

Abstract. Data on activity of the combined adsorbents *Ultrasorb, Pectopal and Carboxykam* for adsorption of the cations Fe^{2+}, Co^{2+}, Cd^{2+}, Pb^{2+}, Zn^{2+}, Cu^{2+}, Ni^{2+} and radioactive isotope ^{137}Cs from a modeling Ringer salt solution are reported. These adsorbents show high adsorption selectivity for ^{137}Cs from biological media (distribution factors achieve 30,000), and also high binding ability for the cations Sr^{2+}, Pb^{2+}, Cd^{2+}, etc. The opportunity of combining properties of sorbents of various natures in combined structures, offered for use as medicinal substances in oral adsorption preparations (enterosorbents) for directed action in treatment of the ecologically dependent diseases connected with the accumulation of heavy metals (HM) and radionuclides (RN) in the organism, is investigated. The efficiency of the preparation *Ultrasorb* for removing RN from the human organism by enterosorption is investigated. It is shown that this preparation increases the natural elimination of incorporated RN by 20%. It is established that a 2 week enterosorption treatment lowers 2-3 times the RN blood content of a patient.

Keywords: enterosorbents; heavy metals; radionuclides; distribution factors; detoxification.

* To whom correspondence should be addressed. Mykola T. Kartel, Institute for Sorption and Problems of Endoecology, NAS of Ukraine, General Naumov street 13, 03164, Kiev, Ukraine; e-mail: kartel@mail.kar.net

J.M. Loureiro and M.T. Kartel (eds.), Combined and Hybrid Adsorbents, 165–179.

1. Introduction

The adverse ecological condition in some regions of Ukraine is often connected to pollution of large territories by radionuclides (RN) and heavy metals (HM), and also by harmful organic substances of technogenic origin. The increase of professional or ecologically linked diseases among the population of the mentioned regions points to the necessity of intensifying complex preventive and medical actions, including an accessible and simple for mass use enterosorption method.[1] Nowadays, enterosorption as an independent method, or more often as part of complex treatments is applied in the therapy of endogenic intoxications caused by acute and chronic peritonitis, pancreatitis, autoimmune diseases, allergies, poisoning by toxic substances, etc. and also in the prophylaxis of occupational diseases.

Meanwhile, the comparative estimation of the functional properties of the enterosorbents available on the Ukrainian market showed that actually all of them are preparations of nonspecific multifunctional action and, apart from ferrocine, do not possess convenient selectivity for radiocesium, let alone radiostrontium, transuranic elements and HM. Therefore the new concept in enterosorption should be, in our opinion, to develop and to apply combined enterosorbents of directed action which, except for general detoxification, are capable to provide selective removal of RN and HM from organism, and also to normalize its basic biochemical parameters.

The creation of high selective sorption materials with surface ion exchange centers, by preparing mechanical mixtures of materials of essentially different natures in strictly proportions, is actually needed. For example, active carbons, which are high capacity adsorbents for substances of molecular type, ion exchangers and catalysts, natural clay minerals possessing a high geometrical surface of disperse (colloidal) particles and exchange properties of selective inorganic cationites, and also plant sorption materials of polysaccharide origin with complexing properties and ability to form inclusion compounds (clatrates).

2. Experimental

In the laboratory of our Institute, under trial conditions, basic elements of technology of synthesis of combined enterosorbents *Ultrasorb*, *Pectopal* and *Carboxykam* (substances and powder or capsules medicinal forms) are worked out.[2-5] Their bases are specially modified active carbon adsorbents such as *UVM* (fibers or cloth) or *KAU* (fruit-stones active carbon), a modified clay mineral *palygorskite*, and also some food additives (*pectin*, *elamin*). The relative proportions of the modified components were obtained experimentally, taking into account an achievement of maximal

adsorption abilities on ^{137}Cs and ^{90}Sr, and preserving the harmlessness of the preparations,[6] confirmed by carrying out pre-acute and chronic experiments on two kinds of animals (rats and mouses), studying some integrated parameters of their general status, namely parameters of functionality for liver, kidneys, blood, and also the remote consequences (embryotoxic, theratogenic and allergenic actions). The compositions of the combined preparations are shown in Table 1.

TABLE 1. The composition of combined enterosorbents

Enterosorbent	1st component	2nd component
Ultrasorb	UVMo-Z – 40 wt.% (Fiber active carbon UVM oxidized, charged by cations of potassium, magnesium and zinc and dispersed by milling)	Palygorskite-M – 60 wt.% (Clay mineral palygorskite impregnated by copper ferrocyanide, dispersed by milling)
Pectopal	Palygorskite-M – 50 wt.% (Clay mineral palygorskite impregnated by copper ferrocyanide, dispersed by milling)	Pectin – 50 wt.% (Commercial refined product from citrus, apples or beet)
Carboxykam	KAUo-MS –50 wt.% (Fruit-stone active carbon KAU oxidized, charged by cations of potassium, magnesium, copper and selenate-anions and dispersed by milling	Elamin – 50 wt. % (Commercial hydrolyzed product of laminaria)

Adsorption experiments were conducted in static conditions: continuous hashing of sorbents in a solution of the corresponding salt with various initial concentrations on a background of standard Ringer salt solution (NaCl – 0.8 %, KCl – 0.042 %, $CaCl_2$ – 0.024 %, $NaHCO_3$ – 0.1 %). The ratio of solid and liquid phases was 1:200. Initial and equilibrium concentrations of metals were determined by atomic absorption spectroscopy with a KAS-120.1 apparatus (Selmi, Ukraine); a complexometry method was also used for the control of the data. The radioactivity of ^{137}Cs in solutions before and after contact with a sorbent was determined on a γ-radiometer RUG-4. An initial solution of ^{137}Cs with initial activity 2.55-5.25 $kBq \cdot L^{-1}$ was used.

Isotherm results on adsorption of HM ions at 20 °C were determined, from which the ions distribution factors (K_d, $mL \cdot g^{-1}$) were calculated for standard conditions, when the equilibrium concentrations of solutions equal 1 $mM \cdot L^{-1}$ within the physiological norm of the content of each ion in an organism blood.[7,8] The experimental data allowed also the determination of

the adsorption selectivity of the combined material in relation to HM toxic ions. This enabled an estimation of the efficiency of each adsorption preparation on concrete metals and the comparison with other known analogues.

According to the decision of the State Pharmacological Center at the Ministry of Public Health of Ukraine the expanded clinical tests of the named preparations, and also researches of their action on an organism of patients (volunteers) were carried out. For testing experiment with *Ultrasorb*, for example, the group of inhabitants of areas from Zhitomir and Rivno Regions, workers of the forestry, undergone to long action of small dozes of radiation from pollution after Chernobyl accident have been selected. The tested group received the combined preparation during 14 days. The dosage was a spoon (7-8 g) of a preparation 3 times per day one hour before meals.

An estimation of the decorporation dynamics and efficiency was carried measuring the integral radioactivity of human body (the so called SICh-measurements) during the 14-days test. Simultaneously, the radioactivity levels of feaces, urine and blood of examinees before reception and, like with SICh-data, on the 7^{th} and 14^{th} day of reception of a preparation were measured. Measurements followed the procedure of the Department of Radiological Analysis of the Institute of Nuclear Researches, NAS of Ukraine. To study radionuclides spectrum of persons undergone to long action of small dozes of radiation it was carried out a fence of venous blood (5 mL) and gathering feaces and urine in the morning. The testing media were placed in special hermetic tubes, weighed and delivered to measurement of activity.

Testing of γ-radioactivity was carried out by an EG8G ORTEX (ORTEX, USA) analyzer using photon detectors from superpure germanium, with special computer treatment of data (software GEV, GMX).

3. Results and Discussion

As the researched binary enterosorbents have been synthesized on the basis of a modified carbon material - high dispersed *oxidized carbon* in the salt form, capable to bind ions of the majority of d-metals effectively even from complex solutions (*Ultrasorb, Carboxykam*), a modified clay mineral - high dispersed *palygorskite* impregnated by copper ferrocyanide (*Ultrasorb, Pectopal*), selective on binding cesium ions, and food additives *pectin* and *elamin* (*Pectopal, Carboxykam*), one of the overall objectives of this research was the determination of quantitative data on the adsorption selectivity of various HM ions and radioactive cesium by these combined preparations. The results for *Ultrasorb* are especially interesting.

First of all, the adsorption isotherms of some metal ions from the corresponding solutions by the combined adsorbent *Ultrasorb* were obtained. In the equilibrium concentration interval of 0.1-0.5 $mM \cdot L^{-1}$ the curves follow the Freundlich empirical equation. The amounts adsorbed are quite close for several ions in a wide interval of concentration, achieving a maximum level within the limits of 0.2-0.4 $mM \cdot g^{-1}$. From the experimental values of adsorption it is possible to calculate the distribution factors and track their changes in a wide concentration interval. Moreover, the use of a logarithmic scale allows extrapolating the dependences for wider intervals of equilibrium concentrations. This is especially important for lower concentrations of ions in solutions for which the relative experimental errors are larger.

From the obtained data on distribution factors for various ions it is possible to order the selectivity of adsorption of HM ions by *Ultrasorb* in an interval of concentration 10^{-2}-1 $mM \cdot L^{-1}$ as:

$$Pb^{2+} > Fe^{2+} > Co^{2+} \sim Cu^{2+} > Ni^{2+} > Cd^{2+} > Zn^{2+}$$

This selectivity order is typical for the majority of oxidized carbons of various genesis.[9] Thus the clay component, the second component of the combined *Ultrasorb* sorbent, actually does not change the HM ions adsorption character of the *UVMo-Z* modified carbon. The special experiments executed to define the sorption activity of the specified ions on the individual clay component *palygorskite-M* have shown that this component practically does not adsorb ions of HM – the K_d value for practically all multivalent cations did not exceed 10. It means that the *Ultrasorb* clay component is an indifferent material in relation to the modified carbon adsorbent and that it reduces only 2-2.5 times the absolute values of adsorption and distribution factors of ions by *Ultrasorb* in comparison with the individual carbon material *UVMo-Z* since the weight of the last in the combined preparation is less than 50%. Calculated values of K_d for ions, obtained at standard conditions, C_{eq} = 1 $mM \cdot L^{-1}$ and C_{eq} equal to the "physiological" contents in biological liquids (first of all in blood) of an organism, are shown in Figure 1a. It is necessary to note that the "physiological" norms for the majority of ions in an organism correspond to 10^{-2} $mM \cdot L^{-1}$, and only for Pb^{2+} and Cd^{2+} the allowable levels are essentially lower - correspondingly 10^{-3} and 10^{-4} $mM \cdot L^{-1}$.

The results on fig. 1a characterize the combined sorbent *Ultrasorb* as a quite high selective material for HM ions, especially for Pb^{2+}, Fe^{2+}, Cu^{2+} and Co^{2+}. Actually such adsorption material, being an adsorbing preparation, is capable to lower quite effectively the increased concentration of the specified metals in an organism (at so-called metalosis) to the required (physiological) level.

The question and influence of the carbon component on the adsorption properties of the mineral components in the combined sorbent *Ultrasorb* is also interesting. As it is known,[10] *palygorskite-M* is a high selective adsorbent for cesium ions. Therefore its assignment in the combined sorbent is to bind selectively radiocesium in liquid media, including biological liquids. Here we notice a reverse situation since the carbon material is absolutely not selective to radiocesium ($K_d \sim 40$), whereas for *palygorskite-M* the distribution factors achieve values of more than 60,000. In various mass ratio combinations of the two sorbents we really noticed some decrease (1.5-2 times) in the selectivity factor for radiocesium in comparison with the individual *palygorskite-M* due to the decrease of the clay mineral mass fraction in the combined sorbent (see Figure 1b). However, the obtained values of K_d for radiocesium, even at a ratio clay:carbon components of 1:3, were above 30,000. And this is quite suitable for its use as an adsorbing preparation for bonding to and removing radioactive isotopes of cesium from an organism biological media.

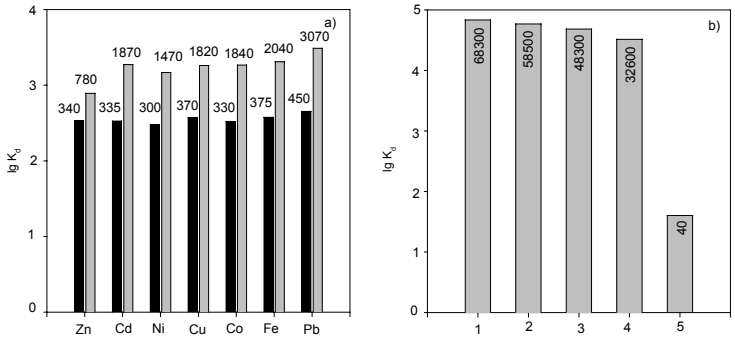

Figure 1. a) Distribution factors (K_d) in the adsorption of HM ions by *Ultrasorb*: dark - under standard conditions (C_{eq} = 1 mM/L), light – at concentrations corresponding to physiological norm; b) Distribution factors in the adsorption of radiocesium by *palygorskite-M* (1), carbon sorbent *UVMo-Z* (5) and "*palygorskite-M : UVMo-Z*" in mass ratio 3:1 (2), 1:1 (3) and 1:3 (4).

Thus, we obtained quantitative characteristics showing the adsorption selectivity of the combined sorbent *Ultrasorb* on HM ions and radiocesium. These data served us for an objective estimation of the properties of this sorbent as a medicinal substance, in comparison with known analogues, and also for a substantiation of the correct dosage for its reception as a medical product. The second purpose of this research was the study of the efficiency of the elimination of RN with a high level of radioactivity from the human organism by enterosorption with the combined preparations.

A number of papers[11-15] for adsorption of HM ions recommends using pure *pectins* or pectin-containing compositions. At the same time, in the literature there are not enough data about quantitative characteristics on the

efficiency of binding ions by pectins, which complicates their correct dosage and strategy of use for preventive and medical purposes. Besides, an essential fact is that the organisms enteric media contain ions of sodium, potassium, calcium, magnesium, etc., which can influence appreciably the selectivity of pectins to the adsorbed ions.

So, the adsorption ability of several types of commercial *pectins* from apples (A), beet (B) and citrus (C) as well as of the pectin-containing adsorbent *Pectopal*, which structure includes the modified clay mineral *palygorskite-M,* was investigated. The selectivity of the pectins and of the *Pectopal* preparation to metal ions was estimated based on distribution factors, obtained from data on adsorption isotherms from aqueous solutions.

In Table 2 values of K_d for systems «*pectin* - solution of HM» in standard conditions (C_{eq} = 1 mM·L^{-1}) and for concentrations corresponding to the physiological norm of human organisms are presented. The selectivity orders both for standard conditions and for physiological concentrations on *Pectopal* are practically identical:

$$Pb^{2+}\ (C>A\sim B) > Cu^{2+}\ (B>A>C) \sim Co^{2+}\ (A>C>B) > Ni^{2+}\ (C>A>B) >$$
$$> Cd^{2+}\ (B>A>C) \sim Zn^{2+}\ (C>A\sim B)$$

at C_{eq} = 1 мМ·L^{-1} and

$$Pb^{2+}\ (B>C>A) >> Cu^{2+}\ (B>C>A) > Co^{2+}\ (A>C>B) > Ni^{2+}\ (C>A>B) >>$$
$$>> Zn^{2+}\ (C\sim A\sim B) \sim Cd^{2+}\ (B>A\sim C)$$

at C_{eq} equal to the physiological norm of metal in organism.

TABLE 2. Distribution factors for HM ions on pectins and *Pectopal*

Metal Ion	Equilibrium Concentration (C_{eq}), mM·L^{-1}	Distribution factor (K_d), mL·g^{-1}			
		Apple *pectin*	Beet *pectin*	Citrus *pectin*	*Pectopal*
Ni^{2+}	1	1.8×10^2	1.6×10^2	2.0×10^2	5.0×10^2
	10^{-2}	2.0×10^2	1.2×10^2	3.2×10^2	1.7×10^3
Co^{2+}	1	4.1×10^2	2.2×10^2	3.5×10^2	4.5×10^2
	10^{-2}	3.1×10^3	2.6×10^2	8.7×10^2	1.3×10^3
Cu^{2+}	1	3.0×10^2	4.4×10^2	2.6×10^2	6.2×10^2
	10^{-2}	2.9×10^3	4.7×10^3	3.1×10^3	4.2×10^3
Zn^{2+}	1	$0.7*10^2$	0.6×10^2	0.7×10^2	3.9×10^2
	10^{-2}	0.3×10^2	0.2×10^2	0.4×10^2	8.2×10^2
Cd^{2+}	1	0.8×10^2	1.5×10^2	0.6×10^2	6.1×10^2
	10^{-4}	$<0.1 \times 10^2$	0.2×10^2	$<0.1 \times 10^2$	1.9×10^3
Pb^{2+}	1	4.1×10^2	4.0×10^2	5.5×10^2	6.5×10^2
	10^{-3}	1.2×10^4	5.9×10^4	4.1×10^4	6.4×10^4

The adsorption activity of the preparation in comparison with that of pectins is much higher. K_d values for standard conditions achieve 10^3 and this is essentially higher than for pure *pectins* (Figure 2).

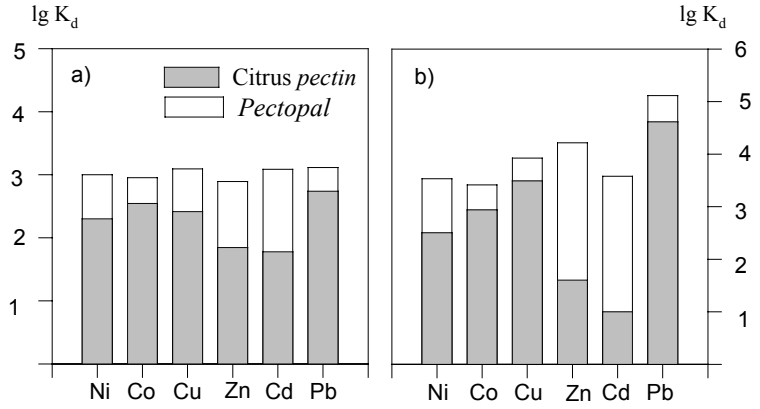

Figure 2. Diagrams of K_d values for various HM ions on pure citrus *pectin* and *Pectopal*: a) standard conditions (C_{eq} = 1 mM L^{-1}), b) physiological concentrations of ions.

Individual *palygorskite-M* has insignificant selectivity to HM ions (K_d = 30-50). In the combined preparation *Pectopal* it plays the role of binder for the cesium radioactive isotopes (K_d achieves $3\text{-}6\cdot10^4$).[10] Positive influence of *palygorskite-M* on binding ions of HM by pectin can be caused by an increase in the amount of a deposit due to the formation of complex compounds not only with the high-molecular fractions, but also with the middle-molecular (partially soluble) pectins. The effect is probably also amplified by the colloid-chemical properties of clay minerals, causing coagulation of complex compounds of pectin with metal ions, with the formation of large conglomerates.

Therefore for the production of pectin based preparations it is common to use disperse mineral additives, for example, a clay mineral or a powdered active carbon. Selectivity of such preparations can be much higher than that of pure pectins.

For effective removal of HM and RN from the organism, alginates (polysaccharides with acid groups produced from seaweeds - *laminaria*) are also recommended. Alginates have ability to selectively adsorb also organic toxic substances (slags, nitrogenous compounds, etc.); moreover, they do not impoverish the organism on microelements and maintain within norm its electrolyte status on vital important cations of calcium, magnesium, potassium and sodium.[16,17]

We have carried out a study on the alginates ability to bind some HM ions (cadmium, lead and strontium) from water solutions of the corresponding soluble salts (chlorides, nitrates) on a background of standard Ringer salt solution. In this study the commercial sample alginates

Manugel-SFB, *Kelgin-HV*, *Kelgin-LV*, and also the food additive *elamin* (alginate-enriched product of *laminaria* processing) have been used. From the obtained adsorption isotherms, using concentrations of the ions in the range of 0.1-5 $mM.L^{-1}$ and reducing the alginates to hydrocolloid state, the constants of the Freundlich equation were determined, and values of distribution factors for the systems «*alginate* -solution of HM ions» were calculated for the standard conditions (C_{eq} = 1 $mM \cdot L^{-1}$) and for C_{eq} corresponding to the physiological norm of the respective metals in the human organism. The analysis of these data enables to compare the abilities of different alginates to bind HM ions. The obtained orders are the following:

Pb^{2+}: *Manugel-SFB > Kelgin-HV > Kelgin-LV > elamin*

Cd^{2+}: *Kelgin-LV > Kelgin-HV > Manugel-SFB > elamin*

Sr^{2+} : *Kelgin-LV > Kelgin-HV > Manugel-SFB > elamin*

It is necessary, however, to note that under conditions of low HM ions concentrations (within the range of the physiological norms for an organism) the orders of binding abilities are different:

Pb^{2+}: *Kelgin-LV > Kelgin-HV > Manugel-SFB > elamin*

Cd^{2+}: *elamin > Kelgin-HV > Manugel-SFB = Kelgin-LV*

Sr^{2+}: *Kelgin-LV > Manugel-SFB > elamin > Kelgin-HV*

The obtained results on selectivity of HM adsorption are shown in Table 3.

TABLE 3. Distribution factors (K_d, $mL.g^{-1}$) for HM ions on alginates, *elamin* and *Carboxykam*

Sorbent	Cd^{2+}		Pb^{2+}		Sr^{2+}	
	$lgC_{eq} = 0$	$lgC_{ph} = -4$	$lgC_{eq} = 0$	$lgC_{ph} = -3$	$lgC_{eq} = 0$	$lgC_{ph} = -5$
Manugel-SFB	450	50,000	770	17,000	250	165,000
Kelgin-HV	550	70,000	900	21,000	300	105,000
Kelgin-LV	850	50,000	770	34,000	400	200,000
Elamin	300	95,000	400	9,000	200	135,000
Carboxykam	900	105,000	7,500	15,000	900	250,000

Adsorption activity of alginates is defined, most likely, by quantitative contents of guluronic and manuric acids in polysaccharide matrix, and also radicals, which can attach HM ions or be replaced by them.

It is argued that the excessive use of refined polysaccharide sorbents such as pectins and alginates can cause some pauperization of an organism

in calcium, magnesium, microelements (zinc, copper, iron, etc.), that can become one of the reasons for the development of hypomicroelementosis in the organism.[18,19] Therefore when producing treatment-and-prophylactic preparations of combined type with the participation of vegetative type sorbents it is meaningful to use not the pure (refined) polysaccharides, but the products of processing vegetative raw material enriched with them, for example, a beet processing product - gom (*pectin-cellulose* complex), a hydrolyzed product of *laminar* (food additive *elamin*), products of hydrolyzed chitin-containing materials (*chitosan* products), etc. It is important to note that processing such products is quite simple and essentially cheaper than refined polysaccharides. So, for example, the production of *elamin* is approximately 10 times cheaper than the pure alginates.

It is interesting that, as well as in the case of *Pectopal*, the *Carboxykam* preparation possesses higher selectivity factors to lead, cadmium and strontium, than pure *elamin* (Figure 3), though the 50% carbon component of the preparation contributes essentially to the selectivity to heavy metals and it should logically reduce the activity of the binary preparation. The strengthening action of the carbon component on the ability of *elamin* to bind heavy metals is caused, apparently, by coagulation influence of colloid particles on partially soluble complexes of alginates of *elamin* with metal ions.

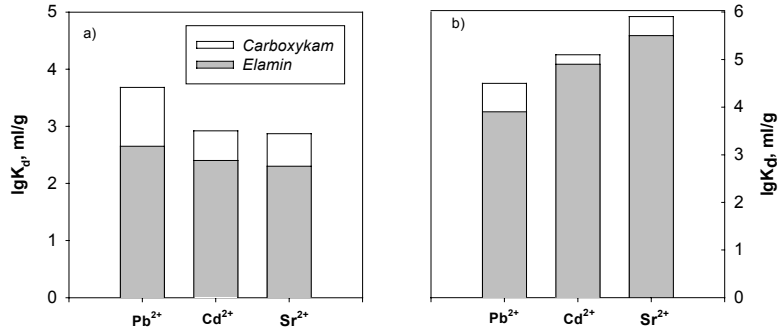

Figure 3. Diagrams of K_d values for various HM ions on *elamin* and *Carboxykam*: a) standard conditions (C_{eq} = 1 mM·L^{-1}), b) physiological concentrations of ions.

Thus, the obtained quantitative characteristics of HM and RN adsorption by pectins and alginates of different origin (or natural sorbents after enriching their acidic polysaccharides, as in the case of *elamin*) enable to purposely use them in a complex with inorganic or carbon sorbents as food additives and medical preparations intended for effective removing the referred toxic products from an organism with simultaneous correction of some biochemical parameters of the organism (for example, according to a blood analysis of the patients accepting such combined preparations).

The efficiency of the therapeutic action, connected with the removing of incorporated RN from an organism, can be observed by the example of use of the combined enterosorbent *Ultrasorb*, according to the dynamics of change of the total radioactivity (SICh-data) and γ-activity on separate isotopes; some of the obtained results are shown in Table 4 and in Figure 4.

The analysis of these data allows asserting that the reception of *Ultrasorb* essentially improves the elimination of RN from the organism of patients who stayed a long time on a polluted territory. The degree of RN elimination achieved 26.5% (see Table 4), while in the control group, which was not accepting enterosorbent, this parameter remained practically unchanged. The average degree of RN elimination from the organisms of volunteers was about 20%. Figure 4 displays the changes in the γ-activity level of the group surveyed (a) and of the control group (b), on the 1st, 7th, and 14th days of supervision. The rate of removing the incorporated RN is a little larger in the first period of enterosorption, i.e. in the first 7 days, and then there is some deceleration of the elimination process.

TABLE 4. Dynamics of change of the total γ-activity (SICh-data) for persons that undergone a long influence of small doses of incorporated radionuclides

NN	Initial level of radioactivity, kBq	Level of radioactivity after enterosorption, kBq			
		7th day	Elimination, %	14th day	Elimination, %
Group that accepted enterosorbent Ultrasorb					
1	47.4±9.5	40.4±8.1	-14.6	37.4±7.5	-21.1
2	27.8±5.8	23.1±4.8	-16.9	20.4±4.2	-26.5
3	92.5±1.8	77.6±15.8	-16.1	70.6±1.4	-23.7
4	12.5±2.8	10.9±2.3	-12.8	9.9±0.2	-21.0
5	31.5±5.9	27.9±5.3	-11.4	25.1±4.9	-20.4
Control group (without enterosorbent)					
1	45.4±9.6	44.8±9.4	-1.2	44.9±9.4	-1.0
2	25.9±5.5	25.5±5.4	-1.6	25.7±5.5	-0.9
3	11.8±2.3	11.9±2.3	-1.2	11.7±2.4	-0.9
4	4.7±0.9	4.7±0.9	-0.4	4.8±0.9	-1.0
5	84.5±17.6	84.1±17.3	-0.5	83.8±17.2	-0.8

There was a special interest in studying the γ-activity dynamic evolution in the blood, urine and feaces of patients who were taking the new enterosorption preparation. In this study, the main contribution from the incorporated RN to the γ-activity of people subjected to a long time exposure of small dozes of radiation was evaluated through the ^{137}Cs, ^{134}Cs, ^{226}Ra and ^{232}Th isotopes. The main way of receipt of RN in an organism is

through the gastroenteric path, where by virtue of physiological features the majority of the RN arrive not only with water and food, but also with aerosols penetrating into the organism through the lungs.[20-22] Therefore, it should be expectable that the contents of RN, taken out with intestinal media (feaces) with an effectively "working" enterosorbent, would be higher.

In Figure 4 a,b the diagrams illustrate the changing activity of feaces, urine and blood on some RN (^{137}Cs+^{134}Cs, ^{226}Ra+^{232}Th). It is visible, for example, that radiocesium is intensively removed from an organism during the course of enterosorption.

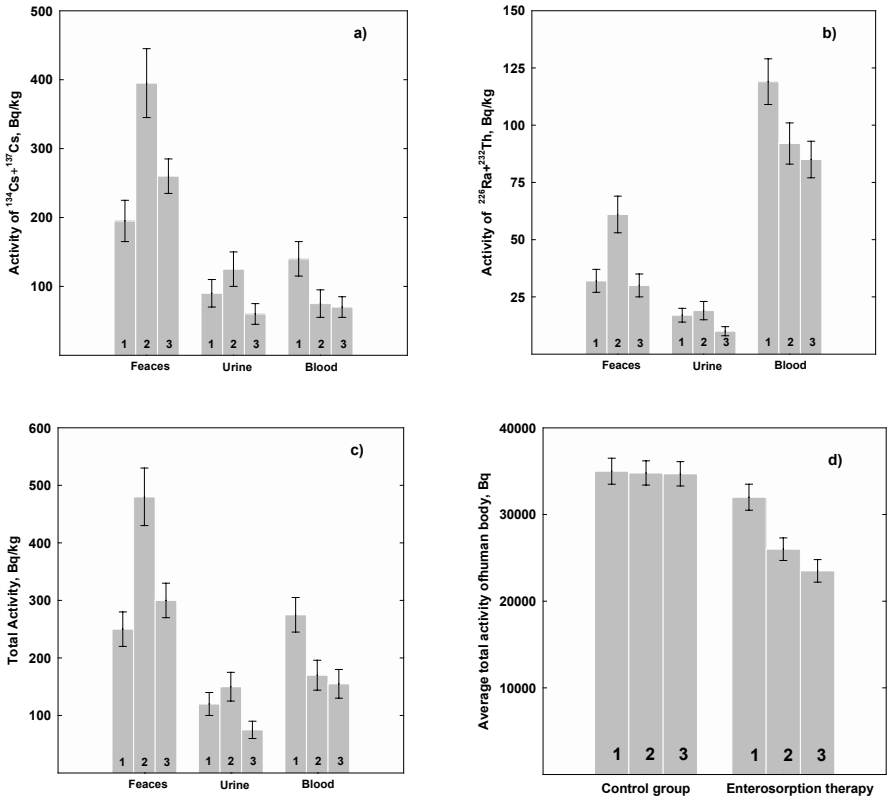

Figure 4. Dynamics of content of ^{137}Cs+^{134}Cs (a), ^{226}Ra+^{232}Th (b) and total activity of RN (c) in biological media of an organism, and average total γ-activity of patient body (d) at the 1st, 7th and 14th days of enterosorption with the *Ultrasorb* preparation.

So, by the seventh day of carrying out a curative course, the contents of radiocesium (ratio ^{137}Cs :^{134}Cs ≈ 10:1) sharply grows in feaces and in urine which testifies the effective work of the used preparation. In the same period, the blood radioactivity reduced. Upon termination of the test, the radioactivity of feaces and urine sharply falls down to a level close to the

initial one, while the activity of blood reduces insignificantly. This testifies that the process of radiocesium removal during enterosorption is accompanied by a constant washing out of new portions of these radionuclides from tissue depots to the blood of the organism.

Comparing the γ-activity changes of radium and thorium (ratio ^{226}Ra : $^{232}Th \approx 1:1$) it is possible to note that their removing from an organism is complicated. The character of changing activities of feaces, urine and blood is similar, but the contents of these RN in blood during enterosorption though decreasing, remains higher than the activity of feaces, the basic parameter of removing RN from an organism.

In Figure 4 c,d the diagrams of changes of total activity of feaces, urine and blood as well as the average total activity of human body are displayed. From the shown diagrams it is visible that by the seventh day of enterosorption with *Ultrasorb* there is a substantial growth of activity of feaces and that the activity of urine also grows. This confirms the effective removing of RN from the organism. Activity of blood thus is appreciably reduced. By the 14^{th} day of carrying out of enterosorption the activity of feaces is reduced, remaining above its initial level. This testifies that the RN removing process still proceeds.

The activity level of urine falls below its initial value. The blood activity decreases, though only scarcely, apparently due to the receipt in blood of new portions of RN washed out from tissue depots of the organism. The character of change of the contents of RN in urine upon reception of *Ultrasorb* is caused, apparently, by a general detoxification action of the enterosorbent, providing "purification" of cell membranes and, as a consequence, an improvement in the transport of ions.

The studied parameters of γ-activity in tests of physiological media for persons of the control group (without enterosorption) have remained practically unchanged.

Medical and biologic researches have confirmed the high adsorption ability of the developed *Ultrasorb* preparation to several harmful metabolites and toxic substances, and also a corrective action on protein, lipid and electrolyte status of the patients.

4. Conclusion

The analysis of obtained data on influence of combined preparations on the human organism shows their efficiency on removing HM and RN from the organism, and also their harmlessness, expressed detoxification and corrective properties. They can be recommended to use in complex therapy of intoxications of various genesis, especially ecology dependent diseases.

Taking into account the effective ability of the combined preparations to remove heavy metals and radiocesium and to provide general detoxification and sometimes corrective action on the organism, they should be recommended in medical practice of extreme situations (medicine of accidents), for example, at carrying out the scheduled and emergency works on object "Shelter" in Chernobyl.

REFERENCES

1. *Enterosorption*, edited by N.A. Belyakov (Center of the Sorption Technologies, Leningrad, 1991).
2. *Patent of Ukraine N20718*. Adsorption preparation “Ultrasorb” to remove radionuclides from organism, V.V.Strelko, M.T.Kartel, S.S.Stavitskaya et al., bul. N6 (2001).
3. *Patent of Ukraine N42137*. Adsorption preparation for decorporation of radionuclides and ions of heavy metals from organism “Pectopal”, V.V.Strelko, V.K.Mardanenko, M.T.Kartel et al., bul. N11 (2003).
4. N.T. Kartel, V.V. Strelko, S.S. Stavitskaya et al., Combined enterosorbent “Carboxykam” for prophylaxis and treatment of ishemia of heart. In *Search and Development of Cardio-Vascular Means. Proceedings* (Alushta, NAS of Ukraine, 2001), pp.17-21.
5. V.V. Strelko, and N.T. Kartel, Active carbon of medical assignment. In *Scientific Principles of Drugs Elaboration* (Osnova, Kharkiv, 1998), pp. 490-516.
6. S.S. Stavitskaya, V.V. Kirsenko, V.N. Karpenko et al., Influence of new combined enterosorbent “Ultrasorb” on biochemical and morphologic parameters of blood, *Ukrainian Biochemical Journal* 68 (N4), 95-100 (1996).
7. *Some Aspects of Toxicity of Metal Ions*, edited by H. Sigel and A. Zigel (Mir, Moscow, 1993).
8. Yu.V. Chmelevsky, and O.K. Usatenko, *Main Biochemical Constants of Human Organism in Norm and Pathology* (Zdorov’ya, Kyiv, 1987).
9. I.A. Tarkovskaya, *Oxidized Carbon* (Naukova dumka, Kiev, 1980).
10. V.V. Strelko, New sorbents for ecological protection of human and animals. In *Sorption Means and Methods of Ecological Protection of Human and Animals. Proceedings* (Homel’1992), pp. 9-10,
11. I.M. Trachtenberg, Pectin-containing oral adsorbents against radionuclides and heavy metals action, *Physician Matter* 4, 23-29 (1992).
12. N.L. Aizenberg, I.A. Trachtenberg, S.A. Sedina et al, Pectin’s and pectinases. In *Progress in Biotechnology-14. Proceedings* (Wageningen, 1995), pp. 947-954.
13. B.D. Levchenko, L.M. Timonova, *Pectin. Pectin Prophylaxis*. (Znanie, Krasnodar, 1992).
14. I.M. Trachtenberg, P.I. Demchenko, V.V. Strelko et al, Modern trends of use of composite pectin-containing adsorbents at influence of xenobiotics. In *Efferent Methods in Medicine. Proceedings* (Anapa, 1992), pp. 131-132.
15. M. Kartel, L. Kupchik, and B. Veisov, Evaluation of pectin binding of heavy metal ions in aqueous solutions, *Chemosphere* 38, 2591-2596 (1999).
16. V. Rudichenko, *Natural Food Adsorbents as a Modern Base of Human Health* (Vyshcha shkola, Kyiv, 1997).
17. L.P. Derevyanko, Use of “Elamin” for healthening people in adverse ecological conditions, *Medicine News* 4, 59-61 (1998).

18. V.I. Smolyar, *Hypo- and Hypermicroelementosis* (Zdorov'ya, Kyiv, 1989).
19. L.R. Nozdryukhina, *Biological Role of Microelements in Organism of Human and Animals* (Soviet medicine, Moscow, 1977).
20. Yu.I. Moskalev, *Radioactive Isotopes in External Media and in Organism* (Atomizdat, Moscow, 1970).
21. E.I. Safronov, *Ray Disease from Internal Irradiation* (Meditsina, Leningrad, 1972).
22. I.K. Dedenko, A.V. Starikov, and V.V. Strelko, *Efferent Methods in Treatment of Radiation Injures*. (Nora-print, Kiev, 1996).

SYNTHESIS OF NEW LOW DENSITY CARBON MATERIALS WITH MOLECULAR SIEVING PROPERTIES

SVETLANA S. STAVITSKAYA*, MYKOLA T. KARTEL, VALENTINA E. GOBA, OLGA N. BAKALINSKAYA AND NINEL M. KOVAL
Institute for Sorption and Problems of Endoecology, NAS of Ukraine, General Naumov str., 13, Kiev, 03164, Ukraine

Abstract. New ways of preparation of carbon adsorbents with molecular-sieving properties, with low apparent densities, are developed. High-dispersed samples are produced using various types of processing at various stages of manufacturing; their structural-sorptive characteristics are determined.

Keywords: Density; carbon materials; structure characteristics; molecular-sieving properties

1. Introduction

Recently intensive researches on the synthesis of sorptive-active carbon sorbents with developed pore volume of molecular dimensions, new carbon materials (CM), nanotubes with adjustable size of entrance apertures[1-6] which can show molecular-sieving effect were conducted.

The development of new ways of synthesis of such CM, the search of new nanodimensions CM with sieving properties, with low density, and the investigation of their features is the subject of this work.

The initial raw material for the preparation of carbon molecular sieving materials can be most of the carbon containing materials: brown coal and coal, including anthracite, lignin, wood, and peat, both synthetic and natural polymers, and other organic substances.

* To whom correspondence should be addressed. Svetlana Stavitskaya, Institute for Sorption and Problems of Endoecology, NAS of Ukraine, General Naumov str., 13, Kiev, 03164, Ukraine. E-mail: ispe@ispe.kiev.ua

J.M. Loureiro and M.T. Kartel (eds.), Combined and Hybrid Adsorbents, 181–186.

2. Experimental

In the present work various methods of preparation of carbon adsorbents with molecular-sieving properties (with given fixed porosity) starting from phenol formaldehyde pitches and using thin dispersed KCI as an applicator have been investigated. Samples have been prepared by two ways.

The first way was: an initial sample of polymer processed by boiling KCI saturated water solutions during 2 h. The prepared sample left in a solution at room temperature during 8 h, then filtered, and dried at 120 ^{o}C. The dried sample was subjected to heat treatment at 200 ^{o}C during 1 h in an inert atmosphere furnace, then 1/2 h at 600 ^{o}C, the heat treatment finishing under an Ar flow at 1000 ^{o}C during 1/2 h. After the heat treatment the salt was removed by washing the sample with hot distilled water.

The second way was: the initial pitch is processed by KCI saturated water solutions during 2.5 h, the solution is filtered, the sample dried at 120 ^{o}C and subjected to heat treatment at T=600 ^{o}C in an inert atmosphere during 1.5 h. The prepared material is also washed by distilled water to remove the HCI.

3. Results and Discussion

Parameters of the porous structure of the prepared CM, determined by sorption of standard vapor (benzene at different P/P_s), and the apparent densities of these sorbents (d) before and after carbonization, are shown in Table 1. Some initial samples with different densities from 40 up to 250 mg cm^{-3} have been chosen for research. It was shown that the density of the samples processed by potassium chloride, after carbonization, was considerably smaller in comparison with the raw samples density. Thus, the limiting adsorptive volume (V_s) equal to the sum $V_{mi}+V_{me}$, practically does not depend on d. The ratio between the volumes of micro- and mesopores also changes only slightly. The carbon materials macropore volume was determined by the difference between the total pore volume, found by the moisture capacity of the carbons, and the maximal adsorbed volume of the benzene standard vapor. It is necessary to note that the structural characteristics of the samples prepared by the second way were much better. Obviously it is connected with the fact that in the first way KCI is less washed and blocks the pores. However CM with similar micropore volumes were prepared both in the first and in the second cases.

The reaction activity and the thermostability of such carbon aerogels in different oxidizing media (CO_2, O_2, HNO_3) were investigated. This gives the possibility to regulate the structure and the nature of the surface of CM

prepared at different temperatures. Samples of various densities were subjected to high-temperature activation by CO_2 for development of microporosity and to increase their sorptive activity. Key parameters of the activation process were determined as well as the kinetic data on density changes during activation at various temperatures from 500 up to 950 ^oC.

TABLE 1. Parameters of porous structure and density of carbon materials at different stages of processing

Sample of polymer	d, mg cm^{-3}		Structural characteristics after carbonization				
	Before carbonization	After carbonization	V_s, cm^3g^{-1}	V_{mi}, cm^3g^{-1}	V_{me}, cm^3g^{-1}	V_{ma}, cm^3g^{-1}	S_g, m^2g^{-1}
			I way				
Initial	147	106	0.054	0.013	0.041	0.315	31.2
Processed by KCl	134	97	0.077	0.033	0.044	0.305	76.8
Initial	83	193	0.062	0.020	0.042	0.410	55.2
Processed by KCl	190	158	0.088	0.049	0.039	0.299	122.4
Initial	246	254	0.037	0.032	0.015	0.245	38.4
Processed by KCl	220	169	0.066	0.029	0.037	0.250	108.0
			II way				
Initial	40	28	0.170	0.160	0.010	0.805	37.0
Processed by KCl	91	54	0.190	0.180	0.010	0.765	98.0
Initial	122	100	0.220	0.200	0.020	0.650	104.0
Processed by KCl	246	190	0.360	0.340	0.020	0.559	80.0

V_s – limiting adsorptive volume equal to (V_{mi} + V_{me}), V_{mi} – micropores volume, V_{me} – mesopores volume, V^{ma} – macropores volume, S^g – a geometrical micropores surface.

Apparently, till a certain moment the density of samples decreased due to burning out most of the amorphous reactive part of the carbon with the subsequent development of porosity. However, with the increase of the processing temperature the d value grew (Figure 1). This can be caused by a change of the textural features of the carbon aerogels. Most likely, the basic part of aromatic layers starts to participate already during the heat treatment at T=750-950 ^oC in the presence of CO_2 together with the destruction of the lateral radicals of the polymeric carbon material. Thus, there is an ordering structure of carbon samples which is characterized by growth of the linear sizes of the polymerized aromatic carbon grids, reduction of interplane distances and increase in true density of synthesized CM. To support these assumptions the roentgenograms of such materials demonstrate the increased contents of crystalline carbon in the structure.

The structural characteristics of CM prepared at different processing temperatures in flowing CO_2, calculated from benzene and water vapors adsorption isotherms are in Table 2: the geometrical micropore surface (S_g), cracks half-width (x), structural constants of the Dubinin-Radushkevich equation (W_o and B), which are the major micropore characteristics, and

also the characteristic energy of adsorption (E_o). The small sizes of the structural constants W_o and B testify that the synthesized CM possess more developed microporous structure; the micropores half-width changes from 0.5 up to 0.8 nm. These sizes are characteristic for molecular-sieving adsorbents.[6]

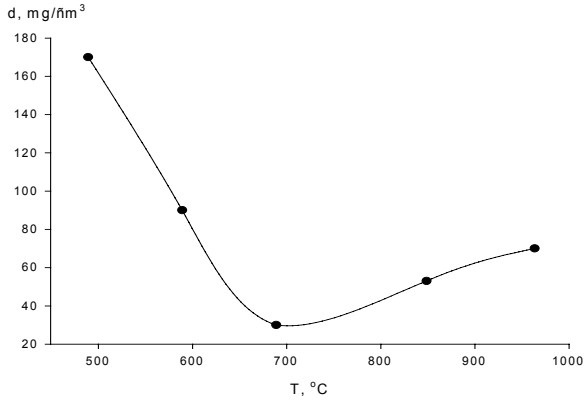

Figure 1. Change of samples density (d, mg/cm^3) depending on activation in flowing CO_2 at temperature T (^{o}C).

TABLE 2. Dependence of CM structural characteristics on the temperature (T) of their CO_2 heat treatments

T^{o}C	S_g, m^2 g^{-1}	W_o, cm^3 g^{-1}	E_o, kJ mol^{-1}	B 10^6	x, nm
400	367	0.15	25.5	0.56	0.70
500	418	0.22	23.6	0.66	0.53
600	370	0.22	21.2	1.40	0.76
700	220	0.15	16.6	1.18	0.47
850	235	0.19	15.6	1.50	0.80
950	265	0.14	23.6	0.66	0.59

CM samples subjected to the action of oxygen from air at T=450-500 ^{o}C and nitric acid in the liquid phase have been prepared apart from the CM thermal treated (activated) at high temperatures in flowing CO_2. The cation exchange capacity (CEC) of the prepared oxidized samples, and also the acidity distribution of the surface functional groups (SFG) formed during oxidation were determined by titration of the carbons with bases of various strengths. The structural-sorptive characteristics of the prepared oxidized CM are shown in Table 3.

Formation of micro- and mesopores is observed during oxidation for all samples. Their limiting adsorptive volume (V_s) depends on the oxidation procedure: the liquid phase oxidation by nitric acid conduces to a V_s value that is twice as big as the one obtained during oxidation by oxygen from air. The micropore volume prevails on all researched CM.

In the present work a method was used for preparation of new forms of microporous carbon materials besides using intercalation process – filling the initial phenolformaldehyde pitches by potassium chloride with subsequent carbonization at various temperature and time modes, thermoactivation and oxidation in the presence of various oxidizing agents. It is supposed that, as a result of this process, there will be a destruction of macro- and partially mesopores and formation of carbon nanoparticles with microporous structure.

TABLE 3. Structural-sorptive characteristics of the oxidized carbon materials

Way and time of oxidation	CEC, $mM\ g^{-1}$	Quantity of SFG, $mM\ g^{-1}$			V_s, $cm^3\ g^{-1}$	V_{mi}, $cm^3\ g^{-1}$	V_{me}, $cm^3\ g^{-1}$	S_g, $m^2\ g^{-1}$
		I	II	III				
Oxidized by HNO_3	4.0	2.70	0.50	1.40	0.071	0.053	0.010	120
Oxidized by O_2, 8 h	3.0	1.60	0.30	1.10	0.038	0.030	0.019	192
Oxidized by O_2, 12 h	3.25	1.75	0.36	1.15	0.036	0.030	0.006	144

I – strong acidic carboxylic groups, II – weak acidic carboxylic groups, III – phenol groups.

A method of ultrasonic processing during various times (from 15 up to 720 min) have been used besides mechanical crushing (Table 4).

New carbon materials – "carbon powders" – high dispersed powders like (nanoparticle size) materials with low apparent density have been synthesized. Their microstructure considerably differs from that of known carbon powders, for example, from technical carbon (soot). With the increase of the thermoactivation time the value of d of the prepared carbon powders decreases (Table 4). They have high micropore surface (~ 400 $m^2\ g^{-1}$). Low values of constants W_o and B confirm the developed microporous structure of the synthesized samples.

TABLE 4. The apparent density and structural characteristics of "carbon powders", prepared by ultrasonic processing of carbonized CM samples during various times

Time of processing, min	d, $mg\ m^{-3}$	W_o, $cm^3\ g^{-1}$	S_g, $m^2\ g^{-1}$	E_o, $kJ\ mol^{-1}$	B 10^6
60	42.8	0.192	400	26.04	0.54
120	34.3	0.197	418	27.48	0.52
180	33.5	0.189	423	27.90	0.47
300	30.2	0.173	408	27.14	0.63
480	28.1	0.217	400	24.19	0.66
720	27.4	0.192	390	23.58	0.48

Micropore sizes increase both after mechanical (from 12.6 up to 14.7Å) and ultrasonic (from 10 up to 17.7 Å) processing. In the latter case, the pore sizes are larger than those of any of the samples prepared by mechanical crushing.

4. Conclusions

New methods and conditions of synthesis of monoporous CM with sieving properties – nanoparticles with low apparent densities starting from phenolformaldehyde pitches are developed. Density, porosity, microstructure, electroconductivity and reactivity of new carbon aerogels have been determined by methods of electronic microscopy, X-ray and thermal analyses, adsorptive-structure, etc. It is found that the final characteristics of the synthesized samples are influenced by the reaction activity and origin of the initial substances, and also by the heat treatment conditions (temperature, time of processing, nature of the environment gas), preliminary impregnation by activating additives and inorganic templates – metals salts.

Adsorbents, having homogeneous porous structure with a micropore size of the order of the sizes of adsorbed molecules are prepared using various types of processing procedures at various stages of manufacturing: thermal, oxidizing, mechanical, ultrasonic.

REFERENCES

1. Wen-Cui Li, An-Hui Lu, and Shu-Cai Gu, Characterization of the microstructures of organic and carbon aerogels based upon mixed cresol-formaldehyde, Carbon 39 (13), 1989-2001 (2001).
2. Gnotong Qin and Shucai Guo, Preparation of RF organic aerogels and carbon aerogels by alcoholic sol-gel process, Carbon 39(12), 1935-1937 (2001).
3. R. Petricevic, M. Glora, and J. Fricke, Planar fibre reinforced carbon aerogels, Carbon 39 (6), 857-867 (2001).
4. J. Jamashita, T. Ojima, M. Shioya, H. Hatori, and Y. Yamada, Organic and carbon aerogels – derived from polyvinylchloride, Carbon 41 (2), 285-295 (2003).
5. N.D. Drozhalina, Carbon molecular sieve on the base of peat, Science and Technique, Minsk, 1984.
6. Nanoparticle systems. Electronics, atomic construction and properties, Proceedings of the NANSYS 2004, NAS of Ukraine, Kiev, 2004.

GRANULAR ACTIVATED CARBON FROM DECIDUOUS WOOD LIGNOCELLULOSE

JANIS RIZHIKOVS*, J. ZANDERSONS, M. PUKE, N. VEDERNIKOVS, G. DOBELE, A. TARDENAKA AND B. SPINCE
Latvian State Institute of Wood Chemistry, 27 Dzerbenes St., LV-1006, Riga, Latvia

Abstract. Since the capacity of an adsorbent is expressed in terms of the surface area or the amount adsorbed per weight unit, high-density adsorbents are required. The dried leftover lignocellulose of furfural production, due to its good self-binding properties, can be granulated or pelletized and used as a potential raw material for production of high-density activated carbon sorbents with double density, in comparison with activated carbon from charcoal. These high-density microporous sorbents are appropriate for purifying gaseous media. The chemical and mechanical pre-treatment of lignocellulose imparts new properties to the porous structure of the carbon material and to the activated carbon prepared from it.

Keywords: high-density sorbent; lignocellulose; granular activated carbon; micropores

1. Introduction

Our recent studies revealed a chance to improve the methods for lignocellulose (LC) thermochemical conversion into sorbents, published elsewhere.[1,2] Some physical and chemical properties of birch LC provide a

* To whom correspondence should be addressed. Janis Rizhikovs, Latvian State Institute of Wood Chemistry, 27 Dzerbenes St., LV-1006, Riga, Latvia; e-mail: tpd@edi.lv

J.M. Loureiro and M.T. Kartel (eds.), Combined and Hybrid Adsorbents, 187–193.

possibility of using this leftover by-product as a raw material for production of high density sorbent. In general, the capacity of an adsorbent is expressed in terms of the surface area or the amount adsorbed per unit weight. In order to improve the adsorption capacity per unit volume of a carbonaceous adsorbent, an attempt was made to prepare activated carbon of increased density from compression- treated wood as a starting raw material.[3] The differences in the apparent density and pore volume between wood and compressed wood did not influence the steam activation reaction, while the apparent density of the microporous carbon made from compressed wood was about double that of the charcoal made from uncompressed wood.

Three major forms of activated carbon, namely, powder, granular and palletized ones are currently available on the market. The granular and palletized ones are appropriate for a packed filter apparatus giving the lowest pressure drop and a high regeneration recovery. In our studies, an attempt was made to use the self-binding properties of the LC left directly after furfural had been distilled-off,[4,5] to prepare a dense LC raw material for production of high density granular or slab form sorbents. The yield of the carbonized intermediate product as well as the sorption properties and porous structure of activated carbon materials were studied.

The impact of the catalyst (concentrated sulfuric acid) in prehydrolysis experiments was investigated not only to elucidate the optimum conditions for ensuring high yields of furfural, but also for obtaining LC with appropriate properties. Lignocellulose was also leached with water before granulation to see the impact of water-soluble substances on the activated carbon properties.

2. Experimental

2.1. OBTAINING OF FURFURAL

Veneer shorts were used as the raw material. The initial material was mixed with sulfuric acid in a special mixer and treated in a steam flow at a temperature of 167 ^{o}C for 60 min.

2.2. LIGNOCELLULOSE

Two parallel samples of LC were prepared, of which one was leached with water. Wet LC containing 45 to 50% (wet basis) was dried at ambient temperature and at 50 to 60 ^{o}C up to the moisture 7–8%. The chips were milled to a particle size less than 2 mm.

2.3. MOULDING OF PANELS AND GRANULATION

Panels were made on a hydraulic hot plate press with electrical heating platens. A transformer realized the temperature adjustment. Thermocouples and a vertical face recorder controlled the moulding temperature. Granulation of LC (moisture 7-8%, wet basis) was carried out in an extruder type apparatus.

2.4. CARBONIZATION

The specimens of granules were carbonized in an electrically heated reactor with a stirrer at the maximum temperature 600 ^{o}C for 60 min.

2.5. ACTIVATION

The granules of the carbonized LC were inserted in a stationary kiln with a steam-superheating device. The superheated steam, heated-up to 850 ^{o}C, was let into the kiln at a speed corresponding to the chosen oxidizing agent – charcoal ratio and the time of activation. Sorption capacity was determined by using conventional methods and a sorptometer.

3. Results and Discussion

The initial assignment to develop a sorbent with a high density is to study the process parameters of making a pressed LC material. The apparent density and bending strength are directly proportional to the moulding temperature and pressure. The carbonized specimens demonstrate the apparent density up to almost 1.0 g/cm^3 (birch charcoal - 0.424 g/cm^3 on the average). The shrinkage of panels during the carbonization process is equal in all dimensions. The same particle volume ratio of approximately 65% has been ascertained in the case of carbonized granules of LC.

Carbonization of densified LC materials is performed in an externally heated apparatus, and the pyroligneous vapor should be burned in a furnace to eliminate noxious emissions and to utilize the production refuse for generation of a heat carrier. The low yield of acids as well as the lack of furfural may be attributed to the hydrolysis of xylan during prehydrolysis, while the more than four-fold decrease in the tar yield, undoubtedly, is a result of the catalytic action of sulfuric acid as a carbonization catalyst and simultaneously ensure a high charcoal yield of 49.5% on the o. d. LC basis (Table 1).

The activated carbon prepared by short term steam activation of carbonized pressed LC materials has properties of microporous sorbents of high density appropriate for purifying gaseous media.[6]

TABLE 1. Lignocellulose processing parameters and products yield (moulding pressure 25 MPa, carbonization temperature 610 °C, activation temperature 870 °C, steam – carbon ratio 3:1)

Moulding		Carbonization		Activation	
Temperature (°C)	Apparent density of panels (g/cm^3)	Yield of carbonized panels (% on the o.d. LC basis)	Apparent density of carbonized panels (g/cm^3)	Time (min)	Yield of activated panels (% on the carbonized panels basis)
120	1.318	49.2	0.950	75	67.4
170	1.430	49.5	0.980	50	65.0

During our experimental works, three different samples of LC charcoal (granularity 3-5 mm) were investigated. The difference was in the concentration of the catalyst used in prehydrolysis experiments (1%, 2% and 3% of sulfuric acid on the o.d. wood basis). The composition of these charcoal samples was almost identical, namely, fixed carbon content and volatiles 84.2-86.1% and 10.1-11.7%, respectively. A minor increase in the ash content parallel to the catalyst concentration increase has been observed (2.9%, 3.8% and 4.7%, respectively). To study the impact of the catalyst concentration, the superheated steam and charcoal ratio 3:1 was taken. Our aim was to achieve the maximum adsorption capacity as well as high enough crushing strength and activated carbon yield.

The results demonstrate that the best activated carbon yield is obtained from the LC prepared by using 2% of sulfuric acid. The mass loss is by 10 to 15% lower at the same conditions of activation. Therefore, if microporous sorbents with a narrow distribution of pores' dimensions are necessary, the prehydrolysis with 2% of the sulfuric acid catalyst is preferable. Since the yield of this activated carbon is 55% (initial charcoal mass basis), the ash content is comparatively low, i.e. 7%, which meets the requirements of most standards for the gas cleaning activated carbon.[7]

To elucidate the impact of water-soluble substances of LC on the potential of pore formation, two parallel sets of samples of LC were prepared (sulfuric acid modulus 0.02, temperature 167 °C, process duration 60 minutes), from which one set was leached with water.

Approximately 25% of the LC mass is lost due to leaching. The greater activated carbon yield from leached LC charcoal, calculated on the amount of the fixed carbon mass (49.8 and 40.7% respectively) does not compensate the LC mass loss caused by the removal of water-soluble components and the lower charcoal yield during the carbonization due to the elimination of sulfuric acid being a carbonization catalyst (Table 2).

The speed of steam in the prehydrolysis reactor did not influence the sorption properties of the activated carbon (respective dyes' sorption activities are listed in Table 3, and the characteristics of the micropores and the total porosity of activated carbon in Table 4). The granular activated carbon prepared from leached LC, in comparison with untreated LC granulated specimens, had minimum sorption activity differences of dyes and somewhat greater pores' volume differences, demonstrated by a sorptometer.

TABLE 2. Carbonization and activation of birch lignocellulose

Speed of steam in wood bulk, m/s	Carbonization T = 600 °C						Activation (T = 850-870 °C)			
	Untreated			Leached			Untreated		Leached	
	Yield, % o.d. LC mass	Fixed carbon %	Ash %	Yield, % o.d. LC mass	Fixed carbon%	Ash %	Yield % char mass	Burn-off, % fixed carbon mass basis	Yield% char mass	Burn-off, % fixed carbon mass basis
0.040	47.1	69.3	2.3	42.8	79.8	0.74	37.9	45.3	44.0	44.9
0.080	51.4	71.0	2.3	42.9	75.6	0.84	41.7	41.3	55.2	29.4
0.120	45.7	74.1	2.4	42.5	78.2	0.62	39.5	46.7	53.3	29.5
0.243	48.1	71.0	2.8	43.6	75.6	0.84	43.8	38.3	46.7	39.6
Mean yield	48.1	71.3		42.9	77.3		40.7	42.9	49.8	35.8

Unfortunately, the granular activated carbon prepared from leached LC demonstrated low mechanical strength properties. Granular activated carbon had a high bulk density, i.e. 320-390 g/L. The carbonized granules of leached LC had a low ash content, i.e. 2.3-2.8% and 0.6-0.8%, respectively. This advantage is a very serious positive characteristic but, in this case, it has practical sense if activated carbon is used in a powder form.

TABLE 3. Impact of prehydrolysis conditions and lignocellulose pre-treatment on the sorptivity of activated carbon

Pre-treatment of LC	Speed of steam in wood bulk, m/s	Burn-off, % o. d. fixed C mass	Yield of activated carbon, % o. d. LC mass	Adsorption capacity of activated carbon, mg/g			
				Iodine (<1.48 nm)[1]	Methylene blue (1.52 nm)[1]	Methyl-violet (2.16 nm)[1]	Congo red (2.26 nm)[1]
non	0.040	45.3	20.1	1105	88	36	22
	0.080	41.3	19.7	1003	72	38	13
	0.120	46.7	19.0	1114	80	32	19
	0.243	38.3	20.0	993	62	27	13
Leached with water	0.040	44.9	15.6	1083	99	32	10
	0.080	29.4	23.5	1005	33	8	2
	0.120	29.5	23.2	1022	27	5	1
	0.243	38.2	20.1	1080	92	23	12

[1] critical pore diameter in molecular sieving adsorption

TABLE 4. Porosity characteristics of activated carbon prepared from granulated untreated and leached lignocellulose (m = 0.02; 167 ^{o}C; 60 min; v = 0.120 m/s)

Characteristics	Units of measure	Untreated LC	Leached LC
BET surface area	m^2/g	925.03	841.52
Langmuir surface area	m^2/g	1205.77	1095.45
Total pore volume	mm^3/g	671.31	522.54
Micropore volume	mm^3/g	265.99	250.18

4. Conclusions

It has been elucidated that a 2% catalyst (H_2SO_4 modulus 0.02) concentration at 167 ^{o}C ensures the best quality of LC for production of activated carbon.

The activated carbon LC charcoal retains high mechanical properties and bulk density.

LC charcoal is appropriate for production of microporous activated carbon.

The activated carbon from leached LC specimens contains less ash than that from raw LC, while, unfortunately, its weak mechanical properties made it unacceptable for production of granulated sorbents.

REFERENCES

1. F.H. Tuovinen, R.J. Honkala, and M.-L. Metsarinta, *UK Patent Appl.* GB 2 038 869 A, Published 30 July (1980).
2. Y. Wang, K. Noda, and S. Kagawa, Manufacturing of activated carbon using furfural residue as raw material, *Chemistry Letters* (Japan) 1052-1053 (2001).
3. I. Abe, T. Fukuhara, S. Iwasaki, K. Yasuda, K. Nakagawa, Y. Iwata, H. Kominami, and Y. Kera, Development of a high density carbonaceous adsorbent from compressed wood, *Carbon* 39, 1485-1490 (2001).
4. N.A. Vedernikov, Production of furfural, in: *Hemicelluloses* (Zinatne, Riga, 1991), pp. 209-222 (in Russian).
5. N.A. Vedernikov, *Latvian patent* 11032 (1996).
6. N. Vedernikov, I. Kruma, A. Zandersons, A. Tardenaka, B. Spince, and J. Chirkova, Production of furfural and carbon materials from deciduous tree wood wastes, *Proc. 7th European Workshop on Lignocellulosics and Pulp*, Turku, Finland, pp. 51-54 (2002).
7. J. Zandersons, N. Vedernikov, I. Kruma, M. Puke, and J. Rizhikovs, Impact of birch wood prehydrolysis conditions upon the yield and properties of activated carbon from lignocellulose, *Proc. 8th European Workshop on Lignocellulosics and Pulp*, Riga, Latvia, pp. 543-546 (2004).

SYNTHESIS OF ACTIVATED CARBON FROM SPENT LUBRICATING OIL AND APPLICATION FOR ADSORPTION OF CADMIUM AND LEAD IONS FROM AQUEOUS SOLUTION

REYAD SHAWABKEH*, ABDULAZIZ KHLAIFAT
Department of Chemical Engineering, Mutah University, AL-Karak, 61710, JORDAN

OMAR KHASHMAN
Water & Environment Research Center, Mutah University, AL-Karak, 61710, JORDAN

SALAH TARAWNEH
Chemistry Department, Mutah University, AL-Karak, 61710, JORDAN

Abstract. A novel activated carbon was prepared from spent lubricating oil by chemical activation. Preparation of this material involved the oxidation of lubricating oil with a mixture of sulfuric and nitric acid solutions. FT-IR analysis showed the presence of carboxylic, phenolic and lactonic groups on the surface of this material. Equilibrium sorption isotherms prepared for this carbon demonstrate that it has a significantly high capacity for lead and cadmium sorption. A maximum of 250 mg Pb^{2+} and 150 mg Cd^{2+} were adsorbed per gram of this carbon.

Keywords: Spent Lubricating oil; Activated carbon; Lead; Cadmium

1. Introduction

Spent industrial and automotive lubrication oil is one of the major hazardous wastes that are generated in each country in the world. Improper

* To whom correspondence should be addressed. Reyad A. Shawabkeh, Department of Chemical Engineering, Mutah University, Al-Karak, 61710, Jordan; e-mail: rshawabk@mutah.edu.jo

J.M. Loureiro and M.T. Kartel (eds.), Combined and Hybrid Adsorbents, 195–200.

discharge of this waste would have an adverse impact on environment. It is estimated that one gallon of used oil can contaminate one million gallons of fresh drinking water, and cover eight-acre slick on surface water.[1] Layers of oil-spill on the surface of water can block sunlight and prevent the photocatalytic process. It prevents the replenishment of the dissolved oxygen and kills fish and other living creatures. This contamination to environment can affect the health of humans, animals and plants. Consequently, several attempts were made to properly recycle and dispose the spent oil. These methods include re-refining, incineration, biodegradation, land application and deep well disposal.[2-4] Recycling is a cost-challenging step compared to manufacturing new version of lubricating oil. Moreover, incineration, land application or deep well disposal can cause either air pollution or contaminate groundwater resources.

Jordan, as well as all neighboring countries, suffers from the shortage of drinking water. Thus, it must not only prevent the water resources from spent oil spill, but also treat the wastewater for reusing. Treatment of wastewater from toxic metals and organics is efficiently obtained by adsorption process using an activated carbon as filter. Removal of pollutants by activated carbon as adsorbent is a promising process that can reduce the concentration of toxic metals to sub-part per million.[5]

Commercial activated carbon can be produced from different types of raw materials, including wood, coal, fruit stones, and nutshells.[6-8] The adsorption capacity of activated carbon against a specific target adsorbate is strongly affected by the type of raw material and the processing technique, as well.

This paper discuses the use of spent lubricating oil as a raw material for the synthesis of activated carbon using novel activation technique. The produced carbon is then used for adsorption of Pb^{2+} and Cd^{2+} from aqueous solutions.

2. Experimental

2.1 MATERIALS

Samples of used lubricating oil were collected from vehicles maintenance facilities. Sodium hydroxide pellets and concentrated sulfuric acid were supplied by Sigma Chemical Company. Deionized water was prepared using Milli Q system (Millipore, France). All Chemicals were analytical reagent grade and the glassware were Pyrex washed with soap, rinsed with nitric acid then washed with deionized water.

2.2 METHODS

Two different activation procedures were used for the synthesis of activated carbon. In the first procedure, a sample of 100 mL of spent oil was mixed thoroughly with an equal volume of concentrated sulfuric acid (Analytical reagent, Scharlau-Spain) in 2-liter beaker. The mixture was heated to 200 °C while being agitated. Air was sparged into the mixture during the heating process to assure complete oxidation, as well as to assist with the agitation process. The resulting carbon was allowed to cool to ambient temperature; washed with distilled water; soaked in dilute sodium hydroxide solution for 30 min; washed a second time with distilled water; dried; and finally classified by particle size. The second procedure was similar to the first one except that activation agents were sulfuric acid (95 wt.%) and nitric acid (5 wt.%).

2.3 CADMIUM AND LEAD ISOTHERMS

Adsorption tests were conducted in 100-mL Erlenmeyer flasks. A sample of 0.1 g of the produced carbon was mixed in 50 mL solution of either $Cd(NO_3)_2$ or $Pb(NO_3)_2$ and allowed to equilibrate in an isothermal shaker (22 ±1 ^oC) for 24 h. The pH was adjusted by adding few drops of either hydrochloric acid or sodium hydroxide. Similar procedures for blank solutions containing either metal ions of interest or AC were used for the purpose of comparisons. After 24 h, all solutions were filtered and centrifuged to remove any suspensions and then analyzed using S4 ThermoElemental atomic absorption spectrophotometer. The difference between the initial and final concentration of each ion represents the amount that transferred to the surface of the AC.

3. Results and Discussion

Waste lubricating oil used in this study is composed of three major groups of oils; gear lubricants, transmission fluids and crankcase oil. The physical properties of these lubricants are illustrated in TABLE 1. The studied samples showed a moderate amount of ash as a result of wearing out the internal surface of engines or introducing atmospheric dust during combustion.

TABLE 1. Chemical Analysis of spent lubricating oil

Property	Method	Value
Specific gravity at 20 ^oC	ASTM D 1298–85	0.91
Flash point K	ASTM D 93–94	422
Viscosity at 37.8 ^oC, cSt	ASTM D 445–74	107
Ash content (wt%)	ASTM D 582	1.3
Asphaltene content (wt%)	ASTM D 3279–97	5.9

The oil samples were treated with both sulfuric and nitric acids. The activation was performed by addition of either sulfuric acid or a mixture of both sulfuric and nitric acids to the oil samples at room temperature. In the first case no effect was noticed on the mixture until the mixture was heated to 100 ^{o}C where the chemical reaction took place. In the second case nitric acid was added gradually to the mixture at room temperature, which resulted in a rapid increase in the solution temperature to 150 ^{o}C reached within one minute as a result of exothermic reaction. In both cases the solutions were heated further while carbon monoxide, carbon and sulfur dioxide, and nitrous oxide (noticed in the second procedure) were released out of the solution. Upon activation with these acids, several slufonation and nitrification reactions took place at the surface of the oil shale samples yielding an activated carbon with large surface functional groups according to Scheme 1.[9]

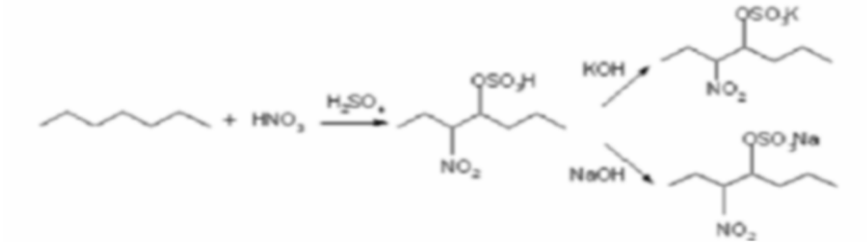

Scheme 1. Sulfonation and nitrification reactions at the surface of carbo-aluminosilicate.

Chemical analysis for the produced AC compared with that of the spent lubricating oil is shown in Table 2. It is clear that activation of the oil with acids followed by washing with water and treatment with sodium hydroxide leached out all heavy metals. Trace amounts were noticed for iron and aluminum on the surface of the carbon. The presence of iron and aluminum in the produced AC could be due to the passivation reaction between the acids and these elements. Moreover, reaction with hydroxide will precipitate these elements as $Fe(OH)_3$ and $Al(OH)_3$.

TABLE 2. Chemical Analysis of the spent lubricating oil and produced activated carbon

Element	Used Lubricating oil	Produced activated carbon
Sulfur	0.4 (wt%)	N/A
Iron	1358 (ppm)	11 (mg/Kg)
Lead	1320 (ppm)	N/A
Calcium	2364 (ppm)	N/A
Zinc	1182 (ppm)	N/A
Magnesium	607 (ppm)	N/A
Copper	17 (ppm)	N/A
Chromium	3.7 (ppm)	N/A
Aluminum	76 (ppm)	2 (mg/Kg)
Barium	11 (ppm)	N/A

A FT-IR spectroscopic study for the activated carbon is shown in *Figure 1*. It is apparent that eight major absorption bands were noticed for this carbon at 3416, 2924, 2852, 1699, 1618, 1458, 1145 and 619 cm^{-1}. The broad band at 3416 cm^{-1} can be assigned to the O-H stretching mode of hydroxyl groups and adsorbed water molecules. Also it may be attributed to the hydrogen-bonded OH group of alcohols and phenols.[10]

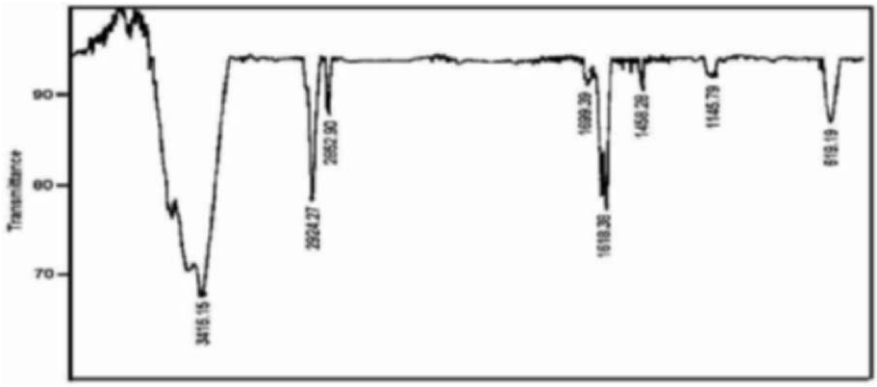

Figure 1. FT-IR spectrum of the activated carbon.

In the region 500-900 cm^{-1}, the AC shows a major peak at 619 cm^{-1}. This peak is assigned to C-H out-of-plane bending in benzene derivative. The peak at 1458 cm^{-1} appeared due to C=C stretch in aromatic rings.[11] It may also result from the C-H bonding mode in the carbon on functionalization with H atom. The peaks at 1600-1700 cm^{-1} are due to the double bond C=O stretching vibrations with aromatic carbons.[12] The absorption peak near 1699 cm^{-1} is attributed to carboxylic group appeared from the oxidation by nitric acid followed by hydroxide treatment.[13]

TABLE 3. Lead and Cadmium uptake by AC at different initial concentrations

Carbon type	Initial concentration (mg/L)	mg Pb^{2+}/g carbon	mg Cd^{2+}/g carbon
Lubricating oil activated with H_2SO_4	0	0	Does not adsorb cadmium
	50	22.5	
	100	45	
	200	85	
Lubricating oil activated with H_2SO_4/HNO_3	0	0	0
	50	22.0	23.5
	100	47.5	41.7
	200	97.5	83.5

Adsorption isotherms for Pb^{2+} and Cd^{2+} are presented in Table 3. It is clear that the carbon produced using sulfuric and nitric acid activation enhanced the amount of uptake for both ions. While, the one produced using only sulfuric acid did not show any removal ability against Cd^{2+}.

4. Conclusions

Spent lubricating oil was used as a raw material for synthesis of activated carbon. The activation agents were sulfuric and nitric acids. The produced carbon demonstrated good adsorption capacity for lead and cadmium ions from aqueous solution. Advantages of this carbon are low cost of raw material and safe operation technique.

REFERENCES

1. C. Harrison, The engineering aspects of a used oil recycling project**,** *Waste Management* 14(3-4), 231-235 (1994).
2. M. Ali, F. Rahman, and A. Hamdand, Techno-economic evaluation of waste lube oil rerefining, *Int. J. Production Economics* 42(3), 263-273 (1996).
3. F. Haus, O. Boissel, and G. Junter, Primary and ultimate biodegradabilities of mineral base oils and their relationships with oil viscosity**,** *Int. Biodeterioration & Biodegradation* 54(2-3), 189-192 (2004).
4. L. Khezami, and R. Capart, Removal of chromium(VI) from aqueous solution by activated carbon: Kinetic and equilibrium studies, *J. Hazard. Mat.* 123(1-3), 223-231 (2005).
5. R. Shawabkeh, D. Rockstraw, and R. Bhada, Copper and strontium adsorption by a novel carbon material manufactured from pecan shells, *Carbon* 40(5), 781-786 (2002).
6. J. Barkauskas, S. Tautkus, and A. Kareiva, Residual content of inorganic ions in activated carbons prepared from wood**,** *J. Analyt. Appl. Pyrolysis* 71(1), 201-212 (2004).
7. J. Gañan, C. González-García, J. González, E. Sabio, A. Macías-García, and M. Díaz-Díez, Preparation of activated carbons from bituminous coal pitches, *Appl. Surf. Sci.* 238(1-4), 347-354 (2004).
8. R. Shawabkeh, D. Rockstraw, and R. Bhada, United States Patent number 6,225,256.
9. K. Benak, L., Dominguez, J. Economy, and C. Mangun, Sulfonation of pyropolymeric fibers derived from phenol-formaldehyde resins. *Carbon* 40, 2323–2332 (2002).
10. T. Yang, and A. Lua, Characteristics of activated carbons prepared from pistachio-nut shells by physical activation. *J. Colloid Interf. Sci.* 267(2), 408-417 (2003).
11. J. Guo, and A. Lua, Textural and chemical characterizations of activated carbon prepared from oil-palm stone with H_2SO_4 and KOH impregnation. *Microp. Mesop. Materials* 32, 111-117 (1999).
12. H. Chiang, C. Huang, and P. Chiang, The surface characteristics of activated carbon as affected by ozone and alkaline treatment. *Chemosphere* 47, 257-265 (2002).
13. S. Shin, J. Jang, S. Yoon, and I. Mochida, A study on the effect of heat treatment on functional groups of pitch based activated carbon fiber using FTIR. *Carbon* 35(12), 1739-1743 (1997).

SYNTHESIS AND CATALYTIC PROPERTIES OF N-CONTAINING SYNTHETIC CARBONS ON A BASIS OF COPOLYMER OF STYRENE AND DIVINYLBENZENE

SERGEY V. ZHURAVSKY*, MYKOLA T. KARTEL AND OLEXANDER M. PUZIY
Institute for Sorption and Problems of Endoecology, NAS of Ukraine, General Naumov str., 13, Kiev, 03164, Ukraine

Abstract. Synthetic N-containing carbons designed on the basis of copolymer of styrene and divinylbenzene by thermochemical carbonization, impregnation with N-containing compounds (urea and melamine) followed by heat treatment or activation are prepared. The yields of carbons, volumes of sorption pores, specific surface area and content of nitrogen are obtained. The examination of their catalytic properties on the decomposition of hydrogen peroxide test reaction showed that the activity of these carbons is caused by the content of nitrogen atoms introduced into the structure of the prepared sorbent.

Keywords: Synthetic carbons; content of nitrogen atoms; catalytic activity

1. Introduction

From the literature it is known that carbons which contain heteroatoms (such as nitrogen) in their composition have interesting physicochemical properties. According to quantum-chemical calculations[1] and experimental data,[2-4] the introduction of nitrogen atoms in a carbon matrix results in the enhancement of the basicity of the carbon surface, considerably raising its catalytic activity in redox type reactions.

Synthetic N-containing carbons can be obtained by several methods:

* To whom correspondence should be addressed. Sergey Zhuravsky, Institute for Sorption and Problems of Endoecology, NAS of Ukraine, General Naumov street 13, 03164, Kiev, Ukraine; e-mail: s_zhur@ukr.net

J.M. Loureiro and M.T. Kartel (eds.), Combined and Hybrid Adsorbents, 201–206.

1. by carbonization of N-containing copolymers and resins (matrix of acrylonitrile, vinylpyridine etc.);[5]
2. by heat treatment of finished carbons in an atmosphere of N-containing gases - $(CN)_2$, NH_3 and others;[6]
3. by heat treatment of oxidized carbons, impregnated with N-containing compounds.[7]

The synthetic carbons SCN, obtained by the first method, have unique porous structure, surface chemistry and mechanical characteristics; however, their obtaining includes an expensive and ecologically unsafe compound, the 2-methyl,5-vinylpyridine. Most similar on porous structure and mechanical characteristics to carbons SCN are carbons such as the SCS, obtained from porous styrene matrixes; however, these carbons do not contain nitrogen. A problem therefore was put to synthesize samples of N-containing carbons with advanced porous system, on the basis of such raw material as chloromethylated copolymer (CMC) of styrene and divinylbenzene, for further studying their sorption and catalytic properties, and evaluating the opportunity of using them as sorbents of medical assignment.

2. Experimental

The usual scheme of obtaining SCS carbons includes sulfonation of CMC of styrene and divinylbenzene followed by carbonization and activation. Thus, for introduction of the N-containing additive the following paths were studied:

1. CMC - sulfonation - impregnation by the N-containing additive - carbonization - activation;
2. CMC - sulfonation - carbonization - impregnation by the N-containing additive - heat treatment - activation;
3. CMC - sulfonation - carbonization - oxidizing (by nitric acid) - impregnation by the N-containing additive - heat treatment - activation.

As a feedstock, porous CMC, made on the State Enterprise "SMOLY", Dneprodzerginsk (Ukraine), was taken. It is in the form of white spherical granules with size approximately 0.5-1mm. The water content of the copolymer was about 23%. Physical characteristics of the copolymer according to the producer certificate are given in the Table 1.

As the N-containing additive urea and melamine were used, since they are accessible compounds with high nitrogen content and with amino groups. The presence of amino groups is necessary for chemical interlinking of molecules of urea or melamine with the CMC sulfonation

surface groups (mainly sulfo- and carboxylic groups) or its oxidized carbonisate (mainly carboxylic and phenol groups):

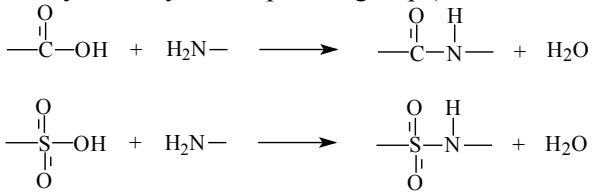

TABLE 1. Physical data of styrene and divinylbenzene porous CMC

Characteristic	Value
Crosslinking, %	10
Porophore, %	90
Particle size, mm	0.5-1.0
Main fraction, %	98
Chlorine percentage, %	17

3. Results and Discussion

3.1. PREPARATION OF NITROGEN CONTAINING CARBONS

The N-containing carbons prepared from styrene-divinylbenzene copolymers are obtained in three stages:

1. sulfonation of CMC of styrene and divinylbenzene in H_2SO_4 (98%) at T = 180 ^oC during 6 h;
2. impregnation of the sulfonated CMC (SCMC) or of its carbonisate (CSCMC) or oxidized (with nitric acid) carbonisate (OKSCMC), using solutions of urea (20 % water solution) or melamine (10 g of melamine, 100 ml of water, 10 ml of glacial acetic acid, T = 100 ^oC). In the case of the sulfonated CMC: 25, 50, 75 or 100 g of urea on 100 g of SCMC and 10 or 20 g of cyanotriamide (melamine) on 100 g of SCMC; in the case of the carbonisate or of the oxidized carbonisate: 50 g of urea on 100 g of CSCMC or OKSCMC, and 20 g of melamine on 100 g of CSCMC or OKSCMC;
3. carbonization of the impregnated sulfonated CMC or calcination of the impregnated carbonisates and oxidized carbonisates at T = 800^oC in argon atmosphere.

Eleven samples of carbon, ten of which are N-containing carbons, were synthesized; their main characteristics (pore volume, surface area and nitrogen content) are shown in Table 2.

TABLE 2. Porous structure and nitrogen content of the obtained samples

Sample	Bulk density, g/cm^3	Mass yield, %	Pore volume (V_s), cm^3/g	Surface area (S_{sp}), m^2/g	N content, %
SCMC - carbonization	0.57	73	0.61	733	0
SCMC+0.25 urea - carbonization	0.59	79	0.57	536	3.6
SCMC+0.5 urea - carbonization	0.61	82.5	0.54	568	4.2
SCMC+0.75 urea - carbonization	0.61	82	0.56	603	4.4
SCMC+1 urea - carbonization	0.61	82.5	0.56	563	4.8
SCMC+0.1 melamine - carbonization	0.58	79	0.59	605	3.1
SCMC+0.2 melamine - carbonization	0.58	81	0.6	525	4.6
CSCMC+0.5 urea - calcination	0.58	74	0.61	657	2.2
CSCMC+0.2 melamine - calcination	0.59	75	0.57	543	2.8
OKSCMC+0.5 urea - calcination	-	49.3	0.71	924	4.6
OKSCMC+0.2 melamine - calcination	-	52.5	0.68	843	6.2

The values for the bulk density and mass yield of each of the prepared carbons were also determined and are shown in Table 2, as well. The Table shows that at increasing the coefficient of impregnation of copolymer by urea or melamine the mass yields at carbonization grow, and the sorption pore volumes decrease. But at coefficients of impregnation by urea 0.5 and higher the yields at carbonization and the volumes of sorption pores reach stationary values of 82.5% and 0.56 cm^3/g respectively. The degree of introduction of nitrogen for calcinated impregnated carbonisates (CSCMC+0.5 urea, calcination; CSCMC+0.2 melamine, calcination) is much lower than for carbonisate from sulphonated impregnated copolymer and calcinated oxidized and impregnated carbonisate with identical coefficients of impregnation by urea or melamine. It is probably linked to a smaller amount of surface groups on the carbonisate, able to chemically contact with the amino groups of urea and melamine.

3.1.1. *Study of catalytic activity*

The catalytic activity of the obtained carbon materials was studied with the help of the test reaction of hydrogen peroxide decomposition.

Carbon samples of mass 0.25 g are flooded in 25 ml of 1% H_2O_2 solution at constantly mixing. At regular time intervals, solution samples were withdrawn and the concentration of H_2O_2 was determined using a standard procedure (titration by solution of potassium permanganate). From the obtained data the kinetic curves of decomposition of hydrogen peroxide were constructed (Figure 1), from which the rate constant of the catalytic

response (k), and also the rate constant reduced by the surface area (k/S_{sp}) were calculated. The respective values are displayed in Table 3.

The study of the catalytic activity in the reaction of hydrogen peroxide decomposition showed that the catalytic activity of the carbon depends on the nitrogen content; however, the proportionality coefficient can change in a wide interval (Figure 2). From the results displayed in Table 3, it is visible that some samples, having almost identical nitrogen content and surface area (for example SCMC+1 urea - carbonization and SCMC+1 melamine - carbonization), essentially differ on the catalytic activity. Based on this it is possible to assume that for catalytic activity the important factor is not only the total content of nitrogen atoms, but is also related with their energy states (pyridine - inactive, pyrrol and amine - active). The study of the dependence of the catalytic activity of the N-containing carbons on the form in which nitrogen is present, is an interesting direction for further research.

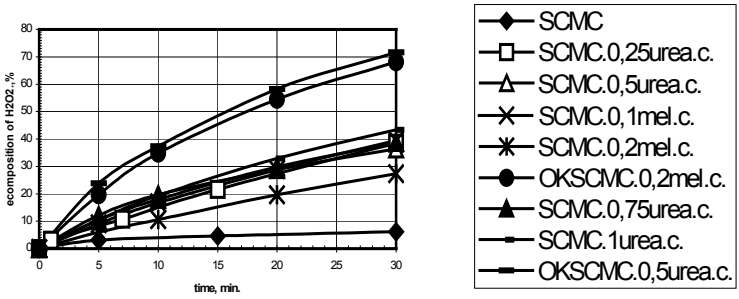

Figure 1. Kinetic curves of hydrogen peroxide decomposition by N-containing carbons.

TABLE 3. Results of catalytic activity studies

Sample	k, min^{-1}	N, %	S_{sp}, $m^2 \cdot g^{-1}$	k/S_{sp}, $(min^{-1} \cdot m^{-2}) \cdot 10^5$
SCMC - carb.	0.002	0	733	0.26
SCMC+0.25 urea - carb.	0.015	3.6	536	2.72
SCMC+0.5 urea - carb.	0.015	4.2	568	2.66
SCMC+0.75 urea - carb.	0.016	4.4	603	2.67
SCMC+1 urea - carb.	0.019	4.8	563	3.34
SCMC+0.1 melamine - carb.	0.016	3.1	605	2.73
SCMC+0.2 melamine - carb.	0.010	4.6	525	2.00
OKSCMC+0.2 melamine - calc.	0.038	6.2	843	4.48
OKSCMC+0.5 urea - calc.	0.041	4.6	924	4.47

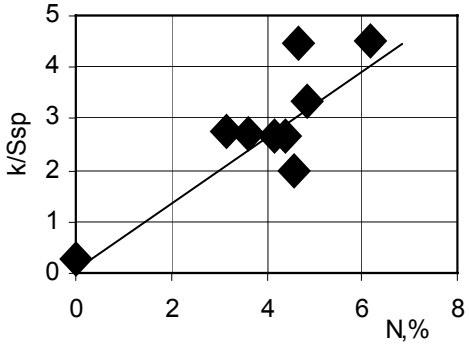

Figure 2. Dependence of the specific reaction rate of hydrogen peroxide decomposition reduced by the surface area (k/S_{sp}, $min^{-1} \cdot m^{-2}$), on the nitrogen content in a series of modified samples.

4. Conclusions

Original procedures of obtaining synthetic carbons on basis of styrene and divinylbenzene CMC are reported, in which carbons samples with nitrogen contents of up to 6 wt% are synthesized. The mass yields of such sorbents is within the limits of 50 to 80% with sorption pore volumes of 0.5-0.7 cm^3/g and specific surface areas of 500-900 m^2/g, that allow to consider them practically identical to the relevant brands of SCN carbons.

The examination of the catalytic activity of the obtained N-containing carbon sorbents in the reaction of hydrogen peroxide decomposition was carried out, showing that their catalytic ability is much higher, than for analogs which do not contain chemically bonded nitrogen. This confirms the presence of active forms of nitrogen atoms in the matrix of the obtained carbons.

REFERENCES

1. V.V. Strelko, V.S. Kuts, and P.A. Thrower, *Carbon* 38, 1499-1524 (2000).
2. S.V. Mikhalovsky, and Yu.P. Zaitsev, *Carbon* 35, 1367-1374 (1997).
3. M.C. Huang, and H. Teng, *Carbon* 41, 951-957 (2003).
4. A.M. Puziy, and S.V. Mihailovsky, *Oil Processing and Petrochemistry* 31, 36-39 (1986).
5. N.T. Kartel, *Carbon Hemosobents on the Basis of Synthetic Activated Carbons*. *Dr. Sci. Thesis*, Kiev, Inst. General & Inorg. Chem., Acad. Sci. of Ukr.SSR, 1989.
6. A.I. Loskutov, and I.A. Kuzin, Reception and examination of ion-exchange properties of nitrogen compound activated carbon, *Synthesis and Properties of Ion-Exchange Materials*, Moscow, Science, 1968, 95-101.
7. A. Bagreev, J.A. Menendez, S. Kopyl, et al., *Carbon* 42, 469-476 (2004).

ADSORPTION PROPERTIES OF MODIFIED FILTRATION MATERIALS IN WATER TREATMENT

YURIY I. TARASEVICH*, ZINAIDA M. SHKAVRO, OLENA O. SHEVCHUK
Institute of Colloid Chemistry and Chemistry of Water, National Academy of Sciences of Ukraine, 42 Vernadsky Ave., Kyiv 03680 Ukraine

YURIY L. ZUB
Institute of Surface Chemistry, National Academy of Sciences of Ukraine, 17 General Naumov Str., Kyiv 03164 Ukraine

Abstract. Modification of filtration materials and sediments in order to change adsorption and adhesion surface properties are proposed. The structure and sorption characteristics of the resulting materials are discussed. Experimental investigation of their application in water treatment and sewage purification has been carried out. The improvement of the adsorption properties and of the effectiveness of water treatment from highly dispersed insoluble and soluble organic contaminations is observed.

Keywords: surface modification; contact filtration; filter; coagulation; clarifier with up-flow layer; sediment; water treatment; sewage purification

1. Introduction

The regulation of interface interactions is the basis for coagulation and filtration intensification in water treatment and sewage purification. Changing of adsorption and adhesion surface properties of the solid phase under the contact with impurities is achieved by its modification.

* To whom correspondence should be addressed. Yuriy I. Tarasevich, Institute of Colloid Chemistry and Chemistry of Water, Ukrainian National Academy of Sciences, 42 Vernadsky Avenue, Kyiv 03680, Ukraine; e-mail: Yuitaras@thomascat.kiev.ua

J.M. Loureiro and M.T. Kartel (eds.), Combined and Hybrid Adsorbents, 207–212.

The purpose of this work is to increase the effectiveness of water treatment from organic compounds by changing adsorption properties of separating medium in rapid and slow filters as well as macroporous sediments in the up-flow layer of clarifiers.

2. Experimental

The adsorption capacity of filtration material was estimated by the residual concentration of organic compounds in water. The p-nitro-aniline sorption isotherms were used as the standard for adsorption from nonelectrolyte solutions. The concentration of dyes in water was determined by spectrophotometry using a Specord UV-Vis. The sediment structure was investigated by spectroscopy. Spectra of electronic paramagnetic resonance were obtained on TSN−254. The concentration of oil products was determined by IR-spectroscopy with preliminary extraction by chlorinated carbon.[1]

The investigations were carried out with different dyes in water (the initial concentration was 24 mg/dm^3) such as acid black, direct black and blue, dispersed black, blue and red. For modeling oil products, we used fuel oil F-100, which was dispersed in water by ultrasound with frequency 2200 Hz.

In order to increase the effectiveness of granular filter operation, the carbon-mineral sorbent (CMS) was used as separation media. This material has been obtained from waste products of percolation oil purification. Aluminum silicate sorbent with coke remains on the surface is formed after its rinsing from oil by ligroin. Soft temperature treatment of this material improved the CMS adsorption properties as the result of reactions of dehydrogenation, cyclization, and condensation. In this research, we used CMS, which has been obtained in ICCWC NASU by Yu.I. Tarasevich, V.M. Rudenko and by the research workers from Russia Z.A. Lityaeva, R.V. Alekseeva and M.M. Kuvaeva.[2] It was activated under 500 ºC. As the result a mixture of montmorillonite and palygorskite with coke in quantity 8.5 w% was obtained. CMS has a porous mineral matrix in which the internal and external surfaces are modified by carbon.

3. Results and Discussion

The adsorption isotherms for p–nitro-aniline solutions by activated and inactivated CMS are presented in Figure 1. As curve (2) shows, CMS adsorbs 0.13 mmol/g of p–nitro-aniline. The carbon layer in CMS represents 6 % of the total adsorbent weight. Taking into consideration that

mineral clays do not adsorb p–nitro-aniline the capacity of the carbon layer is 2 mmol/g.

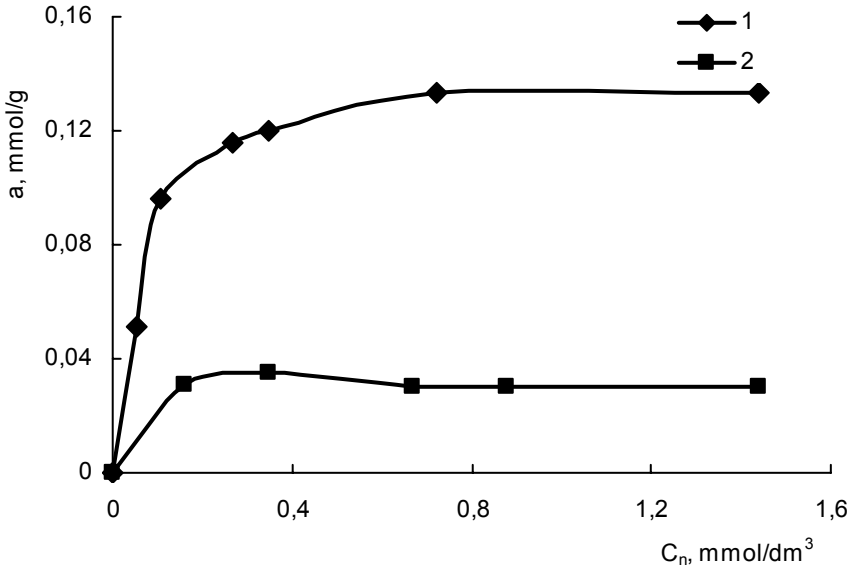

Figure 1. Adsorption isotherms of p–nitro-aniline from aqueous solutions on CMS (1) and spent montmorillonite – palygorskite clay (2).

There are adsorption centers of organic as well as mineral components in CMS. Carbon clusters modify the surface of minerals and have acid as well as basic centers so the range of adsorbed substances increases. Besides acid and basic properties as well as attachment of organic compounds to CMS by ion exchange mechanism, they can interact on chemical sorption mechanism forming donor-acceptor binds. As a result of high temperature activation, the clusters of carbon layer in large mesopores of the mineral matrix are getting their own micro porosity; due to this fact, their high adsorption capacity close to that of the KAD charcoal can be explained.[2] Such properties of CMS allow to remove organic contaminations in ion-soluble as well as in colloid state (Figure 2). As it is shown, the adsorption of humus substances, which cause strong color of water, on CMS (curve 1) increases 2 – 6 times in comparison with quartz sand (curve 2).

The advantage of using CMS in dynamics due to thin carbon layer on large surface of mineral matrix is connected with the possibility of full exhausting for carbon layer. Technological investigations have been carried out where CMS is used as filtration material in rapid filters with highly developed surface of granular and large inter granular porosity. Full saturation of CMS filter is 2 times longer than for quartz sand one. Therefore, CMS provides high capturing ability and increasing duration of

protective action of the granular filter. Filter operation increases 1.3 times along with better quality of the filtrate (20 - 40%) in comparison with sand.

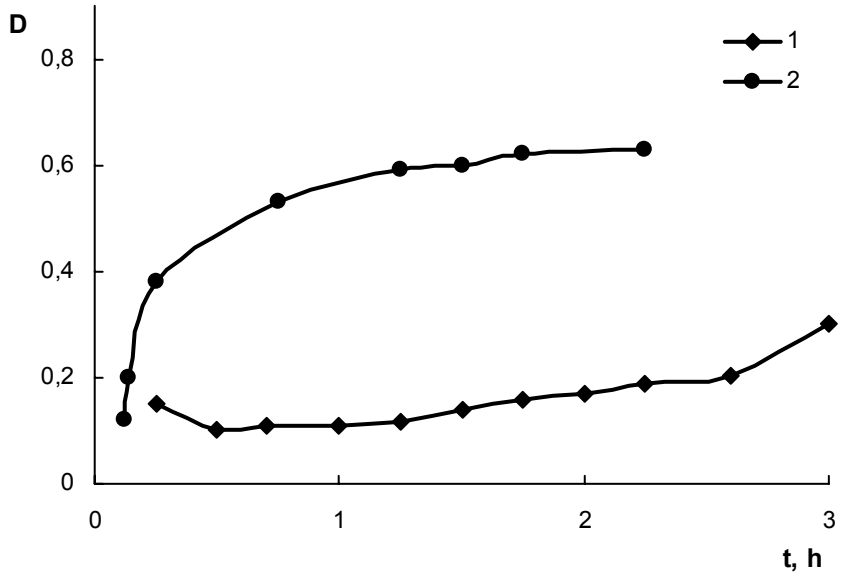

Figure 2. Dynamics of strong color water treatment by filtration through granular CMS filter (1) and quartz sand one (2).

Some technological experiments were carried out for water with emulated and soluble oil products. We used multistage filtration through three filters connected in series with different granular materials. It is evident that the granular material with the highest adsorption properties should be used on the final stage after preliminary filtration through traditional granular material (quartz sand). The preliminary stage can clarify from suspended particles the finishing stage should provide removing of soluble impurities. Initial concentration of oil products in water is 25 mg/dm^3. This laboratory unit of multistage filters with shallow beds (from 0.1 to 0.25 m) can provide a degree of water treatment up to 98 %. According to the quality of filtrate, granular CMS approaches activated carbon AC-3 and has essential advantages compared to coke or anthracite. The filter with CMS operates 1.3 –1.8 times longer than the filter with coke and anthracite.

Mineral oil capacity for different materials was determined; for AC-3 its value is 0.8, for CMS – 0.55, for anthracite – 0.2, for quartz sand – 0.06 g/g. Therefore, it is evident that the adsorption properties of CMS are slightly lower than those of AC-3 and much higher than those of the other granular materials.

In water treatment technology, macro porous sediments as contact up-flow flock blanket of clarifiers are often used. The regulation of their adsorption properties is accomplished by injecting aids for modification purposes.

During our investigations for separation impurities in up-flow solids-contact clarifier, using the sediment of magnesium hydroxide without any modification causes increasing adsorption degree in the following dyes sequence: acid (soluble), direct, dispersed ones. Due to modification of the surface of magnesium hydroxide by two-valence iron ions, the degree of water treatment from organic impurities can increase from 90% up to 99 %. The effectiveness of water treatment from dispersed and acid dyes by magnesium hydroxide (concentration 3 meq/L) modified by different concentrations of iron salts is presented in Fig. 3.

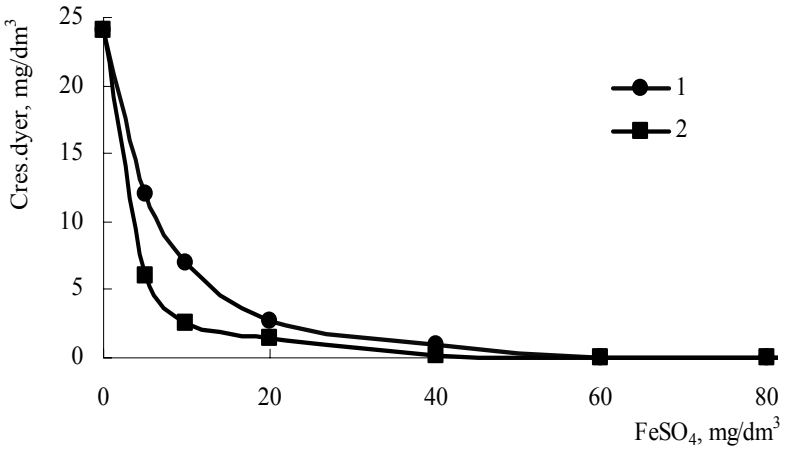

Figure 3. Correlation between the residual concentration of dyes and concentration of $FeSO_4$ upon pH=11, $MgCl_2$ and NaOH 3 meq/L: 1 – for acid black dye, 2 – for dispersed red dye.

The increase of the water treatment degree by iron hydroxide is impossible because the insoluble iron complexes do not form under pH 11. Under this pH as the result of magnesium salts hydrolysis and polymerization, the structures of polynuclear complexes with iron ions in adsorption layer are formed. The last ones have high coordination number (6) in comparison with magnesium ions (4) so they are able to orient and keep a number of organic molecules in polynuclear complexes. The suggestion of such magnesium hydroxide layer structure for adsorption is based on chemical analyzes as well as spectra of electronic paramagnetic resonance. In spectra of acid black dye with $FeSO_4$ the signal in the range of g–2 is absent but in sediments its value increases 10 times. About transition of Fe^{2+} ions into Fe^{3+} we can conclude from intensity of g–2 signal EPR spectra.

Similarly to the acid black the dispersed red dye adsorbs on the surface of sediments following an ion exchange mechanism. The firmness of its attachment to the adsorption layer increases due to forming of chelate cycles.[3]

It is recognized that adsorption of organic compounds as well as the degree of their removing from water increases with the rising of oxygen-bearing functional groups in their structure. During the adsorption of dispersed dyes, the above-mentioned effects are enhanced for such of them which attach to the polynuclear molecules of hydroxide by forming chelate cycles. Such effects are observed not only for dyes but for humic substances too. Interactions between humic substances and hydro complexes of iron and magnesium take place not only due to electrostatic attraction but also to ligand exchange.[4] Due to fulvic acid molecular mass (if steric factor does not balk) they also form ion chelate cycles with the above mentioned metal.

4. Conclusions

Adsorption and filtration are highly effective and ecological safe technologies that are widely used in water treatment and sewage purification. It is an urgent task to intensify these technologies by using new materials and reagents as well as by their modification.

It has been shown that modification of the contact surfaces gives essential increasing degree of adsorption from aqueous solutions during removing organic compounds in ion-soluble and colloid state (humic, acid dyes), in suspended and emulated state (oil products), and highly dispersed ones (dispersed dyes).

A second utilization of exhausted natural mineral clays after oil percolation and catalysis cracking mineral oil as well as sewage water purification gives high economical and ecological effect.

REFERENCES

1. G.A. Roef, and V.A. Yufin, *Sewage water purification and second utilization of oil products* (Resources, Moscow, 1987).
2. Yu.I. Tarasevich, *Natural sorbents in processes of water treatment* (Naukova dumka, Kiev, 1981).
3. V.V. Lukachina, *Ligand-ligand interactions and stability of different ligand complexes* (Naukova dumka, Kiev, 1988).
4. Yu.I. Tarasevich. Mechanism of interaction for humic acids with laminated silicates and coagulants, *Khimiya i technologiya vodu* **2** (4), 297-303 (1980).

PROPERTIES OF COMBINED SORBENT - "ZEOLITE IN FIBER"

V.A. NIKASHINA*, G.V. MYASOEDOVA,
E.V. KULBACHEVSKAYA, E.M. KATS
Vernadsky Institute of Geochemistry and Analytical Chemistry RAS, Kosygin str. 19, Moscow, Russia

V.L. TZIPERMAN, R.K. IDIATULOV
Institute of Synthetic Fiber, Moscow shosse 157, Tver 170032, Russia

Abstract. To employ the pulverized zeolites in dynamic conditions it was obtained the composite material - polyacrylonitrile fiber filled by natural zeolite powder - clinoptilolite-bearing tuff according to earlier developed methods. The ion-exchange and adsorption properties of the new combined sorbent, "zeolite in fiber", on the examples of sorption of Cu^{2+} from 0.5 N NaCl and of oil products from the waste water of car-washing stations, were studied. The distribution coefficients and diffusion coefficients of Cu^{2+} and the distribution coefficients of oil products on the sorbent were determined. It was shown that the ion-exchange rate of Cu^{2+} ions for the new sorbent increased considerably. The filtrating properties are very good. The sorbent is characterized by high selectivity to the oil products.

Keywords: pulverized zeolite; polyacrylonitrile; fiber; ion-exchange; adsorption; oil products of car-washing station; distribution coefficients; kinetics

1. Introduction

The clinoptilolite-containing tuff [CT] is used usually in the form of ground sorbent with grain size of 0.25-2.0 mm. Ion exchange process on these zeolites is characterized by slow kinetics. The pulverized fraction of zeolite can

* To whom correspondence should be addressed. V.A. Nikashina, Vernadsky Institute of Geochemistry and Analytical Chemistry RAS, Kosygin str.19, Moscow119991, Russia; e-mail: nikashina@geokhi.ru

J.M. Loureiro and M.T. Kartel (eds.), Combined and Hybrid Adsorbents, 213–217.

not be used in dynamic conditions. To employ the pulverized zeolites in dynamic conditions a composite material, polyacrylonitrile fiber (PAN) filled by pulverized zeolite according to the previously developed methods was obtained.[1-2] The ion-exchange and adsorption properties of the obtained combined fibrous sorbent based on CT and PAN are investigated in this work.

2. Materials and Methods

A pulverized CT from Shivirtuyiskoye deposit (Russia) of known composition with particles of 20-40 μm in size was used for producing combined fibrous sorbent - CT-PAN. The content of CT in PAN-fiber is 50% (sample 1) and 70% (sample 2). The cation-exchange capacity of the CT-PAN was determined for NH_4^+ ions according to the method described elsewhere.[3] The composition of the investigated solution was as follows: 6-30 mg/L of Cu^{2+} + 0.5 N NaCl, at pH=6. The sorption isotherm of Cu^{2+} ions on the CT-PAN was obtained from this solution. The ion-exchange kinetics of Cu^{2+} ions on this sorbent was studied by the "thin layer"[4] method. Breakthrough curves of Cu^{2+} were obtained for several solution flow rates and CT-PAN bed depths. The adsorption properties were investigated in static conditions on the example of oil products adsorption from car-washing station waste waters. The total organic content (TOC) in water was determined by a method using a solid-electrolyte analyzer described elsewhere.[5]

3. Results and Discussion

3.1. ION-EXCHANGE PROPERTIES

3.1.1. *Cation-exchange capacity and equilibrium characteristics of Cu^{2+} sorption on CT-PAN*

It was established that the total cation exchange capacity of CT-PAN (at 50% of CT) is 0.78 meq/g, and the total cation exchange capacity of CT-PAN (at 70% of CT) is 1.23 meq/g. The total cation-exchange capacity of initial CT was 1.60 meq/g. The sorption isotherm of Cu^{2+} by CT-PAN from a 0.5 N NaCl solution is presented in the Figure 1.

As shown in Figure 1, the ion-exchange sorption of Cu^{2+} by CT-PAN from 0.5 N NaCl is described by a convex isotherm, and the linear section of the

isotherm is characterized by a distribution coefficient of 3-4x10^4 mL/g. The maximum equilibrium capacity for Cu^{2+} from 0.5 N NaCl at pH=6 on CT-PAN (at 50% of CT) was 21-23 mg/g.

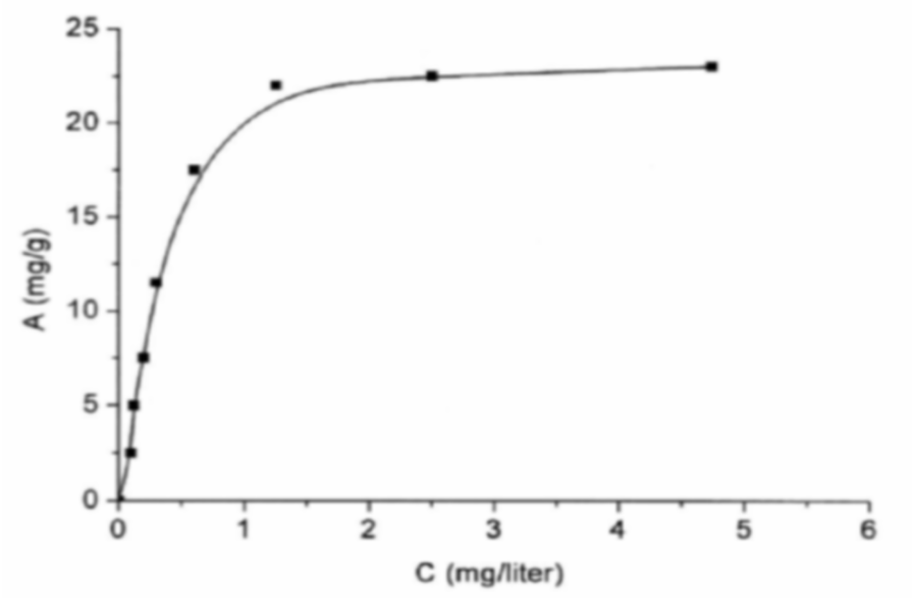

Figure 1. Sorption isotherm of Cu^{2+} from 0.5 N NaCl on CT-PAN (at 50% CT). Experimental conditions: contact time = 8 days, V/m = 500.

3.1.2. *Kinetic characteristics of Cu^{2+} sorption on CT-PAN*

The comparative kinetic dependences of Cu^{2+} ion-exchange for the CT-PAN and for the CT with grain size of 0.25-0.50 mm from 0.5 N NaCl are presented in Figure 2.

As shown in Figure 2, the Cu^{2+} ion-exchange rate for CT-PAN is increased approximately 30 times in comparison with ground CT with grain size 0.25-0.5 mm. The particle diffusion coefficient of Cu^{2+} ions for CT-PAN calculated from obtained experimental data was 2.8x$10^{-12}$$cm^2$/s. The obtained equilibrium distribution and kinetic coefficients make possible to select the corresponding mathematical model of ion-exchange process and to calculate the breakthrough curves of Cu for CT-PAN[6] depending on the solution flow rate, the bed depth, etc.

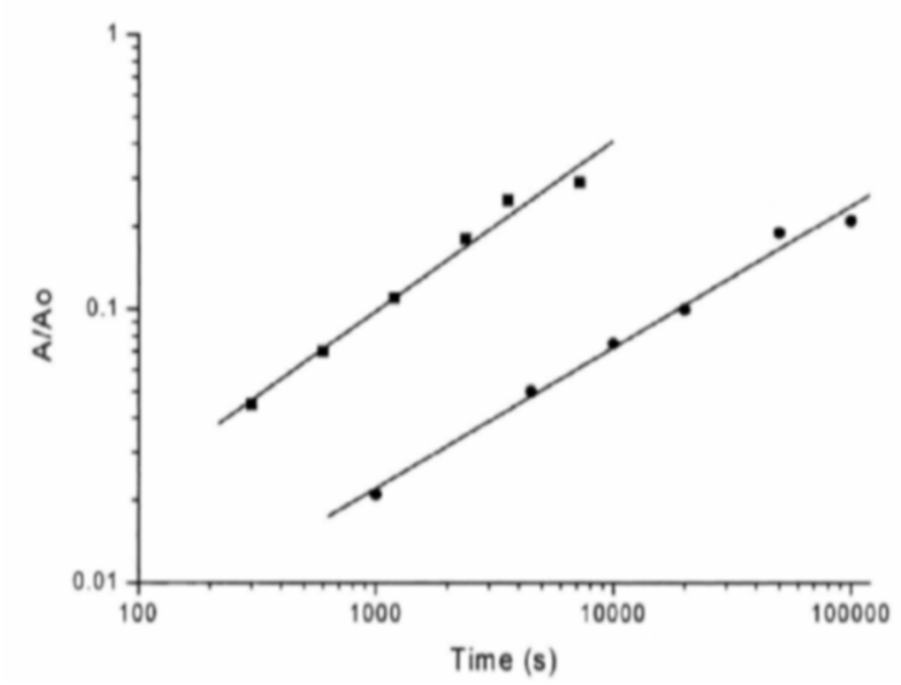

Figure 2. Sorption of Cu^{2+} (A/Ao) by CT-PAN (■-■) and CT (●-●) *vs.* time.

3.2. ADSORPTION PROPERTIES OF CT-PAN

The adsorption properties of CT-PAN in respect to oil products contained in the waste water of car-washing stations were estimated previously in the static experiments as distribution coefficients. For comparison, in Table 1 the distribution coefficients for an active carbon and a natural zeolite are also presented.

TABLE 1. Distribution coefficients of oil products from car washing stations waste waters for CT-PAN, active carbon, and a natural zeolite (TOC data)*

Sorbent	Light organic matter	Heavy organic matter	Total organic matter
CT-PAN	1400	2300	1870
CT-natural	45	250	130
Active carbon	200	700	400

* Experimental conditions: V/m=800, t=1.5 days. Oil products concentration in initial waste water is 78 mg/L.

As shown in Table 1, the distribution coefficient of the light organic matter for CT-PAN was 1400 and of the heavy organic matter was 2300, while for an active carbon the distribution coefficients were only 200 and 700, respectively.

4. Conclusions

The new fiber sorbent is characterized by a very satisfactory ion-exchange capacity (from 0.78 to 1.23 meq/g).

The rate of ion-exchange process for CT-PAN increased approximately 30-fold in comparison with zeolite with grain size 0.25-0.50 mm.

The high selectivity of CT-PAN to oil products of car-washing stations waste waters is demonstrated.

REFERENCES

1. M.S. Mezhirov, A.S. Chegolya, R.K. Idiatulov, A.N. Phedorova, O.I. Baranova, and N.V. Rodina, in: *3th Inter. Symposium on the Chemical Fibres, Tver,* 1981, V.5 (1981) pp. 13-20 (in Russian).
2. M.S. Mezhirov, R.K. Idiatulov, I.F. Babich, and A.S. Chegolya, in: *4th Inter. Symposium on the Chemical Fibres, Tver,* 1986, V.3 (1986), pp. 304-308 (in Russian).
3. V.I. Bogdanova, I.A. Belitskii, L.M. Predeina, G.I. Galay, and I.B. Drobot, *Cation-exchange capacity determination of zeolite-containing rock by absorbed ammonium*, Instruction N 24 (Inst. Miner. Petrogr. of Siberian Department of Russian Academy of Sciences, Novosibirsk, 1993), pp. 18 (in Russian).
4. G.E. Boyd, A.W. Adamson, and L.S. Meyers, The exchange adsorption of ions from aqueous solutions by organic zeolites. 2. Kinetics, *J. Am. Chem. Soc.* 69, 2836-2848 (1947).
5. B.K. Zuev, E.V. Kulbachevskaya, and O.K. Timonina, Analytical possibilities of a solid - electrolyte analyzer for the determination of the total organic content in water, *J. Anal. Chem*. 54(1), 81-84, (1999).
6. V.A. Nikashina, N.K. Galkina, and M.M. Senyavin, The Calculating of the Sorption of Metals by Ion-Exchange Filter, Russian Institute of Scientific and Technical Information, Moscow, Article No. 3668, 1977, 44 pp. (in Russian).

ENHANCEMENT OF ADSORPTION CAPACITY BY USE OF PHASE CHANGE MATERIAL (PCM) AS ADDITIVE IN AN ACTIVATED CARBON (AC) FIXED BED ADSORBER

W. ZIMMERMANN* AND J.U. KELLER
Institute of Fluid- und Thermodynamics, University of Siegen, 57068 Siegen, Germany

Abstract. To avoid emission of volatile hydrocarbons from automotive tank systems, canisters filled with activated carbon (AC) are placed as a buffer to the environment. During the loading of the filter the heat of adsorption released leads to a temperature rise of the AC and hence to an unwanted decrease of storage capacity. By mixing an optimized amount of phase change material (PCM) to the AC the heat effect can be diminished and thus the adsorption capacity of the filter compared with a fixed bed consisting of pure AC increased by more than 15%. Also, the desorption process is enhanced by the PCM, as part of the desorption energy is provided by the latent heat stored in it. The differential and integral heats for n-butane adsorption on activated carbon have been determined by use of a novel sensor gas calorimeter.[1] In knowledge of the data, an optimized amount of PCM to be added to the carbon could be specified. Both, effectiveness of PCM addition as well as the most appropriate melting, i. e. phase changing temperature of the PCM have been investigated in a special testing equipment by systematic experimental work.

Keywords: gasoline vapor; hydrocarbon retention; activated carbon; fixed bed adsorber; heat of adsorption; fuel tank; storage capacity

* To whom correspondence should be addressed: Dr. Wolfgang Zimmermann, Institute of Fluid- and Thermodynamics, University of Siegen, Paul-Bonatz-Strasse 9-11, 57068 Siegen, Germany; e-mail: zimmermann@ift.maschinenbau.uni-siegen.de

J.M. Loureiro and M.T. Kartel (eds.), Combined and Hybrid Adsorbents, 219–224.

1. Introduction

Adsorption filters are widely used for environmental protection by retention of harmful gases or vapors released in technical processes. One example of application is the use of activated carbon (AC) filled canisters to adsorb volatile fuel components evaporated in the tank vessels of cars driven by combustion engines.

The total adsorption capacity of these vessels depends on the canister volume and the adsorbent material used for the fixed bed adsorption process. Since it is important to adjust the adsorption capacity to many different types of cars, the canisters usually are tested using n-butane as a representative substitute for the volatile fuel. Such charging experiments mainly yield the n-butane working capacity (bwc) as a result. The bwc-value is the total amount of n-butane that can be adsorbed by a given fixed bed volume until break through effects occur. The bwc is normally somewhat lower than the gasoline working capacity (gwc) but easily allows evaluation and comparison of the performance of different types of AC-canisters when used as buffers in car tanks.

2. Basics

Volatile hydrocarbons being emitted from a car tank can be adsorbed in the pores of an AC-filter. Since adsorption is an exothermic process, the filter may be heated up to 90 °C or more by the heat of adsorption released. The amount of gas that can be adsorbed decreases with temperature. Thus the temperature rise will lead to a decrease in adsorption capacity of the filter which may come up to more than 50 % of the filter's capacity so that the filter needs to be oversized. A crucial situation may occur during refilling of the car's tank. Then the volatile hydrocarbon/air mixture above the surface of the remnant liquid/gas in the tank is replaced by the incoming liquid fuel. Hence, a considerable amount of volatile hydrocarbons has to be adsorbed completely by the AC. To avoid break-through effects of hydrocarbons to the environment and also simultaneously to increase the storage capacity of the filter and/or decrease its weight and size, microencapsulated paraffin was added to the AC to store part of the heat of adsorption as latent heat in the paraffin acting as a phase change material (PCM).

Under normal conditions, the PCM incorporated in the microcapsules is a solid material with a melting temperature just above ambient temperature. When adsorption takes place and the temperature of the filter increases, the PCM melts and hence most of the heat of adsorption is stored as latent heat. During the unloading cycle of the filter by exposing it to a flow of "dry" air,

which after loading with the prior adsorbed hydrocarbons is now sent to the combustion engine, the temperature of the filter decreases since the desorption process is endothermic. This temperature drop causes solidification of the paraffin in the PCM material as the heat stored during adsorption is now released to the AC and the air flow again.

3. Experimental

To examine the effect of PCM addition to the temperature and the adsorption capacity of the AC-fixed bed, a testing device has been designed. The main part of this device is a commercially used AC-canister, equipped with 13 KTY-temperature sensors on various positions (Figure 1).

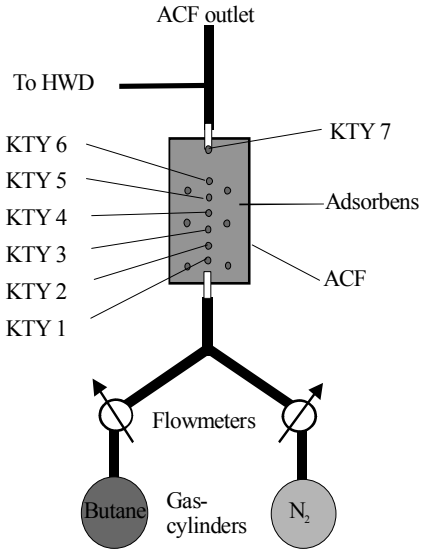

Figure 1. Sketch of the testing device used for activated carbon filter (ACF) performance enhancement.

A gas supply system is connected to the canister feeding it with a mixture of nitrogen and n-butane, both 50% in volume. By switching of the solenoid-valves (not shown in Figure 1), the gas flow can be reversed and thus the canister can be discharged by purging it with dry air. The mass-flow of the gases is adjusted by means of two flow meters, one for the nitrogen and one for the n-butane. At the canister's exit, the leaving gas stream is divided into two parts and the minor flow is leaded into a Hot Wire Detector (HWD) for break through analyses. Supplementary information is given by a balance, on which the canister is placed, recording the weight change caused by ad- or desorption of n-butane. All sensors and

valves are connected to and controlled by a computer. Hence the testing cycle is automated by use of specially developed computer software based on the LabVIEW programming language.

Prior to the determination of the bwc-value, the contents of the canister, i.e. AC and gas have to be conditioned. This is done applying a certain testing cycle several times. This cycle is as follows: first of all, pure AC or the AC/PCM mixture is filled into the canister. After that, the canister is charged by feeding it with the n-butane/nitrogen mixture first and then purging it with dry air. In average, a weight increase of roughly 5% can be stated for the purged canister after 4 – 5 testing cycles.

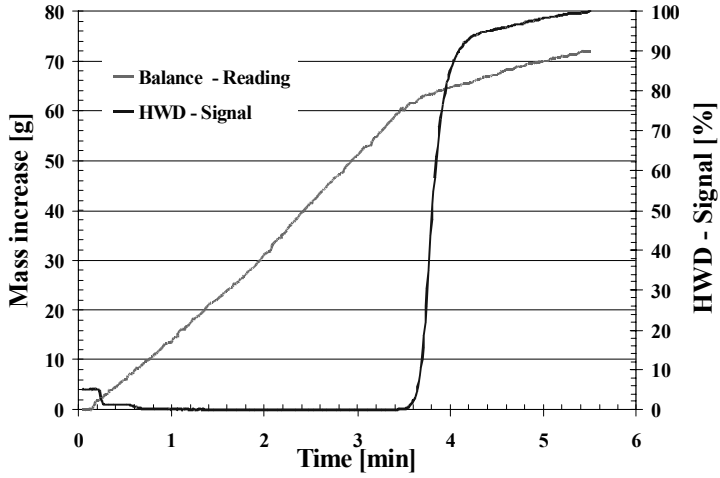

Figure 2. HWD - signal and mass increase for the charging process of a pure carbon filled ACF fed with 1000 g/h n-butane and 50 Vol.-% nitrogen gas flow.

This is caused by the amount of n-butane that is adsorbed irreversibly in the micropores of the clean AC and which can not be removed just by purging the canister with air at ambient conditions. Additionally, the temperatures measured by the KTY-sensors are the highest for the first cycle since the heat of adsorption released is somewhat higher for the clean AC.

When the canister has been conditioned, the bwc-value can be determined by a final charging of the canister with the n-butane/nitrogen mixture. The recorded HWD- curve and the balance signal (Figure 2) have to be evaluated afterwards. The mass uptake of the filter for an increase of the HWD signal line up to 5% is defined as bwc-value. Additionally to the HWD and the balance signal, the temperature curves of the KTY sensors are monitored and recorded by the computer (Figure 3).

From these curves the decrease of the maximum temperatures caused by the addition of PCM to the AC in the fixed bed can be seen. Comparison of

the bwc-value and measured temperatures also reveals, that the adsorption capacity is high when the temperatures are low and vice versa.

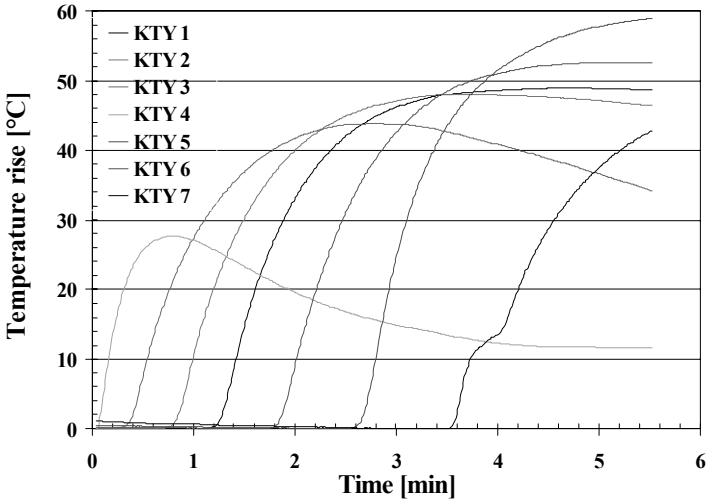

Figure 3. Temperature curves monitored for the canister filled with pure carbon.

4. Results

As a result, the adsorption capacity of the canister tested could be increased by more than 15% due to the addition of PCM to the fixed bed. Careful investigation of the measured curves during desorption also revealed, that the purging time for the filter was reduced by 20% and relative temperature changes during loading and unloading by 10% - 15% respectively.

During the experiments, the AC of the canister fixed bed has been replaced by more and more PCM to find out the optimum AC/PCM ratio. It could be seen, that with increasing amount of PCM the maximum temperatures decreased and the adsorption capacities increased up to a maximum. If more PCM was added to the fixed bed, the temperatures still decreased, but also the adsorption capacity. Now the increase in bwc caused by the temperature decrease of the fixed bed is overbalanced by the reduction of AC, which means a loss of adsorptive material.

Fixed bed charge	bwc	Maximum temperature
Pure AC	66,2 g	85,1 °C
AC + 25 wt-% PCM	77,5 g	65,8 °C

5. Outlook

In today's adsorption canisters the PCM is added as pelletized material to the AC pellet, hence the fixed bed of the ACF does not contain a real hybrid material but a physical mixture of AC and PCM pellets.

As experiments have shown that not only the heat capacity of the PCM is of importance, but also the transfer of heat from the AC to the PCM, it would be desirable in future developments to design a real hybrid material including a microscopic mixture of AC and PCM which would lead to optimized heat transfer properties, and thus an optimized kinetics of the gas adsorption – and desorption process.

REFERENCES

1. W. Zimmermann, and J.U. Keller, A new calorimeter for simultaneous measurement of isotherms and heats of adsorption, *Thermochim. Acta* 405, 31- 41 (2003).

THERMOCHEMICAL ACTIVATION OF LIGNINS FOR OBTAINING EFFECTIVE SORBENTS

GALINA DOBELE*, GALINA TELYSHEVA
Latvian State Institute of Wood Chemistry, 27 Dzerbenes Str.,LV-1006 Riga, Latvia

NIKOLAI BOGDANOVICH
Arkhangelsk State Wood Technology University, 17 Severnaja Dvina Str., 163002, Arkhangelsk, Russia

Abstract. It is found that the thermochemical activation of lignins, products of chemical wood processing, leads to the formation of carbon with a developed microporous structure. Active carbons with high adsorption properties and specific area over 2000 m^2/g were obtained. It has been shown that the decreasing oxygen content in the raw material by thermal pre-treatment is a decisive factor providing a lower consumption of activators, the improvement of sorption properties, and increasing the yield of carbon.

Keywords: Active carbon; pyrolysis; lignins; sodium hydroxide; porous structure; sorption activity

1. Introduction

At present, the consumption of active carbons tends to increase worldwide, and the fields of their application are expanding. The global capacities of active carbon production exceed 400 thousand ton per year. The share of wood active carbons makes up only 20-25% despite the possibility to vary their properties in a wide range. It is explained by the high cost of the raw

* To whom correspondence should be addressed. Galina Dobele, Latvian State Institute of Wood Chemistry, 27 Dzerbenes Str., LV-1006 Riga, Latvia; email: gdobele@edi.lv

J.M. Loureiro and M.T. Kartel (eds.), Combined and Hybrid Adsorbents, 225–230.

material, namely, wood raw coal. In this connection, searches for implementing novel technologies of pyrolysis, with the use of the waste of the chemical and mechanical processing of wood biomass, are under way.

The conventional gas-steam activation for obtaining wood-based active carbons makes it possible to obtain products with the specific surface area 700-900 m^2/g. The achievement of higher indices of the porous structure is connected with the decrease in the yield of active carbon.

The use of inorganic substances as activators of the oxidation process upon pyrolysis makes it possible to enhance the quality of the obtained sorbents, promotes the formation of a mesoporous structure, hampers the development of large pores and enables the regulation of the functional composition of the surface groups and the pore size distribution.

The efficiency of alkali metal hydroxides as chemical activators for obtaining carbon sorbents is proved on different carbon raw materials.[1,2]

Lignin, one of the main components of wood, being a polyaromatic polymer, forms, upon pyrolysis, a carbonized residue with a higher yield in comparison with the case of wood and carbohydrate components of wood, more perfect structure and less content of aliphatic fragments.

The aim of the present study was to investigate the possibilities of obtaining effective microporous sorbents on the basis of lignins, products of chemical processing of wood, by the method of thermochemical activation by sodium compounds.

2. Experimental

***Material*:** sodium-based lignosulphonates, hydrolysis lignin.

Chemical activators: sodium sulphate, carbonate and hydroxide.

Thermal treatment: pre-treatment (pre-pyrolysis) - carbonization 100-400 ^oC, time 180 min; pyrolysis - activation - 600-700 ^oC, time 60 min.

Extraction of the mineral components of carbon: carbon obtained by pyrolysis was extracted with deionized water, 4 runs at the temperature 100 ^oC, modulus 1:10.

Porous structure: the isotherms of low-temperature adsorption of nitrogen were obtained on a Sorptometer KELVIN 1042 (COSTECH Instruments); degassing temperature 250 ^oC; adsorptive gas: nitrogen; carrier gas: helium.

Sorption activity: standard tests of the sorption of iodine (I_2), methylene blue (MB) and heptane.

3. Results

3.1. SODIUM-BASED TECHNICAL LIGNOSULPHONATES (LST)

The results obtained in the present study upon pyrolysis of oxidized lignosulphonates, formed as a waste in vanillin production, have shown that, in this case, no additional introduction of a gaseous activating agent is required; moreover, upon the introduction of water vapor, the sorption activity of carbons falls.[3] This is explained by the peculiarities of the composition of the mineral part of oxidized lignosulphonates, namely, sodium carbonate and sulphate (60-65% in terms of oven-dry LST), which act as chemical activators upon pyrolysis.

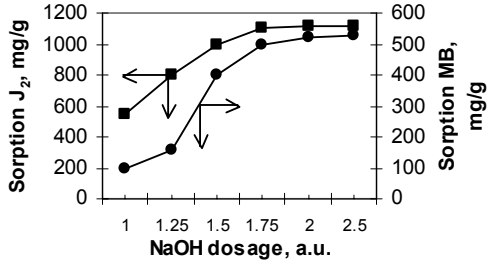

Figure 1. Effect of NaOH on the sorption activity of LST-based carbons relative to methylene blue (1) and iodine (2).

It was found that the active carbons obtained under optimum conditions of pyrolysis (700°C) on the basis of oxidized lignosulphonates and initial lignosulphonates with the addition of sodium salts, in the quantity equivalent to their content in oxidized LST, had practically equal indices: total specific porous structure (BET) - 1500 m^2/g, micropore volume 0.5 cm^3/g, mesopore volume 0.2 cm^3/g, which characterized them as effective sorbents.

The use of sodium hydroxide, which is more active in reaction with oxygen-containing groups of lignin than sodium salts, made it possible to decrease the pyrolysis temperature by 100 °C and enabled the formation of a developed porous surface of carbon and high indices of sorption properties (Fig. 1).

The main components of the mineral substances extracted from the obtained carbon are sodium carbonate and hydroxide (Fig. 2). The quantity of the sulphur-containing sodium compounds is negligible, namely, 2% (in terms of oven-dry LST). The results show that, with increasing quantity of the added alkali, the quantity of the extracted sodium hydroxide grows, with a negligible increase in carbonate. Obviously, it indicates the presence

of definite stoichiometric ratios between the quantity of alkali and the content of reactive sites of lignins. The calculations have shown that practically the whole oxygen present in LST in the chemically bonded state participates in the formation of sodium carbonate.

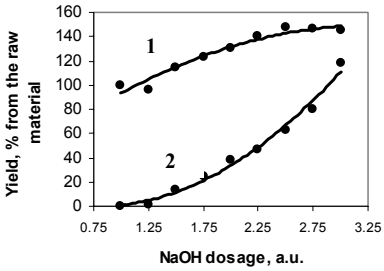

Figure 2. Effect of NaOH dosage on the quantities of sodium carbonate (1) and NaOH (2) extracted from carbon.

Besides that, the chinon-containing structures, both present in the isolated lignins and those formed under the action of alkali, can probably act as traps, as their anion radical form is stabilized by alkali metal ions. As a result of the development of polyconjugation regions, the distinctions between the donor-acceptor properties of the structural elements of lignin are enhanced, and the formation of intramolecular complexes with charge transfer becomes energetically profitable. The presence of intramolecular complexes in the lignin, alkaline treated at temperatures above 300 ^{o}C, is confirmed by ESR-spectroscopy data.[4]

Simultaneously with these reactions, the auto-oxidation process is progressing, and the high-rate formation of gaseous products results in the chemical dispersion of the carbon, its swelling-up and pore formation. Probably, the given mechanism is not the only one according to which the interaction of alkali and lignin is realized. However, it can serve as a tool enabling, taking into account the presence of oxygen in lignin and controlling the quantity of sodium hydroxide and carbonate in aqueous extracts, to regulate the quantity of the added alkali, necessary for obtaining the designed structure of the sorbent.

To verify this suggestion, pre-pyrolysis in the temperature range 100-400 ^{o}C was carried out, which, owing to the decrease in the quantity of oxygen-containing groups in lignin, must favor the decrease in the alkali consumption. At these temperatures, degradation reactions proceed dramatically, and the concentration of elemental carbon occurs. The subsequent pyrolysis – activation of the obtained material in the presence of sodium hydroxide resulted in a considerable growth in the yield of active carbon in terms of the LST organic matter. The highest yield of active

carbon was obtained in the case of using for alkali activation the residue pre-treated in the temperature range 200-300 °C (Fig. 3).

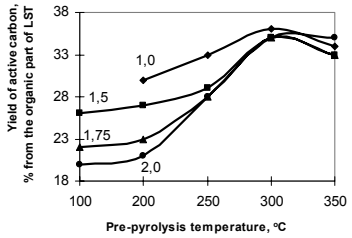

Figure 3. Yield of active carbon on the basis of the carbonized material in the process of thermochemical activation, depending on NaOH dosage.

The pre-pyrolysis temperature 200 °C is enough for the formation of a developed porous structure upon the following pyrolysis (600 °C) of carbonizate. In these conditions, the maximum adsorption of heptane, iodine and methylene blue reaches 1500, 1700 and 600 mg/g, respectively, at the NaOH dosage equal to 2.0 arbitrary units (a.u.).

The change in the pre-treatment temperature makes it possible to vary the bulk density of the obtained carbons. "Heavy" dense charcoal is commonly used for treating liquid media. The highest bulk density of charcoal, namely, 350-450 g/dm^3 was obtained when pre-treatment was performed at 300-400 °C.

"Light" dense sorbents are necessary for obtaining some catalysts as well as spraying disperse carbon. The smallest bulk density of carbon, namely, 150-200 g/dm^3 was obtained when pre-pyrolysis was performed at 100-250 °C.

3.2. HYDROLYSIS LIGNIN

Hydrolysis lignin is a waste of the wood chemical processing aimed at obtaining ethanol and other products of destruction of wood polysaccharides. In contrast to the lignosulphanates formed in the cellulose manufacture, a considerable share of non-hydrolyzed carbohydrates is present in the composition of hydrolysis lignin.

Similarly to the thermal processing of LST described above, pre-pyrolysis of hydrolysis lignin made it possible to decrease oxygen content in the samples from 40.5% for initial lignin to 29.9% and 21.2% for carbonizates obtained at 300 and 400 °C.

The results listed in Table 1 show that the subsequent thermal activation with sodium hydroxide gives active carbons with a highly developed porous surface, namely, above 2000 m^2/g. The regularities of the formation of the

porous structure of active carbons on the basis of hydrolysis lignin and lignosulphonates are similar.

The variation in the pre-pyrolysis temperature and the quantity of the chemical activator makes it possible to obtain active carbons with an equal micropore volume, but with different mesopore volumes. Micropores are represented mainly by super-micropores with a radius of 1.2-1.6 nm. This parameter is the most important one in practice in the case of sorption from solutions. The possibility to regulate the volume of sorbing pores is an important factor in the case of obtaining high-selectivity sorbents.

TABLE 1. Conditions for obtaining of hydrolysis lignin active carbon and characteristics of its porous structure

Pre-pyrolysis temperature, ^oC	Activation temperature, ^oC	Alkali consumption (arbitrary units)	Carbon yield, % from organic substances	Specific surface area, m^2/g	Micro-pores volume, cm^3/g	Meso-pores volume, cm^3/g
400	650	1.7	28.6	2150	1.18	0.01
400	600	1.7	31.2	2070	1.09	0.02
300	650	2.0	20.9	2000	0.97	0.37
300	600	2.0	23.8	2030	0.96	0.41

High-efficient sorbents on the basis of wood were obtained by similar methods, applying pre-pyrolysis and activation by sodium hydroxide.

Thus, it has been shown that sodium hydroxide and salts are effective chemical activators of the thermal transformation of the organic raw material into active carbon. Thermal pre-treatment (pre-pyrolysis) is an effective technique for decrease in the alkaline activators consumption, regulation of the porous structure, pore size distribution and increasing the yield of active carbon.

REFERENCES

1. Patent N 3525961, Japan.
2. Patent N 4937223, USA.
3. Dobele G., Bogdanovich N., et al. Obtaining of carbon sorbents on the basis of oxidized lignosulphonates. In: Proc. 10th European Conference “Biomass for Energy and Industry”, Ed. H.Kopetz, T.Weber, W.Palz, 1998, Wurzburg, Germany, 753-758.
4. Dizhbite T., Telysheva G. ESR application for characterisation of alteration of lignocellulosic matrix structure. In: Proc. 8th International Symposium on Wood and Pulping Chemistry, 1995, Helsinki, Finland, vol. 3, 115-118.

AN OPPORTUNITY FOR REDUCTION OF THE INFLUENCE OF DIFFUSION RESISTANCE WHEN CARRYING OUT CATALYTIC AND ADSORPTION PROCESSES BY USING POROUS WALL TUBES MADE OF ACTIVATED CARBON

LJUTZKAN LJUTZKANOV* AND NIKOLAI KOLEV
Institute of Chemical Engineering, BAS, Acad. G. Bonchev St. 1113 Sofia, BULGARIA

Abstract. A solution has been proposed for eliminating the diffusion resistance by proper structuring of the activated carbon used as catalyst support or as adsorbent. A structured carbon has been obtained in the form of tubes corked from one side. The fluid flow from the space outside the tubes passes through the pores of the pipe walls, enters the tubes and goes out from their openings in the free cross section. If it contains absorbable components, after passing through the tube wall it goes out purified from them. If the activated carbon holds a catalyst, a chemical reaction between the components of the fluid flow on the surface of the catalyst is carried out. Tubes of activated carbon with different adsorption properties have been obtained, the iodine adsorption capacity achieved by now is up to 1150 mg/g and the surface area achieved is up to 1200 m^2/g.

Keywords: diffusion resistance; catalyst support; activated carbon tube; catalysis; adsorption

1. Introduction

It is well known that an increase of a chemical reaction rate, i.e. the development of new and more active catalysts, leads to a process controlled

* To whom correspondence should be addressed; e-mail: ljutzkanov@ice.bas.bg

J.M. Loureiro and M.T. Kartel (eds.), Combined and Hybrid Adsorbents, 231–236.

by the rate of diffusion into pores. In order to reduce the diffusion resistance, ground catalysts are usually used, however they increase pressure drop of the catalyst layer, also channeling and catalyst blowing out takes place.

Recently, the research efforts in developing highly active catalysts on active carbon supports gave very good results in various processes.[1,2]

The aim of the present work is to offer a solution to the problem of eliminating the diffusion resistance by means of appropriate structuring of the active carbon - catalyst support. This new structured active carbon can also be used for designing adsorption apparatuses.

2. Main Ideas for Development of the New Reactor

Let us imagine that it is possible to construct a pipe with thick walls made of porous active carbon sealed up in its upper end. Let us also imagine that a number of such pipes are connected with a pipe grid as it is shown in Figure 1. Let us suppose that the fluid stream enters from the outer part of the pipes 3, mounted to the grid 2, located in the bulk 1. Due to the pipe wall porosity, the stream will pass through them, will enter the pipes lumen and will leave into the apparatus void section. If the stream contains components that can be adsorbed on the active carbon, by passing through the pipe wall it will be purified. If a catalyst, suitable for carrying out a chemical reaction between the gas stream components, is supported on the active carbon, at appropriate pressure and temperature, the desired chemical reaction will be accomplished on the catalyst surface. Moreover, due to gas transfer through the transport pores of the material, that are of micron dimensions, the way passed by the molecules, according to a purely diffusion mechanism, to the corresponding capillary walls where the process takes place, will be similar to the capillary dimensions at both a chemical reaction and adsorption. This way is many orders of magnitude smaller than the way, which would be passed at diffusion into granules of the catalyst, or the adsorbent respectively. This means a simultaneous significant reduction of the corresponding diffusion resistance that will be practically eliminated.

The advantages of the new solution are: the fact that the free volume will be only about 20.8 %; there is a possibility for initial electric heating of the catalyst when carrying out exothermic processes; a constant catalyst temperature is maintained when carrying out endothermic processes; the adsorbent is regenerated with eliminating the steam and condensation stages; furthermore, the problems associated with polluted water, obtained at condensing vapor used for regeneration are avoided; the installation technological scheme is simplified and the time required for the

regeneration process is significantly reduced; due to the high heat conductivity of carbon and the small geometric dimensions of the pores of the catalyst of this type, it will be able to operate practically at isothermal regime during the catalytic process; in case of exothermic processes the temperature of the gas entering the pipe volume can be significantly lower than the temperature needed to carry out the desired chemical reaction; the reactor proposed allows a significant reduction of the heat transfer surface in the apparatus, which is especially important for carrying out high pressure processes; the elimination of the diffusion resistance gives a possibility to carry out a practically instantaneous adsorption process.

The only prerequisite for achieving the advantages of the new apparatus is to synthesize active carbon that allows a flow through the pipe wall at admissible value of the pressure drop.

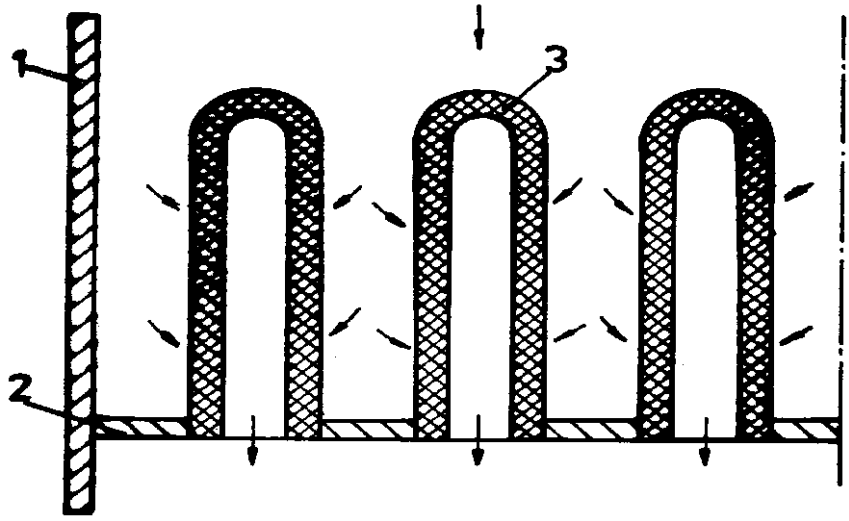

Figure 1. A view of a contact apparatus: 1. Shell; 2. Tube grid; 3. Active carbon tube**.**

3. Experimental

The aim of the experimental work is to study the possibility of developing active carbon with an appropriate geometry that allows a fluid stream passage across its wall capillaries under a sufficiently low pressure drop for practical purposes. It is well know[3-5] that pure highly active carbon can be obtained by gas-steam activation of thermo reactive resins. The opportunity to form a preliminary given geometry makes these materials especially suitable for our purpose.

The investigated activated carbon pipes are prepared by pyrolysis of tubes formed from thermoreactive resin (epoxy, novolak phenol-formaldehyde and phenoplast-bakelite) with different fillings as wood meal and activated carbon. The composition and geometrical characteristics of the tubes before the pyrolysis are given in Table 1. In order to provide a uniform heating of the specimen during its forming, the gas-steam activation was carried out in a rotating tube located in a tubular cylinder furnace.[5,6] The pyrolysis has been carried out for 30 minutes at temperature up to 750°C to homogenize the temperature field and to accomplish the chemical processes. Flue gas containing 35 vol. % water vapor has been used as activating agent.

TABLE 1. Composition and geometrical characteristics of the obtained tubes before the treatment

Investigated materials	Compostion, weight parts of the initial materials	Initial length, mm	Initial diameter, mm	
		δ or H	Outer	Inner
A1	[a]ER 110+ [b]WM 100	8.0	28.0	10
B1	[c]NPR 100+ [d]AC 100	10.0	29.5	10
C1	[e]PB 100+ [b]WF 100+ [d]AC 100	7.3	29.5	10

[a]ER-epoxy resin; [b]WM-wood meal; [c]NPR-novolak phenol-formaldehyde resin; [d]AC- activated carbon; [e]PB - phenoplast-bakelite

The activated carbon tubes are put between the flanges and the gaskets as it is shown in Figure 2. First, the air from the atmosphere has been sucked through the wall of the tube by a vacuum pump. The flowrate has been measured by a rotameter and the pressure drop of the tubes by a differential manometer. The value of mass flowrate is calculated based on the values measured by the rotameter after introducing correction for the pressure. Second, the water is fed into the tube, passes through the wall and the volumes of water are measured at different columns.

A mathematical model has been proposed, describing their permeability in regards to contracting and non-contracting fluids. If the non-contracting fluid stream passes through a porous wall of a cylindrical tube, we can write:

$$K_w = \frac{2\pi\delta.\Delta P}{V\mu \ln(r_2/r_1)} \tag{1}$$

where Δp is the pressure drop of the material in Pa; V is the volumetric flowrate of the passed fluid in m^3/s, μ is the dynamic fluid viscosity in Pa.s, r is radius vector, r_1 and r_2 are inlet and outlet tube radii, respectively, and δ is the thickness of the ring in m.

When the pressure drop of the wall is comparable to the total pressure or when it is not small enough to neglect its influence on the gas density, the equation for the pressure drop in a porous medium in the case of a laminar flow can be written:

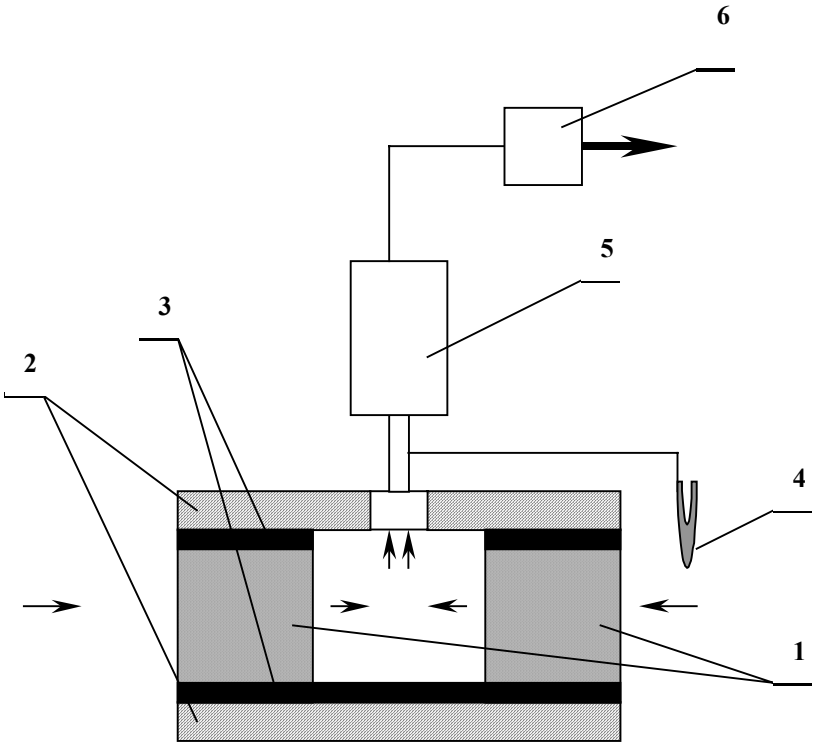

Figure 2. A device for mounting the material studied at determining its pressure drop: 1. Active carbon tube; 2. Flanges; 3. Rubber seals; 4. Manometer; 5. Rotameter; 6. Vacuum pump.

$$K_l = \frac{2\pi H \rho_0}{\mu G p_0 \ln(r_2/r_1)} \cdot \left(p_0^2 - p_1^2\right) \qquad (2)$$

G is the mass flowrate, kg/s; H – total length of the tube, m; r – radius vector, m.

Their permeability is relatively high at practically low pressure drop. The characteristics of the carbon tubes after thermal treatment and the experimentally obtained values of K_w and K_l are presented in Table 2.

Their permeability depends strongly on the initial materials as well as on the conditions of their formation. The values of the constants K_w and K_l,

which are of the order of 10^8 to 10^{13}, vary in the activation process course and become lower with increasing the iodine adsorption capacity that changes from 480 to 1150 mg/g with respect to their specific surface area increasing from 450 to 1200 m^2/g.

TABLE 2. Characteristics of the activated carbon tubes

materials	Radius of the pipes, mm			Yield	Adsorption, J_2	Surface area,	Kp	K_1
	d_2	d_1	δ or H	%	mg/g	m^2/g	Water	Air
A1	19.5	6.1	5.7	15.5	476	452	9.3E+8	1.6e+8
B2	29.1	9.6	11.1	61.1	1157	1195	1.5e+12	1.7e+12
C3	28.0	8.8	6.5	48.0	696	702	1.9e+13	1.5+13

The newly obtained materials and the principle of work are applicable in all branches of chemical industry.

ACKNOWLEDGMENT

This research was financially supported by the Bulgarian National Fund "Scientific Investigations" at the Ministry of Education, Science and Technology under contract No TH 806.

REFERENCES

1. D.L. Trimm, *Design of Industrial Catalysts* (Elsevier, Amsterdam, 1980), p. 94.
2. F. Hinrichsen, A. Rosowski, A. Hornung, M. Muhler, and G. Ertl, The kinetics of ammonia synthesis over Ru-based catalysts. 1. The dissociative chemisorption and associative desorption of N-2, *Journal of Catalysis* 165(1), 33-44 (1997).
3. N. Kolev, and L. Ljutzkanov, Method and frame for elimination of diffusion limited resistant of processes over the pore walls of solid materials. Bulgarian Patent Office, Application Nr. 103707/ 01.09.1999.
4. US-Pat. 4,118,341, v.3.10.78, Jap.-Pror. 25.5.74.
5. R. Jguchik, S. Tsunoda, and S. Takeeshita, *Intern. Chem. Eng.* 14(2), 381-386 (1974).
6. L. Ljutzkanov, and A. Atanasov, Method of treating carbon containing materials, Patent Application No 1101705 /30.06.1997 - The application is published: Patent Office of the Republic of Bulgaria , Official Bulletin N 1/1999 (29.01.99).

USE OF ACTIVE CARBON TO PHENOL REDUCTION FROM WATER SOLUTION

ANNA WOLBORSKA*
Technical University of Lodz, Wolczanska 213, 90-924 Lodz, Poland

Abstract. Efficiency of active carbon applied in water treatment technologies depends on selection of a proper adsorbent, but also on methods and conditions of its use. These subjects are discussed taking as a model example the sorption of phenol on different, also chemically modified (HNO_3, ozone) and biological activated carbons. Ozonation of active carbon changes its porous structure and in the case of phenol it reduces its sorptivity. Strong oxidation of the active carbon with HNO_3, affects also kinetic parameters of the sorption process (the effective diffusion coefficient decreases). The application of biologically active carbon offers wide opportunities. A combination of sorption and biodegradation processes enables advanced removal of phenol from the solution on the one hand, and on the other hand it binds this toxic substance before direct exposure to microorganisms.

Keywords: active carbon; adsorption; biosorption; reduction of phenol

1. Introduction

Sorption of the components of water solutions on active carbon is used in many industrial technologies and is one of the main unit processes in environmental engineering. In the technology of water treatment, active carbon has been used primarily to remove flavor, aroma and color. As

* Anna Wolborska, Technical University of Lodz, Faculty of Process and Environmental Engineering, Wolczanska 213, 90-924 Lodz, Poland, e-mail: wolborsk@wipos.p.lodz.pl

J.M. Loureiro and M.T. Kartel (eds.), Combined and Hybrid Adsorbents, 237–242.

regulations on water quality become more stringent, the application of carbon adsorbents has been extended to the removal of by-products of chemical water disinfection, e.g. products of chlorination and ozonation. Now, special emphasis is put on the reduction of organic micropollutants in water by sorption, due to which doses of disinfectants can be decreased. In sanitary applications there is a tendency not only to minimize the concentration of components removed from the solution, but it is also necessary to observe quality standards and reduce the risk that they will not be met.

A general opinion is that efficiency of the sorption method depends first of all on the selection of proper activated carbon. This is undoubtedly very important, but equally crucial are the conditions and environment in which it is used. Through a proper chemical preparation (modification) of the active carbon itself or through its biological activation, the process can be remarkably changed and can affect both its rate and final result. On the other hand, all accidental situations or emergency related, for instance, to the flow of water solution or process conditions, can also lead to changes of the process, including hazards. This is particularly vital in environmental and toxicological applications.

This subject was discussed using a model example of phenol sorption from aqueous solutions on different, also modified types of activated carbon. Selection of a model adsorbate was determined by its moderate susceptibility to sorption and biodegradation and toxic action on organisms. This study is focused mainly on the equilibrium effects, however in particular cases also the effect of process kinetics on holistic solution of this kind of problems was taken into account.

2. Materials and Methods

Static and kinetic tests of phenol sorption on different types of granulated active carbon were made. An input material were commercial sorbents: F-400 (Chemviron Carbon), AG-5 (Gryfskand), PK 1-3 I ROW-0,8 Supra (Norit). A criterion of sorbent selection was its specific surface area $S_{BET}(N_2)$= 1000 to 1150 m^2/g given in commercial information provided by producers.

Selected types of active carbon were chemically modified by ozonation in a water suspension[1] or by oxidation with nitric acid.[2] Biological activity of the sorbent was achieved by immobilizing a pure bacterial strain of *Pseudomonas putida* from a mineral substrate.[3]

Experimental studies of the equilibrium of phenol sorption on active carbon (determination of adsorption isotherm) were carried out in static conditions at the temperature of 30 °C, preserving a constant ratio of

solution volume to carbon mass. The phases were separated by decanting and centrifuging. The process kinetics was measured in a constant volume closed system in mixing conditions.[5]

3. Results and Discussion

Examples of results obtained in a broad range of research, illustrating the effect of some elements of adsorbent selection and possible changes of its activity in relation to a given substance, are presented. References that provide complete experimental data and theoretical description, which is a basis for a detailed discussion of the subject of this research, are also quoted.

3.1. ACTIVE CARBON TYPE

Figure 1 shows experimental phenol sorption isotherms from water solutions in a broad range of equilibrium concentrations from 0 to 0.6 g/dm^3 on several selected types of commercial active carbon. Convex isotherms approaching monotonically a boundary value, characteristic for adsorption of organic substances with limited solubility, from water were obtained.

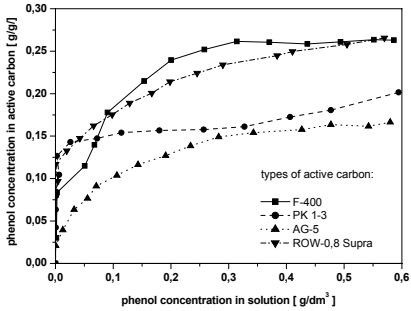

Figure 1. Phenol adsorption isotherms on active carbons.

Worth noting are diversified profiles of the curves and change of their mutual position with an increase of phenol concentration in the water phase. Carbon AG-5 shows the lowest adsorptivity for phenol. In the range of low concentrations the better are the carbons PK 1-3 and ROW-0,8 Supra, but already at equilibrium concentrations >0.1 g/dm^3, carbon F-400 has the highest adsorptivity. Different shapes of particular equilibrium curves illustrate changes in adsorbent-adsorbate interparticle relations. This effect is caused most probably by differences in the chemical nature of adsorbent surfaces. Experience makes us choose carbon ROW-0,8 Supra, which

revealed good adsorptivity and "stable" equilibrium relations in the whole range of concentrations.

It follows from this simple example that already at the initial stage it is difficult to estimate definitely the suitability of a given active carbon even after making a series of basic experiments.

3.2. ACTIVE CARBON OXIDATION

Original active carbon ROW-0,8 Supra was ozonated in an aqueous suspension. Due to ozonation, sorption properties of the tested active carbon for phenol changed (Figure 2).

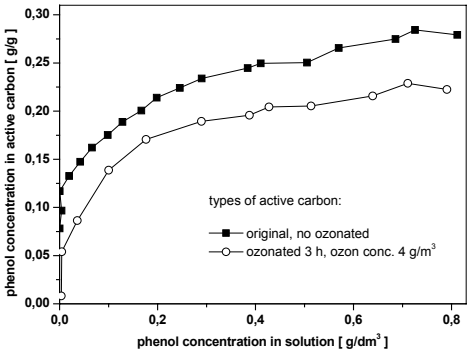

Figure 2. Phenol adsorption isotherms on original and ozonated active carbon ROW 0,8 Supra.

Modification of the sorbent only slightly deteriorated parameters of the porous structure such as specific area, total pore volume, fraction of micro- and macropores in favor of mesopores. These are results of the modification described in literature which was carried out with mild oxidation with other oxidants, e.g. nitric acid.

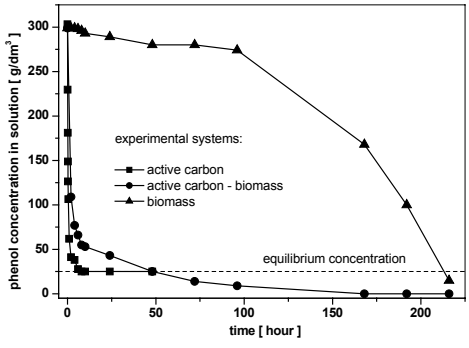

Figure 3. Dependence of effective diffusion coefficient for active carbon AG 5 on the total amount of oxygen on the adsorbent surface.

In general, the change did not refer to the volume of a monolayer, but a tendency towards weakening the adsorbate-adsorbent interaction was observed which led to a decrease of equilibrium adsorptivity.

Intensive oxidation of active carbon with nitric acid resulting in a remarkable increase of oxygen amount present on the sorbent surface induces significant changes in kinetic parameters. Effective surface diffusion coefficient for phenol sorption in carbon decreases with an increase of total oxygen (Figure 3).

3.3. BIOLOGICAL ACTIVE CARBON

A very developed, rough surface of active carbon is an excellent substrate to be inhabited by microorganisms. The mechanism of substance removal from water by biological active carbon (BAC) consists of two processes: sorption and biodegradation by microorganisms that live on the sorbent surface and in its pores. Thus, in this case pollutants present in water should be estimated in view of their susceptibility to each of these processes.

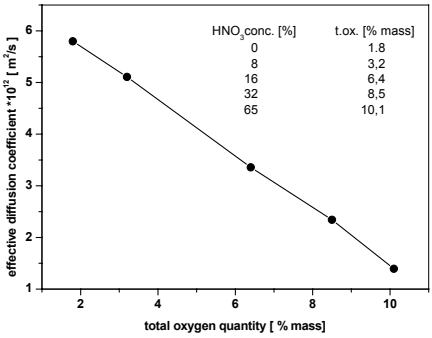

Figure 4. Kinetics of phenol biodegradation and adsorption on active carbon ROW 0,8 Supra.

The presence of biomass on the active carbon surface changes the run, rate and efficiency of phenol reduction in the water solution (Figure 4). A biological film is an additional diffusional layer on the way of transport of a substance from the solution and products of metabolism to the solution. In this case, an increase of mass transfer resistance in the system slows down the process, but due to sorbate biodegradation and sorbent bioregeneration, even a complete phenol reduction in the solution can be achieved (in the case of adsorption, the system can reach only the equilibrium state).

Biodegradation combined with sorption enables quick binding of phenol present in the solution by the sorbent and its gradual uptake by biomass, which decreases the effect of toxicity of the substance occurring at higher concentrations on microorganisms. Particularly advantageous results are obtained when biosorption is carried out in a fixed bed of active carbon.

4. Summary

In view of changing tasks and different criteria, selection of active carbon for a sorption system is a difficult and complex problem. Undoubtedly, it is not enough to know the specific surface area of an adsorbent only. Its operating conditions and various modifications have a vital effect on both equilibrium and kinetic parameters of the process.

For instance, moderate ozonation of the active carbon and oxidation of its surface with nitric acid discussed in this paper, revealed that phenol sorption deteriorated leading to a decrease of equilibrium sorptivity of the sorbent and inner diffusion parameters. In turn, biological carbon activity, despite a significant slow-down of the processes, permitted to use a buffering role of the sorbent for toxic effect of phenol on microorganisms and to reduce to almost nil its presence in the water solution.

In real conditions the effect of different agents (including temperature, pH, phase contact) is naturally much higher and more complex. First of all, we have to deal with multicomponent solutions, in which mutually competitive interactions have always an additional effect on the reduction of sorption of a given substance. Therefore, a versatile estimation of the effect of process conditions on its run and possible applications is so important.

REFERENCES

1. A. Wolborska, K. Maryniak and J. Perkowski, The Effect of Ozonation on Sorption Properties of Active Carbon and Porous Structure. Model Investigations, *Polish Journal of Chemical Technology* 4(2), 42-46 (2002).
2. H. Błasiński, A. Wolborska and J. Kaźmierczak J, Kinetics of Adsorption from Single and Binary Solutions on Activated Carbons with Chemically Different Surfaces, *Adsorption Science and Technology* 12(4), 296-305 (1995).
3. A. Wolborska and T. Jamroz, Immobilization of *Pseudomonas putida* on activated carbon, *Inżynieria i Aparatura Chemiczna* (in Polish) 41(3s), 147-148 (2002).
4. A. Wolborska and K. Pilecka-Bujnowicz, The efficiency of phenol biosorption from water phase on activated carbon, in: *Chemical Industry and Environment IV*, edited by A. M Machin and J. Umbria (Universidad de Las Palmas de Gran Canaria, 2003), pp. 123-131.
5. A. Wolborska and K. Pilecka-Bujnowicz, Sorption of organic compounds from water solutions on activated carbon. Internal diffusion coefficient, in: *Environmental Engineering Studies*, edited by L. Pawłowski, M. Dudzińska and A. Pawłowski (Kluwer Academic/Plenum Publishers, New York, 2003), pp. 141-152.

REMOVAL OF HYDROGEN SULFIDE, AMMONIA AND NITRITE IONS FROM WATER SOLUTIONS USING MODIFIED ACTIVE CARBONS

T. LUPASCU*, RAISA NASTAS, M. CIOBANU, TATIANA ARAPU AND V. RUSU
Institute of Chemistry of the Academy of Sciences of Moldova, Academiei str., 3, Chishinau, 2028 MD, Moldova

Abstract. Modified active carbons were used for removal of hydrogen sulfide, ammonia and nitrite ions from water solutions. Obtained results demonstrate that active carbon oxidized with H_2O_2 following impregnation with Co(II) possesses higher adsorption capacity for NH_4^+ compared with unimpregnated samples. It was established that active carbon obtained from nut shells has better oxidation properties compared with active carbons obtained from plum stones. The optimal conditions for adsorption and oxidation of sulfide and hydro-sulfide ions were established. Active carbons impregnated with Fe^{+3} and Cu^{+2} ions possess higher oxidation capacity demonstrating that these catalysts more effectively catalyze the oxidation of sulfide ions to S^{IV} and S^{VI} species.

Keywords: active carbons; sorption; hydrogen sulfide; ammonia; nitrite ions

1. Introduction

Water treatment technologies require revision, modernization and enriching by utilizing more effective methods and reagents to achieve required standards for drinking water.[1] Basic attention in this program is stressed on a status of the water treatment technologies and their economic aspects

* To whom correspondence should be addressed. T. Lupascu, Institute of Chemistry of the Academy of Sciences of Moldova, Academiei str., 3, Chishinau, 2028 MD, Moldova; email: tlupascu@mail.md

J.M. Loureiro and M.T. Kartel (eds.), Combined and Hybrid Adsorbents, 243–248.

being especially focused on the quality for delivery of potable water to the population. Relevant direction for improving of quality of potable water is application of active carbons at various stages of water treatments. Annually, Moldova imports about 300 tons of active carbons for different purposes. On the other hand, canning and wine plants annually store about 1000 tons of stones of different garden-plants and fruits and about 20000 tons of grape seeds. These agricultural wastes can be used as raw materials to obtain active carbons, ion exchangers and catalysts.

The present researches are focused to develop ion exchangers and catalysts based on new carbon adsorbents derived from fruit stones, and to apply them for removal and oxidation of pollutants in reduced forms - NO_2^-, NH_4^+, species of hydrogen sulfide, from surface and underground waters.

2. Experimental

Oxidation of hydrogen sulfide in aqueous solutions was performed using micro-experimental laboratory installation provided with an air bubbler and recovery flask for aerated hydrogen sulfide. As catalysts were tested commercial activated carbon obtained from birch wood (BAU-A) and active carbons obtained from peach stones (CAP23), following it oxidation (CAPO23) and impregnation with salts $FeCl_3$ (CAPO23Fe) and $Cu(NO_3)_2$ (CAPO23Cu). Also, the catalyst obtained from peach stones and impregnated with NiO oxide (CAP23-NiO) was tested. Elemental sulfur, thiosulfate, sulfite and sulfate ions, and aerated hydrogen sulfide from the recovery flask were determined in the equilibrium solutions by methods from the literature.[2] All sulfur species were recalculated as H_2S.

Active carbons, obtained from nut shells (CAN-7) by chemical activation with phosphoric acid following oxidation with different agents HNO_3, H_2O_2, O_3 (CANO-7) and impregnation with cations Co^{2+}, Ag^+, Ni^{2+} or Cu^{2+} (CANO-7+Me^{n+}), were tested for removal of ammonia ions. Active carbons obtained from nut shells (CAN-7) and plum stones (CAPr-1) by chemical activation with phosphoric acid were tested for researches of nitrite oxidation. Nitrite ions were determined colorimetrically using SPEKOL-211 spectrophotometer.[2]

3. Results and Discussion

Chemical equilibrium of sulfur species $H_2S \Leftrightarrow HS^- \Leftrightarrow S^{2-}$ is shifted to the left at low pH values leading to the raise of H_2S concentration in the solution which may be eliminated by gas bubbling, e.g. by aeration. The analyses using installation provided with an air bubbler and recovery flask

for aerated species demonstrate that at pH values in interval 7.5-8.5 hydrogen sulfide prevails in solution which is eliminated by air bubbling and is trapped in the recovery flask. Thus, the equilibrium concerning oxidation-aeration processes of sulfur species is shifted towards the predominance of aeration process at pH values in interval 7.5-8.5. At higher pH values the chemical equilibrium is shifted to the right, and the oxidation process of sulfur species prevails reaching 86-95% of their content. However, the reaction rate is too low and/or the process is quite long requiring about 24 hours.

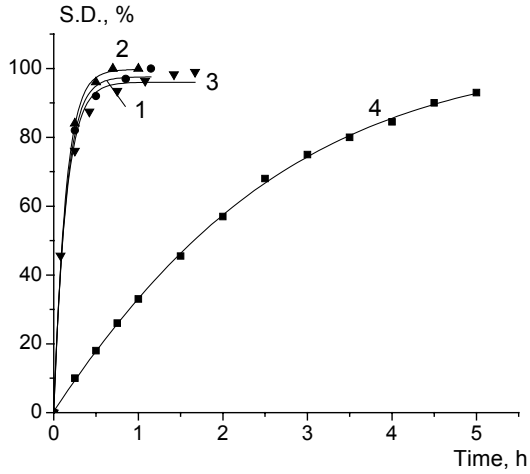

Figure 1. Kinetics of sulfide demand (SD) in the absence (4) and in the presence of active carbon obtained from peach stones CAP23 (1), oxidized active carbon CAPO23 (2), and commercial activated carbon obtained from birch wood BAU-A (3). Initial solution concentration C_0 = 10 mg/L, pH = 8.5, ratio mg O_2/mg H_2S equal to 3/4 in the presence of 1 g of catalysts.

Kinetics of sulfide demand (SD) is modified essentially in the presence of active carbons (Figure 1). The reaction rate considerably raises, about by 14 times, also, the amount of aerated H_2S decreases, reaching only 4-12% of total sulfide content in the presence of active carbons CAP23, CAPO23 (Table 1).

Surface chemistry of the activated carbons exercises considerable influence on type of sulfur species formed in solution. Species of higher oxidation level, S^{IV} and S^{VI}, prevail in the presence of oxidized active carbon CAPO23, and considerably smaller quantities of colloidal sulfur are derived (Table 1). As a whole, this adsorbent possesses higher catalytic activity and is more effective as compared with commercial activated carbon BAU-A.

Catalytic activity of carbons differs, and reaction rate for removal of sulfur species increases as CAPO23Fe< CAPO23Cu< CAP23-NiO (Figure 2)

The type of sulfur species which are formed in solution also differ. High quantities of colloidal sulfur are formed in the presence of catalyst CAP23-NiO. Such species are absent in the presence of catalysts CAPO23Cu and CAPO23Fe for which are characteristic derivation of species of higher oxidation level, S^{IV} and S^{VI}. Data demonstrate that obtained catalyst by impregnation with Cu(II) is the most preferable one for practical purposes for removal of hydrogen sulfide species from underground waters.

TABLE 1. Quantities of H_2S aerated and oxidized to sulfur species in the absence and in the presence of active carbon obtained from peach stones CAP23, oxidized active carbon CAPO23 and commercial activated carbon obtained from birch wood BAU-A. Initial solution concentration C_0 = 10 mg/L, pH = 8.5 and ratio mg O_2/mg H_2S equal to 3/4 in the presence of 1 g of catalysts

Active carbons	Quantity aerated,%	Quantity oxidized,%	Quantities (%) of H_2S oxidized to sulfur species			
			S^0 colloidal	$S_2O_3^{2-}$	SO_3^{2-}	SO_4^{2-}
In the absence of carbons	67.0	33.0	-	-	-	-
CAP23	12.0	88.0	20.4	0	12.5	67.1
CAPO23	4.3	95.6	6.1	11.7	15.4	65.9
BAU-A	9.2	90.8	32.9	32.9	4.5	31.2

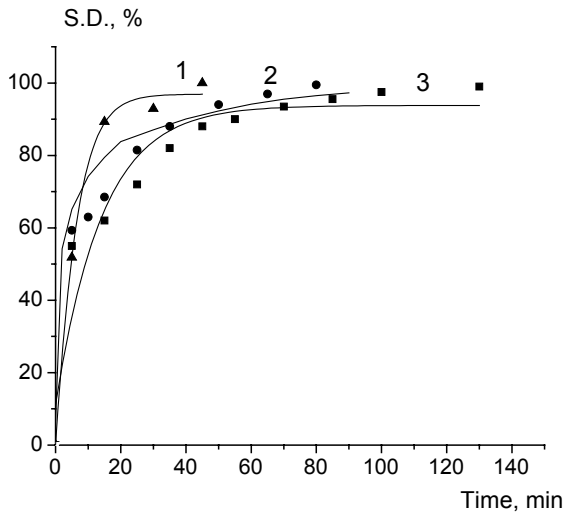

Figure 2. Kinetics of sulfide demand (SD) in the presence of active carbons CAP23-NiO (1), CAPO23Cu (2) and CAPO23Fe (3). Initial solution concentration C_0 = 10 mg/L, pH = 8.5 and ratio mg O_2/mg H_2S equal to 3/4 in the presence of 0.5 g of catalysts.

Surface chemistry of active carbons is influenced both by oxidizing agents and impregnated metals. Higher concentration of the carboxyl groups is obtained after oxidation of active carbons with H_2O_2. Data demonstrate that oxidized active carbon with H_2O_2 following impregnation with Co^{2+} possesses higher adsorption capacity compared with other synthesized active carbons (Figure 3).

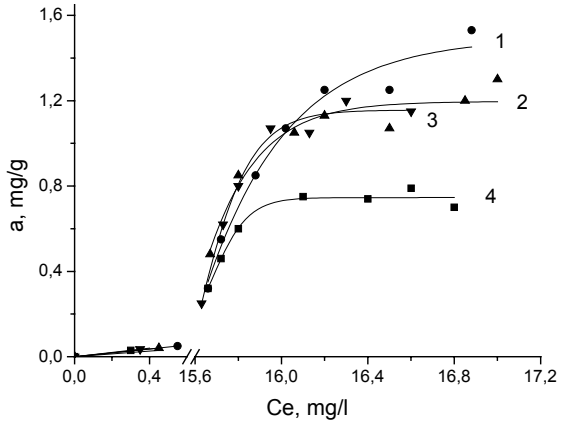

Figure 3. Adsorption isotherms of ammonia ions from water solutions on the oxidized with H_2O_2 active carbons (CANO-7) following impregnation with Co^{2+} (1), Ni^{2+} (2), Ag^{+} (3), Cu^{2+} (4) ions.

Figure 4 presents the kinetics of nitrite oxidation on active carbons. It was establish that active carbons obtained from nut shells (CAN-7) have higher oxidation capacity compared with active carbons obtained from plum stones (CAPr-1). Thus, in the presence of active carbon CAN-7 more than 90% of the initial nitrite in solution is oxidized for about 5 hours, such output in the presence of active carbon CAPr-1 being registered only after about 20 hours.

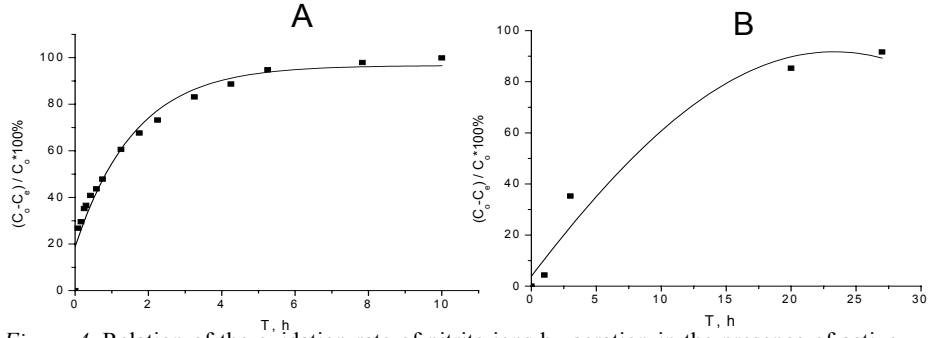

Figure 4. Relation of the oxidation rate of nitrite ions by aeration in the presence of active carbons. **A-** active carbon obtained from nut shells by the chemical method of activation with phosphoric acid (CAN-7), **B-** active carbon obtained from plum stones by the chemical method of activation with phosphoric acid (CAPr-1).

4. Conclusions

Performed researches demonstrate the efficiency of obtained active carbons and catalysts for purification of surface and underground waters from hydrogen sulfide and its salts, ammonia and nitrite ions.

Obtained catalyst by impregnation with Cu(II) ions of oxidized active carbon from peach stones is the most preferable one for practical purposes for removal of hydrogen sulfide species from underground waters.

Oxidized active carbon obtained from nut shells by chemical method of activation with H_3PO_4 and impregnated with Co^{2+} ions is the most preferable one for practical purposes for removal of ammonium ions and ammonia from natural surface waters.

Active carbon obtained from nut shells by chemical method of activation with H_3PO_4 is the most preferable one for practical purposes for removal of nitrite from natural surface waters.

ACKNOWLEDGEMENTS

This work is supported by Bilateral CRDF-MRDA project ME2-3038

REFERENCES

1. Official Monitor of Republic Moldova, 2002, No. 59-61, p. 19-26.
2. Krishnan H.P.N., Ramachanran N.C.G (1970), Vishwakarma, Vol. 11, No. 7, p. 3-8.

ADSORPTION OF CHROMIUM IONS FROM AQUEOUS SOLUTION USING ACTIVATED CARBO-ALUMINOSILICATE MATERIAL

REYAD AWWAD SHAWABKEH*
Department of Chemical Engineering, Mutah University, AL-Karak, 61710, JORDAN

Abstract. A novel activated carbo-aluminosilicate material prepared from oil shale was used as an adsorbent for chromium ions from aqueous solutions. The maximum sorption capacity was found to be 92 mg/g. This value was obtained at pH 4 which is bellow the zero point of charge (pH_{ZPC}) for this material. The pH_{ZPC} was estimated at different mass to solution ratios and ranged from 7.9 to 8.3.

Keywords: Activated carbo-aluminosilicate; adsorption; sulfuric and nitric acid; FT-IR; XRD; Chromium.

1. Introduction

Activated carbon and zeolite are well known materials used extensively in solid-fluid separation and chemical reactions. The microporosity and high surface area and charge for both materials highlighted them as ion exchangers, adsorbents, catalysts and separation media. Activated carbon has been widely used in chemical purification systems to remove solutes and gases from downstream. It has a specific affinity toward non-polar compounds such as organics as it has a hydrophobic property in aqueous solution. The major raw materials for production of activated carbon are wood,[1] coal,[2] nutshells[3] and fruit stones.[4] The main disadvantages of activated carbon are the weak mechanical properties of its surface and the fact that it easily burns at high operating temperatures. On the other hand,

* To whom correspondence should be addressed. Reyad A. Shawabkeh, Department of Chemical Engineering, Mutah University, Al-Karak, 61710, Jordan; e-mail: rshawabk@mutah.edu.jo

J.M. Loureiro and M.T. Kartel (eds.), Combined and Hybrid Adsorbents, 249–254.

zeolites and aluminosilicates are good supporting materials for catalysts and ion exchangers.[5] They have a hydrophilic affinity toward polar molecules as a result of existence of aluminum atoms in their structure. Great efforts were performed to enhance both physical and chemical properties of activated carbon and aluminosilicates materials in order to enhance their surface coverage and selectivity toward target solutes, as well as their catalytic properties.

These research areas focused on either synthesizing new activated carbon and zeolites or impregnating their surfaces with different transition metals.[6] While none, to our knowledge, have paid an attention for producing a material that combines the physical and chemical properties of both activated carbon and zeolites, this research focuses on synthesis of an activated carbo-aluminosilicate material from oil shale and its utilization for remediation of chromium ions from aqueous solutions.

2. Experimental

The activated carbo-aluminosilicate used in this study was synthesized earlier.[7] This material combines the physical and chemical properties of both activated carbon and zeolite. An X-ray diffraction analysis illustrated the formation of zeolite Y, Na-X, and A-types, sodalite, sodium silicate, mullite and cancrinite, while FT-IR spectrum showed the presence of carboxylic, phenolic and lactonic groups on the surface of this material.

Additionally, this material is characterized by its zero point of charge (pH_{ZPC}) by introducing fixed amount of carbo-aluminosilicate material into six 100-mL Erlenmeyer flasks containing 50 mL of 0.1 M potassium nitrate solution. Initial pH values of the six solutions were adjusted to 2, 4, 6, 8, 10 and 12 by adding few drops of either nitric acid or potassium hydroxide. Suspension of different solid to solution samples (1/150 to 1/1000) were allowed to equilibrate for 24 h in an isothermal shaker (22 ±1 ^{o}C). The suspension was filtered and the final pH of these samples was measured again.

Imaging microscope analysis of the surface of the produced carbo-aluminosilicate was accomplished using an Olympus MIC-D Digital Microscope.

2.1 CHROMIUM ISOTHERM

Adsorption tests were conducted in 100-mL Erlenmeyer flasks. A sample of 0.1 g of carbo-aluminosilicate material was mixed in 50 mL solution of potassium dichromate and allowed to equilibrate in an isothermal shaker (22 ±1 ^{o}C) for 24 h. The pH was adjusted by adding few drops of either hydrochloric acid or potassium hydroxide. Similarly, blank solutions were

created for purpose of comparison. After 24 h, all solutions were filtered and centrifuged to remove any suspensions and then analyzed using S4 ThermoElemental atomic absorption spectrophotometer. The difference between the initial and final concentration of each ion represents the amount that transferred to the surface of the carbo-aluminosilicate.

3. Results and Discussion

The chemical analysis of EL-Lajjun oil shale is presented in TABLE 1. The studied samples provided 25.9 wt.% organic and volatile matter with 54.5 wt.% ash. The composition of the ash showed 27.5 wt.% silica, 4.8% alumina while the rest are alkali and alkali earth oxides.

TABLE 1. Chemical Analysis of El-Lajjun oil shale

Property	Value (wt.%)
Organic matter	22
Volatile matter	3.9
Ash	54.5
Moisture	3.1
Sulfur	2.6
Carbonates	13.9

The Zero-point is considered an important factor required for predicting the adsorption property of the surface of this material. This ZPC determines the electrophoretic mobility where the net total particle charge is zero. The produced material is composed of three main constituents, silica which has a pH_{ZPC}=1.9, Alumina (pH_{ZPC}=9.5) and Activated carbon (pH_{ZPC} 5~8).[8] Combining these three constituents resulted in strong attraction between their surfaces due to electrostatic attraction between the opposite sign of these surfaces yielding a pH_{ZPC} value in the range of 7.9~8.3 as shown in Figure 1(a).

It is evident that this surface exhibits amphoteric properties, and acts as a buffer in a wide pH range from 3 to 9 where the pH_{final} remains almost close to the pH_{ZPC} for all values of $pH_{initial}$ in this range. Figure 1(b) shows the variation of pH_{ZPC} with the concentration of carbo-aluminosilicate in solution. An increase in solid to solution ratio from 1:1000 to 1:150 leads to an increase in pH_{PZC} from 7.9 to 8.3, respectively.

Figure 2 shows the imaging microscope photographs for the produced material. It is clear that an irregular and porous surface may be observed where the dark area represents the carbonaceous materials surrounded by the aluminosilicates (white area).

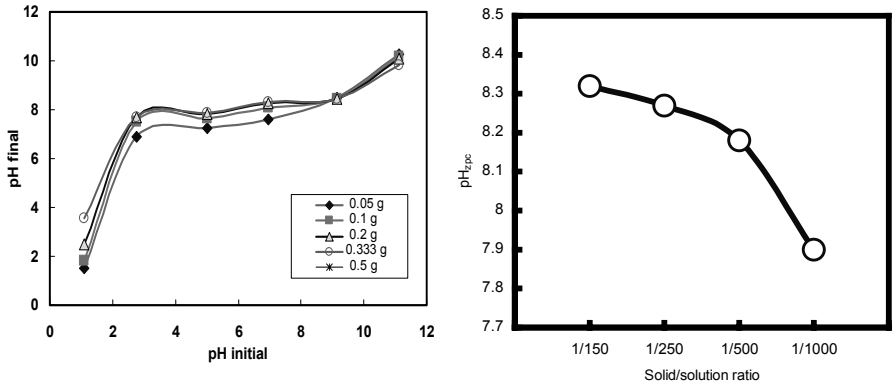

(a) (b)

Figure 1. (a) Variation of ΔpH_{ZPC} vs. $pH_{initial}$ for the activated carbo-aluminosilicate material; (b) Effect of solid to solution ratio on the variation of pH_{ZPC}.

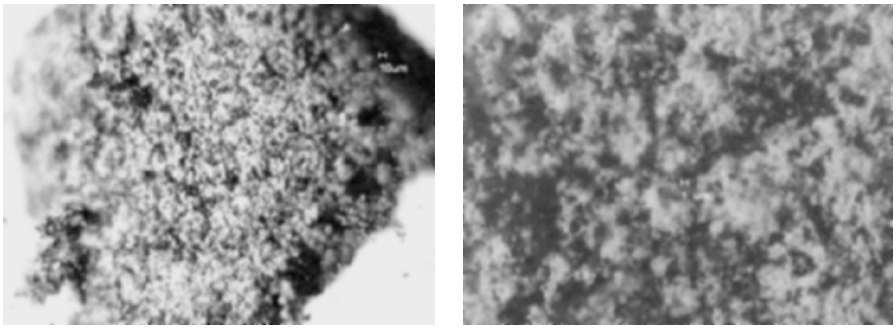

(a) (b)

Figure 2. Imaging microscope photographs of the activated carbo-aluminosilicate.

Chromium adsorption is shown in Figure 3. It is clear that Cr^{6+} was strongly adsorbed at low pH and declined sharply at higher value. The maximum adsorption capacity was 92 mg/g obtained at equilibrium solution concentration of 185 mg/L at pH 4. This value was decreased to 68 mg/g at the same solution concentration but for pH 7.5. The variation of adsorption of chromium ions with pH can be explained by taking into account the isoelectric point of the carbo-aluminosilicate surface and the existing forms of chromium species at different pH values. In an aqueous solution Cr^{6+} exists in the form $HCrO_4^-$, CrO_4^{2-} or $Cr_2O_7^{2-}$ depending of pH value while Cr^{3+} is in the form $Cr(OH)^{2+}$, or CrO_2^-.[9,10] Upon hydration the solid surface develops hydroxyl groups which behave as Bronsted acids according to:[11]

$$CS-OH_2^+ \Leftrightarrow SC-(OH)^0 + H^+$$

$$SC-(OH)^0 \Leftrightarrow SC-O^- + H^+$$

where $CS-OH_2^+$ represents the protonated surface hydroxyl groups when the solution acidity is bellow the pH_{ZPC}, $SC-(OH)^0$ illustrates the neutral surface at the $pH_{ZPC,}$ while $SC-O^-$ is the ionized surface above the pH_{ZPC}. As the solution pH increases or decreases the speciation of the protonated or ionized surface will be increased as a result of increasing the surface charges of the functional groups. This illustrates the increase in adsorption capacity of Cr^{6+} with decreasing the solution pH. At pH 2-6, the surface of the carbo-aluminosilicate material is electropositive and attracts most chromium species existing in solution in the form $HCrO_4^-$ while at higher pH values the surface becomes electronegative and repulses the CrO_4^{2-} species, which becomes predominant in solution. Therefore, the amount of Cr^{6+} uptake by the surface will be higher at pH 4 than at pH 7. On the other hand, at highly acidic solution (pH<2), the hexavalent chromium gets reduced to trivalent one according to:

$$Cr_2O_7^{2-} + 14H^+ + 6e^- \rightarrow 2Cr^{3+} + 7H_2O$$

Aggarwal et al.[12] stated that the maximum adsorption of Cr^{6+} takes place at pH 3 while the maximum reduction of Cr^{6+} to Cr^{3+} happens at pH 1. Therefore, it is expected that at pH 4 only adsorption phenomena takes place at the surface of the activated carbo-aluminosilicate but not reduction reaction.

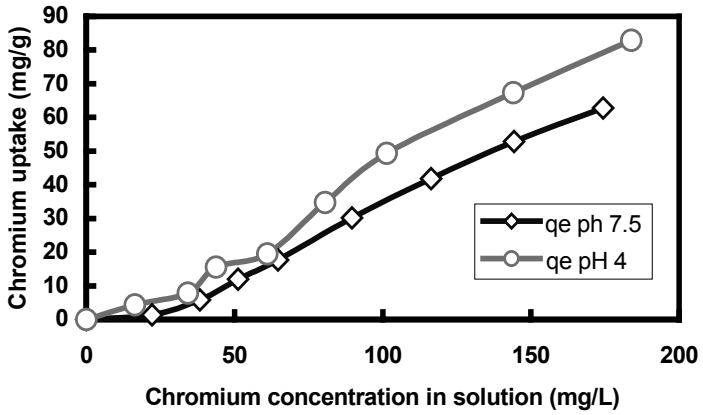

Figure 3. Adsorption isotherms of chromium using carbo-aluminosilicate material.

4. Conclusions

Synthesis and production of activated carbon and zeolite from oil shale can be performed with low cost of raw material and safe operation. This

material proved to be a good adsorbent for chromium ions from aqueous solutions. The removal capacity was 92 mg/g. This material can also be utilized in heterogeneous chemical reactions as a catalyst support. It can tolerate compression and high temperature.

REFERENCES

1. L. Khezami, and R. Capart, Removal of chromium(VI) from aqueous solution by activated carbon: Kinetic and equilibrium studies, *J. Hazard. Mater.* 123(1-3), 223-231 (2005).
2. J. Gañan, C. González-García, J. González, E. Sabio, A. Macías-García, and M. Díaz-Díez, Preparation of activated carbons from bituminous coal pitches, *Appl. Surf. Sci.* 238(1-4), 347-354 (2004).
3. R. Shawabkeh, D. Rockstraw, and R. Bhada, Copper and strontium adsorption by a novel carbon material manufactured from pecan shells, *Carbon* 40(5), 781-786 (2002).
4. C. Durán-Valle, M. Gómez-Corzo, J. Pastor-Villegas, and V. Gómez-Serrano, Study of cherry stones as raw material in preparation of carbonaceous adsorbents, *J. Anal. Appl. Pyrolysis* 73(1), 59-67 (2005).
5. M. Stöcker, Gas phase catalysis by zeolites, *Microp. Mesop. Mater.* 82(3), 257-292 (2005).
6. F. Tomás-Alonso, and J. Latasa, Synthesis and surface properties of zinc ferrite species in supported sorbents for coal gas desulphurization, *Fuel Process. Technol.* 86(2),191-203 (2004).
7. R. Shawabkeh, Synthesis and characterization of activated carbo-aluminosilicate material from oil shale**,** *Microp. Mesop. Mater.* 75(1-2), 107-114 (2004).
8. M. Kosmulski, The pH-dependent surface charging and the Points of Zero Charge, *J. Colloid Interf. Sci.* 253, 77–87 (2002).
9. H. Tel, Y. Alta, and M. Taner, Adsorption characteristics and separation of Cr(III) and Cr(VI) on hydrous titanium(IV) oxide, *J. Hazard. Mater.* 112(3), 225-231 (2004).
10. P. Rana, N. Mohan, and C. Rajagopal, Electrochemical removal of chromium from wastewater by using carbon aerogel electrodes, *Water Research* 38, 2811-2820 (2004).
11. C. Huang, Y. Hsieh, S. Park, M. Corapciogiu, A. Bower, and H. Elliot, in: *Metals Speciation, Separation and Recovery*, edited by J. Patterson and R. Passino. (Lewis Pub, Michigan, 1987), pp. 437-442.
12. D. Aggarwal, M. Goyal, and R. Bansal, Adsorption of chromium by activated carbon from aqueous solution, *Carbon* 37, 1989-1997 (1999).

MODIFIED NATURAL SORBENTS FOR BINDING HEAVY METAL IONS

ALINA A. NIKOLAYCHUK*, LIDIA A. KUPCHIK AND MYKOLA T. KARTEL
Institute for Sorption and Problems Endoecology, NAS of Ukraine, General Naumov str., 13, Kiev, 03164, Ukraine

Abstract. The opportunity of utilizing solid cellulose-containing wastes of food and processing industry for manufacturing sorption materials is considered.

Keywords: Synthesis; biosorbents; cellulose; lignin; vegetative raw

1. Introduction

Taking into account the general pollution of the environment by heavy metals ions and the threat to the health of people and animals, the requirement for manufacture of new effective adsorbents, food and fodder additives of protective, antidote and neutralizing action got actuality social importance. The economic feasibility of carrying out researches in this area is grounded, firstly, on the possibility of using cheap mostly non-utilized waste products of agriculture, food and process industry, and, secondly, on the creation and manufacturing of a wide assortment of new sorption materials with selective action.

Our research is devoted to the development of ways of updating vegetative waste products with the purpose of improving their ability to selectively remove ions of heavy metals. The ways of modifying tested by us are grounded on depolymerization, selective oxidation of alcohol groups of polysaccharides up to carboxylic and obtaining simple ethers with acid properties. Due to such modifications, materials get high reactionary

* To whom correspondence should be addressed. Alina Nikolaychuk, Institute for Sorption and Problems of Endoecology, NAS of Ukraine, General Naumov street 13, Kiev, 03164, Ukraine; e-mail: a_nikolaychuk@ukr.net

J.M. Loureiro and M.T. Kartel (eds.), Combined and Hybrid Adsorbents, 255–260.

ability, easily enter in reactions of connection and replacement and consequently can carry out functions of selective adsorbents or ion exchangers.[1-3]

2. Experimental

In this work, the results of adsorption testing of the modified vegetative materials of cellulose-lignin type, prepared by us in laboratory conditions by chemical and thermal modifying vegetative waste products (nutshells, apricot, peach or plum stones, vegetable, apple and grape rejects, pulp, peels of grain cultures, basket and peel of sunflower, shell of buckwheat, treated corn ears, beer distiller's grain, coffee waste, seaweeds, etc.) are presented.

The specified waste products were chosen because their main chemical components are cellulose and lignin (Table 1), and their fibrous structure has a quite advanced porous structure.[4]

TABLE 1. Chemical composition of the vegetative raw material

Samples	Total ash content, %	Lignin, %	Hemicellulose, %	Cellulose, %
Basket and peel of sunflower	0.4	27.8	24	41
Shell of buckwheat	0.3	19.5	32	36
Wheat straw	6.6	16.7	28.2	39.9
Pulp	4.8	14.3	20.2	54.8
Shell of apricot	5.9	48.6	10.2	33.5
Shell of nuts	5.1	47.5	13.8	31.2

We used the following methods of chemical and temperature modifying the vegetative waste products:

Phosphorilation

The crushed biomass is heated up at 100 ^{o}C in 20% solution of phosphoric acid during 3 h at a ratio of acid:biomass = 5:1; then the biomass is separated, washed out with distilled water to neutral reaction and dried up. The obtained product, which contains cellulose phosphate, has high static exchange capacity (SEC = 4.18 meq/g), and can be used for binding and removal of heavy metals ions from water solutions by an ion exchange, complexing or adsorption mechanism.

Processing by a sulfuric acid

The crushed biomass is heated up at 100 ^{o}C in 20% solution of sulfuric acid during 3 h at a ratio of acid:biomass = 5:1; then the biomass is separated, washed out with distilled water to neutral reaction and dried up.

The obtained product, which contains, in addition to cellulose sulfate, also carboxylic, aldehyde and ketone oxygen-containing groups, has a static exchange capacity around 1.75 meq/g, and its appearance and properties are close to those of activated carbons.

Oxidation by hydrogen peroxide

The crushed biomass is processed by a 30% hydrogen peroxide solution during 20 h at a ratio reagent:biomass = 10:1 (at room temperature); then the biomass separated, washed out with distilled water to neutral reaction and dried up. The obtained oxidized product has a rather high exchange capacity (SEC = 2.77 meq/g), white color without smell and acid taste. It can be used for adsorption of toxic substances and heavy metals in medical and ecological technologies.

Carboxylation

The crushed biomass is processed by a mixture of concentrated nitric and sulfuric acids in the ratio 3:1 during 3 h at a ratio of reagent:biomass = 10:1 (at 100 ^{o}C); then the biomass is separated, washed out with distilled water to neutral reaction and dried up. At such processing there is deeper depolymerization of the carbohydrate complex and its partial oxidation due to dehydration and formation of carboxymethylcellulose. The high exchange capacity of the product (SEC = 3.7 meq/g) makes it a perspective material for adsorption of heavy metals ions.

Alkaline processing (delignification)

The crushed biomass is processed by 15% solution of KOH during 24 h at a ratio of reagent:biomass = 10:1 (at 20 ^{o}C); then the biomass is separated, washed out with distilled water to neutral reaction and dried up.

Obtaining carbonized biomass

The crushed biomass (of particle size 0.2-0.5 mm) is heated up to 800 ^{o}C under an inert gas (argon) atmosphere, in a quartz reactor placed in a hermetic furnace, and maintained 1 h at that temperature. Thus, first, the removal of free as well as of bonded moisture, and also of other volatile compounds (at 100-170 ^{o}C) occur, and second, at the further increasing the temperature up to 800 ^{o}C occurs the structural transformation to pyrolysis products; the weight of the product thus decreases almost 50%. The obtained carbonized product has good characteristics of specific total volume of pores (V_s = 0.09 cm^3/g) and static exchange capacity (SEC = 1.27 meq/g).

Obtaining the activated carbon from the carbonized biomass

The carbonized biomass obtained according to a previous protocol is treated to steam activation at high temperature (800 ^{o}C) during 20 min. Such activation results in the increases of the specific surface area of the material, total volume of pores (V_s = 0.34 cm^3/g) and static exchange capacity (SEC = 2.14 meq/g). The yield of the final activated carbon

achieves 20-25% of the initial mass of the crushed waste material. The carbon activated by steam contains both strong and weak carboxylic as well phenol groups and can be used for the removal of heavy metals ions and their complex compounds by adsorption.

Obtaining biosorbent enriched by lignin

Vegetative raw materials (nutshells, grape and fruit stones, wheat and sunflower peel) are hydrolyzed by mineral or organic acid with 0.5-10% mass concentration at temperature of 80-200 ^{o}C, hydromodule factor from 1 up to 10, during 20-180 min, and then the obtained adsorbent is activated with a water solution of an alkaline metal hydroxide or of an alkaline metal carbonate or bicarbonate with 0.5 up to 15% mass concentrations (calculated on Me_2O, where Me - K, Na) at 70-110 ^{o}C, hydromodule factor from 1 up to 10, during 20-180 min, and the residual alkaline is neutralized by a water solution of mineral or acetic acid or of calcium chloride up to pH 5.5-7.5.

The study of the adsorption ability of the modified materials have been executed in static conditions from solutions of salts of heavy metals (lead, cadmium, nickel, copper, zinc, cobalt, manganese and strontium) in an interval of initial concentration of 12.5-0.3 mM/L. Initial and equilibrium concentrations of ions of heavy metals are determined by atomic-absorption spectroscopy using a KAS-120.1 equipment (Selmi, Ukraine).

3. Results and Discussion

On the diagrams shown in Figure 1, the effects of removing ions of heavy metals under conditions of their initial concentration 100 mg/L are presented.

From the resulted diagrams it is visible that the modified biosorbents from vegetative waste products have rather high parameters of efficiency of clarification of water solutions from ions of heavy metals. For removal of ions of cadmium sorbents modified by alkali and hydrogen peroxide are more suitable. Ions of copper and lead are successfully bonded by carbonaceous types of sorbents, and also carboxylated biomass. For nickel apparently the efficiency is connected with activated carbon and adsorbents modified by alkali.

It is possible to see that the chemical modification allows increasing the sorption capacity of cellulose-containing wastage and gives them selectivity to ions of toxic heavy metals. Comparing the sorption performances of obtained materials with properties of oral adsorbent preparations, which are ordinarily used for binding ions of heavy metals, it is possible to ascertain that selectivity of developed samples is 25-30% higher.

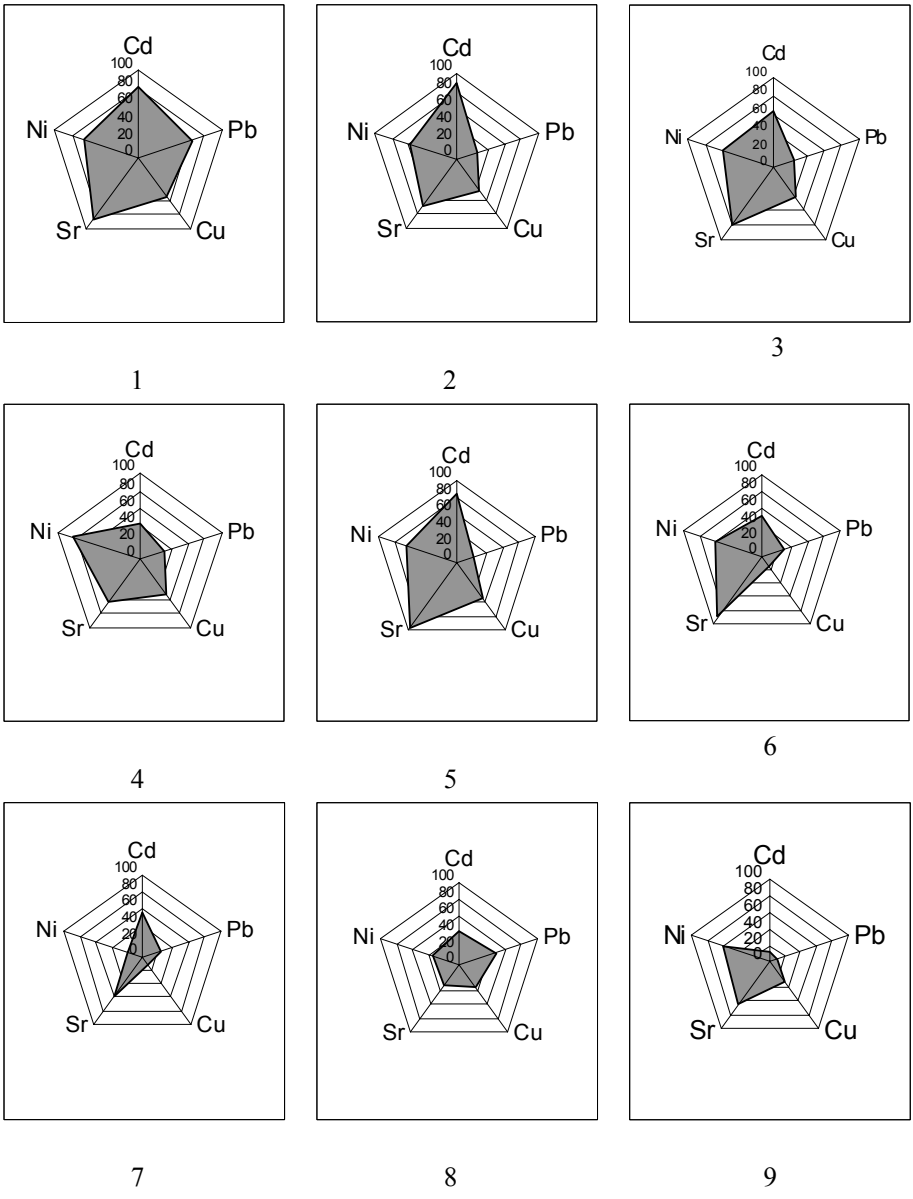

Figure 1. Efficiency of removing ions of heavy metals by different modified biosorbents obtained from waste products of corncobs: 1 - initial biomass; 2 - phosphorilated biomass; 3 - sulfated biomass; 4 - biomass processed by hydrogen peroxide; 5 - carboxylated biomass: 6 - carbonized biomass; 7 - activated carbonizing biomass; 8 - biomass processed by alkali; 9 - biomass enriched by lignin.

The obtained quantitative performances of sorption of toxic metal ions from composite salt solutions suggest the possibility of using modified vegetative wastage from food and processing industries for binding and removal of microimpurities of heavy metals, particularly toxic lead and cadmium, from organism.

4. Conclusions

It is shown that chemical and thermal modifications of biomass from vegetative waste products result in partial destruction of polysaccharide chains and allow improving their ion exchange and adsorption properties. Obtained quantitative characteristics on adsorption of heavy metals ions can be a basis for their use in solving some environmental problems connected with clarification of natural and sewage waters.

Besides the modified biosorbents can find use as components of mixed (combined) enterosorbents (adsorption preparations), food and fodder additives for accelerated detoxification of living organisms from ions of heavy metals which were accumulated in them as consequence of chronic technogenic loadings or probable ecological accidents.

REFERENCES

1. M. Kartel, L. Kupchik, V. Korostyatynets, and V. Strelko, Modifying cellulose-containing raw material - a way to creation of new enterosorbents and food additives, *Scientific Notes of NAUKMA. Chemical Sciences and Technologies,* 19 (2001), 35-42.
2. L.A. Kupchik, V.D. Korostyatynets, M.T. Kartel, et al., Adsorption of heavy metals by natural sorbents of polysaccharide type, *Scientific Works of NUKhT*, 11 (2002), 33-35.
3. N.T. Kartel, L.A. Kupchik, and V.D. Korostyatynets, Chemically modified cellulose as adsorbent for the solving ecological problems, *Fictionalized Materials: Synthesis, Properties and Applications*, *Proc. of Intern. Conf.,* Kiev, 2002, 129-130.
4. V.I. Sharkov, N.I. Kujbina, and Yu.P. Solov'yeva, *Quantitative Chemical Analysis of Vegetative Raw Materials* (Lesnaya promyshlennost', Moscow, 1968).

INFLUENCE OF ADSORPTION OF VIRUSES OF PLANTS ON ELECTRIC PROPERTIES OF POROUS SILICON

YURI A. VASHPANOV*
I.I. Mechnikov National University of Odessa, 27 Paster Str., 65100 Odessa, Ukraine

IGOR P. KONUP
I.I. Mechnikov National University of Odessa, 2 Dvorjanskaja Str., 65100 Odessa, Ukraine

Abstract. We report a method for selective detecting viruses of plants using porous silicon at room temperature. The sizes of pores in porous silicon are larger than those of the researched viruses of plants. The samples of porous silicon have characteristic heterogeneity of porosity and chemical structure along its surface and depth. Adsorbed viruses of plants on the surface of porous silicon induce changes in the measured voltage-current and voltage-farad characteristics. Adsorption of viruses results in the growth of the parameter *c(U)* in the field of voltage greater than 2 V. The characteristic *c(U)* depends on type of the adsorbed viruses.

Keywords: adsorbents; porous silicon; viruses of plants; biosensors

1. Introduction

The physics and electronics of nanobiosensors is one of the most promising and quickly developing areas, causing huge scientific and applied interest all over the world. Semiconductors biosensors controls are a product of achievements of physics and technology of semiconductors, and also of tools, allowing measurements in biological environments and ecological monitoring.

This interest now causes new and prospective semiconductor nanomaterials, such as porous silicon (Por-Si).[1] As is known, single-

* To whom correspondence should be addressed. Yuri Vashpanov, Nanobiosensors Group, Departments of Experimental Physics and Microbiology and Virology, I.I.Mechnikov National University of Odessa, 27 Paster Str., Lab.9, 65100 Odessa, Ukraine; e-mail: vashpanov@mail.ru

J.M. Loureiro and M.T. Kartel (eds.), Combined and Hybrid Adsorbents, 261–267.

crystalline silicon (c-Si) represents the basic material of microelectronic technology. Therefore biosensors on the basis of porous silicon are technologically compatible with modern integrated microcircuits.

Porous silicon has a significant, relatively large, specific surface.[2] This causes a high chemical activity of this material when interacting with its environment.[3] Porous silicon adsorbs especially well organic molecules.[4] That makes it attractive to tests of adsorption of live organisms, as viruses of plants.

The high adsorption sensitivity of porous silicon to polar molecules of organic gases has been established by us.[5,6] Adsorption properties and physical mechanisms of interaction of porous silicon with viruses, bacteria, DNA molecules and other biological objects are investigated now intensively. Absence of full data on physical mechanisms of adsorption sensitivity of porous silicon towards viruses and the nature of the centers of adsorption on the surface of semiconductors sensors require systematic physical, chemical and biological investigations. The purpose of this work is the study of the influence of the adsorption of viruses of plants on the electronic parameters of porous silicon as a method for their detection in a given environment.

2. Methods of Manufacturing of Porous Silicon and Measurements

Samples of porous silicon have been prepared by a method of anodic electrochemical etching of single-crystalline silicon in electrolyte on the basis of 48% hydrogen fluoride aqueous solutions.[7] During etching, additional light and ultrasonic processing of the surface of silicon were used. After manufacturing, the samples passed an additional plasma-chemical processing by ions of fluorine and hydrogen, which essentially increases the adsorption sensitivity to polar molecules.[6] Measurements by a secondary-ionic method of mass-spectrometry have shown that the concentration of ions of fluorine increased up to 3÷4 atomic percent in the surface of the material. Ions of fluorine and hydrogen have a stabilizing effect on the electric properties of this material.[8] The atom of fluorine is more active than oxygen, therefore contact to an air atmosphere is not accompanied by structural changes of the surface of the material. This operation essentially slows down processes of "ageing" of porous silicon in interaction with air. The doping of hydrogen ions of near-surface areas of porous material results in saturation of broken bond on silicon surface and plays an important role in physical properties of porous silicon.

Gas-transparent electric contacts from aluminum (Figure 1) are directly sprayed on the surface of the porous silicon after the end of the technological process of manufacturing.[6] Measurements of voltage-ampere

and voltage-farad characteristics of samples with an error of no more than 1% were made in the special measuring chamber.

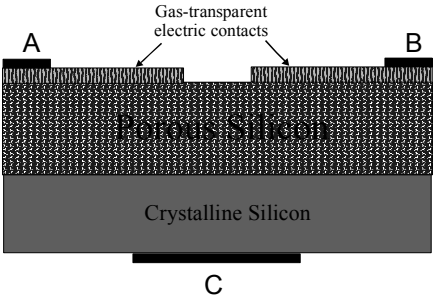

Figure 1. Geometrical structure of the investigated samples of the porous silicon formed on crystal silicon, with electric gas-transparent contacts from aluminum to porous silicon (A, B) and electric contacts to crystal silicon (C).

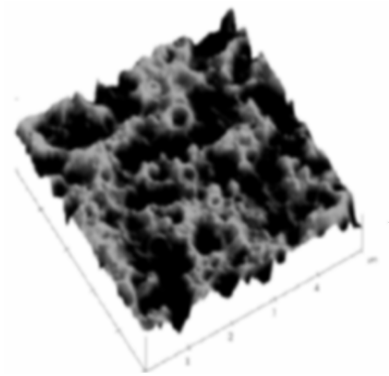

Figure 2. A photo of a surface of the investigated samples of the porous silicon obtained by a method of atomic-force microscopy.

By a method of atomic-force microscopy it is established that the surface of the investigated samples of porous silicon contains pores with diameter up to 300 nanometers (Figure 2).

The investigated viruses of plants were analyzed on the department of microbiology and virology of Odessa I.I. Mechnikov university. Viruses have characteristic diameter from 30 up to 100 nanometers that is less than pore sizes of the semiconductor material. Adsorption of viruses of plants was realized from identical water solutions containing different types of viruses. Regeneration (restoration of properties of the surface) is achieved by dissolution of organic substances and thermal processing in high vacuum.

3. Results and Discussion

In Figure 3 the measured current as a function of the imposed voltage after adsorption of viruses of plants is displayed. As can be seen, the curves show a complex behavior and no known mechanism can describe these dependences.

If we consider that the structure of porous silicon consists of a significant number of wires of different diameters, connected with each other, it is possible to suppose changes of the voltage-ampere

characteristics with the properties of the barriers, formed between them.[9] The significant number consistently included parallel the structures of diodes having variable band gap width and possess an effect of rectification.[7] Then, the character of voltage-ampere characteristics is determined by the passage of an electric current in an assembly of diodes.

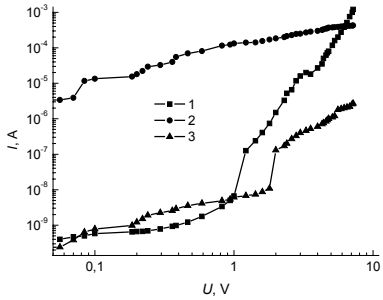

Figure 3. Current *I vs.* voltage *U* after adsorption of TORSV- (curve 1), GPL- (curve 2), SVA- (curve 3) viruses of plants.

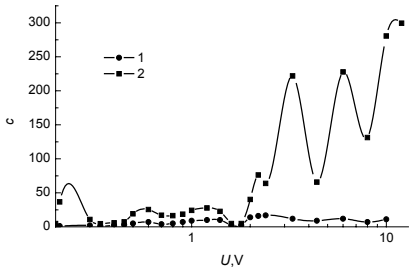

Figure 4. Dependence of the parameter *c* on the voltage *U* of the measurements in vacuum (curve 1) and after adsorption of TORSV-viruses of plants (a curve 2).

A voltage change on a sample results in a *U* redistribution on the diode structures, thus the parameter *c* will be distinct. The parameter *c* can be determined from the characteristics of a voltage-ampere curve through the formula: $c(U)=[\varphi \mathrm{d}(lnI)/\mathrm{d}U]$, where φ= 0.023 V at room temperature.[5] The numerical differentiation of the logarithm of the current can be executed in the Origin program. The dependence *c(U)* has an unusual character testifying for the benefit of the proposed model.

Dependences *c(U)* for adsorption of TORSV-, SVA-, and GPL- viruses of plants are presented in Figures 4 to 6. Under the influence of the researched adsorbed viruses the spectrum of the parameter *c(U)* depends on the type of the viruses. These results are important for the experimental detection of various types of viruses.

Before adsorption of viruses the size of the parameter *c(U)* did not exceed the magnitude of 3. However, under the influence of the researched adsorbed viruses the value of the parameter goes from 1 up to 800. Thus, the character of the change of *c(U)* depends on the type of the viruses. In view of the big displacement of *U*, the value of the current density also increases, as shown by the great values of the parameter *c(U)*. In this case the increase in the direct current can be explained by a process of tunneling of carriers through the conditions on the surface, connected by the adsorbed viruses.

In Figure 7 we display the results of measurements of voltage-farad characteristics (VFC) of porous silicon before and after adsorption of TORCV- viruses (curves 1 and 2). The capacity increases after adsorption of these viruses and has a non-monotone dependence on the imposed voltage. Under adsorption of other viruses, the character of change of VFC was analogous.

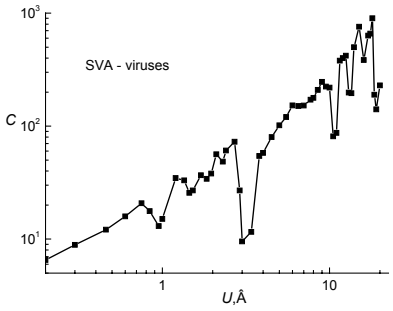

Figure 5. Dependence of the parameter *c* on the voltage *U* of the measurements after adsorption of SVA-viruses of plants.

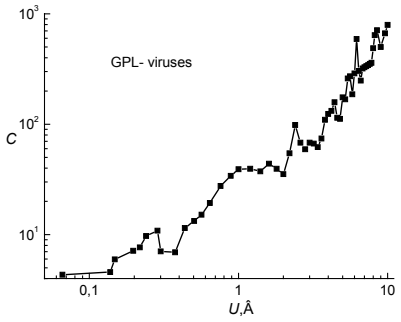

Figure 6. Dependence of the parameter *c* on the voltage *U* of the measurements after adsorption of GPL-viruses of plants.

The physical reason for the increase of the capacity can be connected with the appearance of charged particles (viruses) and the change of the electrostatic permeability inside the porous structure.[10] The non-monotone change of the capacity is possibly explained with the growth of a voltage with inter-localization systems of the located charges. It can occur through superficial conditions by means of tunneling of electrons. The voltage growth to higher located levels eventually reaches the Fermi's level, providing their connection to the tunneling process and resulting in new steps on the voltage-farad characteristics. According to the character of the conditions, formed by adsorbed viruses, the power backlash between levels is reduced in the process of transition from the bottom to the top levels at growth of voltage. Such cycles can be repeated.

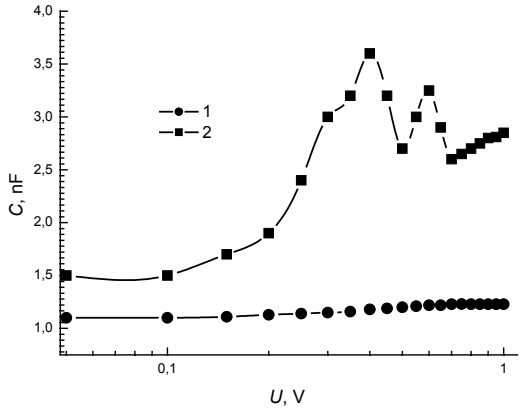

Figure 7. Voltage-farad characteristic of porous silicon before (curve 1) and after adsorption of TORCV- viruses (curve 2).

4. Conclusions

The obtained results testify that adsorption of viruses of plants influences the volt-ampere and volt-farad characteristics of samples of porous silicon. The observable phenomena are connected most likely to changes of characteristics of superficial conditions and barriers, generated between wires of porous silicon. The mechanism of influence of adsorption of charged polar biological molecules (viruses of plants) on voltage-ampere characteristics is connected with the redistribution of voltage on barrier structures and depends on the type of viruses. The measurement of electronic characteristics of porous silicon can be used for the creation of detectors for the presence of viruses in a given environment.

REFERENCES

1. C.A. Betty, R. Lal, D.K. Sharma, J.V. Yakhmi, and J.P. Mittal, Macroporous silicon based capacitive affinity sensors fabrication and electrochemical studies, *Sensors and Actuators B* 97, 334-343(2004).
2. O. Bisi, Porous silicon: a quantum structure for silicon based optoelectronics, *Surface Science Reports* 38, 1-126 (2000).
3. Yu.A.Vashpanov, About gas sensitivity properties of a real surface of silicon modified electrochemical processing in electrolyte on the basis of a HF acid, *Russian Journal* "*Surface*" 12, 87-98 (1998).
4. Yu.A. Vashpanov, Adsorption sensitivity of micro porous silicon to organic and biological molecules with high dipole moment, *International Forum on MicroNano Integration "MINIT 2003",* Potsdam, Germany, P5.2 (2003).
5. Yu.A. Vashpanov, and I.P. Perekrestov, Influence of adsorption polar molecules of ethanol and acetone on electric properties of porous silicon, *Russian Journal* "*Surface*" 10, 108-112 (2005).
6. Yu.A. Vashpanov, and V.A. Smyntyna, *Adsorption sensitivity of semiconductors* (Astroprint, Odessa, Ukraine, 2005).

7. Yu.A. Vashpanov, Electronic properties of microporous silicon under illumination and adsorption of ammonia, *Letters in Russian Journal of Technical Physics* 23(11), 77-82 (1997).
8. Yu.A. Vashpanov, Electronic properties and adsorption sensitivity to ammonia of microporous silicon, *Ukrainian Journal of Physics* 44(4), 468-470 (1999).
9. Yu. Vashpanov, Adsorption sensitivity of porous silicon to polar molecules, *VII Polish-Ukrainian Symposium on Theoretical and Experimental Studies of Interfacial Phenomena and their Technical Applications*, Lublin, Poland, 300-302 (2003).
10. Yu.A. Vashpanov, and A.N. Shushkov, Influence of adsorption of polar molecule on the capacitance of porous silicon, *Journal "The Bulletin of Odessa University"* 7, 234–239 (2003).

ADSORPTION STUDY OF LEAD BY *ASCOPHYLLUM NODOSUM* USING A FACTORIAL EXPERIMENTAL DESIGN

OLGA FREITAS*, RUI BOAVENTURA
LRSE – Laboratory of Separation and Reaction Engineering, Dep. Eng. Química, Faculdade de Engenharia da Universidade do Porto, Rua Dr. Roberto Frias, 4200-465 Porto, Portugal

CRISTINA DELERUE-MATOS
REQUIMTE, Instituto Superior de Engenharia do Porto, Rua Dr. Bernardino de Almeida, 431, 4200-072 Porto, Portugal

Abstract. A factorial design methodology was used to evaluate the effects of temperature, pH and initial concentration of Pb(II) in sorption process onto the marine macro-algae *Ascophyllum nodosum*. The Box-Behnken factorial design method gives a mathematical model that shows the influence of each variable and their interactions on the process efficiency. Study ranges were 10-40 ºC for temperature, 3.00-5.00 for pH and 50-200 mg/L for initial Pb(II) concentration. Within these ranges, the adsorption capacity is slightly dependent on temperature and pH but markedly increases with initial concentration. Maximum adsorption capacity of Pb(II) by *Ascophyllum nodosum* was 180 mg/g, which corresponds to the following values of those variables: temperature = 40 ºC, pH = 5.00 and initial concentration = 200 mg/L.

Keywords: experimental design; Box-Behnken; biosorption optimization; response surface methodology; marine macro-algae

*To whom correspondence should be addressed. Olga Manuela Matos de Freitas, Laboratory of Separation and Reaction Engineering, Departamento de Engenharia Química, Faculdade de Engenharia, Rua Dr. Roberto Frias, 4200-465 Porto, Portugal; e-mail: omf@fe.up.pt

J.M. Loureiro and M.T. Kartel (eds.), Combined and Hybrid Adsorbents, 269–274.

1. Introduction

Heavy metals are major pollutants in marine, ground and surface waters and particularly in urban and industrial wastewaters. Classical physicochemical techniques for heavy metals removal from aqueous solutions, such as precipitation and ion-exchange, are often ineffective and/or very expensive when used for the reduction of the metal content at low concentrations.[1,2]

Considerable research has been carried out in developing cost-effective techniques for heavy metals removal. One of the promising techniques for that purpose is based on the use of biological materials (living or nonliving organisms and their derivates) as biosorbents. Seaweeds present advantages for biosorption because their macroscopic structures offer a convenient basis for the production of biosorbent particles.[3] From all algal biomass available, marine algae are considered to be the most useful as biosorbents due to their abundance.[4] It has been reported that brown algae present a metal binding capacity superior to other organic and inorganic adsorbents.

The effects of various factors on the biosorption process have been studied extensively. Although most existing studies have concentrated on individual effects, it would be useful for understanding the complexity of systems to know the interactive effects of the factors.

The effect of temperature, pH and initial concentration of Pb (II) in sorption process onto marine macro algae *Ascophyllum nodosum* was studied by using a Box-Behnken factorial design method, which gives a mathematical model that shows the influence of each variable and their interactions.

2. Materials and Methods

2.1. PREPARATION OF THE BIOMASS AND METAL SOLUTIONS

Marine macro-algae *Ascophyllum nodosum* were colleted in February 2004 from the coast of the Atlantic sea in northern Portugal (Viana do Castelo). The algae were washed with distilled water in order to remove part of the salts existing in seawater and dried at room temperature. Then, they were ground (centrifugal mill Retsch, model ZM 100) and sieved (Retsch AS 200 siever) to get a fraction of particle size 0.5-1.0 mm. Analytical grade salt, $PbCl_2$, was used to prepare solutions.

2.2. ADSORPTION EXPERIMENTS

Weighted amounts (100 mg) of algae were added to each flask (100 mL capacity) containing 100 mL of metal aqueous solution and the pH was

adjusted to the required value by using NaOH or HCl. The flasks were agitated on a rotary shaker (Multi-stirrer, Velp Scientifica) for 2 hours. The pH of the solution was measured and re-adjusted after 2 hours and the agitation proceeded for 30 minutes more. The suspensions were filtered (cellulose acetate membrane filters, Ref. Albet-AC-045-25-BL) and the metal contents in the filtrates were determined by atomic absorption spectrometry (GBC 932 Plus AAS, Australia). Adsorption capacities (Q, mg/g) were calculated using the values of initial and final metal concentrations in solution.

2.3. EXPERIMENTAL DESIGN

Response Surface Methodology (RSM) is an experimental technique designed to find the optimal response within specified ranges of the factors.

Box-Behnken design was chosen to study the effects of three factors considered to have the most significant effect on the biosorption process: temperature (ºC), pH and metal initial concentration (mg/L). The 2^k factorial design only requires three levels of each factor and is rotatable.[5] Each factor was studied at three different levels (-1, 0, +1). The inclusion of centre points offered a more precise estimate of experimental error and provided a measure for the adequacy of the model (lack of fit). It also enabled the determination of the significance of the interactions between factors. The minimum and maximum range of the investigated factors and the correspondence between real and coded forms are listed in Table 1.

TABLE 1. Experimental range of the factors: actual and coded forms

	Code levels		
Factor	-1	0	1
T - Temperature (ºC)	10	25	40
pH	5.0	4.0	3.0
C - Initial concentration (mg/L)	50	125	200

Using a statistical analysis software package (JMP 5.0.1.) a regression analysis was performed to determine the coefficients of a second-degree polynomial of the form:

$$y = \beta_0 + \sum_{i=1}^{k} \beta_i x_i + \sum_{i=1}^{k} \sum_{j=i}^{k} \beta_{ij} x_i x_j \qquad (1)$$

where y is the response variable, β_0 is the intercept, β_i are coefficients and x_i processing variables.

The statistical analysis of variance (ANOVA) included the Fisher's F-test (overall model significance), its associated probability p>F and the

correlation coefficient R^2, which measures the goodness of fit of regression model and lack of fit. It also includes the Student's t-value for the estimated coefficients and the associated probabilities p>|t|. The combined effect of two factors on the adsorption capacity was plotted as a response surface, for a given value of the third variable.

3. Results and Discussion

The Box-Behnken experimental design required 15 runs in duplicate, three of which correspond to the three factors at their central levels.

Based on F-test and Student's t-test, some effects were discarded, because they did not exhibit any statistical significance. The resulting model is represented by:

$$Q = 110.11833 + 3.93125\left(\frac{T-25}{15}\right) + 2.93125\,(pH-4) + 60.626875\left(\frac{C-125}{75}\right) + 5.1775\left[(pH-4)\left(\frac{C-125}{75}\right)\right] + 2.7833333\left[(pH-4)(pH-4)\right] \quad (2)$$

Figure 1 shows the response surface diagrams of Pb(II) adsorption capacity versus pH and initial concentration, at constant temperature of 40 (a) and 10 ºC (b). The largest Pb adsorption capacity was achieved at the higher levels of pH (5.00) and initial concentration (200 mg/g).

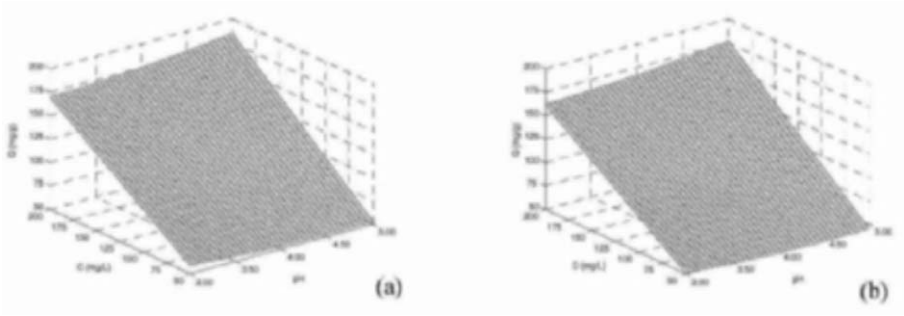

Figure 1. Response surface plots showing the effect of initial concentration and pH on biosorption of Pb(II) at 40 ºC (a) and 10 ºC (b).

Figure 2 illustrates the combined effect of temperature and pH on the biosorption capacity. Pb(II) uptake efficiency increases with pH for a high initial Pb concentration. However, an inverse effect is observed for a low initial Pb concentration. Regardless of the temperature, when increasing of pH from 3.00 to 5.00, the uptake capacity increases approximately 15 mg/g in the first situation and decreases around 6 mg/g in the second one.

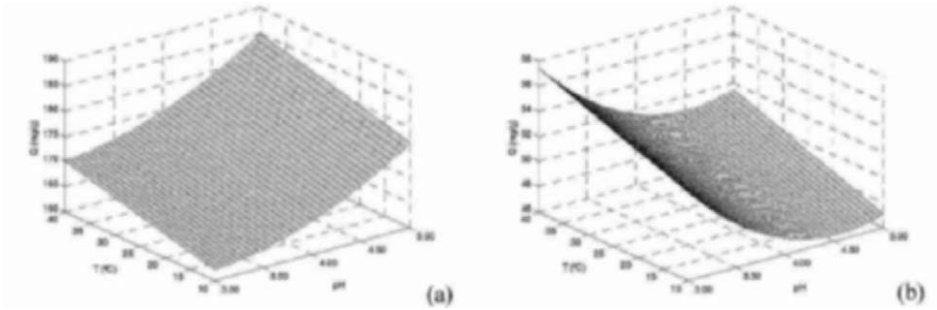

Figure 2. Response surface plots showing the effect of temperature and pH on biosorption of Pb(II) at initial concentration 200 mg/L (a) and 50 mg/L (b).

The response surfaces obtained for variable values of initial concentration and temperature, and constant values of pH - 5.00 (a) and 3.00 (b) - are displayed in Figure 3. Once again it can be observed the strong influence of the initial concentration and the small contribution of temperature.

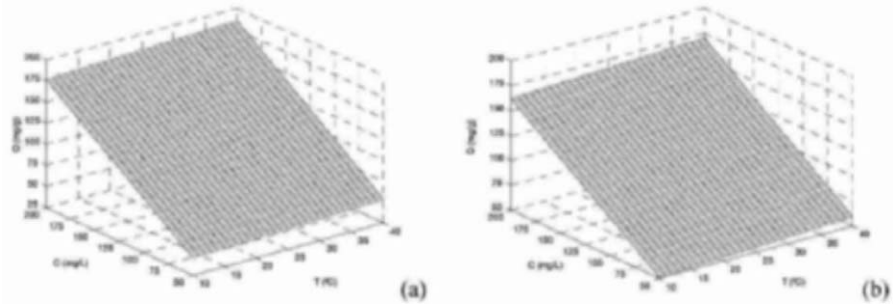

Figure 3. Response surface plots showing the effect of initial concentration and temperature on biosorption of Pb(II) at pH 5.00 (a) and 3.00 (b).

4. Conclusion

The biosorption process of Pb(II) on *Ascophyllum nodosum* is affected by temperature, pH and initial concentration of Pb(II). The influence of these factors on the uptake of lead by the algae decreases as follows: initial concentration > pH > temperature. The largest biosorption capacity (180 mg/g) was obtained at pH = 5.00, temperature = 40 ºC and initial concentration of Pb(II) = 200 mg/g.

ACKNOWLEDGEMENTS

Olga Freitas is grateful to the Ph.D. grant given by PRODEP Program.

REFERENCES

1. G. Çetinkaya Dönmez, Z. Aksu, A. Öztürk, and T. Kutsal, A comparative study on heavy metal biosorption characteristics of some algae, *Process Biochem*. 34, 885-892 (1999).
2. M.E.R. Carmona, M.A.P Silva, and S.G.F Leite, Biosorption of chromium using factorial experimental design, *Process Biochem*. 40, 779-788 (2005).
3. R.H.S.F. Vieira, and B. Volesky, Biosorption: a solution to pollution?, *International Microbiologia* 3, 17-24 (2000).
4. W.B. Amorim, A.M. Hayashi, P.F. Pimentel, and M.G.C. Silva, A study of the process of desorption of hexavalent chromium, *Braz. J. Chem. Eng*. 20(3), 283-289 (2003).
5. G.E.P. Box, W.G. Hunter, and J.S. Hunter, 1978, *Statistics for Experimenters. An Introduction to Design, Data Analysis, and Model Building*, John Wiley & Sons, New York, pp. 453-537.

APPLICATION OF CHITIN CONTAINING SORBENTS FOR TREATMENT OF WATER SOLUTIONS

TATYANA SOLODOVNIK*
Cherkassy State Technological University, 460, Shevchenko Boulevard, 18006, Cherkassy, Ukraine

Abstract. The objective of this work was to study the sorption properties of chitin containing sorbents (ShCS) which were prepared from fungus mycelium of *Aspergillus niger* – waste of biotechnological production of citric acid. These sorbents were used for removing heavy metals (Cu(II), Zn(II), Cr(VI), Cd(II), Pb(II)) from water solutions. For comparison chitosan containing sorbents (ChaCS) from *Aspergillus niger*, which are prepared according to the Muzzarelli method, were used. The influence of the degree of deacetylation (DD) and size of particles on the sorption properties of ChCS and ChaCS was shown. Molecular modeling of chelating complex Pb(II) – chitin was realized by the method of molecular mechanics MM+.

Keywords: chitin; chitosan; sorbent; mycelium; fungus, biomass; *Aspergillus niger*; citric acid; heavy metals, waste

1. Introduction

Last years the concern of scientists and contributors to chitin, chitosan and chitin containing compounds has increased. It is connected to their widespread occurrence in nature, particular properties, and also feasibility in many areas of a national economy. They are widely used as sorbents for sorption of the ions of heavy metals, soluble dyes and petroleum from water

* To whom correspondence should be addressed. Tatyana Solodovnik, Cherkassy State Technological University, 460, Shevchenko Boulevard, 18006, Cherkassy, Ukraine; e-mail: soltav@chiti.uch.net

J.M. Loureiro and M.T. Kartel (eds.), Combined and Hybrid Adsorbents, 275–280.

solutions.[1,2] The raw sources for obtaining chitin containing products are the shell of crabs, lobsters, shrimps, and also green water-plants, funguses.

The researchers of department of chemistry of the Cherkassy State Technological University developed an ecologically safe method of obtaining chitin containing sorbents (ChCS) from fungus mycelium of *Aspergillus niger* which differs by "soft" conditions of processing initial biomass. The aim of this work was the analysis of the physical and chemical characteristics of ChCS and also of their sorbate properties in relation to ions of heavy metals. In earlier works, based on an elemental analysis, it was established that ChCS comprises 31% chitin, 65% glucan, 2.5% melanin and 1.5% proteins.[3,4]

2. Experiment

Insoluble chitin containing sorbents were obtained from waste received during biotechnological production of citric acid. The waste is biomass of *Aspergillus niger*. The biomass was consecutively treated by a hot (60 ºC) 1% NaOH water solution for 90 minutes, washed by distilled water, 1 M HCl solution and finally by organic solvent. The finished product was dried at 40°C for one hour. The degree of deacetylation (DD) of ChCS is 0,8%. ChCS, grinded by a ball mill to the 100-200 mesh size of particles, was used as a raw material for obtaining chitosan containing sorbents (ChaCS) by a known method.[5] This method includes the treatment of an initial raw material by a 40% NaOH water solution for 4 hours at a temperature of 118 ºC. Such conditions of treatment were chosen as the most favorable for obtaining chitosan containing sorbents with good sorption characteristics and with a degree of deacetylation of 96%. The degree of deacetylation was determined based on the sorbent infrared spectra (IR) using the following equation:[6]

$$DD = \left[1 - \left(\frac{A_{1655}}{A_{3450}}\right)\frac{1}{1{,}33}\right] \cdot 100$$

where A_{1655} and A_{3450} are absorbency values at 1655 and 3450 cm^{-1} for the amide I and hydroxyl bands, respectively.

Modelling of chelating complex Pb(II) – chitin was realized by the method of molecular mechanics MM+[7] using the HyperChem program.

In this work the sorption of ions of heavy metals (Cu(II), Zn(II), Cr(VI), Cd(II), Pb(II)) on ChCS in static conditions was studied; 0.02 g of sorbent (ChCS or ChaCS) were shaken in a 0.125 mM solution (100 ml) of the metals salts for 1 hr at 20 ºC and pH = 6,8. After filtration, the analysis was

carried out by flame atomic absorption spectrometry. The sorption capacity q (mg/g) was calculated from:

$$q = \frac{(C_{in} - C_{eq}) \cdot V}{m}$$

where C_{in} is the initial metal concentration in solution (mg/L); C_{eq} is the equilibrium concentration (mg/L); V is the sample volume (L); and m is the sorbent weight (g).

For an estimation of the selective sorbate ability of ChCS and ChaCS, the distribution factor K_d was determined from:

$$q = \frac{(C_{in} - C_{eq}) \cdot V}{C_{eq} \cdot m}$$

3. Results and Discussion

It is known that chitin extracts metals ions from water solutions, forming chelating complexes. However, practically no information exists on which functional groups are involved in this process. In our molecular modeling representation, different atoms of oxygen and nitrogen from two chitin chains, as well as H_2O and Pb^{2+} were involved. Optimization was carried out for four possible structures. The most probable is a complex that consists of the lead ion between two chitin chains, where in the Pb^{2+} coordination participate the ring oxygen (O-5´) and the oxygen of the C-3 hydroxyl (Fig.1). This chelating complex is stable with the minimal energy of conformation of 349.4 kJ/mol. These data agree with those obtained in chitin-cadmium complexation in the wall of a *Neurospora crassa* cell, grown under conditions of Cd-toxicity.[8]

For the assessment of sorbents elective to extract the metals ions, the distribution coefficient K_d was calculated (Table 1).

TABLE 1. Distribution coefficient for ChCS and ChaCS

Sorbent	K_d, mL/g				
	Cu (II)	Zn (II)	Cr (VI)	Cd (II)	Pb (II)
ChCS	2000	410	348	610	2000
ChaCS	49500	500	5750	816	9462

The K_d values shown in Table 1 for the sorbents under study are compatible with chelating sites of a poly-amphoteric nature.

For ChCS: Pb (II) = Cu (II) > Cd (II) > Zn (II) > Cr (VI);

For ChaCS: Cu (II) > Pb (II) > Cr (VI)> Cd (II)> Zn (II).

We think that this can be explained by the fact that the composition of the sorbents includes amino, carboxyl and hydroxyl groups, which will form stable chelating complexes with the metals ions.

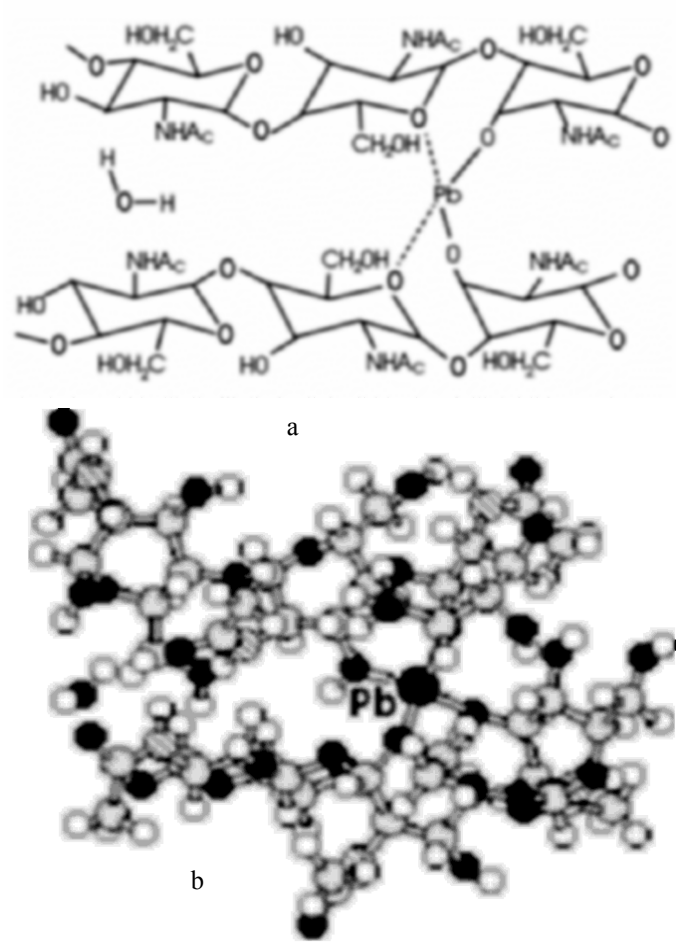

Figure 1. Chelating complexes chitin-lead: a – before optimization; b – after optimization:
- Pb; - N; - C; - H; - O.

The sorption ability of the chitincontaining sorbents for Cu(II), Zn(II), Cr(VI), Cd(II) and Pb(II) ions, obtained with samples of sorbents with different particle sizes after a 1-h contact, are presented in Table 2.

The particles size influences the sorption ability of the sorbents. The decrease of the particles size is accompanied by an increase of the sorption ability of the sorbents for all metals studied. This fact can be ascribed to an

increase of the active surface of the sorbents and by the larger accessibility of the metals to the functional groups.

Increasing the degree of deacetylation (DD) of the sorbents contributes to an increment of their sorption ability, especially for Cr (VI) ions. These results can be explained by the increase of the number of pores within the structure of the sorbents and to a larger access of the metals to the amino groups. The values for the removal of Cr(VI) ions with ChaCS are larger because they complex easily with amino groups than the other metals.

TABLE 2. Dependence of the sorbents sorption ability on the particles size and DD

Sorbent	DD,%	Particle size, μm	q, mg/g				
			Cu(II)	Zn(II)	Cr(VI)	Cd(II)	Pb(II)
ChCS	0,8	710-850	22,4	10,4	3,7	22,4	61,8
		355-500	25,6	13,6	5,1	26,9	80,3
		150-250	32,0	18,2	6,8	38,0	103,6
ChaCS	96	710-850	27,5	11,7	11,3	31,4	88,6
		355-500	30,4	15,6	12,8	35,3	107,1
		150-250	36,8	20,5	15,8	43,1	130,8

4. Conclusions

In this work it is shown that the biomass of the *Aspergillus niger* fungus mycelium, a waste from the biotechnological production of citric acid, may be used for the preparation of chitin-containing sorbents, by a method suggested by the authors; they can also be used for the preparation of chitisan-containing sorbents by previously known methods. These sorbents from *Aspergillus niger* can be an alternative to animal chitin and chitosan for the removal of metal ions from water solutions. It is known that the sorption of metals on chitin and chitosan is accompanied by the formation complexes. Modeling and quantum-chemical computations of these complexes showed that the most probable is a complex which consists of the metal ion between two chitin chains and also that the ring oxygen (O-5′) and the oxygen of C-3 hydroxyl participate in the Me^{2+} coordination. The sorption ability of the sorbents for Cu(II), Zn(II), Cr(VI), Cd(II) and Pb(II) ions is dependent on the degree of deacetylation and on the particles size.

As shown in our earlier works[3,4] ChCS and ChaCS are good petroleum and soluble dyes sorbents from water solutions. Economically and ecologically it is more favourable to use ChCS since, in their production process, the biomass is processed using lower concentration chemical solutions at a temperature of about 60 ºC.

REFERENCES

1. R.A.A. Muzzarelli, F. Tanfani, and G. Scarpini, Chelating, film-forming, and coagulating ability of the chitosan-glucan complex from *Aspergillus niger* industrial wastes. *Biotechnology and Bioengineering* 22, 885-896 (1980).
2. G.A.F. Roberts, *Chitin Chemistry*. MacMillan Press, London (1992).
3. Solodovnik T., Unrod V., Lega Y. Chitin-containing complexes from mycelium of Aspergillus for sorption of petroleum. In: R.A.A.Muzzarelli and C.Muzzarelli (eds), *Chitosan in pharmacy and chemistry*, Atec Edizioni, Grottammare, Italy, 475-478 (2002).
4. T.V. Solodovnik, V.I. Unrod, and S.A. Pakhar, Removal of soluble dyes from solution using chitincontaining complexes. Advances in Chitin science. Vol.VIII. Henryk Struszczyk, Alain Domard, Martin G. Peter, Henryk Pospieszny Eds.: Institute of Plant Protection. Poznan, 379-383 (2005).
5. R.A.A. Muzzarelli, Chitosan-Glucan Komplex und Verfahren zu diesen Herstellung, *Patent FRG*, COSB 37/08, Nº 2923802, 1979.
6. C.Y. Kim, H-M. Choi, and H.T. Cho, Effect of deacetylation on sorption of dyes and chromium on chitin, *J. Appl. Polym. Sci.* 63, 725–736 (1997).
7. P. Gund, D.C. Barry, J.M. Blaney, and N.C. Conen, Guidelines for publications in molecular modeling related to medicinal chemistry, *J. Med. Chem.* 31, 2230–2234 (1988).
8. M. Bhanoori, and G. Venkateswerlu, *In vivo* chitin-cadmium complexation in cell wall of *Neurospora crassa*, *Biochim. Biophys. Acta* 1519: 21-28 (2000).

BIOSORPTION PERFORMANCE OF A BINARY METAL MIXTURE BY ALGAL BIOMASS: COLUMN EXPERIMENTS

VÍTOR VILAR*, CIDÁLIA BOTELHO AND RUI BOAVENTURA
LSRE, Department of Chemical Engineering, University of Porto, Rua Dr. Roberto Frias, 4200-465 Porto, Portugal

Abstract. Raw seaweed *Gelidium sesquipedale* and a composite material prepared from an industrial algal waste have been converted into inexpensive biosorbents, which were used for removal of Pb^{2+}/Cd^{2+} from aqueous solutions. The equilibrium data follow a multi-component discrete model and indicate a good adsorption capacity. The biosorption behavior of both materials during one sorption-desorption cycle of Pb^{2+}/Cd^{2+} has been investigated in a packed-bed flow-through column. In the sorption process, Cd breaks through the column faster than Pb due to its low affinity. An overshoot in the outlet Cd concentration was observed and explained by ion exchange between Pb and Cd, whereby the higher affinity of the Pb ion displaces the Cd ion bounded to the biosorbent. A 0.1 M HNO_3 solution was used as eluant for the desorption process. Desorption was 100% effective for Cd and Pb. A mass transfer model for the adsorption and desorption processes was used to simulate the column performance.

Keywords: Biosorption; Lead; Cadmium; *Gelidium*; Column; Modeling

1. Introduction

Industrialization and urbanization have led to an increase in metal contamination of aquatic environments. Metal removal/recovery is usually achieved by precipitation as hydroxides, sulfides and oxalates; ion

* To whom correspondence should be addressed. Vítor Jorge Pais Vilar, Laboratory of Separation and Reaction Engineering, Department of Chemical Engineering, University of Porto, Rua Dr. Roberto Frias, 4200-465 Porto, Portugal; e-mail: vilar@fe.up.pt

J.M. Loureiro and M.T. Kartel (eds.), Combined and Hybrid Adsorbents, 281–286.

exchange by chemical or electrochemical means; reverse osmosis; chemical or physical adsorption; chemical reduction and biochemical remediation.[1-3] These processes may be ineffective or extremely expensive, especially when concentrations of dissolved metal(s) are in the order of 1 to 100 mg/L.[1-3] Alternative methods based on metal-sequestering properties of certain natural materials of biological origin are under study. Particularly, biosorption processes are potentially advantageous for economical and environmental reasons.

Biosorption on nonliving algal biomass involves a combination of different reactions that can occur in the cell wall, as complexation, coordination, chelation of metals, ion exchange, adsorption and inorganic microprecipitation. Metal uptake is also possible due to electrostatic interactions between metal cations and negatively charged sites at the cell surface.[1-3]

This work aims at studying the biosorption of a binary mixture Pb^{2+}/Cd^{2+} by *Gelidium* algae and by a composite material. Equilibrium isotherms were determined at pH 5.3, 4 and 3 for Pb^{2+}, at pH 6.5, 5.3 and 4 for Cd^{2+} and at pH 5.3 for the mixture Pb^{2+}/Cd^{2+}. Continuous adsorption experiments for the binary mixture were also performed in a packed column.

2. Materials and Methods

2.1. PREPARATION OF BIOSORBENTS AND LEAD/CADMIUM SOLUTION

An algal waste from agar extraction industry was immobilized in Polyacrylonitrile (PAN) and used in this study as well as *Gelidium* algae, the raw material for agar extraction. The characteristics and preparation of both materials were presented in a previous work.[4,5]

Pb(II) and Cd(II) solutions were prepared by dissolving lead and cadmium chloride dehydrate in distilled water. The pH of each test solution was adjusted with diluted HNO_3 and NaOH solutions.

2.2. COLUMN EXPERIMENTS

Column experiments were conducted at constant temperature in a 2.5 cm inner diameter and 15 cm length jacketed glass column, packed with *Gelidium* algae or composite material. Metal solutions ($\approx$ 50 mg L^{-1}) were pumped down through the column at a flow rate of 4 mL min^{-1}. Effluent samples were collected regularly by using a fraction collector and analyzed by AAS. The pH of the effluent was recorded. After column exhaustion, the

biomass loaded with Pb and Cd was regenerated using 0.1 M HNO_3. The flow rate was adjusted to 8 mL min^{-1}.

2.3. EQUILIBRIUM MODEL

A mathematical equilibrium model was developed assuming one kind of active sites (carboxylic groups) in the cell wall, which are responsible for metal biosorption at pH < 6.0, and competition between metal ions and protons. The model is based on apparent equilibrium binding constants, K_H and K_M for H^+ and M^{2+}, respectively. The total metal uptake can be calculated as:

$$q_{M_i} = \frac{Q_{max}\ K_{M_i}\ C_{M_i}}{1 + K_H\ C_H + \sum_{i=1}^{n} K_{M_i}\ C_{M_i}} \tag{1}$$

This equation can be converted in the binary Langmuir equation:

$$q_{M_i} = \frac{Q_{max}\ K'_{M_i}\ C_{M_i}}{1 + \sum_{i=1}^{n} K'_{M_i}\ C_{M_i}}\ ;\ \text{where}\ K'_{M_i} = \frac{K_{M_i}}{1 + K_H\ C_H} \tag{2}$$

From the values of K_M and K_H it is possible to calculate the Langmuir equilibrium constant for a given pH value (pH = -log C_H).

2.4. COLUMN OPERATION

A model was developed assuming isothermal operation, axial dispersed plug flow of the fluid phase, adsorption equilibrium described by Eq. (2) for a binary system, external and internal mass transfer resistances described by the LDF approximation. The dimensionless model equations are:

Mass conservation in the fluid around particles

$$\frac{\partial y_{b_i}}{\partial \theta} = \frac{1}{Pe}\frac{\partial^2 y_{b_i}}{\partial x^2} - \frac{\partial y_{b_i}}{\partial x} - \xi_i\ N_{d_i}\left[y_{M_i} - \langle y_i \rangle\right] \tag{3}$$

Mass conservation inside particles (LDF-Linear Driving Force)

$$\frac{d\langle y_i \rangle}{dt} = N_{d_i}\left[y_{M_i} - \langle y_i \rangle\right] \tag{4}$$

If there is no accumulation in the fluid film surrounding particles

$$\frac{d\langle y_i\rangle}{d\theta} = \frac{N_{f_i}}{\xi_i}\left(y_{b_i} - y_{f_i}\right) \tag{5}$$

Equaling Eq. (4) to Eq. (5) and deriving in order to time we will get:

$$\frac{d\, y_{b_i}}{d\theta} - \frac{d\, y_{f_i}}{d\theta} = \frac{N_{d_i}\, \xi_i}{N_{f_i}}\left[\sum_{i=1}^{2} \frac{\partial\, y_{M_i}}{\partial\, y_{f_i}} \frac{\partial\, y_{f_i}}{\partial\, \theta} - \frac{d\langle y_i\rangle}{d\theta}\right] \tag{6}$$

Solving the linear system of two variables, we obtain:

$$\frac{d\, y_{f_1}}{d\theta} = \frac{\left[\gamma_1 \frac{d\langle y_1\rangle}{d\theta} + \frac{d\, y_{b_1}}{da}\right] D + \left[\gamma_2 \frac{d\langle y_2\rangle}{d\theta} + \frac{d\, y_{b_2}}{da}\right]\left[\left(1+\gamma_1\,\alpha_1\right)\gamma_1\,\alpha_2\right]}{\left[1+\gamma_1\,\alpha_1+\gamma_2\,\beta_2+\gamma_1\,\gamma_2\left(\alpha_1\,\beta_2-\alpha_2\,\beta_1\right)\right]\left(1+\gamma_1\,\alpha_1\right)} \tag{7}$$

$$\frac{d\, y_{f_2}}{d\theta} = \frac{\left[\gamma_1 \frac{d\langle y_1\rangle}{d\theta} + \frac{d\, y_{b_1}}{da}\right]\left(\gamma_2\,\beta_1\right) + \left[\gamma_2 \frac{d\langle y_2\rangle}{d\theta} + \frac{d\, y_{b_2}}{da}\right]\left(1+\gamma_1\,\alpha_1\right)}{\left[1+\gamma_1\,\alpha_1+\gamma_2\,\beta_2+\gamma_1\,\gamma_2\left(\alpha_1\,\beta_2-\alpha_2\,\beta_1\right)\right]} \tag{8}$$

where D, α_1, α_2, β_1 and β_2 are model constants.

Initial and boundary conditions are:

$$\theta = 0 \qquad y_{b_i} = y_{f_i} = \langle y_i\rangle = 0 \tag{9}$$

$$x = 0 \qquad -\frac{1}{Pe}\frac{\partial\, y_{b_i}}{\partial\, x} + y_{b_i} = 1 \tag{10}$$

$$x = 1 \qquad \left.\frac{\partial\, y_{b_i}}{\partial\, x}\right|_{x=1} = 0 \tag{11}$$

The dimensionless variables are defined as:

$$x = \frac{z}{L},\ \theta = \frac{t}{\tau},\ y_{b_i} = \frac{C_{b_i}}{C_{E_i}},\ y_{f_i} = \frac{C_{f_i}}{C_{E_i}},\ \langle y_i\rangle = \frac{\langle q_i\rangle}{Q_{max}},\ y_{M_i} = \frac{q_{M_i}}{Q_{max}} \tag{12}$$

And the dimensionless parameters as:

$$\tau_{d_i} = \frac{R^2}{D_{h_i}},\ \xi_i = \frac{(1-\varepsilon)}{\varepsilon}\rho_{ap}\frac{Q_{max}}{C_{E_i}},\ N_{f_i} = \frac{(1-\varepsilon)}{\varepsilon}k_{f_i}a_p\tau,$$

$$N_{d_i} = k_{p_i}a_p\tau = \frac{3}{\tau_{d_i}}\tau = 3\frac{D_{h_i}}{R^2}\tau,\ Pe = \frac{u_i L}{D_{ax}} \quad (13)$$

The partial differential Eqs. (3) and (4) for each component, and Eqs. (7) and (8) in conjunction with the initial and boundary conditions (Eqs. 9-11) for each component, were solved by the FORSIM package.[6]

3. Results and Discussion

The experimental equilibrium results for single biosorption of lead at pH 5.3 and 4 and cadmium at pH 6.5, 5.3 and 4 were fitted to the discrete model (Eq. 1). The model parameters obtained for the Pb(II)/Cd(II) biosorption at pH 5.3 were: Q_{max} = 0.28 ± 0.01 and 0.098 ± 0.002 mmol/g, pK_H = 4.1 ± 0.1 and 4.6 ± 0.1, pK_{Pb}= 4.0 ± 0.1 and 4.5 ± 0.1 and pK_{Cd}= 3.2 ± 0.1 and 3.4 ± 0.1 (with the K values in L/mol), respectively for algae *Gelidium* and composite material. Comparison among experimental data and predicted values by the discrete equilibrium model is shown in Figure 1.

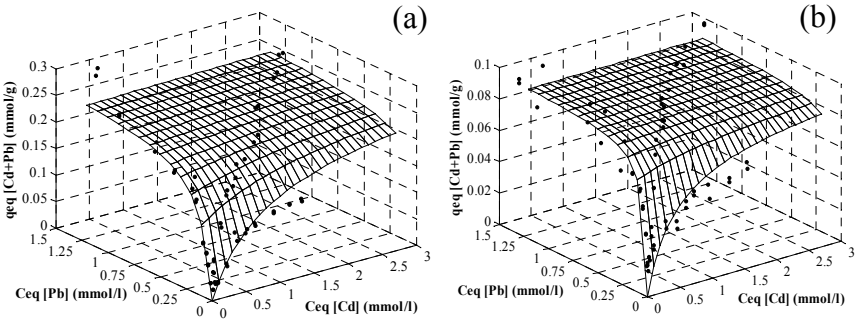

Figure 1. Pb(II)/Cd(II) sorption isotherm surface at pH 5.3: experimental data and predicted by the discrete model for algae (a) and composite material (b).

The breakthrough curves for the binary system (0.24 mmol/L of Pb and 0.43 mmol/L of Cd) at pH 5.6, flow rate = 4 mL/min and T = 20ºC, are presented in Figure 2. Cadmium breaks through the column faster than lead due to its low affinity. The overshoot of the Cd exit concentration is explained by ion exchange between Pb and Cd, whereby the higher affinity of Pb displaces Cd already bound to the biosorbent. The proton concentration profile is due to ion exchange between the metal ions and the

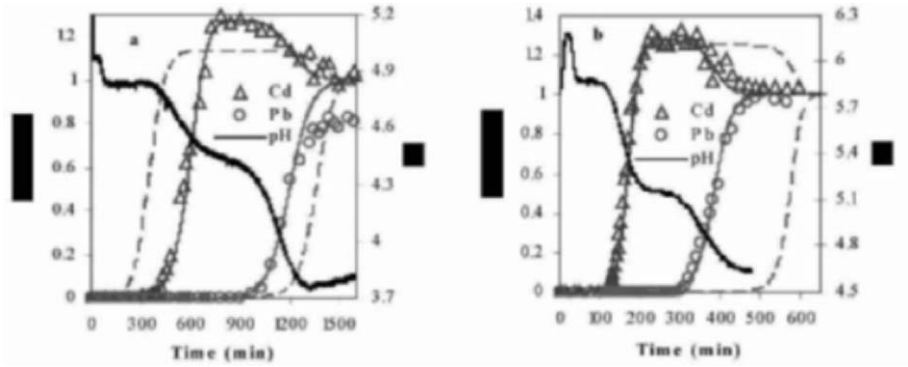

Figure 2. Comparison of experimental Pb(II)/Cd(II) breakthrough curves with predicted ones by the mass transfer model and the pH breakthrough curve; (a) – algae; (b) - composite material.

protons bounded to the active sites. In practice, the pH breakthrough curve may be used as an indication of metal breakthrough. The curves predicted by the mass transfer model are also shown in Figure 2. The dotted lines correspond to the equilibrium parameters presented above. Simulations for algae using K_{Cd} = 1.2 L/mmol (instead of 0.54 L/mmol) and K_{Pb} = 4.8 L/mmol (instead of 11.8 L/mmol) are shown as solid lines. The equilibrium parameters were determined at the equilibrium pH values (3.8 and 4.6), observed at the end of the experiments. As metal mixture biosorption was performed at pH 5.3, those values can only be considered as first estimates.

Elution of the biomass loaded with Pb and Cd can be 100% effective using as eluant HNO_3 0.1 M, and occurs rapidly in the first minutes.

REFERENCES

1. B. Volesky, *Biosorption of Heavy Metals* (CRC Press, Montreal, 1990).
2. B. Volesky, *Sorption and Biosorption* (BV Sorbex, Inc., Montreal, 2003).
3. J. Wase, C. Forster, *Biosorbents for Metal Ions* (Taylor & Francis, London, 1997).
4. V.J.P. Vilar, F. Sebesta, C.M.S. Botelho, and R.A.R. Boaventura, Equilibrium and kinetic modelling of Pb^{2+} biosorption by granulated agar extraction algal waste, *Proc. Biochem.*40, 3276-3284 (2005).
5. V.J.P. Vilar, C.M.S. Botelho, and R.A R. Boaventura, Influence of pH, ionic strength and temperature on lead biosorption by *Gelidium* and agar extraction algal waste, *Proc. Biochem.*40, 3267-3275 (2005).
6. M.B.Carver, D.G. Stewart, J.M. Blair, and W.N. Selander, A Fortran-oriented simulation package for the automated solution of partial and ordinary differential equation systems, Atomic Energy of Canada Limited-5821, 1979.

REMOVAL OF SELENIUM AND ANTIMONY SPECIES FROM AQUEOUS SOLUTIONS BY MEANS OF A WEAKLY BASIC ION EXCHANGER

MERCY S. DZUL EROSA* AND WOLFGANG H. HÖLL
Forschungszentrum Karlsruhe, Institute for Technical Chemistry, Section WGT, P.O. Box 3640, D-76021 Karlsruhe, Germany

Abstract. The removal of Se(IV), Se(VI), Sb(III) and Sb(V) from aqueous solutions by ion exchange using the commercially available weakly basic anion exchanger Duolite A7 with secondary amino groups has been investigated. This work comprises investigations of the equilibria of the sorption of Se and Sb and of the kinetics of uptake. The efficiency of sorption of selenium and antimony species depend strong on the pH. Se(IV) is well sorbed in a narrow range between pH 2.5 and 5.5 whereas Se(VI) is well sorbed between pH = 1 and 6. Sb(III) shows a maximum sorption between pH = 1 and 7, and for Sb(V) optimum sorption is obtained for pH < 5. The kinetic studies show that Se(VI) was removed almost completely in 20 min while sorption of the other species developed slowlier. Studies on sorption equilibria from pure solutions revealed the highest exchanger loadings for Se(VI) and smaller ones for the other species.

Keywords: Selenium; Antimony; Ion Exchange

1. Introduction

Selenium is a trace element, which occurs naturally in the environment. Selenium can be either an essential element or a potential toxicant for organisms, depending on its concentration and chemical form.[1] Antimony is

* To whom correspondence should be addressed. Mercy S. Dzul Erosa, Forschungszentrum Karlsruhe, Institute for Technical Chemistry, Section WGT, P.O. Box 3640, D-76021 Karlsruhe, Germany; e-mail: mercy-sugey.dzul@itc-wgt.fzk.de

J.M. Loureiro and M.T. Kartel (eds.), Combined and Hybrid Adsorbents, 287–292.

ubiquitously present in the environment as a result of natural processes and human activities. Sb(III) and Sb(V) and their compounds are of priority pollution interest. The USEPA drinking water standards recommended maximum contaminant levels of 6 μg/L for antimony and 0.05 mg/L for selenium.[1-3] To meet the standards, different methods have been proposed for removal of selenium and antimony species. These include coagulation with alum and ferric sulfate, lime soda softening, reverse osmosis and activated alumina adsorption,[3] which exhibit efficiencies varying with the speciation of selenium and antimony. The limited efficiencies encountered in these methods are sludge or use of large quantities of reactants, led to research for new methods for selenium and antimony separation.[1,4] Ion exchange offers another possibility. The use of strongly and medium basic anion exchanger as well as of chelating exchanger has been described.[6,7] Contrary to these investigations, the application of a weakly basic exchanger has been studied in this work.

2. Materials and Methods

Experiments for selenium and antimony species removal from water were carried out using the commercially available weakly basic anion exchanger Duolite A7 with secondary amino groups.

For the experiments, the resin was first pretreated with hydrochloric acid and sodium hydroxide to remove impurities from their synthesis. After extensive rinsing with demineralized water the exchanger was applied for the experiments. The resin material has been sieved and divided into 7 fractions.

3. Sorption Experiments

The study of the pH influence was carried out using twenty 0.2 L samples with initial pH values between 0 – 5 and with an initial concentration of 8 μmol L^{-1} for antimony and 12.66 μmol L^{-1} for selenium in contact with 1 g of exchange material for 48 h. After this time the pH and the selenium or antimony concentrations were determined.

The equilibrium sorption results were obtained by mixing various quantities of resin between 0.01 and 4 g with 0.2 L of aqueous solutions. The initial pH was 2.5 for Se(IV), Se(VI) and Sb(III) and 1.5 for Sb(V) and was adjusted with HCl. The samples were shaken for 48 hours.

The sorption kinetics was analyzed by contacting 6 g of sorbent in a rotating basket stirrer with 2 L of an aqueous solution containing selenium or antimony species with an initial concentration of 8 μmol L^{-1} for

antimony and 12.66 μmol L^{-1} for selenium at initial pH of 2.5 for Se(IV), Se(VI) and Sb(III) and 1.5 for Sb(V).

After the times necessary for equilibrium, samples were filtered and analyzed for selenium and antimony species by Hydride Generation-Atomic Absorption Spectrometry. Se(VI) was quantitatively reduced to Se(IV) by heating with concentrated hydrochloric acid. Sb(VI) was reduced to Sb(III) with potassium iodide and L(+) Ascorbic acid. The selenium and antimony concentrations in the sorbent were determined by mass balance between liquid and solid.

4. Results and Discussion

4.1. INFLUENCE OF PH

Figure 1 shows the influence of pH on the sorption of selenium in the pH range between 0 and 12. The impact of pH can be explained by taking into account the different species of selenium and antimony in aqueous solution as a function of pH. Selenous acid, H_2SeO_3 is a weak acid, which dissociates in water into $HSeO_3^-$ and SeO_3^{2-}. The concentration of $HSeO_3^-$ and SeO_3^{2-} are pH dependent, with SeO_3^- occurring predominantly at pH 7. Selenic acid, H_2SeO_4 is a strong acid that dissociates to give SeO_4^{2-} (Table 1). With antimony the neutral species $Sb(OH)_3$ is the principal species over a very wide range (pH= 1 to 11); $Sb(OH)_4^-$ dominates only above pH 11.8, and below pH 1.4 the cationic form $Sb(OH)_2^+$ is predominant. In the presence of chloride, Sb(III) forms a complex predominantly as $SbCl_4^-$; only for pH below pH 2.7 the species $HSb(OH)_6$ dominates, whereas $Sb(OH)_5$ (aq) predominates at pH over 2.7.

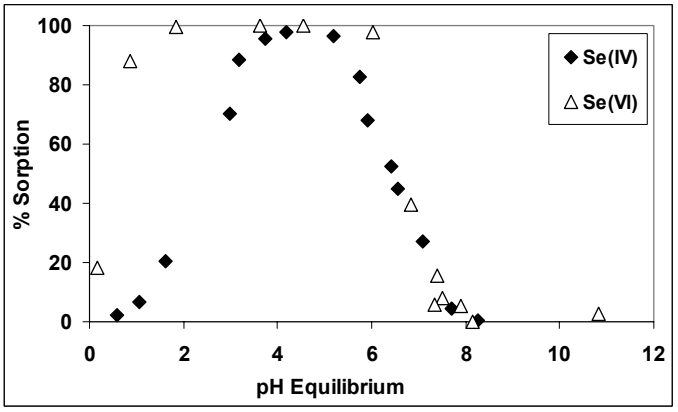

Figure 1. Relative removal of Selenium species as a function of pH; C_0 = 1 mg/L, sorbent mass: 1 g, volume: 0.2 L, temperature 25 ºC.

TABLE 1. Acid-base equilibrium constants for Selenium at 25 °C and 1 bar pressure

Species	pKa
$H_2SeO_3 \Leftrightarrow H^+ + HSeO_3^-$	2.75
$HSeO_3^- \Leftrightarrow H^+ + SeO_3^{2-}$	8.50
$H_2SeO_4 \Leftrightarrow H^+ + HSeO_4^-$	-3.0
$HSeO_4^- \Leftrightarrow H^+ + SeO_4^{2-}$	1.66

Se(IV) is well sorbed in a narrow range between pH = 3 and 5.5. On the other hand, the adsorption of Se(VI) occurs in a wide interval of pH values between 2 and 6.5. From pH 7, the adsorption starts to decrease, while from pH 8 there is no sorption. Figure 2 shows the results for antimony species. The adsorption of Sb(III) is almost 100 % between pH 1 and 7.5. Sb(III) presents almost 20 % of sorption in basic mediums (pH = 12). Sb(V) is efficiently adsorbed in the pH range between 0.5 and 4.

4.2. SORPTION KINETICS

Figure 3 shows the sorption kinetics of Selenium and Antimony species in a batch system. Se(VI) was removed almost 100% in only 20 min, while Se(IV) needs 24 h to reach equilibrium. Se(IV) was only 90% eliminated. In case of antimony species, Sb(III) and Sb(V) are completely adsorbed if the experiments are extended to 24 h.

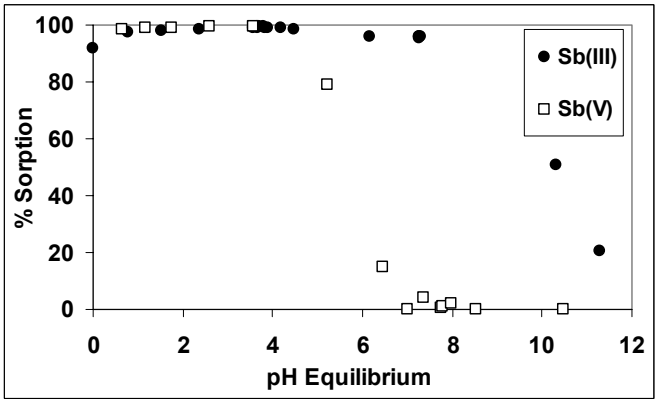

Figure 2. Relative removal of Antimony species as a function of pH; C_0= 1 mg/L, sorbent mass: 1 g, volume: 0.2 L, temperature 25 °C.

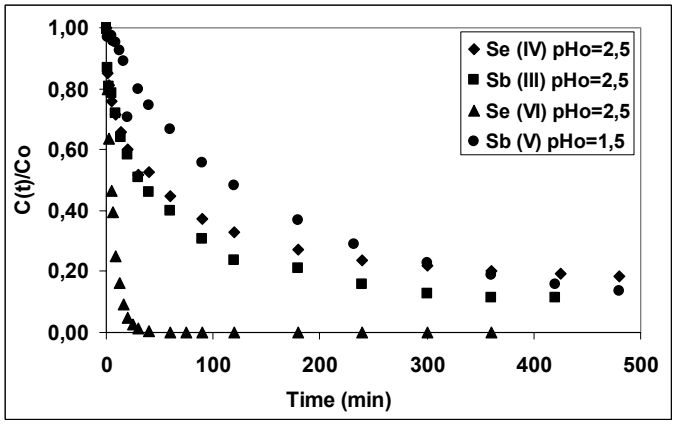

Figure 3. Development of sorption of Selenium and Antimony species in a batch system; C_0 = 1 mg/L, particle size: 0.5 mm; solutions volume: 2 L; temperature: 25 °C.

4.3. SORPTION ISOTHERMS

Figure 4 shows the sorption isotherm of the system selenium/HCl/water. The obtained results show the highest exchanger loadings for Se(VI), with an initially linear increase at small concentrations. The system does not present a maximum value corresponding to the saturation of the sorbent. The sorbed amount of Se(IV) is small because the sorption equilibrium strongly depends on the pH.

Figure 5 shows the results obtained for the system antimony/HCl/water. Duolite A7 has a high affinity for Sb(III) and Sb(V) but none of the curves shows the saturation of the sorbent.

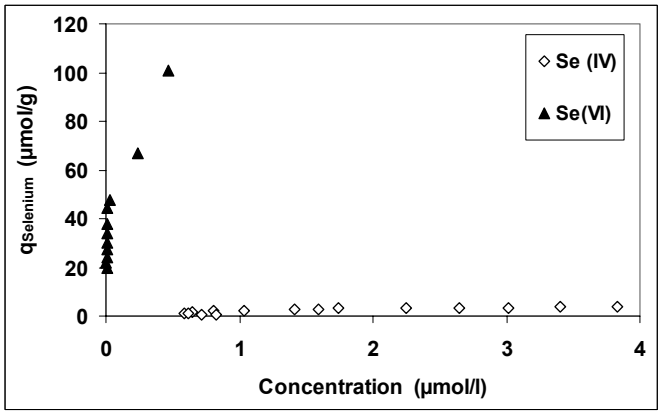

Figure 4. Sorption isotherm of Selenium after 48 h; 0.2 L solutions with Co= 12.66 µmol L^{-1} and pHo = 2.5, temperature: 25 °C.

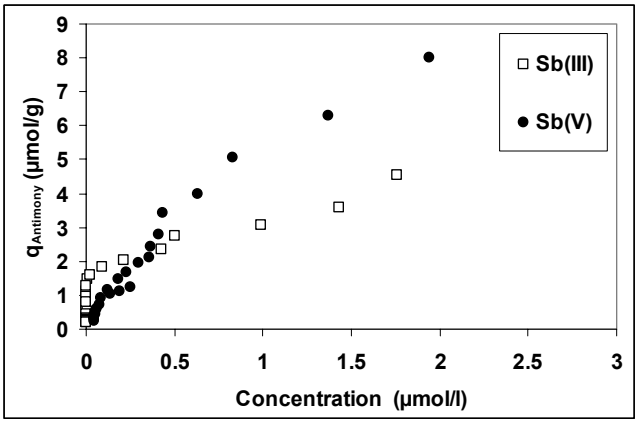

Figure 5. Sorption isotherm of Antimony after 48 h; 0.2 L solutions with Co= 8 µmol L^{-1}, pHo = 2.5 for Sb(III) and pHo = 1.5 for Sb(V), temperature: 25 °C.

5. Conclusions

The weakly basic exchanger Duolite A7 offers a good possibility of elimination of Se(VI) species, while the sorption of Se(IV), Sb(III) and Sb(V) is considerably smaller. Further investigations have to be carried out with respect to the removal of selenium and antimony species from real waters and wastewaters.

REFERENCES

1. U.S. Department of the Interior, Bureau of Reclamation. Water Treatment Engineering and Research Group. Fact Sheet. Revision Date: 9 September 2001.
2. M. Filella, N. Belzile, and C. Yu-Wei, Atimony in the Environment: a reviuw focused on natural waters; I Occurrence, *Earth-Science Reviews* 57, 125-176 (2002).
3. M. Filella, N. Belzile, and C. Yu-Wei, Antimony in the Environment: a review focused on natural waters; II Relevant solution chemistry, *Earth-Science Reviews* 59, 265-285 (2002).
4. K. Gannon and D. J. Wilson, Removal of Antimony from aqueous systems, *Sep. Sci. Technol.* 21(5), 475-493 (1986).
5. A. Kapoors, S. Tanjore, and T. Viraragahvan, Removal of Selenium from water and wastewater, *Int. J. Env. Stud.* 49, 137-147 (1995).
6. P.J. Marcantonio, Process for removing Selenium from wastewater effluent, Patent No. 4,915,928; Apr.10, 1990.
7. W.H. Goodman, Removal of Selenium from water by ion exchange, Patent No. 5,494,582; Feb. 27, 1996.

PART III

MODELING ADSORBENTS, ADSORPTION AND ADSORPTION PROCESSES

THE POROUS STRUCTURE OF HARD AND DEFORMED ADSORBENTS AND MOBILITY OF ADSORBED MOLECULES

R.SH. VARTAPETYAN* AND E.V. KHOZINA
Institute of Physical Chemistry RAS, Leniskij Prospect,31, 119991, Moscow, Russia

Abstract. The opportunities of pulsed NMR methods for studying the mobility of adsorbed molecules and porous structure of microporous rigid and non-rigid adsorbents of different nature are considered. The distribution of nuclear magnetic relaxation times were used to determine the distribution of water and benzene molecules adsorbed in active carbons and in polymer sorbents. The dimensions of the areas corresponding to different porosities have been estimated from the self-diffusion data of water and benzene in AC. The self-diffusion study of water and benzene in the synthetic opals indicate the existence of ultramicropores. The obtained data of nuclear magnetic relaxation and self-diffusion of the adsorbed water and benzene in the different adsorbents are in accordance with the adsorption investigations and complement them.

Keywords: porous structure; adsorbed molecules; mobility; NMR spin-spin and spin-lattice relaxation times; self-diffusion

1. Introduction

The structural analysis of adsorbents (in particular carbon adsorbents) is based on the experimental adsorption isotherm for standard vapors – nitrogen vapor at 77 K or benzene at 293 K.[1-3]

The data of water vapor adsorption were used for estimation of micropore width[4] and mesopore surface of active carbons[5] (AC). The method is based on a comparison of the isotherms of water vapor adsorption in the AC under study with that on a surface of non-porous

* To whom correspondence should be addressed; e-mail: vartapet@phyche.ac.ru

J.M. Loureiro and M.T. Kartel (eds.), Combined and Hybrid Adsorbents, 295–308.

graphitized carbon black (Vulkan-7H, graphitized at 2800 °C).[4] The number of molecules in a cluster, or the number of molecules which are adsorbed at a single primary adsorption site (PAS), is the ratio of the adsorption value, a, to the number of PAS, a_m. It is convenient to represent the adsorption on the surface of graphitized carbon black, expressed in a/a_m units, as abscissa. The adsorption on AC measured at the same relative pressures is used as ordinate. Figure 1 shows an example of the comparison plots for adsorption of water vapor on the series of AC samples.[6]

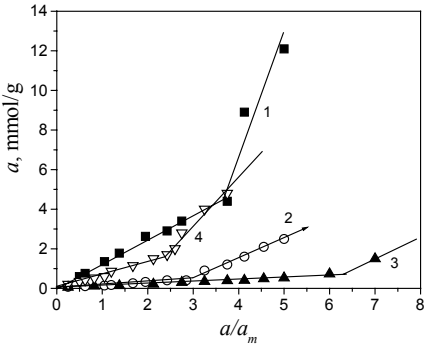

Figure 1. Comparative plots of water vapor adsorption on different samples of AC: (1) - Carboline-1, (2) - FAS-2, (3) - FAS-3, and (4) - SKT- 6A.

The comparison plots are the straight lines starting from the coordinates origin. Their ordinates at $a/a_m = 1$ correspond to the number of PAS per gram of the AC and the inflection upward in the comparison plots indicates the onset of the bridging between water molecules adsorbed on PAS located on the opposite walls of a micropore.[4]

An additional important information about adsorbed molecules and properties of porous media can be given by pulsed nuclear magnetic resonance (NMR) methods.[6-8] This work observed the opportunities of nuclear magnetic relaxation and self-diffusion measurements for determining the mobility of adsorbed molecules with different adsorption mechanisms (water and benzene) and the pore structure parameters of microporous adsorbents with rigid (AC) and non-rigid (polymer adsorbents) framework.

1.1. NUCLEAR MAGNETIC RELAXATION OF MOLECULES IN POROUS MEDIA

The pulsed NMR techniques are based on registration of the response of a spin system in a constant magnetic field to a sequence of radio frequency (RF) pulses and pulsed gradients of the magnetic field (PFG). The evolution of nuclear transverse or longitudinal magnetization to an

equilibrium value is characterized by the recovery times of thermodynamic equilibrium between the spins themselves, and the spins with their environment (lattice) – the spin-spin (T_2) and spin-lattice relaxation times (T_1), correspondingly.[7] The spin relaxation processes are influenced by the intensity of molecular motion.

A theory by Brownstein and Tarr[9,10] established that the evolution of total nuclear magnetization is governed by diffusion and relaxation processes and is sensitive to the geometry of the pore space. An exchange between the molecules in a surface layer and in the pore volume is due to self-diffusion. Under conditions of fast diffusion, when the relaxation time of a molecule in the pore considerably exceeds the time it takes for moving distances comparable to the pore size, the relaxation of a molecule in the pore is characterized by a single relaxation time. The value of this time is proportional to the characteristic pore size, x, viz., the ratio of the pore volume V to the surface S:

$$T_{1,2} = V/\mu S \sim x \tag{1}$$

where μ is the so-called surface relaxation strength.

The fast diffusion conditions are valid for pores smaller than 1 μm.[8] Equation (1) served as a basis for the nuclear magnetic relaxation measurements in different mesoporous materials.[11-14] We make an attempt to estimate the pore size of microporous adsorbents using the values T_1 and/or T_2 of the adsorbed molecules, taking into account the theoretical approach.[9,10]

1.2. SELF-DIFFUSION OF MOLECULES IN POROUS MEDIA

The information about self-diffusion in the NMR PFG experiments is obtained from a response of the spin system of the substance to a stimulated spin-echo sequence of RF pulses ($\pi/2$-τ_1-$\pi/2$-τ_2-$\pi/2$-τ_1-echo).[15,16] Two identical pulses of magnetic field gradient of duration δ and amplitude g are applied after the first and the third RF $\pi/2$-pulse. The time interval between PFG is the so called diffusion observation time: $t_d = \tau_1 + \tau_2$. For sufficiently short field gradient pulses, a normalized spin echo amplitude $A(k, t_d)$ obeys to the relation:

$$A(k,t_d) = \int \exp\left[i\,k(r)\right] P(r,t_d)\,dr \tag{2}$$

where $k = \delta\gamma g$, and γ is the gyromagnetic ratio. $P(r, t_d)$ denotes the propagator, i.e. the probability density for molecular displacements r during observation time t_d.[15]

In free diffusion, the propagator is a Gaussian function with the mean square displacement given by the Einstein equation:

$$\langle r^2 \rangle = 6\, D\, t_d \tag{3}$$

Here D is the self-diffusion coefficient (SDC) that does not depend on the t_d. In this case, the diffusional decay of the spin-echo (DD) is presented as:[15]

$$A(k, t_d)=\exp[-(\gamma\delta g)^2 D t_d)] \tag{4}$$

The pore geometry sensitivity of the NMR PMFG method is defined by the ratio between the resolution of PMFG NMR $l_{PMFG}=(2k)^{-1}$, the root mean-square displacement $l_{Diff}=(2Dt_d)^{1/2}$ and, the mean pore size x.[16]

The micropores are smaller than the resolution of the NMR PMFG method, so the effective value of SDC is averaged over the microporous structure.[16]

2. Experimental

2.1. ADSORPTION OF WATER AND BENZENE IN MICROPOROUS ACTIVE CARBONS AND THE PARAMETERS OF POROUS STRUCTURE

The AC samples of different microporous structure were under consideration of the adsorption and NMR studies.[6,17] The AC samples of different activation were prepared from furfural and were denoted as FAS-1, FAS-2, FAS-3, FAS-H. Carboline -1 and -2 were produced from hydrolyzed lignin. The commercial sample SKT-6A was studied, too.

The parameters of the porous structure of these AC are given in Table 1.

The specific surface area (S_{BET}), the surface area of mesopores (S_{me}), the volume (W_0) and the width (x_0) of a slit-like model of micropores and the dispersion (δ) of the micropore volume distribution of the AC samples were calculated from the adsorption isotherms of nitrogen at 77 K according to the Dubinin-Radushkevich[2] (DR) and Dubinin-Stoeckli[3] (DS) equations and by the adsorption isotherms of water.[4] The pore width is connected to the adsorption energy by a Stoeckli relationship:[3] $x_0 = 10.8/(E_0-11.4)$.

As can be seen from Table 1, the samples FAS-1 and FAS-2 refer to a typical microporous AC. FAS-2 is characterized by larger micropores, a broader size distribution of the micropores (δ), and a larger mesopore surface. Note that FAS-1 and SKT-6A contain mostly micropores.

The BET equation and the comparison method[18] were used for an estimation of the porous structure parameters of FAS-3.

TABLE 1. The parameters of the porous structure of AC calculated from the adsorption isotherms of nitrogen at 77 K and of water vapor at 293 K

AC	Nitrogen adsorption isotherm							Water adsorption isotherm		
	Dubinin-Radushkevich equation				Dubinin-Stoeckli equation					
	$S_{me}+S_g$, m^2/g	S_{me}, m^2/g	W_0, cm^3/g	x, nm	W_0, cm^3/g	x, nm	δ, nm	S_{me}, m^2/g	a_m, mmol/g	x, nm
FAS-1	1363	30	0.32	0.48	0.32	0.48	0.06	28	0.24	0.50
FAS-2	1029	120	0.60	1.32	0.62	1.34	0.30	150	0.15	1.30
FAS-3	2300[a]	–	–	–	–	–	–	360	0.13	1.80
	2100[b]			1.60[b]						
FAS-H	1154	80	0.58	1.08	0.61	1.20	0.28	95	0.28	1.12
SKT-6A	1142	50	0.59	1.08	0.60	1.12	0.13	55	0.60	1.12
carbolin-1	–	–	–	–	–	–	–	65	1.21	1.46
carbolin-2	2530[a]	90	0.89	1.74	–	–	–	120	0.43	0.90
	2330[b]									

[a] determined by BET equation, [b] determined by the comparative method.[18]

2.2. NUCLEAR MAGNETIC RELAXATION MEASUREMENTS OF WATER AND BENZENE IN AC

The spin-spin relaxation processes were examined by free induction decay (FID) signals, which followed the sequences of RF pulses 90^0_x-τ-90^0_y-«solid-echo».[19] It has been found that the FID signal observed in water (benzene)-AC systems is a sum of two functions. The usage of the modified Goldman-Shen sequences to the systems under study found that the fast decaying component in FID corresponds to protons that belong to AC.[17] The application of the Carr-Purcell-Meiboom-Gill (CPMG) pulse sequence [19,20] excluded this component. Figure 2 shows the decay of nuclear transverse magnetization in benzene in FAS-2.

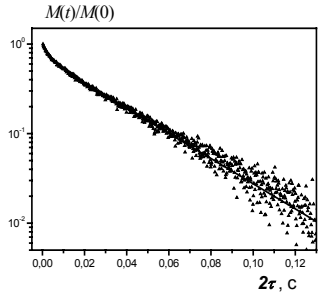

Figure 2. Decay of the transverse magnetization in the sample FAS-2-benzene at Θ=0.6 resulted from the application of the CPMG pulse sequence (the interval between the π-pulses is 100 μs). The solid line is the approximation by the sum of two exponential functions with the relaxation times T_{2min} and T_{2max}. Temperature of measurements is 303 K.

The observed signal was approximated by the sum of two exponentials with relaxation times T_{2min} and T_{2max}:

$$M(t)=p_1\exp(-t/T_{2min}) + p_2\exp(-t/T_{2max});\ \ p_1+p_2=1 \tag{5}$$

where $p_{1,2}$ are the relative fraction of protons with the corresponding relaxation times.

According to theory,[9,10] nuclear magnetic relaxation of a molecule in a pore is characterized by a single relaxation time T_1 or T_2 , defined by Eq. (1).

Therefore, the observed distribution of relaxation times is defined by the pore size distribution:

$$P(T_{1,2i})\rightarrow P(x_i) \tag{6}$$

In addition, the areas of large and small pores are divided in space. In opposite case, when they are mixed, the relaxation is described by an averaged relaxation time.[8]

Thus, a proportion based on Eq. (1) for each adsorption system with specified benzene or water loadings of pores is obtained:

$$\frac{T_{2max}}{x_{max}} = \frac{T_{2min}}{x_{min}} \tag{7}$$

The size of the smallest pores, x_{min}, where benzene or water molecules could be found, were assumed to be no less than their sizes, i.e. 0.3 nm for water (an average value over the molecule size range from different authors[21]) and 0.37 nm for benzene (the thickness).[1] The largest size of micropores in AC, where benzene or water molecules were adsorbed, x_{max}, were calculated by Eq. (7) to be equal to 1.4, 3.2 and 2.2 nm in FAS-1, -2, -3, correspondingly.

The broadest pore size distribution was observed in FAS-2 system (T_2 varied from 3.5 ms to 31.0 ms). This conclusion agreed with the data obtained from nitrogen and water adsorption (see Table 1).

Thus, the distribution of the relaxation time $P(T_2)$ was used to find the relative fraction of molecules over pores of one or another size, *i.e.*, estimate the pore size distribution $P(x)$ (Fig. 3).

The comparison of $P(x)$ for water and benzene in FAS-1, 2, 3 indicated that FAS-1 disposes of the largest fraction of micropores ($x \leq 2.1$ nm) within the total pore volume. At the same time, FAS-2 is characterized by the broadest pore size distribution.

According to the adsorption data, benzene is predominantly adsorbed in micropores, while the water adsorption is determined by the presence of PAS.

The important characteristic of the adsorption system is an average spin-spin or spin-lattice relaxation times $T_{1,2}$ defined as

$$1/T_{1,\,2av}=\Sigma p_i/\,T_{1,\,2i} \tag{8}$$

where p_i is a relative fraction of protons with the relaxation time $T_{1,\,2i}$.

The study of the value of $T_{1,2av}$ of water adsorbed in FAS-3 allowed following the peculiarities of water adsorption on the sample FAS-3 that contains the areas of different porosities.[22]

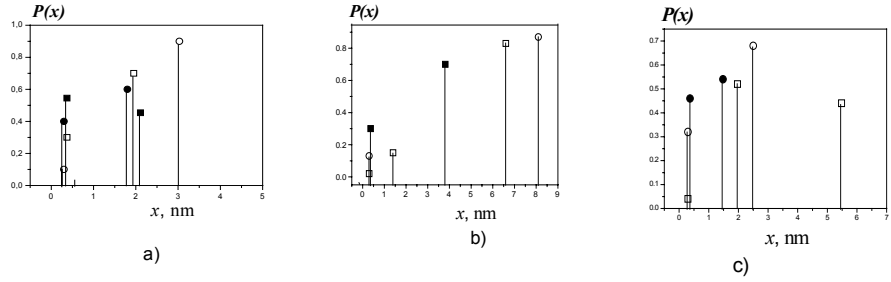

Figure 3. The water and benzene distribution over pores of FAS-1(a) defined from T_2 data for benzene at $\Theta = 0.05$ (•), 1 (■) and for water at $\Theta = 0.05$ (□), 0.89 (o); in FAS-2 (b) at $\Theta = 0.6$ (■ – benzene, □ – water) and in FAS-2 saturated by water (o); in FAS-3 (c) at $\Theta = 0.1$ (• – benzene, o – water) and 1 (□ – water) at $T = 303$ K.

The dependence of the T_{2av} values on the water adsorption values differs from that observed in the others AC of FAS-type. T_{1av} increased with the rise of a/a_m stage by stage. Thus, the formation of the second layer of water clusters was accomplished by the abrupt increase of T_{1av} over an order of magnitude.[22] This happened at $a/a_m = 6.3$ that is the value at which water clusters united in micropores due to the formation of bridges between clusters on the opposite walls of slit-like pores (Fig. 1). The analysis of

dependence $T_{2av}(a)$ at the large adsorption values determined the clusters merging along a mesopore surface in FAS-3.[22]

Note that the equal values of $T_{1,2}$ measured in different adsorbents for one adsorbate do not mean the existence of equal pores in them. The proportion (Eq. 7) must be applied for a certain adsorbate-adsorbent system with a certain adsorption value.

Indeed, the different chemical nature of the surfaces of different adsorbents implies the distinct μ values. The parameter μ was found to be a linear function of the relative fraction of the surface occupied by paramagnetic ions, n_m.[12] Figure 4 presents the dependence of T_{2v} at complete micropore saturation on the volume density of PAS (a_m/W_0) for various AC.[7] The linear feature of the observed dependence $T_2 = f(a_m/W_0)$ indicates the dominant role of the PAS as sinks of nuclear magnetization of the adsorbed water.

In our approach, two assumptions were made. The first is that the PAS distribution (sinks of nuclear magnetization) over the adsorbent pore volume is uniform.

The second assumption is an uncertainty of the smallest pore size corresponding to $T_{1,2min}$. It has been found, that the ultramicropores with the sizes close to the molecular sizes exist in microporous AC and serve as the germs of the formation of larger pores under activation.[23] The existence of ultramicropores of ~0.3 nm in AC was confirmed by the water adsorption in the microporous carbon sensors of oxygen.[24]

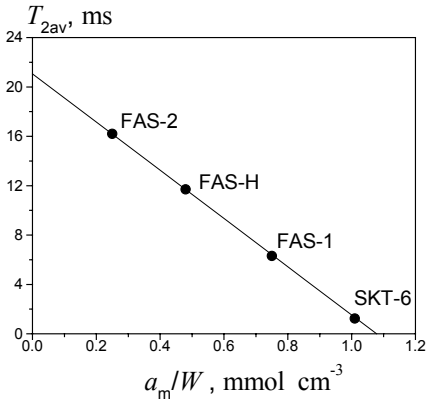

Figure 4. Dependences of T_{2av} values of water on the volume density of PAS, a_m/W_0, for FAS-1, FAS-2 , FAS-H and SKT-6.

2.3. NMR RELAXATION OF WATER AND BENZENE IN THE POLYMER SORBENTS

The super-crosslinked polystyrene "Styrosorb", MN-100 and MT-65 and functionalized porous methacrylate polymer sorbents[25] were considered. The distributions of the water and benzene molecules over the pores of MN-100 and MT-65 were defined for different weight content of adsorbate (see Fig. 5a,b).

It is obvious that the interval of the filled pores of MT-65 (0.3 nm ≤ x <60 nm) is broader than in MN-100 (0.3 nm ≤ x <25 nm), that indicates the wider pore size distribution in MT-65. (MN-100 differs from MT-65 by the presence of amino groups in quantity of 0.2-0.4 mg-eq/g). It is obvious that benzene molecules adsorbed in the larger pores compared with water.

The data obtained indicated a definite difference between the adsorption properties of rigid AC and deformable PS.

The distributions of benzene molecules in MPS were obtained from the two exponential decay of magnetization. The results of $P(x)$ for benzene in MPS at the weight content w~0.7 are presented in Fig. 6.

The largest value of x_{max}, 17 nm, is observed in initial MPS sample, G-60, (17 nm), the smallest, 4 nm, in MPS modified with diethylenetriamine groups, G-60-DETA. The G-60-Bzl sample contains the benzyl groups. Nevertheless, benzene adsorbed predominantly in the smaller pores of PS.

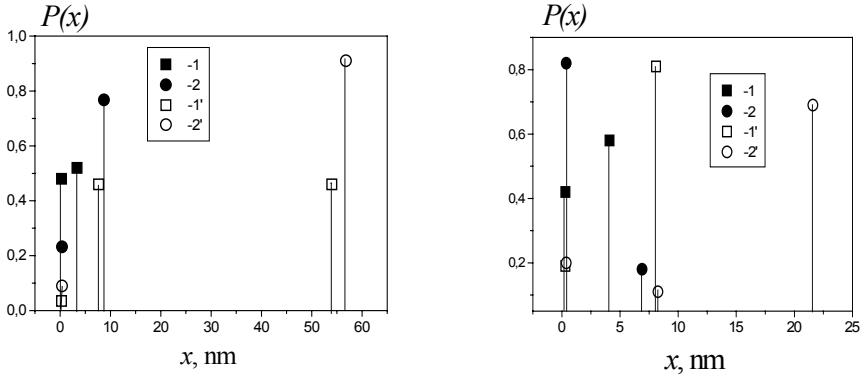

Figure 5. Distribution of water (1, 1') and benzene (2, 2') in the MT-65 (a) and in the MN-100 (b) samples at different weight content of adsorbate: 1, 2 – w = 0.05, 1', 2' – w=0.34 (a) and 1, 2 – w= 0.03; 1', 2' – w = 0.20 (b), calculated from the $P(T_2)$ data at T = 303 K.

In contrast to benzene in MPS, adsorbed water molecules revealed a single relaxation time, which is shorter than that of benzene. Thus, water molecules adsorbed in pores of close sizes.

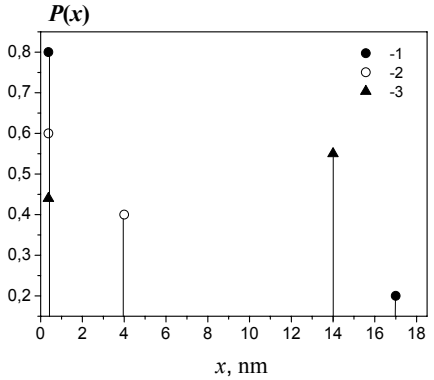

Figure 6. Distribution of benzene in the G-60 pores at w=0.63 (1), G-60-DETA at w=0.7 (2) and G-60-Bzl at w =0.7 (3) calculated from the $P(T_2)$ at T=303 K.

3. Self-Diffusion Measurements of Adsorbed Molecules

3.1. NMR PMFG MEASUREMENTS OF SELF-DIFFUSION OF WATER AND BENZENE IN AC

Figure 7 shows examples of the diffusion decays (DD), $A(g^2)/A(0)$, of water adsorbed in pores of FAS-1 and FAS-3 at the two pore fillings.

The observed diffusion decays of spin-echo (DD) deflected from the exponential behavior (Eq. 4).

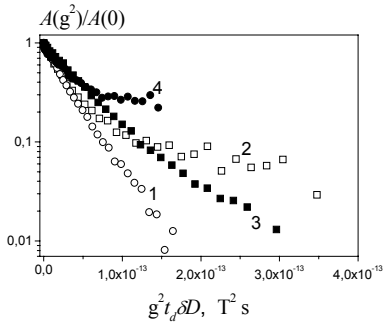

Figure 7. Diffusion spin-echo decays $A(g^2)/A(0)$ of water in pores of FAS-1 (curves 1,2) and FAS-3 (3,4) at the filling degrees Θ = 0.89 (1); 0.06 (2); 1 (3) and 0.02 (4). The diffusion time t_d = 4 ms.

The multiexponential DD reflects the multiphase system.[26] Each phase corresponds to an area of a certain porosity that defines a certain value of SDC. In this case, the diffusional spin-echo decays are described by a spectrum of SDC:

$$A(g^2)/A(0)=\int p(D)[\exp(-\gamma^2\delta^2 g^2 t_d D)]\mathrm{d}D \qquad (9)$$

The width of spectrum, $\ln^2\sigma$, is defined using the log-normal distribution $p(D)$ of diffusivities:

$$p(D) = \frac{1}{\sqrt{2\pi \ln^2 \sigma}} \exp\left(- \frac{\ln^2\left(D/D_0\right)}{2\ln^2 \sigma} \right)$$

The average value of SDC, D_{av}, is defined from the initial slope of DD.[26]

Note that the existence of areas of different porosities in AC was indicated by the multiexponential relaxation. The exchange processes between these areas were found from the examinations of DD at different diffusion times.[27] Figure 8 represents the DD in FAS-3 saturated by water and by benzene observed at different values of t_d. The exchange processes lead to the exponential DD as the diffusion time is increased with the mean value of the SDC being constant.

The SDC distribution of water in FAS-3 was rather narrow ($\ln^2\sigma$= 0.15) and did not depend on t_d in the interval from 1.4 to 326 ms. Hence, fast exchange leads to an averaging over the diffusivity distribution for t_d< 1.4 ms. Using the Einstein relationship with D_{av} for water and t_d=1.4 ms, the extension of FAS-3 pores filled by water characterized by a single SDC, L, one obtained: $L \sim 3$ μm.

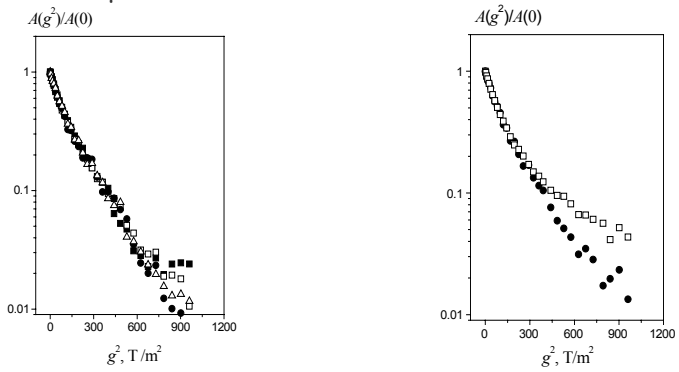

Figure 8. Diffusion spin-echo decays in the samples of FAS- 3 saturated by water (a) and benzene (b), observed at different diffusion times, (a): t_d = 1.4 ms (●), 5 (□), 120 (▌) and 300 ms (Δ); (b): t_d = 1.4 (□) and 326 ms (●) at the condition that $t_d\delta^2$ = const. The temperature is 303K.

The relative width of SDC spectrum observed in FAS-1, 2, 3 saturated by water was not large: 0.12, 0.16 and 0.15, respectively.

When investigating the DD at different t_d in the FAS-3–benzene sample for θ = 1, the value $\ln^2\sigma$ decreased from 0.41 up to 0.19 with increasing t_d from 5 to 326 ms (Fig. 8b). At the same time, D_{av} for different t_d remains

unchanged, so there is no relaxation influence on DD. Therefore, molecular exchange between regions with different benzene diffusivities in FAS-3 occurred at a much slower rate. The further increase of the diffusion time up to 400 ms does not reveal any changes in the DD shape. Using the Einstein relation, one obtained the dimensions of heterogeneities in the FAS-3-benzene system, $L \approx 32$ μm. The molecular exchange between these areas was hampered.

As follows from Fig. 7, the deviation of DD from the exponential form increased with decreasing pore filling. In FAS-1, -2, -3 at water loadings θ<0.09, the DD (curves 2 and 4 on Figure 7) could be approximated only as a sum of two exponentials:

$$A(g^2)/A(0)=p_1\exp(-\gamma^2\delta^2g^2t_dD_1)+ p_2\exp(-\gamma^2\delta^2g^2t_dD_2) \qquad (10)$$

where p_1 and p_2 are the fractions of molecules with D_1 and D_2, respectively; $p_1 + p_2 = 1$.

The values of D_1 and D_2 were related to the diffusion processes in the regions significantly differing in their porosity. These data indicated a loss of connectivity between these regions with decreasing adsorbate content. The extensions of these regions for FAS-3–water at $\theta = 0.02$ are equal to the mean-square displacements of water with D_1 and D_2 during the longest observation time in the experiment t_d=100 ms, namely, 19 and 5μm.

3.2. THE ESTIMATION OF PORE SIZES IN THE SAMPLES OF OPALS

The NMR PFG self-diffusion measurements of adsorbed water and benzene molecules were used for determining the pore sizes in a new class of adsorbents – synthetic opals.[28]

The shapes of DD for water in the opal were described by the sum (eq. 10) with $D_{min} \sim 10^{-11}$ m^2/s and $D_{max} \sim 0.8 \div 2\ 10^{-9}$ m^2/s that indicated two porosities in the opal sample. D_{min} corresponds to water in the ultramicropores. At the same time the exponential DD with $D \sim 10^{-9}$ m^2/s describes the mobility of benzene adsorbed in the opal. Consequently, the ultramicroporous areas of the opal occurred to be inaccessible for benzene. Thus the minimum sizes of the ultramicropores, where water adsorbed, were estimated as no less than 0.3 nm, the size of water molecule,[21] and no more than the thickness of benzene molecule, 0.37 nm.[1]

The self-diffusion data confirmed the electron-positron annihilation as well as the water adsorption studies, which found the coexistence of the pores between the opal nanospheres and the ultramicropores on the surface of nanospheres.

4. Conclusion

Measurements of the nuclear magnetic relaxation times of benzene and water in pores of active carbons were used in order to determine the distribution of adsorbed molecules over pores. The obtained estimates agreed with the water and benzene adsorption data on AC. Further, the porous structure of polymer sorbents with deformed framework was examined based on the proposed approach.

The self-diffusion data of water and benzene in AC were used for the examination of the heterogeneities in the adsorption systems AC–water and AC–benzene. The water adsorption in the ultramicropores of the synthetic opals was established from the self-diffusion measurements. The sizes of the ultramicropores were determined as no less that the water molecule and no more that the benzene molecule.

REFERENCES

1. S.J. Gregg, and K.S.W. Sing, *Adsorption, Surface Area and Porosity*, 2nd ed. (Academic Press, New York, 1982).
2. M.M. Dubinin, Microporous structures and adsorption properties of carbonaceous adsorbents, *Carbon* 21(4), 359-366 (1983).
3. H.F. Stoeckli, P. Rebstein, and L. Ballerini, On the assessment of microporosity in active carbons; a comparison of theoretical and experimental data, *Carbon* 28, 907-909 (1990).
4. R.Sh. Vartapetyan, and A.M. Voloshchuk, The mechanism of adsorption of water molecules on carbon adsorbents, *Russian Chemical Reviews* 64, 985-1001 (1995).
5. R.Sh. Vartapetyan, A.M. Voloshchuk, A.A. Isirikyan, N.S. Polyakov, and Y.I. Tarasevich, Chemistry of carbon surface and mechanism of water molecule adsorption, *Colloids and Surfaces A* 101, 227-232 (1995).
6. G.Sh. Gogelashvili, R.Sh. Vartapetyan, D.V. Ladychuk, Yu.B. Grunin, and E.V. Khozina, Specific features of the adsorption and nuclear magnetic relaxation of water molecules in active carbons: 1. Relation between the spin-spin relaxation of adsorbed water molecules and structural parameters of microporous active carbons, *Colloid. J*. 65, 545-551 (2003).
7. V.V. Mank, and N.I. Lebovka, *Spectroscopy of nuclear magnetic resonance of water in heterogeneous systems* (Naukova Dumka, Kiev, 1988) (in Russian).
8. F. D'Orazio, J.C. Tarcson, W. Halperin et al., Application of nuclear magnetic resonance pore structure analysis to porous silica glasses, *J. Appl. Phys.* 65, 742-751 (1989).
9. K.R. Brownstein, and C.E. Tarr, Spin-lattice relaxation in a system governed by diffusion, *J. Magn. Reson.* 26, 17-24 (1977).
10. K.R. Brownstein, and C.E. Tarr, Importance of classical diffusion in NMR studies of water in biological cells, *Phys. Rev. A* 19, 2446-2453 (1979).
11. W.E. Kenyon, Nuclear magnetic resonance as a petrophysical measurements, *Nuclear Geophysics* 6, 153-171 (1992).
12. R.L. Kleinberg, W.E. Kenyon, and P.P. Mitra, Mechanism of NMR relaxation of fluids in rocks, *J. Magn. Reson. Ser. A* 108, 206-214 (1994).

13. S. Godefroy, J.-P. Korb, M. Fleury, and R.G. Bryant, Surface nuclear relaxation and dynamics of water and oil in macroporous media, *Phys. Rev. E* 64, 21605-21618 (2001).
14. D. Chang, and M.A. Ioannidis, Magnetization evolution in network models of porous rock under conditions of drainage and imbition, *J. Coll. Int. Sci.* 253, 159-170 (2002).
15. J. Karger, and D.M. Ruthven, *Diffusion in Zeolites and other Microporous Solids* (John Wiley, New York, 1992).
16. F. Stallmach, and J.Karger, The potentials of pulsed field gradient NMR for investigation of porous media, *Adsorption* 5, 117-133 (1999).
17. E.V. Khozina, R.Sh. Vartapetian, and D.Sh. Idiyatullin, Features of nuclear magnetic relaxation of water and benzene molecules during absorption on activated carbons and estimation of pore size distribution in adsorbents, *Russ. Chem. Bull.* 51, 2036-2043 (2002).
18. R.Sh. Michail, S. Brunauer, and E.E. Bodor, Investigations of a complete pore structure analysis: I. Analysis of micropores, *J. Colloid. Int. Sci.* 26, 45-53 (1968).
19. H.Y. Carr, and E.M. Purcell, Effects of diffusion on free precession in nuclear magnetic resonance experiments, *Phys. Rev.* 94, 630-638 (1954).
20. S. Meiboom, and D. Gill, Modified spin-echo method for measurement of nuclear relaxation times, *Rev. Sci. Instr.* 29, 688-691 (1958)
21. A.N. Ainscough, and D. Dollimore, Adsorption capacity of molecular sieve type carbons, *Langmuir* 3**,** 708-713 (1987).
22. G.Sh. Gogelashvili, R.Sh. Vartapetyan, D.V. Ladychuk, Yu.B. Grunin, and E.V. Khozina, Specific features of the adsorption and nuclear magnetic relaxation of the water molecules in active carbons: 2. The state of water in active carbon with relatively large pores according to the NMR relaxation data, *Colloid. J.* 66, 271-276 (2004).
23. R.Sh. Vartapetyan, A.M. Voloshchuk, N.A. Limonov, and Yu.A. Romanov, Bimodal micropore size distribution in active carbons, *Russian Chemical Bull.* 42(3), 424-427 (1993).
24. R.Sh. Vartapetyan, A.M. Voloshchuk, A.K. Buryak, C.D. Artamonova, R.L. Belford, P.J. Ceroke, D.V. Kholine, R.B. Clarkson, and B.M. Odintsov, Water vapor adsorption on chars and active carbons - oxygen sensors prepared from a tropical tree wood, *Carbon* 43(10), 2152-2159 (2005).
25. R.Sh. Vartapetyan, E.V. Khozina, M.P. Tsyrupa, and V.A. Davankov, Mobility of Benzene and Water Molecules in Highly Crosslinked Polystyrene Adsorbents, *Russian Journ. of Phys. Chem.* 76(9), 1523-1531 **(**2002)
26. A.I. Maklakov, V.D. Skirda, and N.F. Fatkullin. *Self-diffusion in Polymer systems* in: *Encyclopedia of Fluid Mechanics,* vol. 9., edited by N.P. Cheremisinoff (Gulf-Publishing CO, Houston, 1999) pp. 705-745.
27. E.V. Khozina, R.Sh. Vartapetyan, and A.M. Voloshchuk, Specific features of self-diffusion of molecules of water and benzene in active carbons, *Colloid. J.* 59, 230-235 (1997).
28. R.Sh. Vartapetyan, E.V. Khozina, and I.I. Bardyshev, Self-diffusion of water and benzene molecules adsorbed in the synthetic opal samples, *Appl. Magn. Res.* 29(3), 471-480 (2005).

CHARACTERIZATION OF HARD AND SOFT POROUS MATERIALS AND TISSUE SCAFFOLDS

SERGEY V. MIKHALOVSKY*, LYUBA I. MIKHALOVSKA, STUART L. JAMES
University of Brighton, Lewes Road, Brighton, BN2 4GJ, UK

PAUL E. TOMLINS, PAUL V. GRANT
National Physical Laboratory, Hampton Road, Teddington, Middlesex, TW11 0LW, UK

PANKAJ VADGAMA
Queen Mary, University of London, Mile End Road, London, E1 4NS, UK

VLAD M. GUN'KO
Institute of Surface Chemistry, 17 General Naumov str., 03164 Kiev, Ukraine

Abstract. Porous structure of tissue scaffolds is essential to ensure normal cell functioning providing them with nutrients, oxygen and optimal growth conditions and removing waste products. Characterization of the porous structure of hard implants is less of a problem compared to soft polymer hydrogels. In this work the results of the evaluation of the porous structure of two polymers widely used as implants or scaffolds, polycaprolactone as a hard material and collagen based hydrogel as a soft material are presented. The characterization was carried out using electron, fluorescence and confocal microscopy, quartz crystal microbalance technique and diffusion of macro-molecules.

Keywords: soft hydrogels; collagen; polycaprolactone; tissue scaffolds

* To whom correspondence should be addressed. Sergey V. Mikhalovsky, School of Pharmacy and Biomolecular Sciences, University of Brighton, Cockcroft Building, Lewes Road, Brighton BN2 4GJ, UK; e-mail: s.mikhalovsky@brighton.ac.uk

J.M. Loureiro and M.T. Kartel (eds.), Combined and Hybrid Adsorbents, 309–320.

1. Introduction

Tissue engineering offers novel opportunities for repairing damaged or diseased tissues and organs by incorporating the patient's own healthy cells or donor cells into porous biocompatible materials used as tissue scaffolds. Along with other properties, the porous structure of tissue scaffolds is essential to ensure normal cell functioning providing them with nutrients, oxygen and optimal growth conditions and for removing waste products. It was shown recently that collagen scaffolds with pore size ranging from 20 μm to 200 μm are suitable for cell accommodation and growth.[1,2]

Characterization of the porous structure of hard implants such as ceramics and composites seems to be less of a problem compared to soft polymer hydrogels, for which even the definition of pores is difficult to formulate. With the biomaterials industry booming, the standardization of porous tissue scaffolds becomes a critical issue. In this work we present results of the evaluation of the porous structure of two polymers widely used as implants or scaffolds, an in-house polycaprolactone (PCL) as a hard material and a commercial collagen hydrogel used for wound healing as a soft material.[3,4]

2. Experimental

2.1. MATERIALS

To make a porous polymer we used a water soluble porogen, sodium chloride.[5] Polycaprolactone (PCL, specific gravity 1.145, Aldrich, M_n=86.8 kDa, M_w=136 kDa) was dissolved in chloroform (weight ratio 1:9) and the solution was poured over previously sieved particles of sodium chloride contained within a Petri dish. Evaporation of the solvent resulted in the formation of a polymer matrix containing a high proportion of incorporated NaCl particles. This soluble porogen was then removed by soaking the polymer-salt composite in deionized water which was changed at regular intervals, for at least 48 h. The level of porosity in the PCL matrix was controlled by adjusting the amount of NaCl used in the manufacturing process. The pore size distribution of the porogen was adjusted by sieving.

An artificial skin with the dermal part comprising a copolymer of bovine collagen with chondroitin-6-sulfate (Integra® Life Science Corp., Plainsboro, NJ, USA) was used as the initial collagenous material. The 'dermal' part, i.e., the protein hydrogel separated from the silicone membrane was thoroughly washed with distilled water and freeze-dried. The water and protein plus chondroitin-6-sulfate contents calculated from the dried mass of the initial hydrogel were found to be 98.5% and 1.5%

(w/w), respectively. The mass ratio of chondroitin-6-sulfate to collagen is below 0.10;[6,7] therefore we can consider the material as being a collagen gel. Integra gel is normally stored in isopropanol, which was successively washed in several volumes of sterile PBS for a final period of 24 hours, in order to remove the solvent and fully hydrate the matrix.

2.2. METHODS

2.2.1. Microscopy

Gel samples were prepared for analysis by scanning electron microscopy, SEM, by CO_2 critical point drying as follows. The samples were dehydrated by washing with acetone, placed into an air-tight container filled with acetone. The container was cooled down to -8 ^oC and acetone was replaced by liquid carbon dioxide. Once the container was filled with liquid CO_2 at 70% of the total volume, it was sealed and the temperature was increased stepwise to 20 ^oC and 38 ^oC. At 38 ^oC the internal pressure in the container reached 90 atm, at which point the outlet valve of the container was opened to reduce the internal pressure to the atmospheric level. After that the container with the dried sample was cooled down to room temperature. For SEM analysis the dried gel samples were sputter coated with 50-nm thick layer of gold and examined using SEM JSM-6310 (Japan Electron Optics Ltd).

For confocal microscopy, a Confocal Laser Scanning Microscope Zeiss LSM410 was used. The collagen sample was stained with aqueous fluorescein solution.

Cell distribution in tissue scaffolds was studied using 3T3 mouse fibroblast cells, suspension of which (2.0×10^6 cell mL^{-1}) was incubated for two hours in the collagen hydrogel. The hydrogel with cells was fixed, stained with DAPI stain and photographs taken using a fluorescent microscope at 488 nm.

2.2.2. Diffusion measurements

The collagen hydrogel was characterized by the ability of protein molecules with different size to pass through the hydrogel. Diffusion experiments were carried out in the diffusion cell as shown in Fig. 1. Two glass compartments of 8 mL volume each were separated by a hydrogel membrane. The membrane was reinforced by two meshes and two rubber rings; the diffusion cell was agitated on a shaker at 300 rpm and room temperature. The membrane thickness in the diffusion cell was about 1.0 mm. The protein solution added into compartment 1 (feeder) diffused through the membrane into compartment 2. Aliquots of 0.1 mL were taken

from the compartment 2 at different times and their optical density, OD at 280 nm was measured. To keep the volume of the diffusion system constant, 0.1 mL of phosphate buffered saline, PBS was added each time into compartment 2.

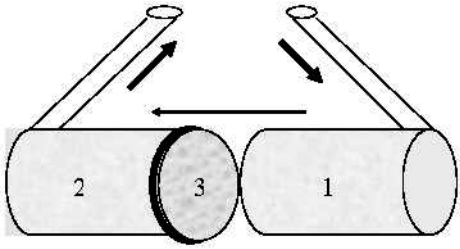

Figure 1. Diffusion cell with compartment 1 (feeder), compartment 2 and hydrogel membrane 3.

Three molecular markers were used in the diffusion experiments: aprotinin, a protein with MW 6.7 kDa; bovine serum albumin (BSA) with MW 67 kDa and fibrinogen (Fg) with MW 340 kDa. The diffusion of proteins was studied using fresh gel samples and gels after a Fg or Fg/BSA run.

2.2.3. Quartz crystal microbalance (QCM) measurements

Quartz crystals, 8.6 mm, 10 MHz (Crystal Works, Oklahoma, USA) were mounted in custom PEEK™ holders using a low viscosity elastomer (RS, Corby, UK), and 5 μm silver wires to yield a pressure-free cartridge crystal assembly. Cartridges were mounted within a temperature controlled block, held at 37 ± 0.1 ºC, electrical connections being made via gold plated pins.[8]

3. Results and Discussion

3.1. ANALYSIS OF THE POROUS STRUCTURE OF POLYMERS

3.1.1. Scanning electron microscopy

Scanning electron micrographs of collagen gel and PCL are given in Fig. 2 and Fig. 3. The porous structure of both materials is clearly visible on the micrographs. SEM resolution is insufficient to see micro- and mesopores* but it provides useful information about the porous structure in the range

* Here the word micropores is used according to the IUPAC terminology for pores with the size below 2 nm, and mesopores are pores with the size between 2 and 50 nm.

from 1 to 100 microns. These pores are important for cell accommodation and growth. Whether preparation of samples according to the procedure described in Section 2.2.1 damages their intact porous structure or not deserves special attention, however in general critical point drying is considered to be a gentle procedure preserving the intact structure of hydrogels.

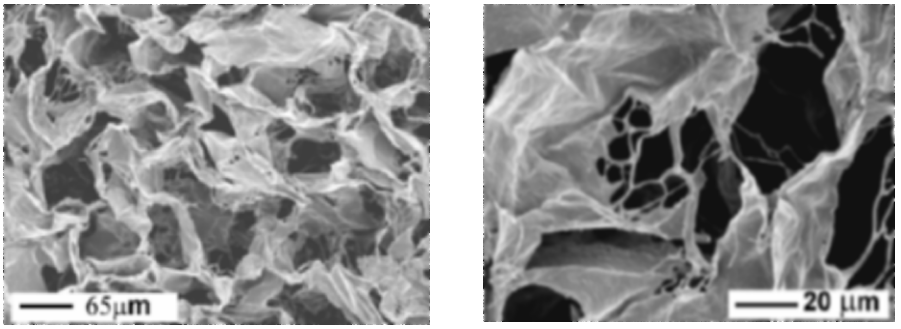

(a) (b)

Figure 2. Scanning electron micrographs of collagen gel at x 250 (a) and x 1000 (b) magnification.

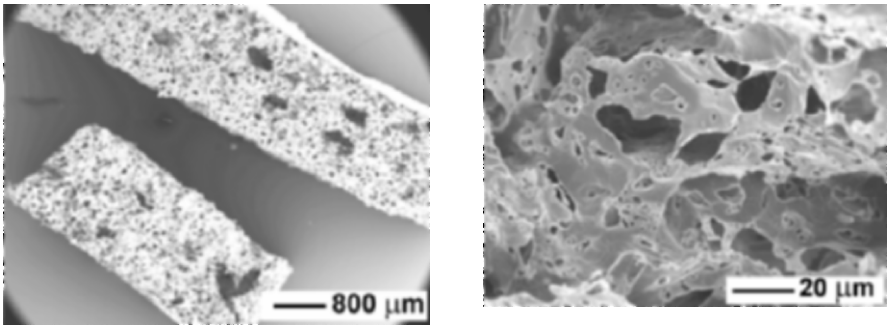

(a) (b)

Figure 3. Scanning electron micrographs of PCL at x20 (a) and x1000 (b) magnification.

3.1.2. Confocal microscopy

The advantage of confocal microscopy over SEM is the ability to examine the hydrogel structure in its aqueous environment. Its obvious disadvantage

is a much lower magnification power, however pores in the micrometer range can be easily visualized (Fig. 4).

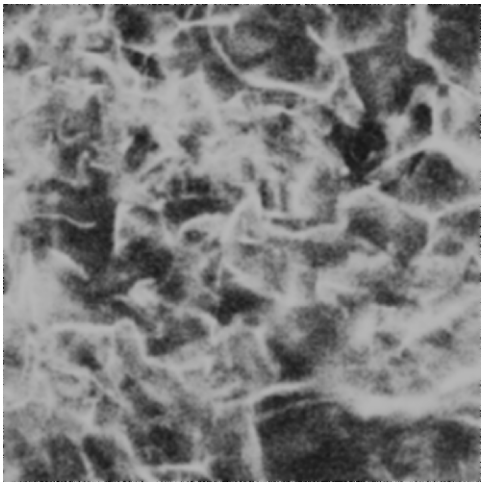

Figure 4. Confocal micrograph of the collagen hydrogel at x150 magnification.

3.2. CELL DISTRIBUTION IN TISSUE SCAFFOLDS

3.2.1. Fluorescence microscopy

In Fig. 5 a micrograph of the distribution of 3T3 mouse fibroblast cells after two hours incubation of the cell suspension with collagen hydrogel is shown. It is clear that the cells penetrated the gel and spread throughout it. This result confirms that the porous structure revealed by SEM and confocal microscopy is suitable for cell migration and growth in this material.

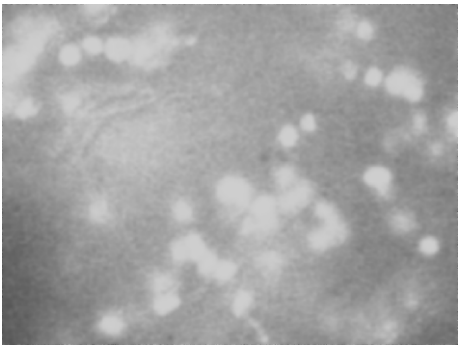

Figure 5. Fibroblast cell distribution in the collagen gel.

3.3. QCM STUDIES

The introduction of cells to quartz crystals with associated collagen hydrogel overlayers reduced the oscillation frequency by 110 ± 1.0 Hz and increased the auto-gain controller voltage, indicating cell interaction with the collagen matrix (Fig. 6). These shifts can be interpreted in terms of mass addition at the sensor surface. The response of the QCM also reflects the dissipation of energy within the system and hence changes of viscoelastic properties of the matrix and cellular overlayers.

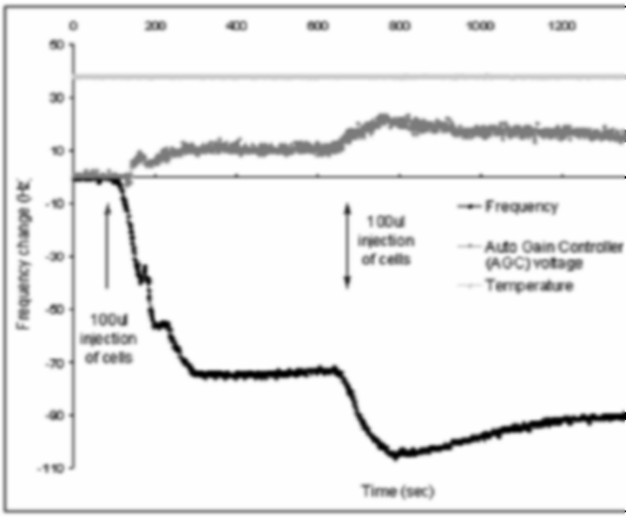

Figure 6. Composite frequency (black), auto-gain controller voltage (AGC) (mid-grey) and temperature (light-grey) trace for the addition of 0.1 mL aliquot of 3T3 fibroblast suspension (2.0×10^6 cell mL^{-1}) upon an unsupported section of collagen hydrogel laid the surface of a 10 MHz gold coated crystal. Flow injection rate 0.01 mL min^{-1}, 37 ± 0.1 ºC, pH 7.2, PBS.

3.4. DIFFUSION EXPERIMENTS

3.4.1. Experimental results

The dynamics of aprotinin, Apr, and Fg diffusion are shown in Figures 7 and 8 (data for BSA diffusion are not shown). Within 60-65 min of diffusion of relatively small aprotinin molecules the system reaches equilibrium for both (1.3 and 2.6 mg/ml) initial concentrations (Fig. 7). The larger BSA molecules need about 75 minutes to reach equilibrium and Fg molecules equilibrate within 90 minutes (Fig. 8). This pattern is characteristic of the relationship between the diffusion coefficient and the molecular mass of solute; the larger the molecules the slower their motion. For example, the diffusion coefficients, D_0 for BSA and Fg in aqueous

media are 1.0×10^{-6} cm^2/s and 1.94×10^{-7} cm^2/s, respectively. The diffusion of aprotinin through the hydrogel membrane is slower after a pre-run of Fg, and particularly after a pre-run of BSA and Fg (Fig. 7).

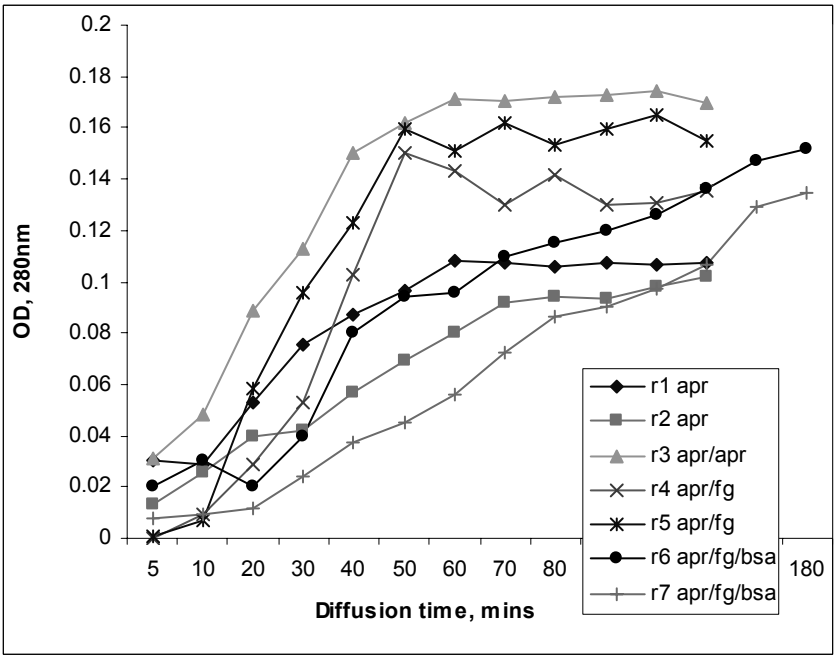

Figure 7. Dynamics of aprotinin diffusion through the collagen hydrogel. 1 & 2 are for starting concentration of 1.23 mg/mL in the feeder cell (OD=0.09). 3-7 are for starting concentration of 2.46 mg/mL (OD =0.18). 3 - Apr run after Apr; 4 and 5 – Apr run after Fg; 6 and 7 - Apr run after Fg and BSA.

Similar patterns were observed in the experiments with BSA diffusion after Fg (not shown). This could be explained by the blocking of small pores and channels in the hydrogel matrix by adsorbed or physically trapped protein molecules from the previous run.

3.4.2. Mathematical description

If the diffusion through open pores is straightforward with molecules moving to reduce a concentration gradient, it can be described by First Fick's Law, *i.e.*

$$J = -D\Delta c \tag{1}$$

where the flux, J depends on the concentration gradient, Δc over a specific distance through a proportionality constant, the diffusion coefficient, D. The applicability of this simple relationship to tissue scaffolds depends on the effective path length of an open pore that is often substantially longer

than the sample dimensions, due to the interconnectivity of pores. In this case, the diffusion coefficient measured for a straight through pore diffusion needs to be reduced by appropriate amount, i.e.

$$D_{porous} = \frac{\varepsilon}{\tau} D_{free} \tag{2}$$

where ε/τ is the porosity tortuosity factor. The tortuosity factor in a tissue scaffold will differ for different molecular species due to both size and charge effects. It will change with time due to changes in the pore size distribution and tortuosity that will occur due to cell growth, protein adsorption and scaffold degradation.

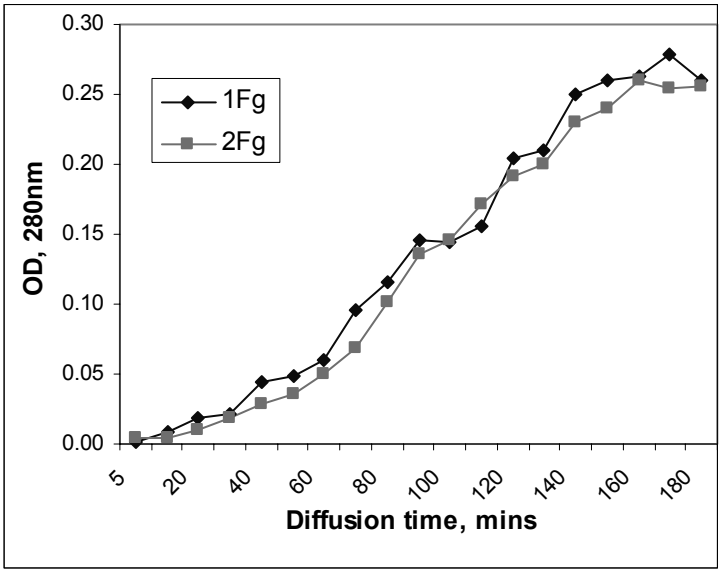

Figure 8. Dynamics of fibrinogen diffusion through the collagen hydrogel. Initial Fg concentration 1.7 mg/mL.

To gain more information from the diffusion kinetics data the distribution function of the diffusion coefficient *f(D)* was calculated using an integral equation (3):

$$c(x,t) = \frac{c_0}{2\sqrt{\pi}} \int_{D_{min}}^{D_{max}} \frac{1}{\sqrt{Dt}} exp\left(-\frac{x^2}{4Dt}\right) f(D)dD \tag{3}$$

where c_0 is the initial concentration in the feeder cell, x is the membrane (hydrogel) thickness, and D_{min} and D_{max} are the minimal and maximal values of the diffusion coefficient, respectively. This equation was solved using a regularization procedure. The diffusion of proteins through the

membrane is limiting; therefore, the Brownian diffusion of protein molecules in the cells was neglected. Distribution functions of the diffusion coefficient for aprotinin and Fg are shown in Figures 9 and 10.

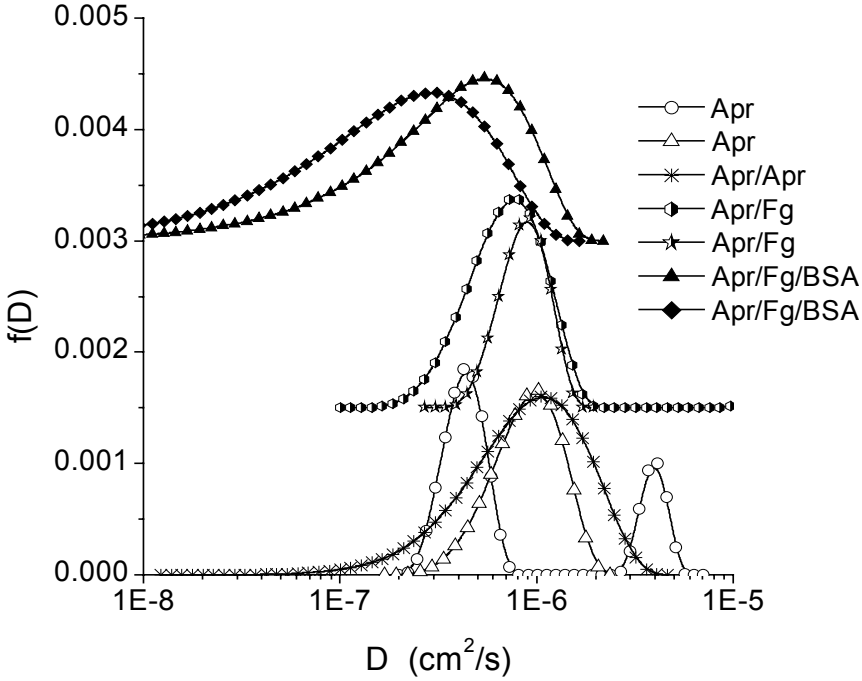

Figure 9. Distribution function of the diffusion coefficient *f(D)* for aprotinin through the collagen hydrogel.

The appearance of several peaks on the *f(D)* curves for certain runs can be explained by the mechanism of protein diffusion through hydrogel. The peaks of the distribution function *f(D)* for Fg and BSA (not shown) reveal that the corresponding diffusion coefficients are close to D_0, *i.e.* the diffusion of Fg and BSA occurs as diffusion of free monomers in the aqueous solution without the membrane. This confirms that proteins of different molecular weight such as aprotinin, BSA (14×6×4 nm) and even Fg (45×9×6 nm) can penetrate through the collagen hydrogel without significant retardation. The left peak or the left shoulder of *f(D)* curves in the case of monomodal distributions at $D < D_0$ values indicates that the diffusion of a portion of protein molecules through the hydrogel is slower than in the aqueous solution because of the protein adsorption within the collagen network. This adsorption reduces the pore size of the hydrogel matrix and causes retardation of the diffusion of the next portion of molecules through the membrane. This effect is maximal in the aprotinin run after BSA and Fg (Fig. 7) because large protein molecules block the membrane passage more effectively than smaller molecules.

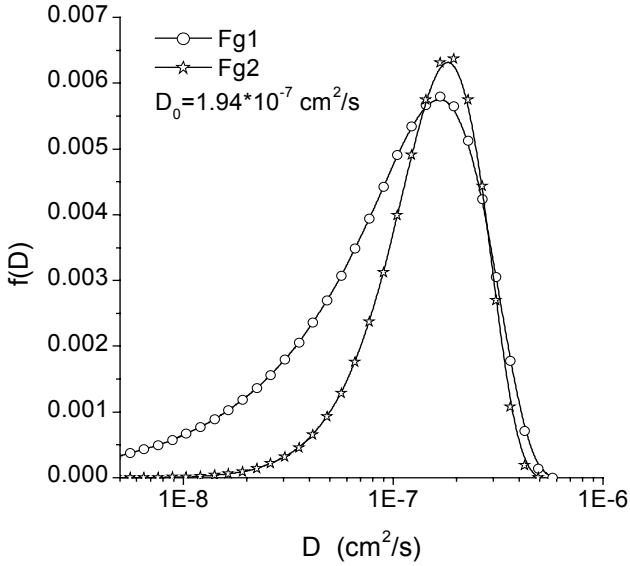

Figure 10. Distribution function of the diffusion coefficient *f(D)* for fibrinogen through the collagen hydrogel.

4. Conclusions

Measurement of the porous structure of soft hydrogels is a challenging task which is of extreme importance for predicting their performance and optimizing their properties as tissue scaffolds. No single method can provide all the necessary information, however combining data obtained using modern experimental techniques would help to solve this problem.

ACKNOWLEDGEMENTS

Authors express their thanks to Dr. K. D. Pavey (University of Brighton) for discussion of the QCM data and to Mr. V. I. Chernyshev (Palladin Institute of Biochemistry, Kiev) for sample preparation for electron microscopy.

This work has been funded by the Department of Trade and Industry (UK), project MPP4.2.

Prof. V. M. Gun'ko acknowledges financial support of his visit to Brighton by NATO Collaborative Linkage Grant N979845.

REFERENCES

1. R. Stern, M. McPherson, and M. T. Longaker, Histological study of artificial skin used in the treatment of full-thickness thermal injury, *J. Burn Care Rehabil.* 11(1), 7-13 (1990).
2. I. V. Yannas, E. Lee, D. P. Orgill, E. M. Skrabut, and G. F. Murphy, Synthesis and characterization of a model extracellular matrix that induces partial regeneration of adult mammalian skin, *Proc. Natl. Acad. Sci. USA* 86(3), 933-937 (1989).
3. I. Jones, L. Currie, and R. Martin, A guide to biological skin substitutes, *Br. J. Plast. Surg.* 55(3), 185-193 (2002).
4. B. L. Seal, T. C. Otero, and A. Panitch, Polymeric biomaterials for tissue and organ regeneration, Review, *Materials Sci. Eng. R* 34, 147-230 (2001).
5. E. Sachlos, and J. T. Czerhuszka, Making tissue scaffolds work. Review on the application of solid free form fabrication technology to the production of tissue engineering scaffolds, *Eur. Cells Materials* **5**, 29-40 (2003).
6. D. Michaeli, and M. McPherson, Immunological study of artificial skin used in the treatment of thermal injuries, J. Burn Care Rehabil. 11(1), 21-26 (1990).
7. F.J. O'Brien, B.A. Harley, I.V. Yannas, and L. Gibson, Influence of freezing rate on pore structure in freeze-dried collagen-GAG scaffolds, *Biomaterials* 25(6), 1077-1086 (2004).
8. K. D. Pavey, S. L. James, S. E. James, L. I. Mikhalovska, P. Tomlins, F. Paul, and S. V. Mikhalovsky, Real-time monitoring of cellular integration within bulk soft tissue scaffold materials, *J. Mater. Chem*. 13, 654-656 (2003).

MODELING GAS PHASE ADSORPTION IN INDUSTRIAL AND MILITARY APPLICATIONS

PETER LODEWYCKX*
Dept. of Chemistry, Royal Military Academy,
Renaissancelaan 30, B-1000 Brussels, Belgium

Abstract. This paper deals with the current state of modeling the breakthrough behavior of activated carbon beds. Different models are discussed as well as the differences between dealing with industrial dangers and with military/terrorist threats. Finally some of the problems are highlighted. These are mainly the result of the real-life, i.e. non-ideal, conditions of use of the protective mask-activated carbon canister combination.

Keywords: adsorption; activated carbon; mathematical modeling

1. Introduction

Modeling gas phase adsorption on activated carbon filters is necessary, both in an industrial environment and for the protection of military and civilian personnel in military operations and/or under terrorist threat. The broad range of toxic agents, environmental conditions and types of activated carbon simply does not allow laboratory testing of each and every possible combination. In order to evaluate the protection provided by a specific activated carbon filter in a well-defined environment it is necessary to trust the results of mathematical modeling, taking into account the necessary safety margins.

There are however marked differences between the modeling in an industrial environment and in a military one. In general it is safe to state

* E-mail: Peter.Lodewyckx@rma.ac.be

J.M. Loureiro and M.T. Kartel (eds.), Combined and Hybrid Adsorbents, 321–335.

that most problems are encountered in the latter one, resulting in less accurate but more robust models.

2. Particularities of Modeling in an Industrial Environment

2.1. TOXIC AGENTS

The big advantage of modeling in an industrial environment is the prior knowledge of the danger, more specifically the nature and the concentration of the toxic agents and the composition of the air. Industrial safety and health regulations require chemical plants and other industrial installations posing chemical risks to have emergency plans. These are based on an elaborate risk analysis and will give good estimates of what to expect in case of an incident (leakage, explosion,…). Usually it is possible to allocate the 'right' filter to each worker, i.e. to maximize the protection provided by a mask-filter combination, as the number of toxic agents is both limited and well defined. The same being true for the concentration range.

A supplementary advantage of knowing the threat is the increased possibility to use ESLI's (End of Service Life Indicators). These devices can give the bearer a signal (acoustic, odor,…) when the filter reaches the end of its adsorption capacity and decreases the need for reliable modeling.

2.2. EXPOSURE TIME OF THE FILTER

The time of exposure of the activated carbon filter to the toxic agent is either limited, or well-defined, or both. When the worker needs respiratory protection during his normal task, the exposure time will be regulated by work instructions (based on a risk analysis). Usually only a very limited part of the filter capacity will be used. There is however a risk when re-using the filter as the behavior of an activated carbon bed at intermittent use is still an area of very little research.[1]

When using a filter in the case of an incident, the exposure time will be limited: workers will only use activated carbon filters to escape from a toxic environment. Intervention teams will be, almost exclusively, equipped with self-contained breathing apparatus.

3. Particularities of Modeling in a Military Environment

3.1. TOXIC AGENTS

In contrast to the industrial environment, the toxic agents and their concentrations are usually not known prior to the exposure. There is also no unique view on exactly what property makes a gas a Chemical Warfare Agent or CWA. It is certainly not its lethality, as many very dangerous gases (e.g. dioxins) are not considered to be CWAs. Nor is there a direct link with the production process, as some gases (e.g. CNCl and HCN) are commonly classed as CWAs, but have a widespread use in industry. Even the actual use as a chemical weapon does not suffice. For example, even chlorine is no longer considered a CWA. The only thing they all have in common is their high toxicity.

Apart from the CWA, toxic industrial chemicals (TIC) can pose a severe threat to troops and civilian population in a zone of operations or as a result of a terrorist attack. Even though careful planning and reconnaissance will yield a lot of useful information on the type of TIC and the quantities likely to be released, uncertainty will be higher than in the case of a pure industrial environment.

3.2. EXPOSURE TIME OF THE FILTER

In general, for military personnel the mission will prevail, even in the case of a chemical attack or incident. Therefore, bed exposure times will tend to be (much) longer than in the case of industrial applications.

Another difference resides in the moment the protective equipment is put to use. In an industrial environment this will be just before entering a contaminated area or just after the incident. Military personnel can be wearing its protective equipment for hours prior to an imminent attack. This results in the filter being exposed to the humidity in the ambient air prior to its actual use (see 8.1).

4. Chemical Engineering Models

4.1. EQUATIONS

The chemical engineering models consider the filter as a chemical reactor, using the conventional equations for mass and heat transfer to describe the transport processes through the filter. Even with modern computational techniques, one has to make some assumptions and simplifications to the real phenomena:[2-6]

- There is no radial dispersion, i.e. one uses a unidimensional model of a plug flow. This is generally true, as the (usually) cylindrical shape of the filter, in combination with a high flow rate, will result in a negligible radial dispersion. Axial dispersion, however, can not be neglected.
- There is no pressure drop over the filter. Of course this is not true, but the influence of pressure drop on the different equations (e.g. by changing the partial pressure values) is very small.
- The heat capacities (c_p and c_v) remain constant. In the range of the measured differences in pressure and temperature this assumption is correct.
- The contaminant is passive. This means the contaminant will not change the macroscopic dynamic parameters of the carrier gas (usually air). The limited amount of the toxic compound will not change gas parameters such as viscosity and density, hence one can use the known parameters of dry or humid air to calculate the dynamics of the gas flow.
- The filter is considered to be adiabatic, i.e. there is no heat exchange between the activated carbon bed and the environment. This is certainly not true, and some models do take the heat exchange (loss) with the environment into account. However, this is not a feature of the activated carbon bed, but is directly related to the filter housing or canister.
- The temperature of the gas and the activated carbon, at a certain spot inside the filter, are always equal. This presumes an infinitely fast heat exchange between the gas (heated by the exothermic reactions) and the carbon. This would also mean that all the carbon downstream from the adsorption front would have the same temperature as the gas in the adsorption front. Experimental evidence shows clearly this is not the case.[7] However, as this heat exchange is very case sensitive, it is in most cases impossible to calculate it correctly.

With these provisos, one can rely on the following set of equations:

- A mass balance over the filter (interparticle diffusion)
- An energy (heat) balance over the filter
- A mass balance over one carbon particle (intraparticle diffusion)
- An energy (heat) balance over one carbon particle

As one can see, this is a system of coupled differential equations. Some of these balances can even involve more than one equation, e.g. intraparticle diffusion that can be a combination of Knudsen diffusion and surface diffusion. A supplementary equation is needed to describe the adsorption itself. In the case of pure physisorption, this is simply the mathematical description of the adsorption isotherm, e.g. the Dubinin-Radushkevich

equation.[8] In the case of chemisorption, one has to find an equation to describe the interaction between the carbon (and the impregnants) and the specific gas. In most cases chemisorption equilibrium conditions can be fitted with a Langmuir-type isotherm. A combination of these equations, including a correct set of boundary conditions, will yield a time-concentration profile through the filter.

These models have two main advantages: they simulate the complete breakthrough curve (see 5.1) and they are, within the limits of the assumptions and simplifications, physically correct. The first one is not really needed in the case of protection of military personnel since the most important parameter that has to be determined is the breakthrough time (see 5.1). The complete breakthrough curve is of particular interest in gas separation applications and more complex systems such as PTSA (Pressure and Temperature Swing Adsorption).

4.2. PARAMETERS TO BE ESTIMATED/MEASURED

The main advantage, the physical correctness, of these models comes at a price as one has to describe, in detail, every physical and chemical phenomenon inside the carbon and one has to know all the interaction parameters. Some of these, such as the tortuosity, the different diffusion coefficients, the flow pattern and any chemical interactions, are difficult to calculate or even to evaluate from a limited number of experiments. As a result, these models that are supposed to be very general can only be used for a limited number of very specific adsorbent-adsorbate couples. If either changes, one has to go back to the drawing board, estimating, guessing or determining experimentally the missing parameters. Even though this limits the practical use of these models, their importance should not be underestimated. A detailed comparison between the results of the model and experimental breakthrough curves can yield very important information about the adsorption and transport processes, especially if one is interested in the values and effects of adsorption heats and heat transport through the bed. It goes without saying that these equations are best suited for industrial applications where the adsorbent and adsorbate are well known and remain unchanged.

5. Breakthrough (curve) Modeling

5.1. BREAKTHROUGH AND BREAKTHROUGH CURVE

An important feature in filter modeling is the breakthrough curve (concentration at the filter outlet as a function of time). This curve is nothing more than the mirror image of the adsorption front (see Fig. 1).

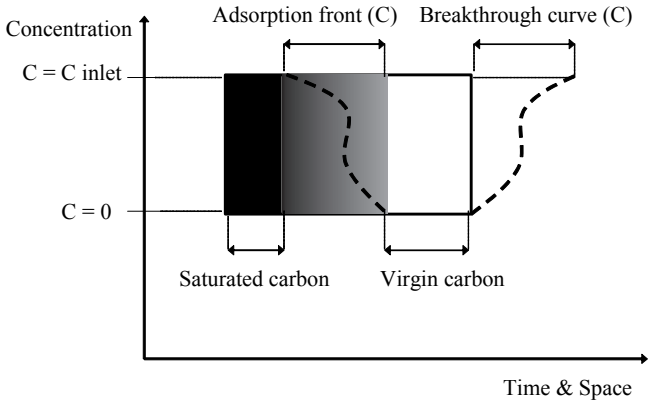

Figure 1. Adsorption front and breakthrough curve for an activated carbon bed.

For most military applications, and for protective purposes in general, there is no need to simulate the complete breakthrough curve. The point of interest is when the breakthrough curve reaches a certain concentration, the so-called breakthrough concentration. This is a predetermined value, different for each toxic compound. Logically, it is the concentration at which the person wearing the protective equipment starts to experience adverse effects. For industrial chemicals these are normally tabulated values, such as TLV (Threshold Limit Value) or MAK (Maksimale Arbeitsplatz Konzentration), that take into account long term effects on safety and health. For the chemical warfare agents these are typically IDLH-values (Immediate Danger to Life and Health). This is purely a practical approach, as, sadly enough, for many CWA these are the only thresholds that have been established experimentally. Once this value is reached at the filter outlet, the protection is considered compromised and the filter has to be exchanged for a new one.

5.2. EXISTING MODELS

Nearly all the breakthrough models are based on some sort of mass balance over the filter. In other words, all other mass and energy balances (see 4.1) are either ignored, or are not treated separately. Usually these equations,

especially the ones related to diffusion, only influence adsorption kinetics. The capacity of the activated carbon bed is then determined by a combination of the mass balance over the filter, combined with an expression defining the maximum uptake per unit of carbon, i.e. the adsorption isotherm. All kinetic terms are usually combined into one or two parameters that "correct" the capacity of the filter in order to give the proper breakthrough time. Some of the references give a very good, and comprehensive, overview of these models and equations.[9,10]

6. Wheeler-Jonas or Reaction Kinetic Model

6.1. EQUATION AND PHYSICO-CHEMICAL BACKGROUND

One of the most commonly used models is the one proposed by Wheeler and Jonas in the early 70s.[11] This equation, also known as the Reaction Kinetic equation, can be expressed in several forms. The most explicit one is given in Eq. (1).

$$t_b = \frac{W_e \cdot W}{Q \cdot c_{in}} - \frac{W_e \cdot \rho_b}{k_v \cdot c_{in}} \ln\left(\frac{c_{in} - c_{out}}{c_{out}}\right) \quad (1)$$

The breakthrough time t_b (min) is expressed as a function of the sorption capacity W_e (g_{gas} per g_{carbon}), the total mass of carbon in the filter W (g_{carbon}), the volumetric flow rate Q ($cm^3.min^{-1}$), the inlet concentration c_{in} ($g_{gas}.cm^{-3}$), the bulk density of the carbon in the filter ρ_b ($g_{carbon}.cm^{-3}$), the breakthrough concentration c_{out} ($g_{gas}.cm^{-3}$) and the overall mass transfer coefficient k_v (min^{-1}). There are some limitations to this equation:

- The flow pattern has to be a perfect plug flow with axial, but no radial diffusion. This is normally satisfied when the diameter of the bed is not too small compared to the bed length. For filter systems it is commonly accepted that diameters have to exceed 2 cm to be considered plug flow.
- The original equation was based on physisorption into micropores.
- The rate constant k_v has to be of a first order with respect to the number of gas molecules (= c_{in}). For pure physisorption this is usually true in the first, convex, part of the sigmoidal breakthrough curve, i.e. for values of c_{out}/c_{in} < 5 to 10 %.

The specific arrangement of the different terms clearly shows the rationale of the model: the first term is the total capacity of the carbon ($W.W_e$) for a given vapor divided by the total amount of this vapor entering the filter per unit of time ($Q.c_{in}$). In other words, this is the time the filter

would resist if the adsorption was instantaneous and the adsorption front (see Fig. 1) would have zero depth. After $t = t_b$ the concentration at the outlet of the filter would jump from zero to c_{in}. In reality, the adsorption front has a certain width, and there are vapor molecules in front of the saturated part of the filter. Consequently, the breakthrough time will be shortened by the second term. This term is of course a function of the reduction factor R ($c_{in}.c_{out}^{-1}$), i.e. the point chosen on the breakthrough curve to define the breakthrough time. But the most important parameter here is the overall mass transfer coefficient k_v. This factor accounts for all possible resistances against mass transport during the adsorption process. In this way it covers both the interparticle and intraparticle diffusion.

The Wheeler-Jonas equation can be used as such to extrapolate experimental data to other circumstances, varying airflow, concentration, bed depth, etc. To do this, W_e and k_v can be treated as fitting parameters and derived from a number of breakthrough experiments. Then, the obtained values can be used to make the necessary extrapolations. However, if one really wants to predict breakthrough times for a given filter-toxic vapor system, there has to be a way to calculate W_e and k_v without any prior breakthrough experiment. For W_e this problem is not too difficult to solve[12] as the dynamic capacity, in the case of physisorption, can be approximated by the static capacity as given by the adsorption isotherm. Accordingly, W_e can be calculated, rather straightforwardly, from the Dubinin-Radushkevich equation (Eq. 2):

$$W_e = W_o\, d_L \exp\left[\frac{-B\,T^2}{\beta^2}\log^2\left(\frac{c_S}{c_{in}}\right)\right] \qquad (2)$$

The only unknown parameters are W_o and B. These can be derived from any known isotherm of the activated carbon (e.g. N_2 at 77K). The affinity coefficient β can be found in the literature or calculated, the liquid density d_L and the saturation concentration c_S are tabulated.

Estimating the overall mass transfer coefficient k_v is more difficult. It is, a priori, impossible to differentiate between the different diffusion steps in the adsorption process. Therefore k_v is estimated on the basis of semi-empirical equations. Up to now, the most complete one is given by Eq. (3).[13] In this equation, k_v is the overall mass transfer coefficient (min^{-1}), β is the affinity coefficient of the Dubinin-Radushkevich equation , d_p the mean diameter of the carbon particles (cm), v_L the linear velocity of the air stream through the bed ($cm.s^{-1}$), W_e the equilibrium adsorption capacity (g_{vapor}/g_{carbon}) and M_W the molar mass of the toxic organic vapor ($g.mol^{-1}$).

$$k_v = 800.\beta^{0.33}.d_p^{-1.5}.v_L^{0.75}.\left(\frac{W_e}{M_w}\right)^{0.5} \quad (3)$$

6.2. ADVANTAGES AND WEAKNESSES

The weaknesses of this equation are obvious: as one does not differentiate between the different diffusion mechanics there is no way to correlate k_v with theoretical or experimental diffusion models. In other words, the model lacks physical correctness.

On the other hand, the explicit differentiation between capacity and kinetics is very useful when studying new systems and/or the influence of certain parameters (see 8) on the adsorption behavior. As it is essentially a 2-parameter equation (all parameters beside W_e and k_v can be calculated for any given system), it is very adequate to be used for extrapolations in the cases where Eq. (2) and/or (3) are not valid (see 8.3).

7. Modeling Different Forms of Carbon

7.1. GRANULAR ACTIVATED CARBON

For the physisorption on granular activated carbon the Wheeler-Jonas equation and Eq. (2) and (3) can be used as such. All parameters can be either measured directly or derived from a N_2- isotherm.

7.2. CARBON FIBERS AND CARBON CLOTH

Carbon fibers are gaining a lot of attention lately for protective purposes. For certain applications their low weight, high capacity and good adsorption kinetics outweigh their disadvantages (high pressure drop and difficulties to use impregnations). For modeling purposes Eq. (1) and (2) can be used without any special precaution. Even though one has to be very careful with the exact definition of the different parameters. E.g. the value of ρ_b will be very low for a bed of activated carbon fibers.

The application of Eq. (3) is less straightforward, especially the determination of d_p, as a fiber is very different from a spherical particle. However, it is clear that the diameter of a particle is a measure for its external surface and hence for the boundary layer governing diffusion. According to this, for activated carbon fibers d_p can be calculated as the diameter of a sphere with the same external surface as the fiber. Given the

ratio between fiber diameter and length, there is a direct relation between the fiber length and the parameter d_p from Eq. (3).[14-16]

For modeling purposes carbon cloths can be treated as carbon fibers, using the appropriate values of bulk density and fiber length.

7.3. CARBON MONOLITHS

Like fibers, activated carbon monoliths attract much attention for military applications. Especially the very good adsorption kinetics, combined with a low breathing resistance, look promising. Downsides are the difficulties to impregnate the carbon and leakage (= very low concentrations coming through the monolith long before the actual breakthrough time) when confronted with highly toxic chemicals.

The modeling problem is essentially the same as for fibers: estimating the value of d_p. As the gas is flowing on the inside of the channels, rather than on the outside of spherical particles, it seems logical to link d_p to the diameter of the monolith channels. This has been investigated and, for specific monoliths, the relation was found[17] to be d_p = channel diameter/π.

7.4. THIN LAYERS (PROTECTIVE SUITS)

Preliminary results indicate that Eq. (1), (2) and (3) are also valid when calculating breakthrough of thin layers of activated carbon, such as can be found inside semi-permeable chemical protective suits.

7.5. NON-CARBON ADSORBENTS

When using non-carbon adsorbents (such as zeolites), or hybrid adsorbents, Eq. (1) stays valid. In most cases the two supporting equations are valid too, sometimes with minor adjustments, but this has to be examined case by case.

8. Problems with Breakthrough Modeling

8.1. HUMIDITY

Humidity has a marked effect on breakthrough times. This is not in the least due to the abundance of moisture in the ambient air. A relative humidity of 60% at 296 K, which is not at all exaggerated and quite normal in most parts of the world, is equivalent to a concentration of approximately 16500 ppmv of water molecules. For a filter, this concentration comes into contact

with the activated carbon through the inhaled air stream. For clothing, the transpiration going out will be an additional source of water "contamination" of the activated carbon. Thus even in the absence of any toxic compound, the activated carbon in filters and clothing will be exposed to water vapor. This is often referred to as pre-wetting, or prehumidification, of the carbon bed. When a chemical incident occurs, the toxic compound will be in competition with the water vapor in the air stream, and with the pre-adsorbed water, if any, for available adsorption space. This can be "real" space, i.e. micropore volume in the case of physisorption, or reactive/catalytic species on the surface of the carbon (e.g. Cu ions on whetlerite).

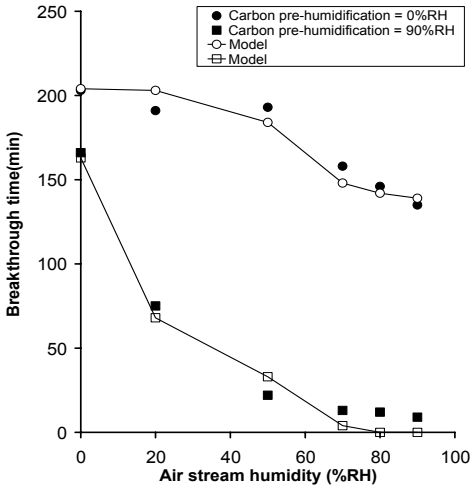

Figure 2. Example of modeling the breakthrough time of physisorbed vapors under humid conditions using the Wheeler-Jonas equation and adapted forms of Eq. (2) and (3).

In the case of physisorption, the loss of adsorption capacity (Eq. 2) can be modeled. The most successful way of doing this is by volume exclusion.[18-20] The more volatile the toxic compound, the more it will be influenced by water adsorption as it is unable to replace the more strongly adsorbed water molecules. The available micropore volume in the presence of water can be calculated from the dry micropore volume, the amount of pre-adsorbed water, the amount of water in the contaminated air stream and the amount of water replaced by the vapor. The latter being function of the total amount of water on the carbon, the ratio of the amounts of water and vapor in the air stream and the ratio of their saturation vapor pressures. The new value of the micropore volume thus obtained can be used in Eq. (2) to calculate the capacity under humid conditions.

The water adsorbed on the carbon will also influence adsorption kinetics by slowing down mass transfer. The overall mass transfer coefficient, k_v, of

the Wheeler-Jonas equation does not differentiate between the different types of diffusion. Consequently, every impact of water on the adsorption kinetics will be translated into a drop of k_v values. The mass transfer coefficient under humid conditions can be expressed as a function of this coefficient in the absence of water, the total pore volume of the carbon and the total amount of water adsorbed.[21] Combining the adapted models to calculate W_e and k_v it is possible to obtain very good predictions for the breakthrough time of physisorbed agents. This is illustrated in Fig. 2.

8.2. DISCONTINUOUS FLOW PATTERN

There has been much debate about the influence of the flow type on breakthrough times of activated carbon beds: in some cases experimentally determined breakthrough times with a "breather" flow (discontinuous or half-sine flow) have been shown to be significantly shorter than the corresponding breakthrough times with a continuous flow.[22-24] This is of particular interest as this type of flow is typical for activated carbon canisters used in combination with a gas mask. It has been demonstrated that this difference is primarily due to a change in the overall mass transfer coefficient k_v.

This can be explained by the difference between the mean value of the real (discontinuous) air stream velocity through the bed (v_L - see Eq. 3) and the value of v_L calculated from a continuous flow. Simulations show that the ratio of these two values is a constant factor of 1.22. Taking this into account, it is possible to make accurate predictions of real life breakthrough times of gas mask canisters. Providing, of course, that Eq. (3) is valid (see 8.3).

8.3. CHEMISORPTION, CHEMICAL REACTIONS AND TRACE QUANTITIES

The Wheeler-Jonas equation is based on a mass balance over the carbon bed. As such, it should remain valid in the case of chemisorption. But, a priori, neither Eq. (2) nor Eq. (3) can be used in this case. Capacity is a function of specific interactions, rather than micropore volume. This means Eq. (1) cannot calculate breakthrough times "ab initio" but is still able to be used for the extrapolation of a limited set of experimental data.[25,26] In some cases Eq. (3) seems to remain valid, undoubtedly when diffusion rather than the chemical reaction is the rate controlling step in the chemisorption process.

When chemical reactions take place on the carbon in the presence of water (such as hydrolysis of the toxic compound), or when the compound is

highly soluble in water, Eq. (1) through (3) remain valid in the absence of water vapor. As in real conditions of use this is seldom the case, and the derived equations that take the water vapor into account (see 8.1) are certainly not valid, it is very difficult to model adsorption behavior under these circumstances. Even extrapolations of breakthrough times are to be treated with great care.

When only trace quantities of a gas are present in the air stream, surface groups are known to play a role in the adsorption process, even for gases that are "purely" physisorbed at higher concentrations.[27] This means the equations that have been developed to estimate capacity and kinetics are no longer valid. However, usually the surface groups enhance the capacity at low inlet concentrations. As a result the estimated breakthrough times are lower than the real ones, which means the error is towards an increased safety for the user.

9. Conclusions

The huge amount of different toxic vapors, coupled to the marked influence of environmental conditions, makes it impossible to rely exclusively on laboratory testing to estimate breakthrough times of activated carbon filters. In many cases accurate predictions are possible, even when based on a very limited number of experimentally determined parameters of the carbon. In other cases it is only possible to use some of these equations to extrapolate the results of actual filter testing. And in some cases it is still, at this time, impossible to give any accurate prediction of the adsorption behavior of the activated carbon bed.

REFERENCES

1. F.A.P Maggs, and M.E. Smith, The use and regeneration of type-O canisters for protection against methyl bromide, *Ann. Occup. Hyg.* 18, 111-119, 1974.
2. M.J.G. Linders, Prediction of breakthrough curves of activated carbon based sorption systems: from elementary steps to process design, TU Delft (The Netherlands), PhD thesis, 1999.
3. P. Lodewyckx, Simulatie van de fysische adsorptie van gassen en dampen op een aktieve koolfilter [Simulation of the physical adsorption of gases and vapours on an activated carbon filter]. Katholieke Universiteit Leuven (Belgium) – FTW-CIT, MSc thesis, 1991.
4. A. Lavanchy, R. Touzani, and M. Stöckli, Numerical simulation of dynamic physisorption on activated carbon beds, *Int. Carbon Conference*, Santa Barbara CA (USA), 38-39, 1991.
5. U. Huber, Ueber die numerische simulation von dynamischen sorptionsprozessen im festbett [About the numerical simulation of dynamic sorption processes in a fixed bed], GRD AC-Labor, Bericht TA-8-SIG Wo/Le no. 8143, Spiez (Switzerland), 1981.

6. R.H. Van Dongen, and P.C. Stamperius, The dynamics of adsorption of vapours by porous adsorbents in fixed beds - Breakthrough curves of sarin on charcoal in the very low concentration region, Report 1974-4, Chemisch Laboratorium, TNO, Rijswijk (The Netherlands), 1974.
7. L. Verhoeven, D. Van Rompaey, and P. Lodewyckx, The temperature effects of the adsorption of phosgene on military filters, *Int. Carbon Conference,* Lexington KY (USA), 2001.
8. M.M. Dubinin, The potential theory of adsorption of gases and vapors for adsorbents with energetically nonuniform surfaces, *Chem. Rev.* 60, 235-241, 1960.
9. E. Balieu, Fundamental aspects on air filtration and purification by means of activated carbon filters, *Int. Symp. on Gas Separation Technology*, Antwerp (Belgium), 91-136, 1989.
10. M. Van Zelm, and J. Medema, Analysis of breakthrough curves of benzene on active charcoal, in: *Protection Against Toxic Compounds - Chemical and Technological Aspects*, Chemical Laboratory TNO, Rijswijk (The Netherlands), 104-119, 1973.
11. L.A. Jonas, and J.A. Rehrmann, The kinetics of adsorption of organo-phosphorous vapors from air mixtures by activated carbons, *Carbon* 10, 657-663, 1972.
12. G.O. Wood, Activated carbon adsorption capacities for vapors, *Carbon* 30, 593-599, 1992.
13. G.O. Wood, and P. Lodewyckx, An extended equation for rate coefficients for adsorption of organic vapors and gases on activated carbons in air-purifying respirator cartridges, *Am. Ind. Hyg. Assoc. J.* 64, 646-650, 2003.
14. P. Lodewyckx, G.O. Wood, and S.K Ryu, The Wheeler-Jonas equation: a versatile tool for the prediction of carbon bed breakthrough times, *Carbon* 42, 1345-1349, 2004.
15. C. Martin, J.-P. Joly, and A. Perrard, The Wheeler-Jonas model for interpreting breakthrough curves of SO_2 traces in air through carbon beds, *Carbon Conference*, Oviedo (Spain), 2003.
16. P. Lodewyckx, and S.K. Ryu, Modelisation of the adsorption of organic vapours on activated carbon fibres by means of the reaction kinetic equation, *Abstracts Carbon Conference*, Beijing (PRC), 2002.
17. P. Lodewyckx,T. Valdés-Solis, M.J.G. Linders, and F. Kapteijn, Application of the Wheeler-Jonas equation for the calculation of carbon monolith breakthrough times, *Int. Carbon Conference*, Providence RI (USA), 2004.
18. M. Manes, Estimation of the effects of humidity on the adsorption onto activated carbon of the vapors of water-immiscible organic liquids, *Engineering Foundation Conference on Fundamentals of Adsorption*, Schloss Elmau (Germany), 1983.
19. R.J. Grant, R.S. Joyce, and J.E. Urbanic, The effect of relative humidity on the adsorption of water-immiscible organic vapors on activated carbon, *Engineering Foundation Conference on Fundamentals of Adsorption*, Schloss Elmau (Germany), 1983.
20. P. Lodewyckx, and E.F. Vansant, The influence of humidity on the adsorption capacity from the Wheeler-Jonas model for the prediction of breakthrough times of activated carbon beds, *Am. Ind. Hyg. Assoc. J.* 60, 612-617, 1999.
21. P. Lodewyckx, and E.F. Vansant, The influence of humidity on the overall mass transfer coefficient of the Wheeler-Jonas equation, *Am. Ind. Hyg. Assoc. J.* 61, 461-468, 2000.
22. Y. Suzin, I. Nir, and D. Kaplan, The effect of flow pattern on the adsorption of DMMP in activated carbon beds and canisters, *Carbon* 38, 1129-1133, 2000.

23. M.J.G. Linders, E.P.J. Mallens, J.J.G.M. van Bokhoven, F. Kapteijn, and J.A. Moulijn, Breakthrough of shallow activated carbon beds under constant and pulsating flow, *Am. Ind. Hyg. Assoc. J.* 66 (March/April), 173-180, 2003.
24. I. Nir, D. Kaplan, and Y. Suzin, Extension of the Wheeler-Jonas model (WJM) for dynamic adsorption to pulsating flow, *Proceedings of the 7th International Conference on Fundamentals of Adsorption - FOA 7*, Nagasaki (Japan), 2001.
25. P. Lodewyckx, and L. Verhoeven, Using the Wheeler-Jonas equation to describe the adsorption of inorganic molecules: Chlorine, *Carbon* 41, 1215-1219, 2003.
26. L. Verhoeven, and P. Lodewyckx, Using the Wheeler-Jonas equation to describe adsorption of inorganic molecules: Ammonia, *Int. Carbon Conference*, Lexington, KY (USA), 2001.
27. D. Cazorla-Amoroz, M.A. Lillo-Rodenas, and A. Linares-Solano, Adsorption of VOCs at low concentration by porous carbons. Relevance of surface chemistry and porosity, *International Carbon Conference*, Kyeongju (Korea), 2005.

FOCUSING MATERIALS RESEARCH THROUGH PROCESS MODELING

JOSÉ MIGUEL LOUREIRO*, ANA MAFALDA RIBEIRO
LSRE, Department of Chemical Engineering, University of Porto, 4200-465 Porto, Portugal

SÓNIA ADRIANA FIGUEIREDO
ISEP, Polytechnic Institute of Porto, 4200-465 Porto, Portugal

Abstract. A brief introduction to chemical engineering modeling is given. It is then applied to several systems, showing that the introduction of dimensionless variables in the model equations enable the identification of the parameters that control the systems behavior. These parameters can generally be determined by independent experiments for a given system and the behavior of the system can be reasonably predicted through simulation. The systems here considered are the removal of color from liquid streams using natural waste materials from the Portuguese seafood industry, carbon filters for individuals protection in toxic environments, a class of polyacrilic gel beads reinforced by a polyamide membrane for metals extraction from aqueous media and the use of exhausted resins from an industrial demineralizing plant in the recovery of gold. The eventual weaknesses of the materials used in those processes are evidenced by simulation, showing the limiting parameters and in what sense should they be changed in order to improve the system behavior.

Keywords: process modeling; color removal; carbon filters; gold recovery; materials' research

* To whom correspondence should be addressed. José Miguel Loureiro, Laboratory of Separation and Reaction Engineering, Department of Chemical Engineering, University of Porto, Rua Dr. Roberto Frias, 4200-465 Porto, Portugal; e-mail: loureiro@fe.up.pt

J.M. Loureiro and M.T. Kartel (eds.), Combined and Hybrid Adsorbents, 337–348.

1. Introduction

Process modeling, i.e., the construction of a mathematical model for a physico-chemical system is a well established procedure in Chemical Engineering.[1] The model itself is no more than an ensemble of equations describing the process within the assumptions (or hypotheses) made. When dealing with a process, these equations are of utmost four categories:

- Conservation equations, describing the conservation of mass, energy, momentum, etc.
- Equilibrium relations, describing the (Thermodynamic) limits for the system progress;
- Rate equations, describing the chemical (reaction) and physical (transport) kinetics;
- Initial and boundary conditions linking the system (dependent variables) to its surroundings (specific values of the independent variables).

The model complexity should be intrinsically linked to the objectives pursued by the model itself, i.e., it should not include phenomena that can be neglected in view of the objectives nor should the reverse happen.

After writing the model equations in terms of physical quantities with dimensions, the following step is normally the introduction of dimensionless variables. Quoting Aris:[2] "it is only when quantities are made dimensionless that their magnitudes acquire an intrinsic meaning in the context of the model". This is a sometimes forgotten step but it should be stressed that it is essential in order to identify the independent (dimensionless) parameters controlling the process behavior. Their identification is straightforward and the influence of each parameter on the process behavior can then be studied independently of each other. These model parameters can, in principle, be classified as operating or intrinsic (those which cannot be changed by the change of one or more operating variables).

The objective of this work is to show that the information assessed by the parametric study referred to above can be used, in a feedback way, to focus materials research since it enables the identification of the eventual weaknesses of the materials used. This will be done with the help of several examples, namely:

- the removal of color from liquid streams using natural waste materials from the Portuguese seafood industry, where it will be shown that a biochemical reaction develops, superimposing its effects to the adsorption on the materials surface, an effect commonly referred as bioregeneration,[3]

- carbon filters for individuals protection in toxic environments, a gas phase system where adsorption and chemical reaction cooperate to enhance the protection time provided by the filter,
- a class of polyacrilic gel beads reinforced by a polyamide membrane for metals extraction from aqueous media, where the intraparticle resistance can be reduced by the development of intraparticle convection, and
- the use of exhausted resins from an industrial demineralizing plant in the recovery of gold, where the concepts of recycling and reuse are applied.

2. Color Removal with Natural Waste Materials[4]

In the framework of an environmental engineering project we decided to investigate the possibility of removing color from textile wastewaters using natural waste materials from the Portuguese seafood industry. With this purpose, three materials were selected, namely the Squid (*Loligo vulgaris*) and Sepia (*Sepia officinalis*) pens and the Anodonta (*Anodonta cygnea*) shell. These are chitin containing materials and chitin was shown to be a convenient adsorbent for dyes,[5] almost equivalent to activated carbon, the most used adsorbent in this context, even if expensive. After a previous screening test, two dyestuffs from CIBA-GEIGY, one reactive, the Cibacron green T3G-E (CI reactive green 12) and one direct, the Solophenyl green BLE 155% (CI direct green 26), were also selected to conduct the study.[6]

2.1. EQUILIBRIUM AND KINETICS

In order to predict the behavior of a fixed bed system for the removal of color using the above mentioned natural materials, adsorption equilibrium and kinetics should be determined.

Equilibrium was experimentally determined[7] at two temperatures (20 and 50 ºC) by contacting different amounts of the adsorbents with dye solutions with given concentration in closed flasks; two different grain sizes were used. Interestingly enough, smaller particles adsorbed more than larger particles, an unexpected result since, in principle, equilibrium should be independent of particle size. The observed result indicates a large contribution of the external surface for adsorption, probably due to the large molecular dimensions of the dyestuffs which cannot reach the inner surface of the adsorbents.

The Langmuir and Freundlich equations were shown to represent with reasonable accuracy the equilibrium data and the respective parameters were obtained by optimization.[6]

The next step was the experimental determination of the kinetics of adsorption. To this end, experimental runs were conducted in a perfectly mixed continuous adsorber. Using the previously determined equilibrium and a pore diffusion model to represent the adsorption kinetics, the effective diffusivities for each dye in each adsorbent were determined through the comparison between the experimental and the simulated response curves to a step input in the inlet dye concentration.[8] The obtained intraparticle effective diffusivity was invariably very low, coherently with the large dimensions of the dye molecules, corresponding to a very slow adsorption kinetics.

2.2. COLUMN EXPERIMENTS AND MODELING

With the equilibrium and kinetic data independently determined, a model can be built for the column experiments which, hopefully, will be able to represent the respective operation. This was true for several experiments, where the slow kinetics controlled the process. For these adsorbent/dye pairs, a further step was tried, mainly a chemical treatment (deproteinization or demineralization) of the materials in order to open the respective pores and to increase their relative chitin content; this procedure enhanced the dyes removal but the gain was hardly worth the effort.[9]

Column experiments for the removal of the direct dyestuff (Solophenyl green BLE 155%) with the Anodonta shell and with the Sepia pen gave unexpected results: when saturating the column, the outlet dye concentration first increased and then decreased to a plateau. This raised the question if a biochemical reaction was evolving inside the column; in order to confirm this hypothesis the flowrate to the column was changed and the height of the outlet plateau changed accordingly, a first confirmation of the hypothesis. The final confirmation was obtained after the experiments, when microorganisms were seen to develop in culture medium.

A model, considering axial dispersed plug flow of the fluid phase, external (film) and internal (homogeneous diffusion) resistances and taking into account the observed biodegradation of the direct dye, was then developed.[7,10] The dimensionless form of this model is:

$$\frac{1}{Pe}\frac{\partial^2 X}{\partial Z^2} = \frac{u_i}{u_{io}}\frac{\partial X}{\partial Z} + \frac{\partial X}{\partial \theta} + N_f (X - X^*) + \frac{k}{k_\infty} N_r X \qquad (1)$$

$$\frac{\partial Y}{\partial \theta} = N_d (Y^* - Y) \tag{2}$$

$$Y^* - Y = \frac{N_f}{\xi N_d} (X - X^*) \tag{3}$$

where X and Y are the dimensionless fluid and adsorbed phase concentrations, X* and Y* being the respective values in equilibrium, Z is the dimensionless axial coordinate and θ is time normalized by the column space time. From these equations it is evident that five dimensionless parameters control the system behavior; their definitions and names are:[10]

- $Pe = u_{io} L / D_{ax}$, axial Peclet number;
- $\xi = [(1-\varepsilon)/\varepsilon](q_E / c_E)\rho_{ap}$, column capacity factor;
- $N_f = (1-\varepsilon) k_f a_p \tau_o / \varepsilon$, number of mass transfer units by film diffusion;
- $N_d = 60 D_{he} \tau_o / d_p^2$, number of mass transfer units by internal diffusion;
- $N_r = k_\infty \tau_o$, number of reaction units or Damköhler number.

Both the axial dispersion and the film mass transfer coefficients can be determined by correlations.[10] The equilibrium (Langmuir) and kinetic (effective diffusivity) parameters determined before were used in the model. The value of the terminal biodegradation kinetic constant, k_∞, was obtained from the plateau concentration reached with one of the flowrates. Since the outlet concentration increased and then decreased, an induction period (t*) for the biomass growth (from an initial fraction $r_o = m / m_\infty$) following a first order mechanism was also introduced. This gives:

$$0 \le t < t^* \qquad k = k_\infty \exp\left[\left(1 - \frac{t}{t^*}\right) \ln(r_o)\right] \tag{4}$$

$$t \ge t^* \qquad k = k_\infty \tag{5}$$

This model is able to represent with reasonable accuracy the experimental results obtained.[7,10]

2.3. DISCUSSION

The interesting observation to retain from the simulations of the systems where biodegradation (bioregeneration[3]) occurs is that increasing the adsorbing capabilities of the materials does not contribute to increase the dye removal, since, e.g., only 0.8% of the Anodonta adsorption capacity is

really used.[10] As a matter of fact, even with smaller molecules, since the microorganisms block the access to the pores, the internal surface of the adsorbent is hardly accessible by the solutes. The removal occurs almost exclusively by the biochemical reaction and the chemical treatment of the materials although improving their adsorbing characteristics, apart from increasing the costs, also reduces or eliminates the development of the microorganisms responsible for the biodegradation. Since the steady state plateau is a function of the column space time, there is a simpler way to control the outlet concentration by just manipulating one operating parameter, the flowrate.

3. Carbon Filters for Individuals Protection in Toxic Environments

3.1. MODELING AND SIMULATION

When considering nonlinear adsorption coupled with chemical reaction in fixed beds, equilibrium models were developed and solved for Langmuir adsorption with zero[11], first[12] and second[13] order chemical reactions. It was shown that, for first order reaction, the breakthrough time normalized by space time is given by:[12]

$$\theta_{Bp} = 1 + \xi K \left[1 + \frac{1}{N_r} \ln \left| \frac{1 + (K-1)\exp(-N_r)}{K} \right| \right] \qquad (6)$$

where ξ is the mass capacity factor, K is the dimensionless adsorption constant and N_r is the number of reaction units. This equation shows that the breakthrough time increases with both the number of reaction units (Damköhler number) and the nonlinearity of the isotherm. The limit values are $\theta_{Bp} = 1+\xi$ in the absence of chemical reaction ($N_r = 0$) and $\theta_{Bp} = 1+\xi K$ for very large Nr ($N_r \to \infty$).

Carbon filters used in masks for individual protection in toxic environments are a special case of adsorptive reactors, where the toxic is adsorbed on the support (active carbon) and simultaneously consumed by chemical reaction on (or with) the impregnants. An example is the system studied by Friday[14] where the impregnant material (a metal salt) is consumed in a global second order reaction with the adsorbed solute (cyanogen chloride). A model was developed and solved for this system, including external (film) and internal (linear driving force approximation) mass transfer resistances.[13]

Carbon filters are shallow beds and the breakthrough concentration is generally very low due to the toxicity of the gases or vapors involved; as a

consequence, axial dispersion cannot be neglected. The model was then extended by the inclusion of axial dispersion, seven dimensionless parameters identified, and their influence on the breakthrough time of the filter assessed.[15]

Simulation results show that, again, apart from the axial dispersion which should be carefully evaluated, the nonlinearity of the equilibrium adsorption isotherm and the number of reaction units are the main parameters controlling the useful time of the filters.

The fixed bed was then considered to operate with axial or radial (inner and outer) flow and three models (ideal, dispersion and resistances) were solved for each geometry and flow. It was shown that the classical fixed bed arrangement with axial flow gives generally the best protection (longer useful time), except for some special cases (high values of the product ξN_r), where the radial outer-flow arrangement can be better.[16] It was also concluded that, since human lives depend on the correct functioning of these devices, a complex model, including as many physical and operating characteristics as possible should be used.

3.2. DISCUSSION

Since carbon filters are mainly applied for the life protection of individuals, the aforementioned systematic simulation of the dynamic behavior of carbon filters with several models shows that axial dispersion can never be neglected when building a model of these systems. It also shows that the knowledge of both the intrinsic (equilibrium and kinetic) as well as the operating (bed height, flowrate) parameters are of paramount importance to estimate with confidence the breakthrough time of a carbon filter. The operating parameters are generally known a-priori, but the intrinsic parameters should be estimated (based on correlations) or experimentally determined. Finally, the useful operating time of these systems can be drastically improved increasing both the number of reaction units and the nonlinearity of the adsorption equilibrium isotherm. This constitutes a challenge to the field of materials research.

4. Complexing Capsules for Metals Extraction

The Ph.D. thesis of Laguecir[17] involved the synthesis of polyamide complexing capsules containing a poly(acrylic acid) gel for the extraction of heavy metals from liquid streams. Polyacrylic acid is known to have excellent chelating properties but low mechanical resistance which limits its use in extraction processes. Although crosslinking can increase the mechanical resistance it also decreases the chelating capacity. This problem

was overcome by encapsulating the polyacrylic acid gel in rigid polyamide porous capsules.

4.1. EQUILIBRIUM AND KINETIC MODELING

Before the metals extraction, the gel is in sodium form and ion exchange occurs during chelation, sodium being substituted by the metals in the ionic sites of the gel. Experimental equilibrium points were determined in a stirred batch vessel and, given that an ion exchange process is taking place, the mass action law was used to model equilibrium; an excellent agreement was obtained between experimental and calculated points.[18]

Kinetic experiments of copper extraction were also carried out in a closed system; the liquid solution was well stirred in order to eliminate the external (film) resistances. A model, using the Nernst-Planck equation for intraparticle diffusion,[19] was built to simulate the histories of the fluid concentrations in the vessel.[20] This model was able to represent the experimental results with reasonable accuracy, enabling the determination of the effective diffusivity of copper ions in the polyacrylic acid gel. This effective diffusivity is almost three orders of magnitude lower than the diffusivity of copper in water, leading to the conclusion that diffusion, if homogeneous, is taking place in the dense gel phase.

Another (non reported) model was also built where the resistance of the polyamide membrane was included in series with the resistance to diffusion of the gel phase. This new model was not able to simulate the experimental results, i.e., apparently the resistance to mass transfer in the outer shell is negligible when compared to the resistance in the gel phase.

The characteristic time for intraparticle diffusion (also called time constant for intraparticle diffusion) for species i is given by:

$$\tau_d = \frac{R^2}{D_i} \tag{7}$$

where R is the particle radius (distance that an ion has to move from the liquid phase until the center of the particle) and D_i is the ion diffusivity inside the particle. Remembering that the gel phase is, in this case, encapsulated inside porous rigid polyamide spheres, the particles resemble the Hyper D media developed for preparative liquid chromatography.[21] These “soft gel in a rigid shell” materials present an enhanced diffusivity due to the development of intraparticle convection which increases with flowrate (pressure drop), conserving their dynamic capacities even with high flowrates. Physically, one can say that when flowrate increases the distance that ions have to move until the gel exchange sites decreases

(without changing the particle diameter), and so does the time constant for intraparticle diffusion.[22]

4.2. DISCUSSION

These encapsulated polyacrylic gel beads show a high static resistance to mass transfer. It is true that they can be produced in several dimensions[20] but the pressure drop through a fixed bed increases with the decrease of the particle diameter and so flowrate (productivity) cannot be increased without a cost. But since the polyamide membranes are highly porous, as a matter of fact, higher flowrates can be used without productivity losses due to the development of intraparticle convection. Unfortunately no experimental runs were conducted in order to test this hypothesis and to evaluate the intraparticle Peclet number, a measure of intraparticle flow.[22] It seems, however, that materials of this kind, where intraparticle convection will develop, can be an alternative in several reaction[23] and/or separation[24] applications when the intraparticle resistance is the controlling step.

5. Gold Recovery with Exhausted Resins[25]

Improvements in environmental quality are currently achieved by an in-source elimination or reduction of the pollutants generation as well as by recycling and reusing those which cannot be eliminated. To expand the useful life of products contributes decisively to a cleaner environment and is an essential requirement for any self-sustainable policy. Resins that completed their life-cycle in industrial water demineralizing plants are candidates for recycling and reuse to recover metals from wastewaters since their composition is known and, after a convenient regeneration step, they still show ion-exchange capacity. Gold and silver can in principle be recovered by the anionic resins from plating wastewaters and rinsing solutions since these resins show a high affinity to cyanide complexes, the form in which gold and silver can be found in solutions from both the mining and the electroplating industries.

A research work was then conducted with the objective of recovering gold from cyanide solutions using the anionic weak base macroporous Purolite A-100 resin, exhausted in an industrial demineralizing plant.

5.1. EQUILIBRIUM AND KINETICS

Isotherm equilibrium data were obtained in batch stirred flasks using different amounts of resin and equal amounts of a fixed concentration

mother solution. The resin exhibits a very high capacity for gold (more than 400 mg Au/g of dry resin).

Given that a weak electrolyte solution is used, both the Langmuir and the Freundlich isotherm equations can be and were used to represent the ion exchange equilibrium data,[19] but only the Freundlich equation was able to do that within the experimental errors, enabling the determination of the respective parameters.[25]

Since the recovery of gold is pursued in this work and the common practice of incinerating the saturated resin[26] is discarded for environmental reasons, the resin regeneration to recover gold was envisaged using an alkaline solution. This regenerating solution is no more a weak electrolyte and, furthermore, the Freundlich equation does not fix a limit to the resin capacity. Then, a mass action law isotherm (typical for ion exchange systems), also able to represent the experimental equilibrium data with reasonable accuracy, was used in the simulation of the regeneration step.

A kinetic experiment was then conducted in an agitated closed vessel; since the resin presents a very high capacity for gold, the amount of resin used (1 g) was very low when compared to the amount of solution (900 cm^3) with a 100 ppm gold cyanide concentration. In order to prevent physical attrition, the resin was placed inside a tea bag. Both these facts contribute to a non complete mixing, i.e., the film resistance to mass transfer was not eliminated. A model was then developed, including external and internal mass transfer resistances. The intraparticle mass transfer resistance was estimated with a fickian equivalent diffusivity based on the Nernst-Planck equation[27] and the linear driving force approximation was used. The model was able to follow very well the experimental results, enabling the determination of the film mass transfer coefficient.

5.2. COLUMN EXPERIMENTS AND MODELING

A column saturation experiment was run and simulated using a model considering axial dispersed plug flow of the fluid phase and incorporating the previously determined expressions for equilibrium (Freundlich isotherm) and kinetics (linear driving force with the equivalent diffusivity). The model is able to follow accurately the experimental saturation history of gold concentrations at the column outlet.

Finally a regeneration experiment was run, using a solution of potassium hydroxide and potassium cyanide (5 wt% in each) and simulated using the model developed for saturation but including now the mass action law isotherm for describing equilibrium. Moreover, a new equivalent Fick diffusivity was determined since the exchange is now in the reverse sense,

i.e., the most mobile ion is now replacing the less mobile ion in the resin.[27] Also, a mass balance equation, stating that total concentration is conserved in the fluid phase, was added. The model solution was not able to follow the experimental results when the determined equivalent diffusivity was used. This happens probably because di-hydrated potassium aurocyanide precipitates inside the pores of the resin, drastically increasing the intraparticle resistance. As a matter of fact, when the diffusivity used in the model solution is decreased 140 times, the model accurately follows the experimental results.

5.3. DISCUSSION

This work shows that a resin already considered as a waste from an industrial demineralizing plant can indeed be used to recover and concentrate gold from low concentrated solutions. The advantages, both from the economical and the environmental points of view are evident. As a matter of fact, the resin itself has a null (or even negative) cost and its useful life time is extended by recycling and reusing it in the recovery of a high value material (gold); moreover pollution is reduced.

Again, a convenient model is able to accurately predict the system behavior and simulations with the model enable the search of ideal conditions for the envisaged purpose.

REFERENCES

1. A.E. Rodrigues, and M. Minceva, Modelling and Simulation in chemical engineering: tools for process innovation, *Comp. Chem. Eng.* 29, 1167-1183 (2005).
2. R. Aris, *Mathematical Modeling Techniques* (Dover Publications, New York, 1994).
3. W.A. Chudyk, and V.L. Snoeyink, Bioregeneration of activated carbon saturated with phenol, *Environ. Sci. Technol.* 18, 1-5 (1984).
4. S.A. Figueiredo, Remoção de Corantes Têxteis em Solução Aquosa Usando Materiais Naturais Contendo Quitina, *Ph.D. Thesis*, FEUP, Univ. Porto, Portugal, 2002.
5. G. McKay, and H.S. Blair, The adsorption of dyes onto chitin in fixed bed columns and batch adsorbers, *J. Appl. Polymer Sci.* 29, 1499-1514 (1984).
6. S.A. Figueiredo, Remoção de Cor em Efluentes de Tinturarias Têxteis Usando Adsorventes de Baixo Custo, *M.Sc. Thesis*, FEUP, Univ. Porto, Portugal, 1997.
7. S.A. Figueiredo, R.A. Boaventura and J.M. Loureiro, The removal of dyestsuffs from textile wastewaters using low cost adsorbents, in *Fundamentals of Adsorption 6*, edited by F. Meunier (Elsevier, Paris, France, 1998), pp. 1023-1028.
8. S.A. Figueiredo, R.A. Boaventura, and J.M. Loureiro, The application of natural waste materials as adsorbents for textile dyestsuffs removal – kinetic studies, in *Fundamentals of Adsorption 7*, edited by K. Kaneko, H. Kanoh and Y. Hanzawa (IK International, Chiba, Japan, 2002), pp. 810-817.
9. S.A. Figueiredo, J.M. Loureiro, and R.A. Boaventura, Natural waste materials containing chitin as adsorbents for textile dyestuffs: batch and continuous studies, *Water Research* 39, 4142-4152 (2005).

10. S.A. Figueiredo, R.A. Boaventura, and J.M. Loureiro, Color removal with natural adsorbents: modelling, simulation and experimental, *Sep. Pur. Technol.* 20, 129-141 (2000).
11. J. Loureiro, C. Costa, and A. Rodrigues, Dynamics of adsorptive reactors. I-Instantaneous nonlinear adsorption and finite zero order irreversible reaction, *Can. J. Chem. Eng.* 68, 127-138 (1990).
12. J. Loureiro, C. Costa, and A. Rodrigues, Propagation of concentration waves in fixed-bed adsorptive reactors, *The Chem. Eng. J.* 27, 135-148 (1983).
13. J.M. Loureiro, and A.E. Rodrigues, in: *Fundamentals of Adsorption*, edited by A.B. Mersmann and S.E. Scholl (Un. Eng. Trustees, N. York, USA, 1991), pp. 507-516.
14. D.K. Friday, The breakthrough behaviour of a light gas in a fixed-bed adsorptive reactor, *AICHE Symp. Series* 84, 89-93 (1988).
15. R.C. Soares, J.M. Loureiro, C. Sereno, and A.E. Rodrigues, Modeling and simulation of carbon mask adsorptive reactors, *Ind. Eng. Chem. Res.* 34, 2762-2768 (1995).
16. A.M. Ribeiro, and J.M. Loureiro, Simulation of toxic gases and vapours removal by activated carbon filters, *Chem. Eng. Sci.* 57, 1621-1626 (2002).
17. A. Laguecir, Synthèse de capsules complexantes en polyamide à base d'un gel d'acide polyacrylique. Application à l'extraction de métaux lourds et modélisation du transfert d'ions, *Ph.D. Thesis*, ECPM, Univ. Louis Pasteur, Strasbourg, France, 2001.
18. Y. Frère, L. Danicher, A. Laguecir, J.M. Loureiro, and M. Burgard, Complexing capsules – metal extraction and modelling of ion transfer, *Int. J. Pharmaceutics* 242, 393-397 (2002).
19. F. Helfferich, *Ion Exchange* (Dover Publications, New York, 1995).
20. A. Laguecir, Y. Frère, L. Danicher, J.M. Loureiro, B. Ernst, and M. Burgard, Polyacrylic gel beads reinforced by a polyamide membrane: application to copper removal in aqueous media, *Desalination* 146, 311-317 (2002).
21. E. Boschetti, Advanced sorbents for preparative protein separation purposes*, J. Chromatogr. A* 658, 207-236 (1994).
22. M. Rendueles de la Vega, C. Chenou, J.M. Loureiro, and A.E Rodrigues, Mass transfer mechanisms in Hyper D media for chromatographic proteins separation, *Bioch. Eng. J.* 1, 11-23 (1998).
23. A.E. Rodrigues, J.M. Loureiro, and R.Q. Ferreira, Intraparticle convection revisited, *Chem. Eng. Comm.* 107, 21-33 (1991).
24. Z. Lu, J.M. Loureiro, M.D. LeVan, and A.E. Rodrigues, Pressure swing adsorption processes: intraparticle diffusion/convection models, *Ind. Eng. Chem. Res.* 32, 2740-2751 (1993).
25. C.P. Gomes, M.F. Almeida, and J.M. Loureiro, Gold recovery with ion exchange used resins, *Sep. Pur. Technol.* 24, 35-57 (2001).
26. B. Bolto, and L. Pawlowski, in: *Fundamentals and applications of ion exchange*, edited by L. Liberti and J.R. Millar (Martinus Nijhoff Pubs., Dordrecht, The Netherlands, 1985), pp. 144-176.
27. M. Rendueles de la Vega, J.M. Loureiro, and A.E. Rodrigues, Equivalence between Nernst-Planck and 'corrected' Fick's law in modelling fixed-bed ion exchange processes, *The Chem. Eng. J.* 61, 123-132, 1996.

SOME ASPECTS OF PHYSICAL AND CHEMICAL ADSORPTION ON SURFACE OF AMORPHOUS SOLID

TAMAZ A. MARSAGISHVILI*, M.N. MACHAVARIANI
Institute of Inorganic Chemistry and Electrochemistry of Georgian Academy of Sciences, 11, Mindeli str., Tbilisi, 0186, Georgia

S.A. KIRILLOV
Institute for Sorption and Problems of Endoecology, Ukrainian National Academy of Sciences, 13, General Naumov St., 03680 Kyiv, Ukraine

Abstract. Theoretical calculation of rate constant of adsorption of polyatomic particles on the surface of amorphous solid is carried out in this work. Calculation is conducted within the frames of quantum theory. The question of the characteristics (geometric parameters and frequencies of intramolecular vibrations) of polyatomic polarizable adsorbing particles in polar medium is considered. Calculations are carried out taking into account the interaction of intramolecular vibrations of the particle with polarization fluctuations of the medium. The proposed scheme of calculations allows taking into account the effects of frequency and spatial dispersion of amorphous solid. Events of physical and chemical adsorption are considered.

Keywords: physical adsorption; chemical adsorption; amorphous solid

1. Introduction

Sorbents, which are able to adsorb in pores impurity particles are used for liquid, first of all water, purification process from impurities. Adsorption of different impurities on channel's walls in amorphous solid depends considerably on electrostatic field of charges distributed on channel's walls.

* To whom correspondence should be addressed. E-mail: tmars@geo.net.ge

J.M. Loureiro and M.T. Kartel (eds.), Combined and Hybrid Adsorbents, 349–356.

Adsorption may be physical or chemical depending on the form of interaction of adsorbed particles with adsorbent. Too many monographs and articles are devoted to theoretical investigations of physical and chemical adsorption, in order to quote them in the present work. Advisedly we will restrictly consider only some quantum aspects of interaction of particles with the surface of amorphous solid, which allow to see the complexity of the problem of conducting analytical calculations.

2. System's Hamiltonian

The adsorption problem for polyatomic charged particles is of interest theoretically. The existence of electrostatic interaction between the adsorbing particle and the medium (amorphous solid and liquid) induces medium polarization. Polarized medium influences adsorbed particle, in its turn, and polarizes it. System's Hamiltonian can be presented as follows:

$$H = H_m^s + H_p - \int \left\langle \vec{P}(\vec{r}) \right\rangle_0 \vec{E}(\vec{r}, Q_0) d\vec{r} - \int \delta\vec{P}(\vec{r}) \vec{E}(\vec{r}, Q_0) d\vec{r} \qquad (1)$$

where H_m^s is system's Hamiltonian; H_p is Hamiltonian of the particle; $\langle P(r) \rangle_0$ is average value of system's polarization, stimulated by electric field of the particle with field intensity $E(r,Q_0)$, (Q_0 is set of intramolecular coordinates of the particle). Transforming from the Hamiltonian of nonpolarized medium H_m^s to Hamiltonian of polarized medium H_m, in dielectric approximation we have:

$$H = H_m + H_p - \frac{1}{2} \int \left\langle \vec{P}(\vec{r}) \right\rangle_0 \vec{E}(\vec{r}, Q_0) d\vec{r} - \int \delta\vec{P}\vec{E}(\vec{r}, Q_0) d\vec{r} \qquad (2)$$

For electric field intensity of particle in dipole approximation we can use the expression:

$$\varepsilon_\alpha(\vec{r}) = -\int d\vec{r} G_{E_\alpha E_\beta}(\vec{r}, \vec{r}') \sum_{i=1}^{N} \mu_\beta^i(\vec{R}_i) \delta(\vec{r} - \vec{R}_i) + G_{E_\alpha \varphi}(\vec{r}, R) \rho(\vec{R}) \qquad (3)$$

Here G_{EE} and G_{E_φ} are Green functions of the electric field intensity operators and of the condensed medium scalar potential; μ^i is the dipole moment of the i-th bond of the particle, R_i is the radius vector of the i-th dipole of the particle, ρ, R are the charge of the particle and the radius vector of the charge localization point.

For the polarizable particle the value of μ^i is different from the corresponding vacuum value μ_0^i, it can be defined from

$$\mu_\alpha^i = \mu_0^i + \sum_{j=1}^{N} \alpha_{\alpha\beta}^i \left\{ G_{E_\beta E_\gamma} \mu_\gamma^i + G_{E_\alpha \varphi} \rho \right\} \quad (4)$$

where $\alpha_{\alpha\beta}^i$ is the polarizability tensor of the i-th bond of the particle. It is obvious that if all the components of the polarizability tensor and vacuum values of the bond dipole moments are known, then it is possible to find all the *3N* values of μ from the system (4). As Green functions we can use the corresponding solutions of the electrostatic problems of model functions which allow taking into account the effects of the spatial dispersion of the medium (amorphous solid and liquid in channels). Further on, substituting the found values of μ_α^i in the correlation (3) we define thus the intensity of the system's electric field $\varepsilon(r, R_{i,})$ and find mean polarization of the medium $\langle P(r) \rangle_0$ using fluctuation-dissipation theorem.

Hamiltonian of the system may be written as follows:

$$H = H_m + H_p + \frac{1}{2} \int \vec{E}(\vec{r}, Q) G_{PP}^R(\vec{r}, \vec{r}') \vec{E}(\vec{r}, Q) d\vec{r} d\vec{r}' - \int \delta \vec{P}(\vec{r}) \vec{E}(\vec{r}, Q) d\vec{r} \quad (5)$$

In this formula we expand the intensity of the electric field in a power series of Q^0 up to linear terms,

$$H = \delta\Omega_0 + H_p + H_m - \int d\vec{r} \delta \vec{P}(\vec{r}) \vec{E}(\vec{r}, Q) \quad (6)$$

Here H_p is the Hamiltonian of the polarized solvated particle,

$$H^p = H^{p0} + \sum_n d_n Q_n^0 + \sum_{nn'} h_{nn'} Q_n^0 Q_{n'}^0 \quad (7)$$

where

$$h_{nn'} = \frac{1}{2} \frac{\partial E^0}{\partial Q_n^0} G_{PP}^R \frac{\partial E^0}{\partial Q_m^0}_{Q_n^0 = Q_{n0}^0},$$

$$d_n = \frac{1}{2} (E^0 G_{PP}^R \frac{\partial E^0}{\partial Q_n^0} + \frac{\partial E^0}{\partial Q_n^0} G_{PP}^R E^0)_{Q_n^0 = Q_{n0}^0} \quad (8)$$

In (6) $\delta\Omega_0$ is free energy of the solvated particle, it has the form:

$$\delta\Omega_0 = \frac{1}{2} \int dt dt' \int d\vec{r} d\vec{r}' E_\alpha(\vec{r}, Q_0^0) G_{P_\alpha P_\beta}^R(\vec{r}, \vec{r}', t - t') E_\beta(\vec{r}, Q_0^0) \quad (9)$$

With the help of some transformation of coordinates (shifting and turning) the Hamiltonian H_p can be reduced to a quadratic form with frequencies ω_s and coordinates Q_s.

$$H_p = \frac{1}{2}\sum_s \omega_s \left[(Q_s - Q_{so})^2 - \frac{\partial^2}{\partial Q_s^2} \right] + J \tag{10}$$

where Q_{s0} is the equilibrium value of the Q_s coordinate, J is minimal energy of the particle.

It is obvious that the influence of the solvated polarized particle upon the medium leads to additional medium polarization. Because of this it is necessary to use the characteristics of polarized particle in (6)-(10) and to bring in $E(Q_0)$ instead of $E(Q)$.

In formula (6) we expand the intensity of the electric field E in a power series of $Q - Q_0$ up to the linear term. As a result we have:

$$H = \delta\Omega_0 + H_m + H_p + H_{int}^{(1)} + H_{int}^{(2)} \tag{11}$$

where

$$H_{int}^{(1)} = -\int \delta\vec{P}\vec{E}(\vec{r}, Q_0)d\vec{r} \tag{12}$$

is the interaction of medium polarization fluctuation with impurity static field and

$$H_{int}^{(2)} = -\sum_s \int d\vec{r}\delta\vec{P}(\vec{r})\delta Q_s \vec{V}_s(\vec{r}); \quad \vec{V}_s(\vec{r}) = \frac{\partial\vec{E}(\vec{r}, Q)}{\partial Q_s}_{Q_s = Q_{s0}} \tag{13}$$

is the interaction of medium polarization fluctuation with intramolecular vibrations of impurity.

Hamiltonian of initial state we will write down as:

$$H = H_m^i + H_{sol}^i + H_p^i + H_{m,p}^{int} + H_{p,sol}^{int} + H_{m,sol}^{int} \tag{14}$$

where H_m^i is Hamiltonian of medium (liquid), where is placed the adsorbing particle; H_p^i is Hamiltonian of this particle; H_{sol}^i is Hamiltonian of amorphous solid; $H_{m,p}^{int}$ is interaction of the particle with liquid medium; $H_{p,sol}^{int}$ is interaction of the particle with amorphous solid; $H_{m,sol}^{int}$ is interaction Hamiltonian of liquid medium with amorphous solid.

Hamiltonian in final state has the form:

$$H = H_m^f + H_{sol}^f + H_{m,sol}^{int} \tag{15}$$

Within the frames of this model, the particle is adsorbed on channel's wall of amorphous solid in final state. Amorphous solid can be characterized by additional intramolecular vibration (one or several) appeared as a result of chemical adsorption in final state.

3. Physical Adsorption on the Channel's Surface of Amorphous Solid

First of all let's consider the process of physical adsorption of the particle on the channel's surface of amorphous solid from liquid. It will be assumed, at that, that additional vibrating degree of freedom does not appear in the system in adsorption state. It is assumed that number of vibrating degrees of freedom at the beginning and at the end of the process is equal. Even with this assumption general expression for the rate constant of the process has rather bulky character. The case when intramolecular oscillations may be considered as classical will be regarded for simplicity.

Rate constant of adsorption process can be expressed as:

$$K_a = \left|V_{fi}(\vec{R}^*,\psi^*)\right|^2 \Phi(\vec{R}^*,\psi^*)U(\vec{R}^*,\Psi^*)\exp\Bigg\{-\beta\theta^*\Delta F - \psi^m(\vec{R}^*,\psi^*;\theta) -$$
$$-\beta\sum_{n=1}^{N} E_{rn}\frac{\theta^*(1-\theta^*)\omega_n^i\omega_n^f}{(1-\theta^*)(\omega_n^i)^2+\theta^*(\omega_n^f)^2} - \theta\sum_{k=1}^{N}\ln(\omega_n^f/\omega_n^i) - \theta^*\ln\Big[1+$$
$$+\beta\sum_{k=1}^{N}(G_k(\vec{R}^*,\psi^*)+\frac{\omega_k^f}{\omega_k^i}\overline{G}_k(\vec{R}^*,\psi^*))\frac{\sqrt{2E_{rk}\omega_k^i}}{\omega_k^f}\Big]\Bigg\}(2\pi)^{1/2}$$
$$\left[\prod_{s=1}^{N}\frac{\omega_s^i}{\sqrt{(1-\theta^*)(\omega_s^i)^2+\theta^*(\omega_s^f)^2}}\right]\Bigg\{1+\sum_{k=1}^{N}\left[G_k(\vec{R}^*,\psi^*)+\frac{\omega_k^f}{\omega_k^i}\overline{G}_k(\vec{R}^*,\psi^*)\right]$$
$$(\beta\theta^*-F_\omega(\theta^*))\sqrt{2E_{rk}\omega_k^i}\,\theta^*(\omega_k^f)^2\Big[(1-\theta^*)(\omega_k^i)^2+\theta^*(\omega_k^f)^2\Big]^{3/2}\Bigg\} \tag{16}$$

where point of inflection θ^* may be found from equation:

$$\beta\Delta F + \frac{\partial\psi^m(R^*,\psi^*;\theta)}{\partial\theta} + \frac{\partial}{\partial\theta}\sum_{k=1}^{N}\beta E_{rk}\frac{\theta(1-\theta)\omega_k^i\omega_k^f}{(1-\theta)(\omega_k^i)^2+\theta(\omega_k^f)^2} +$$
$$\ln\prod_{k=1}^{N}\frac{\omega_k^f}{\omega_k^i} + \ln\left\{1+\beta\sum_{k=1}^{N}\left[G_k\left(\vec{R}^*,\psi^*\right)+\frac{\omega_k^f}{\omega_k^i}\overline{G}_k\left(\vec{R}^*,\psi^*\right)\right]\frac{\sqrt{2E_{rk}\omega_k^i}}{\omega_k^f}\right\} = 0 \tag{17}$$

In these formulas V_{fi} is resonance integral of interaction of adsorbing particle with the surface (with some particle or group of particles) of amorphous solid. Matrix element is calculated with use of wave functions in frames of concrete model for amorphous solid. Resonance integral V_{fi} can be considered as some phenomenological parameter. Arguments of this resonance integral characterize geometric characteristics of the process, distance to surface, spatial orientation of the particle during adsorption.

Function $\Phi(\vec{R}^*,\psi^*)$ is distribution function (model function may be selected as this function) of adsorbing particles. If geometric dimensions of the channel are big enough for motion of the particles along the channel, distribution of particles will be approximately uniform. If channel dimensions don't allow free passing of particles, then distribution will be determined by mechanism of transfer of particles along the channel (see above previous part). $\Psi^m(\vec{R}^*,\psi^*;\theta)$ is function of medium reorganization. It includes reorganization of two subsystems: amorphous solid, on the wall of which takes place adsorption, and liquid, where the adsorbing particle is placed. Formal expression of it is:

$$\Psi^m(\vec{R}^*,\psi^*,\theta)=\frac{1}{\pi}\int d\vec{r}d\vec{r}'\Delta E_i(\vec{r},\vec{R}^*,\psi^*)\Delta E_k(\vec{r}',\vec{R}^*,\psi^*)$$
$$\int_{-\infty}^{\infty} d\omega\, Im\, g_{ik}{}^R(\vec{r},\vec{r}';\omega)\frac{sh\frac{\beta\omega(1-\theta)}{2}sh\frac{\beta\omega\theta}{2}}{\omega^2 sh\frac{\beta\omega}{2}} \qquad (18)$$

For charge transfer processes there is kinetic parameter – medium reorganization energy, which is determined by formula:

$$E_r^m\left(\vec{R},\psi\right)=-\frac{1}{2}\int d\vec{r}d\vec{r}'\Delta E_i\left(\vec{r};\vec{R},\psi\right)g^R{}_{ik}\ \ (\vec{r},\vec{r}';\omega=0)\Delta E_k(\vec{r}';\vec{R},\psi) \qquad (19)$$

Here $\Delta E_i\left(\vec{r};\vec{R},\psi\right)$ is change of system's electrostatic field strength during transfer process and Green function g^R is temporal function of polarization fluctuations operators of amorphous solid and liquid at finite temperature. In factorization approximation for g^R function we have:

$$g_{ik}{}^R\ (\vec{r},\vec{r}';\omega)=g_{ik}{}^R(\vec{r},\vec{r}';\omega=0)f(\omega) \qquad (20)$$

Reorganization function of medium can be expressed as:

$$\Psi^m(\vec{R}^*,\psi^*,\theta)=E_r^m\frac{2}{\hbar}\int_{-\infty}^{\infty}d\omega f(\omega)\frac{sh\frac{\beta\omega(1-\theta)}{2}sh\frac{\beta\omega\theta}{2}}{\omega^2 sh\frac{\beta\omega}{2}} \qquad (21)$$

When taking the integrals over r and r' it is necessary to consider geometry of channel and that circumstance, that as effects of spatial dispersion of medium (function g(r, r')), so effects of frequency dispersion (function f(ω)) must be described by different model functions for amorphous solid and liquid.

E_{rn} is reorganization energy of n-th intramolecular degree of freedom of adsorbing particle, and ω^i and ω^f are correspondingly the frequencies of intramolecular vibration in the beginning and at the end of the process.

Reorganization functions G and $\overline{G}$ are defined from the formulas:

$$\begin{aligned} G\left(\vec{R},\psi\right) &= -\frac{1}{2}\int d\vec{r}d\vec{r}'\frac{\partial E_i}{\partial Q}\left(\vec{r};\vec{R},\psi\right)g^R{}_{ik}\ \ (\vec{r},\vec{r}';\omega=0)\Delta E_k(\vec{r}';\vec{R},\psi) \\ \overline{G}\left(\vec{R},\psi\right) &= -\frac{1}{2}\int d\vec{r}d\vec{r}'\Delta E_i\left(\vec{r};\vec{R},\psi\right)g^R{}_{ik}\ \ (\vec{r},\vec{r}';\omega=0)\frac{\partial E_k}{\partial Q}(\vec{r}';\vec{R},\psi) \end{aligned} \tag{22}$$

Q – is normal coordinate of intramolecular vibration of the system.

Everything that is concerned with medium reorganization must be considered at their calculation.

Damped functions and oscillated damped functions were applied as model functions for description of effects of frequency and spatial dispersion of medium. As conducted calculations have shown, carrying out of analytical calculations to the end is impossible, and it is necessary to conduct numerical integration.

Activation energy of the process is determined by formula:

$$\begin{aligned} E_a = \theta^*\left(1-\theta^*\right)E_r^m - \Delta F\theta^* + \sum_{k=1}^{N} E_{rk}\theta^*(1-\theta^*)\omega_k^i\omega_k^f\left[\left(1-\theta^*\right)(\omega_k^i)^2+\theta^*(\omega_k^f)^2\right]^{-1} + \\ kT\theta^*\ln\left[1+\beta\sum_{k=1}^{N}\left(G_k+(\omega_k^f/\omega_k^i)\overline{G}_k\right)\right]\left(2E_{rk}\omega_k^i\right)^{1/2}(\omega_k^f)^{-1}+\theta^*\sum_{k=1}^{N}\ln(\omega_k^f/\omega_k^i) \end{aligned} \tag{23}$$

Expression of rate constant will be considerably simplified, if we neglect the interaction of intramolecular vibrations of the particle with fluctuations of medium polarization:

$$E_a = \theta^*\left(1-\theta^*\right)E_r^m - \Delta F\theta^* + \sum_{k=1}^{N} E_{rk}\theta^*(1-\theta^*)\omega_k^i\omega_k^f\left[\left(1-\theta^*\right)(\omega_k^i)^2+\theta^*(\omega_k^f)^2\right]^{-1} \tag{24}$$

Equation for determination of θ^* correspondingly will take the form:

$$\beta\Delta F + \frac{\partial\psi^m(R^*,\psi^*;\theta)}{\partial\theta} + \frac{\partial}{\partial\theta}\sum_{k=1}^{N}\beta E_{rk}\frac{\theta(1-\theta)\omega_k^i\omega_k^f}{(1-\theta)(\omega_k^i)^2+\theta(\omega_k^f)^2} = 0 \tag{25}$$

If intramolecular reorganization of particle may be also neglected, or if the particle is monoatomic, then:

$$E_a = \theta^*\left(1-\theta^*\right)E_r^m - \Delta F\theta^* \tag{26}$$

and for determination of θ^* we have the following equation:

$$\beta\Delta F + \frac{\partial \psi^{m}(R^{*}, \psi^{*}; \theta)}{\partial \theta} = 0 \tag{27}$$

4. Chemical Adsorption on the Surface of the Channel of Amorphous Solid

The following functional equation is obtained for rate constant of the process:

$$K_a = \frac{\left|V_{fi}(\vec{R}^{*}, \psi^{*})\right|^2}{\sqrt{\left|\psi''_{\theta\theta}\right|}} \Phi(\vec{R}^{*}, \psi^{*}) \exp\left\{-\beta\theta^{*}\Delta F - \psi^{m}(\vec{R}^{*}, \psi^{*}; \theta) - \right. \tag{28}$$

$$\left. \Psi^{v}(\vec{R}^{*}, \psi^{*}; \theta) - \Psi^{mv}(\vec{R}^{*}, \psi^{*}; \theta) \right\} * N(\vec{R}^{*}, \psi^{*}; \theta; \omega_n)$$

Functions $\Psi^{v}(\vec{R}^{*}, \psi^{*}; \theta)$ and $\Psi^{mv}(\vec{R}^{*}, \psi^{*}; \theta)$ have rather complex form and are reorganization functions of vibration subsystem. Electron resonance integral $\left|V_{fi}(\vec{R}^{*}, \psi^{*})\right|$ is calculated as non-diagonal matrix element of interaction of adsorbed particle by electron wave-functions of initial and final states of the system. Function $N(\vec{R}^{*}, \psi^{*}; \theta; \omega_n)$ is calculated for concrete processes with consideration of geometry of channel and particles.

5. Conclusions

Processes of physical and chemical adsorption of polyatomic particles on the surface of amorphous solid are considered. Analytical expressions for kinetic parameters, characterizing adsorption processes are obtained. As it is obvious from the analysis of obtained results, interaction of intramolecular vibrations of adsorbed substance with polarization fluctuations of amorphous solid and liquid, from which adsorption takes place, has considerable influence on the process during adsorption.

ACKNOWLEDGMENTS

We are deeply thankful to STCU for financing of works (Project GR-85(j)). We express our thanks to NATO ARW for financial support for participation in conference and possibility of presentation of the results.

BREAKTHROUGH BEHAVIOR OF WATER VAPOR ON ACTIVATED CARBON FILTERS

ANA MAFALDA RIBEIRO AND JOSÉ MIGUEL LOUREIRO*
LSRE, Department of Chemical Engineering, University of Porto, 4200-465 Porto, Portugal

Abstract. The dynamic behavior of water vapor adsorption on activated carbon filters is studied by simulation. A model, that includes axial dispersion and where the adsorption equilibrium is represented by the Dubinin-Serpinski equation, is developed. The influence of the axial Peclet number on the breakthrough curve is evaluated.

Keywords: dynamic simulation; carbon filters; water adsorption

1. Introduction

Activated carbon, being one of the best adsorbents for organic chemicals, is used in gas mask filters for purifying contaminated air. As human lives depend on the correct use of these filters it is crucial to be able to predict their breakthrough time accurately.

During normal use of these filters, water is generally present, either pre-adsorbed or as humidity in the feed stream (or both). It is well known[1-3] that its presence can affect the breakthrough curves of the toxic compounds significantly.

The purpose of this work is to simulate the dynamic adsorption of water vapor on activated carbon filters and to assess the influence of the axial Peclet number on the obtained breakthrough curves.

* To whom correspondence should be addressed. José Miguel Loureiro, Laboratory of Separation and Reaction Engineering, Department of Chemical Engineering, University of Porto, Rua Dr. Roberto Frias, 4200-465 Porto, Portugal; e-mail: loureiro@fe.up.pt

J.M. Loureiro and M.T. Kartel (eds.), Combined and Hybrid Adsorbents, 357–360.

2. Model Equations

In order to describe the behavior of the filter, a mathematical model was developed which considers axial dispersed plug flow of the fluid phase and absence of resistances. The dimensionless form of the model is:

$$\frac{1}{Pe}\frac{\partial^2 f}{\partial x^2} - \frac{\partial f}{\partial x} - (1+\xi D)\frac{\partial f}{\partial \theta} = 0 \tag{1}$$

with the initial (2) and boundary (3) conditions,

$$\theta = 0 \qquad f = 0 \tag{2}$$

$$x = 0 \qquad 1 = f - \frac{1}{Pe}\frac{\partial f}{\partial x} \tag{3a}$$

$$x = 1 \qquad \frac{\partial f}{\partial x} = 0 \tag{3b}$$

and where f is the dimensionless fluid concentration, x is the dimensionless axial coordinate, θ is time normalized by the column space time and D is the derivate of the adsorption isotherm in respect to f. The model parameters are:

- $Pe = u_i L / D_{ax}$, axial Peclet number;
- $\xi = \left[(1-\varepsilon)/\varepsilon\right](q_E / c_E)\,\rho_{ap}$, column capacity factor.

The equilibrium adsorption isotherm was represented by the Dubinin-Serpinski equation (4), using the parameters values for the BPL activated carbon at 28 ºC previously determined.[4]

$$\frac{P}{P_0} = \frac{q}{K_1 (q_0 + q)(1 - K_2 q)} \tag{4}$$

When solving the model equation, a numerical problem arises at $f = 0$, that was overcame using the l'Hôpital rule to calculate the limit of D at that point, which is given by (5).

$$\lim_{f \to 0} D = \frac{q_0 K_1 R_g T C_E}{q_E P_0} \tag{5}$$

The limiting case, i.e. infinite Peclet number, was also determined using the equilibrium theory for a single solute.[5]

3. Simulation Results and Discussion

The commercial package PDECOL[6] was used to numerically integrate the model equation. The influence of the Peclet number on the breakthrough behavior was evaluated for different feed humidity contents. The results are shown in Figures 1 to 3.

The shape of the breakthrough curves is a result of the shape of the isotherm and is, in this case, composed of two parts, as expected from the equilibrium theory. The first is a dispersive and the second a compressive front or shock.

When axial dispersion is present, a competitive effect between the dispersion and the equilibrium appears. As the Peclet number decreases, broader curves result and eventually the effect of the shock is no longer visible on the breakthrough curve.

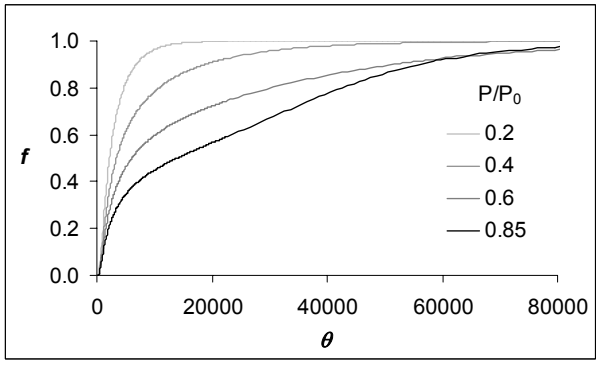

Figure 1. Breakthrough curves of water vapor for *Pe* = 3 and different feed humidity values.

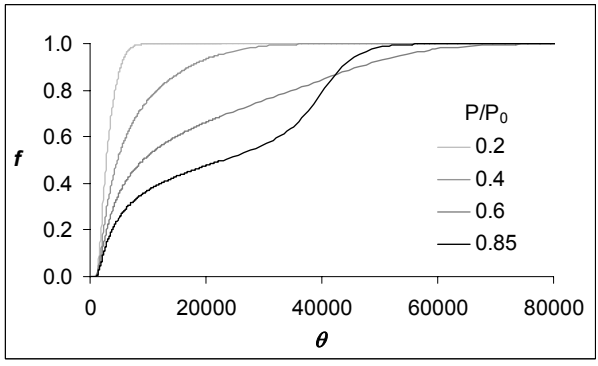

Figure 2. Breakthrough curves of water vapor for *Pe* = 30 and different feed humidity values.

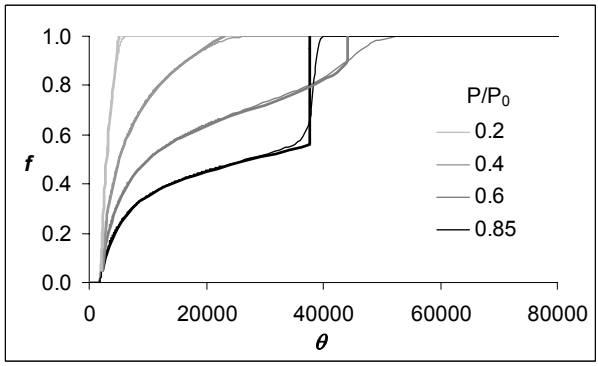

Figure 3. Breakthrough curves of water vapor for: —— *Pe* = 300, ▬▬ Pe = ∞ and different feed humidity values.

A qualitative comparison can be made between these simulation results and the experimental curves obtained by Qi[7], where the shape of the breakthrough curve is well reproduced with this simple model.

These results also show that distinct feed humidity contents produce significantly different breakthrough curves, making it an important variable when the competitive adsorption with the toxic compounds is considered.

REFERENCES

1. P. Lodewyckx, The Influence of Water Vapour on the Adsorption of Organic Vapours by Activated Carbon, *Ph.D. Thesis*, University of Antwerpen, Belgium, 1998.
2. E. Biron and M.J.B. Evans, Dynamic adsorption of water-soluble and insoluble vapours on activated carbon, *Carbon* 36 (7-8), 1191-1197 (1998).
3. M.D. Werner, The effects of relative humidity on the vapor phase adsorption of trichloroethylene by activated carbon, *Am. Ind. Hyg. Assoc. J.* 46 (10), 585-590 (1985).
4. A.M. Ribeiro, M. Vilarinho, and J.M. Loureiro, Adsorption isotherms of MTBE and water vapors on BPL, ASC and ASC-Teda Carbons. *International Conference on Carbon*, Gyeongju (Korea), 2005.
5. A.E. Rodrigues, Modeling of percolation processes, in: *Percolation Processes: Theory and Applications*, edited by A.E. Rodrigues and D. Tondeur (Sithoff & Noordhoff, Alphen aan den Rijn, 1981) pp. 31-81.
6. N. Madsen, .K. and R.F. Sincovec, PDECOL: General collocation software for partial differential equations, *ACM Transactions on Mathematical Software* 5, 326-351 (1979).
7. N. Qi, Adsorption of Organic Coumpounds and Water Vapor on Activated Carbon: Equilibria and Fixed-Bed Humidity Steps, *Ph.D. Thesis*, Vanderbilt University, USA, 2003.

LIST OF PARTICIPANTS

BAKALINSKAYA, Olga N.	Institute for Sorption & Problems of Endoecology, NAS of Ukraine, General Naumov Street 13, Kiev 03164, UKRAINE
BANDOSZ, Teresa	The City College of the City University of New York, Dept. of Chemistry; Convent Avenue & 138 Street, New York, NY 10031, USA
CHMIELEWSKA, Eva	Comenius University, Faculty of Natural Sciences, Mlynská dolina, 842 15 Bratislava, SLOVAKIA
CHUBAR, Natalia I.	Institute for Sorption & Problems of Endoecology, NAS of Ukraine, General Naumov Street 13, Kiev 03164, UKRAINE
DIZHBITE, Tatiana	Latvian State Institute of Wood Chemistry, 27 Dzerbenes str., Riga, LV 1006, LATVIA
DOBELE, Galina	Latvian State Institute of Wood Chemistry, 27 Dzerbenes str., Riga, LV 1006, LATVIA
DZUL EROSA, Mercy-Sugey	Forshchungszentrum Karlsruhe, University of Karlsruhe, P.O. Box 3640, 76021, GERMANY
FREITAS, Olga M.	REQUIMTE, Instituto Superior de Engenharia do Porto, Rua Dr. Bernardino de Almeida, 431, 4200-072 Porto, PORTUGAL
JARONIEC, Mietek J.	Kent State University, Dept. of Chemistry; P.O. Box 5190, Kent, OH 44242-0001, USA
KANELLOPOULOS, Nikos	Materials & Membranes for Environmental Applications Laboratory, NCSR "Demokritos"; Aghia Paraskevi GR 153 10, GREECE
KARTEL, Mykola T.	Institute for Sorption and Problems of Endoecology, NAS of Ukraine, 13 Gen. Naumov Str., 03164 Kiyv, UKRAINE
KOIVULA, Risto	University of Helsinki; P.O.Box 55, A.I.Virtasen aukio 1, 00014 Helsinki, FINLAND
LASZLO-NAGY, Krisztina	Budapest University of Technology and Economics, Dept. of Phys. Chemistry; Budafoki ut 8, H-1521 Budapest, HUNGARY

LJUTZKANOV, Ljutzkan A.	Inst. of Chem. Engineering, Bulgarian Academy of Sciences, Acad. G. Bonchev St., Bl. 103, 1113 Sofia, BULGARIA
LODEWICKX, Peter	Royal Military Academy, Department of Chemistry, Renaissancelaan 30, B-1000 Brussels, BELGIUM
LOUREIRO, José M.	LSRE/DEQ, Faculdade de Engenharia daUniversidade do Porto, Rua Dr. Roberto Frias, 4200-465 Porto, PORTUGAL
LUPASCU, Tudor	Institute of Chemistry, Academy Science of Moldova, Academiei str. 3, Chishinau, 2028 MD, MOLDOVA
MALYSHEV, Michail E.	Boreskov Institute of Catalysis, Siberian Branch of RAS, Pr. Akademika Lavrentieva 5, Novosibirsk 630090, RUSSIA
MARSAGISHVILI, Tamaz	Algadze Institute of Inorganic Chemistry and Electrochemistry, Georgian Academy of Sciences, 11 Mindeli str., Tbilisi 0186, GEORGIA
MATIS, Kostas A.	Laboratory of General & Inorganic Chemical Technology, Department of Chemistry, Aristotle University, GR-54124 Thessaloniki, GREECE
MIKHALOVSKY, Sergey V.	University of Brighton, School of Pharmacy & Biomol. Sciences; Cockcroft Building, Lewes Road, Brighton BN2 4GJ, Sussex, UK
NAVRATIL, James D.	Clemson University, Dpt. of Environmental Engineering & Science, 432 Computer Court, Anderson, SC 29625-6510, USA
NIKASHINA, Valentina A.	Vernadsky Institute of Geochemistry and Analytical Chemistry of RAS, Kosygin str. 19, Moscow 119991, RUSSIA
NIKOLAYCHUK, Antonina	Institute for Sorption & Problems of Endoecology, NAS of Ukraine, General Naumov Str. 13, Kiev 03164, UKRAINE
PELEKA, Froso	Lab. of General & Inorganic Chem. Technology, Dept. of Chemistry, Aristotle University, GR-54124 Thessaloniki, GREECE

PENDELYUK, O.	Institute for Sorption & Problems of Endoecology, NAS of Ukraine, General Naumov Str. 13, Kiev 03164, UKRAINE
RIBEIRO, Ana Mafalda	LSRE, Department of Chemical Engineering, University of Porto; Rua Dr. Roberto Frias, 4200-465 Porto, PORTUGAL
RIBEIRO, M. Madalena	Rua Tomaz Ribeiro, 65, 6º Esq., 4450-296 Matosinhos, PORTUGAL
RIZHIKOVS, Janis	Latvian State Institute of Wood Chemistry, 27 Dzerbenes str., Riga, LV 1006, LATVIA
RODRGUEZ-REINOSO, F.	Universidad de Alicante, Dept. de Quimica Inorganica; Apdo. Correos 99, E-03080 Alicante, SPAIN
RUSSKOVA, Julia	Lomonosov Moscow State University, Biological Faculty, Department of Microbiology, Vorobievi gori 1/12, Moscow 119992, RUSSIA
RUZIMURADOV, Olim N.	Scientific-Technological Complex “Science and Progress” at Tashkent State University, 7a Mirza Golib str., Tashkent 700174, UZBEKISTAN
SANTOS, Silvia C.R.	Lab. of Separation & Reaction Engineering, Universidade do Porto, Rua Dr. Roberto Frias 4200-465 Porto, PORTUGAL
SHAWABKEH, Reyad A.	Mutah University, Department of Chemical Engineering, AL-Karak, 61710, JORDAN
SHEA, Kenneth J.	University of California, Dept. of Chemistry; 5021 Frederick Reines Hall; Irvine, CA 92697-4575, USA
SOLODOVNIK, Tatyana V.	Cherkassy State Technological University; 460 Shevchenko Boulevard, 18006 Cherkassy, UKRAINE
STRELKO, Volodymyr V.	Institute for Sorption & Problems of Endoecology, NAS of Ukraine; Gen. Naumov Str. 13, Kiev 03164, UKRAINE
SZERBIN, Pavel	"Frédéric Joliot-Curie" National Research Institute for Radiobiology and Radiohygiene, POB 101, 1775 Budapest, HUNGARY
TELYSHEVA, Galina	Latvian State Institute of Wood Chemistry, 27 Dzerbenes str., Riga, LV 1006, LATVIA
TENNISON, Stephen	MAST Carbon Technology Ltd., Henley Park, Guidford GU3 2AF, Surrey, UK

VARTAPETIAN, Ruben Sh.	Institute of Physical Chemistry, Russian Academy of Sciences; Leninsky Prospect 31, Moscow 119991, RUSSIA
VASHPANOV, Yuriy	Mechnikov National University of Odessa, Department of Experimental Physics, 27 Paster Str., Lab. 9, Odessa 65100, UKRAINE
VILAR, Vítor	Lab. of Separation and Reaction Engineering, Universidade do Porto, Rua Dr. Roberto Frias, 4200-465 Porto, PORTUGAL
WOLBORSKA, Anna	Technical University of Lodz, Faculty of Process and Environmental Engineering, Ul. Wolczanska 213, Lodz, 90-924, POLAND
ZAITSEVA, Hanna O.	Institute for Sorption & Problems of Endoecology, NAS of Ukraine, General Naumov Street 13, Kiev 03164, UKRAINE
ZHURAVLYEV, Igor Z.	Institute for Sorption & Problems of Endoecology, NAS of Ukraine, General Naumov Str. 13, Kiev 03164, UKRAINE
ZIMMERMANN, Wolfgang	University of Siegen, Dept. of Mechan. Engineering, Inst. of Fuid- & Thermodynamics; Paul-Bonatz-Str. 9-11, 57068 Siegen, GERMANY
ZUB, V.	Institute of Surface Chemistry, NAS of Ukraine; Gen. Naumov Str. 17, Kiev 03164, UKRAINE
ZUB, Yuriy L.	Institute of Surface Chemistry, NAS of Ukraine; Gen. Naumov Str. 17, Kiev 03164, UKRAINE

INDEX

Acetic acid, glacial 202
Activated
  carbo-aluminosilicate 249
  carbon 249–251, 253, 257, 258, 295, 296, 298, 302, 307, 321, 322, 324, 325, 327–331, 333, 337, 339, 342, 343, 357, 358
Activation
  thermochemical 225
Adsorber
  fixed bed 219
Adsorption
  benzene 307
  cadmium and lead 189
  capacity 24, 27–29, 113, 116, 129, 136, 138
  cations 39, 47, 50
  characteristics 50, 52
  chemical 349, 350
  chromium ions 249, 250
  combined preparations 167, 168
  dye 191, 212
  equilibrium 283, 339, 343, 357
  filters 220
  formaldehyde 126, 182
  front 324
  gas phase 325
  heat 325
  isotherms 64, 79, 109, 113, 131, 169, 171, 173, 183
  kinetics 327, 329, 330
  lead 269
  n-butane 219
  nitrogen 220, 295
  oral preparations 165
  phenol 63, 119, 231
  physical 145, 152
  process 155, 156, 196
  properties 207, 208, 210, 211, 213, 214, 216, 225, 231
  radioactive cesium 41
  sulfur containing species 145
  viruses of plants 261
  water 301, 302
Agent
  structure forming 4–6, 9
  toxic 321–323
Akaganéite
  iron precursor 105
Algal
  biomass 270
  waste 281
Algae
  marine, macro 270
Antimony removal 287
Arsenate
  oxyanions, removal 65
  pollutants removal 63
Ascophyllum nodosum 269
Aspergillus niger 275
Axial
  dispersion 324, 341
  Peclet number 341
Bactericide
  cations 71
Bentonite
  adsorbent 106, 111
Benzene
  adsorption 307
  self-diffusion data 307
Biodegradation 340
Biosensors 261
Biosorption
  biosorbent 270
  optimization 269
  performance 281
  process 282
Bis(trialkoxysilanes)
  structure-forming agent 4
Box-Behnken 269
Breakthrough
  behavior 321, 357
  curve 357, 359, 360
  modeling 330
  time 330
Cadmium
  cations, removal 105, 107, 108
Calixarenes 51

and their derivatives 49
Calorimeter
sensor gas 219
Canister, activated carbon 220
Car washing stations
oil products 213
waste water 214
Carbon
activated 219, 220, 234, 235, 237, 238, 245, 249, 250, 253
bed 321
biologically active 78, 237
canister 321
chemically treated 119
cloth 329
dioxide, sequestration 23
fiber 151, 153
filter 321, 322, 333
functionalized 117
granular 321
in gas separation and storage 133
materials, low density 181
mineral sorbent 208
modified, active 168
molecular sieve 78, 133
monolith 330
N-containing 155, 201
nanoporous 30, 119
surface chemistry 147
synthetic 201
thin layer 330
tube 231
Carboxykam 165
Catalytic
activity 201, 204
processes 232
support 232
Cations
adsorption 155
bactericide 71, 72
template effect 93
three charge 93
Cesium
selective removal 37
radioactive, 41
Characterization
hard porous materials 309
hybrid polymer-silica 55
mesoporous materials 23
methods 57
porous structure 307
soft porous materials 309
tissue scaffolds 309
Chitin
containing sorbent 275
Chitosan 275, 276
Chromatography
hybrid adsorbent 55
Chromium
adsorption 252
chromate, removal 64
ions, adsorption 249
isotherm 250
Citric acid 275
Clinoptilolite
tuff 63, 66
Collagen 309
Color removal 337, 339
Combined
adsorption preparations 165
sorbent 169
Complexing capsules 343
Corrosion
products, removal 37
Design
Box-Behnken 269
factorial expertimental 269
mesoporous materials 23
Desorption
energy 219
process 219
Desulfurization
carbonaceous materials 145
Diffusion
cell 304
coefficient 315, 316
experiments 311
macromolecules 294
measurements 296
resistance 231
self 295
Dimensionless variable 337
Distribution factors 165, 167, 169
Dubinin-Astakov equation 129

Dubinin-Radushkevich equation 125, 183
Dubinin-Serpinski equation 357
Dye
  cationic, astrazon red 111
  adsorption 111
Effluent
  nuclear waste 37
Enterosorbents 165
Environmental
  applications 23, 24, 26
  conditions 321
  constraints 106
  pollution 112
  protection 220
Equilibrium
  adsorption isotherms 64, 79, 109, 113, 131, 169, 171, 298
  characteristics 214
  chemical 244
  model 283, 285, 342
  sorption 195, 288
Fiber
  polyacrilonitrile 213
Filter
  carbon 321, 322
  loading 219
Filtration
  contact 207
  materials, modified 207
Freundlich equation 173, 346
Fuel tanks 31
Fungus mycelium 275
Furfural 187, 298
Gas
  purification 207
  separation 120, 325
  storage 135, 138
Gasoline
  vapor 219
Gelidium sesquipedale 281
Gold recovery 337, 345
Hamiltonian 350
Hard porous materials 309
Heat
  adsorption 213
  effect 219
  latent 219
Hot wire detector 221
Humidity 323
Hybrid
  adsorbents 49, 330
  organic-inorganic materials 3
Hydrogels 309
Hydrogen
  peroxide 257, 258
  sulfide 243, 244
Hydrophobization
  external surface 63
Identification
  polysiloxane xerogels 49
Industrial applications 151, 323
Inorganic
  ion exchanger 37–39, 46
  adsorbent 270
Ion exchange
  properties 93, 155
  radionuclides removal 37
  removal of Se and Sb 279
  selectivity 95
  uranium complex 85
Iron
  nanoadsorbents 105
  precursor 105
Kinetics
  adsorption 133, 136, 327
  characteristics 213
  diffusion 85, 317
  ion exchange 214
  film diffusion 88, 341
  modeling 333
  of sulfide demand 245
  parameters 242
  pseudo second order 111, 114
  sorption 133
  uptake 282
Langmuir equation 109, 283
Lead
  adsorption 269, 273
Lignin 225, 298
  hydrolysis 226
Lignocellulose
  materials 71
  modification 71, 73
Lignosulphonates
  sodium-based 226
Lubricating oil, spent 195

Mask, protective 321
Melamine 201
Mesoporous
carbons 23
hydrothermostability 77
mesophase materials 77
ordered materials 23, 24
silicas and organosilicas 24
volume 99
Metal
catalytic 145
extraction 337
heavy metal ions 23, 105, 255
microprobe technique 14
mixture, binary 282
Microprobe
metal 14
technique 14
Microscopy
confocal 309, 311
electron 311
fluorescence 314
imaging 250
SEM 107, 122, 303, 304
TEM 79, 107
Military
applications 321
threats 323
Mobility of adsorbed molecules 295
Model
chemical engineering 323, 337
column 340
Dubinin-Astakov 129
Dubinin-Radushkevich 125, 183
equations
Freundlich 169, 173, 340
Langmuir 109, 111, 115, 340
mathematical 89, 91, 215
multi-component 281
process 332
reaction kinetic 327
Wheeler-Jonas 327
Molecular sieve 78
Muzzarelli method 275
Neurospora crassa 276
Nitric acid 119, 122, 126, 137, 184, 195, 197
Nuclear
magnetic relaxation times 295
waste effluents 37
Palygorskite 166
Peclet number, axial 341
Pectin 166
apple 171, 256
beet 171
citrus 171
Pectopal 171
Phase change material 219
Polyacrilic gel beads 337
Polyamide membrane 337
Polysiloxane
xerogels 3, 5, 14, 49
Properties
acid/base 119
adsorption 3, 14, 27, 71, 97, 120, 170, 201, 207, 208, 210, 267
catalytic 250
ion exchange 250, 256, 260
molecular sieving 181
of porous silicon 261
Pseudomonas putida 238
Pyrolysis 257
Quantum theory 349
Quartz crystal microbalance 309
Radionuclides
selective removal 37, 166
Recovery of gold 337
Relaxation times 295
Removal
ammonia 243
antimony 287
arsenate oxyanions 105, 109
cadmium cations 105, 107
chromate pollutants 63
color 327
corrosion products 37
formaldehyde 126
heavy metals 165, 174
hydrogen sulfide 243
lead 258
metal ions 260, 279
nitrite ions 243
phenol 121
selective, radionuclides 37

selenium 287
sulfur compounds 145, 239
waste products 208, 309
Resin, exhausted 337
Response surface methodology 269
Ringer salt solution 165
Scaffolds 309, 314
Seafood industry 337
Selectivity
cesium 37, 168
ion exchanger 38, 244
organozeolites 85
Selenium removal 287
Self-diffusion 295
Sequestration
carbon dioxide 23
Silica
characteristics 24
for VOCs 27
hybrid polymer 55
mesoporous 24, 26, 27, 77
organosilica 24
porous silicon 261
synthesis 24
Soft porous materials 301
Sol-gel
method 3, 49, 55, 91, 98
transition time 93
Solid-state
NMR spectroscopy 11
Spectroscopy
ESCA 66
FT-IR 195, 249
IR 51
NMR 11, 287
SAXS 117
solid-state NMR 11
vibrational 10
XPS 63, 66, 117
Spin
lattice 295, 297
spin 297
relaxation times 297
Strontium
selective removal 37
Structure
characteristics 181
chemical 256
crystal 99
mesophase 77
microporous 135, 154, 184
porous 93, 95, 100, 101
polysiloxane xerogels 3, 10, 14
Sulfur
compounds, removal 145
hydrogen sulfide 144, 145, 150, 237
methyl mercaptans 145
species, chemical equilibrium 243
sulfide ions 243
sulfur dioxide 145, 151
sulfuric acid 151, 153, 188
Surface
amorphous solid 349–351
chemistry 245, 247
modification 147, 207
response, methodology 269
Synthesis
high dispersed phosphates 94
hybrid polymer-silica 55
iron-based adsorbents 105
mesoporous materials 23
polysiloxane xerogels 3, 5, 6, 9
titanium phosphates 94
zirconium phosphates 96
Technique
CVD 136
immersion calorimetry 137
metal microprobe 14
quartz crystal microbalance 309
XRD 79, 81, 107
Template
effect 93
Terrorist threats 321
Tetraalkoxysilane
structure-forming agent 6
Tissue scaffolds 309, 310
Titanium
phosphate 99
Toxic
agents 321, 322
environments 337, 339
Treatment
chemical 340
hydrothermal 77

water 85, 86, 88, 89, 91, 94
Tubes
porous wall 231
Tuff
clinoptilolite 63, 69
Ultrasorb 165, 166
Uranium
carbonate complex 85
sorption 85
Viruses
of plants, adsorption 261
Volatile
fuel components 220
organic compounds 27
Wall
porous, tubes 225
Waste
effluents, nuclear 37
natural 337, 338
products removal 292
water treatment 106, 208, 210–212
wood chemical processing 229
Water
adsorption 301, 302
car washing station 213
self-diffusion data 295
vapor, adsorption 295
waste, treatment 46, 99
Wheeler-Jonas model 327
Xerogels
polysiloxane 3, 5, 14, 49
synthesis 3, 5
structure 3
sorption properties 3
Zeolite
in fiber 213
mesoporous 77
organo 83
powder 213
pulverized 213
surface phenomena 66
Zirconium
phosphate 91